Molecular Basis of Redox Signaling

Lead Guest Editor: Maria C. Franco
Guest Editors: Maria C. Carreras and Luciana Hannibal

Molecular Basis of Redox Signaling
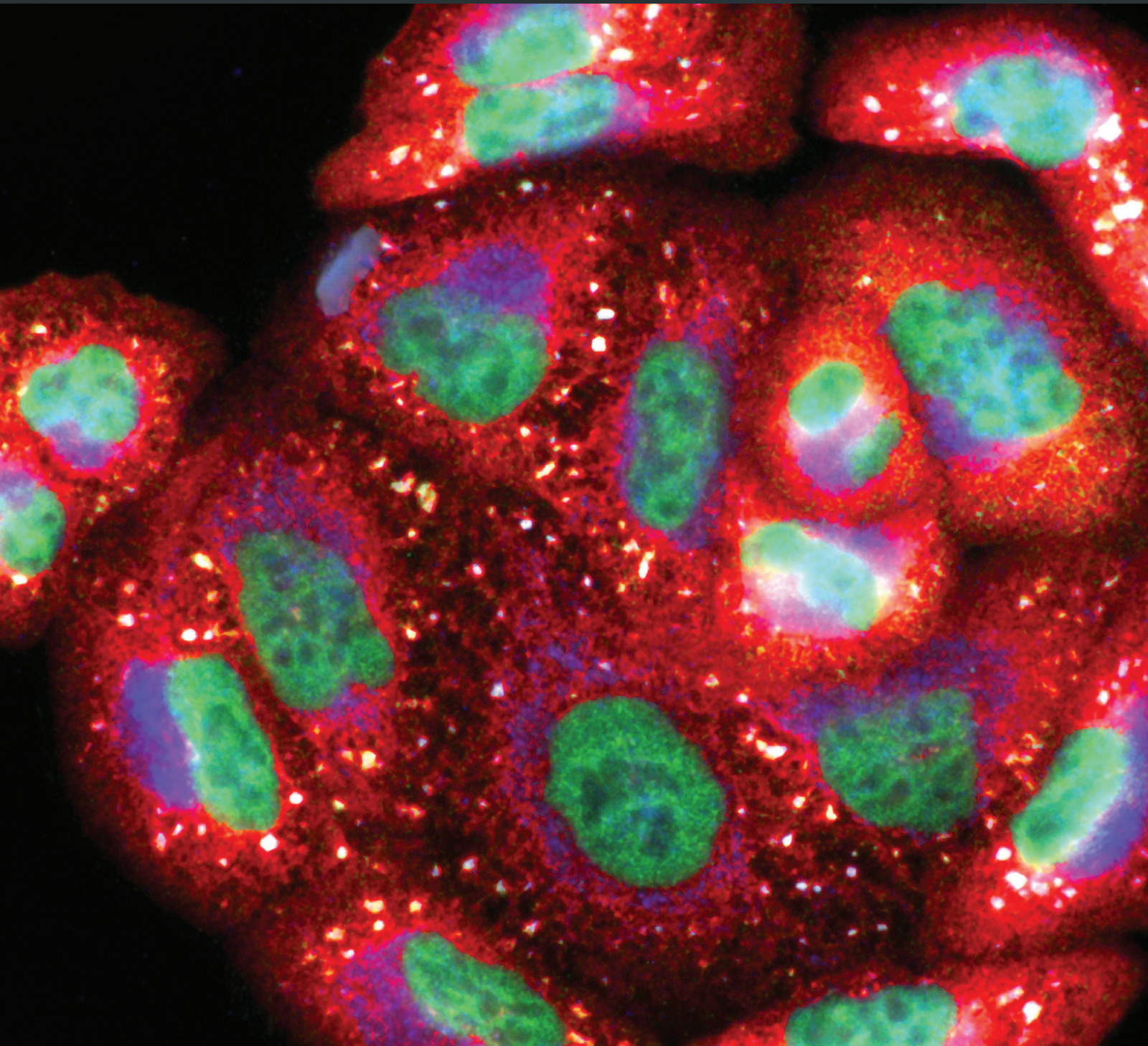
Molecular Basis of Redox Signaling

Lead Guest Editor: Maria C. Franco
Guest Editors: Maria C. Carreras and Luciana Hannibal

Editorial Board

Contents

Editorial
Molecular Basis of Redox Signaling

Maria Clara Franco (ID),[1] Maria C. Carreras (ID),[2] and Luciana Hannibal (ID)[3]

[1]Department of Biochemistry and Biophysics, College of Science, Oregon State University, Corvallis, OR, USA
[2]Departamento de Bioquímica Clínica, Facultad de Farmacia y Bioquímica, Universidad de Buenos Aires, Buenos Aires, Argentina
[3]University Medical Center Freiburg, Freiburg im Breisgau, Germany

Correspondence should be addressed to Maria Clara Franco; maria.franco@oregonstate.edu

Oxidants are produced in physiological and pathological conditions. The production of reactive nitrogen and oxygen species (RNS and ROS, respectively) can lead to vastly different cellular outcomes depending on their subcellular location, half-life, reactivity, gradients, and the antioxidant defenses. While oxidative stress caused by general oxidative damage is often nonspecific and linked to cell death by necrosis, at lower concentrations, ROS and RNS can act as second messengers regulating redox-sensitive signaling pathways, which elicit very specific cellular responses [1, 2]. Redox signaling is an intrinsic, tightly regulated component of cell metabolism, controlling cell growth, differentiation, and death. The interplay between the production of oxidants and the antioxidant defenses is highly regulated to maintain cellular redox homeostasis [3, 4]; thus, its dysregulation underlies many pathological conditions, including cancer, neurodegeneration, and cardiovascular and metabolic diseases. This special issue is focused on redox signaling in pathology and developments in redox-based therapies.

In this issue, H. Pérez et al. examined the molecular basis of the role of p66Shc in brain mitochondrial dysfunction, showing a connection with ROS/RNS production, Sirt 3 activity modulation, and mitochondrial dynamics and biogenesis. The modulation of p66shc activity could be a candidate for therapeutic intervention for longer lifespan or higher quality of life. In an article exploring the stimulatory role of nitric oxide (NO) on protein synthesis in the muscle, R. Wang et al. show that protein synthesis is regulated in a NO-dependent manner in differentiated C2C12 myoblasts by the mTOR/p70S6K pathway, highlighting the potential

clinical applications of targeting the production of NO in muscle metabolism. Also, by a thorough examination of heart function and metabolites in a mouse Nrf2 knock-out model, R. Erkens et al. show that inhibition of NO synthesis at the onset of ischemia (I) and during early reperfusion (R) worsened myocardial damage and systolic dysfunction in Nrf2-deficient animals. The study reveals that eNOS upregulation under conditions of compromised antioxidant capacity may afford cardioprotection against I/R. K. Xu et al. discuss tryptophan and its metabolites as a source of antioxidant defense in the placenta. The authors summarize data on mechanisms that involve tryptophan and 3-hydroxyanthranilic acid, a metabolite of the tryptophan-kynurenine pathway, as initiators of signaling events that activate Nrf2 in the placenta, stimulating the expression of antioxidant proteins and proteins responsible for the biosynthesis of low molecular weight antioxidants.

In relation to cancer, S. V. Kostyuk et al. examined the penetration of easily oxidizable GC-rich DNA fragments (GC-DNA) into breast cancer cells and their potential for therapeutic development. Results from the study indicate that GC-DNA provided in the cell culture medium interacts with the cell surface, induces NOX4 expression, and undergoes oxidation by augmentation of reactive oxygen production. Thus, the incorporation and expression of cell-free DNA in cancer cells may harbor utility for therapeutic development.

Additional articles in this special issue address fundamental aspects of redox signaling in physiological conditions. P. V. Avdonin et al. uncovered that H_2O_2 synergizes with

calcium-mobilizing agonists of the 5-hydroxytryptamine receptors 5-HT1B and 5-HT2B through the induction of endogenous oxidative stress in human umbilical vein endothelial cells and suggested that H_2O_2 potentiation of agonist-induced calcium signaling in endothelial cells may contribute to vasorelaxation. In another study by C. Urbainsky et al., the authors performed a comprehensive analysis of the substrates and functions of the oxidoreductase nucleoredoxin (Nrx) in neuronal cells. Their results suggest that Nrx may be involved in the redox regulation of cell morphology and metabolism.

Four review articles cover current knowledge of the role of oxidants and redox signaling in pathology. S. Boukhenouna et al. discuss the biological role of reactive oxygen species in the progression of chronic obstructive pulmonary disease (COPD) and cellular mechanisms to repair oxidative damage. A primary factor in the development of COPD is exposure to cigarette smoke that induces oxidative stress and epithelial cell damage. Cigarette smoke is the leading risk factor of lung injury and pulmonary emphysema. Sustained oxidative damage to biomolecules forces chronic upregulation of antioxidant and other cytoprotective responses. Under the high oxidative stress conditions documented in patients with COPD, defense systems can reach exhaustion failing to halt further disease deterioration. E. Richard et al. summarize the current knowledge on the pathophysiological role of reactive oxygen species and redox imbalance in inborn errors of metabolism (IEM), with a focus on selected branched-chain amino acid disorders, organic acidurias, and homocystinuria. The authors also cover the source of ROS in these IEMs and evaluate the efficacy of antioxidant therapies and mitochondria-targeted approaches in these diseases. Also, A. Giuffrè and J. B. Vicente present a comprehensive review of the biochemistry of hydrogen sulfide and its intricate interactions with other gasotransmitters. The work covers hydrogen sulfide occurrence in biological fluids and tissues, biogenesis and catabolism by specialized enzymes, partition in intra- and extracellular compartments, signaling, abnormal homeostasis in cardiovascular disease, neurodegenerative disorders and cancer, and reactivity with NO and CO. The review by R. Manoharan et al. describes the role of serine-threonine kinase receptor-associated protein (STRAP) in the regulation of cell proliferation and death in normal and cancer cells. While STRAP interacts with many redox-sensitive proteins to promote cell survival and proliferation in both normal and cancer cells, under conditions that affect the redox balance, STRAP may also induce cell death. This dual role of STRAP in cancer cells may uncover novel therapeutic options for cancer treatment.

Therapeutic strategies aimed at restoring redox homeostasis have been pursued for many years, albeit with very limited success. In this special issue, N. E. Buglak et al. present a critical review of the literature, evaluating successful and unsuccessful approaches, including patient selection, dose, and delivery route. The authors also focus on the development of local targeted delivery of antioxidants as a promising therapeutic approach to address local redox dysfunction. For example, J. Paprocki et al. study how different markers of the oxidant-antioxidant equilibrium are modulated after repeated stimulation with hyperbaric oxygen (HBO), a therapy associated with increased production of reactive oxygen species used to treat sudden sensorineural hearing loss. Another example is the use of cold physical plasma (CAP), a therapeutic strategy that generates reactive oxygen and nitrogen species, used for chronic and acute wound treatment. In this issue, A. Schmidt et al. show that CAP activates a complex cellular response and discuss the functional consequences of the clinical use of plasmas for wound treatment.

The lack of tools to isolate specific oxidative modifications has hindered our understanding of the functional consequences of such modifications for many years. Here, J. J. Porter and R. A. Mehl summarize current knowledge of oxidative posttranslational protein modifications and the development of new tools through genetic code expansion, for the genetically encoded, site-specific incorporation of amino acids carrying oxidative modifications into proteins. These tools enable the accurate determination of the role of a particular posttranslational modification at unique positions in a protein of choice.

In summary, this special issue highlights the importance of understanding the molecular basis of redox signaling and the need for targeted therapies that have so far remained a major challenge in the field.

Conflicts of Interest

The editors declare that they have no conflicts of interest regarding the publication of this special issue.

Acknowledgments

References

[1] M. Schieber and N. S. Chandel, "ROS function in redox signaling and oxidative stress," *Current Biology*, vol. 24, no. 10, pp. R453–R462, 2014.

[2] N. T. Moldogazieva, I. M. Mokhosoev, N. B. Feldman, and S. V. Lutsenko, "ROS and RNS signalling: adaptive redox switches through oxidative/nitrosative protein modifications," *Free Radical Research*, vol. 52, no. 5, pp. 507–543, 2018.

[3] C. Espinosa-Diez, V. Miguel, D. Mennerich et al., "Antioxidant responses and cellular adjustments to oxidative stress," *Redox Biology*, vol. 6, pp. 183–197, 2015.

[4] H. Sies, C. Berndt, and D. P. Jones, "Oxidative stress," *Annual Review of Biochemistry*, vol. 86, no. 1, pp. 715–748, 2017.

Research Article

Enhancement by Hydrogen Peroxide of Calcium Signals in Endothelial Cells Induced by 5-HT1B and 5-HT2B Receptor Agonists

Pavel V. Avdonin [ID],[1] **Alexander D. Nadeev,**[2] **Galina Yu. Mironova** [ID],[1] **Irina L. Zharkikh,**[3] **Piotr P. Avdonin,**[1] **and Nikolay V. Goncharov** [ID][2]

[1]*Koltsov Institute of Developmental Biology RAS, Moscow, Russia*
[2]*Sechenov Institute of Evolutionary Physiology and Biochemistry RAS, Saint Petersburg, Russia*
[3]*Institute of General Pathology and Pathophysiology RAMS, Moscow, Russia*

Correspondence should be addressed to Pavel V. Avdonin; pvavdonin@yandex.ru

Hydrogen peroxide, formed in the endothelium, acts as a factor contributing to the relaxation of blood vessels. The reason for this vasodilatory effect could be modulation by H_2O_2 of calcium metabolism, since mobilization of calcium ions in endothelial cells is a trigger of endothelium-dependent relaxation. The aim of this work was to investigate the influence of H_2O_2 on the effects of Ca^{2+}-mobilizing agonists in human umbilical vein endothelial cells (HUVEC). We have found that H_2O_2 in concentration range 10-100 μM increases the rise of $[Ca^{2+}]_i$ induced by 5-hydroxytryptamine (5-HT) and carbachol and does not affect the calcium signals of ATP, agonist of type 1 protease-activated receptor SFLLRN, histamine and bradykinin. Using specific agonists of 5-HT1B and 5-HT2B receptors CGS12066B and BW723C86, we have demonstrated that H_2O_2 potentiates the effects mediated by these types of 5-HT receptors. Potentiation of the effect of BW723C86 can be produced by the induction of endogenous oxidative stress in HUVEC. We have shown that the activation of 5-HT2B receptor by BW723C86 causes production of reactive oxygen species (ROS). Inhibitor of NADPH oxidases VAS2870 suppressed formation of ROS and partially inhibited $[Ca^{2+}]_i$ rise induced by BW723C86. Thus, it can be assumed that vasorelaxation induced by endogenous H_2O_2 in endothelial cells partially occurs due to the potentiation of the agonist-induced calcium signaling.

1. Introduction

In the early 1930s, the phenomenon of oxidative (respiratory) burst at phagocytosis was described [1]. This work initiated enormous number of studies of the role of ROS in biological processes and systems. High concentrations of ROS normally are characteristic function of the so-called professional phagocytes—cells of innate immunity; in other cells, high concentration of ROS is a sign of oxidative stress and a cause of cell death [2]. Low concentrations of ROS are permanently formed in almost all cells of the body and perform the functions of second messengers in redox-sensitive signaling pathways [3, 4]. The vascular endothelium plays a crucial role in maintaining homeostasis, and it is often

both the main target and one of the sources of ROS [5, 6]. In physiological conditions, the synthesis of ROS by NADPH oxidases (NOX) carries out a signaling function [7]; however, the disturbance of its metabolism and associated signaling pathways is the cause of many vascular pathologies [8]. In terms of signaling, H_2O_2 is considered as the most stable and important kind of ROS. According to some data, the concentration of both endogenous and exogenous H_2O_2 can reach hundred micromoles [9–11]. In vascular endothelial cells H_2O_2 is produced by NOX4, and it was demonstrated that its targeted overexpression in endothelial cells results in a decrease in blood pressure and potentiation of relaxation under the action of acetylcholine and histamine [12]. It was assumed that the cause of

vasodilation is hyperpolarization of the plasma membrane of smooth muscle cells induced by H_2O_2. However, there are some indications that H_2O_2 can cause the relaxation of vessels, acting directly on endothelial cells. In a number of studies, it was shown that exogenous H_2O_2 caused the increase of $[Ca^{2+}]_i$ in endothelial cells and modulated calcium signaling in response to physiological agonists [13–17]. The increase of $[Ca^{2+}]_i$ in endothelial cells induced by H_2O_2 can amplify the synthesis and release of relaxing factors. The data on the influence of H_2O_2 on calcium metabolism in endothelial cells are controversial. According to [16], H_2O_2 inhibits agonist-induced $[Ca^{2+}]_i$ rise in EC. However, such effects are observed at very high unphysiological concentrations of H_2O_2 [13]. Recently, we demonstrated that H_2O_2 in concentration range of 10 to $100\,\mu M$ stimulated mobilization of Ca^{2+} in HUVEC partially due to the activation of two-pore calcium channels [18]. Calcium ions released from endolysosomal vesicles via two-pore channels are operating as a trigger promoting Ca^{2+} mobilization from more capacious intracellular calcium depots. The aim of this study was to estimate how H_2O_2 influences upon the action of Ca^{2+}-mobilizing agonists in HUVEC.

2. Materials and Methods

2.1. Reagents. The reagents used were as follows: BW723C86 and CGS12066B from Tocris; DCFH-DA and CalciumGreen/AM from Molecular Probes; serotonin, bradykinin, N-Acetyl-L-cysteine, VAS2870, Na_3VO_4, and BVT948 from Sigma-Aldrich.

2.2. Cell Culture. The endothelial cells were isolated from the human umbilical vein as described previously [19] with modifications [20]. The umbilical veins were washed with Hanks balanced salt solution containing antibiotics, filled with a M199 medium supplied with 0.1% collagenase (Sigma-Aldrich), and incubated at room temperature for 40 min. The cells were washed and grown in plastic vessels covered with 0.2% gelatin in M199 medium. The medium contained Earle's salts, 20% fetal bovine serum (Invitrogen, United States); $300\,\mu g/mL$ endothelial growth supplement from the rabbit brain obtained according to [21]; $100\,\mu g/mL$ heparin; and $100\,\mu g/mL$ gentamycin.

2.3. Registration of $[Ca^{2+}]_i$ Changes. The changes in $[Ca^{2+}]_i$ were registered in HUVEC of 2-4 passages with the use of the fluorescent probe CalciumGreen (Thermo Fisher Scientific, USA) and a microplate spectrofluorometer Synergy 4 (BioTech, USA). The cells grown in 96-well plates were loaded with the probe at 37°C for 1 h in M199 medium, containing $1\,\mu M$ CalciumGreen/AM and $100\,\mu g/mL$ Pluronic F127. After that, the physiological salt solution (PSS, pH 7.4) containing 145 mM NaCl, 5 mM KCl, 10 mM Hepes, 1 mM $MgCl_2$, 1 mM $CaCl_2$, and 10 mM glucose was added to the cells. The cells were preliminarily washed with the PSS solution to remove the M199 medium. Fluorescence was registered at 485 nm (excitation) and 530 nm (emission) at room temperature. All data are represented as ratios of two values ($\Delta F/Fo$): the increase in the fluorescence in

response to an agonist (ΔF) and the basal fluorescence of the unstimulated cells (Fo). The plots show the averages of three or more measurements.

2.4. Detection of ROS in HUVEC. ROS generation in HUVEC was assessed using $2',7'$-dichlorodihydrofluorescein diacetate (DCFH-DA) as a probe. The cells grown in 96-well plates were incubated with $2\,\mu M$ of DCFH-DA during 1 h at room temperature. The formation of ROS in the cells was determined by measuring the rate of DCFH oxidation into $2',7'$-dichlorofluorescein (DCF). DCF fluorescence was measured at excitation wavelength of 485 ± 20 nm and with emitter bandpass of 527 ± 15 nm. The rate of fluorescence rise was taken as an index of ROS generation.

2.5. Statistics. Data are presented as mean ± SEM of 6–12 measurements. Statistical significance was calculated using Excel and MedCalc statistical software according the Student-Newman-Keuls test.

3. Results

In HUVEC, $[Ca^{2+}]_i$ is strongly increased in response to ADP, histamine, and the agonist of type 1 protease-activated receptor SFLLRN and to a lesser degree to bradykinin (Figure 1(a)). The responses to these agonists are not affected by H_2O_2. 5-hydroxytryptamine and carbachol induced substantially less elevation of $[Ca^{2+}]_i$ in HUVEC, and H_2O_2 caused a significant potentiation of their effects (Figure 1(a)). In some preparations of HUVEC, the rise of $[Ca^{2+}]_i$ in response to 5-HT was negligible, but in the presence of H_2O_2 it increased severalfold (Figure 1(b)). The reason for such strong potentiation of the $[Ca^{2+}]_i$ rise induced by 5-HT is not clear. We suppose that it might depend on the quality of the contacts between the cells in monolayer and the degree of synchronization of Ca^{2+} responses of single cells. The synchronization of calcium signaling of endothelial cells in monolayer has been demonstrated earlier [22]. The increase in $[Ca^{2+}]_i$ in response to 5-HT and carbachol occurred when the H_2O_2 concentration changed from 10 to $100\,\mu M$ (Figure 2(a)). At $200\,\mu M$ H_2O_2 did not cause additional potentiation, while its own effect on the level of $[Ca^{2+}]_i$ was growing (Figure 2(b)). Catalase prevents potentiation by H_2O_2 of 5-HT calcium signaling (Figure S1).

The vascular endothelium expresses serotonin 5-HT1B and 5-HT2B receptors. It is known that serotonin or its selective agonists activate NO synthase and cause vascular relaxation [23, 24]. In general, serotonin receptors of endothelial cells are very poorly investigated. There is no information in the literature on the participation of 5-HT1B receptors in the regulation of $[Ca^{2+}]_i$ in endothelial cells. Regarding 5-HT2B receptors, there is an evidence that their activation in human pulmonary artery endothelial cells causes elevation of $[Ca^{2+}]_i$ [25]. We investigated effects of 5-HT1B and 5-HT2B receptor agonists CGS12066B and BW723C86 in order to determine which of these receptors could be responsible for the enhancement of the Ca^{2+}-mobilizing activity by H_2O_2 (Figure 3). The 5-HT1B receptor agonist CGS12066B caused a very weak rise of $[Ca^{2+}]_i$.

(a)

(b)
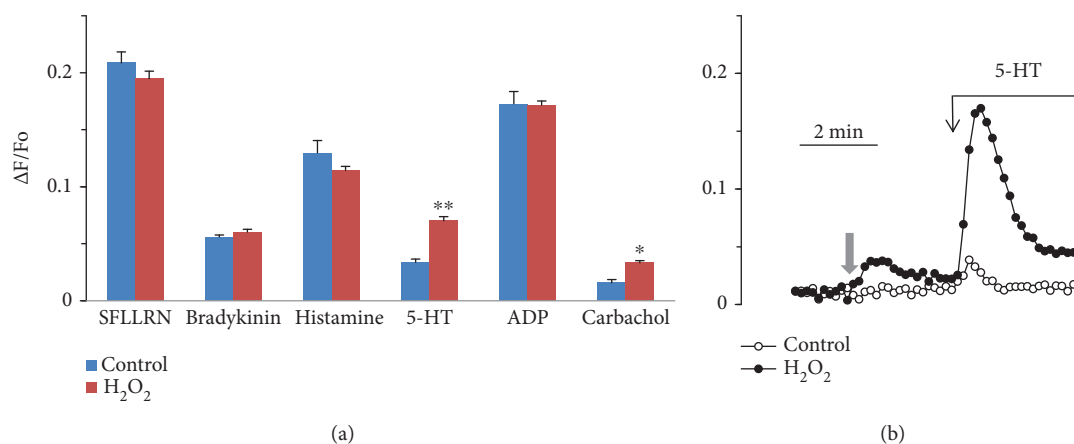
FIGURE 1: (a) Effect of the agonists on $[Ca^{2+}]_i$ in HUVEC in the absence and presence of H_2O_2. (b) Kinetics of calcium response to 5-HT in the absence and presence of H_2O_2. Concentration of H_2O_2 was 100 μM. Grey arrow indicates addition of H_2O_2 or vehicle. Concentrations of the agonists were 5 μg/mL for SFLLRN, 10^{-7} M for bradykinin, and 10^{-5} M for histamine, 5-HT, carbachol, or ADP. Each value is the mean of 6 to 9 measurements ± SEM ($^*p < 0.05$; $^{**}p < 0.01$).

(a)

(b)
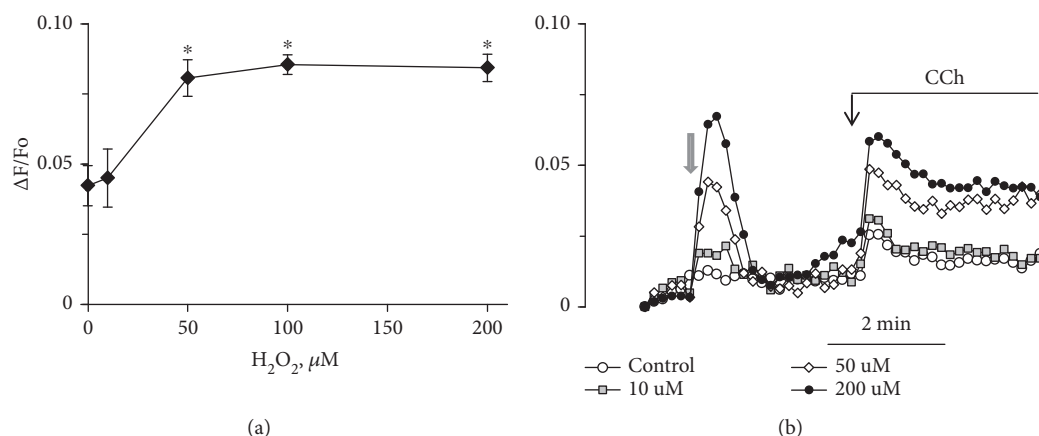
FIGURE 2: Dependence of $[Ca2+]_i$ rise in HUVEC in response to 5-HT (a) or carbachol (b) on concentration of H_2O_2. Grey arrow indicates addition of H_2O_2 or vehicle in control. Concentrations of added H_2O_2 in (b) were 10, 50, and 200 μM. The concentration of 5-HT and carbachol was 10 μM. Each value in (a) is the mean of 4-6 measurements ± SEM ($^*p < 0.01$).

However, its effect sharply increased in the presence of H_2O_2. BW723C86 at a concentration of 50 μM induced the elevation of $[Ca^{2+}]_i$ and H_2O_2 further enhanced its effect near twofold. Alpha-methyl-5-hydroxytryptamine (αMHT) is a relatively specific agonist toward 5-HT2B receptors and its effect was also enhanced by H_2O_2. These results indicate that the Ca^{2+}-mobilizing activity of both receptors is potentiated in the presence of H_2O_2.

The increase in $[Ca^{2+}]_i$ caused by the agonists in the presence of H_2O_2 does not disappear with the removal of calcium ions from the extracellular medium, which indicates mobilization of calcium ions from the intracellular depots (Figure S2). The withdrawal of extracellular calcium did not affect the effective concentration of H_2O_2. The full potentiation of $[Ca^{2+}]_i$ rise in response to CGS12066B and BW723C86 was observed at 50 μM H_2O_2 both at normal and low level of extracellular Ca^{2+} (Figure S3) as in the case of 5-HT (Figure 2(a)). The potentiating effect of H_2O_2 is suppressed by the antioxidant N-acetylcysteine (Figures 4 and 5). In some HUVEC preparations, the calcium signals

in response to CGS12066B and BW723C86 were quite strong. We suggested that this may be due to the formation of endogenous ROS, which might increase the calcium-mobilizing activity of 5-HT1B and 5-HT2B receptors in a manner similar to exogenous H_2O_2. In favor of this point of view, there is a data on the inhibition by N-acetylcysteine of $[Ca^{2+}]_i$ rise in response to CGS12066B and BW723C86 (Figure 6). On the other hand, there was no suppression of the effect caused by the agonist of type 1 protease-activated receptor SFLLRN. These data assume the existence of a specific mechanism through which an increase in $[Ca^{2+}]_i$ occurs when 5-HT1B and 5-HT2B receptors are activated in HUVEC.

In order to test the hypothesis of an increase in the functional activity of 5-HT1B and 5-HT2B receptors under the action of endogenous ROS, we investigated whether their formation in HUVEC occurred in conditions of $[Ca^{2+}]_i$ measurement. For registration of the ROS, the fluorescent probe DCFH-DA penetrating into the cells was used. The increase in the fluorescence due to
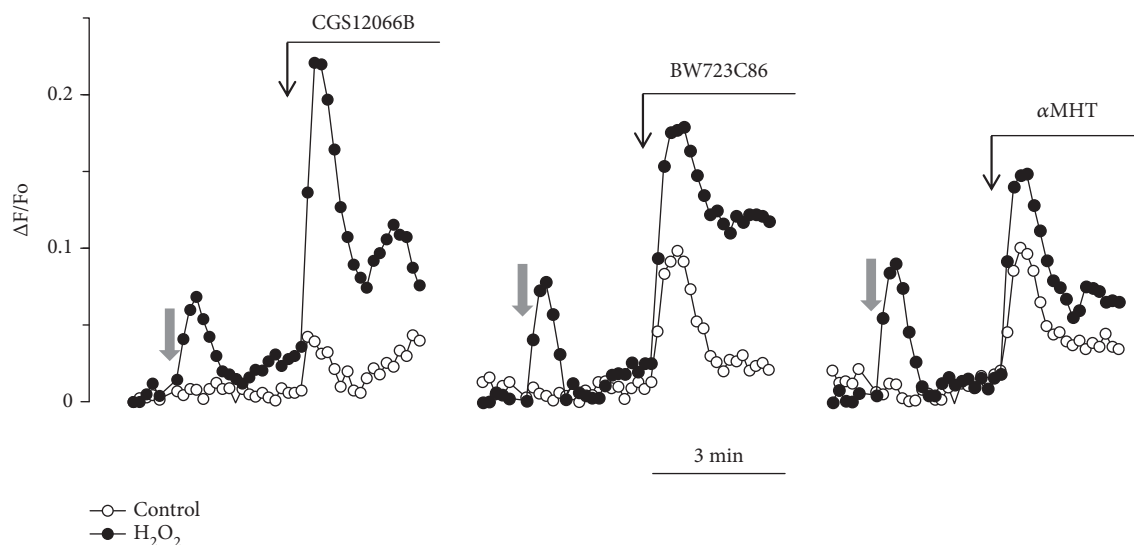
FIGURE 3: An increase in $[Ca^{2+}]_i$ in HUVEC in response to CGS12066B, BW723C86, and alpha-methyl-5-hydroxytryptamine (αMHT) upon the action of H_2O_2. The concentration of CGS12066B, BW723C86, and H_2O_2 is 50 μM; αMHT: 10 μM. Grey arrow indicates addition of H_2O_2 or vehicle. For each agonist, a typical response of 3–6 experiments is presented.

(a)

(b)
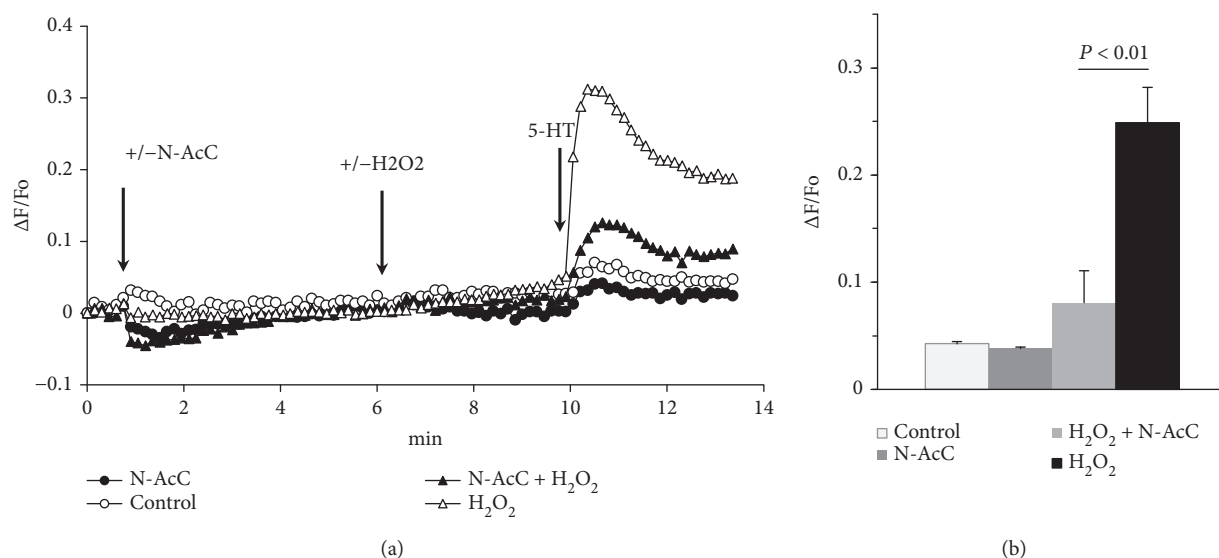
FIGURE 4: Suppression by N-acetyl cysteine (N-AcC) of H_2O_2-induced potentiation of $[Ca^{2+}]_i$ rise in response to 5-HT. Concentrations of H_2O_2, N-AcC, and 5-HT were 50 μM, 2 mM, and 10 μM, respectively.

oxidation DCFH into 2′,7′-dichlorofluorescein (DCF) reflects the accumulation of ROS in the cytoplasm. As can be seen in Figure 6(a), spontaneous formation of ROS occurs in HUVEC. In the presence of CGS12066B, the oxidation rate of the H2DCF does not change. We found that BW723C86 at a concentration of 100 μM increased the formation of ROS severalfold in HUVEC (Figure 6). VAS2870, a selective inhibitor of NOX, almost completely blocked the formation of ROS induced by BW723C86 (Figure 6(b)). Thus, the data suggest the coupling of 5-HT2B receptors with NOX.

The next task was to find out whether endogenous ROS generated by NOX can affect the calcium signaling in HUVEC. As shown in Figure 7(a), the NOX inhibitor VAS2870 does not change the response to 30 μM BW7323C86 and decreases by 15.4 + 3.8% ($n = 12$; $p < 0.01$) the $[Ca^{2+}]_i$ elevation caused by BW723C86 at a concentration of 100 μM. This indicates the contribution of NOX to the regulation of calcium signaling from 5-HT2B receptors. To evaluate the role of ROS endogenously formed in HUVEC in $[Ca^{2+}]_i$ regulation via 5-HT2B receptors, we used another approach: inducers of ROS formation were applied. Such properties are possessed by orthovanadate (Na_3VO_4) [26] and substance BVT948 [27]. Na_3VO_4 and BVT948 potentiated the rise of $[Ca^{2+}]_i$ in HUVEC caused by 30 μM BW723C86 by 1.7 and 2.5 times (Figure 7), respectively.
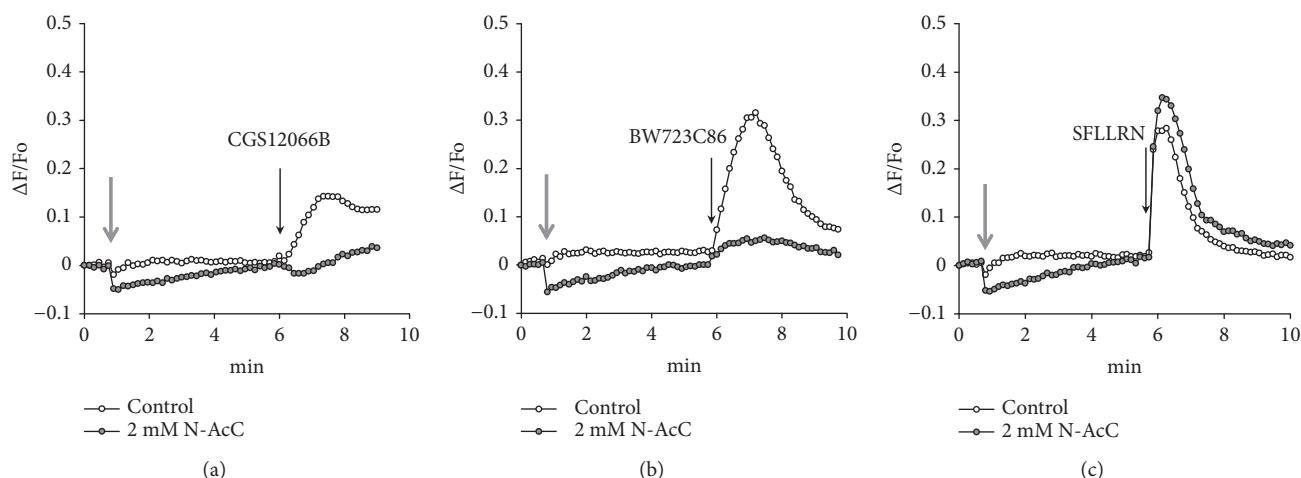
FIGURE 5: Effect of N-acetyl cysteine on $[Ca2+]_i$ elevation in response to CGS12066B (50 μM), BW723C86 (100 μM), and SFLLRN (10 μg/mL). Typical data of 3-4 experiments are presented.
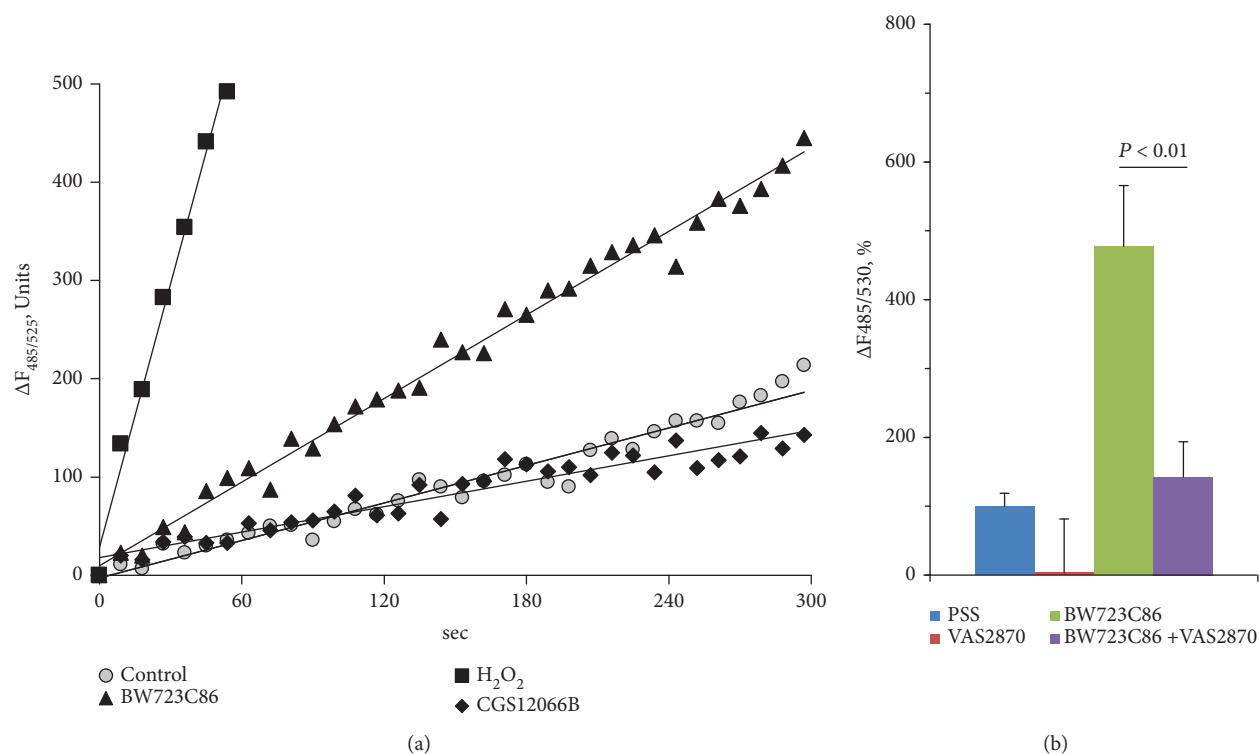
FIGURE 6: (a) Increase in the fluorescence of DCFH in HUVEC in control conditions, with the addition of exogenous H_2O_2 (200 μM), BW723C86 (100 μM), or CGS12066B (100 μM). The data of one of four independent experiments are presented. (b) Inhibition of BW723C86-induced formation of ROS by inhibitor of NADPH oxidase VAS2870. The concentrations were H_2O_2 200 μM, BW723C86 and CGS12066B 100 μM, and VAS2870 10 μM.

4. Discussion

In this paper, we have demonstrated that hydrogen peroxide dramatically increases the rise of $[Ca^{2+}]_i$ in endothelial cells in response to serotonin. It was found that the reason for this could be an increase in the functional activity of 5-HT1B and 5-HT2B receptors. To the best of our knowledge, this is the first demonstration of Ca-mobilizing activity of 5-HT1B

receptors in endothelial cells. There is only one experimental work demonstrating that 5-HT2B receptors stimulate calcium mobilization in endothelial cells, which was conducted on the cells isolated from the human pulmonary artery [25]. The reason for the lack of published data on this topic seems to be the low functional activity of 5-HT1B and 5-HT2B receptors. Earlier we showed that in smooth muscle cells of blood vessels 5-HT2B receptors are functionally inactive and their
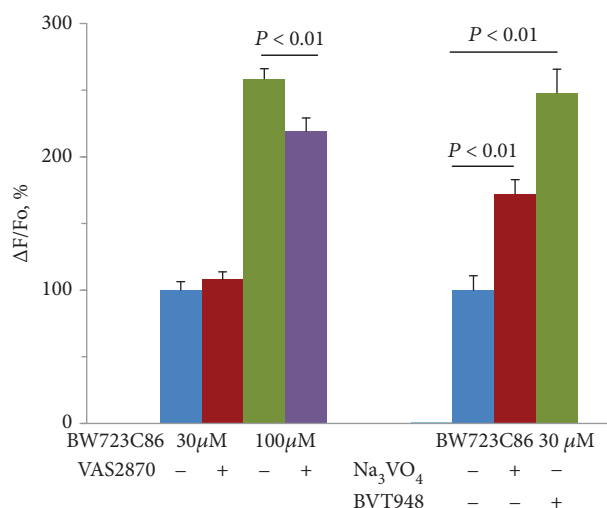
FIGURE 7: Inhibition of calcium signaling mediated by 5-HT2B receptors by VAS2870 and potentiation by Na_3VO_4 and BVT948. Concentrations of VAS2870, Na_3VO_4, and BVT948 were 10, 200, and 1 μM, respectively.

transition to the active state occurs under the influence of ROS [28]. The results presented in this paper show that the same pattern of 5-HT receptor regulation exists in HUVEC.

The increase in calcium signaling upon exposure to H_2O_2 is selective with respect to the action of serotonin. There is an increase in the level of $[Ca^{2+}]_i$ in response to carbachol, though it is extremely low even in the presence of H_2O_2. The difference in the effect of ROS on the functional properties of 5-HT receptors, on the one hand, and histamine, ADP, and PAR1 receptors, on the other hand, is indicative of differences in the mechanisms of signal transduction. In the paper of Ullmer et al. [25], data were presented according to which 5-HT2B receptors induce the activation of ryanodine-sensitive channels in human pulmonary endothelial cells. We have shown that the main source of increasing $[Ca^{2+}]_i$ in HUVEC in response to the activation of 5-HT1B and 5-HT2B receptors could certainly be intracellular stores, but their nature has not yet been established.

In many cases, H_2O_2 initially causes a transient rise of $[Ca^{2+}]_i$, but its potentiating effect can be manifested without an apparent increase in the level of $[Ca^{2+}]_i$ in HUVEC. In a recent paper, we showed that H_2O_2 activated two-pore calcium channels in HUVEC [18]. It was assumed that calcium ions released from endolysosomal vesicles through the two-pore channels serve as a trigger opening of the endo-/sarcoplasmic reticulum channels. Perhaps this mechanism is implemented in this case, too.

Presently, it is a well-known fact that H_2O_2 at low nontoxic concentrations can serve as a second messenger. The enhancement of $[Ca^{2+}]_i$ is one of the terminal links in serotonergic signaling. The primary targets of H_2O_2 are known to be SH groups of PTEN and tyrosine phosphatases [29]. Moreover, tyrosine phosphatases are the target for different inducers of ROS formation, such as Na_3VO_4 and BVT946 [27, 30]. These substances have the same effect as H_2O_2, so there is a reason to think that the tyrosine phosphorylation system is involved in the serotonergic regulation of $[Ca^{2+}]_i$

in HUVEC. The involvement of tyrosine protein phosphatases and protein kinases of the Src family in calcium signaling of 5-HT2B receptors was shown in vascular smooth muscle cells [28].

In this work, we have shown that the activation of 5-HT2B receptor by BW723C86 induces ROS accumulation in the cytoplasm of HUVEC. Earlier, we showed the same effect of BW723C86 in rat aorta smooth muscle cells [28]. The formation of ROS in both cell types is suppressed specifically by the NADPH oxidase inhibitor VAS2870. This suggests the coupling of 5-HT2B receptors with this enzyme. The question about the type of NOX interacting with the 5-HT2B receptors requires further investigation.

Based on the data obtained, it might be suggested that the excessive production of H_2O_2 by leukocytes as well as the formation of endogenous ROS in endothelial cells could influence the serotoninergic regulation of vascular tone and secretion from endothelial cells. Serotonin stimulates von Willebrand factor secretion via 5-HT1B receptors and the mechanism of this process is not completely clear [31]. Oxidative stress and simultaneous release of 5-HT from platelets could be a pathogenic factor of microvascular thrombosis. The stimulation of 5-HT2B receptors in endothelial progenitors by nordexfenfluramine and some other pharmacological agents causes valvular heart disease [32]. The potentiation of calcium response via 5-HT2B receptors in progenitors by H_2O_2 can probably accelerate its development. On the other hand, the moderate formation of H_2O_2 in endothelial cells can cause a physiologically relevant increase of $[Ca^{2+}]_i$ and promote vascular relaxation. Future work will be required to uncover whether H_2O_2 potentiates vasorelaxation via 5-HT receptors.

Data Availability

The data used to support the findings of this study are available from the corresponding author upon request.

Conflicts of Interest

The authors confirm that there are no conflicts of interest.

Acknowledgments

Supplementary Materials

Figure S1: inhibition by catalase of H_2O_2-induced $[Ca^{2+}]_i$ elevation and its effect on 5-HT-induced calcium signaling in HUVECs. (A) Kinetics of $[Ca^{2+}]_i$ changes. (B) Decrease in 5-HT-induced calcium signal. Catalase at concentration 150 units/mL or buffer was added 5 min before H_2O_2. Concentrations of H_2O_2 and 5-HT were 100 and 10 μM, respectively. $^*p < 0.01$ compared to control without H_2O_2, $n = 4$. Figure S2: the increase in $[Ca^{2+}]_i$ in HUVEC incubated with 200 μM H_2O_2 in response to CGS12066A (50 μM) and BW723C86 (100 μM) in a medium with calcium ions (1.25 mM $CaCl_2$) and in a medium without calcium in the

presence of $100\,\mu M$ EGTA. The average of 3 parallel measurements $\pm$ SEM is presented. Figure S3: the influence of different concentrations of H_2O_2 on $[Ca^{2+}]_i$ elevation in HUVECs induced by $50\,\mu M$ CGS12066B (A) and $30\,\mu M$ BW723C86 (B). The magnitude of the response in the presence of calcium ions and in the absence of H_2O_2 is taken as 100%. Each value is a mean of 6 measurements. The increments of $\Delta F/Fo$ in the presence of H_2O_2 significantly differ from control values ($p < 0.01$). (Supplementary Materials)

References

[1] C. W. Baldridge and R. W. Gerard, "The extra respiration of phagocytosis," American Journal of Physiology-Legacy Content, vol. 103, no. 1, pp. 235-236, 1932.

[2] S. Magder, "Reactive oxygen species: toxic molecules or spark of life?," Critical Care, vol. 10, no. 1, p. 208, 2006.

[3] A. Petry, M. Weitnauer, and A. Gorlach, "Receptor activation of NADPH oxidases," Antioxidants & Redox Signaling, vol. 13, no. 4, pp. 467–487, 2010.

[4] V. J. Thannickal and B. L. Fanburg, "Reactive oxygen species in cell signaling," American Journal of Physiology-Lung Cellular and Molecular Physiology, vol. 279, no. 6, pp. L1005–L1028, 2000.

[5] M. Feletou and P. M. Vanhoutte, "Endothelial dysfunction: a multifaceted disorder (the Wiggers award lecture)," American Journal of Physiology. Heart and Circulatory Physiology, vol. 291, no. 3, pp. H985–1002, 2006.

[6] J. M. Li and A. M. Shah, "Endothelial cell superoxide generation: regulation and relevance for cardiovascular pathophysiology," American Journal of Physiology-Regulatory, Integrative and Comparative Physiology, vol. 287, no. 5, pp. R1014–R1030, 2004.

[7] R. P. Brandes, N. Weissmann, and K. Schroder, "NADPH oxidases in cardiovascular disease," Free Radical Biology & Medicine, vol. 49, no. 5, pp. 687–706, 2010.

[8] Y. J. Gao and R. M. Lee, "Hydrogen peroxide induces a greater contraction in mesenteric arteries of spontaneously hypertensive rats through thromboxane A_2 production," British Journal of Pharmacology, vol. 134, no. 8, pp. 1639–1646, 2001.

[9] D. P. Jones, "Radical-free biology of oxidative stress," American Journal of Physiology-Cell Physiology, vol. 295, no. 4, pp. C849–C868, 2008.

[10] S. B. Shappell, C. Toman, D. C. Anderson, A. A. Taylor, M. L. Entman, and C. W. Smith, "Mac-1 (CD11b/CD18) mediates adherence-dependent hydrogen peroxide production by human and canine neutrophils," The Journal of Immunology, vol. 144, no. 7, pp. 2702–2711, 1990.

[11] S. J. Weiss, J. Young, A. F. LoBuglio, A. Slivka, and N. F. Nimeh, "Role of hydrogen peroxide in neutrophil-mediated destruction of cultured endothelial cells," The Journal of Clinical Investigation, vol. 68, no. 3, pp. 714–721, 1981.

[12] R. Ray, C. E. Murdoch, M. Wang et al., "Endothelial Nox 4 NADPH oxidase enhances vasodilatation and reduces blood pressure in vivo," Arteriosclerosis, Thrombosis, and Vascular Biology, vol. 31, no. 6, pp. 1368–1376, 2011.

[13] T. N. Doan, D. L. Gentry, A. A. Taylor, and S. J. Elliott, "Hydrogen peroxide activates agonist-sensitive Ca^{2+}-flux pathways in canine venous endothelial cells," Biochemical Journal, vol. 297, no. 1, pp. 209–215, 1994.

[14] Q. Hu, S. Corda, J. L. Zweier, M. C. Capogrossi, and R. C. Ziegelstein, "Hydrogen peroxide induces intracellular calcium oscillations in human aortic endothelial cells," Circulation, vol. 97, no. 3, pp. 268–275, 1998.

[15] T. Volk, M. Hensel, and W. J. Kox, "Transient Ca2+ changes in endothelial cells induced by low doses of reactive oxygen species: role of hydrogen peroxide," Molecular and Cellular Biochemistry, vol. 171, no. 1/2, pp. 11–21, 1997.

[16] D. E. Wesson and S. J. Elliott, "The H_2O_2-generating enzyme, xanthine oxidase, decreases luminal Ca^{2+} content of the IP_3-sensitive Ca^{2+} store in vascular endothelial cells," Microcirculation, vol. 2, no. 2, pp. 195–203, 1995.

[17] Y. Zheng and X. Shen, "H_2O_2 directly activates inositol 1, 4, 5-trisphosphate receptors in endothelial cells," Redox Report, vol. 10, no. 1, pp. 29–36, 2005.

[18] P. V. Avdonin, A. D. Nadeev, E. B. Tsitrin et al., "Involvement of two-pore channels in hydrogen peroxide-induced increase in the level of calcium ions in the cytoplasm of human umbilical vein endothelial cells," Doklady Biochemistry and Biophysics, vol. 474, no. 1, pp. 209–212, 2017.

[19] E. A. Jaffe, R. L. Nachman, C. G. Becker, and C. R. Minick, "Culture of human endothelial cells derived from umbilical veins. Identification by morphologic and immunologic criteria," The Journal of Clinical Investigation, vol. 52, no. 11, pp. 2745–2756, 1973.

[20] N. V. Goncharov, I. Sakharov, S. M. Danilov, and O. G. Sakandelidze, "Use of collagenase from the hepatopancreas of the Kamchatka crab for isolating and culturing endothelial cells of the large vessels in man," Biulleten' Eksperimental'noĭ Biologii i Meditsiny, vol. 104, no. 9, pp. 376–378, 1987.

[21] T. Maciag, J. Cerundolo, S. Ilsley, P. R. Kelley, and R. Forand, "An endothelial cell growth factor from bovine hypothalamus: identification and partial characterization," Proceedings of the National Academy of Sciences of the United States of America, vol. 76, no. 11, pp. 5674–5678, 1979.

[22] R. E. Laskey, D. J. Adams, M. Cannell, and C. van Breemen, "Calcium entry-dependent oscillations of cytoplasmic calcium concentration in cultured endothelial cell monolayers," Proceedings of the National Academy of Sciences of the United States of America, vol. 89, no. 5, pp. 1690–1694, 1992.

[23] A. Bhattacharya, K. W. Schenck, Y. C. Xu, L. Nisenbaum, E. Galbreath, and M. L. Cohen, "5-Hydroxytryptamine$_{1B}$ receptor-mediated contraction of rabbit saphenous vein and basilar artery: role of vascular endothelium," The Journal of Pharmacology and Experimental Therapeutics, vol. 309, no. 2, pp. 825–832, 2004.

[24] E. Glusa and H. H. Pertz, "Further evidence that 5-HT-induced relaxation of pig pulmonary artery is mediated by endothelial 5-HT$_{2B}$ receptors," British Journal of Pharmacology, vol. 130, no. 3, pp. 692–698, 2000.

[25] C. Ullmer, H. G. Boddeke, K. Schmuck, and H. Lubbert, "5-HT$_{2B}$ receptor-mediated calcium release from ryanodine-sensitive intracellular stores in human pulmonary artery endothelial cells," British Journal of Pharmacology, vol. 117, no. 6, pp. 1081–1088, 1996.

[26] R. A. Coulombe Jr., D. P. Briskin, R. J. Keller, W. R. Thornley, and R. P. Sharma, "Vanadate-dependent oxidation of pyridine nucleotides in rat liver microsomal membranes," Archives of Biochemistry and Biophysics, vol. 255, no. 2, pp. 267–273, 1987.

[27] C. Liljebris, P. Baranczewski, E. Bjorkstrand et al., "Oxidation of protein tyrosine phosphatases as a pharmaceutical mechanism

of action: a study using 4-hydroxy-3, 3-dimethyl-2*H*-benzo[*g*]indole-2, 5(3*H*)-dione," *The Journal of Pharmacology and Experimental Therapeutics*, vol. 309, no. 2, pp. 711–719, 2004.

[28] G. Y. Mironova, P. P. Avdonin, N. V. Goncharov, R. O. Jenkins, and P. V. Avdonin, "Inhibition of protein tyrosine phosphatases unmasks vasoconstriction and potentiates calcium signaling in rat aorta smooth muscle cells in response to an agonist of 5-HT2B receptors BW723C86," *Biochemical and Biophysical Research Communications*, vol. 483, no. 1, pp. 700–705, 2017.

[29] S. G. Rhee, "Cell signaling. H_2O_2, a necessary evil for cell signaling," *Science*, vol. 312, no. 5782, pp. 1882-1883, 2006.

[30] D. Hecht and Y. Zick, "Selective inhibition of protein tyrosine phosphatase activities by H_2O_2 and vanadate *in vitro*," *Biochemical and Biophysical Research Communications*, vol. 188, no. 2, pp. 773–779, 1992.

[31] T. Schluter and R. Bohnensack, "Serotonin-induced secretion of von Willebrand factor from human umbilical vein endothelial cells via the cyclic AMP-signaling systems independent of increased cytoplasmic calcium concentration," *Biochemical Pharmacology*, vol. 57, no. 10, pp. 1191–1197, 1999.

[32] E. Ayme-Dietrich, R. Lawson, F. Cote et al., "The role of 5-HT$_{2B}$ receptors in mitral valvulopathy: bone marrow mobilization of endothelial progenitors," *British Journal of Pharmacology*, vol. 174, no. 22, pp. 4123–4139, 2017.

Research Article

Markers of Oxidant-Antioxidant Equilibrium in Patients with Sudden Sensorineural Hearing Loss Treated with Hyperbaric Oxygen Therapy

Jarosław Paprocki [ID],[1] **Paweł Sutkowy** [ID],[1] **Jacek Piechocki,**[2] **and Alina Woźniak** [ID][1]

[1]*Department of Medical Biology and Biochemistry, Collegium Medicum of Nicolaus Copernicus University, Karłowicza 24, 85-092 Bydgoszcz, Poland*
[2]*Mazovian Centre for Hyperbaric Therapy and Wound Treatment in Warsaw, Wołoska 137, bud. "O", 02-507 Warszawa, Poland*

Correspondence should be addressed to Jarosław Paprocki; jaroslawpaprocki@interia.pl

The concentration of thiobarbituric acid reactive substances (TBARSs) in plasma and erythrocytes, the activity of selected antioxidant enzymes in erythrocytes: catalase (CAT), superoxide dismutase (SOD), and glutathione peroxidase (GPx), and the levels of hemoglobin (HGB) and haematocrit (HCT) were determined in 40 patients with sudden sensorineural hearing loss (SSNHL) subjected to 14 treatment sessions in a Haux Starmed 2200 hyperbaric chamber. Hyperbaric oxygen (HBO) therapy involved breathing 100% oxygen at 0.25 MPa. Blood for analysis was collected from the basilic vein at three time points: before the first HBO session, approximately 5 min after the first session, and after the 14th session. The control group included 20 healthy individuals never before treated with HBO therapy. Compared to the pre-HBO values, a 10% increase ($P < 0.05$) in the TBARS concentration in erythrocytes, a 28% increase in the GPx activity ($P < 0.05$), and a 7% decrease in the SOD activity ($P < 0.05$) were observed after 14 HBO sessions. The CAT activity decreased by 6% ($P < 0.05$) after the first session. The TBARS concentration in plasma was 13% higher ($P < 0.01$), while that in erythrocytes was 24% lower ($P < 0.001$) in the SSNHL patients before the first HBO session compared to the control group. The CAT activity in the SSNHL patients before HBO therapy was 26% higher ($P < 0.001$) than that in the control group. A statistically significant reduction in HGB and HCT after 14 HBO sessions ($P < 0.01$) compared to the pre-HBO values was demonstrated. SSNHL is accompanied by disturbance in the oxidant-antioxidant equilibrium. Repeated stimulation with hyperbaric oxygen modulates the activity of antioxidant enzymes. It seems that the increased generation of hydrogen peroxide is responsible for the changes in the activity of antioxidant barrier enzymes observed after HBO sessions.

1. Introduction

Sudden sensorineural hearing loss (SSNHL) is impairment of the hearing of unknown aetiology, developing over 72 hours. It usually affects one ear, less often both. The age group most frequently affected is people aged 30 to 60 years [1]. The main audiometric criterion of SSNHL is hearing impairment no deeper than 30 dB affecting at least 3 neighbouring frequencies [2, 3]. The incidence of SSNHL in Poland is 5–20 cases per 100,000 people per year [2]. There is no clearly understood cause of this condition, but the most common aetiologies

mentioned in the literature include vascular, viral, and autoimmune factors. SSNHL is treated pharmacologically using corticosteroids, antiviral drugs, thrombolytic agents, and vitamins [1]. Hyperbaric oxygen (HBO) therapy, increasingly used by otolaryngologists in treating SSNHL, consists of breathing 100% oxygen in a specially adapted chamber in which the pressure is approximately 2.5 ATA [4]. HBO therapy can be used directly after the occurrence of SSNHL as a primary treatment, alone or together with pharmacotherapy, or as a secondary treatment [2]. In studies, the beneficial effect of this method in treating SSNHL has been associated with

improved microcirculation and facilitated diffusion of oxygen from capillary vessels to tissues. After HBO sessions, an increase in the partial pressure of oxygen in the cochlea and reduced hypoxia and oedema of tissues are observed. Moreover, the response to infections and ischaemia in the patient is altered [1].

The purpose of aerobic metabolism is the production of chemical energy stored in ATP, mainly in the process of oxidative phosphorylation [5]. A side effect of this process is the formation of reactive oxygen species (ROS), including oxygen free radicals (OFR), particularly during an incomplete reduction of oxygen in the oxidative chain [5]. The condition in which the generation of ROS exceeds the antioxidant capacity of the body is called oxidative stress [6]. Antioxidant enzymes, such as catalase (CAT), superoxide dismutase (SOD), and glutathione peroxidase (GPx), are responsible for scavenging ROS in the human body [6]. One of the consequences of oxidative stress is increased intensity of lipid peroxidation—free radical chain reactions leading to the oxidation of polyunsaturated fatty acids that form, e.g., cell membranes. Oxidation of polyunsaturated fatty acids leads to the enzymatic or nonenzymatic production of multiple final α,β-unsaturated aldehyde products, such as malondialdehyde (MDA)—a mutagen commonly used as a biomarker of lipid peroxidation [7]. It has already been seen that HBO increases the production of oxygen free radicals whose effect on the body can be both beneficial and adverse. Therefore, it is possible that this form of therapy induces oxidative stress [8].

The aim of the study was to determine the effect of 14 HBO therapy sessions on the concentration of thiobarbituric acid reactive substances (TBARSs) in plasma and erythrocytes, the activity of key antioxidant enzymes: SOD, CAT, and GPx, and the levels of haemoglobin (HGB) and haematocrit (HCT) in patients with SSNHL.

2. Material and Methods

The study was approved by the Bioethics Committee of Ludwik Rydygier Collegium Medicum in Bydgoszcz, Nicolaus Copernicus University, in Torun, Poland (approval no.: KB 260/2016).

2.1. Study Subject. The study was conducted in 40 patients (23 men and 17 women; mean age: 43.2 ± 16.0 years) of the Mazovian Centre for Hyperbaric Therapy and Wound Treatment in Warsaw, Poland, treated with HBO therapy for SSNHL. HBO therapy was initiated no later than 5 days after the onset of SSNHL. The patients underwent 14 sessions (conducted daily, one per day) in the hyperbaric chamber, Haux Starmed 2200 used at the Mazovian Centre for Hyperbaric Therapy and Wound Treatment in Warsaw (Figures 1 and 2). The patients received systemic corticosteroidotherapy recommended as the first-line therapy in SSNHL. For the duration of the experiment, the patients were orally administered prednisone (a loading dose of 1 mg/kg of body weight per day, with the usual maximum dose of 60 mg/day) at a gradually tapered dosage until discontinuation. Corticosteroidotherapy was initiated immediately after the diagnosis of

Figure 1: Inside the hyperbaric chamber at the Mazovian Centre for Hyperbaric Therapy and Wound Treatment in Warsaw, Poland (photograph: J. Paprocki).
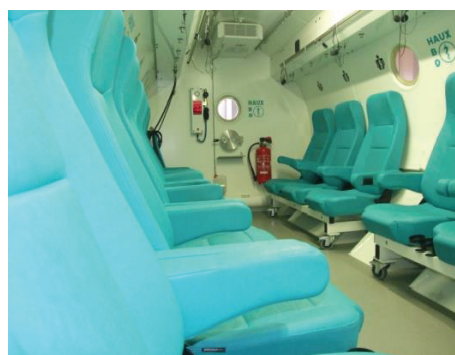
Figure 2: The hyperbaric chamber at the Mazovian Centre for Hyperbaric Therapy and Wound Treatment in Warsaw, Poland (photograph: J. Paprocki).

SSNHL and continued for 2 weeks. The first and second time points of the study occurred during prednisone therapy, while the third time point occurred after the completion of prednisone therapy. When therapy was completed, an improvement in hearing (within the range of 10–20 dB) was observed in 30 patients.

Participants with other health problems characterised by a proven disruption of the oxidant-antioxidant equilibrium were excluded from the study.

The control group consisted of 20 healthy volunteers (12 men and 8 women; mean age: 28.1 ± 7.1 years) never before treated with HBO therapy.

The employed hyperbaric chamber allowed maintaining equal environmental conditions, i.e., pressure, temperature, and air humidity, and enabled breathing 100% oxygen for the same period for each participant. The inside of the chamber was filled with a breathing gas mixture in which the concentration of oxygen did not exceed 23%, but the study participants breathed 100% oxygen using masks. Hyperbaric oxygen (HBO) therapy involved breathing 100% oxygen at 0.25 MPa. The sessions lasted 90 min and included two 10-minute periods of compression and decompression. Three HBO therapy subsessions, lasting 20 minutes each, were separated by two 5-minute breaks during which the participants breathed the air inside the chamber. Each complete HBO session cycle was as follows: 10 min compression+20 min oxygen

TABLE 1: Markers of oxidative stress in the blood of healthy members of the control group and patients with sudden sensorineural hearing loss (SSNHL) treated with hyperbaric oxygen (HBO) therapy and the values of haemoglobin concentration and haematocrit in the SSNHL patients.

Parameters	Control	SSNHL patients		
		Before HBO therapy	~5 min after first HBO session	After 14 HBO sessions
TBARS in plasma (nmol MDA/mL)	0.38 ± 0.07	$0.43 \pm 0.10^{++}$	$0.45 \pm 0.08^{+++}$	$0.42 \pm 0.10^{+}$
TBARS in erythr. (nmol MDA/g Hb)	32.60 ± 6.77	$24.70 \pm 8.25^{+++}$	$24.47 \pm 8.07^{+++}$	$27.06 \pm 8.39^{+++*}$
CAT (10^4 IU/g Hb)	52.97 ± 6.09	$66.64 \pm 10.25^{+++}$	$62.93 \pm 8.23^{+++*}$	$64.75 \pm 10.07^{+++}$
SOD (U/g Hb)	816.73 ± 128.64	764.44 ± 159.00	757.06 ± 141.50	$713.26 \pm 72.89^{+++*\dagger}$
GPx (U/g Hb)	5.54 ± 4.05	7.51 ± 4.64	$8.97 \pm 4.42^{+}$	$9.61 \pm 4.75^{+++*}$
HGB (g/mL)		15.58 ± 1.39		$14.64 \pm 1.43^{**}$
HCT (%)		43.88 ± 3.47		$41.29 \pm 3.60^{**}$

TBARS: thiobarbituric acid reactive substances; CAT: catalase; GPx: glutathione peroxidase; SOD: superoxide dismutase; HGB: haemoglobin; HCT: haematocrit. The values are expressed as means ± standard deviations (SD) of the means. $^{+}$Statistically significant difference compared to the control group ($^{+}P < 0.05$; $^{++}P < 0.01$; $^{+++}P < 0.001$). *Statistically significant difference compared to parameters measured before the HBO therapy ($^{*}P < 0.05$; $^{**}P < 0.01$). †Statistically significant difference compared to the parameters measured after the 1st HBO session ($^{\dagger}P < 0.05$).

therapy+5 min breathing the air inside the chamber+20 min oxygen therapy+5 min breathing the air inside the chamber +20 min oxygen therapy+10 min decompression.

In the SSNHL patients, blood for analysis was collected from the basilic vein at three time points: before the first HBO session, approximately 5 min after the first session, and after the full series of 14 sessions. The biochemical analyses were conducted at a laboratory of biochemistry at the Department of Medical Biology and Biochemistry of the Collegium Medicum of Nicolaus Copernicus University, Poland. In the control group members, blood samples were taken once. The samples were analysed for the concentration of TBARS in erythrocytes and plasma, the activity of CAT, SOD, and GPx in erythrocytes, and the HGB and HCT values.

2.2. Methods. The TBARS concentration was determined following a method by Buege and Aust [9] as modified by Esterbauer and Cheeseman [10]. Lipid peroxidation products were identified using thiobarbituric acid (TBA). Malondialdehyde (MDA) is the main but not the only lipid peroxidation product that reacts with TBA. For the sake of simplicity, the level of all substances reacting with TBA was presented as the MDA concentration.

The CAT activity was determined by measuring the decrease in the absorbance of a solution of hydrogen peroxide (H_2O_2) decomposed by the enzyme. The decrease in the absorbance value is directly proportional to the reduction of the H_2O_2 concentration in the solution [11]. The CAT activity was expressed in IU/g Hb.

The SOD activity was determined based on the inhibition of adrenaline autoxidation to adrenochrome in alkaline conditions. To measure the SOD activity, a previously obtained haemolysate after removal of haemoglobin with a chloroform-ethanol mixture was used. After centrifugation, two layers were obtained: lower layer containing denatured haemoglobin and chloroform and upper layer containing the enzyme [12]. To determine the SOD activity, continuous recording of the reaction was conducted using a reaction

kinetics programme on a Varian spectrophotometer. The SOD activity was expressed in U/g Hb.

The GPx activity was determined at 20°C using a method based on the decomposition of hydrogen peroxide by the enzyme with the concurrent oxidation of reduced glutathione [13]. The results were expressed in U/g Hb.

2.3. Statistical Analysis. The TBARS concentration in plasma and erythrocytes and the activities of CAT, SOD, and GPx were analysed using the comparative analysis of variance (ANOVA; Tukey's range test) (STATISTICA v. 9.1). For the assessment of the statistical significance of the HGB and HCT values measured before the first and after the 14th HBO sessions, Student's t-test was used. Differences at significance level $P < 0.05$ were presumed as statistically significant. Dependencies between the analysed parameters were assessed using correlation matrices. A statistical hypothesis of the significance of the correlation coefficients (r) was tested.

3. Results

The TBARS concentration in the plasma of the SSNHL patients before the HBO therapy was 13% higher than in the healthy members of the control group, and the difference was statistically significant ($P < 0.01$) (Table 1). Approximately 5 min after the first HBO session and then after 14 HBO sessions, the plasma TBARS concentration did not change in a statistically significant manner compared to the that in the pretreatment level and was significantly higher than that in the control group (by 18%, $P < 0.001$, and 11%, $P < 0.05$, respectively).

The TBARS concentration in the erythrocytes of the SSNHL patients before the HBO therapy was 24% lower than that in the control group, and the difference was statistically significant ($P < 0.001$). Approximately 5 min after the first HBO session, the erythrocytic TBARS concentration did not change in a statistically significant manner compared to the level measured before HBO while after

the 14th session, it was increased by 10% ($P < 0.05$). The TBARS concentration in the erythrocytes of the SSNHL patients after the 14th HBO session was 17% lower than that in the control group, and the difference remained statistically significant ($P < 0.01$).

The CAT activity in the erythrocytes of the SSNHL patients before the HBO therapy was 26% higher than that in the control group, and the difference was statistically significant ($P < 0.001$). Approximately 5 minutes after the first HBO session, the CAT activity decreased by 6% ($P < 0.05$) compared to that determined before treatment, while after 14 sessions, it showed a slight increasing trend ($P > 0.05$) compared to that measured after the first session and was nonsignificantly lower than that before the HBO therapy. After both the first and 14th HBO sessions, the CAT activity in the SSNHL patients was significantly higher than that in the control group by 19% ($P < 0.001$) and 22% ($P < 0.001$), respectively.

No statistically significant differences were found in the erythrocytic SOD activity before the HBO therapy in the SSNHL patients and the control group. However, the SOD activity was nonsignificantly lower in the SSNHL patients. Approximately 5 min after the first HBO session, the SOD activity decreased in a statistically nonsignificant manner, while after 14 sessions, it was 7% lower compared to that in the pretreatment level, and the difference was statistically significant ($P < 0.05$). The SOD activity after 14 HBO sessions was 6% lower than that after the first session and 13% lower than that in the control group, and both differences were statistically significant ($P < 0.05$ and $P < 0.001$, respectively).

No statistically significant differences were found in the erythrocytic GPx activity in the SSNHL patients and the control group. However, the GPx activity was nonsignificantly higher in the SSNHL patients than in the control group. Approximately 5 min after the first HBO session, the GPx activity was nonsignificantly ($P > 0.05$) increased compared to the pretreatment value and was significantly higher by 62% ($P < 0.05$) than that in the control group. After 14 HBO sessions, a nonsignificant increasing tendency in the GPx activity compared to that after the first HBO session was observed. The GPx activity at that time point of the study was 28% higher ($P < 0.05$) than that of before the HBO therapy and 73% higher ($P < 0.001$) than that in the control group.

The HGB concentration in the SSNHL patients after the 14th HBO session was 6% lower than that of before the HBO therapy, and the difference was statistically significant ($P < 0.01$). The HCT value determined at that time point was also 6% lower ($P < 0.01$) than that of before treatment.

4. Discussion

In this study, no statistically significant changes in the TBARS concentration in the plasma of the SSNHL patients were observed. However, in erythrocytes, the concentration of TBARS after 14 HBO sessions increased compared to the value determined before the HBO therapy, which can indicate an enhanced peroxidation of membrane lipids in these cells. Yet, the erythrocytic TBARS concentration in the

TABLE 2: Statistically significant correlation coefficients between the parameters measured in the patients with SSNHL (studied group).

	Parameters	r
	TBARS in plasma/SOD	0.458**
Before HBO therapy	TBARS in erythrocytes/SOD	−0.318*
	CAT/GPx	0.395*
~5 min after first	TBARS in plasma/SOD	0.365*
HBO session	CAT/GPx	0.317*
After 14 HBO sessions	SOD/GPx	0.356*

TBARS: thiobarbituric acid reactive substances; CAT: catalase; GPx: glutathione peroxidase; SOD: superoxide dismutase. *$P < 0.05$. **$P < 0.01$.

SSNHL patients was lower in a statistically significant manner than that in the control group at all time points. Therefore, the observed increase in the TBARS concentration in erythrocytes can also be interpreted as normalisation of redox processes, and the reduced level of TBARS could be a result of intensified antioxidant mechanisms accompanying the oxidative processes occurring in SSNHL. This hypothesis is supported by the significantly higher CAT activity in the SSNHL patients measured before the HBO therapy compared to the control group. Another fact supporting the hypothesis of effective removal of ROS by scavenging mechanisms in the SSNHL patients was also the statistically significant negative correlation between the SOD activity and the TBARS concentration in erythrocytes observed before the HBO therapy ($r = −0.318$; $P < 0.05$) (Table 2, Figure 3).

Despite the proven increase in the generation of ROS in the blood induced by hyperbaric oxygen [14, 15], changes in the levels of TBARS and MDA after HBO therapy reported in the literature are not clear. Both an increase and a decrease in the levels of lipid peroxidation products after this type of treatment have been reported. An increase in, e.g., MDA level in the erythrocytes of divers subjected to hyperbaric exposure was demonstrated by Kozakiewicz et al. [16]. In turn, Benedetti et al. [15] observed an increased level of TBARS in the plasma of patients before their 15th HBO session compared to that of before the first HBO session, with the erythrocytic TBARS concentration showing no significant change. In patients with diabetes mellitus, a statistically significant increase in the MDA concentration in plasma was shown after the first HBO session, while changes observed after the 15th session were not statistically significant [17]. In their study, Paprocki et al. [18] did not demonstrate statistically significant changes in the concentration of TBARS in either the erythrocytes or the plasma of patients subjected to an HBO session, regardless of the fact whether before the experiment, the patients had undergone HBO sessions of no more than 3 times, or more than 23 times. In experimental studies conducted in animals treated with hyperbaric oxygen, as in humans, the observed changes in the concentrations of lipid peroxidation products have varied. A reduction in the concentration of MDA in erythrocytes after HBO therapy compared to the group not treated with HBO has been shown, e.g., in rats with experimentally induced Crohn's disease
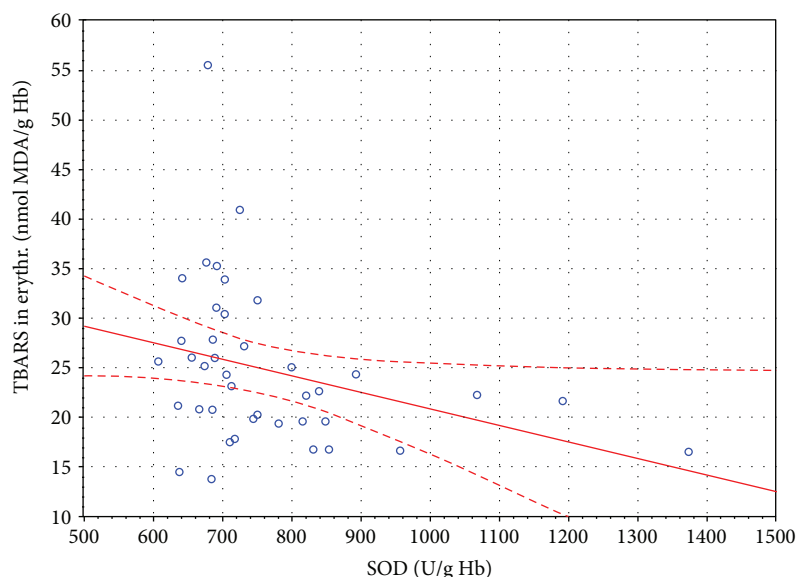
FIGURE 3: Linear regression of superoxide dismutase (SOD) activity versus thiobarbituric acid reactive substances (TBARS) concentration in the erythrocytes of SSNHL patients before HBO therapy ($r = -0.318$, $P < 0.05$).

[19] and with experimentally induced pancreatitis [20]. In turn, an increase in the TBARS concentration has been found in the erythrocytes of rats with streptozotocin- (STZ-) induced diabetes after HBO [21].

Therefore, it seems that the use of HBO generates ROS, but the functioning antioxidant mechanisms protect membrane lipids from excessive peroxidation. Differences reported in various publications can also be associated with the value of pressure at which the HBO sessions are conducted or with the formation of potential adaptive mechanisms with respect to hyperbaric oxygen. It cannot be excluded that the observed differences were affected by the time onset of SSNHL and the initiation of HBO therapy. In this study, HBO therapy was initiated no later than 5 days after the onset of SSNHL, which was in line with the guidelines of the Polish Society of Audiology and Phoniatrics. According to the guidelines, HBO therapy should be used only as supportive treatment during the first two weeks after the onset of SSNHL [1]. However, the effectiveness of HBO therapy in improving hearing is also observed in cases in which this treatment is introduced later, e.g., within 20 days of the onset of hearing loss [22]. Moreover, Topuz et al. [23] demonstrated that HBO therapy increases the effectiveness of conventional therapy when the treatment is started early after the onset of SSNHL.

The level of lipid peroxidation products observed in this study could also be affected by the use of corticosteroids (prednisone) by the patients at a tapered dose. Studies employing experimental models have proven that short-term use of corticosteroids protects various tissues against oxidative damage, but their longer use intensifies lipid peroxidation [24]. In this experiment, the patients took corticosteroids for a short period of time, i.e., up to two weeks. Other studies have also shown that corticosteroids reduce the intensity of lipid peroxidation. Keles et al. [25] demonstrated a decrease

in the serum and cerebrospinal fluid concentrations of MDA in patients with multiple sclerosis after corticosteroid therapy. A decrease in lipid hydroperoxide (ROOH) and normalisation of the H_2O_2 and TBARS levels have been observed after corticotherapy in Graves' disease patients [26]. The above effects of corticotherapy may be due to the fact that corticosteroids, among other actions, increase the levels of antioxidant enzymes in leukocytes [27] and inhibit the release of superoxide anion by human monocytes [28].

In the study presented in this paper, a statistically significant decrease of 6% ($P < 0.05$) in the CAT activity in the erythrocytes of patients with SSNHL after the first HBO stimulation was observed. After 14 HBO sessions, the CAT activity showed a statistically nonsignificant tendency to increase compared to that determined after the first HBO session. It was higher in a statistically significant manner in the SSNHL patients compared to that in the control group at all time points. In turn, the SOD activity decreased significantly after 14 HBO sessions. It was 7% lower ($P < 0.05$) than that of before the HBO therapy and 6% lower ($P < 0.05$) than that of after the first session. Concurrently, the GPx activity after 14 HBO sessions increased by 26% compared to that measured before the HBO therapy, and the difference was statistically significant ($P < 0.05$). The higher CAT activity in the erythrocytes of the SSNHL patients before the HBO therapy compared to the control group may imply the excessive H_2O_2 generation in the course of SSNHL. This was also confirmed by the higher, although statistically nonsignificant, GPx activity in the erythrocytes of the SSNHL patients. Both enzymes are involved in the removal of H_2O_2, and erythrocytes are considered as a circulating sink of H_2O_2 [29]. Hydrogen peroxide, which is electrically neutral and more stable than superoxide anion, easily passes through biological membranes [5] and, therefore, can migrate from the environment into erythrocytes. Further
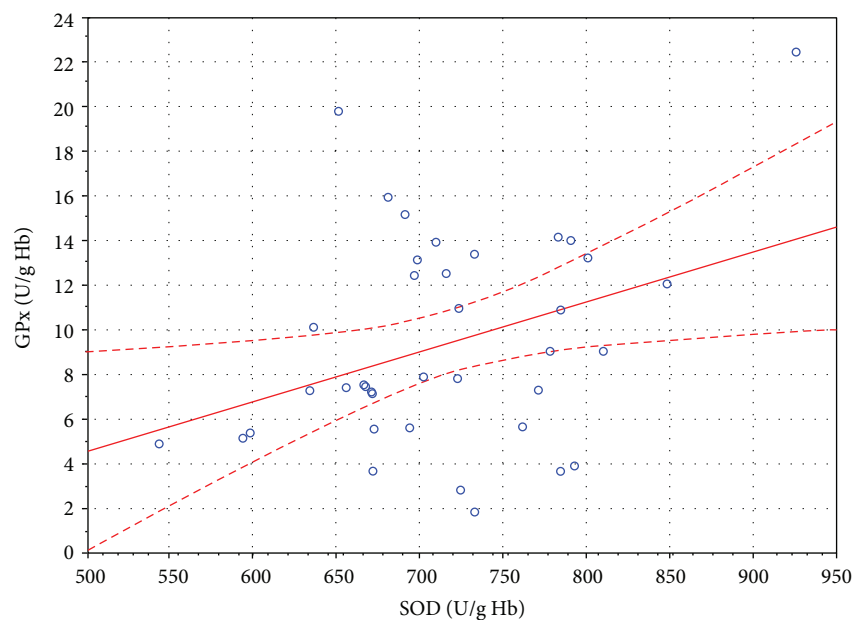
FIGURE 4: Linear regression of superoxide dismutase (SOD) activity versus glutathione peroxidase (GPx) activity in the erythrocytes of SSNHL patients after 14 HBO sessions ($r = 0.356$, $P < 0.05$).

increase in the GPx activity in erythrocytes to significantly higher values after the 14th HBO session, compared to that measured before the HBO therapy, may indicate potential increase in H_2O_2 generation also due to hyperbaric oxygen therapy. Increased H_2O_2 generation may be also verified by the statistically significant positive correlation between the activities of GPx and SOD in the erythrocytes of the SSNHL patients after 14 HBO sessions ($r = 0.356$, $P < 0.05$) (Table 2, Figure 4). Hydrogen peroxide can initiate a nonenzymatic degradation of haem, while the products of this degradation initiate oxidative processes in erythrocytes [30].

Paprocki et al. [31], in a preliminary study in patients with SSNHL, demonstrated a reduction of the CAT activity approximately 5 minutes after the completion of a single HBO session. The largest reduction of the CAT activity was observed in patients under 35 years of age. Similarly, in people with different diseases, only the CAT activity decreased approximately 5 min after a single HBO session, but this phenomenon regarded only those patients who had been in HBO sessions no more than 3 times prior to the experiment [18]. In turn, no changes in the CAT activity were observed in people subjected to HBO therapy multiple times (over 23 sessions) before the experiment. The activities of GPx and SOD in the erythrocytes of those patients did not change in a statistically significant manner after the experimental HBO session [18]. No statistically significant changes in the activities of SOD, GPx, and CAT 24 hours after a single HBO session were found in the erythrocytes of healthy people [32]. In another study conducted in healthy people, the GPx activity in erythrocytes increased significantly during HBO therapy, but not after its completion [33]. In studies conducted in animals, changes in the activity of antioxidant enzymes after HBO therapy have not been clear either. For example, an increase in the SOD activity in rapidly contracting muscles and a decrease in the CAT activity in slowly

contracting muscles have been observed in rats [34]. Matsunami et al. [35] demonstrated a decrease in the Cu-Zn SOD and CAT gene expression and an increase in the GPx gene expression in all tested organs of rats with experimentally induced diabetes treated with HBO therapy compared to a group of rats with experimentally induced diabetes that were not treated with HBO therapy.

In the SSNHL patients, a statistically significant reduction of haematocrit and haemoglobin after 14 HBO sessions compared to the values measured before the first session was observed. The results obtained by other authors are not definitive. For example, Handy et al. [36] did not demonstrate changes in the haematocrit value and the concentration of haemoglobin in the blood of chronically ill patients with problematic wounds after 20 HBO sessions. In turn, Sinan et al. [37] showed a large reduction in haematocrit in patients after 20 HBO sessions compared to their baseline values, but the difference was not statistically significant. Conversely, a statistically significant decrease in haematocrit and haemoglobin was demonstrated in 16 selected patients after 21 days of HBO therapy [38]. It is possible that long-term, repeated treatment with hyperbaric oxygen affects the process of erythropoiesis, which can be an adaptive mechanism of the body to high pressure and high oxygen concentration.

5. Conclusions

SSNHL is accompanied by disturbance in the oxidant-antioxidant equilibrium. Repeated stimulation with hyperbaric oxygen modulates the activity of antioxidant enzymes. It seems that increased generation of hydrogen peroxide is responsible for the changes in the activity of antioxidant barrier enzymes observed after HBO sessions.

Data Availability

The study data used to support the findings of this study are included within the article.

Conflicts of Interest

The authors declare that they have no conflict of interests. The study did not receive specific funding but was performed as part of the employment of the authors in Ludwik Rydygier Collegium Medicum in Bydgoszcz, Nicolaus Copernicus University, Toruń, Poland.

References

[1] J. Śliwińska-Kowalska, W. Narożny, A. Sekula et al., "Sudden sensorineural hearing loss – position paper of the polish Society of Audiology and Phoniatrics on the diagnostic and therapeutic recommendations," *Otorynolaryngologia*, vol. 14, no. 2, pp. 65–73, 2015.

[2] M. Pezzoli, M. Magnano, L. Maffi et al., "Hyperbaric oxygen therapy as salvage treatment for sudden sensorineural hearing loss: a prospective controlled study," *European Archives of Oto-Rhino-Laryngology*, vol. 272, no. 7, pp. 1659–1666, 2015.

[3] H. Sun, X. Qiu, J. Hu, and Z. Ma, "Comparison of intratympanic dexamethasone therapy and hyperbaric oxygen therapy for the salvage treatment of refractory high-frequency sudden sensorineural hearing loss," *American Journal of Otolaryngology*, vol. 39, no. 5, pp. 531–535, 2018.

[4] J. Paprocki, M. Gackowska, M. Pawłowska, and A. Woźniak, "The current use of hyperbaric oxygen treatment," *Medycyna Rodzinna*, vol. 4, pp. 217–222, 2016.

[5] A. Sarniak, J. Lipińska, K. Tytman, and S. Lipińska, "Endogenous mechanisms of reactive oxygen species (ROS) generation," *Postepy Higieny i Medycyny Doswiadczalnej*, vol. 70, no. 0, pp. 1150–1165, 2016.

[6] D. Martini, C. Del Bo, M. Tassotti et al., "Coffee consumption and oxidative stress: a review of human intervention studies," *Molecules*, vol. 21, no. 8, p. 979, 2016.

[7] C. A. Cobb and M. P. Cole, "Oxidative and nitrative stress in neurodegeneration," *Neurobiology of Disease*, vol. 84, pp. 4–21, 2015.

[8] S. R. Thom, "Oxidative stress is fundamental to hyperbaric oxygen therapy," *Journal of Applied Physiology*, vol. 106, no. 3, pp. 988–995, 2009.

[9] J. A. Buege and S. D. Aust, "Microsomal lipid peroxidation," *Methods in Enzymology*, vol. 52, pp. 302–310, 1978.

[10] H. Esterbauer and K. H. Cheeseman, "Determination of aldehydic lipid peroxidation products: malonaldehyde and 4-hydroxynonenal," *Methods in Enzymology*, vol. 186, pp. 407–421, 1990.

[11] R. F. Beers and J. Sizer, "Spectrophotometric method for measuring the breakdown of hydrogen peroxide by catalase," *Journal of Biological Chemistry*, vol. 195, no. 1, pp. 133–140, 1952.

[12] H. P. Misra and I. Fridovich, "The role of superoxide anion in the autoxidation of epinephrine and a simple assay for superoxide dismutase," *Journal of Biological Chemistry*, vol. 247, no. 10, pp. 3170–3175, 1972.

[13] D. E. Paglia and W. N. Valentine, "Studies on the quantitative and qualitative characterization of erythrocyte glutathione peroxidase," *Journal of Laboratory and Clinical Medicine*, vol. 70, no. 1, pp. 158–169, 1967.

[14] C. K. Narkowicz, J. H. Vial, and P. W. McCartney, "Hyperbaric oxygen therapy increases free radical levels in the blood of humans," *Free Radical Research Communications*, vol. 19, no. 2, pp. 71–80, 1993.

[15] S. Benedetti, A. Lamorgese, M. Piersantelli, S. Pagliarani, F. Benvenuti, and F. Canestrari, "Oxidative stress and antioxidant status in patients undergoing prolonged exposure to hyperbaric oxygen," *Clinical Biochemistry*, vol. 37, no. 4, pp. 312–317, 2004.

[16] M. Kozakiewicz, J. Kędziora, K. Kędziora-Kornatowska et al., "Effect of hyperbary on chosen prameters of oxidative stress in divers blood," *Polish Hyperbaric Research*, vol. 12, no. 3, pp. 7–12, 2005.

[17] F. Gürdöl, M. Cimşit, Y. Öner-İyidoğan, Ş. Körpinar, S. Yalçinkaya, and H. Koçak, "Early and late effects of hyperbaric oxygen treatment on oxidative stress parameters in diabetic patients," *Physiological Research*, vol. 57, no. 1, pp. 41–47, 2008.

[18] J. Paprocki, P. Sutkowy, E. Krzyżańska-Malinowska, J. Piechocki, and A. Woźniak, "The indicators of oxidant – antioxidant balance in patients performed hyperbaric oxygenation," *Polish Hyperbaric Research*, vol. 43, no. 2, pp. 23–38, 2013.

[19] B. Gulec, M. Yasar, S. Yildiz et al., "Effect of hyperbaric oxygen on experimental acute distal colitis," *Physiological Research*, vol. 53, no. 5, pp. 493–499, 2004.

[20] M. Yasar, S. Yildiz, R. Mas et al., "The effect of hyperbaric oxygen treatment on oxidative stress in experimental acute necrotizing pancreatitis," *Physiological Research*, vol. 52, no. 1, pp. 111–116, 2003.

[21] T. Matsunami, Y. Sato, T. Sato, and M. Yukawa, "Antioxidant status and lipid peroxidation in diabetic rats under hyperbaric oxygen exposure," *Physiological Research*, vol. 59, no. 1, pp. 97–104, 2010.

[22] J. Ajduk, M. Ries, R. Trotic, I. Marinac, K. Vlatka, and V. Bedekovic, "Hyperbaric oxygen therapy as salvage therapy for sudden sensorineural hearing loss," *The Journal of International Advanced Otology*, vol. 13, no. 1, pp. 61–64, 2017.

[23] E. Topuz, O. Yigit, U. Cinar, and H. Seven, "Should hyperbaric oxygen be added to treatment in idiopathic sudden sensorineural hearing loss?," *European Archives of Oto-Rhino-Laryngology and Head & Neck*, vol. 261, no. 7, pp. 393–396, 2004.

[24] R. L. Torres, I. L. Torres, G. Laste, M. B. Ferreira, P. F. Cardoso, and A. Belló-Klein, "Effects of acute and chronic administration of methylprednisolone on oxidative stress in rat lungs," *Jornal Brasileiro de Pneumologia*, vol. 40, no. 3, pp. 238–243, 2014.

[25] M. S. Keles, S. Taysi, N. Sen, H. Aksoy, and F. Akçay, "Effect of corticosteroid therapy on serum and CSF malondialdehyde and antioxidant proteins in multiple sclerosis," *The Canadian Journal of Neurological Sciences*, vol. 28, no. 2, pp. 141–143, 2001.

[26] J. Bednarek, H. Wysocki, and J. Sowiński, "Peripheral parameters of oxidative stress in patients with infiltrative Graves' ophthalmopathy treated with corticosteroids," *Immunology Letters*, vol. 93, no. 2-3, pp. 227–232, 2004.

[27] A. A. Youssef and D. N. Baron, "Leucocyte superoxide dismutase in rheumatoid arthritis," *Annals of the Rheumatic Diseases*, vol. 42, no. 5, pp. 558–562, 1983.

[28] S. J. Szefler, C. E. Norton, B. Ball, J. M. Gross, Y. Aida, and M. J. Pabst, "IFN-gamma and LPS overcome glucocorticoid inhibition of priming for superoxide release in human monocytes. Evidence that secretion of IL-1 and tumor necrosis factor-alpha is not essential for monocyte priming," *The Journal of Immunology*, vol. 142, no. 11, pp. 3985–3992, 1989.

[29] F. Orrico, M. N. Möller, A. Cassina, A. Denicola, and L. Thomson, "Kinetic and stoichiometric constraints determine the pathway of H_2O_2 consumption by red blood cells," *Free Radical Biology and Medicine*, vol. 121, no. 6, pp. 231–239, 2018.

[30] E. Zapora and I. Jarocka, "Hemoglobin – source of reactive oxygen species," *Postepy Higieny i Medycyny Doswiadczalnej (online)*, vol. 67, pp. 214–220, 2013.

[31] J. Paprocki, M. Pawłowska, P. Sutkowy, J. Piechocki, and A. Woźniak, "The oxidant–antioxidant equilibrium in the blood of people with sudden sensorineural hearing loss after the first hyperbaric oxygen therapy session – a preliminary study," *Polish Hyperbaric Research*, vol. 61, no. 4, pp. 15–24, 2017.

[32] C. Dennog, P. Radermacher, Y. A. Barnett, and G. Speit, "Antioxidant status in humans after exposure to hyperbaric oxygen," *Mutation Research*, vol. 428, no. 1-2, pp. 83–89, 1999.

[33] V. Matzi, J. F. Greilberger, J. Lindenmann et al., "Application of hyperbaric oxygen reduce oxidative damage of plasmatic carbonyl proteins and 8-OHdG by activating glutathion peroxidase," *Clinical Laboratory*, vol. 61, pp. 587–593, 2015.

[34] P. Gregorevic, G. Lynch, and D. A. Williams, "Hyperbaric oxygen modulates antioxidant enzyme activity in rat skeletal muscles," *European Journal of Applied Physiology*, vol. 86, no. 1, pp. 24–27, 2001.

[35] T. Matsunami, Y. Sato, T. Sato, S. Ariga, T. Shimomura, and M. Yukawa, "Oxidative stress and gene expression of antioxidant enzymes in the streptozotocin - induced diabetic rats under hyperbaric oxygen exposure," *International Journal of Clinical and Experimental Pathology*, vol. 3, no. 2, pp. 177–188, 2009.

[36] R. D. Handy, P. Bryson, A. J. Moody, L. M. Handy, and J. R. Sneyd, "Oxidative metabolism in platelets, platelet aggregation, and hematology in patients undergoing multiple hyperbaricoxygen exposures," *Undersea & Hyperbaric Medicine*, vol. 32, no. 5, pp. 327–340, 2005.

[37] M. Sinan, N. Z. Ertan, B. Mirasoglu et al., "Acute and long-term effects of hyperbaric oxygen therapy on hemorheological parameters in patients with various disorders," *Clinical Hemorheology and Microcirculation*, vol. 62, no. 1, pp. 79–88, 2016.

[38] E. Thorsen, H. Haave, D. Hofsø, and R. J. Ulvik, "Exposure to hyperoxia in diving and hyperbaric medicine – effects on blood cell counts and serum ferritin," *Undresea & Hyperbaric Medicine*, vol. 28, no. 2, pp. 57–62, 2001.

Research Article

Increased Transfection of the Easily Oxidizable GC-Rich DNA Fragments into the MCF7 Breast Cancer Cell

Svetlana V. Kostyuk [1], **Nadezhda N. Mordkovich,**[2] **Natalya A. Okorokova,**[2]
Vladimir P. Veiko,[2] **Elena M. Malinovskaya,**[1] **Elizaveta S. Ershova,**[1] **Marina S. Konkova** [1],
Ekaterina A. Savinova,[1,3] **Maria A. Borzikova,**[1,4] **Tatiana A. Muzaffarova,**[1]
Lev N. Porokhovnik [1], **Nataly N. Veiko,**[1] **and Serguey I. Kutsev**[1,3]

[1]*Research Centre for Medical Genetics (RCMG), Moscow 115478, Russia*
[2]*Bach Institute of Biochemistry, Biotechnology Research Center, Russian Academy of Sciences, Moscow 119071, Russia*
[3]*N. I. Pirogov Russian National Research Medical University, Moscow 117997, Russia*
[4]*I.M. Sechenov First Moscow State Medical University (Sechenov University), Moscow 119991, Russia*

Correspondence should be addressed to Svetlana V. Kostyuk; svet.kostyuk@gmail.com

Received 28 June 2018; Revised 16 October 2018; Accepted 14 November 2018; Published 5 February 2019

Guest Editor: Luciana Hannibal

Objective. Easily oxidizable GC-rich DNA (GC-DNA) fragments accumulate in the cell-free DNA (cfDNA) of patients with various diseases. The human oxidized DNA penetrates the MCF7 breast cancer cells and significantly changes their physiology. It can be assumed that readily oxidizable GC-DNA fragments can penetrate the cancer cells and be expressed. *Methods.* MCF7 cells were cultured in the presence of two types of GC-DNA probes: (1) vectors pBR322 and pEGFP and (2) plasmids carrying inserted human rDNA (pBR322-rDNA and pEGFP-rDNA). pEGFP and pEGFP-rDNA contained a CMV promoter and a fluorescent protein gene *EGFP*. ROS generation rate, accumulation of the DNA probes in MCF7, 8-oxodG content, expression of *EGFP* and *NOX4*, and localization of EGFP, NOX4, and 8-oxodG in MCF7 were explored. The applied methods were qPCR, fluorescent microscopy (FM), immunoassay, and flow cytometry (FCA). *Results.* When GC-DNA is added to the cell culture medium, it interacts with the cell surface. At the site of GC-DNA contact with the cell, NOX4 is expressed, and ROS level increases. The ROS oxidize the GC-DNA. When using the plasmids pEGFP and pEGFP-rDNA, an increase in the amount of the DNA *EGFP*, RNA *EGFP*, and EGFP proteins was detected in the cells. These facts suggest that GC-DNA penetrates the cells and the *EGFP* gene is expressed. Insertions of the rDNA significantly increase the GC-DNA oxidation degree as well as the rate of plasmid transfection into the cells and the *EGFP* expression level. In the nucleus, the oxidized GC-rDNA fragments, but not the vectors, are localized within the nucleolus. *Conclusions.* GC-rich cfDNA fragments that are prone to oxidation can easily penetrate the cancer cells and be expressed. The cfDNA should become a target for the antitumor therapy.

1. Introduction

In the 1940s, it was discovered that mammalian DNA not only is contained in the cell nuclei but could be also found in the serum of peripheral blood [1]. The human cell-free DNA (cfDNA) is known to be enriched with GC-pairs. Mean GC-pair content in cfDNA of healthy controls is 53.7% [2], whereas gDNA contains 42% of GC-pairs [3]. In pathology and under the action of harmful environmental factors, cfDNA becomes increasingly enriched with GC-rich motifs (GC-DNA) [4]. A hallmark of accumulation of GC-DNA as part of cfDNA can be two highly repetitive sequences, which are present in hundreds of copies in the human genome: mitochondrial DNA [5, 6] and ribosomal genes (rDNA) [7]. The rDNA is easier to use, because its abundance in the genome is constant and does not depend on the current state of the cell.

A several fold increase in rDNA content within cfDNA is observed in chronic pathologies followed by exaggerated cell

death (ischemic heart disease, chronic arterial hypertension, and rheumatic arthritis [7–9]), as well as in case of a chronic exposure to ionizing radiation or smoking [10, 11]. In some cases, the content of rDNA fraction within cfDNA can increase by more than an order of magnitude.

As a result of the change in CG-composition of cfDNA observed in autoimmune and cardiovascular pathologies, the cfDNA becomes biologically active. Both models GC-DNA and cfDNA from the patients induce changes in the functional activity of human endothelial cells [12], rat cardiomyocytes [13], neurons [14], human stem cells [15], and lymphocytes [16]. The first and major sign of the GC-DNA impact is elevated ROS production [15].

In spite of intensive studies of cfDNA in oncological diseases [17], whether GC-DNA fragments possess biological activity in respect of cancer cells remains elusive. We showed previously that exposure to the oxidized human gDNA enhances both genome instability and survival in MCF7 cancer cells [18]. Nonoxidized human gDNA did not possess such properties. Since human GC-DNA contains a high number of most easily oxidizable dGn ($n > 2$) motifs [15], one can expect that these oxidized DNA fragments exhibit activity with regard to cancer cells.

The biological activity of oxidized human gDNA is manifested as a consequence of its more effective penetration into the cells [18]. GC-DNA can be also expected to penetrate easily the cells owing to its higher oxidation degree. Alongside with that, promotors of approximately 40% of human genes are known to include CpG islets (about 1.5 kbp long), which are identical to rDNA with respect to their GC-composition and could accumulate within cfDNA. The accumulation of a fraction of the genes with GC-rich promotors within cfDNA can result in the expression of these genes in the cells. In addition, DNA fragments, when penetrating the cells, can bind and exhaust the pool of factors that regulate the expression of some specific genes. As a result, the gene expression patterns can change.

Thus, in this study, we intended to obtain answers for the following questions: (1) Does the GC-DNA, containing rDNA, have an ability to penetrate MCF7 cancer cells? (2) Can the genes contained in the extracellular GC-DNA be expressed inside MCF7 cells? (3) Can the extracellular GC-DNA containing the genes modulate the expression of the same genes in the nucleus?

2. Methods

2.1. Cell Culture. ER/PR-positive MCF7 breast cancer cells were purchased at ATCC, Manassas, USA (Cat: HTB-22). MCF7 cells were cultured in DMEM medium supplemented with 10% (v/v) fetal calf serum, 2 mM L-glutamine, 100 units/mL penicillin, and 100 μg/mL of streptomycin. Cells were grown in a humidified atmosphere with 5% CO_2 in air at 37°C. Before the treatment with GC-DNA probes, cells were grown for 48 h in slide flasks.

2.2. Model GC-DNA. Plasmid pEGFP-C1 (pEGFP) that contains the EGFP gene (http://www.bdbiosciences.com, GenBank accession number U55763) was used as a vector

(Figure 1(b)). The DNA fragment to be inserted was synthesized and consisted of 420 base pairs flanked with BamHI restriction sites and containing the rDNA. Cloned rDNA fragment covers positions from 601 to 1021 b of human rDNA (Figure 1(a)).

Plasmid pBR322 is the commercial product (Sigma-Aldrich). pBR322-rDNA (plasmid DNA) contains rDNA sequences cloned into the EcoRI site of pBR322 vector. Cloned rDNA fragment covers positions from −515 to 5321 of human rDNA (Figure 1(a)).

2.2.1. Plasmid Clearance from Endotoxins. All the GC-DNA samples were subjected to the purification procedure removing lipopolysaccharides; this included sequential treatment with Triton X114 (Merck, Germany) followed by gel filtration on the HW 85 [19] or the use of an Endotoxin Extractor (Sileks, Russia). In order to prove that the observed response was caused exclusively by DNA, not by endotoxin residuals, additional experiments were set up. (1) A sample of plasmid DNA underwent complete hydrolysis down to nucleosides using DNA exonucleases and phosphatase. The resultant plasmid hydrolysates had no biological activity, which is intrinsic to an intact DNA.

(2) We analyzed the expression of TLR4 gene, which is always activated in the presence of the endotoxin. The samples of plasmid DNA induced no increase of TLR4 expression.

2.3. The cfDNA Samples Obtained from Blood Plasma. We used four blood plasma samples derived from healthy donors and four blood plasma samples from untreated breast cancer patients, who had applied for genetic tests in RCMG. The investigation was carried out in accordance with the latest version of the Declaration of Helsinki and approved by the Regional Ethics Committee of RCMG (Approval #5). All participants signed an informed written consent to participate after the nature of the procedures had been completely explained to them. CfDNA isolation from blood plasma and quantification of rDNA in the cfDNA was performed as described earlier [10]. The content of the transcribed region of rDNA was presented as pg rDNA/ng cfDNA.

2.4. Flow Cytometry

2.4.1. EGFP. Nonfixed cells were analyzed at 488 nm. To quantify the background fluorescence, the control cells were analyzed.

2.4.2. 8-oxodG and NOX4. Staining of the cells with antibodies was performed as previously described [18]. To quantify the background fluorescence, we stained a portion of the cells with secondary FITC- (PE) conjugated antibodies only.

Cells were analyzed at CyFlow Space (Partec, Germany).

2.5. Quantification of mRNA. Total mRNA was isolated using RNeasy Mini kits (Qiagen, Germany), treated with DNAse I, and reverse transcribed by a Reverse Transcriptase kit (Sileks, Russia). The expression profiles were obtained using qRT-PCR with SYBR Green PCR Master Mix (Applied Biosystems). The mRNA levels were analyzed using the StepOnePlus (Applied Biosystems); the technical error
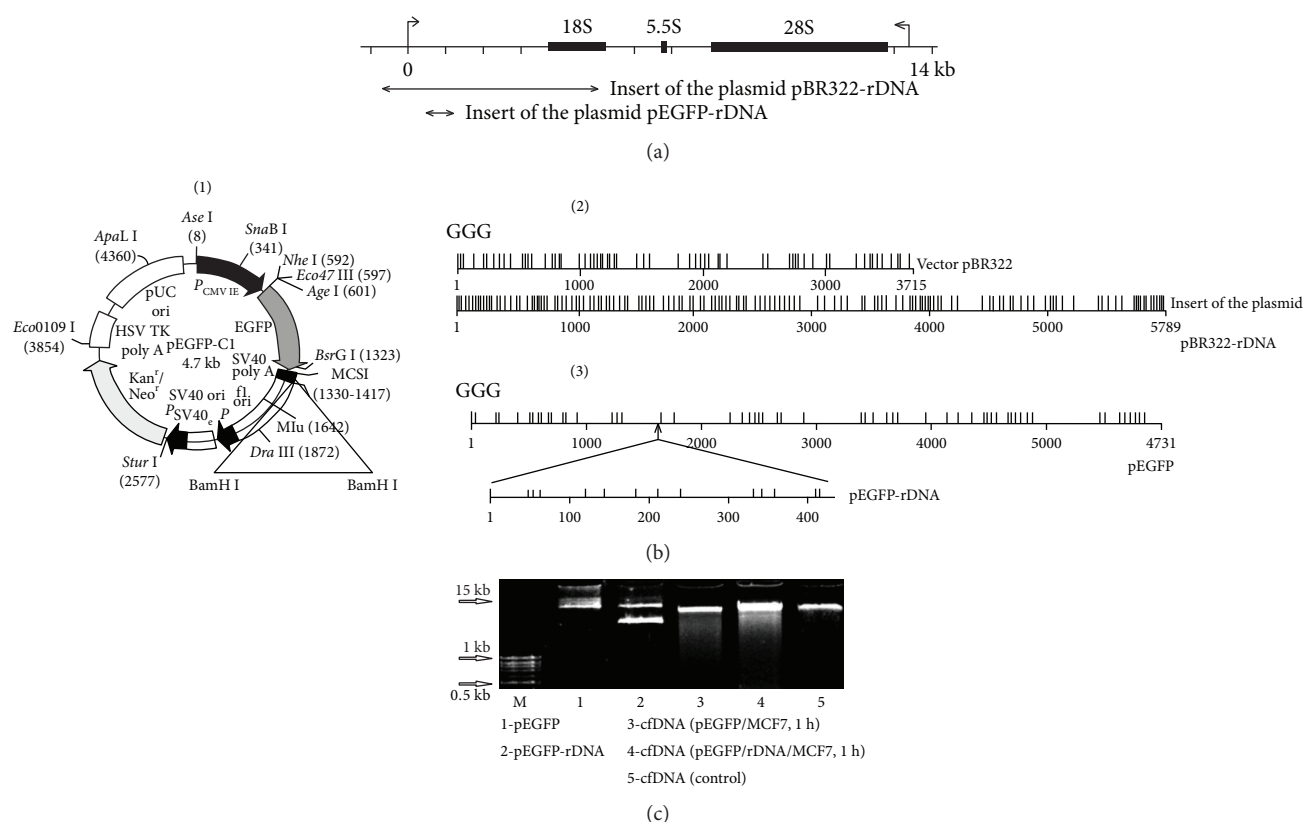
FIGURE 1: (a) Scheme of the human ribosomal repeat. Segments—the inserts of the model GC-DNA analyzed are shown. (b) (1)—plasmid pEGFP-C1 (pEGFP) (http://www.bdbiosciences.com, GenBank accession number U55763). The site BamH1 is marked. (2) and (3)—distribution of the easily oxidizable GGG-motifs within pBR322, pBR322-rDNA, pEGFP, and pEGFP-rDNA. (c) Determination of the plasmid fragmentation in the extracellular DNA after 1 h of MCF7 incubation with 50 ng/mL pEGFP or pEGFP-rDNA. The total DNA was isolated from the cell culture medium. Electrophoresis of DNA was carried out in a 2% agarose gel stained with ethidium bromide. Gel tracks 1 and 2—plasmid solutions in water were applied.

was approximately 2%. The following primers were used (Sintol, Russia):

(1) EGFP (F TACGGCAAGCTGACCCTGAAG; R TG AAGCACTGCACGCCGTAGG)

(2) NOX4 (F:TTGGGGCTAGGATTGTGTCTA; R:GA GTGTTCGGCACATGGGTA)

(3) TBP (reference gene) (F: GCCCGAAACGCCGAAT AT; R: CCGTGGTTCGTGGCTCTCT)

2.6. Quantification of pEGFP and pEGFP-rDNA in the Cells and Medium

2.6.1. The Cells.
After incubation medium removal by centrifugation at 460 g, cells were mixed with the solution (1 mL) containing 0.2% sodium lauryl sarcosylate, 0.002 M EDTA, and 75 μg/mL RNAse A (Sigma-Aldrich, USA) and incubated for 45 min, then treated at 37°C with proteinase K (200 μg/mL, Promega, USA) for 24 h. After two cycles of the purification with saturated phenolic solution, DNA fragments were precipitated by adding two volumes of ethanol in the presence of 2 M ammonium acetate. The precipitate was then washed with 75% ethanol twice, dried, and dissolved in water. The concentration of DNA was determined by

measuring fluorescence intensity after DNA staining with the PicoGreen (Molecular Probes/Invitrogen, CA, USA). The contents of pEGFP and pEGFP-rDNA were obtained using qPCR with SYBR Green PCR Master Mix (Applied Biosystems). The following primers were used (Sintol, Russia):

(1) EGFP (F: TACGGCAAGCTGACCCTGAAG; R: TG AAGCACTGCACGCCGTAGG)

(2) Human B2M (reference gene, accession number M17987) (F: GCTGGGTAGCTCTAAACAATGTA TTCA; R: CATGTACTAACAAATGTCTAAAAT GG)

2.6.2. Culture Medium.
For the isolation of DNA from the cell culture medium, a procedure similar to that described above for the cells was used. DNA underwent electrophoresis in a 2% agarose gel stained with ethidium bromide.

2.7. 8-oxodG Levels in pEGFP and pEGFP-rDNA

2.7.1. MCF7 1 h (Figure 2(c)).
MCF7 were cultured in the presence of plasmids for one hour. The RNA fraction which contained fragments of plasmid DNA was isolated using YellowSolve (Sileks, Russia). RNA was digested (1 h, 37°, 75 μg/mL RNAse A), and DNA was precipitated with 75%

(a)

(b)

(c)
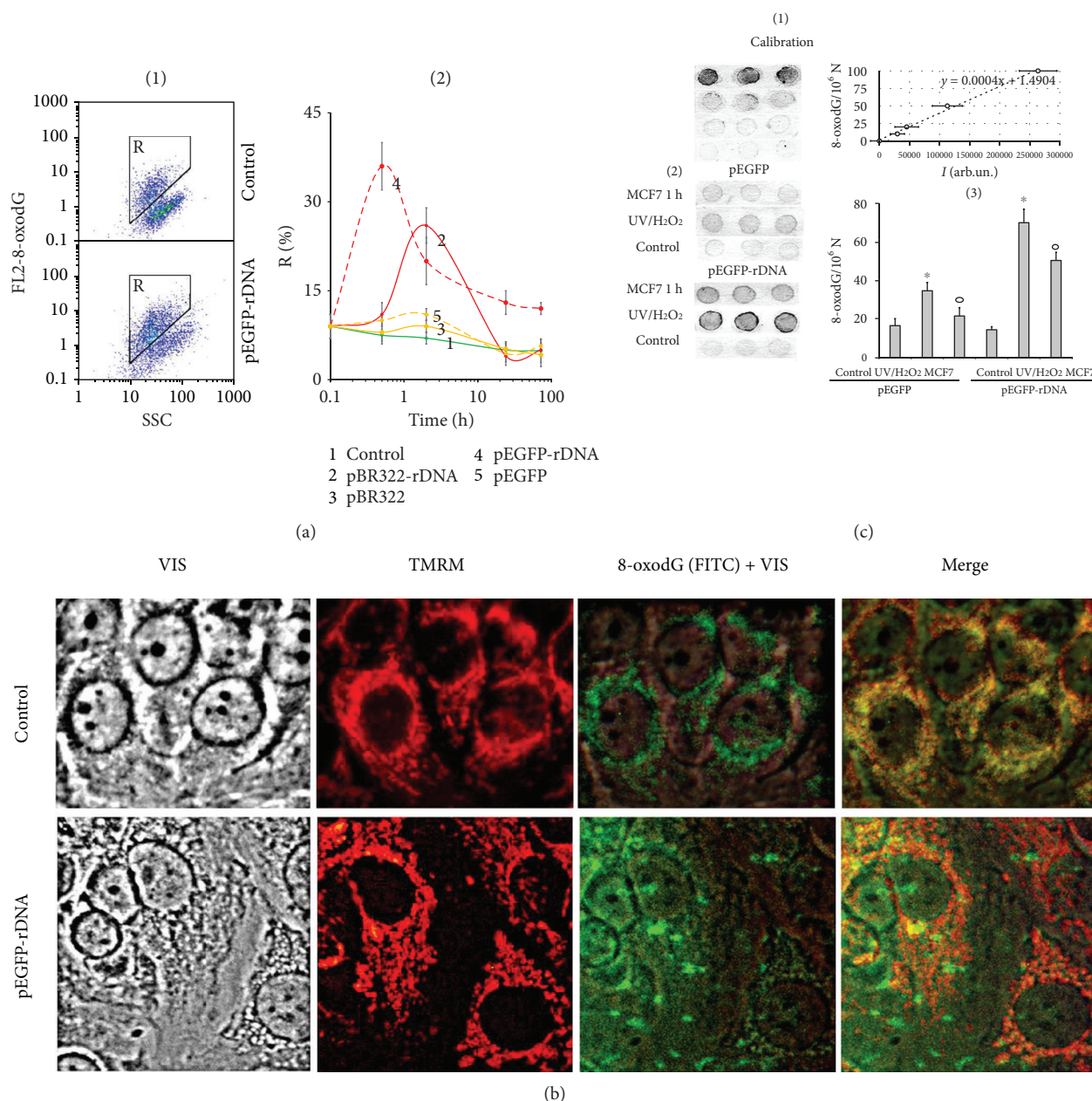
Figure 2: 8-oxodG levels in MCF7. (a) FCA: (1)—cell plots: FL2 (8-oxodG-PE) versus SSC. R: gated area. (2)—relative proportions of 8-oxodG-positive cells in R gate (change with time). (b) FM-based evaluation of mitochondria and 8-oxodG (FITC) in the cells treated with pEGFP-rDNA for 1 h (×40). Unfixed cells were stained with MitoTracker TMRM (15 min, 37° C) and photographed. Next, cells were fixed with 3% paraformaldehyde, treated with 0.1% Triton X100, and 8-oxodG was detected using antibodies (FITC). Photographed in the same field. (c) 8-oxodG levels in pEGFP and pEGFP-rDNA. Immunoassay technique on nitrocellulose membranes using 8-oxodG antibodies conjugated with alkaline phosphatase was used. (1 and 2)—four standard samples of oxidized genomic DNA (10 ng/dot) with a known content of 8-oxodG (was determined by ESI-MS/MS using AB SCIEX 3200 Qtrap machine [18]) were applied in order to plot a calibration curve for the dependence of the signal intensity on the number of 8-oxodG bases. (3 and 4)—the samples of oxidized and nonoxidized (control) pEGFP and pEGFP-rDNA (10 ng/dot) were applied. MCF7 1 h—pEGFP or pEGFP-rDNA after 1 h of incubation with MCF7; UV/H_2O_2—plasmids were oxidized in 0.1% H_2O_2 solution with UV irradiation ($\lambda > 312$ nm) for 3 minutes at 25°C (Vilber Lourmat equipment, TCP-20.LM).

ethanol. The contents of pEGFP and pEGFP-rDNA were obtained using qPCR.

2.7.2. UV/H_2O_2 (Figure 2(c)). The method for DNA oxidation was specified previously [18]. Briefly, plasmids pEGFP and pEGFP-Gn (100 ng/μL) were oxidized in 0.1% H_2O_2 solution

with UV irradiation ($\lambda > 312$ nm) for 3 minutes at 25°C. Modified DNA was precipitated with two volumes of ethanol in the presence of 2 M ammonium acetate. The precipitate was washed twice with 75% ethanol, then dried, and dissolved in water. Resulting DNA concentrations were quantified by an analysis of the UV spectra.

The method for 8-oxodG quantitation was specified in details previously [20]. Briefly, the DNA samples were applied to a prepared filter (Optitran BA-S85, GE Healthcare). Three dots (10 ng/dot) were applied per each sample. Four standard samples of the oxidized genomic DNA (10 ng/dot) with a known content of 8-oxodG (determined by ESI-MS/MS using AB SCIEX 3200 Qtrap machine [18]) were applied onto the same filter, in order to plot a calibration curve for the dependence of the signal intensity on the number of 8-oxodG copies in a particular sample. The filter was heated at 80°C in vacuum for 1.5 h. 8-oxodG antibody conjugated with alkaline phosphatase was used. Then the filter was placed into a solution of substrates for alkaline phosphatase NBT and BCIP. Upon the completion of reaction, the filter was washed with water and dried in the darkness. The dried filter was scanned. For the quantitative analysis of the dots, special software was used (Images6, RCMG, Moscow). Signals from several dots for the same sample are averaged. The 8-oxodG content in a studied sample is calculated using the calibration curve equation. A relative standard error was $15\% \pm 5\%$.

2.8. Fluorescence Microscopy

2.8.1. Immunocytochemistry. MCF7 cells were fixed in 3% formaldehyde (4°C) for 20 min, washed with PBS, and then permeabilized with 0.1% Triton X-100 in PBS for 15 min at room temperature, followed by blocking with 0.5% BSA in PBS for 1 h and incubated overnight at 4°C with the NOX4 and 8-oxodG antibody. After washing with 0.01% Triton X-100 in PBS, MCF7 cells were incubated for 2 h at room temperature with the FITC/PE goat anti-mouse IgG, washed with PBS, and then stained with DAPI.

2.8.2. Intracelullar Localization of Labeled GC-DNA Fragments. Labeling of pBRR322 and pBR322-rDNA was performed by nick translation using a CGH Nick Translation Kit (Abbott Molecular) under the manufacturer's protocol. Labels pBR322^{green} and pBR322-rDNA^{green} or pBR322-rDNA^{red} were added to the cultivation media for 30 min. Cells were washed three times with PBS, fixed in 3% paraformaldehyde (4°C) for 10 min, washed with PBS, and stained with 2 μg/mL DAPI.

2.8.3. EGFP. Nonfixed cells were analyzed at 488 nm. To quantify the background fluorescence, the control cells were analyzed.

2.8.4. Mitochondria. The cells were stained with 30 nM TMRM (tetramethylrhodamine methyl ester) (Molecular Probes) for 20 min at 37°C.

2.9. ROS Assay. The cells were analyzed using a total fluorescence assay in the 96-well plate format at $\lambda ex = 488$ nm and $\lambda em = 528$ nm (EnSpire equipment, Finland). The cultivation medium was replaced by 5 μm H$_2$DCFH-DA (Molecular Probes/Invitrogen, CA, USA) in PBS solution, and a relative fluorescence intensity increase was detected at 37°C. 16 (8×2) repeated measurements were provided for each GC-DNA concentration, and 24 for the control. The mean absolute intensities were divided by the average value of the intensity corresponding to $t = 0$, obtaining the values of I_0. The graphs are presented in the coordinates $I -$ time. The obtained data were approximated by linear dependence; the value of the tangent of the slope (index k_i) together with the error of determination was calculated. k_0 is reaction rate constant for DCF formation in control cells: $\Delta k = k_i - k_0$.

2.10. Statistics. All reported results for qPCR, PT-qPCR, immunoassay, and FCA were reproduced at least three times as independent biological replicates. The significance of the observed differences was analyzed using nonparametric Mann–Whitney U tests. The data were analyzed with StatPlus2007 Professional software (http://www.analystsoft.com/). All p values were considered statistically significant at $p < 0.05$. The software for "Imager 6" was designed by R. Veiko (RCMG, Moscow).

3. Results

3.1. Experimental Design. In order to study the eventual biological activity of GC-DNA towards MCF7 cancer cells, four model GC-DNA constructs were used (Figures 1(a) and 1(b)):

(1) pBR322-rDNA: plasmid DNA (10,197 bp) contains rDNA sequences (5836 bp, 73% GC) cloned into the EcoRI site of pBR322 vector. The rDNA fragment clone covers the positions from −515 to 5321 of human rDNA (Figure 1(a))

(2) pBR322: vector (4361 bp, 53% GC) served as a control for pBR322-rDNA

(3) pEGFP-rDNA: plasmid DNA (5151 bp) contains GC-rich rDNA sequences (420 bp, 91.9% GC) cloned into the BamH1 site of pEGFP-C1 vector. Cloned rDNA fragment covers positions from 601 to 1021b of human rDNA (Figure 1(a))

(4) pEGFP: plasmid pEGFP-C1 (53.4% GC) contains EGFP gene used as a control for pEGFP-rDNA

All the plasmids are enriched with GC-pairs compared to human gDNA (42% GC). Plasmid sequencing showed multiple GGG motifs, Figure 1(b), (2) and (3). The dG bases included in such motifs are known to have the lowest oxidation potentials among all the bases in the DNA molecule [21].

In addition to plasmids, cfDNA samples isolated from the blood plasma of healthy donors ($N = 4$) and the blood plasma of untreated breast cancer patients ($N = 4$) were also used. In the cfDNA samples, rDNA content was determined. The cfDNA samples derived from the cancer patients contained more rDNA, than the samples from healthy donors (1.3–2.1 pg/ng cfDNA vs 3.1–4.2 pg/ng cfDNA).

The MCF7 culture medium contained 320 ± 40 ng/mL cfDNA 48 h after the start of culture growth. The rDNA content in gDNA and cfDNA was, respectively, 1.47 pg/ng gDNA [22] and 2.5 pg/ng cfDNA. GC-DNA was added to the MCF7 culture medium in a concentration of 50 ng/mL. So the total cfDNA content slightly increased (by a factor of

1.15, up to 370 ± 40 ng/mL), while the GC-rDNA content substantially elevated (approximately 20-fold compared to the cfDNA content in the control cells). The cells were cultured with GC-DNA for 0.5 to 72 h.

A question whether plasmid DNA requires linearization before adding to the culture medium was considered specially. Our first tests failed to show any difference between the rates of accumulation of intact GC-DNA and their linearized forms in the cells. We examined the conformation of plasmids, which had remained in the medium after one-hour cell incubation, using electrophoresis in a 2% agarose gel (Figure 1(c), data for pEGFP and pEGFP-rDNA are presented). The initial plasmid pool contained various circular forms (tracks 1 and 2, Figure 1(c)). However, following incubation with the cells, almost only one form remained (tracks 3 and 4), which was partially fragmented. Thus, when the cells were present in the medium, the supercoiled circular plasmid DNA is rapidly hydrolyzed down to linear molecules of different length that roughly corresponds to the length of fragments of cell's own cfDNA accruing in the culture medium (track 5). On the basis of these data, we added nonlinearized plasmids to the culture medium during the major experiments.

3.2. Interaction of GC-DNA with the Cells. The probes pBR322-rDNA[green], pBR322-rDNA[red], and pBR322[green] were labeled with SpectrumRed and SpectrumGreen [18]. After 30 minutes of incubation with MCF7, BR322-rDNA[green] and pBR322[green] demonstrated approximately the same MCF7 binding pattern: the signals were situated as separate grains over the cytoplasm periphery (Figures 3(a) and 3(b)) and could be observed approximately in half of the cells. More detailed simultaneous analysis showed that GC-DNA binding to the cell depended on the base sequence (Figure 3(c)). Not all signals observed in the cell after binding to pBR322-rDNA[red] and pBR322[green] probes coincide: signals from pBR322-rDNA[red] probe are more numerous. As early as 3 h after, the fluorescence of DNA-probed in MCF7 considerably decreased and was not detected at all 24 h later.

Thus, firstly, rDNA fragments selectively interact with some cellular structures and, secondly, fluorescent label in GC-DNA probe quickly degrades. The latter can suggest an elevated level of ROS, which oxidize and/or quench the dye fluorescence.

3.3. GC-DNA Induces a Transient Oxidative Stress in MCF7. To study the possible influence of GC-DNA on the intracellular levels of ROS, the ROS were measured using dichlorodihydrofluorescin diacetate (H_2DCFH-DA) dye that rapidly penetrates cell membranes and gets trapped in the cytosol in its deacetylated form. In the cytosol, nonfluorescent DCFH serves as a sensitive intracellular marker for oxidative stress upon its oxidation to DCF by a variety of ROS [23]. Figure 4(a) shows the results of ROS assay in living cells using a plate reader.

When we added DNA samples after adding H_2DCFH-DA to the medium, we observed a signal increase in the presence of GC-DNA compared to the control. The peak rate of DCF production was observed within the first 20 min after adding

GC-DNA to the cells (Figure 4(a)). Later, the curve slope diminished several times. But if the cells were at first exposed to DNA samples during 30 min and then added H_2DCFH-DA, the effect lacked (Figure 4(a), (2)).

Both cfDNA samples from controls and patients stimulated ROS synthesis in the cells. The cell response for the exposure to the cancer cfDNA samples was higher than for the exposure of the control cfDNA and comparable to the cell response for the exposure to the model GC-DNA. The ROS synthesis level positively correlated with the rDNA content in cfDNA (Figure 4(a), (3)).

Figure 4(b) displays the results of ROS assay in the living cells using fluorescence microscopy. H_2DCFH-DA dye stains the control cells mainly along the surface of the cell membrane. GC-DNA initiates stained grains in the cytoplasm. The localization of green DCF grains mainly coincides with the localization of red grains of the tagged DNA-probe GC-DNA[red] (Figure 4(b)). It seems that the interaction of GC-DNA with the cellular structures stimulates ROS production in the place of the contact.

One can conclude, firstly, that GC-DNA is an inducer of quick ROS synthesis in MCF7 cells. Secondly, in parallel with the active ROS production, a process is initiated in the cells, which is aimed at reducing the ROS level.

3.4. GC-DNA Evoked an Increase in NOX4 Expression. The amount of NOX4 protein in the cells was evaluated using FCA (Figure 5(a)). MCF7 cell culture harbors two cell subpopulations: with high (gate R1, approximately 10% of the cells) and low (gate R2) contents of NOX4 protein (Figure 5(a), (1)). GC-DNA induced an increase of NOX4 amount. The effect was maximum in 24 h after the start of exposure and decreased by 72 hours down to the baseline. The pEGFP and pBR322 plasmids that carried no rDNA inserts evoked an increase of the rate of cells with high level of NOX4 expression by a factor of two and five, respectively. The plasmids that carried rDNA inserts stimulated the NOX4 protein synthesis in a less degree.

The level of RNA *NOX4* in 24 h after an exposure to GC-DNA is shown in Figure 5(b). In the presence of pEGFP-rDNA and pBR322-rDNA plasmids, the RNA *NOX4* amount increased by a factor of 2 to 4, whereas in the presence of pEGFP and pBR322, increased by a factor of 9 to 10.

In control cells, NOX4 is located on the cellular surface and in the cytoplasm. In the presence of GC-DNA, this protein is expressed on the cellular surface, in the cytoplasm, and in the nucleus (Figure 5(c)).

Thus, all the types of GC-DNA induced an increase in *NOX4* expression; however, the presence of rDNA inserts reduced this effect.

3.5. GC-DNA Induced an Increase in 8-oxodG Content in the Cells. The 8-oxodG content in the cells was determined using FCA (Figure 2(a)). pEGFP-rDNA and pBR322-rDNA increased the fraction of cells with high 8-oxodG content (gate R, Figure 2(a), (1)) by a factor of 2-3 ($p < 0.05$). The effect reached the peak in the first several hours and decreased in 24 h (Figure 2(a), (2)). An exposure to the
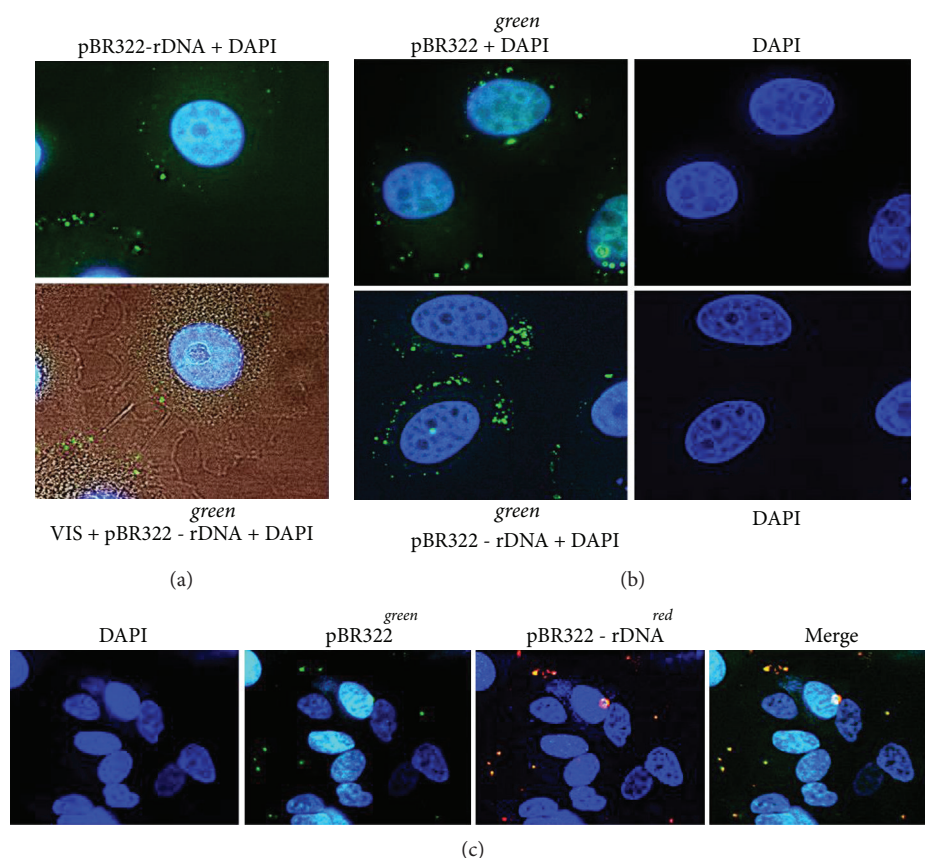
FIGURE 3: Staining of MCF7 cells with various types of labeled GC-DNA. (a) Top photo: pBR322-rDNA^{green}, nuclei are stained with DAPI. Bottom photo: merged staining patterns of pBR322-rDNA^{green}, DAPI and the image of the cell in visible light (×100). (b) pBR322^{green} (top photo) and pBR322-rDNA^{green} (bottom photo). (c) Merged staining patterns of pBR322^{green} and pBR322-rDNA^{red} (×40). Labeling of pBRR322 and pBR322-rDNA was performed by nick translation using a CGH Nick Translation Kit (Abbott Molecular). Labels pBR322^{green} and pBR322-rDNA^{green} or pBR322-rDNA^{red} were added to the cultivation media (50 ng/mL) for 30 min. Cells were washed three times with PBS, fixed in 3% paraformaldehyde (4°C) for 10 min, washed with PBS, and stained with 2 μg/mL DAPI.

plasmids pEGFP and pBR322 slightly influenced the 8-oxodG content in the cells ($p > 0.05$).

The elevation of intracellular 8-oxodG signal after an exposure to pEGFP-rDNA and pBR322-rDNA within the first hours can be associated with an increased oxidation level of the cellular DNA (mitochondrial and nuclear) and/or with an increased oxidation level of the plasmid itself followed by interaction with the cells. In order to elucidate this question, we determined the localization of 8-oxodG signals in the cells using fluorescence microscopy (Figures 2(b) and 6). In the control cells, 8-oxodG (FITC) was detected in the mitochondria (MitoTracker TMRM). Within the first 30 minutes after the beginning of exposure to GC-DNA, additional compact single signals were detected in the cellular cytoplasm. Their localization only partially coincided with the mitochondria. These signals were more abundant in case of exposure to pEGFP-rDNA and pBR322-rDNA. 24 h later, these signals were not detected. Signals from 8-oxodG detected in the mitochondria insignificantly differed from the control sample by intensity.

Thus, the increase of 8-oxodG content in the cells (Figure 2(a)) is induced by an elevated oxidation level of GC-DNA itself. It should be noted that the cell treatment

before FCA (washing with a solution containing trypsin and EDTA) led to detaching the superficially bound cfDNA and complexes of cfDNA with proteins from the cellular surface [24, 25]. Using FCA, it was possible to detect only those fragments of oxidized GC-DNA, which had already penetrated the cytoplasm through the cell membrane.

In order to find out finally the cause of the difference in 8-oxodG content between the cells exposed to vectors or to pEGFP-rDNA and pBR322-rDNA, we compared oxidability of pEGFP-rDNA plasmid and pEGFP vector (Figure 2(c)). The 8-oxodG content in DNA was analyzed using immunoassay on nitrocellulose membranes using antibodies to 8-oxodG conjugated with alkaline phosphatase. For measurement calibration, DNA samples with known 8-oxodG content were used (Figure 2(c), (1)). Plasmids pEGFP and pEGFP-rDNA were oxidized in 0.1% H_2O_2 solution at UV treatment ($\lambda > 312$ nm) or added for 1 h to the MCF7 culture medium. The plasmids were isolated from the cells as part of RNA fraction (see Methods) separating the high-molecular fraction of cellular DNA. Then hydrolysis was conducted using RNAse 1, and 8-oxodG content was assayed in DNA (Figure 2(c), (2)). In both experiments, pEGFP-rDNA plasmid contained more 8-oxodG than the pEGFP vector
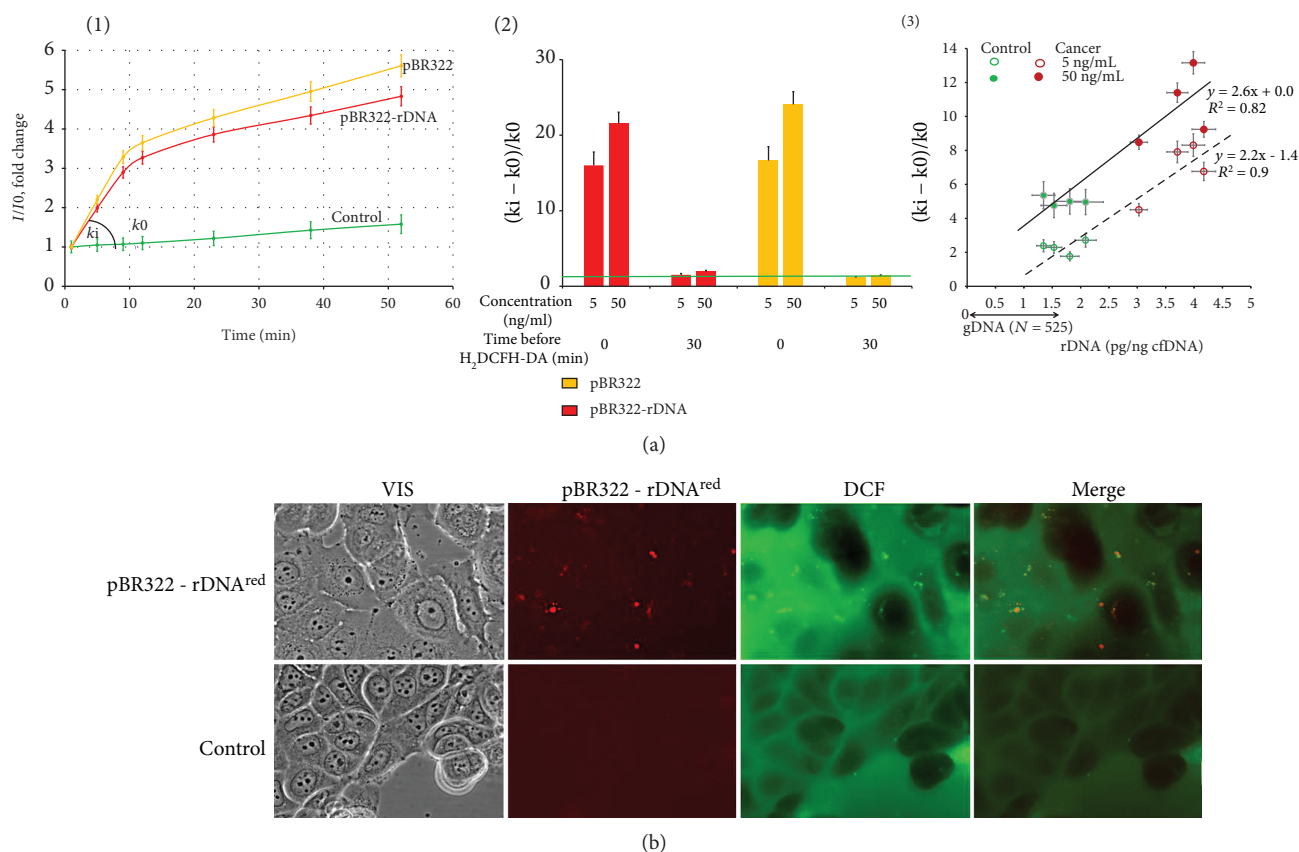
FIGURE 4: The exposure of MCF7 cells to GC-DNA leads to an increase in ROS production. (a) FL-plate reader. The cells were analyzed using total fluorescence assay in the 96-well plate format at λ_{ex} = 488 nm and λ_{em} = 528 nm (EnSpire equipment). (1)—an example of reaction rate constant determination for DCF formation. The cultivation medium was replaced with 5 μm H$_2$DCFH-DA in PBS solution, GC-DNA was immediately added to the solution (50 ng/mL), and a relative fluorescence intensity increase was detected at 37°C. I and I_0—sample's signal at time t and immediately after H$_2$DCFH-DA and GC-DNA addition, respectively. The line slope-reaction rate constant for DCF formation (k). ROS index $\Delta k/k_0 = (k_i - k_0)/k_0$. (2)—ROS index for pBR322-rDNA and pBR322. Time of cultivation with GC-DNA before adding H$_2$DCFH-DA and plasmid concentration is shown in the figure. (3)—dependence of ROS index on the rDNA content in cfDNA samples. The cfDNA samples (5 or 50 ng/mL) were added after H$_2$DCFH-DA addition. (b) FM-based evaluation of MCF7 cells sequentially treated with 5 μm H$_2$DCFH-DA and pBR322-rDNA^{red} (50 ng/mL) and incubated for 30 min (×40). Top photo: red granules—pBR322-rDNA localization in the cells; green granules—synthesis of DCF. Some of the signals are the same, indicating DCF synthesis at the site of DNA contact with the cell. In the presence of pBR322-rDNA, it increases the overall intensity of green fluorescence, compared with the control (bottom photo).

(Figure 2(c), (3)). After 1 h long incubation with cells, pEGFP-rDNA and pEGFP contained, respectively, 0.10 and 0.26 of 8-oxodG per one plasmid molecule. In other words, as a minimum, one 8-oxodG was contained in approximately one of four pEGFP-rDNA molecules and only one of 10 pEGFP molecules. One can suppose that rDNA contains still unidentified motifs, within which dG has even lower potential, than within the known GGG motif [21].

Thus, the compact single signals in the cellular cytoplasm (Figure 2(b)) and the considerable increase of 8-oxodG signal within the first hours of MCF7 incubation with GC-rDNA (Figure 2(a)) can be explained by stronger oxidation of GC-rDNA and, correspondingly, a higher rate of penetration of oxidized GC-rDNA fragments into the cells as compared to vectors.

Figure 6 shows the data on the localization of 8-oxodG in the cells exposed for 24 h to plasmids that carried and did not

carry rDNA insertions. The localization of 8-oxodG in the presence of vectors pBR322 and pEGFP did not differ from the control cells: 8-oxodG signals were located in the cytoplasm (in mitochondrial DNA). However, in case of pEGFP-rDNA and pBR322-rDNA probes, we observed 8-oxodG in the nucleus (within the nucleolus area, Figure 6(c)) of approximately half of the cells.

Thus, oxidized GC-rDNA fragments penetrate the cells and are localized in the structures of nucleolus organizer regions. The appearance of extra rDNA fragments—potential competitors for binding to nucleolar proteins in the nucleolus—can result in a decline in the performance of the ribosome biogenesis.

3.6. GC-DNA Modulates the Performance of Ribosome Biogenesis in MCF7.

For the quantification of intracellular 18S rRNA, the RT-qPCR technique was applied

(a)

(b)

(c)
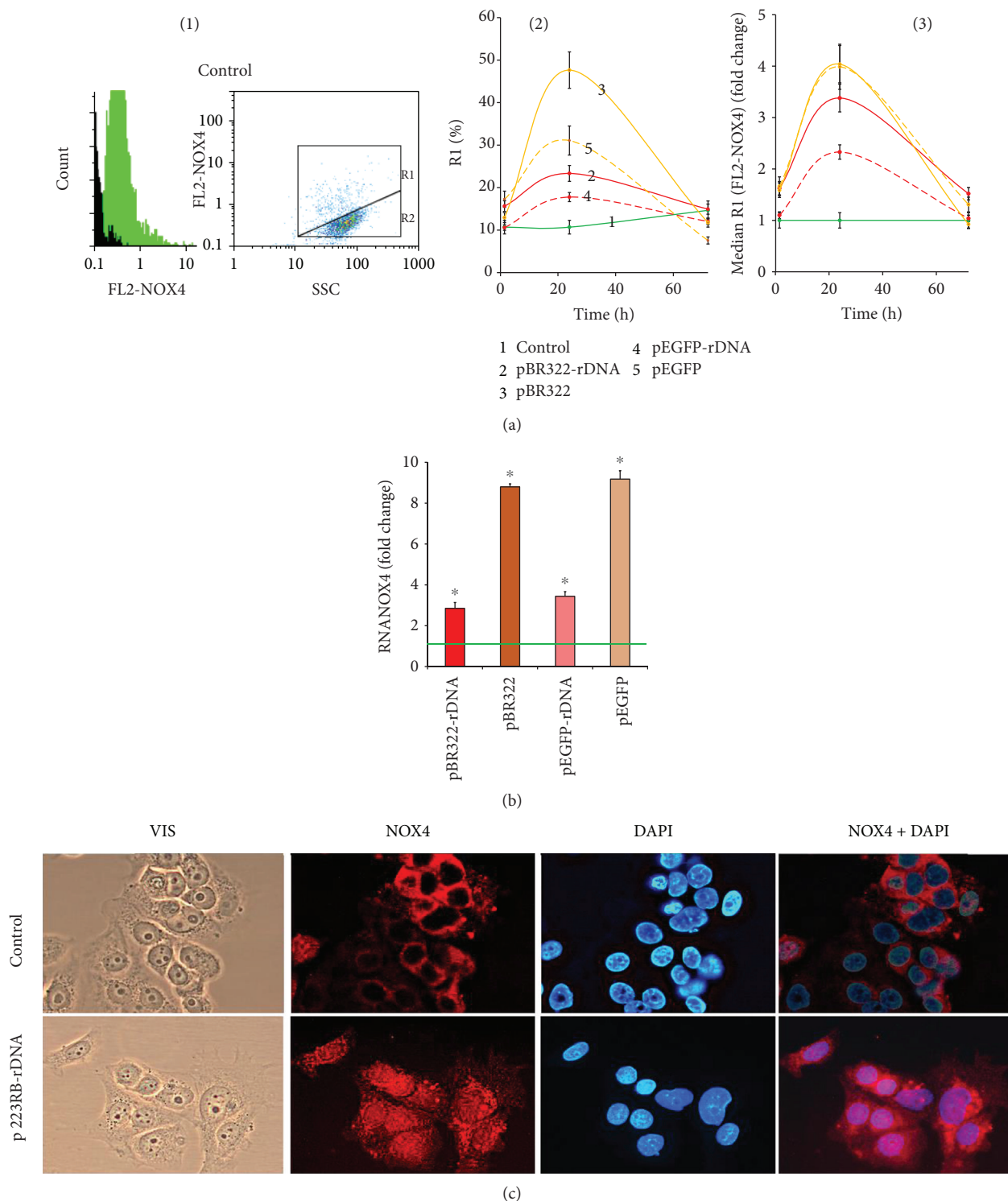
FIGURE 5: Expression of *NOX4* in MCF7. (a) FCA. (1)—the distribution of FL2-NOX4 fluorescence intensities; black: background fluorescence (PE-conjugated secondary antibodies). Cells plots: FL2 (NOX4-PE) versus SSC; R1 and R2: gated areas. (2)—relative fractions of NOX4-positive cells in R1 gate. (3)—median signal intensity of FL2-NOX4 in R1 gate. (b) RT-qPCR. The levels of NOX4-encoding RNAs in the cells exposed to GC-DNA for 24 h. The data are normalized by the content of RNA *NOX4* in the control. (c) FM-based evaluation of NOX4 (PE) in the cells treated with pEGFP-rDNA for 24 h (×40). $^*p < 0.05$ against control group of cells (nonparametric U test).

(a)

(b)

(c)   (d)
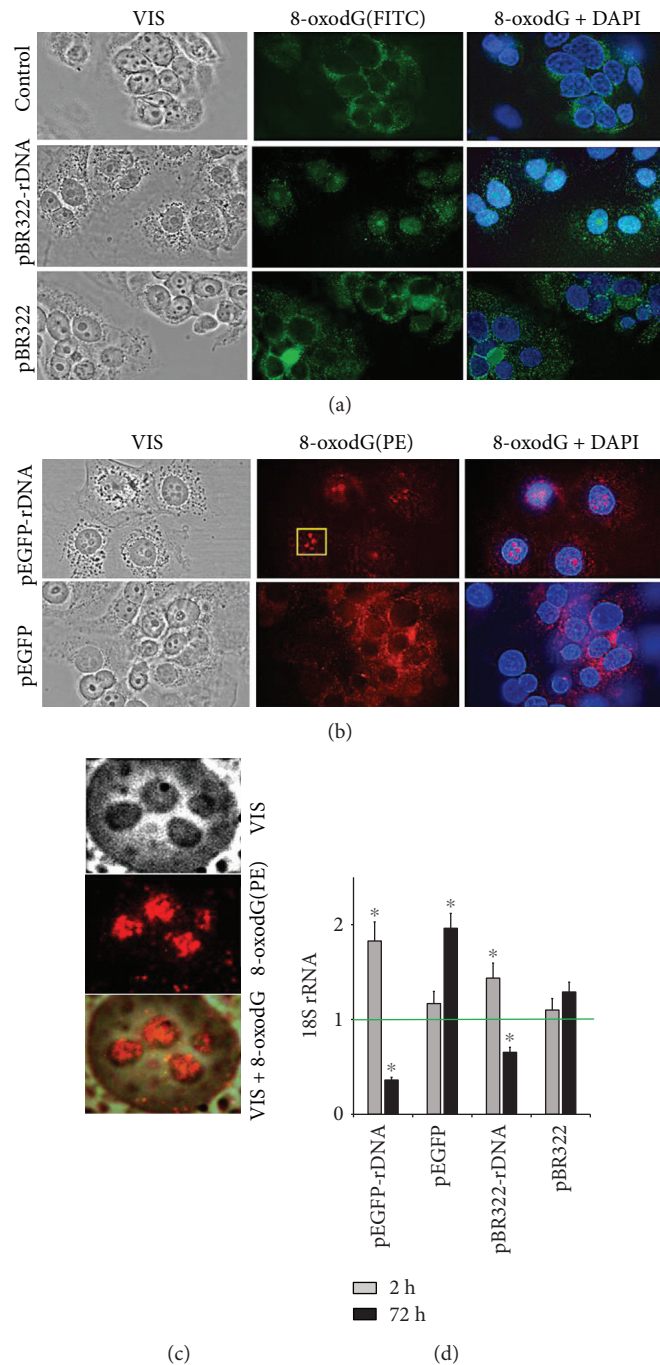
FIGURE 6: FM-based evaluation of 8-oxodG in the cells treated with pBR322 and pBR322-rDNA (a) and pEGFP and pEGFP-rDNA (b) for 24 h (×40). (c) For the analysis of the selected area of the photo, the image size was increased via computer processing. (d) RT-qPCR. The levels of 18S rRNA in the cells exposed to GC-DNA for 2 h and 24 h. The data are normalized by the content of 18Sr RNA in the control.

(Figure 6(d)). pEGFP-rDNA and pBR322-rDNA within the first hours after adding to the culture medium augmented the rRNA content in the cells by a factor of 1.5 to 2.0. pBR322 and pEGFP induced an increase of rRNA by 10%–15% (the difference from the controls is not significant, $p > 0.05$). After 72 h of cell exposure to pEGFP-rDNA and pBR322-rDNA, the rRNA content demonstrated a 2- or 3-fold decrease;

pBR322 and pEGFP did not decrease or even increase the rRNA content in the cells.

3.7. The Expression of EGFP Gene from pEGFP and pEGFP-rDNA. The constructions pEGFP and pEGFP-rDNA contain CMV-promotor and EGFP gene (Figure 1), rendering a possibility to study EGFP expression in the cells.

Successful expression requires DNA penetration into the cells. Therefore, we determined the rate of accumulation of pEGFP-rDNA and pEGFP plasmids inside the cells using qPCR (Figure 7(a)). Unlike the pEGFP vector, the pEGFP-rDNA accumulated inside the cells abundantly and could be detected even after 72 h.

After 24 h of cultivation in the presence of pEGFP-rDNA and pEGFP, the content of RNA *EGFP* increased (Figure 7(b)). The plasmid pEGFP-rDNA stimulated *EGFP* transcription in a greater degree, than pEGFP. We determined the amount of EGFP protein in the cells using flow cytometry (Figure 7(c)). For comparison, we performed pEGFP-rDNA plasmid transfection with the help of a Turbo Fect kit. We determined the ratio of highly fluorescent cells (gate R2, Figure 7(c), (1)) and mean fluorescence intensity of all the cells (gate R1). After 24 h, the cells cultivated in the presence of pEGFP-rDNA demonstrated a several times higher content of the EGFP protein, than in the presence of pEGFP vector, but lower, than in the case of transfection pEGFP-rDNA conducted with the aid of the Turbo Fect kit. In the presence of pEGFP-rDNA, the cell culture contained a larger fraction of cells with a relatively low amount of the EGFP protein. The data of fluorescence microscopy corroborated this conclusion (Figure 7(d)).

4. Discussion

4.1. GC-DNA Induces a Transient ROS Burst and Becomes Oxidized in MCF7. The model GC-DNA, regardless of the presence of rDNA insertions, induced a ROS burst in the first hour of cultivation with the cells (Figure 4, scheme in Figure 8). The blood plasma cfDNA samples stimulate ROS synthesis as well; moreover, the higher rDNA content in the cfDNA is, the higher the ROS level is (Figure 4(a), (3)). Extremely intense ROS synthesis was observed in the places of the contact of GC-DNA fragments with the cells (Figure 4(b)). NADPH-oxidase NOX4, which plays an essential role in the cancer cell physiology [26, 27], is likely a key participant in this process. NOX4 catalyzes hydrogen peroxide synthesis in the cells. The NOX family enzymes are localized on cell membranes and in other places [28]. In the presence of GC-DNA, *NOX4* gene expression noticeably elevated at the levels of both transcription (Figure 5(b)) and translation (Figures 5(a) and 5(c)).

Both vectors stimulate NOX4 expression stronger and longer than plasmids with an rDNA insertion. This fact can be explained by the slower process of oxidation of the vector compared to rDNA (Figure 2). A negative feedback can be assumed that already oxidized cfDNA fragments send back to the cell a signal for reducing the ROS synthesis with NADPH-oxidase NOX4 enzyme. It can be hypothesized that the main objective (biological sense) of the elevation of ROS content in the presence of cfDNA is the oxidation of the latter in order to impart to cfDNA some novel biologic properties.

In the literature, the matter of influence of the DNA sequence on its oxidability is poorly explored. There are reports that within GGG motifs, deoxyguanosine has a very low oxidation potential, the minimum of all the bases [21]. In case of pEGFP-rDNA plasmid, an insertion of rDNA does not change significantly the ratio of GGG motif (Figure 1(b), (3)). However, the oxidation level of pEGFP-rDNA is notably higher, than that of pEGFP (Figure 2(c)). One can suppose that rDNA carries motifs with even lower oxidation potential. Besides, the type of oxidative modification may be also of importance. In recent years, great attention is paid to the oxidative modification of cytosine [29]. However, this is still unclear, if the oxidation potential of cytosine changed when cytosine is included in the GC-rich DNA regions and if the oxidation of cytosine has an effect on the oxidation potential of guanosine within the same GC-pair. This interesting issue needs further investigation.

4.2. GC-rDNA Has the Increased Property to Penetrate and Be Expressed in the Cancer Cells. CfDNA oxidation is a key event in the further development of cfDNA biological effects. The cfDNA fragments that harbour oxidized bases [18] penetrate inside the cell. The mechanism of penetration of oxidized DNA fragments through the cell membrane remains elusive. An existence of DNA sensors in the cells, which recognize the oxidized cfDNA bases, is suggested [18, 30, 31].

A number of facts suggest an elevated accumulation of GC-rDNA in MCF7 compared to the vectors. Sites of localization of GC-rDNA in the cells are more abundant, than sites of localization of the vector (Figure 3). The cells contain much more oxidized fragments of GC-rDNA, than oxidized fragments of the vectors (Figure 2(a)). GC-rDNA content in MCF7 is several times higher, than the vector content (Figure 7(a)). One of the major causes of more active transfection of MCF7 with GC-rDNA compared to the vectors is the increased oxidability of rDNA fragments (Figure 2(c)).

Nonoxidized DNA fragments have virtually no ability to pass through the cell membrane from the culture medium and be expressed in the cells. For efficient transfection of DNA, various techniques are usually applied. The exaggerated rate of GC-rDNA penetration into the cells also suggests a higher level of expression of genes carried by GC-rDNA. Indeed, we revealed a high level of expression of *EGFP* gene within pEGFP-rDNA even compared to the use of the common transfection technique (Figures 7(b), 7(c), and 7(d)) that correlated with the elevated content of pEGFP-rDNA in the cells (Figure 7(a)). Obviously, effective expression requires, in addition to DNA penetration to the cell, the intact promoter and gene itself. These conditions seem to be met in case of pEGFP-rDNA. The elevated oxidability of inserted rDNA guarantees rapid penetration of the plasmid into the cell; meanwhile, the promoter and gene itself become oxidized in a less number of plasmid molecules.

The above-mentioned possibility in principle to express genes from external cfDNA fragments is of importance for the understanding of processes of cancer cell survival during therapy. Earlier, we and other authors quoted data related to the influence of cfDNA on tumor therapy. CfDNA favors cancer cell survival under the conditions of deleterious impacts, evoking an adaptive response [18, 32].

4.3. Potential Use of the Study Findings in Antitumor Therapy. Thus, the total body of facts reported here suggests that GC-DNA could become a tool in antitumor therapy.

(a)

(b)

(c)

(d)
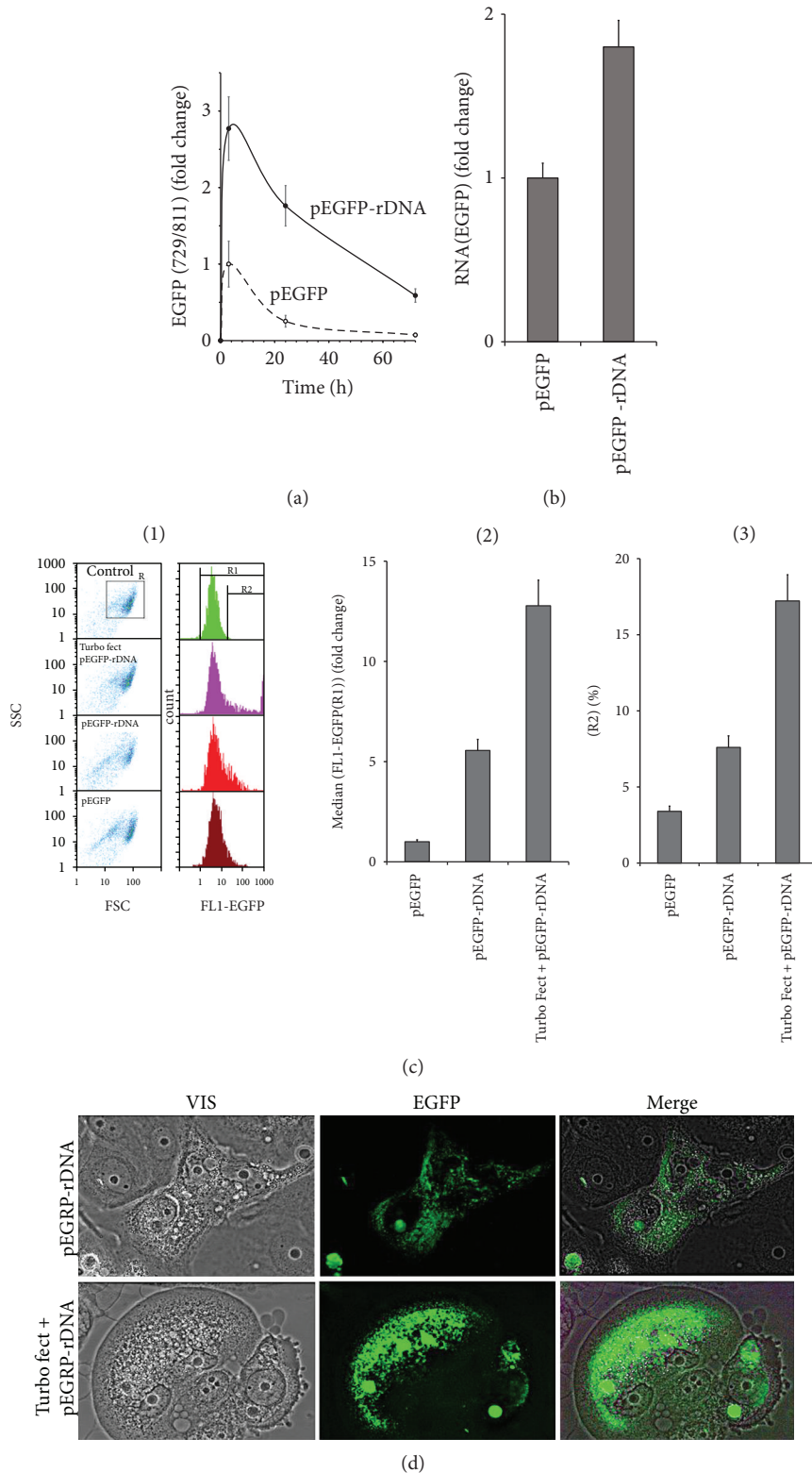
FIGURE 7: Expression of EGFP in MCF7 treated with pEGFP-rDNA or pEGFP for 24 h. (a) qPCR. Quantitation of pEGFP and pEGFP-rDNA in the cellular DNA after 3, 24, and 72 hours of incubation. pEGFP content (3 h) is taken as one unit. (b) RT-qPCR. The levels of EGFP-encoding RNAs in the cells exposed to pEGFP or pEGFP-rDNA. (c) FCA. (1)—nonfixed cell plots: SSC versus FCS; R—the analyzed cell subpopulation. Distribution of FL1-EGFP fluorescence intensities. R1- and R2-gated areas. (2)—median signal intensity of FL1-EGFP (gate R1). (3)—relative fractions of EGFP-positive cells (R2 gate). (d) FM-based evaluation of EGFP in the cells treated with pEGFP-rDNA or pEGFP-rDNA/Turbo Fect (×40).
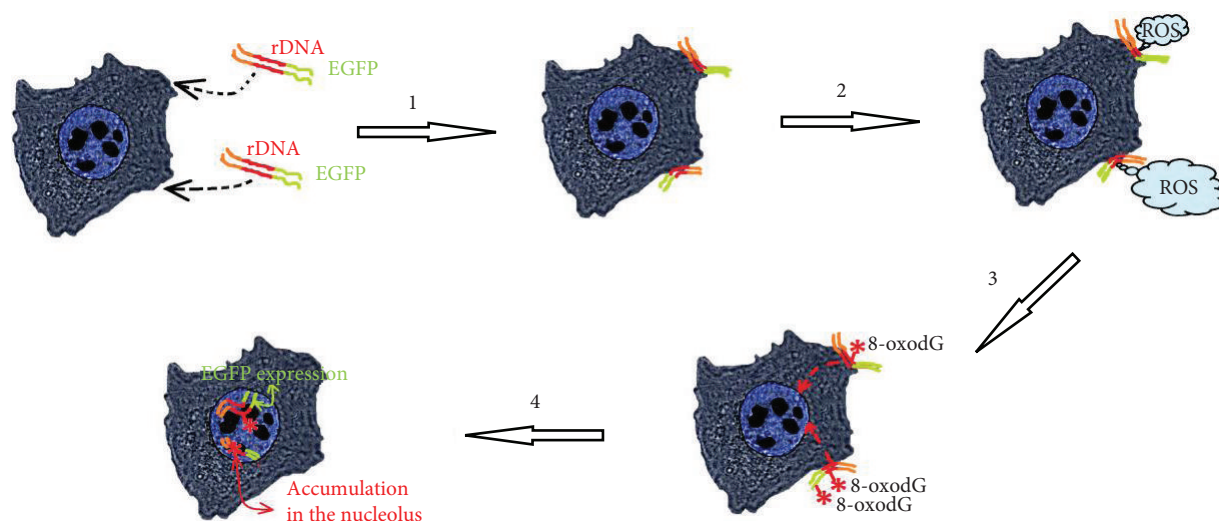
FIGURE 8: A summary of events that occur in MCF7 cells exposed to GC-DNA (pEGFP-rDNA as an example), which harbor genes that can be transcribed. (1)—GC-DNA approaches and interacts with the cell surface. (2)—GC-DNA stimulates a burst of ROS generation at the site of contact with the cell. ROS level is independent of the presence of easily oxidizable motifs. (3)—the easily oxidizable bases of rDNA (or other human easily oxidizable DNA sequences) are oxidized. GC-DNA without an easily oxidizable rDNA insert is oxidized to a lesser degree. (4)—oxidized GC-DNA is transfected into the cell nucleus and can be expressed (*EGFP* gene in pEGFP-rDNA molecules with intact promoter is expressed). GC-rDNA molecules are accumulated in the nucleolus.

Altering the properties of cfDNA could contribute to more effective tumor elimination and metastasis prevention. Several approaches can be suggested.

4.3.1. Modulation of the Transcriptional Activity of Tumor Genes. Data shown in Figure 6 suggest a possibility of penetration of oxidized cf-rDNA fragments into the cell nucleus. When they reached the nucleus, rDNA fragments interact with the nucleolar proteins, which possess binding selectivity with respect to rDNA motifs. Moreover, cf-rDNA fragments can compete with the nuclear ribosomal genes for binding to and exhaust the cell pool of factors necessary for the ribosome biogenesis. An indirect evidence in favor of this speculation is the decline of rRNA content in the cells cultivated in the presence of GC-rDNA, but not plasmid vectors (Figure 6(b)). Other motifs within GC-cfDNA could be expected to modulate expression of other genes by competing for binding to transcription factors in the respective nuclear areas.

Transfection effectiveness of plasmids carrying easily oxidizable regions and motifs, which can affect the expression of the tumor genes, can be increased via preliminary oxidation of the plasmids *in vitro*. The modern methods allow selective oxidation of DNA bases with different oxidation potentials [33]. Such conditions can be found, when easily oxidizable DNA fragments only are oxidized.

4.3.2. Blocking Adaptive cfDNA Action on Tumor Cells. Earlier cfDNA was shown to induce an adaptive response, which increases the survival rate of cancer cells, during chemotherapy [18, 32]. Oxidized DNA induces much higher adaptive response than unoxidized. The adaptive response is induced by a short-time elevation of ROS synthesis under the action of cfDNA [32]. The elevated ROS level induces a network of DNA damage response (DDR) mechanisms that counteract toxicity and safeguard genome integrity [34]. If the ROS burst is blocked, then the adaptive response does not develop [18]. In this context, the use of natural low-toxic antioxidants, which quench ROS and have anticancer properties, seems a perspective [35].

CfDNA can carry mutant genes from the tumor genome, which trigger cancerogenesis in healthy cells. Penetration of cfDNA into the healthy cells can result in metastases. Previously, we showed that GC-DNA considerably altered the functional activity of human stem cells [15]. Antioxidants, which prevent cfDNA oxidation, can thus preclude its penetration to the healthy cells.

Abbreviations

CfDNA: Cell-free DNA of MCF7 culture medium
GC-cfDNA: GC-rich fragments of cell-free DNA
GC-DNA: A generic term for all DNA probes used in this study
GC-rDNA: Plasmids carrying rDNA insertions.

Data Availability

The data used to support the findings of this study are available from the corresponding author upon request.

Conflicts of Interest

The authors declare that they have no conflict of interest.

Authors' Contributions

Nadezhda N. Mordkovich, Natalya A. Okorokova, Vladimir P. Veiko, Elena M. Malinovskaya, Elizaveta S. Ershova, Marina S. Konkova, Ekaterina A. Savinova, Maria A. Borzikova, Tatiana A. Muzaffarova, and Lev N. Porokhovnik participated in designing and carrying out most experimental procedures and helped in drafting the manuscript. Nataly N. Veiko and Kostyuk contributed to performing the statistical tests, interpretation of the results, and writing the first draft of the manuscript. Serguey I. Kutsev participated in the coordination and design of the study and helped in drafting the manuscript. Lev N. Porokhovnik translated the manuscript to English. All authors read and approved the final version of the manuscript.

Acknowledgments

References

[1] J. Aucamp, A. J. Bronkhorst, C. P. S. Badenhorst, and P. J. Pretorius, "A historical and evolutionary perspective on the biological significance of circulating DNA and extracellular vesicles," *Cellular and Molecular Life Sciences*, vol. 73, no. 23, pp. 4355–4381, 2016.

[2] N. Suzuki, A. Kamataki, J. Yamaki, and Y. Homma, "Characterization of circulating DNA in healthy human plasma," *Clinica Chimica Acta*, vol. 387, no. 1-2, pp. 55–58, 2008.

[3] E. S. Lander, L. M. Linton, B. Birren et al., "Initial sequencing and analysis of the human genome," *Nature*, vol. 409, no. 6822, pp. 860–921, 2001.

[4] F. E. Krapf, M. Herrmann, W. Leitmann, and J. R. Kalden, "Are retroviruses involved in the pathogenesis of SLE? Evidence demonstrated by molecular analysis of nucleic acids from SLE patients' plasma," *Rheumatology International*, vol. 9, no. 3–5, pp. 115–121, 1989.

[5] N. Alvarado-Vásquez, "Circulating cell-free mitochondrial DNA as the probable inducer of early endothelial dysfunction in the prediabetic patient," *Experimental Gerontology*, vol. 69, pp. 70–78, 2015.

[6] E. Tuboly, D. McIlroy, G. Briggs, N. Lott, and Z. J. Balogh, "Clinical implications and pathological associations of circulating mitochondrial DNA," *Frontiers in Bioscience*, vol. 22, pp. 1011–1022, 2017.

[7] N. N. Veiko, N. A. Bulycheva, O. A. Roginko et al., "Ribosomal repeat in cell free DNA as a marker for cell death," *Biochemistry*, vol. 2, no. 2, pp. 198–207, 2008.

[8] N. N. Veiko, N. O. Shubaeva, S. M. Ivanova, A. I. Speranskii, N. A. Lyapunova, and D. M. Spitkovskii, "Blood serum DNA in patients with rheumatoid arthritis is considerably enriched with fragments of ribosomal repeats containing immunostimulatory CpG-motifs," *Bulletin of Experimental Biology and Medicine*, vol. 142, no. 3, pp. 313–316, 2006.

[9] N. N. Veiko, I. L. Konorova, M. E. Neverova et al., "The effect of CpG-rich DNA fragments on the development of hypertension in spontaneously hypertensive rats (SHR)," *Biochemistry*, vol. 4, no. 3, pp. 269–278, 2010.

[10] I. B. Korzeneva, S. V. Kostuyk, E. S. Ershova et al., "Human circulating ribosomal DNA content significantly increases while circulating satellite III (1q12) content decreases under chronic occupational exposure to low-dose gamma- neutron and tritium beta-radiation," *Mutation Research/Fundamental and Molecular Mechanisms of Mutagenesis*, vol. 791-792, pp. 49–60, 2016.

[11] I. V. Chestkov, N. N. Veiko, L. S. Ershova et al., "The method for analysis of the copy number variations of GC-rich repeat of human genome in damaged DNA. Detection of increasing copy number of ribosomal genes in extracellular DNA circulating in blood plasma of smokers' humans," *Medical Genetics*, vol. 15, pp. 43–50, 2016.

[12] S. V. Kostyuk, A. Y. Alekseeva, M. S. Kon'kova et al., "Oxidized extracellular DNA suppresses nitric oxide production by endothelial NO synthase (eNOS) in human endothelial cells (HUVEC)," *Bulletin of Experimental Biology and Medicine*, vol. 157, no. 2, pp. 202–206, 2014.

[13] N. Bulicheva, O. Fidelina, N. Mkrtumova et al., "Effect of cell-free DNA of patients with cardiomyopathy and rDNA on the frequency of contraction of electrically paced neonatal rat ventricular myocytes in culture," *Annals of the New York Academy of Sciences*, vol. 1137, no. 1, pp. 273–277, 2008.

[14] L. V. Efremova, S. V. Kostyuk, L. G. Khaspekov, and N. N. Veiko, "Accumulating fragments of extracellular DNA (ecDNA) influence rat primary cerebellum granule cell culture," in *Circulating Nucleic Acids in Plasma and Serum*, P. B. Gahan, Ed., pp. 213–218, Springer, 2010.

[15] S. Kostyuk, T. Smirnova, L. Kameneva et al., "GC-rich extracellular DNA induces oxidative stress, double-strand DNA breaks, and DNA damage response in human adipose-derived mesenchymal stem cells," *Oxidative Medicine and Cellular Longevity*, vol. 2015, Article ID 782123, 15 pages, 2015.

[16] A. I. Speranskii, S. V. Kostyuk, E. A. Kalashnikova, and N. N. Veiko, "Erichment of extracellular DNA from the cultivation medium of human peripheral blood mononuclears with genomic CpG rich fragments results in increased cell production of IL6 and TNFα via activation of the NF-κB signaling pathway," *Biochemistry*, vol. 9, no. 2, pp. 174–184, 2015.

[17] R. Aarthy, S. Mani, S. Velusami, S. Sundarsingh, and T. Rajkumar, "Role of circulating cell-free DNA in cancers," *Molecular Diagnosis & Therapy*, vol. 19, no. 6, pp. 339–350, 2015.

[18] S. V. Kostyuk, M. S. Konkova, E. S. Ershova et al., "An exposure to the oxidized DNA enhances both instability of genome and survival in cancer cells," *PLoS One*, vol. 8, no. 10, article e77469, 2013.

[19] R. Ma, J. Zhao, H. C. Du, S. Tian, and L. W. Li, "Removing endotoxin from plasmid samples by Triton X-114 isothermal extraction," *Analytical Biochemistry*, vol. 424, no. 2, pp. 124–126, 2012.

[20] E. S. Ershova, E. M. Jestkova, I. V. Chestkov et al., "Quantification of cell-free DNA in blood plasma and DNA damage degree in lymphocytes to evaluate dysregulation of apoptosis in schizophrenia patients," *Journal of Psychiatric Research*, vol. 87, pp. 15–22, 2017.

[21] C. von Sonntag, *Free-Radical-Induced DNA Damage and Its Repair. A Chemical Perspective*, Springer, 2006.

[22] S. V. Kostyuk, M. A. Kvasha, D. A. Khrabrova et al., "Symmetric dimeric bisbenzimidazoles DBP(n) reduce methylation of *RARB* and *PTEN* while significantly increase methylation of

rRNA genes in MCF-7 cancer cells," *PLoS One*, vol. 13, no. 1, article e0189826, 2018.

[23] C. P. LeBel, H. Ischiropoulos, and S. C. Bondy, "Evaluation of the probe 2′,7′-dichlorofluorescin as an indicator of reactive oxygen species formation and oxidative stress," *Chemical Research in Toxicology*, vol. 5, no. 2, pp. 227–231, 1992.

[24] E. Y. Rykova, E. S. Morozkin, A. A. Ponomaryova et al., "Cell-free and cell-bound circulating nucleic acid complexes: mechanisms of generation, concentration and content," *Expert Opinion on Biological Therapy*, vol. 12, Supplement 1, pp. S141–S153, 2012.

[25] O. E. Bryzgunova, S. N. Tamkovich, A. V. Cherepanova et al., "Redistribution of free- and cell-surface-bound DNA in blood of benign and malignant prostate tumor patients," *Acta Naturae*, vol. 7, no. 2, pp. 115–118, 2015.

[26] K. Shanmugasundaram, B. K. Nayak, W. E. Friedrichs, D. Kaushik, R. Rodriguez, and K. Block, "NOX4 functions as a mitochondrial energetic sensor coupling cancer metabolic reprogramming to drug resistance," *Nature Communications*, vol. 8, no. 1, p. 997, 2017.

[27] N. Tobar, J. Guerrero, P. C. Smith, and J. Martínez, "NOX4-dependent ROS production by stromal mammary cells modulates epithelial MCF-7 cell migration," *British Journal of Cancer*, vol. 103, no. 7, pp. 1040–1047, 2010.

[28] L. Zhang, M. V. C. Nguyen, B. Lardy et al., "New insight into the Nox4 subcellular localization in HEK293 cells: first monoclonal antibodies against Nox4," *Biochimie*, vol. 93, no. 3, pp. 457–468, 2011.

[29] T. Äijö, R. Bonneau, and H. Lähdesmäki, "Generative models for quantification of DNA modifications," *Methods in Molecular Biology*, vol. 1807, pp. 37–50, 2018.

[30] A. V. Ermakov, M. S. Konkova, S. V. Kostyuk, V. L. Izevskaya, A. Baranova, and N. N. Veiko, "Oxidized extracellular DNA as a stress signal in human cells," *Oxidative Medicine and Cellular Longevity*, vol. 2013, Article ID 649747, 12 pages, 2013.

[31] K. Glebova, N. Veiko, S. Kostyuk, V. Izhevskaya, and A. Baranova, "Oxidized extracellular DNA as a stress signal that may modify response to anticancer therapy," *Cancer Letters*, vol. 356, no. 1, pp. 22–33, 2015.

[32] R. Anunobi, B. A. Boone, N. Cheh et al., "Extracellular DNA promotes colorectal tumor cell survival after cytotoxic chemotherapy," *The Journal of Surgical Research*, vol. 226, no. 18, pp. 181–191, 2018.

[33] Z. Chang, Y. Yang, J. He, and J. F. Rusling, "Gold nanocatalysts supported on carbon for electrocatalytic oxidation of organic molecules including guanines in DNA," *Dalton Transactions*, vol. 47, no. 40, pp. 14139–14152, 2018.

[34] L. H. F. Mullenders, "Solar UV damage to cellular DNA: from mechanisms to biological effects," *Photochemical & Photobiological Sciences*, vol. 17, no. 12, pp. 1842–1852, 2018.

[35] A. M. Mahgoub, M. G. Mahmoud, M. S. Selim, and M. E. EL Awady, "Exopolysaccharide from marine Bacillus velezensis MHM3 induces apoptosis of human breast cancer MCF-7 cells through a mitochondrial pathway," *Asian Pacific Journal of Cancer Prevention*, vol. 19, no. 7, pp. 1957–1963, 2018.

Research Article

Cold Physical Plasma Modulates p53 and Mitogen-Activated Protein Kinase Signaling in Keratinocytes

Anke Schmidt,[1] **Sander Bekeschus** ⓘ**,**[1,2] **Katja Jarick,**[1,2] **Sybille Hasse,**[1]
Thomas von Woedtke,[1,3] **and Kristian Wende** ⓘ[1,2]

[1]*Leibniz-Institute for Plasma Science and Technology e. V., Felix-Hausdorff-Str. 2, 17489 Greifswald, Germany*
[2]*ZIK Plasmatis at Leibniz-Institute for Plasma Science and Technology e. V, Felix-Hausdorff-Str. 2, 17489 Greifswald, Germany*
[3]*Department of Hygiene and Environmental Medicine, University Medicine Greifswald, 17475 Greifswald, Germany*

Correspondence should be addressed to Kristian Wende; kristian.wende@inp-greifswald.de

Small reactive oxygen and nitrogen species (ROS/RNS) driven signaling plays a significant role in wound healing processes by controlling cell functionality and wound phase transitions. The application of cold atmospheric pressure plasma (CAP), a partially ionized gas expelling a variety of ROS and RNS, was shown to be effective in chronic wound management and contrastingly also in malignant diseases. The underlying molecular mechanisms are not well understood but redox signaling events are involved. As a central player, the cellular tumor antigen p53 governs regulatory networks controlling proliferation, death, or metabolism, all of which are grossly modulated by anti- and prooxidant signals. Using a human skin cell model, a transient phosphorylation and nuclear translocation of p53, preceded by the phosphorylation of upstream serine- (ATM) and serine/threonine-protein kinase (ATR), was detected after CAP treatment. Results indicate that ATM acts as a direct redox sensor without relevant contribution of phosphorylation of the histone A2X, a marker of DNA damage. Downstream events are the activation of checkpoint kinases Chk1/2 and several mitogen-activated (MAP) kinases. Subsequently, the expression of MAP kinase signaling effectors (e.g., heat shock protein Hsp27), epithelium derived growth factors, and cytokines (Interleukins 6 + 8) was increased. A number of p53 downstream effectors pointed at a decrease of cell growth due to DNA repair processes. In summary, CAP treatment led to an activation of cell repair and defense mechanisms including a modulation of paracrine inflammatory signals emphasizing the role of prooxidant species in CAP-related cell signaling.

1. Introduction

Cold physical plasma (CAP) is an emerging biomedical technique and found to interfere with processes controlled by redox signaling *in vivo*, such as wound healing, immune modulation, and cancer [1–6]. Different source geometries and discharge types (barrier discharges and plasma jets) have been developed with some being accredited medical products [7–10]. In principle, energy is introduced into a noble gas or a molecular gas resulting in the ionization of a fraction of it. CAP expels various forms of energy: light (UV, visible, and IR), electromagnetic fields, and small chemical entities like electrons, ions, and molecules. To the current knowledge, the short- and long-lived reactive oxygen and nitrogen species (e.g., $NO\bullet$, $\bullet O_2^-$, N_xO_y, $HO\bullet$, $ONOO^-$, and H_2O_2)

are the major contributors to the described effects both *in vitro* and *in vivo*. Their occurrence can be controlled by plasma source design and discharge parameter engineering, especially the composition of the working gas. In vivo, stimulatory effects in chronic or acute wound healing (animal models) or in humans (clinical trials) were reported [5, 11–14]. The biochemical background of these observations is so far not fully investigated. In vitro, an impact on cell viability and cell cycle progression is frequently observed, along with changes in cell metabolism, redox signaling, and protein secretion [15–20]. Increasing knowledge is gathered regarding cellular redox signaling pathways [21, 22]. The cellular tumor antigen p53 is basically a transcription factor with a major role in DNA damage sensing and control, hypoxia, or nutrient fluctuation [23]. Further roles have been

reported, e.g., interaction with apoptotic effectors in the cytosol [24, 25]. A wide range of posttranslational modifications adjusts p53's transcriptional and transcription-independent functions. Accordingly, p53 regulation is fundamentally involved in processes requiring cell repair, cell proliferation, or cell migration, such as acute and chronic wounds [26–28].

A complex, not fully understood relationship evolved around p53 and redox signal transduction checking free reactive oxygen or nitrogen species (ROS/RNS) levels and controlling cell fate [29]. The activation of p53 sparks both pro- and antioxidant downstream effects. Prooxidant measures promote autophagy and apoptosis, while antioxidant effects comprise increased protein expression involved in NADPH and glutathione metabolism, mitochondrial membrane stabilization, and modulation of nuclear factor-(erythroid-derived 2-) like 2 (NFE2L2 or NRF2) related signaling [30–32]. This major antioxidant pathway is protective against oxidative damages and is activated by natural and xenobiotic triggers, e.g., photodynamic therapy, small molecules like sulforaphane, or cold atmospheric plasma (CAP) as source for ROS/RNS [16, 33, 34].

Published data on CAP effects in cells or tissues suggest a role for p53, its downstream targets, and connected pathways such as the mitogen-activated protein (MAP) kinases in governing the cellular response towards CAP-derived ROS/RNS [35]. Potentially, via oxidative signals, an activation of major MAP kinases [36] precedes a kinase-driven posttranslational modification of p53 activity [37–39] and establishes a crosstalk between the MAP kinase and the p53 signaling pathways [40–42], even influencing cell migration [43]. To test this hypothesis, a well-described human epithelial model cell line (HaCaT) was used to analyze p53 phosphorylation, activation of up- and downstream targets of the p53, and the expression of related genes or proteins in response to CAP.

A strong activation of the MAPK – p53 axis was found after CAP, emphasizing that plasma-derived ROS/RNS have a significant impact on cell fate and performance. The involvement of p53 phosphorylation indicates a substantial impact on cellular processes necessary to adapt to CAP treatment. An activation of cell protective processes accompanied by an increased expression of growth factors and cytokines relevant in wound underlines the use of CAP in wound management and other redox-signaling related conditions.

2. Materials and Methods

2.1. Cell Culture Cells and Cold Plasma Treatment. HaCaT keratinocytes were cultivated in RPMI 1640 cell culture medium containing 8% fetal bovine serum (Sigma-Aldrich, Germany), 2 mM glutamine, 0.1 mg/ml streptomycin, and 100 U/ml penicillin (PAN Biotech, Germany) at 37°C, 95% relative humidity, and 5% CO_2 [16]. Twenty-four hours prior to experiment, 1×10^6 cells were seeded in 60 mm dishes (Sarstedt, Germany). As cold physical plasma source, the kINPen 09 (neoplas tools, Germany) was utilized. This plasma jet consists of a central pin-type electrode that ignited a plasma by applying a voltage of 2–6 kV at a frequency of around 1 MHz. Argon (Air Liquide, France) was used as feed gas (3 standard liters per minute). For all experiments, an

indirect treatment regimen was chosen to assure homogeneity of the treatment and it was achieved by exposing 5 ml of RPMI w/ all supplements to the plasma effluent at a distance of 9 mm using an automated xyz-table. The treated liquid was transferred immediately to the prepared cells.

2.2. Cellular Viability, ROS Levels, and Apoptosis. Changes of intracellular redox levels were determined using CM-H_2DCF-DA (Life Technologies, CA, USA). Cells were stained with 1μM of dye for 20 min, prior to plasma-treated medium was added, and evaluated 5 min thereafter by fluorescence microscopy. Cell viability was assessed using the CellTox™ Green Cytotoxicity Assay (Promega, Germany). Briefly, 15,000 cells were seeded in 96 well plates 24 h prior to experiment. 24 h after indirect treatment, the dye was added. After 15 min, the fluorescence intensity was measured at λ_{ex} 490 nm and λ_{em} 525 nm using a microplate reader (Infinite 200, Tecan, Switzerland). To determine late apoptosis, a *Gallios* flow cytometer and *Kaluza* software (Beckman Coulter, CA, USA) were applied 18 hours after indirect treatment using Green Caspase-3 Kit (Promokine, Germany) according to the manufacturer's protocol.

2.3. Immunofluorescence Microscopy. HaCaT cells were grown on glass coverslips for 24 h, and plasma treated as indicated. After appropriate time points, cells were fixated with 4% (w/v) paraformaldehyde for 20 min, permeabilized with PBS/0.1% Triton X-100 for 20 min, and treated with 3% bovine serum albumin (BSA) in PBS. Slides were washed twice with 1% BSA in PBS and incubated at 4°C overnight with p53 antibody (NEB, Germany, 1 : 1.600). Afterwards, cells were washed twice with PBS and incubated with secondary antibody Alexa Fluor 488-conjugated goat anti-rabbit (Life Technology, Germany, 1 : 700) for 1 h. Coverslips were washed again with PBS and mounted using VECTA-SHIELD® with DAPI (Vector Labs, CA, USA). Samples were observed using an Axio Observer Z1 (Zeiss, Germany).

2.4. Gene Expression Analysis by Quantitative Real-Time PCR. RNA was isolated using RNA Mini Kit (Bio&SELL, Germany), and total mRNA was reversely transcribed using Transcriptor First Strand Synthesis Kit (Roche, Germany). Primer specificity was confirmed by separating PCR amplification products in an agarose gel. Quantitative real-time PCR was performed using the Fast Sybr Kit (Kapa Biosystems, MA, U.S.A.) and a LightCycler 480 (Roche, Germany). Gene specific primers for BAX, BBC3, GADD45, and CDKN1A were used [44–47] at a concentration of 200 nM (Suppl. Table 1). The samples were preincubated at 95°C for 3 min, followed by 40 amplification cycles of 10 s denaturing at 95°C, 30 s annealing at 55°C, and amplification for 1 s at 72°C. Finally, a melting curve was performed with five acquisitions/°C from 65°C to 97°C. All samples were performed in triplicates. To calculate relative gene expression, the data of the threshold cycles was analyzed using the $\Delta\Delta C_T$ method.

2.5. Western Blot and ELISA. Cells were plasma-treated, rinsed with ice-cold PBS, and then lysed in ice-cold RIPA lysis buffer containing protease and phosphatase
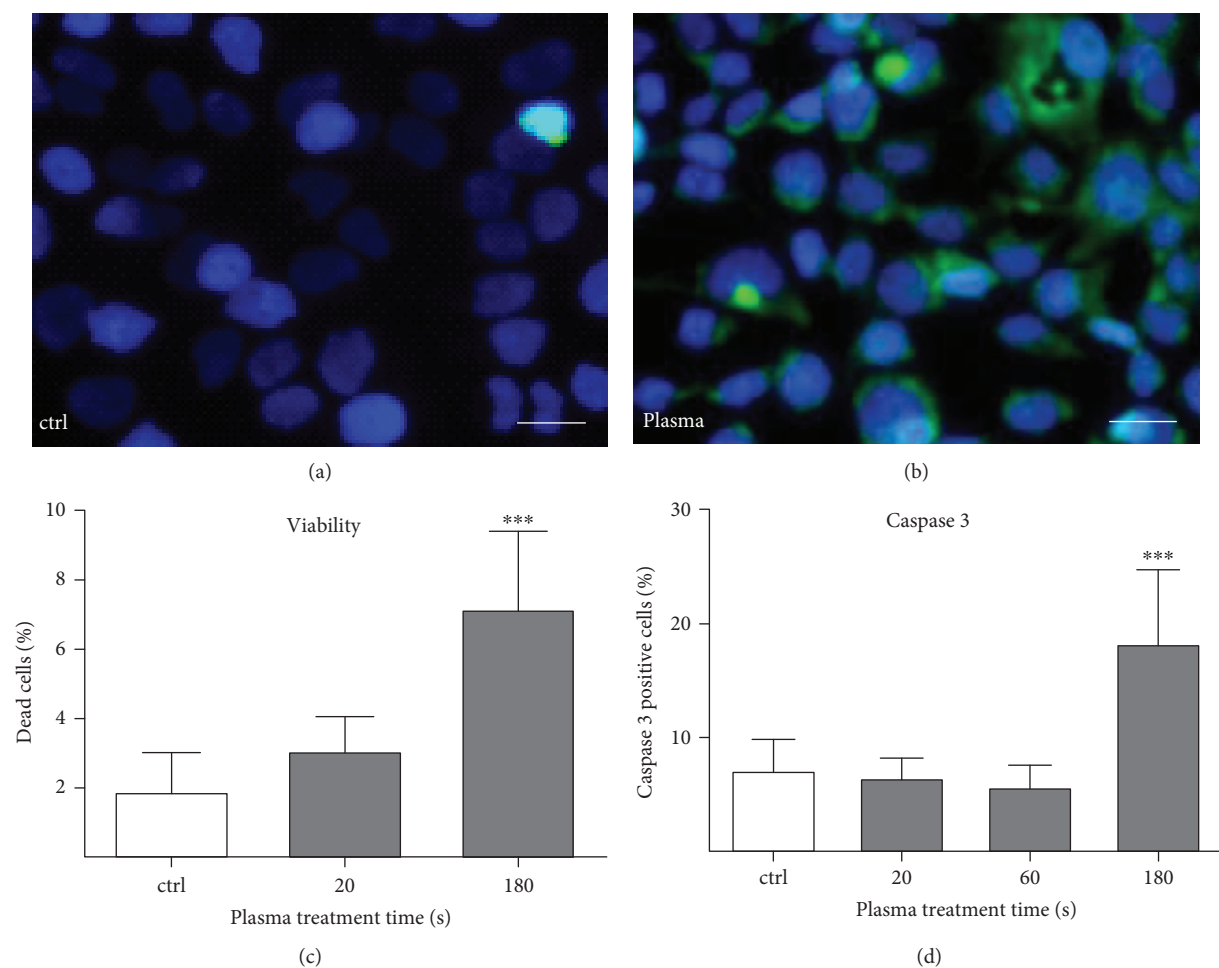
FIGURE 1: Cold plasma oxidized keratinocytes and altered cell viability. The intracellular ROS level was detected by CM-H$_2$DCFDA fluorescence staining for control (a) and indirectly plasma-treated HaCaT keratinocytes (using kINPen 09 plasma jet) (b). For assessment of cell viability, the CellTox™ Green Dye was used and showed a 1.5 to 3.5-fold increase of death cells after 20 s or 180 s of plasma treatment, respectively (c). To quantitate apoptosis, plasma-treated cells were stained with active caspase 3-detecting reagents and examined by flow cytometry. A significant 2.1-fold of caspase 3-positive cells was detected after 180 s of plasma treatment (d). Data are presented as mean + S.E. of four independent experiments; statistical comparison was done using one-way ANOVA (***$p < 0.001$). Scale bar 50 μm.

inhibitors (cOmplete/PhosSTOP; Roche, Germany) and 2 mM phenylmethanesulfonylfluoride (PMSF; Carl Roth, Germany). The protein concentrations were equalized and samples were heated to 95°C for 5 min in Laemmli buffer (0.25 mM Tris, 2% SDS, 10% glycerol, 2% β-mercaptoethanol, 0.001% bromophenol blue). Proteins were separated on a 10% SDS-PAGE Gel (Anamed GmbH, Germany) and blotted onto a Roti®PVDF membrane (Carl Roth, Germany). After blocking in TBS-T (0.05% nonfat milk powder in TRIS-buffered saline pH 7.6/0.05% Tween 20, TBS-T), blots were incubated with Erk1/2 (#9102), Mek1/2 (#9126), Sapk/Jnk (#9258), p38 (#9212), p53 (#2527) as well as phospho-specific antibodies for p-ATM (S1981, #5883), p-ATR (S428, #2853), p-Chk1 (S296, #2349), p-Chk2 (T68, #2661), p-Erk1/2 (T202/Y204, #4370), p-p38 (T180/Y182, #9216), p-Mek1/2 (S217/S221, #9154), p-Sapk/Jnk (T183/Y185, #4668), p-HSP27 (S78,# 2405), p-p53 (S15, # 9286), and p-p53 (S37, #2989), all 1 : 1000 in TBS-T at 4°C overnight (Cell Signaling Technologies, Germany). Then, procedure was preceded by 1 h incubation with secondary antibody (Jackson Europe, UK) 1 : 10,000 in TBS-T and followed by incubation with ECL reagent. Chemiluminescence was detected by ImageQuant LAS 4000 and analyzed by ImageQuantTL (GE Healthcare, UK). Phosphorylated protein levels of p53-dependent kinases were normalized to β-actin (housekeeping). Analyses of secreted proteins were performed using the enzyme-linked immunosorbent assay (ELISA). Human IL-6, IL-8, and GM-CSF were detected using ELISA Max™ kits (BioLegend, UK) and human VEGF-A using ELISA (Thermo Scientific, Germany). Procedures were performed according to the manufacturers protocols.

2.6. Statistical Analysis. At least three independent experiments were performed in all assays. Bar graphs represent arithmetic mean + standard deviation (S.D.). Statistical comparison between experimental groups was done using

(a)

(b)

(c)

(d)
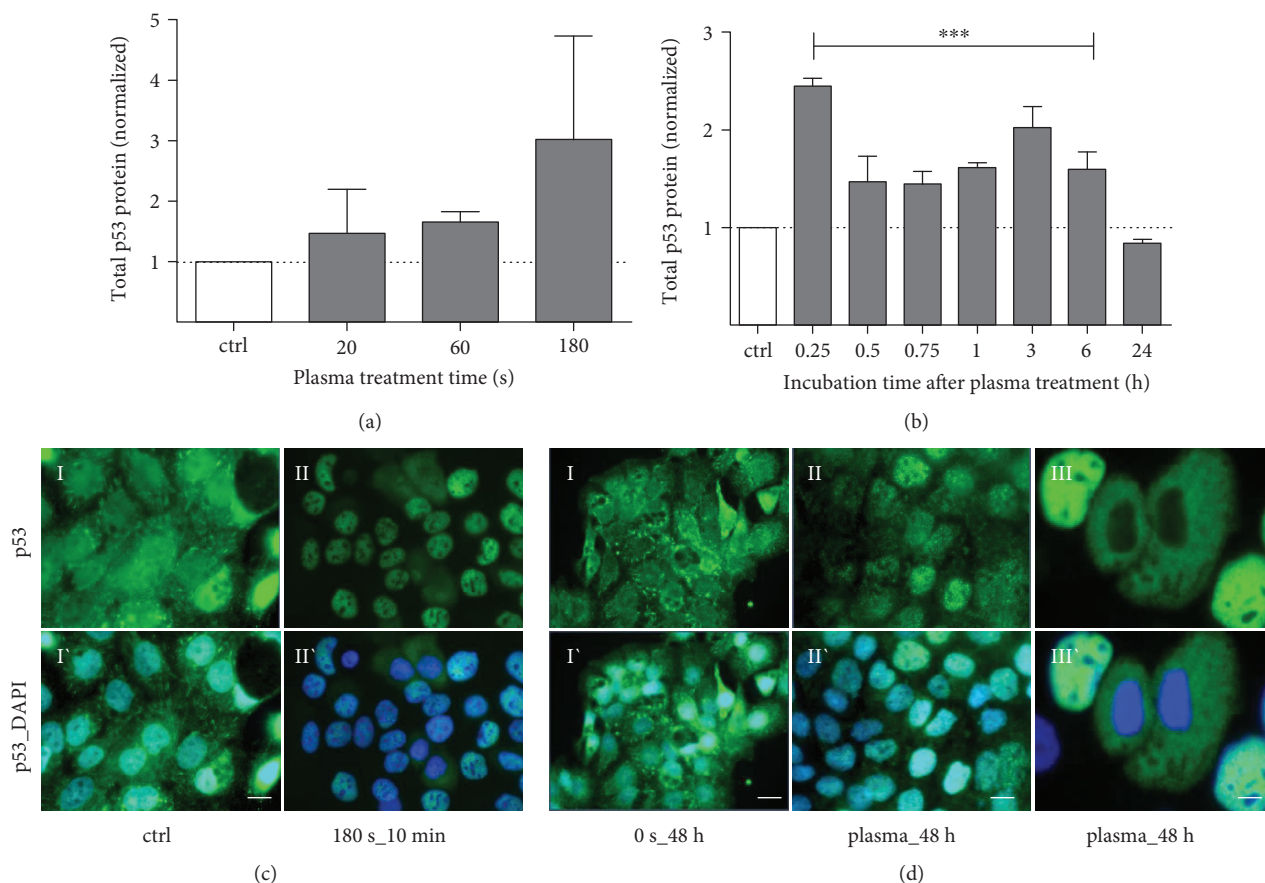
Figure 2: Cold plasma transiently enhanced total p53 protein expression and induced nuclear translocation. Total expression of p53 showed a treatment time-depending increase (a, after 3 h), in particular, 3 h after plasma exposure (b, 180 s). Immune fluorescent microscopy of HaCaT cells revealed a strong translocation of p53 (green) from cytoplasm into the nucleus in dependence of treatment and incubation time (CII) in contrast to control (CI). After 30 min, p53 was exclusively detected in nuclei. Forty-eight hours after plasma exposure, p53 was redistributed in the cytoplasm of HaCaT cells. Data are presented as mean + S.D. of two analyses (a, b) or as one representative (c, d). Statistical analysis was done using one-way ANOVA with *Dunnett* corrections for multiple comparisons to untreated, normalized control (***$p < 0.001$). Scale bar 50 μm (CII, DI-II) and 20 μm (CI, DIII).

one-way analysis of variances followed by *Dunnett* post-testing comparing treated samples to untreated control samples. When investigations were carried out at different time points, statistical analysis was done for each time point independently. A p value of ≤0.05 was considered statistically significant.

3. Results

3.1. Intracellular ROS, Cell Viability, and Apoptosis. Microscopic evaluation of the HaCaT cells after treatment showed an increased fluorescence signal of the redox-sensitive dye CM-H$_2$DCF (Figures 1(a) and 1(b)`). This increased ROS prevalence could also be detected in a treatment time-dependent manner by flow cytometry using the same dye (data not shown). After 24 h, a significant 3.5-fold increase in dead cell numbers was detected for high-treatment intensity 180 s (Figure 1(c)). In parallel, the late apoptosis marker caspase 3 activity increased significantly to 18% (Figure 1(d),

basal level ≈ 6–8%). Early apoptotic signs like phosphatidyl-serine externalization remain scarce (data not shown).

3.2. Plasma-Induced Accumulation and Nuclear Translocation of the Tumor Suppressor p53. Three hours after plasma, a treatment time-depending increase of total p53 protein expression was observed (Figure 2(a)). On a timeline, p53 protein expression levels fluctuated with peaks 15 min (2.3-fold) and 3 h (1.9-fold) after treatment and returned to the baseline level within 24 h (Figure 2(b), 180 s of treatment). Immunofluorescence staining with an anti-p53 antibody showed the subcellular localization of endogenous total p53 after plasma exposure (Figure 2(c)). While control cells showed a predominant localization of p53 in the cytosol (Figure 2(c), I), an immediate and rapid cytoplasmic-nuclear trafficking was observed already 10 min after treatment (Figure 2(c), II). The nuclear localization of p53 was observed up to 24 h after treatment, changing to a predominantly cytoplasmic distribution about 48 h after treatment (Figure 2(d)).

(a)

(b)

(c)

(d)
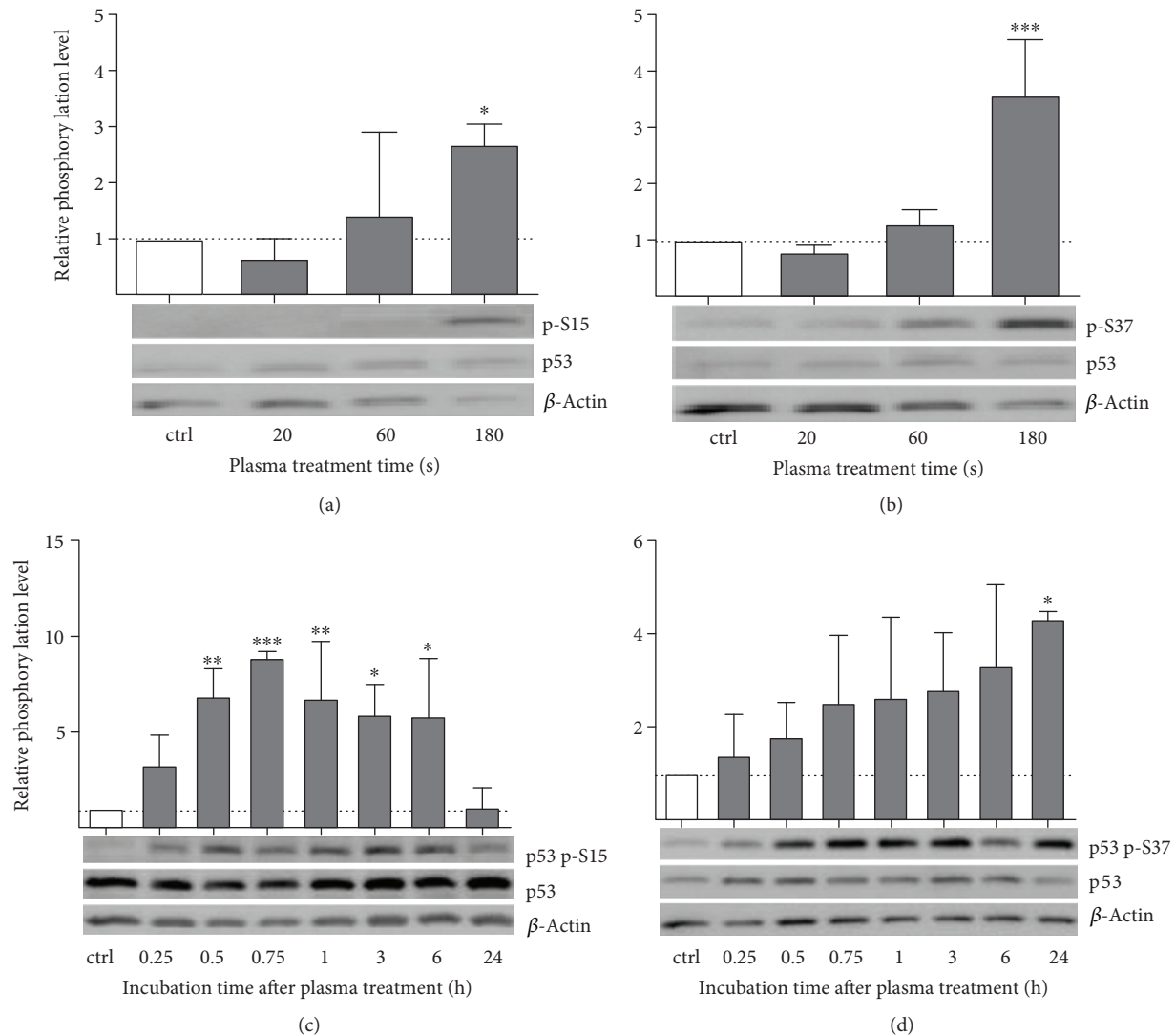
FIGURE 3: Cold plasma alters phosphorylation level of p53 in a treatment and incubation time-dependent manner. The upper graphs showed the treatment time-dependent activation of p53. Displayed are relative p53 phosphorylation levels of residues Ser15 (a) and Ser37 (b) normalized to total p53 and β-actin expression. Bottom graphs displayed the time courses of relative phosphorylation after longest plasma treatment of relative p53-Ser15 (c) and Ser37 phosphorylation (d). Untreated samples were included as negative control (ctrl). Data are presented as mean + S.D. of two independent experiments. The x-axis represents treatment time (a, b) or incubation after plasma treatment (c, d). Statistical comparison was done using one-way ANOVA with *Dunnett* corrections for multiple comparison to untreated control, normalized control ($^*p < 0.05$, $^{**}p < 0.01$, $^{***}p < 0.001$).

3.3. Plasma Treatment Contributes to p53 Phosphorylation on Serine 15 and 37.

The nuclear localization of p53 is caused by activation of p53 through phosphorylation of serine 15 (Ser15) and serine 37 (Ser37). The phosphorylation levels one hour after plasma treatment showed a clear dependence on treatment intensity. Phosphorylation on Ser15 was increased after 60 s and more clearly after 180 s (Figure 3(a)). In comparison, phosphorylation level of p53 on Ser37 was only slightly increased after 60 s but raised fourfold after 180 s of treatment (Figure 3(b)). On a time axis, a rapid increase in Ser15 phosphorylation, reaching a maximum eightfold increase after 45 min, was observed. This level remained until 6 h after treatment and returned to the baseline level after 24 h (Figure 3(c)). For Ser37 phosphorylation, a slow and constant increase

was observed which lasted for more than 24 h (Figure 3(d)). The positive control H_2O_2 (100 μM) showed an intensely increased Ser37 phosphorylation, whereas Ser15 phosphorylation level was not affected (data not shown).

3.4. Phosphorylation of p53 Upstream Kinases after Plasma Treatment.

Several sensors and upstream activators of p53 were analyzed regarding their plasma-induced activation pattern. A treatment time-dependent induction of ATR and ATM phosphorylation was observed one hour after plasma treatment (Figures 4(a) and 4(b)). The phosphorylation of ATR/ATM was transient and returned to baseline 24 h after treatment. The control (100 μM H_2O_2) led to a very slight rise in p-ATR, whereas the p-ATM levels raised profoundly (data not shown). No impact on phosphorylation status

(a)

(b)

(c)
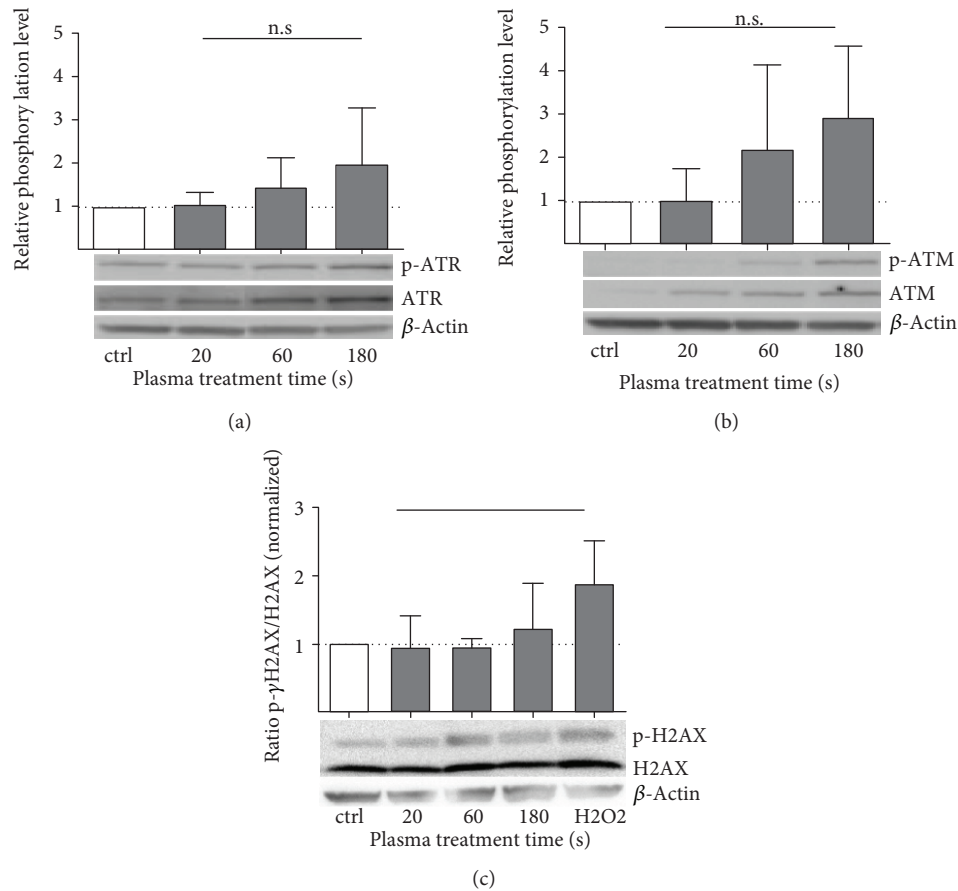
FIGURE 4: Cold plasma activates upstream activators of p53 regardless of γ-H2AX function. Relative phosphorylation of ATR (p-S428) was slightly enhanced in comparison to control (a). Quantification of Western blot has shown a treatment time-dependent induction of phosphorylation of ATM (p-S1981) in HaCaT cells (b, not significant). Phosphorylated H2AX (γH2AX), as a key factor in sensing double strand DNA breaks, was not significantly enhanced after plasma treatment (c). Representative blots are shown. Data are presented as mean + S.D. of two analyses. The x-axis represents treatment time with plasma or control (ctrl)/positive control (H2O2). Statistical analysis was done using one-way ANOVA with *Dunnett* corrections for multiple comparisons to untreated, normalized control.

and total protein expression of γ-H2AX by indirect plasma treatment was detected (Figure 4(c)).

Phosphorylation level of Chk1, the kinase downstream of ATM, was tightly coupled to plasma treatment and incubation time. A more than twofold increase of Chk1 phosphorylation after 60 s and a sixfold upregulation after 180 s of treatment was detected (Figure 5(a)). After treatment, phospho-Chk1 levels increased rapidly and reached a plateau after 45 min (about fourfold increase), where levels remained almost constant for the following hours. Beginning 6 hours after the treatment baseline level was reestablished 24 h post-plasma treatment (Figure 5(c)). Chk2, the checkpoint kinase downstream of ATR, was phosphorylated rapidly and transiently. A just over threefold increase after 60 s and more than sevenfold increase in p-Chk2 levels after 180 s of treatment was found (Figure 5(b)). Timewise, the levels of p-Chk2 increased even more rapidly than those of p-Chk1. The maximum was reached around 30 min after plasma treatment (5-fold increase), followed by a rapid decline in p-Chk2 levels so that by three hours after plasma treatment,

the levels of p-Chk2 had returned to nearly baseline level (Figure 5(d)). In addition, both molecules were strongly phosphorylated in the H_2O_2 control (data not shown).

3.5. Cold Plasma Activates Mitogen-Activated Protein (MAP) Kinase Signaling. The phosphorylation level of the mitogen-activated protein kinases Erk1/2 (MAPK1/2) increased steadily with treatment intensity and peaked at nearly five-fold increase after 180 s (Figure 6(a)). A similar behavior was observed for p38 and Jnk phosphorylation, which both peak at 180 s of treatment (Figures 6(b) and 6(c)). Unlike the more continuous increase observed for Erk phosphorylation levels, Jnk shows an abrupt escalation in phosphorylation level up to 14-fold after 180 s of treatment compared to 20 s (1.5-fold) or 60 s (4.8-fold). Kinase p38 phosphorylation was increased 7-fold (60 s) and 11-fold (180 s), respectively. The positive control (100 μM H2O2) led to an increase of the phosphorylation levels in all three kinases (data not shown). The time course of the MAP kinase phosphorylation triggered by 180 s of treatment was found to differ between

(a)

(b)

(c)

(d)
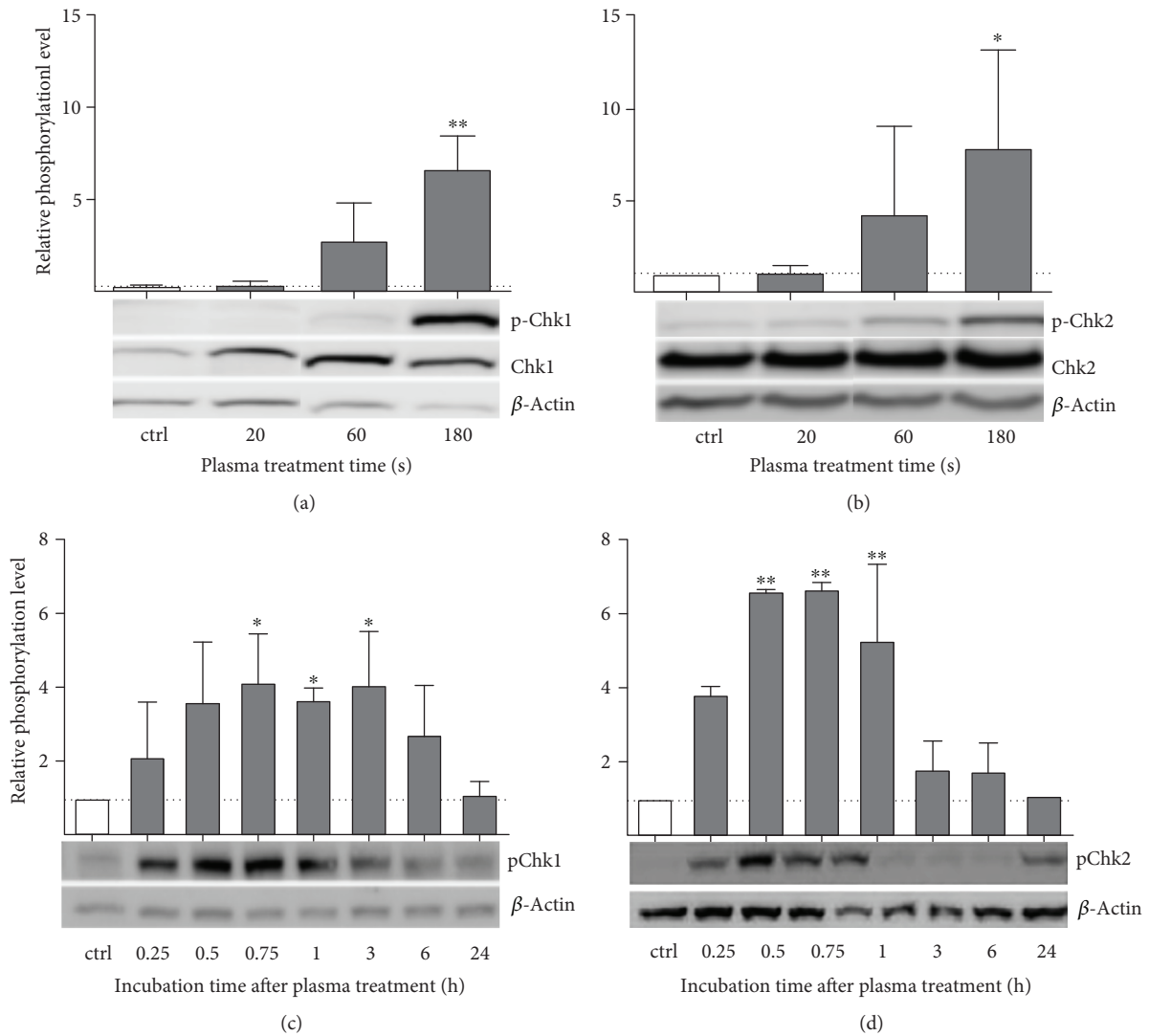
FIGURE 5: Cold plasma-induced activation of checkpoint kinases 1 and 2 downstream of ATM/ATR in HaCaT cells. Displayed are the increase of the relative phosphorylation levels of Chk1 (a, p-S296) and Chk2 (b, p-T68) after different treatment times, and time course of phosphorylated Chk1 (c) and Chk2 (d) protein after 180 s of plasma treatment over 24 h. Phosphorylated proteins were normalized to β-actin. Data are presented as mean + S.D. of three analyses. The x-axis represents treatment time (a, b) or incubation after plasma treatment (c, d). Statistical analysis was done using one-way ANOVA with *Dunnett* corrections for multiple comparisons to untreated, normalized control ($^{*}p < 0.05$, $^{**}p < 0.01$).

the three kinases; while Erk1/2 phosphorylation increased rapidly, peaking between 15 and 30 min (Figure 6(d)), Jnk phosphorylation levels rose slowly but constantly, peaking after 3–6 h posttreatment. In contrast, p38 levels showed a more flat and biphasic behavior with similar levels up to 1 h past treatment and higher levels for 3–6 h after treatment (Figures 6(e) and 6(f)). The positive control H_2O_2 did not lead to increased Erk phosphorylation but induced phosphorylation of p38 and Jnk only (data not shown). All three MAP kinase phosphorylation levels returned to their baseline 24 h after plasma treatment.

3.6. Downstream Effects of p53 Activation upon Plasma Treatment. To clarify the signaling cascade, we checked the downstream activation of p53 target genes by quantitative real-time PCR (qPCR). The expression levels of BAX and

BBC3 (proapoptotic pathway), GADD45 (DNA repair), and CDKN1A/p21 (cell cycle control, senescence) were not significantly altered by 60 s of plasma treatment after 3–12 h (Figure 7(a)). The six-hour time point was chosen for further analysis: a significant, roughly 5-fold increase in BBC3 and GADD45 as well as CDKN1A mRNA expression was induced by long (180 s) treatment. With shorter treatments (20 s and 60 s), target gene expression was slightly but nonsignificantly reduced. BAX expression remained unaltered (Figure 7(b)). Additionally, the cellular protein levels of Bax, Puma (the gene product of BBC3), Gadd45, and p21 (the gene product of CDKN1A) were analyzed by Western blotting. The pattern observed on the transcriptional level was confirmed by an increased expression of BBC3/Puma (Figure 7(c)), Gadd45 (Figure 7(d)), and CDKNA1/p21 (Figure 7(e)) while Bax remained unchanged (data not

(a)

(b)

(c)

(d)

(e)

(f)
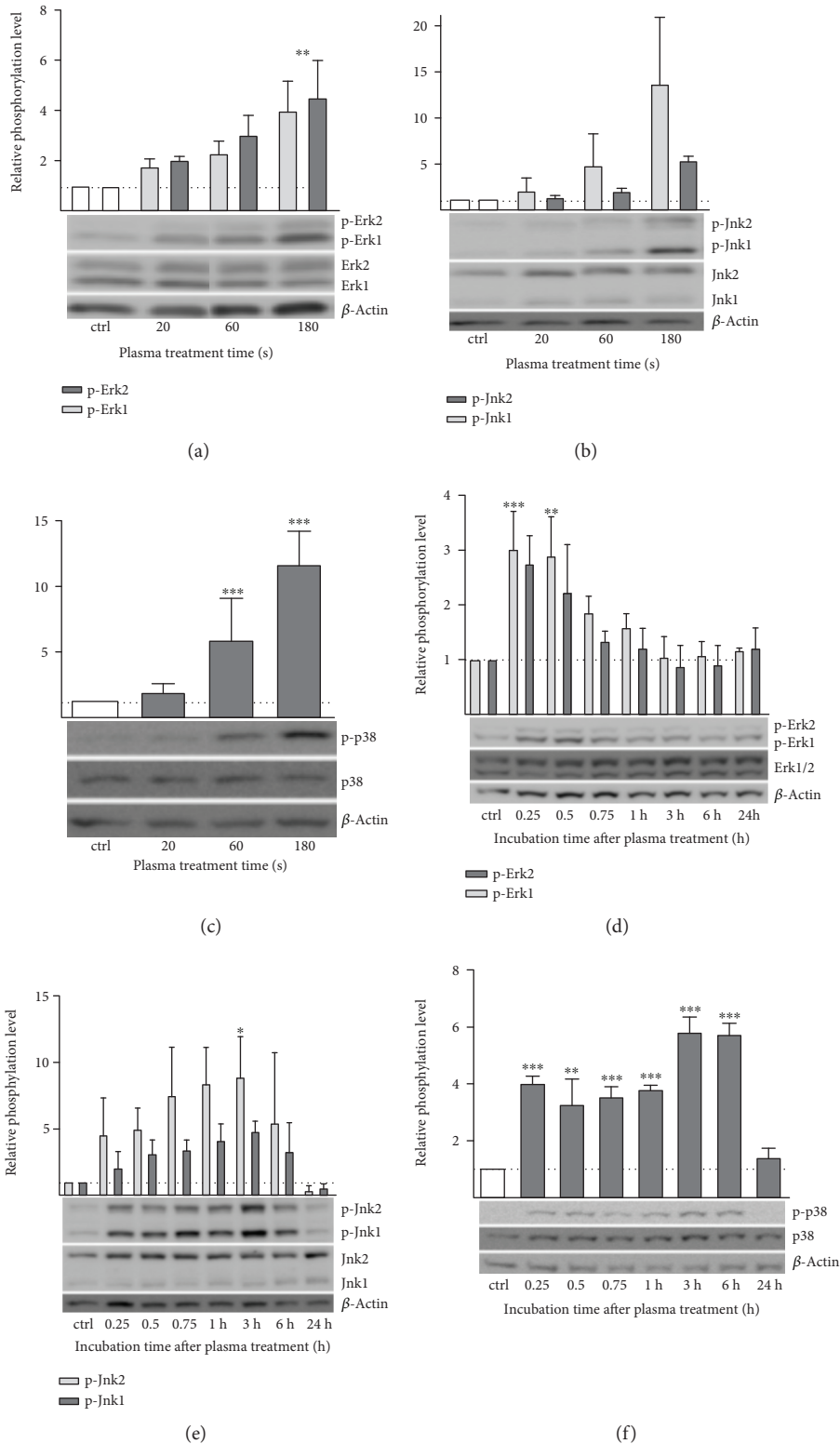
FIGURE 6: Plasma-induced activation of MAP kinase signaling in HaCaT keratinocytes. Displayed are relative phosphorylation levels of Erk (p-T202/Y204, a), Jnk (p-T183/Y185 (b)), and p38 (p-T180/Y182, (c) kinases after different treatment times. Lower panels showed the results for time course of relative phosphorylation levels after 180 s of plasma treatment for Erk (d), Jnk (e), and p38 (f). Each expression was normalized to total protein expression. Representative blots are shown. Data are presented as mean + S.D. of two analyses. The x-axis represents treatment time (a–c) or incubation after plasma treatment (d–f). Statistical analysis was done using one-way ANOVA with *Dunnett* corrections for multiple comparisons to untreated, normalized control ($^*p < 0.05$, $^{**}p < 0.01$, $^{***}p < 0.001$).

(a)

(b)

(c)

(d)

(e)

(f)
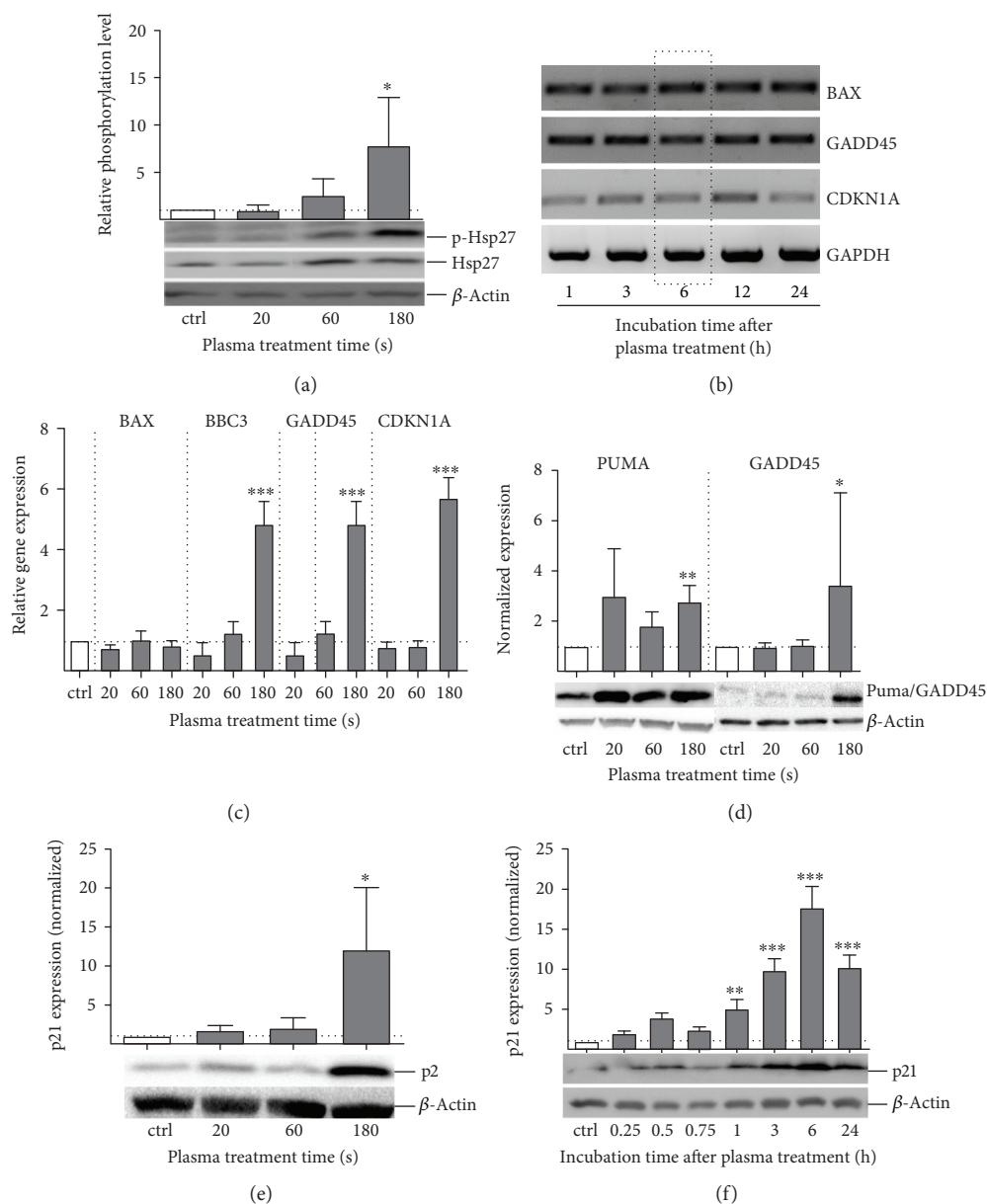
FIGURE 7: Cold plasma-induced impact on major p53 downstream targets. The total amount and the phosphorylated form of the stress-related protein HSP27 was significantly enhanced after plasma treatment (a). Agarose gel showing semiquantitative PCR of BAX, BBC3, GADD45, and CDKN1A after 1 to 24 h posttreatment of HaCaT cells with 60 s plasma (b). mRNA copy numbers of all four targets were measured 6 h after plasma treatment by qPCR and normalized to the relative gene expression ($\Delta\Delta$CT values on a log2 scale) (c). Puma (protein of BBC3), Gadd45 (d), and p21 (e) expression was significantly enhanced after plasma exposure (180 s). p21 (protein of CDKN1A) increased until 6 hours after plasma treatment, declining afterwards (f). Representative blots are shown. The x-axis represents treatment time (a, c, d, and e) or incubation after plasma treatment (b, f). Data are presented as mean + S.D. of two (c, d) or three (b) analyses. Statistical analysis was done using one-way ANOVA with *Dunnett* corrections for multiple comparisons to untreated, normalized control ($^*p < 0.05$, $^{**}p < 0.01$, $^{***}p < 0.001$).

shown). For p21, a maximal upregulation of protein was visible six hours after plasma exposure (Figure 7(f)). In contrast to transcriptional regulation, Gadd45 protein expression was not altered for investigated time points and treatment times.

The MAP kinase and ROS/RNS-associated heat shock protein 27 (Hsp27), a downstream effector of the p38 signaling cascade, showed a clear correlation of phosphorylation level with treatment time. Similar to the p38, the maximal phosphorylation level was reached after 180 s of treatment

(Figure 8(a)). In H$_2$O$_2$ control, phosphorylation of Hsp27 was only mildly stimulated (data not shown).

Gene expression and protein secretion of several cell-signaling molecules, *e.g.*, growth factors, and cytokines are strongly regulated by the MAP kinase activity. The plasma treatment had a significant impact on mRNA level resulting in a three- to fivefold upregulation of growth factors such as the vascular endothelial VEGFA and heparin-binding growth factor HBEGF as well as the colony-stimulating

(a)

(b)

(c)
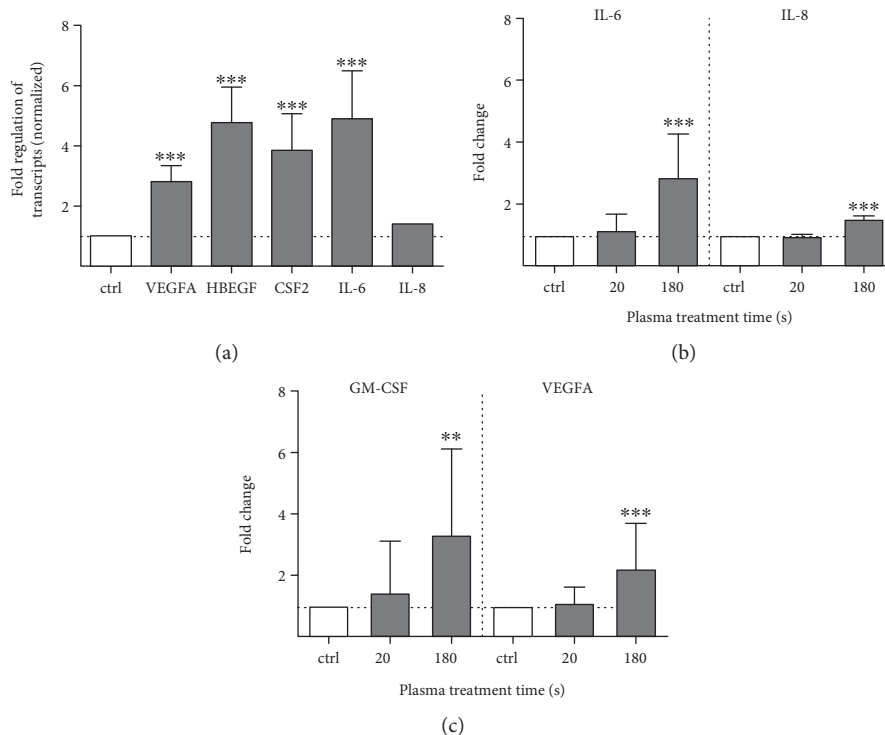
FIGURE 8: Plasma-induced changes of downstream effectors of MAP kinase signaling cascade in HaCaT keratinocytes. Transcription of several growth factors and cytokines was measured using qPCR. VEGFA, HBEGF, CSF2, and IL-6 were mainly upregulated after plasma treatment in contrast to nonregulated IL-8 (a). Results of secretion of IL-6 and IL-8 (b) cytokines as well as GM-CSF and VEGFA (c) growth factors using ELISA measurements confirmed the mRNA expression profiles. Data in diagrams are presented as mean + S.D. of at least three independent experiments. Statistical analysis was performed using one-way ANOVA with *Dunnett* corrections for multiple testing to untreated, normalized control ($^*p < 0.05$, $^{**}p < 0.01$, $^{***}p < 0.001$).

factor CSF2. For IL-6 as a proinflammatory cytokine, the mRNA levels showed a significant upregulation of DNA transcription, in contrast to IL-8.

The secretion of the two cytokines (IL-6/8) and growth factors (GM-CSF and VEGFA) was further measured using ELISA. Cytokine profiling indicated that IL-6 and IL-8 are most significantly increased in 180 s treated cells after 12 h (Figure 8(b)). The secretion of GM-CSF and VEGFA was found to be maximal 12 h after 180 s of treatment (Figure 8(c))

4. Discussion

Cold atmospheric plasma generates a mixture of reactive oxygen or nitrogen species (ROS/RNS) in the gas phase that in contact with liquids lead to the deposition of secondary/ tertiary species. Among those, singlet oxygen, atomic oxygen, hydroxyl radicals, and hydrogen peroxide are major contributors [48–50]. Since several years, CAP is used and investigated in biomedical research and clinics, especially for targeting chronic and acute wound management [2, 5, 10, 13, 51]. While it is a long-standing axiom that CAP has antimicrobial properties [52–54], its role and biochemical interaction with mammalian cells are less clear. Depending on treatment intensity and model system, CAP induces cell death and senescence or sparks cell activation and differentiation [16, 55–57]. Latest research

seeks to connect CAP with inflammatory processes and immune system control [58–61].

After CAP treatment, an increase of intracellular ROS was observed in HaCaT cells using an unspecific redox-sensitive dye which is in line with previous findings [62, 63]. However, it remains to be elucidated, which reactive species of which origin contribute to the oxidation of intracellular CM-H$_2$-DCF (after ester cleavage) since no reporter dyes that are accepted of being able to distinguish between different intracellular ROS are commercially available. Intracellular compartmentalization increases complexity that is not addressed by the simple dye. A promising but demanding approach in this regard is thiol switch dyes (HyPER) [64]. Subsequently, a rapid yet transient increase of total p53 expression accompanied by its nuclear accumulation was observed. Parallel to the nuclear trafficking, serine phosphorylation (Ser15 and Ser37) indicated an activation of p53 via external stimuli, which has been described for UV light stimulation previously [65]. Reports also demonstrate that p53 serine 15/37 sites are phosphorylated by stress-related c-Jun N-terminal kinase (Jnk) and mitogen-activated protein kinase p38 (p38) as well as several upstream kinases, especially ataxia telangiectasia mutated (ATM), ataxia telangiectasia and Rad3-related (ATR), and checkpoint kinase 1/2 (Chk1/2) [66]. Besides DNA damage transduction, ATM and ATR act as cellular redox sensor signals [67–69]. It was found that the ATM protein kinase activity
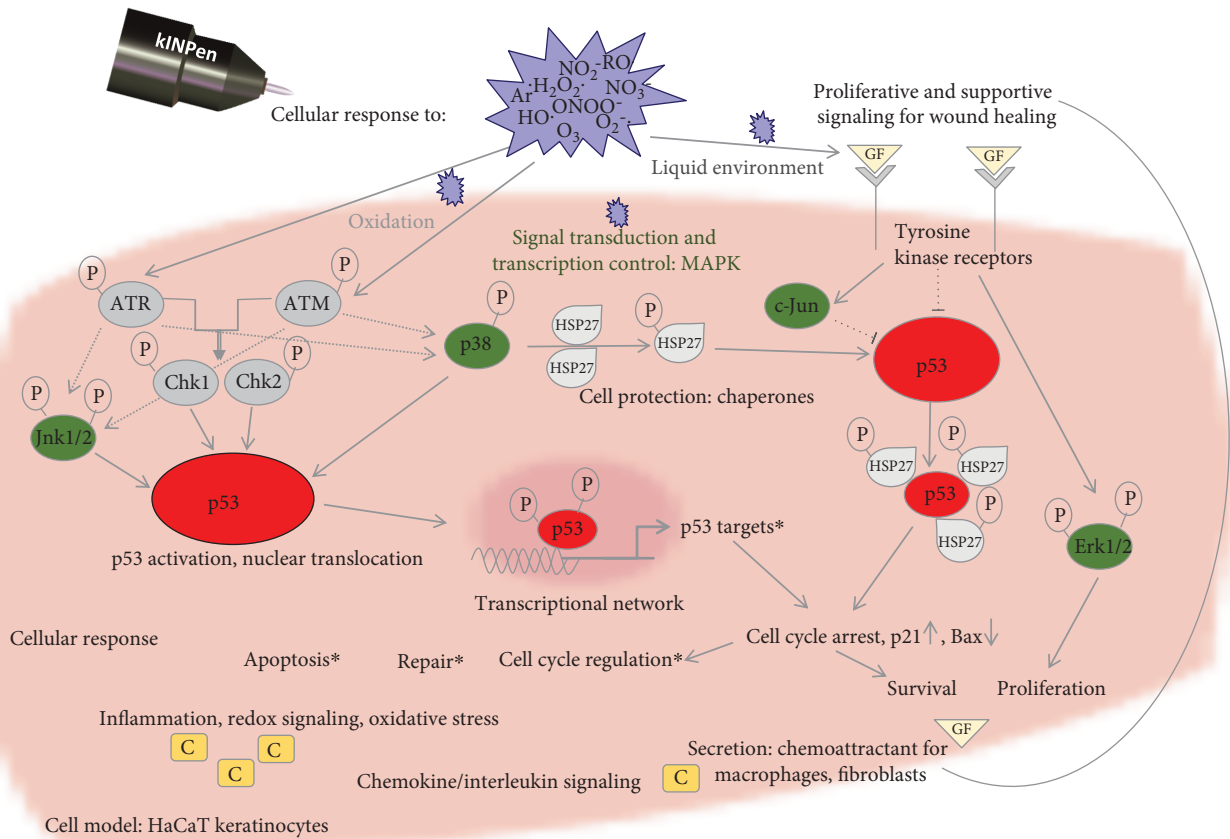
FIGURE 9: Schema of proposed cold plasma-induced regulation of p53. The primary event in the described pathways is the recognition of plasma-generated reactive oxygen species (ROS) by specific ROS sensors in keratinocytes (*e.g.*, transcription factors p53 and Nrf2 and kinases ATM or Keap1). Plasma generates ROS which in turn activate and phosphorylate p53 via upstream kinases. Activation of p53 increases transcription of p53 targets (BAX, CDKN1A, and GADD45), which increases p53-dependent apoptosis and cell death. Increased expression and phosphorylation of heat shock protein HSP27 by p38 MAP kinase result in p53 binding. HSP27 protects HaCaT cells from plasma-induced apoptosis by increased transcription of p21 resulting in cell cycle arrest, DNA repair, and cell survival. Plasma-induced activation and phosphorylation of MAP kinases (*e.g.*, signal transduction and transcription control) modulates the expression of genes and proteins related to proliferation and cell survival via Erk1/2. Therefore, p53 acts as an anti- and prooxidant.

was directly activated after exposure of cells to H_2O_2 without the presence of DNA strand breaks [70]. Observations point to the importance of ATM in oxidative stress response regulation in addition to its DNA damage sensing [71]. In an ATM-deficient mice model, increased levels of ROS and signs of oxidative stress within the central nervous system were detected [72, 73]. Predominantly after long CAP treatment, the phosphorylation of ATM and the subsequent activation of the checkpoint kinase Chk1 were observed, which is in good agreement with the finding that ATM is a relevant sensor for reactive oxygen (or nitrogen) species. The direct activation of ATM may trigger protective downstream effects in mammalian cells that potentially cross-correlate with the NFE2L2 pathway [16]. It remains to be established whether ATM signaling occurs upstream of NFE2L2 thiol oxidation and is a necessary precondition or if both pathways are activated in parallel. The fact that the phosphorylation of the histone γ-H2AX was only nonsignificantly increased by CAP seems to contribute to the above conclusion as only a strong γ-H2AX activation points at DNA damage as initial effect. Additionally, DNA damage was not reported a major route

in vitro and in vivo for the plasma device investigated here [74–76]. However, a robust activation of checkpoint kinases 1 and 2 was detected together with an increase of G2 phase cells in cell cycle. This is only in part in agreement to findings reported from a nitrogen plasma jet, which led to a strong γ-H2AX phosphorylation in human colon cells, combined with an increase of Chk2 activation [77]. In contrast to the noble gas plasma used in this work, nitrogen plasmas in contact with physiological liquids produce high amounts of peroxynitrite and hypochlorite, facilitating oxidative processes in biomolecules that are subsequently reflected by the activation of γ-H2AX seen by the authors. Paralleling the low increase of γ-H2AX, only small changes in ATR phosphorylation were seen for all plasma treatment times. This indicates that only a limited and transient oxidative damage to cellular DNA occurred. The activation of ATR is also reflected by the Ser37 phosphorylation of p53 that the kinase can be responsible for; yet, also ATM is able to phosphorylate p53 at Ser37 to a minor extent [69]. On these grounds, it can be argued that plasma treatment triggers redox signaling and such increases the "awareness" of prooxidant species [78].

Indicative for transcriptionally active p53 is the detected transcription of apoptosis pathway proteins (BBC3 and PUMA but not BAX), cell cycle arrest (CDKN1A gene and p21 protein), and DNA repair (GADD45). Of note, previous studies using the kINPen and another noble gas plasma source demonstrated the absence of mutagenic effects in plasma-treated cells [74, 75, 79].

A connected pathway is the mitogen-activated protein (MAP) kinase signaling. MAP kinases have a direct role in translating physical stimuli into biochemical signals. The phosphorylation of p53 at serine 15 by p38 kinase was detected after UVB irradiation [66]. In addition, CAP treatment as a physical-chemical stimulus was shown to lead to the activation of MAP kinases both in normal and in cancer cells [80–84]. In this work, a time and treatment intensity-related activation profile of the kinases p38, Jnk, and Erk was observed. The activity pattern of the stress-activated protein kinases p38 and Jnk was similar to each other while Erk phosphorylation showed an inverted time course. Notably, Erk activation occurs faster and at lower treatment intensity than Jnk and p38 activation but is less persistent. It can be assumed that this reflects the activity of short-lived reactive species (O, O_2^-, $^1O_2$) at the cell membrane via oxidation of the epidermal growth factor receptor [85] or lipid peroxidation products like oxidized phospholipids [86, 87]. The prolonged activation of Jnk and p38 can be related to H_2O_2 which is able to cross the cell membrane via aquaporins [88]. Downstream of the MAP kinase signaling an activation of the antiapoptotic heat shock protein Hsp27 was observed. The molecule serves various functions and acts as a mediator between ROS, p53, and MAPK signaling [89–91]. Hsp27 is also involved in cytoskeleton remodeling and cell migration, which is modulated by CAP treatment [5, 92]. Further, an increase of transcription and secretion of signal molecules involved in wound healing processes and cell migration has been observed. The acute-phase cytokines IL-6 and IL-8 are closely interwoven with MAPK-related signaling [93]. Having chemotactic impact, they also stimulate neutrophil trafficking and T-cell differentiation. IL-6 is the more robustly increased of the two, although also IL-8 is reported to be controlled by ATM [94]. Plasma treatment induces upregulation of GM-CSF and VEGFA in normal keratinocytes, which this study confirmed [81]. An overview of the impact of CAP treatment on the cellular redox signaling based on the present data is given in Figure 9.

There is mounting evidence that p53 modulates the wound healing processes [27], and the data presented here further motivate the use of CAP in wound management. In acute wounds, a transient inhibition of the p53 occurs to support cell proliferation. This could not be observed in the cell model used, instead the activation of the p53 signaling cascade led to a decrease of cellularity that is relevant for wound maturation in order to avoid the development of scar tissue [95, 96]. Along the same avenue, a decrease of cell proliferation and metabolism is welcomed to reduce fibrosis in healing wounds [97]. As discussed, p53 signals in cell migration. CAP resulted in a transiently enhanced migratory activity of normal cells [5, 11]. Finally, the secretion of chemotactic interleukins triggers immune cell invasion and

activation. Taken together, CAP treatment leads to a number of functional consequences that are in part due to the concerted action of MAPK pathway and p53 signaling, which was presumably triggered by short-lived reactive species expelled from the plasma source.

5. Conclusion

Cold plasma treatment leads to complex, interwoven redox signaling events in mammalian cells via the impact of short- and long-lived ROS/RNS. Signaling related to the p53 axis was found to be a major hub of cold plasma-cell interaction, along with the upstream redox sensors ATM and ATR. Further, MAP kinase signaling accompanied and modulated the p53 signals. Both, negative (p53 activation) as well as positive (Erk activation) effects on cellular longevity were detected for human keratinocytes. A treatment intensity dependence of the observed proapoptotic, proinflammatory, and prosurvival effects as well as a general activation of redox-related proteins showed a timeline dependency of all changes. Functional consequences with regard to the clinical use of plasmas in wound treatment are a reduction in cell proliferation, a transient increase in cell migration, and secretion of immunomodulatory signal proteins.

Abbreviations

ATM:	Ataxia telangiectasia mutated
ATR:	Ataxia telangiectasia and Rad3-related
Chk1/2:	Checkpoint kinase 1/2
Erk:	Extracellular signal-regulated kinase
Hsp27:	Heat shock protein 27
Jnk:	c-Jun N-terminal kinase
MAPK (p38):	Mitogen-activated protein kinase
p53:	Tumor suppressor protein
RNS:	Reactive nitrogen species
ROS:	Reactive oxygen species.

Data Availability

No -omics data were used; most other data can be found in the manuscript. Further data (Western blot scans, etc.) are available upon request.

Conflicts of Interest

The authors declare that they have no conflicts of interest.

Acknowledgments

Supplementary Materials

Table 1: primer sequences for downstream targets of p53, which were used in quantitative RT-PCR analyses. *(Supplementary Materials)*

References

[1] H.-R. Metelmann, C. Seebauer, V. Miller et al., "Clinical experience with cold plasma in the treatment of locally advanced head and neck cancer," *Clinical Plasma Medicine*, vol. 9, pp. 6–13, 2018.

[2] G. Isbary, G. Morfill, H. U. Schmidt et al., "A first prospective randomized controlled trial to decrease bacterial load using cold atmospheric argon plasma on chronic wounds in patients," *British Journal of Dermatology*, vol. 163, no. 1, pp. 78–82, 2010.

[3] J. Schlegel, J. Köritzer, and V. Boxhammer, "Plasma in cancer treatment," *Clinical Plasma Medicine*, vol. 1, no. 2, pp. 2–7, 2013.

[4] D. Yan, J. H. Sherman, and M. Keidar, "Cold atmospheric plasma, a novel promising anti-cancer treatment modality," *Oncotarget*, vol. 8, no. 9, pp. 15977–15995, 2017.

[5] A. Schmidt, S. Bekeschus, K. Wende, B. Vollmar, and T. von Woedtke, "A cold plasma jet accelerates wound healing in a murine model of full-thickness skin wounds," *Experimental Dermatology*, vol. 26, no. 2, pp. 156–162, 2017.

[6] R. K. Gandhirajan, S. K. Sagwal, Y. Bodnar, and S. Bekeschus, "Induction of immunogenic cell death upon combinatorial therapy with cold physical plasma and chemotherapeutic agents in melanoma," *Free Radical Biology & Medicine*, vol. 112, pp. 92-93, 2017.

[7] S. Reuter, T. von Woedtke, and K.-D. Weltmann, "The kIN-Pen—a review on physics and chemistry of the atmospheric pressure plasma jet and its applications," *Journal of Physics D: Applied Physics*, vol. 51, no. 23, p. 233001, 2018.

[8] K. D. Weltmann and T. von Woedtke, "Plasma medicine—current state of research and medical application," *Plasma Physics and Controlled Fusion*, vol. 59, no. 1, 2017.

[9] G. Isbary, J. L. Zimmermann, T. Shimizu et al., "Non-thermal plasma—more than five years of clinical experience," *Clinical Plasma Medicine*, vol. 1, no. 1, pp. 19–23, 2013.

[10] S. Emmert, F. Brehmer, H. Hänßle et al., "Atmospheric pressure plasma in dermatology: ulcus treatment and much more," *Clinical Plasma Medicine*, vol. 1, no. 1, pp. 24–29, 2013.

[11] A. Schmidt, S. Bekeschus, H. Jablonowski, A. Barton, K. D. Weltmann, and K. Wende, "Role of ambient gas composition on cold physical plasma-elicited cell signaling in keratinocytes," *Biophysical Journal*, vol. 112, no. 11, pp. 2397–2407, 2017.

[12] S. Hartwig, C. Doll, J. O. Voss, M. Hertel, S. Preissner, and J. D. Raguse, "Treatment of wound healing disorders of radial forearm free flap donor sites using cold atmospheric plasma: a proof of concept," *Journal of Oral and Maxillofacial Surgery*, vol. 75, no. 2, pp. 429–435, 2017.

[13] C. Ulrich, F. Kluschke, A. Patzelt et al., "Clinical use of cold atmospheric pressure argon plasma in chronic leg ulcers: a pilot study," *Journal of Wound Care*, vol. 24, no. 5, pp. 196–203, 2015.

[14] G. Isbary, J. Heinlin, T. Shimizu et al., "Successful and safe use of 2 min cold atmospheric argon plasma in chronic wounds: results of a randomized controlled trial," *British Journal of Dermatology*, vol. 167, no. 2, pp. 404–410, 2012.

[15] X. Cheng, J. Sherman, W. Murphy, E. Ratovitski, J. Canady, and M. Keidar, "The effect of tuning cold plasma composition on glioblastoma cell viability," *PLoS One*, vol. 9, no. 5, article e98652, 2014.

[16] A. Schmidt, S. Dietrich, A. Steuer et al., "Non-thermal plasma activates human keratinocytes by stimulation of antioxidant and phase II pathways," *Journal of Biological Chemistry*, vol. 290, no. 11, pp. 6731–6750, 2015.

[17] M. Vandamme, E. Robert, S. Lerondel et al., "ROS implication in a new antitumor strategy based on non-thermal plasma," *International Journal of Cancer*, vol. 130, no. 9, pp. 2185–2194, 2012.

[18] A. M. Hirst, F. M. Frame, M. Arya, N. J. Maitland, and D. O'Connell, "Low temperature plasmas as emerging cancer therapeutics: the state of play and thoughts for the future," *Tumor Biology*, vol. 37, no. 6, pp. 7021–7031, 2016.

[19] G. Bauer and D. B. Graves, "Mechanisms of selective antitumor action of cold atmospheric plasma-derived reactive oxygen and nitrogen species," *Plasma Processes and Polymers*, vol. 13, no. 12, pp. 1157–1178, 2016.

[20] D. B. Graves, "The emerging role of reactive oxygen and nitrogen species in redox biology and some implications for plasma applications to medicine and biology," *Journal of Physics D: Applied Physics*, vol. 45, no. 26, p. 263001, 2012.

[21] C. S. Pillay, B. D. Eagling, S. R. E. Driscoll, and J. M. Rohwer, "Quantitative measures for redox signaling," *Free Radical Biology & Medicine*, vol. 96, pp. 290–303, 2016.

[22] J. Navarro-Yepes, M. Burns, A. Anandhan et al., "Oxidative stress, redox signaling, and autophagy: cell death versus survival," *Antioxidants & Redox Signaling*, vol. 21, no. 1, pp. 66–85, 2014.

[23] F. Kruiswijk, C. F. Labuschagne, and K. H. Vousden, "p53 in survival, death and metabolic health: a lifeguard with a licence to kill," *Nature Reviews Molecular Cell Biology*, vol. 16, no. 7, pp. 393–405, 2015.

[24] L. Shi, L. Yu, F. Zou, H. Hu, K. Liu, and Z. Lin, "Gene expression profiling and functional analysis reveals that p53 pathway-related gene expression is highly activated in cancer cells treated by cold atmospheric plasma-activated medium," *PeerJ*, vol. 5, article e3751, 2017.

[25] A. E. Hall, W. T. Lu, J. D. Godfrey et al., "The cytoskeleton adaptor protein ankyrin-1 is upregulated by p53 following DNA damage and alters cell migration," *Cell Death & Disease*, vol. 7, no. 4, article e2184, 2016.

[26] D. G. Greenhalgh, "The role of apoptosis in wound healing," *The International Journal of Biochemistry & Cell Biology*, vol. 30, no. 9, pp. 1019–1030, 1998.

[27] P. D. Nguyen, J. P. Tutela, V. D. Thanik et al., "Improved diabetic wound healing through topical silencing of p53 is associated with augmented vasculogenic mediators," *Wound Repair and Regeneration*, vol. 18, no. 6, pp. 553–559, 2010.

[28] D. Thomasova, S. R. Mulay, H. Bruns, and H.-J. Anders, "p53-independent roles of MDM2 in NF-κB signaling: implications for cancer therapy, wound healing, and autoimmune diseases," *Neoplasia*, vol. 14, no. 12, pp. 1097–1101, 2012.

[29] W. Chen, T. Jiang, H. Wang et al., "Does Nrf2 Contribute to p53-mediated control of cell survival and death?," *Antioxidants & Redox Signaling*, vol. 17, no. 12, pp. 1670–1675, 2012.

[30] W. Chen et al., Mary Ann Liebert, Inc., New Rochelle, NY, USA, 2012.

[31] Y. Song, X. Li, Y. Li et al., "Non-esterified fatty acids activate the ROS–p38-p53/Nrf2 signaling pathway to induce bovine hepatocyte apoptosis in vitro," *Apoptosis*, vol. 19, no. 6, pp. 984–997, 2014.

[32] K. Lisek, E. Campaner, Y. Ciani, D. Walerych, and G. del Sal, "Mutant p53 tunes the NRF2-dependent antioxidant response to support survival of cancer cells," *Oncotarget*, vol. 9, no. 29, pp. 20508–20523, 2018.

[33] N. Rubio, J. Verrax, M. Dewaele et al., "p38^{MAPK}-regulated induction of p62 and NBR1 after photodynamic therapy promotes autophagic clearance of ubiquitin aggregates and reduces reactive oxygen species levels by supporting Nrf2–antioxidant signaling," *Free Radical Biology & Medicine*, vol. 67, pp. 292–303, 2014.

[34] Y.-J. Surh, J. Kundu, and H.-K. Na, "Nrf2 as a master redox switch in turning on the cellular signaling involved in the induction of cytoprotective genes by some chemopreventive phytochemicals," *Planta Medica*, vol. 74, no. 13, pp. 1526–1539, 2008.

[35] I. A. Olovnikov, J. E. Kravchenko, and P. M. Chumakov, "Homeostatic functions of the p53 tumor suppressor: regulation of energy metabolism and antioxidant defense," *Seminars in Cancer Biology*, vol. 19, no. 1, pp. 32–41, 2009.

[36] A. Matsuzawa and H. Ichijo, "Redox control of cell fate by MAP kinase: physiological roles of ASK1-MAP kinase pathway in stress signaling," *Biochimica et Biophysica Acta (BBA) - General Subjects*, vol. 1780, no. 11, pp. 1325–1336, 2008.

[37] T. Buschmann, O. Potapova, A. Bar-Shira et al., "Jun NH$_2$-terminal kinase phosphorylation of p53 on Thr-81 is important for p53 stabilization and transcriptional activities in response to stress," *Molecular and Cellular Biology*, vol. 21, no. 8, pp. 2743–2754, 2001.

[38] O. Pluquet, S. North, A. Bhoumik, K. Dimas, Z.'. Ronai, and P. Hainaut, "The cytoprotective aminothiol WR1065 activates p53 through a non-genotoxic signaling pathway involving c-Jun N-terminal kinase," *Journal of Biological Chemistry*, vol. 278, no. 14, pp. 11879–11887, 2003.

[39] D. V. Bulavin, Y. Higashimoto, I. J. Popoff et al., "Initiation of a G2/M checkpoint after ultraviolet radiation requires p38 kinase," *Nature*, vol. 411, no. 6833, pp. 102–107, 2001.

[40] H. J. Schaeffer and M. J. Weber, "Mitogen-activated protein kinases: specific messages from ubiquitous messengers," *Molecular and Cellular Biology*, vol. 19, no. 4, pp. 2435–2444, 1999.

[41] R. J. Davis, "Signal transduction by the JNK group of MAP kinases," *Cell*, vol. 103, no. 2, pp. 239–252, 2000.

[42] P. P. Roux and J. Blenis, "ERK and p38 MAPK-activated protein kinases: a family of protein kinases with diverse biological functions," *Microbiology and Molecular Biology Reviews*, vol. 68, no. 2, pp. 320–344, 2004.

[43] L. Roger, G. Gadea, and P. Roux, "Control of cell migration: a tumour suppressor function for p53?," *Biology of the Cell*, vol. 98, no. 3, pp. 141–152, 2006.

[44] A. Loewer, E. Batchelor, G. Gaglia, and G. Lahav, "Basal dynamics of p53 reveal transcriptionally attenuated pulses in cycling cells," *Cell*, vol. 142, no. 1, pp. 89–100, 2010.

[45] K. Ramachandran, G. Gopisetty, E. Gordian et al., "Methylation-mediated repression of *GADD45α* in prostate cancer

[46] A. R. Goloudina, K. Tanoue, A. Hammann et al., "Wip1 promotes RUNX2-dependent apoptosis in p53-negative tumors and protects normal tissues during treatment with anticancer agents," *Proceedings of the National Academy of Sciences of the United States of America*, vol. 109, no. 2, pp. E68–E75, 2012.

[47] S. H. Ibrahim, Y. Akazawa, S. C. Cazanave et al., "Glycogen synthase kinase-3 (GSK-3) inhibition attenuates hepatocyte lipoapoptosis," *Journal of Hepatology*, vol. 54, no. 4, pp. 765–772, 2011.

[48] A. Schmidt-Bleker, J. Winter, A. Bösel, S. Reuter, and K.-D. Weltmann, "On the plasma chemistry of a cold atmospheric argon plasma jet with shielding gas device," *Plasma Sources Science and Technology*, vol. 25, no. 1, 2015.

[49] H. Tresp, M. U. Hammer, J. Winter, K. D. Weltmann, and S. Reuter, "Quantitative detection of plasma-generated radicals in liquids by electron paramagnetic resonance spectroscopy," *Journal of Physics D: Applied Physics*, vol. 46, no. 43, p. 435401, 2013.

[50] H. Jablonowski and T. von Woedtke, "Research on plasma medicine-relevant plasma–liquid interaction: what happened in the past five years?," *Clinical Plasma Medicine*, vol. 3, no. 2, pp. 42–52, 2015.

[51] M. Klebes, C. Ulrich, F. Kluschke et al., "Combined antibacterial effects of tissue-tolerable plasma and a modern conventional liquid antiseptic on chronic wound treatment," *Journal of Biophotonics*, vol. 8, no. 5, pp. 382–391, 2015.

[52] G. Daeschlein, M. Napp, S. von Podewils et al., "In vitro susceptibility of multidrug resistant skin and wound pathogens against low temperature atmospheric pressure plasma jet (APPJ) and dielectric barrier discharge plasma (DBD)," *Plasma Processes and Polymers*, vol. 11, no. 2, pp. 175–183, 2014.

[53] T. Nosenko, T. Shimizu, and G. E. Morfill, "Designing plasmas for chronic wound disinfection," *New Journal of Physics*, vol. 11, no. 11, 2009.

[54] S. Bekeschus, A. Schmidt, K.-D. Weltmann, and T. von Woedtke, "The plasma jet kINPen – a powerful tool for wound healing," *Clinical Plasma Medicine*, vol. 4, no. 1, pp. 19–28, 2016.

[55] N. Kumar, P. Attri, D. K. Yadav, J. Choi, E. H. Choi, and H. S. Uhm, "Induced apoptosis in melanocytes cancer cell and oxidation in biomolecules through deuterium oxide generated from atmospheric pressure non-thermal plasma jet," *Scientific Reports*, vol. 4, no. 1, p. 7589, 2014.

[56] S. Arndt, E. Wacker, Y. F. Li et al., "Cold atmospheric plasma, a new strategy to induce senescence in melanoma cells," *Experimental Dermatology*, vol. 22, no. 4, pp. 284–289, 2013.

[57] I. Yajima, M. Iida, M. Y. Kumasaka et al., "Non-equilibrium atmospheric pressure plasmas modulate cell cycle-related gene expressions in melanocytic tumors of RET-transgenic mice," *Experimental Dermatology*, vol. 23, no. 6, pp. 424-425, 2014.

[58] M. Keidar, D. Yan, I. I. Beilis, B. Trink, and J. H. Sherman, "Plasmas for treating cancer: opportunities for adaptive and self-adaptive approaches," *Trends in Biotechnology*, vol. 36, no. 6, pp. 586–593, 2018.

[59] S. Bekeschus, K. Rödder, A. Schmidt et al., "Cold physical plasma selects for specific T helper cell subsets with distinct cells surface markers in a caspase-dependent and NF-κB-

independent manner," *Plasma Processes and Polymers*, vol. 13, no. 12, pp. 1144–1150, 2016.

[60] V. Miller, A. Lin, and A. Fridman, "Why target immune cells for plasma treatment of cancer," *Plasma Chemistry and Plasma Processing*, vol. 36, no. 1, pp. 259–268, 2016.

[61] S. Bekeschus, A. Mueller, V. Miller, U. Gaipl, and K.-D. Weltmann, "Physical plasma elicits immunogenic cancer cell death and mitochondrial singlet oxygen," *IEEE Transactions on Radiation and Plasma Medical Sciences*, vol. 2, no. 2, pp. 138–146, 2018.

[62] A. Schmidt, T. von Woedtke, and S. Bekeschus, "Periodic exposure of keratinocytes to cold physical plasma: an in vitro model for redox-related diseases of the skin," *Oxidative Medicine and Cellular Longevity*, vol. 2016, Article ID 9816072, 17 pages, 2016.

[63] T. Adachi, H. Tanaka, S. Nonomura, H. Hara, S. I. Kondo, and M. Hori, "Plasma-activated medium induces A549 cell injury via a spiral apoptotic cascade involving the mitochondrial–nuclear network," *Free Radical Biology & Medicine*, vol. 79, pp. 28–44, 2015.

[64] V. V. Belousov, A. F. Fradkov, K. A. Lukyanov et al., "Genetically encoded fluorescent indicator for intracellular hydrogen peroxide," *Nature Methods*, vol. 3, no. 4, pp. 281–286, 2006.

[65] E. Batchelor, A. Loewer, C. Mock, and G. Lahav, "Stimulus-dependent dynamics of p53 in single cells," *Molecular Systems Biology*, vol. 7, no. 1, 2011.

[66] Q. B. She, N. Chen, and Z. Dong, "ERKs and p38 kinase phosphorylate p53 protein at serine 15 in response to UV radiation," *Journal of Biological Chemistry*, vol. 275, no. 27, pp. 20444–20449, 2000.

[67] A. K. Singh, P. Pandey, M. Tewari, H. P. Pandey, I. S. Gambhir, and H. S. Shukla, "Free radicals hasten head and neck cancer risk: a study of total oxidant, total antioxidant, DNA damage, and histological grade," *Journal of Postgraduate Medicine*, vol. 62, no. 2, pp. 96–101, 2016.

[68] C. Pereira, R. Coelho, D. Grácio et al., "DNA damage and oxidative DNA damage in inflammatory bowel disease," *Journal of Crohn's and Colitis*, vol. 10, no. 11, pp. 1316–1323, 2016.

[69] S. Ditch and T. T. Paull, "The ATM protein kinase and cellular redox signaling: beyond the DNA damage response," *Trends in Biochemical Sciences*, vol. 37, no. 1, pp. 15–22, 2012.

[70] Z. Guo, R. Deshpande, and T. T. Paull, "ATM activation in the presence of oxidative stress," *Cell Cycle*, vol. 9, no. 24, pp. 4805–4811, 2010.

[71] K. Ito, A. Hirao, F. Arai et al., "Regulation of oxidative stress by ATM is required for self-renewal of haematopoietic stem cells," *Nature*, vol. 431, no. 7011, pp. 997–1002, 2004.

[72] A. Kamsler, D. Daily, A. Hochman et al., "Increased oxidative stress in ataxia telangiectasia evidenced by alterations in redox state of brains from Atm-deficient mice," *Cancer Research*, vol. 61, no. 5, pp. 1849–1854, 2001.

[73] K. L. Quick and L. L. Dugan, "Superoxide stress identifies neurons at risk in a model of ataxia-telangiectasia," *Annals of Neurology*, vol. 49, no. 5, pp. 627–635, 2001.

[74] K. Wende, S. Bekeschus, A. Schmidt et al., "Risk assessment of a cold argon plasma jet in respect to its mutagenicity," *Mutation Research/Genetic Toxicology and Environmental Mutagenesis*, vol. 798-799, pp. 48–54, 2016.

[75] S. Kluge, S. Bekeschus, C. Bender et al., "Investigating the mutagenicity of a cold argon-plasma jet in an HET-MN model," *PLoS One*, vol. 11, no. 9, article e0160667, 2016.

[76] K. Wende, S. Straßenburg, B. Haertel et al., "Atmospheric pressure plasma jet treatment evokes transient oxidative stress in HaCaT keratinocytes and influences cell physiology," *Cell Biology International*, vol. 38, no. 4, pp. 412–425, 2014.

[77] K. Kim, J. D. Choi, Y. C. Hong et al., "Atmospheric-pressure plasma-jet from micronozzle array and its biological effects on living cells for cancer therapy," *Applied Physics Letters*, vol. 98, no. 7, article 073701, 2011.

[78] B. Liu, Y. Chen, and D. K. St. Clair, "ROS and p53: a versatile partnership," *Free Radical Biology & Medicine*, vol. 44, no. 8, pp. 1529–1535, 2008.

[79] V. Boxhammer, Y. F. Li, J. Köritzer et al., "Investigation of the mutagenic potential of cold atmospheric plasma at bactericidal dosages," *Mutation Research/Genetic Toxicology and Environmental Mutagenesis*, vol. 753, no. 1, pp. 23–28, 2013.

[80] C.-H. Kim, J. H. Bahn, S. H. Lee et al., "Induction of cell growth arrest by atmospheric non-thermal plasma in colorectal cancer cells," *Journal of Biotechnology*, vol. 150, no. 4, pp. 530–538, 2010.

[81] A. Barton, K. Wende, L. Bundscherer et al., "Nonthermal plasma increases expression of wound healing related Genes in a keratinocyte cell line," *Plasma Medicine*, vol. 3, no. 1-2, pp. 125–136, 2013.

[82] L. Chen, S. Guo, M. J. Ranzer, and L. A. Dipietro, "Toll-like receptor 4 has an essential role in early skin wound healing," *The Journal of Investigative Dermatology*, vol. 133, no. 1, pp. 258–267, 2013.

[83] A. Gazel, T. Banno, R. Walsh, and M. Blumenberg, "Inhibition of JNK promotes differentiation of epidermal keratinocytes," *Journal of Biological Chemistry*, vol. 281, no. 29, pp. 20530–20541, 2006.

[84] M. A. Read, M. Z. Whitley, S. Gupta et al., "Tumor necrosis factor α-induced E-selectin expression is activated by the nuclear factor-κB and c-JUN N-terminal kinase/p38 mitogen-activated protein kinase pathways," *Journal of Biological Chemistry*, vol. 272, no. 5, pp. 2753–2761, 1997.

[85] H. Ji, J. Wang, H. Nika et al., "EGF-induced ERK activation promotes CK2-mediated disassociation of α-catenin from β-catenin and transactivation of β-catenin," *Molecular Cell*, vol. 36, no. 4, pp. 547–559, 2009.

[86] G. Leonarduzzi, M. C. Arkan, H. Başağa, E. Chiarpotto, A. Sevanian, and G. Poli, "Lipid oxidation products in cell signaling," *Free Radical Biology & Medicine*, vol. 28, no. 9, pp. 1370–1378, 2000.

[87] V. N. Bochkov, D. Mechtcheriakova, M. Lucerna et al., "Oxidized phospholipids stimulate tissue factor expression in human endothelial cells via activation of ERK/EGR-1 and Ca^{++}/NFAT," *Blood*, vol. 99, no. 1, pp. 199–206, 2002.

[88] H. Sies, "Role of metabolic H_2O_2 generation redox signaling and oxidative stress," *Journal of Biological Chemistry*, vol. 289, no. 13, pp. 8735–8741, 2014.

[89] A. Vidyasagar, N. A. Wilson, and A. Djamali, "Heat shock protein 27 (HSP27): biomarker of disease and therapeutic target," *Fibrogenesis & Tissue Repair*, vol. 5, no. 1, p. 7, 2012.

[90] Y. Xu, Y. Diao, S. Qi et al., "Phosphorylated Hsp27 activates ATM-dependent p53 signaling and mediates the resistance of MCF-7 cells to doxorubicin-induced apoptosis," *Cellular Signalling*, vol. 25, no. 5, pp. 1176–1185, 2013.

[91] Z. Qi, L. Shen, H. Zhou et al., "Phosphorylation of heat shock protein 27 antagonizes TNF-α induced HeLa cell apoptosis via regulating TAK1 ubiquitination and activation of p38 and ERK signaling," *Cellular Signalling*, vol. 26, no. 7, pp. 1616–1625, 2014.

[92] S. Arndt, P. Unger, E. Wacker et al., "Cold atmospheric plasma (CAP) changes gene expression of key molecules of the wound healing machinery and improves wound healing in vitro and in vivo," *PLoS One*, vol. 8, no. 11, article e79325, 2013.

[93] M. Mihara, M. Hashizume, H. Yoshida, M. Suzuki, and M. Shiina, "IL-6/IL-6 receptor system and its role in physiological and pathological conditions," *Clinical Science*, vol. 122, no. 4, pp. 143–159, 2012.

[94] W.-T. Chen, N. D. Ebelt, T. H. Stracker, B. Xhemalce, C. L. van den Berg, and K. M. Miller, "ATM regulation of IL-8 links oxidative stress to cancer cell migration and invasion," *eLife*, vol. 4, article e07270, 2015.

[95] B. Vollmar, A. M. el-Gibaly, C. Scheuer, M. W. Strik, H. P. Bruch, and M. D. Menger, "Acceleration of cutaneous wound healing by transient p53 inhibition," *Laboratory Investigation*, vol. 82, no. 8, pp. 1063–1071, 2002.

[96] A. Desmouliere, M. Redard, I. Darby, and G. Gabbiani, "Apoptosis mediates the decrease in cellularity during the transition between granulation tissue and scar," *The American Journal of Pathology*, vol. 146, no. 1, pp. 56–66, 1995.

[97] J.-I. Jun and L. F. Lau, "The matricellular protein CCN1 induces fibroblast senescence and restricts fibrosis in cutaneous wound healing," *Nature Cell Biology*, vol. 12, no. 7, pp. 676–685, 2010.

Research Article

Nucleoredoxin-Dependent Targets and Processes in Neuronal Cells

Claudia Urbainsky [iD],[1] Rolf Nölker,[2] Marcel Imber,[3] Adrian Lübken,[1] Jörg Mostertz,[2] Falko Hochgräfe,[2] José R. Godoy,[4] Eva-Maria Hanschmann [iD],[1,5] and Christopher Horst Lillig [iD][1]

[1]The Institute for Medical Biochemistry and Molecular Biology, University Medicine, University of Greifswald, Germany
[2]Competence Center Functional Genomics, Junior Research Group Pathoproteomics, University of Greifswald, Germany
[3]Institute for Biology-Microbiology, Freie Universität Berlin, Germany
[4]Faculty of Biomedical Sciences, Ross University School of Veterinary Medicine, Basseterre, Saint Kitts and Nevis
[5]Department of Neurology, Medical Faculty, Heinrich-Heine University Düsseldorf, Germany

Correspondence should be addressed to Eva-Maria Hanschmann; eva-maria.hanschmann@med.uni-duesseldorf.de
and Christopher Horst Lillig; horst@lillig.de

Nucleoredoxin (Nrx) is an oxidoreductase of the thioredoxin family of proteins. It was shown to act as a signal transducer in some pathways; however, so far, no comprehensive analysis of its regulated substrates and functions was available. Here, we used a combination of two different strategies to fill this gap. First, we analyzed the thiol-redox state of the proteome of SH-SY5Y neuroblastoma cells depleted of Nrx compared to control cells using a differential thiol-labeling technique and quantitative mass spectrometry. 171 proteins were identified with an altered redox state; 161 of these were more reduced in the absence of Nrx. This suggests functions of Nrx in the oxidation of protein thiols. Second, we utilized the active site mutant Cys208Ser of Nrx, which stabilizes a mixed disulfide intermediate with its substrates and therefore trapped interacting proteins from the mouse brain (identifying 1710 proteins) and neuronal cell culture extracts (identifying 609 proteins). Profiling of the affected biological processes and molecular functions in cells of neuronal origin suggests numerous functions of Nrx in the redox regulation of metabolic pathways, cellular morphology, and signal transduction. These results characterize Nrx as a cellular oxidase that itself may be oxidized by the formation of disulfide relays with peroxiredoxins.

1. Introduction

Redox signaling constitutes an essential mechanism for the regulation of protein function within specific, rapid, and highly regulated signaling cascades, comparable to de-/phosphorylation. Specific oxidative modifications of proteins, for instance, the formation of allosteric disulfides, are often attributed to the action of reactive oxygen or nitrogen species, most of all hydrogen peroxide (H_2O_2). Due to the low rate constants of H_2O_2 with most protein thiols, however, this oxidation as well as the reduction of disulfides requires catalysis by specific enzymes [1, 2].

Nucleoredoxin (Nrx) is a member of the thioredoxin (Trx) family of proteins. This family includes various oxidoreductases, such as Trxs, glutaredoxins (Grxs), peroxiredoxins (Prxs), and protein disulfide isomerases (PDIs) that catalyze cellular redox signaling [3]. All these proteins share a common structural motif, the so-called Trx fold [4]. The Nrx gene (NXN) encodes a protein of 48 kDa and is ubiquitously expressed [5]. Despite its name, the protein is localized in both the cytosol and the nucleus [5, 6]. The Nrx protein contains three Trx domains organized in a structure similar to those of PDIs that contain three to four Trx domains. The N- and C-terminal domains of Nrx share a high similarity to

the b$'$ domains of PDIs and lack a redox active center. The central domain, however, contains the dithiol active site motif Cys-Pro-Pro-Cys and was shown to be active in the insulin reduction assay [6]. The function of the PDI-like domains in Nrx is unclear; they may be important for substrate recognition, i.e., specific protein-protein interactions.

Up to now, no comprehensive identification of potential Nrx substrates has been presented and only scattered information on the function of the protein is available. Two interaction partners that have been identified are phosphofructokinase 1 and protein phosphatase 2A [7, 8]. The activity of both proteins is affected through direct interactions. Nrx also seems to be part of transcriptional regulation, because it enhances the induction of the three transcription factors CREB (cAMP response element-binding protein), NFκB (nuclear factor kappa B), and AP-1 (activator protein-1) [9]. In addition, Nrx was shown to regulate both the Wnt/PCP (planar cell polarity) and the Wnt/β-catenin pathway [10, 11]. The latter is inhibited through Nrx by binding to the basic PDZ domain of dishevelled (Dvl), thereby suppressing the redirection of the Wnt-induced signaling. This process is redox-dependent, because reducing conditions strengthen and oxidizing conditions weaken this protein-protein interaction [10]. Nrx might not only suppress this pathway but also retain a pool of inactive Dvl by preventing its proteasomal degradation. Binding of Nrx to the PDZ domain of Dvl prevents the possible interaction of Dvl and kelch-like protein 12 (KLHL12), which is part of an E3 ubiquitin ligase complex and leads to the ubiquitination and thus degradation of Dvl [12]. This mechanism may ensure that the pathway can be rapidly activated upon Wnt stimulation.

Here, we present the first comprehensive analysis of potential Nrx interaction partners and regulated pathways using a combination of two different strategies. First, we compared the redox state of the proteome from the human neuroblastoma cell line SH-SY5Y with cells in which the expression of Nrx was silenced. The redox state of the thiol proteome was identified and quantified using a differential thiol-labeling approach followed by quantitative mass spectrometry. Second, we utilized the unique reaction mechanism of Trx proteins to perform an intermediate trapping experiment using a Cys-Pro-Pro-Ser active site mutant of Nrx. With this approach, we trapped potential substrates from the SH-SY5Y cell line, as well as from murine brain tissue. We identified more than 50 proteins by all three approaches. Our findings imply potential functions of Nrx as an oxidase, rather than a reductase, in redox regulation of, e.g., metabolic pathways, cellular morphology, and signal transduction.

2. Material and Methods

2.1. Chemicals and Reagents.
Chemicals and enzymes were purchased from Sigma-Aldrich (St. Louis, USA), unless otherwise stated, and were of analytical grade or better. Cell culture media and supplements were purchased from PAN-Biotech (Aidenbach, Germany) unless otherwise stated. Antibodies detecting Nrx (16128-1-AP, Proteintech, Manchester UK), actin (sc-47778, Santa Cruz Biotechnology,

Dallas, USA), Prx1 (LF-MA0214, AbFrontier, Seoul, South Korea), Prx2 (serum, produced and validated by AG Lillig [5]), and tyrosine hydroxylase (Millipore MAP318) were used, as well as horseradish peroxidase-conjugated anti-rabbit and anti-mouse IgGs (Bio-Rad, Hercules, USA). SDS PAGE and Western blotting kits and equipment were purchased from Bio-Rad (Hercules, USA).

2.2. Cloning, Mutagenesis, Protein Expression, and Purification.
The open reading frame of Nrx was amplified by PCR from mouse cDNA using the oligonucleotides 3$'$catatgtcgggcttcctggag5$'$ and 5$'$ggatccactagatgggctcaggc3$'$. Following A-tailing, the PCR product was ligated into the pGEM-T vector (Promega, Madison, USA) and was further subcloned by restriction ligation into the expression plasmid pET15b (Novagen, Darmstadt, Germany). For the intermediate trapping experiments, the more C-terminal active site cysteinyl residue of mouse Nrx was exchanged for a seryl residue (changing the Cys-Pro-Pro-Cys active site to Cys-Pro-Pro-Ser) by site-directed mutagenesis as described before in [13] using specific oligonucleotides (3$'$gtgtccacccagccgaagcc5$'$ and 5$'$taaggcttcggctgggtggac3$'$). Following the sequence analysis, the plasmid was transformed into the E. coli strain BL21(DE3)pRIL. Mouse Nrx Cys208Ser was expressed as a polyhistidine-tagged fusion protein in E. coli and was purified using the immobilized metal affinity chromatography technique and FPLC (ÄKTAprime, GE Healthcare, Uppsala, Sweden) as described before in [5]. The expression and purification efficiency was analyzed by SDS PAGE.

2.3. Cell Culture and Cell Transfection.
SH-SY5Y cells were cultured in MEM medium without L-glutamine (PAA/GE Healthcare) supplemented with 2 mM L-glutamine and HeLa cells in DMEM at 37°C and 5% CO_2 in a humidified atmosphere. Both media were supplemented with 10% FCS and 0.1 mg/ml streptomycin/100 U/ml penicillin.

Cells were transiently transfected with specific siRNA against Nrx (Eurogentec, Liège, Belgium; test siRNAs: Ambion, Carlsbad, California) (siNrx A sense: GGAUGA CAUGACUGACUCCtt, antisense: GGAGUCAGUCAUGU CAUCCtc; siNrx B sense: GGCCUUUGUGAAUGACUU Ctt, antisense: GAAGUCAUUCACAAAGGCCtc; siNrx C sense: GCCGAUAGCUGAGAAAAUCtt, antisense: GAUU UUCUCAGCUAUCGGCtg), as well as unspecific, scrambled control siRNA (sense: CAUUCACUCAGGUCAUCA Gtt, antisense: CUGAUGACCUGAGUGAAUGtt) using electroporation as described before [14]. In brief, $5 \cdot 10^6$ Mio SH-SY5Y cells or $3.5 \cdot 10^6$ HeLa cells were resuspended in 550 μl electroporation buffer (21 mM HEPES, 137 mM NaCl, 5 mM KCl, 0.7 mM Na2HPO4, 6 mM D-Glucose, pH 7.15), mixed with 15 μg siRNA and transfected using 230 V, 500 Ω, and 1050 μF for SH-SY5Y cells or 250 V, 500 Ω, and 1500 μF for HeLa cells. The cells were mixed with 550 μl prewarmed FCS and seeded in conditioned medium. After 72 h, cells were transfected a second time with the corresponding siRNA. After another 72 h, the cells were harvested using trypsin and were lysed as follows. For Western blot analysis and the 2-Cys Prx redox blot, the

proteins were alkylated for 30 min at 37°C with 100 mM N-ethyl maleimide (NEM) (Pierce, St. Leon-Rot, Germany) in PBS prior to lysis and were then lysed for 30 min at room temperature in 2% CHAPS lysis buffer containing 5 mM NEM (40 mM HEPES, 50 mM NaCl, 1 mM EDTA, 1 mM EGTA, 1-fold protease inhibitor). For the intermediate trapping, cells and also the brain tissue were lysed in NP40 lysis buffer (10 mM Tris, 10 mM NaCl, 3 mM MgCl$_2$, 0.1% NP40, pH 7.4).

2.4. SDS PAGE and Western Blot. The protein concentration of the clarified lysates was determined using the Bradford reagent (Bio-Rad, Hercules, USA). The proteins were diluted in TE buffer (10 mM Tris, 1 mM EDTA, pH 8) and mixed with sample buffer. 20-40 μg proteins were separated by reducing (100 mM DTT) or nonreducing SDS PAGE for 30 min at 200 V using a 4-20% Mini PROTEAN TGX stain-free gel, which was subsequently activated according to the manufacturer's protocol, using the ChemiDoc XRS+ System. The proteins were transferred to a PVDF membrane using the Trans-Blot Turbo RTA Transfer Kit, according to the manufacturer's instructions. Using the ChemiDoc, the transferred proteins were imaged. This picture was used to normalize the Western blot signals to the total protein amount of the sample separated during the SDS PAGE. The membrane was blocked and incubated overnight with the specific primary antibody. The membrane was washed and incubated with HRP-coupled secondary antibody. The membrane was incubated with SuperSignal West Pico/Femto (Thermo Fisher Scientific, Waltham, USA) according to the manufacturer's instruction, to allow the detection of the resulting chemiluminescence with the ChemiDoc system. Western blots were densitometrically analyzed using ImageJ. In the case of the 2-Cys Prx redox blot, cells were treated with NEM prior and during cell lysis, and clarified lysates were subjected to nonreducing SDS PAGE and Western blot using specific antibodies against Prx1 and Prx2. The redox state of Prxs was quantified using ImageJ. The ratio of the reduced monomeric protein and the oxidized dimeric protein was analyzed. The 2-dimensional diagonal redox SDS PAGE was performed modifying the protocol described in [15]. In brief, 40 μg cell lysate was mixed with sample buffer, denatured, and separated using a 4-20% PROTEAN TGX stain-free gel (Bio-Rad) at 200 V for 30 min. The protein lane was cut out and reduced in 250 mM DTT in sample buffer at 65°C. The proteins were alkylated for 20 min using 100 mM NEM in 1-fold sample buffer. Next, the gel was applied to a second 4-20% PROTEAN TGX IPG gel. A molecular weight marker was added, and the gel lane was overlayed with 1% agarose before the proteins were separated again. Following Western blotting, the total protein in the diagonal was visualized using the stain-free technology with the ChemiDoc XRS+ System. Pictures of the total protein in the diagonal (depicted in blue) and the specific protein of interest (in black) were overlayed using ImageLab 5.0 Software (Bio-Rad).

2.5. Immunocyto- and Histochemistry. Immunocyto- and histochemistry were performed as described in [5, 16].

The samples were analyzed with a Leica LCS SP2 confocal microscope (Leica, Wetzlar, Germany). Deconvolution and colocalization analysis was performed with the Huygens software package (Scientific Volume Imaging, Hilversum, Netherlands).

2.6. Intermediate Trapping and Mass Spectrometry. 1.5 g CNBr-activated sepharose (GE Healthcare, Little Chalfont, UK) was prepared for coupling according to the manufacturer's protocol. 1.17 mg purified mNrx Cys208Ser was rebuffered with coupling buffer (0.1 M NaHCO$_3$, 0.5 M NaCl, pH 8.3) using a PD-10 Sephadex G-25 column (GE Healthcare, Little Chalfont, UK) and added to the sepharose for 6 h at 4°C. After blocking the column overnight with 300 μl blocking buffer (50 mM NaH$_2$PO$_4$, 1 mM ethanolamine, 1 mM HCl) and washing it with excess TE buffer, the protein was reduced adding 10 mM DTT in TE buffer (10 mM Tris, 1 mM EDTA, pH 8), followed by washing with TE buffer. After equilibrating the sepharose with 5 ml NP40 lysis buffer, 3 ml clarified SH-SY5Y lysates or mouse brain extracts were added to the column and incubated for 2 h at 4°C. Mouse brain extracts were isolated from Black 6 C57J mice, homogenized, and lysed in NP40 lysis buffer. The column was washed first with Tris buffer (100 mM Tris, 300 mM NaCl, pH 8) and then with TE buffer, before trapped proteins were eluted in 5 ml 10 mM DTT and 10 mM neutralized TCEP. A washing step with 3 ml TE buffer yielded a second eluate. The eluates were combined, and proteins were precipitated adding 10% TCA (final) (Roth, Karlsruhe, Germany). The proteins were pelletized by centrifugation (13300 rpm, 50 min, 4°C) and washed once with ice-cold 100% acetone (Roth, Karlsruhe, Germany) and twice with 80% (room temperature) acetone. Between the washing steps, the proteins were centrifuged for 45 min at 13300 rpm and 4°C. One part of the pellet was resuspended in 100 μl urea buffer (8 M urea, 20 mM HEPES, 1 mM EDTA, pH 8) and separated using a Mini-PROTEAN TGX stain-free gel (Bio-Rad, Hercules, USA) at 100 V for one hour. The PageBlue (Fermentas, St. Leon-Rot, Germany) stained gel was analyzed via mass spectrometry, as well as a part of the pure, nonresuspended protein pellet. Supplementary Figure 2 shows a scheme depicting the intermediate trapping approach.

2.7. Differential Thiol-Redox Labeling with iodoTMT. Differential labeling was performed as described before in [17]. In brief, Nrx-depleted SH-SY5Y cells and scrambled siRNA control cells were harvested, washed with PBS, and lysed by sonication in UHE buffer (8 M urea, 20 mM HEPES, 1 mM EDTA, pH 8.0) containing one vial of iodoTMT™ labeling reagent, see Table 1 (Thermo Fisher Scientific, Waltham, USA), followed by incubation for 1 h at 30°C. The lysate was cleared, and proteins were acetone-precipitated. The precipitate was pelleted and washed with acetone, and the air dried pellet was dissolved, reduced, and alkylated in 100 μl UHT buffer (8 M urea, 20 mM HEPES pH 8.0, 1 mM TCEP) containing a second vial of the iodoTMT™ labeling reagent, followed by incubation for 1 h at 30°C. The protein concentration was determined, equal protein amounts of three biological replicates were mixed, and proteins were

Sample	1st label (reduced)	2nd label (oxidized)	Full label
siCtrl 1	126	129	126
siCtrl 2	127	130	127
siCtrl 3	128	131	128
siNrx 1	126	129	129
siNrx 2	127	130	130
siNrx 3	128	131	131

acetone-precipitated. The pellet was washed with acetone, and the air-dried pellet was loosened in 25 mM ammonium bicarbonate buffer and digested for 2 h at 30°C adding trypsin at a protein to enzyme ratio of 100 : 1. The same amount of trypsin as before was added a second time, and the sample was incubated overnight at 30°C. The reaction was stopped by adding trifluoroacetic acid (TFA), and the proteins were freeze-dried. The pellets were dissolved in TBS, and the iodoTMT™ labeled peptides were purified using an anti-TMT™ antibody (Thermo Fisher Scientific, Waltham, USA). The peptides were eluted adding 400 μl TMT (tandem mass tag) elution buffer (Thermo Fisher Scientific, Waltham, USA), followed by centrifugation. The supernatant was freeze-dried and dissolved in 5% acetonitrile/0.1% TFA. The samples were desalted via stage tipping. The peptides were separated with nano-HPLC and analyzed with an in-line coupled high-accuracy mass spectrometer. Spectra were analyzed with the computational proteomics platform MaxQuant with integrated quantification algorithms for chemical labels. Supplementary Figure 1 shows a scheme of the differential labeling approach.

The iodoTMT™ labels were also used to analyze changes in the abundance of proteins with cysteinyl residues. To do so, the samples were treated as described before except that the TCEP was already added to the lysis buffer with iodoTMT™ reagent to label all thiols in one step.

2.8. Functional Annotation Analyses. Gene ontology (GO) analysis and classification was done using the PANTHER data analysis and classification system. Proteins identified in the differential labeling approach with a p value < 0.05 and identified proteins from the intermediate trapping approaches with at least two determined iBAQs (intensity-based absolute quantification) were loaded separately into the classification tool. Proteins were analyzed for the ontologies' "biological process" and "molecular function" using a human background for the differential labeling and the intermediate trapping with SH-SY5Y extracts and a mouse background for the intermediate trapping data gained with mouse brain extracts.

3. Results and Discussion

Nrx is an active oxidoreductase that catalyzes thiol-disulfide exchange reactions *in vitro* [6]. It was shown to act as a signal transducer in some pathways, e.g., Wnt/Dvl [12]; however, no comprehensive analysis of its substrates and regulated pathways was available.

We applied two distinct strategies for the identification of Nrx targets. First, we performed a differential thiol-labeling approach that allows the specific analysis of the redox state of the whole thiol-redox proteome. We compared cells with siRNA-mediated silencing of Nrx expression to control cells treated with unspecific scrambled siRNA (see Supplementary Fig. 1). Second, we used an active site mutant of Nrx that lacks the C-terminal resolving cysteinyl residue within the dithiol active site motif. This protein was immobilized and allowed to react with potential target proteins. The thiol-disulfide exchange reaction mechanism of Trx family proteins requires the formation of an intermediate mixed disulfide of the N-terminal active site cysteinyl residue with the target protein. This intermediate is trapped in reactions with the mutant protein; hence, we named this approach intermediate trapping [18] (see Supplementary Fig. 2). We focused on redox-regulated targets in neuronal cells. Next to brain tissue from 6-week-old mice, we analyzed the cell line SH-SY5Y that was originally derived from a female patient with neuroblastoma. These cells display a high dopamine-β-hydroxylase activity and are able to form processes resembling dendrites and axons [19].

Nrx-specific RNA interference was established comparing three different siRNAs. All of them were effective in significantly reducing the levels of Nrx in HeLa cells (Figures 1(a) and 1(b)). The most effective one (siRNA C) reduced the levels of Nrx after consecutive rounds of transfections to below 3% compared to control-transfected cells and was used for further experiments. The efficiency of the knockdown was also confirmed in SH-SY5Y cells, where the protein was essentially undetectable following the siRNA treatment (Figure 1(c)).

Nrx was described to act in both the nucleus [6] and cytosol, e.g., [12]. To clarify the localization of the protein in neuronal cells, we have analyzed the subcellular localization of the protein in both neuron-like SH-SY5Y cells and dopaminergic cells of the mouse substantia nigra by immunocyto- and histochemistry and confocal microscopy (Figure 2). In all analyzed cells, Nrx displayed a dual nuclear and cytosolic staining. This confirms previous results from our extensive analysis of redoxins in mouse tissues [5], as well as the data presented in the human protein atlas [20] (https://proteinatlas.org).

To analyze the thiol proteome in Nrx-depleted cells, SH-SY5Y cells were transfected and seeded in flasks for the labeling steps. For each condition, the siRNA-mediated gene-silencing of Nrx was confirmed by Western blot analysis (not shown). The samples were subjected to the differential labeling as described and analyzed by quantitative mass spectrometry; for details, see the experimental procedures, Table 1, and Supplementary Fig. 1. To our surprise, 161, i.e., 94.2%, of the 171 proteins identified with significant changes of the thiol-redox state were more reduced in the samples lacking Nrx expression (Figure 2(a)). These proteins displayed changes in at least one cysteinyl-containing peptide. The full list of these proteins was included in the supplementary material. These unexpected results suggest that Nrx may be involved in the oxidation of these proteins *in vivo*. The oxidation of protein thiols under physiological

(a)

(b)

(c)
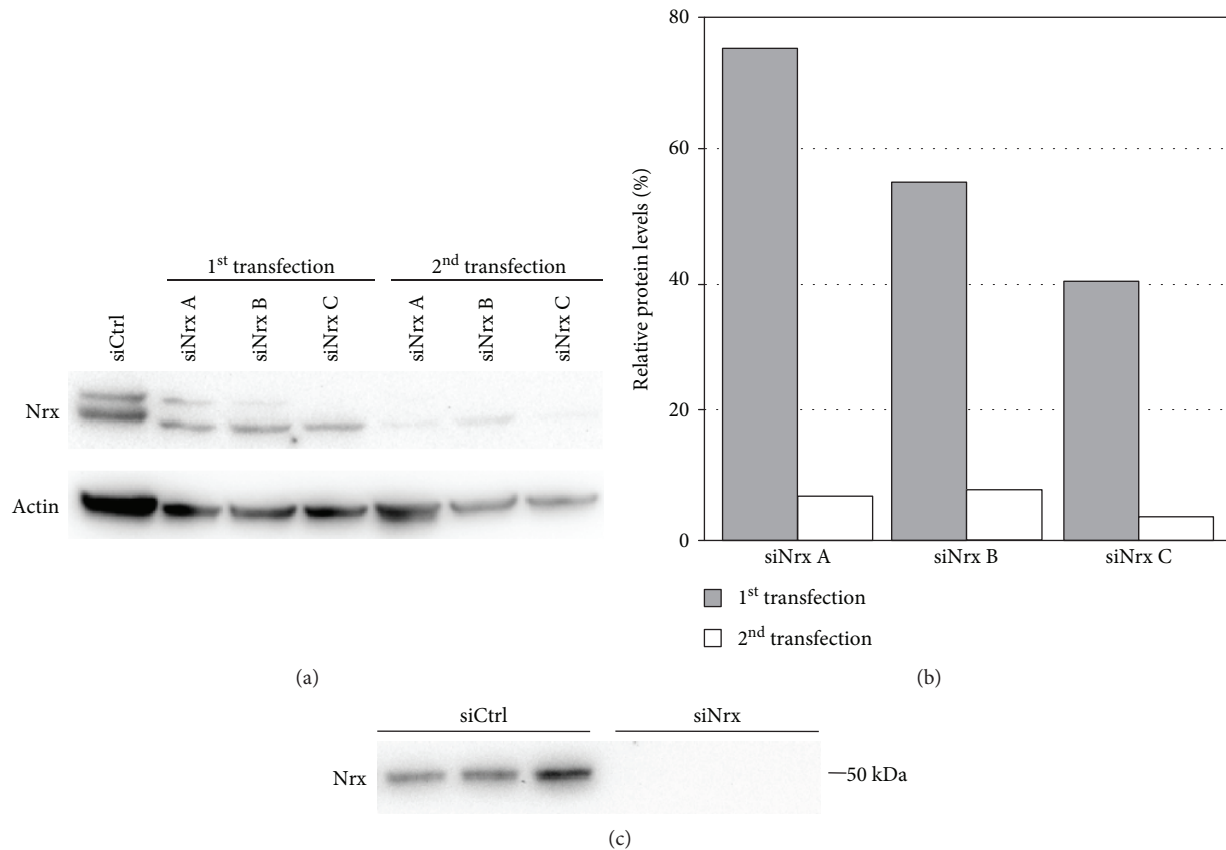
FIGURE 1: Establishment of siRNA-mediated gene-silencing in HeLa cells. Three different siRNAs against Nrx (siNrx A-C) as well as unspecific control siRNA (siCtrl) were used to establish a specific gene-silencing of Nrx. HeLa cells were transfected twice by electroporation, and 72 h after each transfection, cell extracts were prepared. The Nrx protein levels were analyzed by immunoblotting using specific antibodies against Nrx and actin (a). The quantification of the Western blot signals was performed using ImageJ and shows that siNrx C induced the most efficient knockdown of Nrx (b). Confirmation of the siRNA-mediated knockdown of Nrx in SH-SY5Y cells ($n = 3$) (c).

conditions is still a mystery. Although hydrogen peroxide can facilitate this, the low rate constants of most protein thiols with H_2O_2 preclude that this reaction occurs *in vivo* [2, 21, 22]. This led to the proposal that thiol- and selenol-peroxidases may act as sensors or transmitters by transferring the disulfides that form within their active site following the reduction of peroxides to specific target proteins [21]. Thiol-disulfide exchange reactions are fully reversible by nature. The direction of these reactions is determined by thermodynamic constrains such as the redox potential. The velocity of the reactions, however, is determined by the activity of enzymes that catalyze the reactions [22]. In fact, recent reports demonstrated that the oxidation of various protein thiols in cells depends on the presence of active peroxiredoxins [15]. It is tempting to speculate about a catalytic function of Nrx in disulfide relay pathways. In fact, we identified Prx1 as an interaction partner of Nrx in this study.

To analyze the potential role of Nrx as oxidase of protein thiols also in cells of nonneuronal origin, we determined the redox state of both Prx1 and Prx2 in the HeLa cells lacking Nrx using Western blotting following nonreducing SDS PAGE (Figure 3). Prxs form an intermolecular disulfide in their reaction cycle that allows determining their redox state

in samples treated with thiol alkylators during the harvesting and lysis of cells. Prx1, but not Prx2, was slightly more oxidized in the absence of Nrx, 11.1% compared to 7.2% in controls. Albeit statistical power was low (p value = 0.1, unpaired t-test analysis) (Figures 3(a) and 3(b)), the more oxidized Prx1 and the more reduced target proteins support the idea that Prx1 may oxidize Nrx in different cell types. Subsequently, Nrx transfers these oxidation equivalents to other proteins that cannot directly interact with the Prx.

Next to the differences in the redox state, the levels of 58 proteins were significantly altered, i.e., the p value of three independent samples was lower than 0.05. 30 of these proteins were decreased in the cells lacking Nrx compared to the control cells (see supplementary material).

For the second approach, we cloned mouse Nrx, produced the trapping mutant protein Cys208Ser by PCR, and purified the protein by metal affinity chromatography following recombinant expression in *E. coli* (see supplementary Figures 2 and 3). The proteins were immobilized and allowed to react with potential targets that were identified by mass spectrometry. The intermediate trapping of potential targets from mouse brain tissue as well as from the SH-SY5Y cell extracts yielded 1710 and 609 significant

(a)

(b)

(c)

(d)

(e)

(f)
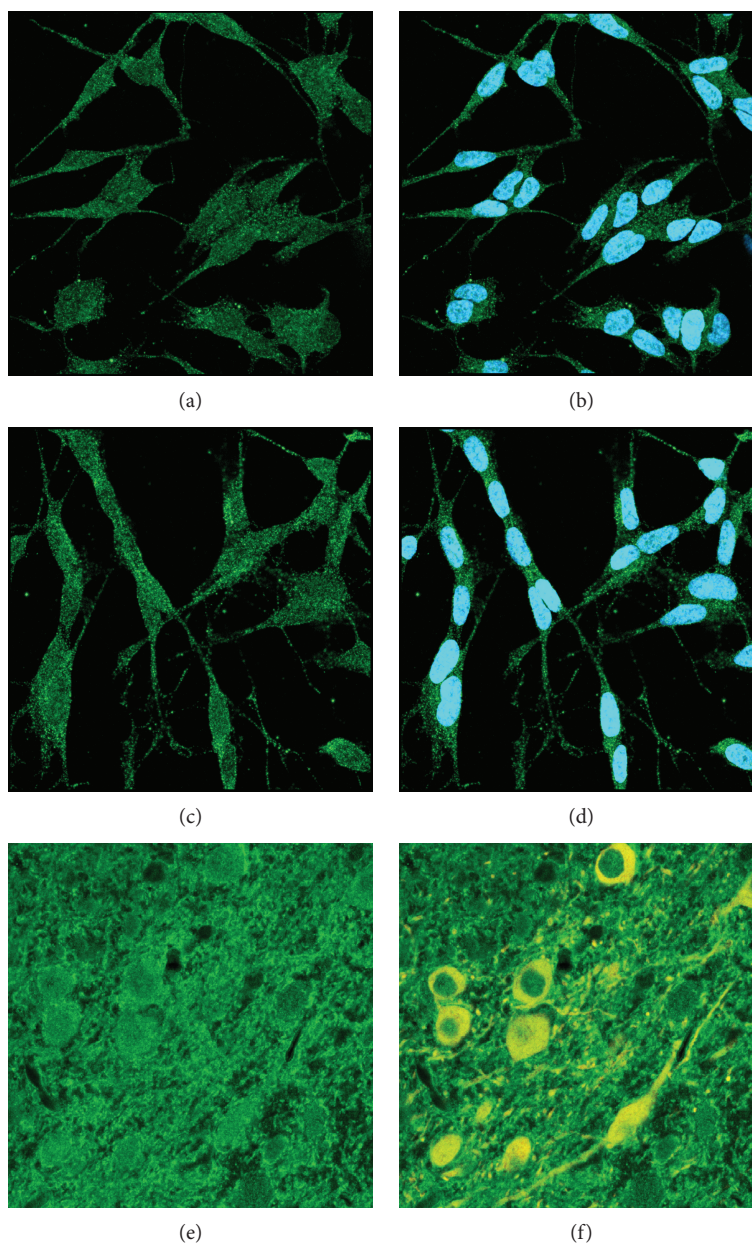
Figure 2: Subcellular localization of Nrx in SH-SY5Y cells and dopaminergic neurons of the mouse CNS. Immunocytochemistry stained for Nrx (green) and nuclei (blue in (b) and (d)) or tyrosine hydroxylase (yellow in (f)), analyzed by confocal microscopy. (a, b) SH-SY5Y control cells. (c, d) SH-SY5Y cells 72 hours after the beginning of neuron-like differentiation induced by retinoic acid. (e, f) Nrx staining in the substantia nigra of the mouse; dopaminergic neurons were labeled for tyrosine hydroxylase (yellow).

hits, respectively, in the databases. In contrast to the differential labeling approach, however, this approach does not allow concluding the direct or indirect reduction or oxidation of target proteins by Nrx due to the reversibility of the thiol-disulfide exchange reactions. The full lists of the identified proteins were also included in the supplementary material.

51 potential Nrx target proteins were identified by all three approaches and are listed in Table 2. Also, the analysis of the affected biological processes and molecular functions using the PANTHER data analysis and classification system [23, 24] yielded a high degree of overlap between the different

experiments; see Figures 2(b) and 2(c). The lists are topped by cellular/metabolic processes and proteins with enzymatic activity, e.g., glyceraldehyde-3-phosphate dehydrogenase (GAPDH) or triose phosphate isomerase. These are followed by structural proteins, many of which function in a cellular component organization, e.g., cofilin 1, fascin 1, or kinesin light chain 1. Also, proteins with functions in the regulation of cellular processes and signal transduction were identified in significant numbers, for instance, guanine nucleotide-binding protein 1 or histone deacetylase 2.

Some of the proteins identified here as potential Nrx targets have been reported before to be regulated by the

(a)

(b)

(c)
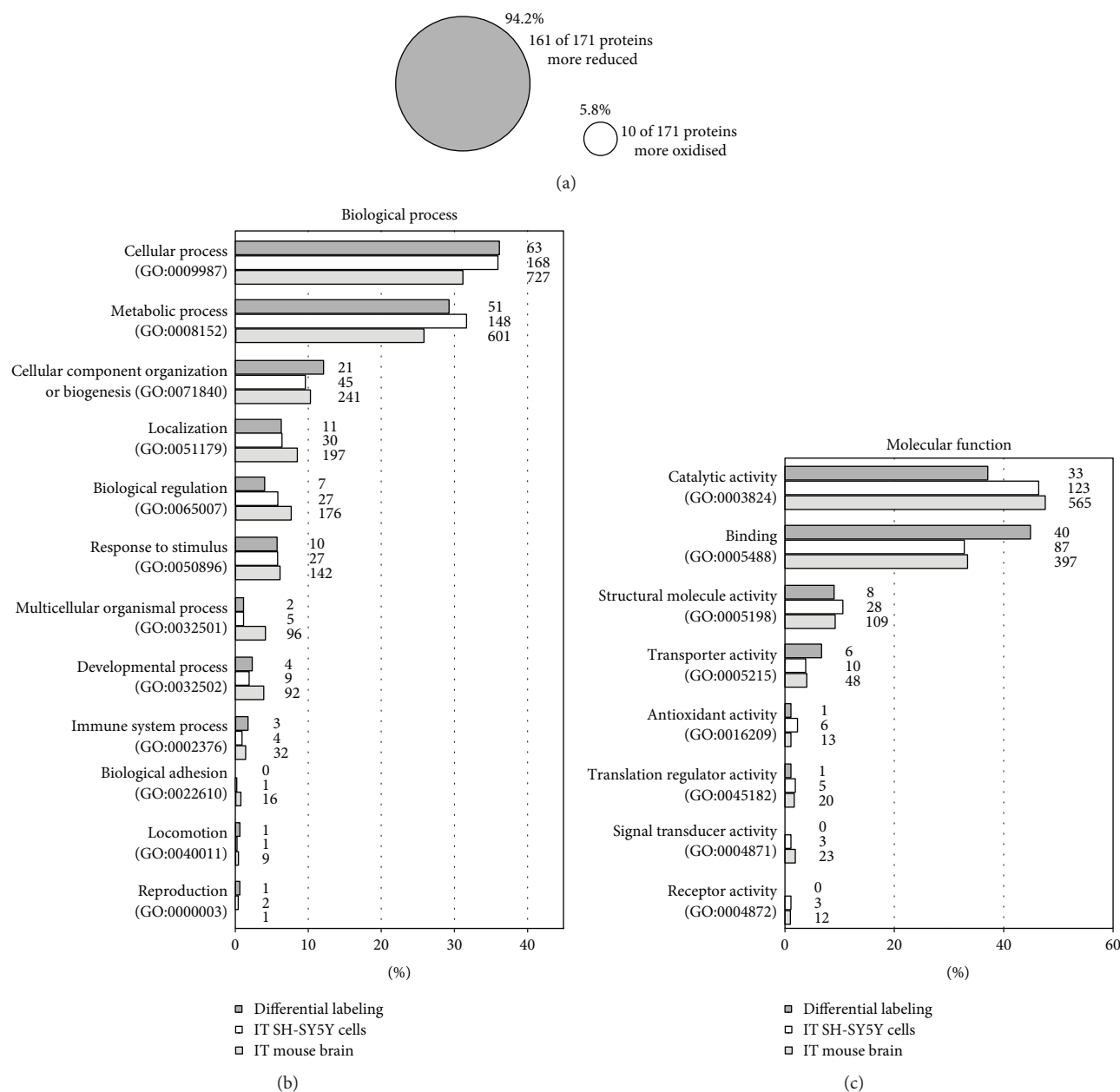
FIGURE 3: Classification of potential Nrx interaction partners identified by mass spectrometric analysis. To identify potential Nrx interaction partners and targets, three mass spectrometric-based approaches were performed, namely, a differential labeling with neuroblastoma SH-SY5Y cells lacking Nrx as well as two intermediate trappings (IT) with recombinant mNrx Cys208Ser using SH-SY5Y cell and mouse brain extracts. The results from the differential labeling were used to analyze the redox proteome of Nrx-depleted cells revealing that 94.2% of the identified cysteine-containing proteins were more reduced in the absence of Nrx (a). The potential interaction partners of Nrx, identified by all three approaches, were compared regarding their biological processes (b) and their molecular function (c) using the PANTHER classification system. There is a big resemblance between the results of the three approaches, with most potential interaction partners having catalytic activities and functions in binding, as well as metabolic and cellular processes.

thiol-redox state. GAPDH, for instance, is inactivated by disulfide formation and other redox modifications of its active site Cys152 [25]. Here, we found this cysteinyl residue to be slightly more reduced (3.4%; p value 0.031) in the absence of Nrx in the cells of neuronal origin (see Supplementary Tables). We have also analyzed the redox state of this protein in the HeLa cell culture model using a 2-dimensional diagonal gel electrophoresis approach as described in [15] (Figures 4(c) and 4(d)). The protein was more oxidized in

the presence of Nrx, as seen from the increased GAPDH staining below the diagonal (Figure 4(c)), compared to cells lacking Nrx (Figure 4(d)). Cofilin 1 was reported to be redox regulated by both glutathionylation [26] and intermolecular disulfide formation [27]. The protein seems to be inhibited by oxidation in its regulation of actin dynamics. Cell migration, for instance, seems to require the reduction of the protein [28]. We have confirmed the more reduced state of cofilin 1 also in the HeLa model using diagonal

TABLE 2: Potential Nrx targets identified by all three approaches. The table contains the 51 proteins that were identified in all three experiments, i.e., the differential thiol labeling in Nrx-depleted SH-SY5Y cells, and the intermediate trapping using SH-SY5Y and mouse brain extracts. The proteins are sorted alphabetically; full lists can be found in the supplementary material.

Protein ID	Gene name	Protein name
P49588	AARS	Alanine-tRNA ligase, cytoplasmic
P23526	AHCY	Adenosylhomocysteinase
P49419	ALDH7A1	Alpha-aminoadipic semialdehyde dehydrogenase
P04075	ALDOA	Fructose-bisphosphate aldolase A
P48444	ARCN1	Coatomer subunit delta
P54687	BCAT1	Branched-chain amino acid aminotransferase, cytosolic
P78371	CCT2	T-Complex protein 1 subunit beta
P50990	CCT8	T-Complex protein 1 subunit theta
P23528	CFL1	Cofilin-1
Q00610	CLTC	Clathrin heavy chain 1
O94760	DDAH1	N(G),N(G)-Dimethylarginine dimethylaminohydrolase 1
P26641	EEF1G	Elongation factor 1-gamma
P13639	EEF2	Elongation factor 2
P09104	ENO2	Gamma-enolase
P21333	FLNA	Filamin-A
Q16658	FSCN1	Fascin
P04406	GAPDH	Glyceraldehyde-3-phosphate dehydrogenase
P62873	GNB1	Guanine nucleotide-binding protein
P17174	GOT1	Aspartate aminotransferase, cytoplasmic
P00505	GOT2	Aspartate aminotransferase, mitochondrial
Q92769	HDAC2	Histone deacetylase 2
Q99714	HSD17B10	3-Hydroxyacyl-CoA dehydrogenase type-2
P07900	HSP90AA1	Heat shock protein HSP 90-alpha
Q9NSE4	IARS2	Isoleucine-tRNA ligase, mitochondrial
P12268	IMPDH2	Inosine-5′-monophosphate dehydrogenase 2
Q07866	KLC1	Kinesin light chain 1
P28838	LAP3	Cytosol aminopeptidase
P55209	NAP1L1	Nucleosome assembly protein 1-like 1
P12955	PEPD	Xaa-Pro dipeptidase
P14618	PKM	Pyruvate kinase
P62937	PPIA	Peptidyl-prolyl cis-trans isomerase A
P53041	PPP5C	Serine/threonine-protein phosphatase 5
Q06830	PRDX1	Peroxiredoxin-1
Q9H6Z4	RANBP3	Ran-binding protein 3
P54136	RARS	Arginine-tRNA ligase, cytoplasmic
P39023	RPL3	60S ribosomal protein L3
P36578	RPL4	60S ribosomal protein L4
P61247	RPS3A	40S ribosomal protein S3a
Q16181	SEPT7	Septin-7

TABLE 2: Continued.

Protein ID	Gene name	Protein name
P37837	TALDO1	Transaldolase
P60174	TPI1	Triosephosphate isomerase
Q71U36	TUBA1A	Tubulin alpha-1A chain
Q9BVA1	TUBB2B	Tubulin beta-2B chain
Q16881	TXNRD1	Thioredoxin reductase 1, cytoplasmic
P62987	UBA52	Ubiquitin-60S ribosomal protein L40
P61088	UBE2N	Ubiquitin-conjugating enzyme E2 N
P45974	USP5	Ubiquitin carboxyl-terminal hydrolase 5
Q99536	VAT1	Synaptic vesicle membrane protein VAT-1 homolog
Q96QK1	VPS35	Vacuolar protein sorting-associated protein 35
P54577	YARS	Tyrosine-tRNA ligase, cytoplasmic
P63104	YWHAZ	14-3-3 protein zeta/delta (protein kinase C inhibitor protein 1)

electrophoresis (Figures 4(e) and 4(f)). Nrx appears to promote the intermolecular disulfide-bonded form of cofilin 1 (Figure 4(e)). Hence, Nrx may, through the oxidation and inhibition of cofilin 1, negatively regulate cytoskelatal dynamics and cell motility.

One of the proteins with the most substantial changes in thiol-redox state was the triose phosphate isomerase. In the absence of Nrx, four cysteinyl residues were found to be more reduced: Cys67 (38.9%, p value 0.0385), Cys87 (29.4%, p value 0.0245), Cys127 (42.1%, p value 0.0125), and Cys218 (38.7%, p value 0.0479). The S-nitrosylation of the latter Cys218 residue has been reported to lead to a reduction in the activity of the human protein by 30% [29]. The glutathionylation of the human enzyme has been described in stressed T-lymphocytes [26]. In the close homologous enzymes from plants and algae, Cys127 and Cys218 can also be modified by glutathionylation [30] and other redox modifications (summarized, e.g., in [31]). The branched-chain amino acid aminotransferase was reported to be inactivated by S-nitrosylation and S-thiolation [32, 33]. In the absence of Nrx, we found the protein to be more reduced at Cys292 (20.1%, p value 0.044). Among the proteins identified here that were not yet reported to be regulated by redox modification of cysteinyl residues were the proteasomal subunit PSMA6 that was more reduced in the absence of Nrx at Cys47 (31.4%, p value 0.0238) and the dynein light chain 1 that was more reduced at Cys56 (23.8%, p value 0.0177). One of the few proteins that was significantly more oxidized in the absence of Nrx was the glutathione S-transferase omega 1 (13.4%, p value 0.0392) at the nonactive site residue Cys159.

We also identified proteins that were described as interaction partners of Nrx before. Nrxs suggested an electron donor in thiol-disulfide exchange reactions; the selenoprotein thioredoxin reductase 1 (TrxR1) [6] was identified in all three experiments. Protein phosphatase 2A was shown to form a stable complex with Nrx that may be important for the regulation of its activity [7]. In our differential labeling
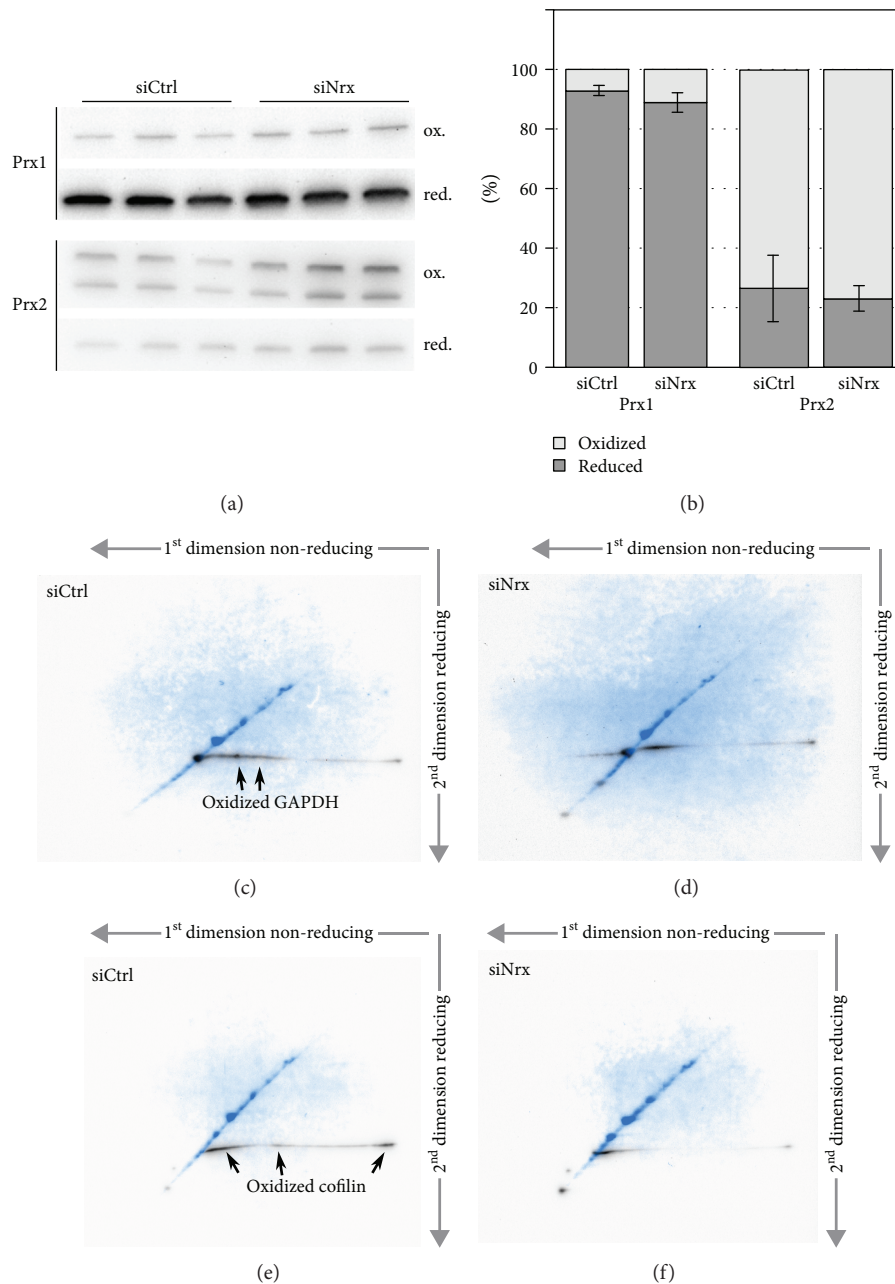
FIGURE 4: Redox state of cytosolic peroxiredoxins, cofilin, and GAPDH in Nrx-depleted HeLa cells. The redox state of Prx1 and Prx2 was analyzed in Nrx-depleted HeLa cells by 2-Cys Prx redox blot (a). Prior to lysis, free thiols were alkylated with NEM, and the monomer and dimer levels of the two proteins were analyzed via the 2-Cys Prx redox blot using specific antibodies against Prx1 and Prx2, respectively (a). The quantification of the Western blot signals using ImageJ (b) shows that more dimeric, i.e., oxidized Prx1, is present in the absence of Nrx (p value = 0.1). (c-f) Analysis of the redox state of potential Nrx targets by 2-dimensional diagonal gel electrophoresis and Western blotting. Both GAPDH and cofilin showed an increased staining of spots that fell below the diagonal in the second dimension in the presence of Nrx (c, e), compared to HeLa cells lacking Nrx (d, f). In the overlayed pictures, the total protein content in the diagonal is depicted in blue, the specific protein of interest in black.

approach, protein phosphatase 2C A was one of the few proteins that was more oxidized in the presence of Nrx (Cys266, 6.6%, p value 0.0258). Interestingly, in plant cells, catalase is maintained in a reduced state by substrate-interaction with the Nrx homologue NRX1 [34].

Nrx has been implied in the redox regulation of cellular differentiation through the Wnt signaling pathway

[10–12]. Our study suggests that it may also function in neuronal development. Reactive oxygen species and the redox state of various proteins contribute to neurogenesis, cell polarization, and maturation of neurons, providing a context for the spatiotemporal control of neural fate; see, for instance, [35]. The production of hydrogen peroxide is not sufficient to oxidize target proteins with significant rates

[21, 22]. Nucleoredoxin may thus be a facilitator of hydrogen peroxide signaling by catalyzing the thiol-disulfide exchange reaction between peroxidases, such as Prxs, as sensors and the downstream target proteins that mediate the biological functions.

In summary, our study presented here suggests a number of specific functions for mammalian Nrx in the redox regulation of metabolic pathways, cellular morphology, and signal transduction pathways in neuronal cells. We identified numerous proteins with an altered thiol-redox state, dependent on the presence of Nrx. Astonishingly, most of these thiols were more reduced in the absence of this Trx family oxidoreductase. These results suggest a function of Nrx in the oxidation of these thiols, rather than their reduction. A possible way for the oxidation of Nrx itself may be the formation of disulfide relays with peroxiredoxins, supported by the direct interactions of the proteins demonstrated here.

Abbreviations

Dvl: Dishevelled
GAPDH: Glyceraldehyde-3-phosphate dehydrogenase
H_2O_2:   Hydrogen peroxide
NEM: N-Ethyl maleimide
Nrx: Nucleoredoxin
PDI: Protein disulfide isomerase
Prx: Peroxiredoxin
TMT: Tandem mass tag
Trx: Thioredoxin.

Data Availability

All data is available in the supplementary material.

Conflicts of Interest

The authors declare that there is no conflict of interest regarding the publication of this paper.

Acknowledgments

Supplementary Materials

Supplementary 1. Supplementary Figure 1: scheme of the differential labeling approach. Supplementary Figure 2: scheme depicting the intermediate trapping approach used to identify potential Nrx interaction partners. Supplementary Figure 3: recombinant expression and purification of mouse Nrx WT and Cys208Ser in *E. coli*.

Supplementary 2. The list contains 171 potential Nrx interaction partners identified using the differential labeling approach in SH-SY5Y cells depleted of Nrx compared to control cells. Included are proteins with a significantly changed redox state, i.e., p values < 0.5. The proteins are in order of the differences in the thiol-redox state, beginning with the more reduced protein thiols.

Supplementary 3. This list shows 58 cysteine-containing proteins whose abundance is significantly changed (p value < 0.5) in SH-SY5Y cells lacking Nrx. The proteins were identified using the differential labeling approach with one iodoTMT™ label and a completely reduced proteome due to addition of the reductant TCEP.

Supplementary 4. Listed are 609 potential Nrx interaction partners that were identified with the intermediate trapping approach using mNrxC208S and SH-SY5Y extracts. Included are proteins, where at least two positive iBAQ (intensity-based absolute quantification) values were recorded. The iBAQ corresponds to the sum of all the peptide intensities divided by the number of observable peptides of a protein.

Supplementary 5. Using the intermediate trapping approach with mNrxC208S and mouse brain extracts, 1710 proteins with at least two positive iBAQ values were identified.

References

[1] R. Brigelius-Flohé and L. Flohé, "Basic principles and emerging concepts in the redox control of transcription factors," *Antioxidants & Redox Signaling*, vol. 15, no. 8, pp. 2335–2381, 2011.

[2] C. Berndt, C. H. Lillig, and L. Flohé, "Redox regulation by glutathione needs enzymes," *Frontiers in Pharmacology*, vol. 5, p. 168, 2014.

[3] E.-M. Hanschmann, J. R. Godoy, C. Berndt, C. Hudemann, and C. H. Lillig, "Thioredoxins, glutaredoxins, and peroxiredoxins—molecular mechanisms and health significance: from cofactors to antioxidants to redox signaling," *Antioxidants & Redox Signaling*, vol. 19, no. 13, pp. 1539–1605, 2013.

[4] J. L. Martin, "Thioredoxin—a fold for all reasons," *Structure*, vol. 3, no. 3, pp. 245–250, 1995.

[5] J. R. Godoy, M. Funke, W. Ackermann et al., "Redox atlas of the mouse: immunohistochemical detection of glutaredoxin-, peroxiredoxin-, and thioredoxin-family proteins in various tissues of the laboratory mouse," *Biochimica et Biophysica Acta*, vol. 1810, no. 1, pp. 2–92, 2011.

[6] H. Kurooka, K. Kato, S. Minoguchi et al., "Cloning and characterization of the nucleoredoxin gene that encodes a novel nuclear protein related to thioredoxin," *Genomics*, vol. 39, no. 3, pp. 331–339, 1997.

[7] K. Lechward, E. Sugajska, I. de Baere, J. Goris, B. A. Hemmings, and S. Zolnierowicz, "Interaction of nucleoredoxin with protein phosphatase 2A," *FEBS Letters*, vol. 580, no. 15, pp. 3631–3637, 2006.

[8] Y. Funato, T. Hayashi, Y. Irino, T. Takenawa, and H. Miki, "Nucleoredoxin regulates glucose metabolism via phosphofructokinase 1," *Biochemical and Biophysical Research Communications*, vol. 440, no. 4, pp. 737–742, 2013.

[9] K. Hirota, M. Matsui, M. Murata et al., "Nucleoredoxin, glutaredoxin, and thioredoxin differentially regulate NF-κB, AP-1, and CREB activation in HEK293 cells," *Biochemical and Biophysical Research Communications*, vol. 274, no. 1, pp. 177–182, 2000.

[10] Y. Funato, T. Michiue, M. Asashima, and H. Miki, "The thioredoxin-related redox-regulating protein nucleoredoxin inhibits Wnt–β-catenin signalling through dishevelled," *Nature Cell Biology*, vol. 8, no. 5, pp. 501–508, 2006.

[11] Y. Funato, T. Michiue, T. Terabayashi et al., "Nucleoredoxin regulates the Wnt/planar cell polarity pathway in Xenopus," *Genes to Cells*, vol. 13, no. 9, pp. 965–975, 2008.

[12] Y. Funato, T. Terabayashi, R. Sakamoto et al., "Nucleoredoxin sustains Wnt/β-catenin signaling by retaining a pool of inactive dishevelled protein," *Current Biology*, vol. 20, no. 21, pp. 1945–1952, 2010.

[13] C. Berndt, C. Hudemann, E.-M. Hanschmann, R. Axelsson, A. Holmgren, and C. H. Lillig, "How does iron–sulfur cluster coordination regulate the activity of human glutaredoxin 2?," *Antioxidants & Redox Signaling*, vol. 9, no. 1, pp. 151–157, 2007.

[14] J. I. Romero, E.-M. Hanschmann, M. Gellert et al., "Thioredoxin 1 and glutaredoxin 2 contribute to maintain the phenotype and integrity of neurons following perinatal asphyxia," *Biochimica et Biophysica Acta (BBA) - General Subjects*, vol. 1850, no. 6, pp. 1274–1285, 2015.

[15] S. Stöcker, M. Maurer, T. Ruppert, and T. P. Dick, "A role for 2-Cys peroxiredoxins in facilitating cytosolic protein thiol oxidation," *Nature Chemical Biology*, vol. 14, no. 2, pp. 148–155, 2018.

[16] C. Hudemann, M. E. Lönn, J. R. Godoy et al., "Identification, expression pattern, and characterization of mouse glutaredoxin 2 isoforms," *Antioxidants & Redox Signaling*, vol. 11, no. 1, pp. 1–14, 2009.

[17] S. Sievers, S. Dittmann, T. Jordt, A. Otto, F. Hochgräfe, and K. Riedel, "Comprehensive redox profiling of the thiol proteome of *Clostridium difficile*," *Molecular & Cellular Proteomics*, vol. 17, no. 5, pp. 1035–1046, 2018.

[18] L. D. Schütte, S. Baumeister, B. Weis, C. Hudemann, E.-M. Hanschmann, and C. H. Lillig, "Identification of potential protein dithiol-disulfide substrates of mammalian Grx2," *Biochimica et Biophysica Acta (BBA) - General Subjects*, vol. 1830, no. 11, pp. 4999–5005, 2013.

[19] J. L. Biedler, L. Helson, and B. A. Spengler, "Morphology and growth, tumorigenicity, and cytogenetics of human neuroblastoma cells in continuous culture," *Cancer Research*, vol. 33, no. 11, pp. 2643–2652, 1973.

[20] F. Pontén, M. Gry, L. Fagerberg et al., "A global view of protein expression in human cells, tissues, and organs," *Molecular Systems Biology*, vol. 5, 2009.

[21] R. Brigelius-Flohé and L. Flohé, "Is there a role of glutathione peroxidases in signaling and differentiation?," *BioFactors*, vol. 17, no. 1–4, pp. 93–102, 2003.

[22] M. Deponte and C. Horst Lillig, "Enzymatic control of cysteinyl thiol switches in proteins," *Biological Chemistry*, vol. 396, no. 5, pp. 401–413, 2015.

[23] H. Mi, X. Huang, A. Muruganujan et al., "PANTHER version 11: expanded annotation data from Gene Ontology and Reactome pathways, and data analysis tool enhancements," *Nucleic Acids Research*, vol. 45, no. D1, pp. D183–D189, 2017.

[24] H. Mi, A. Muruganujan, J. T. Casagrande, and P. D. Thomas, "Large-scale gene function analysis with the PANTHER classification system," *Nature Protocols*, vol. 8, no. 8, pp. 1551–1566, 2013.

[25] N. R. Hwang, S.-H. Yim, Y. M. Kim et al., "Oxidative modifications of glyceraldehyde-3-phosphate dehydrogenase play a key role in its multiple cellular functions," *Biochemical Journal*, vol. 423, no. 2, pp. 253–264, 2009.

[26] M. Fratelli, H. Demol, M. Puype et al., "Identification by redox proteomics of glutathionylated proteins in oxidatively stressed human T lymphocytes," *Proceedings of the National Academy of Sciences of the United States of America*, vol. 99, no. 6, pp. 3505–3510, 2002.

[27] B. W. Bernstein, A. E. Shaw, L. S. Minamide, C. W. Pak, and J. R. Bamburg, "Incorporation of cofilin into rods depends on disulfide intermolecular bonds: implications for actin regulation and neurodegenerative disease," *The Journal of Neuroscience*, vol. 32, no. 19, pp. 6670–6681, 2012.

[28] Y. Samstag, I. John, and G. H. Wabnitz, "Cofilin: a redox sensitive mediator of actin dynamics during T-cell activation and migration," *Immunological Reviews*, vol. 256, no. 1, pp. 30–47, 2013.

[29] J. M. Romero, M. E. Carrizo, and J. A. Curtino, "Characterization of human triosephosphate isomerase S-nitrosylation," *Nitric Oxide*, vol. 77, no. July, pp. 26–34, 2018.

[30] S. Dumont, N. V. Bykova, G. Pelletier, S. Dorion, and J. Rivoal, "Cytosolic triosephosphate isomerase from *Arabidopsis thaliana* is reversibly modified by glutathione on cysteines 127 and 218," *Frontiers in Plant Science*, vol. 7, p. 1942, 2016.

[31] M. Zaffagnini, L. Michelet, C. Sciabolini et al., "High-resolution crystal structure and redox properties of chloroplastic triosephosphate isomerase from *Chlamydomonas reinhardtii*," *Molecular Plant*, vol. 7, no. 1, pp. 101–120, 2014.

[32] M. E. Conway, S. J. Coles, M. M. Islam, and S. M. Hutson, "Regulatory control of human cytosolic branched-chain aminotransferase by oxidation and S-glutathionylation and its interactions with redox sensitive neuronal proteins," *Biochemistry*, vol. 47, no. 19, pp. 5465–5479, 2008.

[33] S. J. Coles, P. Easton, H. Sharrod et al., "S-Nitrosoglutathione inactivation of the mitochondrial and cytosolic BCAT proteins: S-nitrosation and S-thiolation," *Biochemistry*, vol. 48, no. 3, pp. 645–656, 2009.

[34] S. Kneeshaw, R. Keyani, V. Delorme-Hinoux et al., "Nucleoredoxin guards against oxidative stress by protecting antioxidant enzymes," *Proceedings of the National Academy of Sciences of the United States of America*, vol. 114, no. 31, pp. 8414–8419, 2017.

[35] C. Wilson, E. Muñoz-Palma, and C. González-Billault, "From birth to death: a role for reactive oxygen species in neuronal development," *Seminars in Cell & Developmental Biology*, vol. 80, no. August, pp. 43–49, 2018.

Review Article

The Tryptophan Pathway Targeting Antioxidant Capacity in the Placenta

Kang Xu [ID],[1] **Gang Liu** [ID],[1] **and Chenxing Fu** [ID][2,3]

[1]*Laboratory of Animal Nutritional Physiology and Metabolic Process, Key Laboratory of Agro-ecological Processes in Subtropical Region, Institute of Subtropical Agriculture, Chinese Academy of Sciences, National Engineering Laboratory for Pollution Control and Waste Utilization in Livestock and Poultry Production, Changsha, Hunan 410125, China*
[2]*College of Animal Science and Technology, Hunan Agricultural University, Changsha, Hunan 410128, China*
[3]*Hunan Collaborative Innovation Center for Utilization of Botanical Functional Ingredients and Hunan Collaborative Innovation Center of Animal Production Safety, Changsha, Hunan 410128, China*

Correspondence should be addressed to Gang Liu; gangle.liu@gmail.com

The placenta plays a vital role in fetal development during pregnancy. Dysfunction of the placenta can be caused by oxidative stress and can lead to abnormal fetal development. Preventing oxidative stress of the placenta is thus an important measure to ensure positive birth outcomes. Research shows that tryptophan and its metabolites can efficiently clean free radicals (including the reactive oxygen species and activated chlorine). Consequently, tryptophan and its metabolites are suggested to act as potent antioxidants in the placenta. However, the mechanism of these antioxidant properties in the placenta is still unknown. In this review, we summarize research on the antioxidant properties of tryptophan, tryptophan metabolites, and metabolic enzymes. Two predicted mechanisms of tryptophan's antioxidant properties are discussed. (1) Tryptophan could activate the phosphorylation of p62 after the activation of mTORC1; phosphorylated p62 then uncouples the interaction between Nrf2 and Keap1, and activated Nrf2 enters the nucleus to induce expressions of antioxidant proteins, thus improving cellular antioxidation. (2) 3-Hydroxyanthranilic acid, a tryptophan kynurenine pathway metabolite, changes conformation of Keap1, inducing the dissociation of Nrf2 and Keap1, activating Nrf2 to enter the nucleus and induce expressions of antioxidant proteins (such as HO-1), thereby enhancing cellular antioxidant capacity. These mechanisms may enrich the theory of how to apply tryptophan as an antioxidant during pregnancy, providing technical support for its use in regulating the pregnancy's redox status and enriching our understanding of amino acids' nutritional value.

1. Background

During pregnancy, the placenta's nutrient transport and barrier functions have been shown to affect the development and health of the fetus [1]. Because of its import, risks to the placenta can result in further complications. The placenta's oxidative stress leads to metabolic abnormalities, which can generate harmful effects and impede the fetal nutrition and barrier protection functions [2]. A number of studies have indicated that oxidative stress plays an important role in preeclampsia, fetal distress, fetal growth restriction, pathological abortion, and other pregnancy-associated diseases [3].

In the placenta, syncytiotrophoblast mainly serves invasion and endocrine functions but may also be an important part of the placental barrier, ensuring optimal fetal development and pregnancy. During gestation, various factors can induce oxidative stress in syncytiotrophoblast, trophoblast, and other portions of the placenta, thus disturbing the placenta's overall functioning; even worse, these can induce pathological pregnancy [4]. For instance, unreasonable nutrient intake, inflammation, heat stress, high stocking density,

ultraviolet radiation, placental ischemia, and other harmful factors can induce oxidative stress on the placenta during pregnancy [5–8].

In addition to a myriad of external factors, there are numerous internal factors that can affect placental stress. The addition of antioxidants into a diet during pregnancy is important to improve antioxidant capacity of the placenta and fetus and is beneficial for the mother's health. Some traditional antioxidant nutrients (such as vitamin C and vitamin E) are used in the diet and can relieve oxidative stress during pregnancy [9]. However, these traditional antioxidants also have side effects at the population level, including reduced fetal weight, increased blood pressure in pregnant women, and increased risk of premature rupture of membranes [9–11]. The exploration and application of new antioxidative additives in the diet are thus important and significant to prevent oxidative stress and associated diseases during pregnancy [10, 11].

Tryptophan (Trp) is an essential amino acid in animals. It is also a precursor to many active molecules, such as serotonin, melatonin, kynurenic acid, NAD, and NAPD [12]. Studies have reported that Trp and some metabolites (melatonin, kynurenic acid, and xanthurenic acid) can act as effective antioxidants in organisms, removing reactive oxygen, reactive nitrogen, and active chlorine species and enhancing the organism's protection against free radical damage [13–15]. In endotoxic shock mice, Trp acted as an effective scavenger to clear free radicals and alleviated cellular damage caused by free radicals [16]. Watanabe et al. showed that L-Trp was an important antioxidant in the human placenta, as it helps inhibit the lipid peroxidation reaction under oxidative stress [17]. Additionally, Trp catabolism and related metabolic enzymes in the placenta were lower in patients with preeclampsia and eclampsia than in pregnant women without these conditions [18]. Animal experiments have shown that Trp supplements could reduce the mortality and abortion rate of pregnant mice infected by pseudorabies virus, improving both the fetal survival rate and the proportion of litters born alive [19].

These studies reveal that Trp can act as an effective antioxidant. However, the mechanism of how it works is still poorly understood. Accordingly, this review discusses the potential antioxidation mechanisms of Trp in the placenta and other extrahepatic tissues based on related research, with the intent of providing theoretical support and practical reference to improve the antioxidant capacity and reproductive performance of pregnant mammals by controlling Trp metabolism.

2. Antioxidant Property of Trp

In previous research, Trp has been found to be an important antioxidant in certain foods, such as eggs [20], yacon [21], and potatoes [22]. Recent studies have indicated that Trp contributes as an antioxidant in breast milk [23]. Additionally, Trp was proven to be a powerful antioxidant in *in vitro* culture tests of human glioma cells [24]. Under high-density feeding conditions, increased Trp in a diet (0.48%) may significantly improve the antioxidant capacity of ducks, which

increased glutathione peroxidase (GSH-Px) and catalase (CAT) content in the pecloralis muscles and other tissues [25]. These studies have shown that Trp is an effective antioxidant in animals.

To investigate the mechanism of Trp's antioxidation, Perez-Gonzalez et al. showed that Trp cannot be oxidized by hydrogen peroxide across a variety of chemical environments based on quantum mechanical and chemical detection methods. The antioxidant property of Trp *in vivo* is not directly attributable to the radical scavenging activity of Trp molecules per se, but rather the radical scavenging activity of some Trp metabolites [26, 27] or the activation of antioxidative systems in the body after being treated by Trp. Christen et al. demonstrated that some hydroxylated metabolites of Trp (serotonin, 3-hydroxykynurenine, xanthurenic acid, and others) possessed radical scavenging activity, but Trp did not [14].

3. Antioxidant Property of Some Trp Metabolites

In the body, tryptophan (Trp) is catabolized through two primary pathways and generates numerous bioactive molecules in the following ways: (1) by synthesizing indole derivatives, containing serotonin and melatonin, through the biosynthesis pathway of melatonin, and (2) by producing kynurenic acid, xanthurenic acid, anthranilic acid, nicotinic acid, and others through the kynurenine pathway catalyzed by tryptophan 2,3-dioxygenase (TDO) in the liver or indoleamine 2,3-dioxygenase (IDO) in the extrahepatic tissues [14, 28].

Many studies have reported the antioxidant properties of Trp metabolites, especially melatonin. Melatonin can directly remove free radicals and enhance antioxidation capacity by enhancing the expression or activity of antioxidant enzymes [15]. Richter et al. reported that melatonin increased the expression of antioxidant enzymes in the placenta, improving placental efficiency and birth weight when mothers were malnourished [29]. Wang et al. found that melatonin treatment could significantly reduce LPS-induced oxidative and hypoxia stresses in the placenta [30]. Tamura et al. found that the placenta could synthesize a small amount of melatonin, stimulating the synthesis and secretion of melatonin by the pineal gland, thus relieving oxidative stress on the placenta [31].

In the kynurenine pathway, kynurenine [14], kynurenic acid [32], xanthurenic acid [33], 3-hydroxyanthranilic acid (HA), and other Trp metabolites were shown to have the ability to effectively eliminate free radicals *in vivo* and *in vitro*. Weiss et al. found that 3-hydroxyanthranilic acid can effectively remove reactive oxygen species and active chlorine [13].

4. Antioxidant Property of Trp Metabolic Enzymes

In addition to these kynurenine metabolites, the metabolic enzymes IDO and TDO in the kynurenine pathway are also considered "scavengers" of "free radicals" and important antioxidant enzymes. TDO and IDO use superoxide anion

as a cofactor to catalyze the oxidation of Trp to kynurenines [34]. The efficiency of these two enzymes to clear free radicals is even higher than that of SOD [34]. Their enhanced activity was suggested to be a response or adaptation to oxidative stress in the body [34].

5. Trp Metabolism in the Placenta

The expression of IDO is closely associated with the formation of the placenta and is thus found in its greatest abundance in the placenta [35]. During pregnancy, as maternal Trp metabolism and utilization rates increase, plasma Trp concentration is reduced [36, 37] and the ratio of kynurenine/Trp increases throughout the pregnancy [18]. Kudo considered that these changes might be ascribed to increased IDO activity in the placenta, showing that the expression of IDO1 in the placenta increased as gestation proceeded in normal pregnancies [38].

In preeclampsia patients, the mRNA and protein expression of IDO and Trp metabolic activity decreased in the placenta. The decrease extent of Trp metabolic activity was found to be associated with the severity of the disease [39, 40]. Compared with those who were not pregnant, the ratio of plasma kynurenine/Trp was significantly increased in normal pregnant women, but showed no change in preeclampsia patients [18]. Nilsen et al. researched the antioxidant activity of IDO in the placenta and found that oxidative stress was associated with decreased IDO activity in the placenta of pregnant preeclampsia patients [41]. In addition, the mRNA expression of IDO1 was detected in cultured human placental cells *in vitro*. Expression increased after LPS stimulation [42].

6. Trp/mTORC1/Keap1-Nrf2-ARE Pathway

In terms of antioxidation, Trp plays an important regulatory role in restoring the body antioxidant system. In 2016, Jiang et al. found that the level of GSH and GPx in muscle tissue could be enhanced by feeding Trp to grass carp, verifying that some signal molecules in the Nrf2/ARE pathway and mTOR pathway were closely related to Trp-initiated increases in body antioxidant capacity [43].

6.1. Keap1-Nrf2-ARE. The nuclear factor erythroid 2-related factor 2/antioxidant response element (Nrf2/ARE) pathway is the most important endogenous antioxidant pathway in the body. It plays an important role in cellular redox homeostasis and cellular defense against oxidative stress [44–46]. In the Nrf2/ARE pathway, the transcription factor Nrf2 is a key to defense oxidative stress. At least two other essential components are required to induce protective responses and cytoprotective enzymes: (1) antioxidant response elements (AREs), cis-elements with core sequence: TGAG/CNNNGC [47], and (2) Kelch ECH association protein 1 (Keap1), a cytosolic repressor molecule that binds with Nrf2 in the cytoplasm, promoting proteasomal degradation of Nrf2 [46, 48].

At a resting state, Nrf2 and Keap1 molecules combine in the cytoplasm in a nonfree and constantly degraded inactive state. After being stimulated by signals, however, Keap1 and Nrf2 uncouple; Nrf2 transfers into the nucleus from the cytoplasm and heterodimerizes with members of the small musculoaponeurotic fibrosarcoma (Maf) family of transcription factors that bind with the antioxidant response elements (AREs), activating the expression of downstream antioxidant proteins and detoxifying enzymes [44]. Research has suggested that some antioxidant proteins have genes with the cis-element ARE in their promoter regions, such as superoxide dismutase (SOD), NADPH:quinone oxidoreductase 1 (NQO1), glutathione S-transferase A2 (GSTA2), heme oxygenase 1 (HO-1), and glutathione S-transferase (GST); these serve as target genes after Nrf2 activation [49].

In the process of Nrf2 activation, the dissociation of Nrf2-Keap1 is a key step [50]. The dissociation of Keap1-Nrf2 proceeds by two primary patterns: (1) the cysteine residues of Keap1 are modified by electrophiles, inducing a change in Keap1's conformation and a dissociation of Keap1-Nrf2 and then transferring Nrf2 into the nucleus to regulate the transcription of target genes [51], and (2) the phosphorylation of Keap1 and Nrf2 induced by protein kinase C (PKC) regulates the dissociation of Keap1-Nrf2 [50, 52].

6.2. Trp/mTORC1. The mTOR signaling pathway mainly comprises mTOR (mammalian target of rapamycin) and other series of protein kinases. mTOR participates in the composition of two structurally and functionally distinct multiprotein complexes: mTORC1 (mammalian target of rapamycin complex 1) and mTORC2 (mammalian target of rapamycin complex 2) [53]. mTORC1 is composed of the regulatory-associated protein of mTOR (raptor), a member of the FK506-binding protein (FKBP) family, FKBP38, and others [54]. Intracellularly and/or extracellularly, the mTORC1 signaling pathway can be regulated by growth factors, oxygen, energy levels, amino acids, and stress (such as endoplasmic reticulum stress, energy stress, oxidative stress, and genotoxic stress) and plays important roles in controlling numerous important cellular processes, including protein translation, lipid synthesis, stress response, and autophagy [55].

The mTORC1/S6 kinase (S6K) pathway can be activated by amino acids' entry into cells via various signaling cascades. Numerous studies have suggested that a Trp sufficiency signal was associated with activated mTOR activity in mTORC1 [56, 57]. In porcine intestinal epithelial cells, Wang et al. found that L-Trp was not catabolized but can nonetheless induce mTOR activation and increase the expression of the L-Trp transporters (solute carrier family 3 member 1 (SLC3A1), solute carrier family 6 member 14 (SLC6A14), and solute carrier family 6 member 19 (SLC6A19)) [56]. The mesenchymal stromal cells could disrupt mTOR activation by inducing the expression of indoleamine 2,3-dioxygenase (IDO) and Trp depletion, which interferes with a Trp sufficiency signal promoting cellular mTOR activation [57].

6.3. mTORC1/Keap1-Nrf2-ARE. The signaling adaptor p62 is an integral component in the central gated channel of the nuclear pore protein complex. It is also a key factor in
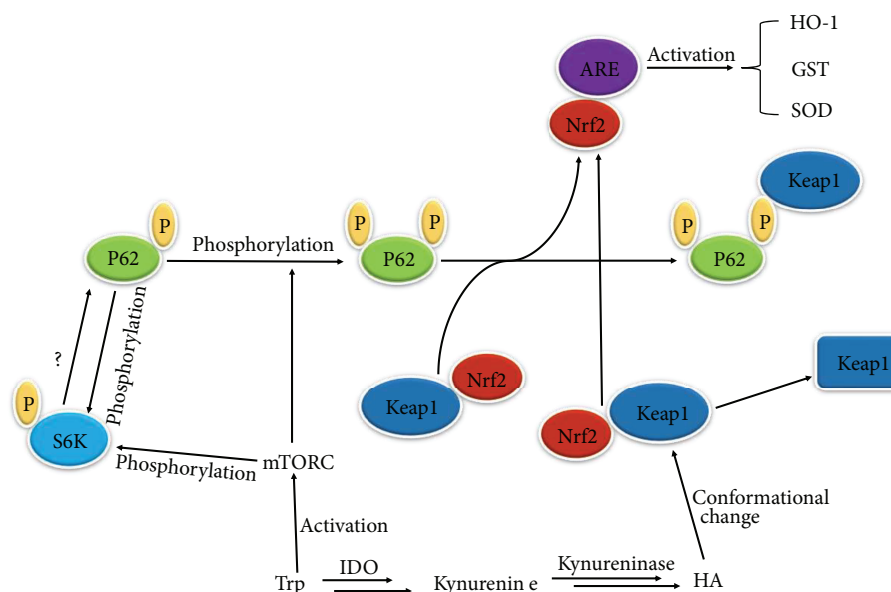
FIGURE 1: The predicted pathways where Trp exerts antioxidant effect in cell. Trp: tryptophan; IDO: indoleamine 2,3-dioxygenase; HA: 3-hydroxyanthranilic acid; HO-1: heme oxygenase 1 gene; GST: glutathione S-transferase gene; SOD: superoxide dismutase.

mediating cellular functions due to its ability to establish interactions with multiple signaling molecules [58, 59]. The protein p62 is an integral part of the mTORC1 complex and is essential for mTORC1 activation in response to amino acids. Studies have shown that in an amino acid-dependent manner, p62 interacted with mTOR and raptor in mTORC1 and mediated amino acid signaling for the activation of S6K1 and 4EBP1 [58]. In addition, p62 was essential for mTORC1 activation in response to amino acids, but may not be essential for mTORC1 activation in response to other stimulations (such as insulin-induced stimulations) [58]. In another report, direct phosphorylation of p62 was at S351 cysteine residue by the mTOR kinase via an *in vitro* kinase assay [60]. This suggests that the increased phosphorylation of p62 might directly reflect the steady-state level of mTORC1 kinase activity when p62 was higher expressing [60]. In mouse embryonic fibroblasts (MEFs), rapamycin (a specific inhibitor of the mTOR kinase) treatment could suppress both the phosphorylation of p62 and the downregulation of Keap1 [60], while also significantly inhibiting the expression of the Nrf2 target HO-1.

Meanwhile, p62 mediates the regulation of the Keap1-Nrf2-ARE signaling pathway via kinase phosphorylation and the uncoupling of the protein kinase [61]. In mouse embryonic fibroblasts, p62 enhances Nrf2 activation by impairing Keap1 activity [61]. PF-4708671, a specific inhibitor of S6K1, induces autophagic Keap1 degradation-mediated Nrf2 activation in a p62-dependent manner, indicating that p62-dependent Nrf2 activation might play a crucial role in protecting cells from PF-4708671-mediated apoptosis [61].

p62 interacts with the Nrf2-binding site of Keap1, competitively inhibiting the interaction between Keap1 and Nrf2 and then activating the expression of numerous genes to encode antioxidant proteins and anti-inflammatory enzymes [62, 63]. Meanwhile, when p62 activates Nrf2, Nrf2 can also positively upregulate the expression of p62, implying a positive feedback loop [64].

Numerous studies have shown that the activation of mTORC1 can lead to the activation of the Keap-Nrf2-ARE pathway in a p62-dependent manner [65, 66]. Ichimura et al. showed that in the mTORC1-dependent manner, the site S351 cysteine residue in p62 was phosphorylated, leading to increases in affinity between p62 and Keap1 and inducing the separation of Keap1 and Nrf2. Then, stable Nrf2 enters the nucleus and induces the expression of the cytoprotective genes [60].

Accordingly, combined with the aforementioned details that Trp could enhance the expression of numerous signal molecules in the Keap-Nrf2-ARE and mTOR pathways, we suggest that in extrahepatic tissue, Trp could activate the phosphorylation of p62 after activation of mTORC1. Phosphorylated p62 would then uncouple the interaction between Nrf2 and Keap1, with activated Nrf2 then entering the nucleus to induce expressions of antioxidant proteins, thus improving the cell's antioxidation capacity (Figure 1).

7. The 3-Hydroxyanthranilic Acid/Nrf2-Keap Pathway

Studies have indicated that the placenta was the most enriched site for indoleamine 2,3-dioxygenase (IDO) in the kynurenine pathway and that the expression of IDO is closely related to placental formation [35]. Kudo demonstrated that IDO1 expressions in the normal placenta increased along with gestational time [38]. Other studies showed that IDO mRNA and protein expression decreases with decreased Trp metabolism in the placentas of pregnant preeclampsia patients [40]. In cultured human placenta cells, the expression of IDO1 mRNA was detected and expression increased
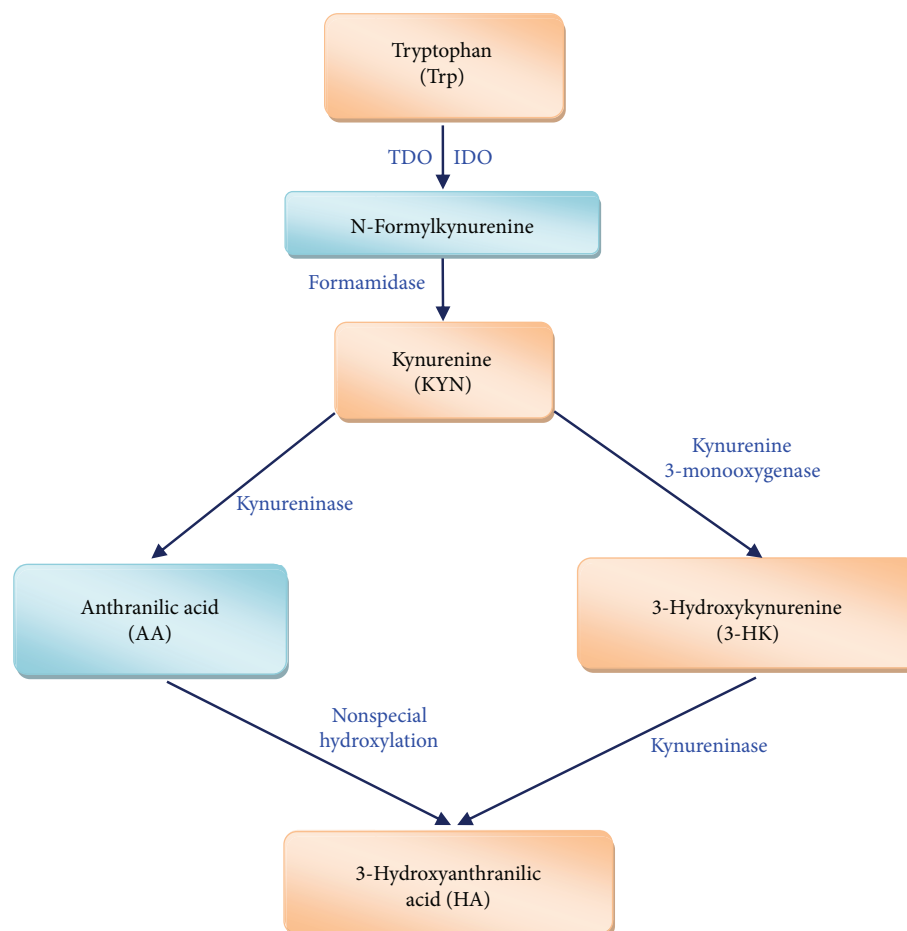
FIGURE 2: The intracellular generation pathway of 3-hydroxyanthranilic acid from tryptophan. TDO: tryptophan 2,3-dioxygenase; IDO: indoleamine 2,3-dioxygenase [19].

after LPS stimulation [42]. Research has also inferred that the induction of IDO may stimulate tissues' antioxidant defense mechanisms. Transcriptome analyses of placentas from patients with preeclampsia and normal pregnancy showed that numerous expression genes were enriched in the Trp metabolism and Nrf2-Keap pathways, indicating that Trp metabolism and the Nrf2 pathway were associated with oxidative stress in the placentas of patients with preeclampsia [67]. Therefore, variations in placental Trp metabolism may affect antioxidant activity in the placenta.

In the extrahepatic tissue, 3-hydroxyanthranilic acid (HA), one of Trp metabolites in the kynurenine pathway, is an effective antioxidant [68] (Figure 2). HA not only directly scavenges for free radicals (hydroxyl radical, peroxynitrite, and other radicals included) within certain density ranges but also induces the expression of heme oxygenase 1 (HO-1), a cellular protection and anti-inflammatory cytokine [68–70]. The capacity of HA to induce HO-1 expression has been shown to correlate with the formation of radicals induced by HA because the radical ROS is essential for the activation of Nrf2. The expression of the HO-1 at transcriptional level is controlled by numerous factors—for instance, the HO-1 promoter coordinates with several transcription-regulating elements in response to redox

sensitivity, including Nrf2-activation. In cultured human astrocytes, HA was able to effectively induce the expression of HO-1 [70]. In human microglia, HA can weakly induce HO-1 expression and LPS-suppressed microglial HO-1 expression [70]. In mammals, inducible nitric oxide synthase (iNOS) is an isoform of NOS, which catalyzes the biosynthesis of nitric oxide (NO) [71, 72]. The production of NO involves increased ROS and reactive nitrogen species (RNS), which can induce oxidative stress, cellular damage, and inflammation [72–74]. In murine macrophages, iNOS, HO-1, and IDO were simultaneously expressed after being stimulated by interferon- (IFN-) γ and LPS [69]. HA dose-dependently suppressed iNOS expression by enhancing HO-1 expression and then increased IDO expression and activity [69]. In the human umbilical vein endothelial cells, HA could induce the expression of HO-1 as an antioxidant by activating the Nrf2/ARE signal pathway and suppressing the activation of NF-κB, which affects the development of diseases such as vascular injury and aortic atherosclerotic inflammation [68].

Therefore, besides Trp activates the expressions of antioxidant proteins through activating the mTORC1 and Nrf2/ARE pathway, we also predict that HA could induce the expression of antioxidant proteins (such as HO-1) to enhance the cellular antioxidant capacity in the extrahepatic

tissues. HA, a Trp metabolite formed along the kynurenine pathway catalyzed by IDO and kynureninase, could modify and change conformation of Keap1, induce the dissociation between Nrf2 and Keap1 after which activated Nrf2 enters into the nucleus, and induce the expression of antioxidant proteins (Figure 1). These two regulation modes may coexist in the tissues or cells and operate in coordination.

8. Conclusion

Overall, although Trp is suggested to be an effective antioxidant and has been used as a functional food additive, the antioxidant efficiency and antioxidant mechanism of Trp in the organism required clarification. Meanwhile, we still lack understanding of the effects of Trp, its metabolites, and metabolic enzymes on the antioxidant properties of extrahepatic tissues. This review summarized early experiments associated with the effect of Trp's antioxidant properties (also including metabolites and metabolic enzymes) to speculate on the antioxidation mechanism of Trp in the placenta. These predicted pathways pave the way for further research on Trp's antioxidant ability in the placenta and are beneficial for further exploring its antioxidation mechanism. Future findings will be useful for recommendations for Trp additives in food as an antioxidant amino acid. The present review should provide theoretical support for practical applications: to relieve oxidative stress and thus improve the reproductive outcomes for female mammals.

Conflicts of Interest

The authors declare that there is no conflict of interest regarding the publication of this paper.

Acknowledgments

References

[1] T. Jansson and T. L. Powell, "Role of the placenta in fetal programming: underlying mechanisms and potential interventional approaches," *Clinical Science*, vol. 113, no. 1, pp. 1–13, 2007.

[2] A. S. Levine, L. Sun, R. Tan et al., "The oxidative DNA damage response: a review of research undertaken with Tsinghua and Xiangya students at the University of Pittsburgh," *Science China Life Sciences*, vol. 60, no. 10, pp. 1077–1080, 2017.

[3] E. Jauniaux, L. Poston, and G. J. Burton, "Placental-related diseases of pregnancy: involvement of oxidative stress and implications in human evolution," *Human Reproduction Update*, vol. 12, no. 6, pp. 747–755, 2006.

[4] L. Poston and M. T. M. Raijmakers, "Trophoblast oxidative stress, antioxidants and pregnancy outcome-a review," *Placenta*, vol. 25, pp. S72–S78, 2004.

[5] J. S. Drukteinis, T. Medrano, E. A. Ablordeppey, J. M. Kitzman, and K. T. Shiverick, "Benzo[*a*]pyrene, but not 2,3,7,8-TCDD, induces G2/M cell cycle arrest, p21^{CIP1} and p53 phosphorylation in human choriocarcinoma JEG-3 cells: a distinct signaling pathway," *Placenta*, vol. 26, pp. S87–S95, 2005.

[6] F. Gundogan, G. Elwood, P. Mark et al., "Ethanol-induced oxidative stress and mitochondrial dysfunction in rat placenta: relevance to pregnancy loss," *Alcoholism: Clinical & Experimental Research*, vol. 34, no. 3, pp. 415–423, 2010.

[7] S.-C. Chen, T.-L. Liao, Y.-H. Wei, C.-R. Tzeng, and S.-H. Kao, "Endocrine disruptor, dioxin (TCDD)-induced mitochondrial dysfunction and apoptosis in human trophoblast-like JAR cells," *Molecular Human Reproduction*, vol. 16, no. 5, pp. 361–372, 2010.

[8] F. Chen, "Induction of oxidative stress and cytotoxicity by PCB126 in JEG-3 human choriocarcinoma cells," *Journal of Environmental Science and Health, Part A*, vol. 45, no. 8, pp. 932–937, 2010.

[9] A. Conde-Agudelo, R. Romero, J. P. Kusanovic, and S. S. Hassan, "Supplementation with vitamins C and E during pregnancy for the prevention of preeclampsia and other adverse maternal and perinatal outcomes: a systematic review and metaanalysis," *American Journal of Obstetrics & Gynecology*, vol. 204, no. 6, pp. 503.e1–503.e12, 2011.

[10] L. Poston, A. L. Briley, P. T. Seed, F. J. Kelly, A. H. Shennan, and FRCOG for the Vitamins in Pre-eclampsia (VIP) Trial Consortium, "Vitamin C and vitamin E in pregnant women at risk for pre-eclampsia (VIP trial): randomised placebo-controlled trial," *The Lancet*, vol. 367, no. 9517, pp. 1145–1154, 2006.

[11] J. M. Roberts, L. Myatt, C. Y. Spong et al., "Vitamins C and E to prevent complications of pregnancy-associated hypertension," *New England Journal of Medicine*, vol. 362, no. 14, pp. 1282–1291, 2010.

[12] G. Liu, S. Chen, J. Zhong, K. Teng, and Y. Yin, "Crosstalk between tryptophan metabolism and cardiovascular disease, mechanisms, and therapeutic implications," *Oxidative Medicine and Cellular Longevity*, vol. 2017, Article ID 1602074, 5 pages, 2017.

[13] G. Weiss, A. Diez-Ruiz, C. Murr, I. Theur, and D. Fuchs, "Tryptophan metabolites as scavengers of reactive oxygen and chlorine species," *Pteridines*, vol. 13, no. 4, pp. 140–143, 2002.

[14] S. Christen, E. Peterhans, and R. Stocker, "Antioxidant activities of some tryptophan metabolites: possible implication for inflammatory diseases," *Proceedings of the National Academy of Sciences*, vol. 87, no. 7, pp. 2506–2510, 1990.

[15] R. J. Reiter, D. X. Tan, J. Cabrera, and D. D'Arpa, "Melatonin and tryptophan derivatives as free radical scavengers and antioxidants," in *Tryptophan, Serotonin, and Melatonin: Basic Aspects and Applications*, G. Huether, W. Kochen, T. J. Simat, and H. Steinhart, Eds., pp. 379–387, Springer, Boston, MA, USA, 1999.

[16] O. K. Bitzer-Quintero, A. J. Dávalos-Marín, G. G. Ortiz et al., "Antioxidant activity of tryptophan in rats under experimental endotoxic shock," *Biomedicine & Pharmacotherapy*, vol. 64, no. 1, pp. 77–81, 2010.

[17] S. Watanabe, S. I. Togashi, N. Takahashi, and T. Fukui, "L-Tryptophan as an antioxidant in human placenta extract," *Journal of Nutritional Science and Vitaminology*, vol. 48, no. 1, pp. 36–39, 2002.

[18] Y. Kudo, C. A. R. Boyd, I. L. Sargent, and C. W. G. Redman, "Decreased tryptophan catabolism by placental indoleamine 2,3-dioxygenase in preeclampsia," *American Journal of Obstetrics & Gynecology*, vol. 188, no. 3, pp. 719–726, 2003.

[19] K. Xu, H. Liu, M. Bai, J. Gao, X. Wu, and Y. Yin, "Redox properties of tryptophan metabolism and the concept of tryptophan use in pregnancy," *International Journal of Molecular Sciences*, vol. 18, no. 7, p. 1595, 2017.

[20] C. Nimalaratne, D. Lopes-Lutz, A. Schieber, and J. Wu, "Free aromatic amino acids in egg yolk show antioxidant properties," *Food Chemistry*, vol. 129, no. 1, pp. 155–161, 2011.

[21] X. Yan, M. Suzuki, M. Ohnishi-Kameyama, Y. Sada, T. Nakanishi, and T. Nagata, "Extraction and identification of antioxidants in the roots of yacon (*Smallanthus sonchifolius*)," *Journal of Agricultural and Food Chemistry*, vol. 47, no. 11, pp. 4711–4713, 1999.

[22] X. Xu, W. Li, Z. Lu, T. Beta, and A. W. Hydamaka, "Phenolic content, composition, antioxidant activity, and their changes during domestic cooking of potatoes," *Journal of Agricultural and Food Chemistry*, vol. 57, no. 21, pp. 10231–10238, 2009.

[23] A. Tsopmo, B. W. Diehl-Jones, R. E. Aluko, D. D. Kitts, I. Elisia, and J. K. Friel, "Tryptophan released from mother's milk has antioxidant properties," *Pediatric Research*, vol. 66, no. 6, pp. 614–618, 2009.

[24] B. N. Nayak and H. S. Buttar, "Evaluation of the antioxidant properties of tryptophan and its metabolites in in vitro assay," *Journal of Complementary and Integrative Medicine*, vol. 13, no. 2, pp. 129–136, 2016.

[25] Y. Liu, J. M. Yuan, L. S. Zhang et al., "Effects of tryptophan supplementation on growth performance, antioxidative activity, and meat quality of ducks under high stocking density," *Poultry Science*, vol. 94, no. 8, pp. 1894–1901, 2015.

[26] A. Perez-Gonzalez, L. Munoz-Rugeles, and J. R. Alvarez-Idaboy, "Tryptophan: antioxidant or target of oxidative stress? A quantum chemistry elucidation," *RSC Advances*, vol. 4, no. 99, pp. 56128–56131, 2014.

[27] A. Pérez-González, J. R. Alvarez-Idaboy, and A. Galano, "Free-radical scavenging by tryptophan and its metabolites through electron transfer based processes," *Journal of Molecular Modeling*, vol. 21, no. 8, p. 213, 2015.

[28] K. Goda, Y. Hamane, R. Kishimoto, and Y. Ogishi, "Radical scavenging properties of tryptophan metabolites," in *Tryptophan, Serotonin, and Melatonin: Basic Aspects and Applications*, G. Huether, W. Kochen, T. J. Simat, and H. Steinhart, Eds., pp. 397–402, Springer, Boston, MA, USA, 1999.

[29] H. G. Richter, J. A. Hansell, S. Raut, and D. A. Giussani, "Melatonin improves placental efficiency and birth weight and increases the placental expression of antioxidant enzymes in undernourished pregnancy," *Journal of Pineal Research*, vol. 46, no. 4, pp. 357–364, 2009.

[30] H. Wang, L. Li, M. Zhao et al., "Melatonin alleviates lipopolysaccharide-induced placental cellular stress response in mice," *Journal of Pineal Research*, vol. 50, no. 4, pp. 418–426, 2011.

[31] H. Tamura, H. Takayama, Y. Nakamura, R. J. Reiter, and N. Sugino, "Fetal/placental regulation of maternal melatonin in rats," *Journal of Pineal Research*, vol. 44, no. 3, pp. 335–340, 2008.

[32] R. Lugo-Huitrón, T. Blanco-Ayala, P. Ugalde-Muñiz et al., "On the antioxidant properties of kynurenic acid: free

[33] V. L. A. Lima, F. Dias, R. D. Nunes et al., "The antioxidant role of xanthurenic acid in the *Aedes aegypti* midgut during digestion of a blood meal," *PLoS One*, vol. 7, no. 6, article e38349, 2012.

[34] A. Britan, V. Maffre, S. Tone, and J. R. Drevet, "Quantitative and spatial differences in the expression of tryptophan-metabolizing enzymes in mouse epididymis," *Cell and Tissue Research*, vol. 324, no. 2, pp. 301–310, 2006.

[35] F. Yamazaki, T. Kuroiwa, O. Takikawa, and R. Kido, "Human indolylamine 2,3-dioxygenase. Its tissue distribution, and characterization of the placental enzyme," *Biochemical Journal*, vol. 230, no. 3, pp. 635–638, 1985.

[36] H. Schröcksnadel, G. Baier-Bitterlich, O. Dapunt, H. Wachter, and D. Fuchs, "Decreased plasma tryptophan in pregnancy," *Obstetrics & Gynecology*, vol. 88, no. 1, pp. 47–50, 1996.

[37] A. A. Badawy, "Effects of pregnancy on tryptophan metabolism and disposition in the rat," *Biochemical Journal*, vol. 255, no. 1, pp. 369–372, 1988.

[38] Y. Kudo, "The role of placental indoleamine 2,3-dioxygenase in human pregnancy," *Obstetrics & Gynecology Science*, vol. 56, no. 4, pp. 209–216, 2013.

[39] D. I. S. Santoso, P. Rogers, E. M. Wallace, U. Manuelpillai, D. Walker, and S. B. Subakir, "Localization of indoleamine 2,3-dioxygenase and 4-hydroxynonenal in normal and preeclamptic placentae," *Placenta*, vol. 23, no. 5, pp. 373–379, 2002.

[40] P. Sedlmayr, A. Blaschitz, and R. Stocker, "The role of placental tryptophan catabolism," *Frontiers in Immunology*, vol. 5, p. 230, 2014.

[41] R. M. Nilsen, A.-L. Bjørke-Monsen, Ø. Midttun et al., "Maternal tryptophan and kynurenine pathway metabolites and risk of preeclampsia," *Obstetrics & Gynecology*, vol. 119, no. 6, pp. 1243–1250, 2012.

[42] P. Dharane, U. Manuelpillai, E. Wallace, and D. W. Walker, "NFκB-dependent increase of kynurenine pathway activity in human placenta: inhibition by sulfasalazine," *Placenta*, vol. 31, no. 11, pp. 997–1002, 2010.

[43] W. D. Jiang, H. L. Wen, Y. Liu et al., "Enhanced muscle nutrient content and flesh quality, resulting from tryptophan, is associated with anti-oxidative damage referred to the Nrf2 and TOR signalling factors in young grass carp (*Ctenopharyngodon idella*): avoid tryptophan deficiency or excess," *Food Chemistry*, vol. 199, pp. 210–219, 2016.

[44] H. Kumar, I. S. Kim, S. V. More, B. W. Kim, and D. K. Choi, "Natural product-derived pharmacological modulators of Nrf2/ARE pathway for chronic diseases," *Natural Product Reports*, vol. 31, no. 1, pp. 109–139, 2014.

[45] S. P. Reddy, "The antioxidant response element and oxidative stress modifiers in airway diseases," *Current Molecular Medicine*, vol. 8, no. 5, pp. 376–383, 2008.

[46] T. Nguyen, P. Nioi, and C. B. Pickett, "The Nrf2-antioxidant response element signaling pathway and its activation by oxidative stress," *Journal of Biological Chemistry*, vol. 284, no. 20, pp. 13291–13295, 2009.

[47] E. E. Vomhof-DeKrey and M. J. Picklo Sr., "The Nrf2-antioxidant response element pathway: a target for regulating energy metabolism," *The Journal of Nutritional Biochemistry*, vol. 23, no. 10, pp. 1201–1206, 2012.

[48] K. Itoh, N. Wakabayashi, Y. Katoh et al., "Keap1 represses nuclear activation of antioxidant responsive elements by Nrf2 through binding to the amino-terminal Neh2 domain," *Genes & Development*, vol. 13, no. 1, pp. 76–86, 1999.

[49] T. W. Kensler, N. Wakabayashi, and S. Biswal, "Cell survival responses to environmental stresses via the Keap1-Nrf2-ARE pathway," *Annual Review of Pharmacology and Toxicology*, vol. 47, no. 1, pp. 89–116, 2007.

[50] K. Umemura, T. Itoh, N. Hamada et al., "Preconditioning by sesquiterpene lactone enhances H_2O_2-induced Nrf2/ARE activation," *Biochemical and Biophysical Research Communications*, vol. 368, no. 4, pp. 948–954, 2008.

[51] B. M. Dietz, D. Liu, G. K. Hagos et al., "*Angelica sinensis* and its alkylphthalides induce the detoxification enzyme NAD(P)H: quinone oxidoreductase 1 by alkylating Keap1," *Chemical Research in Toxicology*, vol. 21, no. 10, pp. 1939–1948, 2008.

[52] T. Nguyen, P. J. Sherratt, and C. B. Pickett, "Regulatory mechanisms controlling gene expression mediated by the antioxidant response element," *Annual Review of Pharmacology and Toxicology*, vol. 43, no. 1, pp. 233–260, 2003.

[53] D. Xie, S. Zhu, and L. Bai, "Lactic acid in tumor microenvironments causes dysfunction of NKT cells by interfering with mTOR signaling," *Science China Life Sciences*, vol. 59, no. 12, pp. 1290–1296, 2016.

[54] Y. Duan, F. Li, K. Tan et al., "Key mediators of intracellular amino acids signaling to mTORC1 activation," *Amino Acids*, vol. 47, no. 5, pp. 857–867, 2015.

[55] K. Uno, T. Yamada, Y. Ishigaki et al., "A hepatic amino acid/mTOR/S6K-dependent signalling pathway modulates systemic lipid metabolism via neuronal signals," *Nature Communications*, vol. 6, no. 1, p. 7940, 2015.

[56] H. Wang, Y. Ji, G. Wu et al., "L-Tryptophan activates mammalian target of rapamycin and enhances expression of tight junction proteins in intestinal porcine epithelial cells," *The Journal of Nutrition*, vol. 145, no. 6, pp. 1156–1162, 2015.

[57] M. Böttcher, A. D. Hofmann, H. Bruns et al., "Mesenchymal stromal cells disrupt mTOR-signaling and aerobic glycolysis during T-cell activation," *Stem Cells*, vol. 34, no. 2, pp. 516–521, 2016.

[58] A. Duran, R. Amanchy, J. F. Linares et al., "p62 is a key regulator of nutrient sensing in the mTORC1 pathway," *Molecular Cell*, vol. 44, no. 1, pp. 134–146, 2011.

[59] L. Wang, L. Liu, L. Qin, Q. Luo, and Z. Zhang, "Visualization of reticulophagy in living cells using an endoplasmic reticulum-targeted p62 mutant," *Science China Life Sciences*, vol. 60, no. 4, pp. 333–344, 2017.

[60] Y. Ichimura, S. Waguri, Y. S. Sou et al., "Phosphorylation of p62 activates the Keap1-Nrf2 pathway during selective autophagy," *Molecular Cell*, vol. 51, no. 5, pp. 618–631, 2013.

[61] J. S. Park, D. H. Kang, D. H. Lee, and S. H. Bae, "PF-4708671, a specific inhibitor of p70 ribosomal S6 kinase 1, activates Nrf2 by promoting p62-dependent autophagic degradation of Keap1," *Biochemical and Biophysical Research Communications*, vol. 466, no. 3, pp. 499–504, 2015.

[62] M. Komatsu, H. Kurokawa, S. Waguri et al., "The selective autophagy substrate p62 activates the stress responsive transcription factor Nrf2 through inactivation of Keap1," *Nature Cell Biology*, vol. 12, pp. 213–223, 2010.

[63] A. Lau, X.-J. Wang, F. Zhao et al., "A noncanonical mechanism of Nrf2 activation by autophagy deficiency: direct interaction between Keap1 and p62," *Molecular and Cellular Biology*, vol. 30, no. 13, pp. 3275–3285, 2010.

[64] A. Jain, T. Lamark, E. Sjøttem et al., "*p62/SQSTM1* is a target gene for transcription factor NRF2 and creates a positive feedback loop by inducing antioxidant response element-driven gene transcription," *Journal of Biological Chemistry*, vol. 285, no. 29, pp. 22576–22591, 2010.

[65] S. H. Bae, S. H. Sung, S. Y. Oh et al., "Sestrins activate Nrf2 by promoting p62-dependent autophagic degradation of Keap1 and prevent oxidative liver damage," *Cell Metabolism*, vol. 17, no. 1, pp. 73–84, 2013.

[66] J. S. Park, D. H. Kang, D. H. Lee, and S. H. Bae, "Fenofibrate activates Nrf2 through p62-dependent Keap1 degradation," *Biochemical and Biophysical Research Communications*, vol. 465, no. 3, pp. 542–547, 2015.

[67] M. Løset, S. B. Mundal, M. P. Johnson et al., "A transcriptional profile of the decidua in preeclampsia," *American Journal of Obstetrics & Gynecology*, vol. 204, no. 1, pp. 84.e1–84.e27, 2011.

[68] H. O. Pae, G. S. Oh, B. S. Lee, J. S. Rim, Y. M. Kim, and H. T. Chung, "3-Hydroxyanthranilic acid, one of l-tryptophan metabolites, inhibits monocyte chemoattractant protein-1 secretion and vascular cell adhesion molecule-1 expression via heme oxygenase-1 induction in human umbilical vein endothelial cells," *Atherosclerosis*, vol. 187, no. 2, pp. 274–284, 2006.

[69] G.-S. Oh, H.-O. Pae, B.-M. Choi et al., "3-Hydroxyanthranilic acid, one of metabolites of tryptophan via indoleamine 2,3-dioxygenase pathway, suppresses inducible nitric oxide synthase expression by enhancing heme oxygenase-1 expression," *Biochemical and Biophysical Research Communications*, vol. 320, no. 4, pp. 1156–1162, 2004.

[70] D. Krause, H.-S. Suh, L. Tarassishin et al., "The tryptophan metabolite 3-hydroxyanthranilic acid plays anti-inflammatory and neuroprotective roles during inflammation," *The American Journal of Pathology*, vol. 179, no. 3, pp. 1360–1372, 2011.

[71] L. Hannibal, R. C. Page, M. M. Haque et al., "Dissecting structural and electronic effects in inducible nitric oxide synthase," *Biochemical Journal*, vol. 467, no. 1, pp. 153–165, 2015.

[72] L. Hannibal, "Nitric oxide homeostasis in neurodegenerative diseases," *Current Alzheimer Research*, vol. 13, no. 2, pp. 135–149, 2016.

[73] M. C. Franco, V. G. A. Arciuch, J. G. Peralta et al., "Hypothyroid phenotype is contributed by mitochondrial complex I inactivation due to translocated neuronal nitric-oxide synthase," *Journal of Biological Chemistry*, vol. 281, no. 8, pp. 4779–4786, 2006.

[74] M. C. Franco and A. G. Estévez, "Reactive nitrogen species in motor neuron apoptosis," in *Amyotrophic Lateral Sclerosis*, pp. 313–334, IntechOpen, 2012.

Review Article

Hydrogen Sulfide Biochemistry and Interplay with Other Gaseous Mediators in Mammalian Physiology

Alessandro Giuffrè (ID) [1] **and João B. Vicente** (ID) [2]

[1]*CNR Institute of Molecular Biology and Pathology, Rome, Italy*
[2]*Instituto de Tecnologia Química e Biológica António Xavier, NOVA University of Lisbon, Av. da República (EAN), 2780-157 Oeiras, Portugal*

Correspondence should be addressed to Alessandro Giuffrè; alessandro.giuffre@uniroma1.it
and João B. Vicente; jvicente@itqb.unl.pt

Hydrogen sulfide (H_2S) has emerged as a relevant signaling molecule in physiology, taking its seat as a bona fide gasotransmitter akin to nitric oxide (NO) and carbon monoxide (CO). After being merely regarded as a toxic poisonous molecule, it is now recognized that mammalian cells are equipped with sophisticated enzymatic systems for H_2S production and breakdown. The signaling role of H_2S is mainly related to its ability to modify different protein targets, particularly by promoting persulfidation of protein cysteine residues and by interacting with metal centers, mostly hemes. H_2S has been shown to regulate a myriad of cellular processes with multiple physiological consequences. As such, dysfunctional H_2S metabolism is increasingly implicated in different pathologies, from cardiovascular and neurodegenerative diseases to cancer. As a highly diffusible reactive species, the intra- and extracellular levels of H_2S have to be kept under tight control and, accordingly, regulation of H_2S metabolism occurs at different levels. Interestingly, even though H_2S, NO, and CO have similar modes of action and parallel regulatory targets or precisely because of that, there is increasing evidence of a crosstalk between the three gasotransmitters. Herein are reviewed the biochemistry, metabolism, and signaling function of hydrogen sulfide, as well as its interplay with the other gasotransmitters, NO and CO.

1. Introduction

1.1. Brief Historical Account of Hydrogen Sulfide. Hydrogen sulfide (H_2S) is known in popular culture as a toxic poisonous gas and a source of foul smell, such as that of rotten eggs, sewers, swamps, and volcanic sources. Ancient alchemic practices produced several preparations now known to release hydrogen sulfide, for example, the H_2S- and ammonia-rich gases released upon distillation to obtain Liquor Hepatis (Balsam of the Soul), made from limestone and camel dung. In his treaty on workers' diseases "De Morbis Artificum," the 17th–18th century Italian physician Bernardino Ramazzini first described painful eye inflammation often leading to secondary bacterial infection and eventually blindness in workers who cleaned privies and cesspits [1]. Ramazzini hypothesized that, when the workers

stirred the excrements, an unknown volatile compound was released which, besides having the undesired health effects, was also responsible for turning black their copper and silver coins on the surface. The same toxic volatile substance, originated in the Paris sewers, was likely responsible for a series of incidents in the late 18th century, ranging from mild eye and mucous membrane inflammation to severe asphyxia. Almost at the same time, in 1777, the Swedish chemist Carl Wilhelm Scheele described the stinking substance (sulfur air) resulting from the reaction of pyrite (ferrous disulfide) with a mineral acid [2].

While long considered a poisonous substance, not only hazardous for workers but also burdensome for some industrial processes (e.g., "oil souring" in oil extraction), hydrogen sulfide was in the late 20th century discovered to be endogenously formed in humans, and in the early 21st century, it

was recognized as an extremely relevant signaling molecule in physiology and general biology.

1.2. General Chemistry of Hydrogen Sulfide. Hydrogen sulfide is a colorless flammable gas. It is a weak acid, existing in aqueous solution in equilibrium with hydrosulfide (HS^-) and sulfide (S^{2-}), according to $pK_{a1} \sim 7.0$ (H_2S/HS^-) and $pK_{a2} \sim 19$ (HS^-/S^{2-}), at 25°C ([3] and references therein). At physiological pH values, the S^{2-} concentration in solution is therefore negligible. According to this equilibrium, at the physiological pH 7.4, c.a. 70% of hydrogen sulfide is in its HS^- form, the remainder occurring as H_2S. In the alkaline mitochondrial matrix (pH 8.0), HS^- reaches 92%, while the remaining 8% corresponds to H_2S. Contrarily, under the acidic conditions in lysosomes (pH 4.7), >99% of hydrogen sulfide is in its H_2S form and is slightly polar, allowing it to freely diffuse across and accumulate in aqueous or hydrophobic milieu such as biological membranes. Herein, unless otherwise stated, the terms "hydrogen sulfide" or "sulfide" and the abbreviation "H_2S" henceforth collectively designate the pool of the H_2S, HS^-, and S^{2-} species.

H_2S is the sulfur species corresponding to the lowest sulfur oxidation state (−2). Sulfur, with its electronic configuration [Ne] $3s^2\,3p^4$, is a highly redox versatile element, with oxidation states ranging from −2 to +6 (as in sulfate), due to the six valence electrons. This versatility certainly accounts for its biological usefulness and is probably related to the major role of sulfur in the emergence and evolution of life on Earth (reviewed in [4]). H_2S is a reducing species, displaying a reduction potential of −280 mV (pH 7.0, against the standard hydrogen electrode) for the two-electron HS^-/S^0 redox couple (−230 mV for H_2S/S^0) [5], close to the values for the glutathione disulfide/glutathione (GSSG/GSH) and the cystine/cysteine redox couples.

Presently, despite major advances, the physiological H_2S concentrations are still a matter of debate, and the posited levels have been decreasing with the increasing sophistication and accuracy of the detection methods. Currently, free H_2S is reported to be submicromolar, although it may exist in equilibrium with a pool of labile sulfur-containing molecules that can liberate H_2S "on demand," that is, under particular physiological conditions [6]. To add more complexity into the role of H_2S in human (patho)physiology, it has become clear that a great part of the signaling effects attributed to H_2S (see below) actually results from the occurrence of persulfides and polysulfides, among other sulfur-containing molecules, that have been collectively termed "reactive sulfur species" (RSS). More details on the formation of persulfides and polysulfides, and their physiological relevance intertwined with that of hydrogen sulfide, are given below.

2. Hydrogen Sulfide Metabolism in Human Physiology

The reactivity and potential toxicity of hydrogen sulfide demand its levels to be kept under strict control. Indeed, even temporary imbalances in local hydrogen sulfide concentrations can trigger a cascade of cellular events with pathological consequences. The production and breakdown of H_2S is thus essentially ensured by specialized enzymes, tightly regulated and compartmentalized. Although H_2S is freely permeable to membranes and thus highly diffusible inside the cell, compartmentalization of its synthesis or breakdown could be relevant to ensure local effects in cellular organelles. A clue for this has been for instance provided by showing that the mitochondria-targeted H_2S donor AP39 ([10-oxo-10-(4-(3-thioxo-3H-1,2-dithiol-5yl)phenoxy)decyl) triphenylphosphonium bromide]), consisting of the H_2S-releasing moiety ADT-OH (5-(4-hydroxyphenyl)-3H-1,2-dithiole-3-thione)coupled to the mitochondria-targeting triphenylphosphonium (TPP$^+$) moiety, protects mitochondria in oxidatively stressed endothelial cells more effectively than ADT-OH itself, not coupled to TPP$^+$ and thus unable to specifically target mitochondria [7]. Despite decades of molecular and cellular studies on the enzymatic systems involved in H_2S synthesis and breakdown, it appears at times that this field of biology is still in its infancy, with new reactive molecules and new targets of H_2S and related species being consistently identified and new mechanistic details and regulatory subtleties being unraveled.

2.1. Human H_2S-Synthesizing Enzymes. The biogenesis of hydrogen sulfide in human physiology occurs via two major routes: by endogenous specialized enzymes and as an end-product or intermediate of microbial metabolic pathways within the gut microbiota, particularly in sulfate-reducing bacteria. Interestingly, by comparing germ-free versus conventional mice, it was shown that the intestinal microbiota regulates H_2S homeostasis not only in the gut but also systemically in various tissues and organs [8]. Namely, the presence of microbiota was found to be associated with higher levels of free H_2S not only in some intestinal tracts (colon and cecum) but also in plasma. Moreover, as compared to germ-free mice, the conventional animals displayed higher levels of bound sulfane sulfur in plasma, fat, and lung, and higher CSE activity and reduced cysteine levels in most organs and tissues [8]. Another secondary source of H_2S is proposed to be persulfides and polysulfides, either endogenously generated or derived from dietary intake (reviewed in, e.g., [9]).

The three human enzymes reported to endogenously generate hydrogen sulfide are cystathionine β-synthase (CBS), cystathionine γ-lyase (CSE, also known as cystathionase), and 3-mercaptopyruvate sulfurtransferase (MST) (Figure 1) [10].

2.1.1. Expression in Cells and Tissues and Cellular Localization. The occurrence of all three H_2S-synthesizing enzymes in cells, tissues, and organs and their cellular distribution remain evolving subjects, particularly taking into account that these may vary under different (patho)physiologic conditions. It is generally considered that CBS regulation occurs at the protein level, the enzyme being a target of multiple posttranslational modifications and having two regulatory domains that respond to different stimuli (reviewed, e.g., in [11]), unlike CSE, for which no posttranslational regulatory mechanisms are known [10]. Moreover, since CBS and CSE employ various combinations of
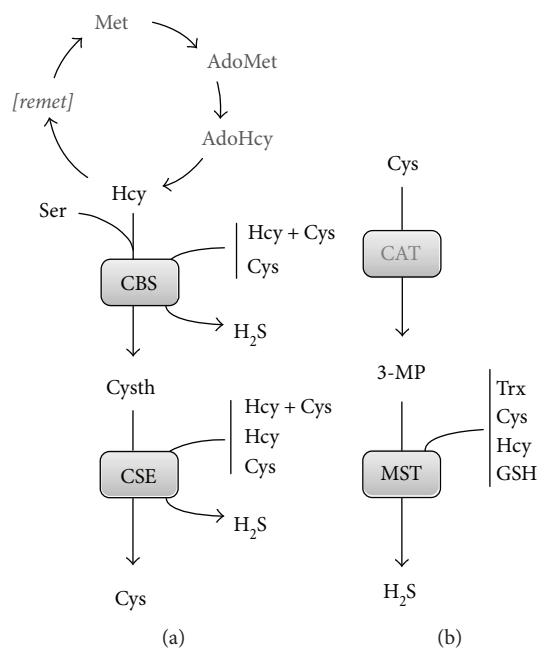
FIGURE 1: Hydrogen sulfide biosynthetic pathways in mammalian physiology. (a) Transsulfuration branch of the methionine cycle. L-Methionine (Met) is converted by L-methionine adenosyltransferase to s-adenosyl-L-methionine (AdoMet), which is used by methyltransferases in methylation reactions, generating s-adenosyl-L-homocysteine (AdoHcy). AdoHcy hydrolase then converts AdoHcy into L-homocysteine (Hcy), which can either be converted back to L-methionine through the remethylation cycle ([remet]), or enter the transsulfuration branch. Cystathionine β-synthase (CBS) converts Hcy and L-serine into L-cystathionine (Cysth), which is taken up by cystathionine γ-lyase (CSE) to generate L-cysteine (Cys). Hydrogen sulfide (H_2S) is synthesized by CBS and CSE in several alternative reactions (see Figure 2). (b) H_2S synthesis by 3-mercaptopyruvate sulfurtransferase (MST). Cys is converted by cysteine aminotransferase (CAT) into 3-mercaptopyruvate (3-MP), which is used by MST to synthesize H_2S along with its cosubstrates thioredoxin (Trx), Cys, Hcy, and l-glutathione (GSH).

the same substrates in their H_2S-generating reactions (Figures 1 and 2), regulation of one enzyme will likely affect the other, due to increased or decreased substrate availability (e.g., in [11]).

The tissue and organ distribution of the H_2S-synthesizing enzymes has been studied for different organisms, employing immunohistochemical detection and analyzing transcriptional levels and H_2S-generating activity. In man and rodents, CBS is mostly abundant in the liver, pancreas, kidney, brain, and nervous system [9, 12–14]. Recently, CBS expression in the carotid body, as well as in uterine and mesenteric and umbilical arteries, was reported [15]. As for CSE, it is mostly expressed in the liver, kidney, and smooth muscle (both vascular and nonvascular), its expression and H_2S-generating activity being negligible in the brain, heart, and spleen [9, 13, 16, 17]. MST tissue distribution has been systematically studied for different organisms. The activity of bovine MST has been reported to be highest in the adrenal cortex, followed by the liver, heart, and kidney [18]. Abundant rat MST expression has

been detected in the kidney (proximal tubular epithelium), liver (pericentral hepatocytes), aorta, and brain glial cells [19]. Recently, Tomita et al. detected abundant murine MST in the brain (neural and glial cells), liver, kidney, testes, and endocrine organs (particularly in pancreatic islets) and lower levels in bronchiolar cells, spleen, thymus, and small intestine [20]. Finally, Western blot analysis and enzymatic assays revealed the presence of active MST, but undetectable CBS and CSE, in red blood cells [21].

In terms of cellular localization, the classical view is that both CBS and CSE are cytosolic enzymes, whereas MST localizes to the mitochondria (e.g., [9, 10, 22]). However, several examples show that this classical view may be challenged. It has been reported that when blood homocysteine levels rise, microvascular endothelial cells and hepatocytes may secrete CBS and CSE, thus circulating as part of the plasma proteome and contributing to H_2S generation [23]. Extracellularly synthesized H_2S was shown to contribute to increased cell viability and decreased oxidative damage to DNA after serum starvation and hypoxia/reoxygenation. Furthermore, immunoprecipitation of circulating CBS and CSE from serum prior to its supplementation with homocysteine enhanced serum-induced stress towards endothelial cells. Altogether, these observations suggest that secreted CBS and CSE have a protective role in the endothelium by both producing H_2S and clearing excess homocysteine. Another notable characteristic of CBS is its ability to be SUMOylated leading to protein accumulation in the nucleus [24]. Perhaps of greatest significance for their role as H_2S-synthesizing enzymes is the observation that both CBS and CSE can translocate to the mitochondria under various (patho)-physiological conditions. This becomes particularly relevant taking into account that H_2S can not only stimulate mitochondrial bioenergetics (i) by supplying electron equivalents to the quinol pool via sulfide:quinone oxidoreductase (reviewed in [10, 25]), (ii) by activating the glycolytic enzyme glyceraldehyde 3-phosphate dehydrogenase [26], and (iii) by persulfidation of ATP synthase [27, 28] but also block mitochondrial respiration by tight inhibition of cytochrome c oxidase (CcOX, reviewed in [29–31]). CBS has been observed to partially localize to liver mitochondria, where the protein transiently accumulates under hypoxia/ischemia, with the resulting increased H_2S generation protecting mitochondria from oxidative stress [32]. Once cells return to normoxia, CBS levels are restored via protein degradation by mitochondrial Lon protease, which recognizes and targets specifically the oxidized form of the regulatory heme at the CBS N-terminal domain [32].

In the colorectal cancer cell line HCT 116, a significant fraction of CBS localizes to the mitochondria, being associated with the outer mitochondrial membrane. The resulting increased H_2S levels are proposed to stimulate cancer cell energy metabolism, particularly oxidative phosphorylation and glycolysis [33]. In line with this observation, CBS has been shown to contribute in various cancer cells to a shift in the fate of glucose utilization from glycolysis to the pentose phosphate pathway [34] (detailed in Section 4.3.1). By also promoting tumor angiogenesis, the increased H_2S availability may contribute to increased oxygen supply to tumor cells.
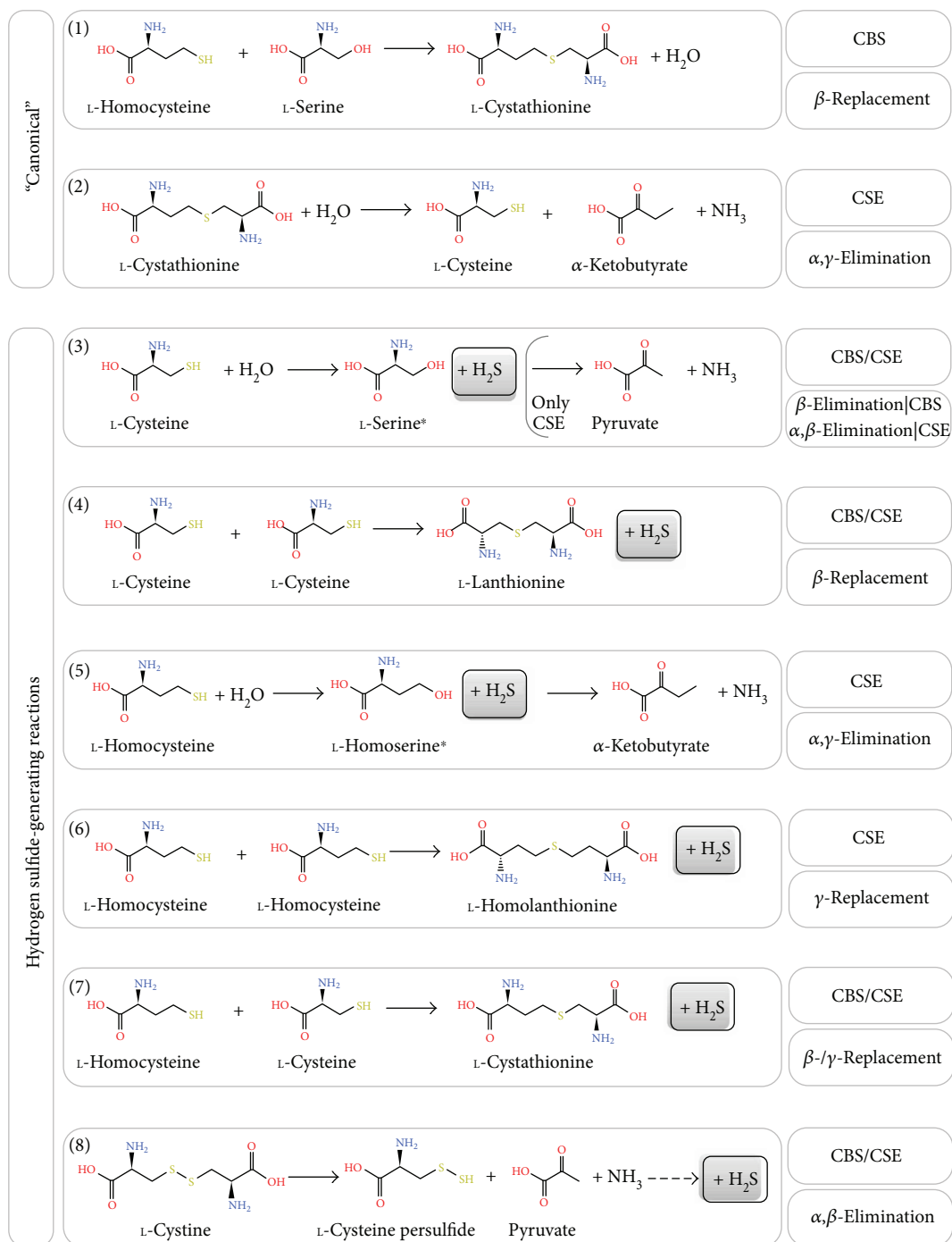
FIGURE 2: Catalytic versatility of the H$_2$S-synthesizing enzymes cystathionine β-synthase (CBS) and cystathionine γ-lyase (CSE). Chemical structure of the metabolites and reaction schemes involved in H$_2$S synthesis by CBS and CSE. Top panel, "canonical" reactions catalyzed by CBS and CSE as part of the transsulfuration branch of the methionine cycle. Center-bottom panel, alternative H$_2$S-generating reactions. Chemical structures labeled as α-ketobutyrate and pyruvate are represented as the α-ketobutyric and pyruvic acid, respectively. *Serine and homoserine have not been detected as intermediates in the CSE-catalyzed reactions 3 and 5, respectively, only their downstream products α-ketobutyric and pyruvic acids (resp.).

In a mouse model of amyotrophic lateral sclerosis, CBS accumulation in mitochondria isolated from the spinal cord and the resulting increased H$_2$S generation are proposed to be related with impaired cytochrome c oxidase-dependent respiration [35].

CSE has been reported to translocate to the mitochondria of vascular smooth muscle cells (SMCs) in response to stimuli that increased intracellular calcium levels. This translocation appears to be mediated by the mitochondrial membrane translocase of the outer membrane 20 (Tom20).

Whereas SMCs display impaired ATP production in hypoxic conditions, the presence of CSE inside the mitochondria contributed to cysteine catabolism, H$_2$S synthesis, and stimulated ATP synthesis under such conditions, suggesting that CSE translocation may sustain mitochondrial bioenergetics in response to certain stresses [28].

MST is generally regarded as a mitochondrial enzyme. However, Fräsdorf et al. have shown that there are actually two splice variants of the protein, MST-Iso1 and MST-Iso2, both of which localize to the cytosol, while only MST-Iso2 also localizes to the mitochondria in HEK293a and HeLa cells [36].

2.1.2. Associated Metabolic Pathways. CBS and CSE participate in the transsulfuration branch of the methionine methylation/remethylation cycle (Figure 1(a)), a key pathway which generates extremely relevant signaling molecules for mammalian physiology. In this cycle, methionine (Met) derived essentially from dietary intake is converted to *s*-adenosyl-*L*-methionine (AdoMet) by methionine adenosyltransferase ([37] and references therein). AdoMet is the methyl group donor for virtually all methylation reactions in mammalian physiology, through the action of methyltransferases. Concurrently with methylation, *s*-adenosyl-*L*-homocysteine (AdoHcy) is generated, which is used by AdoHcy hydrolase (SAHH) to produce homocysteine (Hcy) and adenosine. Homocysteine then either enters the transsulfuration branch or proceeds through the remethylation pathway to revert to methionine, depending on different metabolic fluxes and other physiological conditions. The metabolites AdoMet, AdoHcy, and Hcy participate in the regulation of numerous physiological processes. As detailed below, AdoMet is an allosteric regulator of CBS, increasing its enzymatic activity by 2–5-fold upon binding. This allosteric activation results in an increase in $V_{\max}$, without any notable effect on the substrate affinity (K_M) [38, 39]. The "canonical" reactions attributed to CBS and CSE within the transsulfuration pathway result in conversion of homocysteine into cysteine as follows (Figure 2): CBS catalyzes the β-replacement of serine by homocysteine, yielding cystathionine, and CSE then proceeds by converting cystathionine to cysteine, α-ketobutyrate, and ammonia in an α,γ-elimination reaction. The role of CBS and CSE in hydrogen sulfide production results from an extensive repertoire of alternative reactions that these enzymes are able to catalyze (Figure 2) [39, 40], possibly related to the fact that both are pyridoxal 5′-phosphate-(PLP-) dependent enzymes. This may be perceived as catalytic promiscuity or versatility-based robustness [11]. A notable thorough *in vitro* kinetic characterization of CBS- and CSE-catalyzed H$_2$S-generating reactions combined with kinetic simulations has been carried out by Singh et al., allowing to envisage which reactions are relevant *in vivo* under different (patho)physiological conditions [39]. Both CBS and CSE are able to synthesize H$_2$S through cysteine β-elimination or β-replacement, respectively employing one or two cysteine molecules (Figure 2, reactions (3) and (4)), or through β- or γ-replacement using cysteine and homocysteine (Figure 2, reaction (7)). CSE alone is able to synthesize H$_2$S via homocysteine α,γ-elimination or γ-replacement,

respectively employing one or two homocysteine molecules (Figure 2, reactions (5) and (6)). Both CBS and CSE also catalyze cystine α,β-elimination to yield cysteine persulfide, which ultimately may generate H$_2$S (Figure 2, reaction (8)). Besides H$_2$S synthesis, some of these reactions originate thioether metabolites such as lanthionine and homolanthionine, which may have been suggested as biomarkers of hydrogen sulfide generation in homocystinuric patient samples [41]. Under substrate saturating conditions, the turnover number of recombinant human CBS for the H$_2$S-generating cysteine and homocysteine β-/γ-replacement reaction (reaction (7) in Figure 2) is 3.7-fold higher than that of the cystathionine-generating canonical reaction [39]. Kinetic simulations show that this difference drops to 1.3-fold at physiologically relevant substrate concentrations, which still indicates that CBS-catalyzed H$_2$S synthesis at the expense of homocysteine and cysteine accounts for ~56% of cystathionine production. Notably, reaction (7) is responsible for 96% of the net CBS-catalyzed H$_2$S production, whereas the cysteine-alone-based reactions (reactions (3) and (4) in Figure 2) account for a mere 1.6–2.6% of H$_2$S synthesis. Still, the H$_2$S-producing capacity of CBS appears to be insensitive to the systemic homocysteine levels, possibly related to the fact that homocysteine can only bind to CBS after serine or cysteine. The same kinetic simulations show that, contrarily to CBS, CSE catalyzes the canonical reaction of cysteine synthesis via cystathionine α,γ-elimination (reaction (2) in Figure 2) with a much higher (20–30 fold) catalytic efficiency (k_{cat}/K_M) than determined for the H$_2$S-synthesizing reactions (reactions (3–6) in Figure 2). At physiologically relevant substrate concentrations (10 μM homocysteine, 100 μM cysteine, and 5 μM cystathionine), the canonical reaction turnover is still 5-fold or 12-fold higher than those for H$_2$S-generating cysteine or homocysteine cleavage reactions, respectively. Under those conditions, approximately 70% of CSE-catalyzed H$_2$S production derives from cysteine and 29% from homocysteine. Also in contrast with CBS, the CSE-catalyzed H$_2$S generation depends on homocysteine availability. Indeed, kinetic simulations assuming equimolar CBS (fully activated by AdoMet) and CSE at "normal" homocysteine concentrations (10 μM) reveal that CSE contributes to 32% of the synthesized H$_2$S, whereas the CSE contribution increases to 45% and 74% under conditions of moderate and severe hyperhomocysteinemia, respectively. This indicates that CSE may have a significant role in homocysteine clearance at pathophysiological elevated homocysteine levels, particularly in tissues or organs where CBS is absent or poorly expressed.

Recently, Majtan et al. reported on a thorough kinetic analysis of CBS-catalyzed reactions combined with simulations [38]. This study demonstrated the competitive advantage of serine over cysteine as a substrate for its condensation with homocysteine (to yield H$_2$O or H$_2$S, resp.), with a 2–5-fold higher catalytic efficiency of the canonical reaction compared to the H$_2$S-generating reaction. However, despite this apparent advantage at saturating substrate concentrations, the H$_2$S-producing reaction is able to compete with the canonical reaction under physiologically relevant conditions [38]. Indeed, one of the key findings is that a main determinant

(a)

(b)
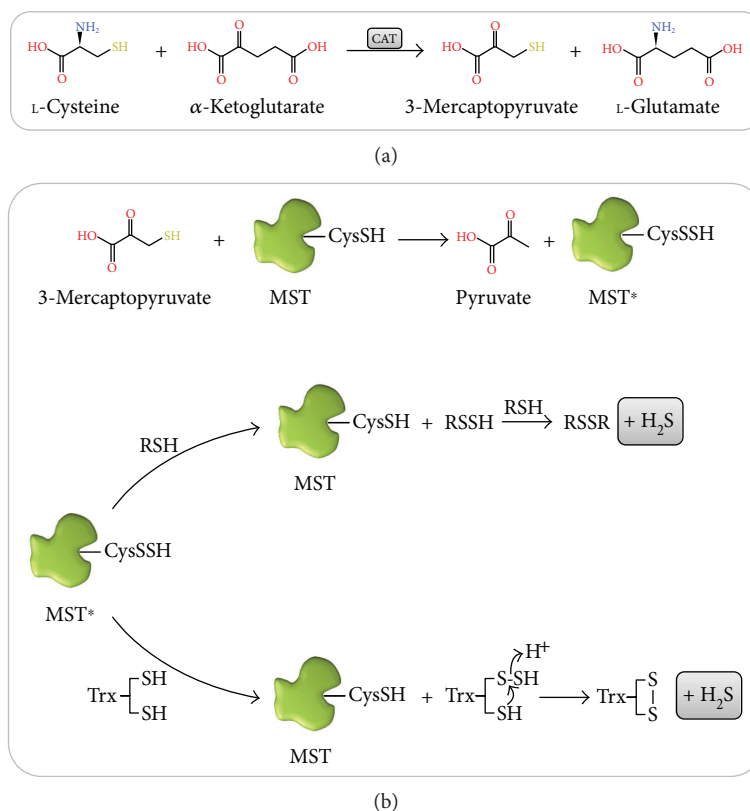
FIGURE 3: Reaction mechanism of H$_2$S production by 3-mercaptopyruvate sulfurtransferase (MST). Chemical structure of the metabolites and reaction schemes involved in H$_2$S synthesis by MST. (a) Production of 3-mercaptopyruvate (3-MP) is catalyzed by cysteine aminotransferase (CAT), with α-ketoglutarate as cosubstrate. (b) MST reaction with its activating substrate 3-MP and acceptor substrates. Upon reacting with 3-MP, the side-chain sulfhydryl of Cys$_{248}$ (CysSH) becomes persulfidated (CysSSH), which activates MST (MST*) towards the reaction with the acceptor substrates. The reaction with low-molecular-weight (LMW) thiol-containing substrates (RSH) involves the sequential reaction with two substrate molecules. In the first step, MST* transfers the sulfane sulfur from the cysteine persulfide to the RSH, regenerating the enzyme and releasing a persulfide RSSH product. In the second step, another RSH reacts with RSSH to yield H$_2$S and oxidized RSSR. The reaction of MST* with reduced thioredoxin (Trx) proceeds similarly to that with LMW RSH molecules. The MST cysteine persulfide is initially transferred to Trx, yielding CysSSH, which is then attacked by a nearby cysteine thiol, releasing H$_2$S and yielding oxidized Trx. Chemical structures labeled as α-ketoglutarate, 3-mercaptopyruvate, and L-glutamate are represented as α-ketoglutaric, 3-mercaptopyruvic, and L-glutamic acids, respectively.

of CBS-catalyzed H$_2$S production is the cysteine to serine ratio, adding another layer of complexity to be taken into account when considering the *in vivo* role of each H$_2$S-producing enzyme.

Despite the remarkable value of these kinetic studies, H$_2$S generation obviously also depends on the relative expression levels of each enzyme in each cell/tissue and on the systemic and local availability of substrates (cysteine, homocysteine, cystine, and serine), regulatory metabolites (e.g., AdoMet), and other effectors which negatively modulate enzymatic activity (e.g., NO and CO inhibit CBS; detailed below).

The role of 3-mercaptopyruvate sulfurtransferase (MST) is also tightly associated with cysteine metabolism. 3-Mercaptopyruvate (3-MP) is generated by cysteine (or aspartate) aminotransferase (CAT, Figure 3(a)) through cysteine deamination, using α-ketoglutarate as cosubstrate and yielding glutamate as coproduct [10]. An additional pathway whereby 3-MP is generated has been recently demonstrated to be present mostly in the cerebellum and the kidney, involving D-cysteine and a D-amino acid oxidase [42].

The interaction between MST and its 3-MP substrate gives rise to an enzyme-bound cysteine persulfide intermediate at Cys$_{248}$ (MST* in Figure 3(b)), concomitantly with pyruvate release [43]. H$_2$S can then be released by transfer of the active site cysteine persulfide to physiologic small thiols like cysteine, homocysteine, and glutathione or reducing molecules such as thioredoxin (Trx) or dihydrolipoic acid (DHLA) or by reaction with nonphysiological reductants like 2-mercaptoethanol and dithiothreitol [43]. The MST persulfide intermediate transfers its persulfide to an acceptor R-SH, forming an R-S-SH intermediate, which then reacts with another acceptor RSH molecule to yield a disulfide (RSSR) and H$_2$S. From the tested physiological acceptor substrates, thioredoxin displays the highest catalytic efficiency, orders of magnitude higher than those for DHLA, cysteine, homocysteine, and glutathione [43]. This observation is consistent with the observation that some protozoan parasites encode MST variants with a fused thioredoxin domain.

The broad impact of H$_2$S on mammalian physiology has been widely assessed in numerous *in vivo* studies,

utilizing knockout mouse models of the three H$_2$S-synthesizing enzymes CBS, CSE, and MST and of ethylmalonic encephalopathy protein 1 (ETHE1, also known as persulfide dioxygenase or sulfur dioxygenase), implicated in H$_2$S breakdown. Making use of these models, particularly the ones for CSE and CBS, H$_2$S has been shown to take part in a huge number of physiological and pathophysiological processes and thus to have a high impact on human health and disease. For a comprehensive overview of the wide spectrum of studies carried out on these models, the readers can refer to [9], a recent review specifically addressing this topic.

2.1.3. Structural and Functional Properties of H$_2$S-Generating Enzymes

(1) Cystathionine β-Synthase (CBS). Human cystathionine β-synthase (CBS) is considered to assemble as a homotetramer of 551 amino acid-long (~61 kDa) monomers, each consisting of three domains (Figure 4(a)): an N-terminal domain (residues 1–70) that binds a noncatalytic heme cofactor, a central catalytic PLP-binding domain (residues 71–381), and a C-terminal regulatory domain (residues 412–551, also known as Bateman module, comprising two motifs, CBS1 and CBS2) responsible for enzyme activation upon AdoMet binding. Structural studies on the human enzyme have revealed that the catalytic domain has a highly conserved structural fold of the β-family of PLP-dependent enzymes, consisting of thirteen α-helices and two β-sheets composed of four and six strands [44, 45]. Several intrinsically flexible regions that were initially not visible in the structure of a truncated human CBS lacking the C-terminal domain became visible in the structure of a "full-length" CBS construct (with a 10-residue deletion at the C-terminus, (Figure 4(a)). These include the strands β4, β5, and β6 preceding the loops L145–148, L171–174, and L191–202, which are proposed to constitute the catalytic site entrance (together with loop L295–316) and are stacked between the catalytic core and the C-terminal domain, as well as helix α7 following the L191–202 loop. The active site PLP moiety is bound to the catalytic core through a Schiff base bond to the ε-amino group of lysine 119 (Figure 4(b)). A long 30-residue α-helical stretch (residues 382–411; helices α15 and α16) tethers the catalytic core to the C-terminal AdoMet-binding domain. The latter actually comprises two so-called CBS domains which share a common structural fold despite the poor sequence identity (~7% over 133 residues). The key finding in the structure of full-length CBS was the revelation that, in AdoMet-free CBS, the C-terminal domain from one monomer blocks the substrate entry site of the opposing monomer within one dimer (Figure 4(c)) [44]. This blockage is accomplished by stabilization of the above mentioned intrinsically flexible region composed by the β4, β5, and β6 strands preceding the loops L145–148, L171–174, and L191–202. Indeed, the interaction between the core and regulatory domains has been shown to involve (i) hydrophobic interactions with residues from the C-terminal domain CBS2 motif and (ii) H-bonds with residues from the C-terminal domain CBS1 motif [44, 46]. Notably, in the presence of AdoMet, the two C-terminal domains assemble

(a)

(b)

(c)
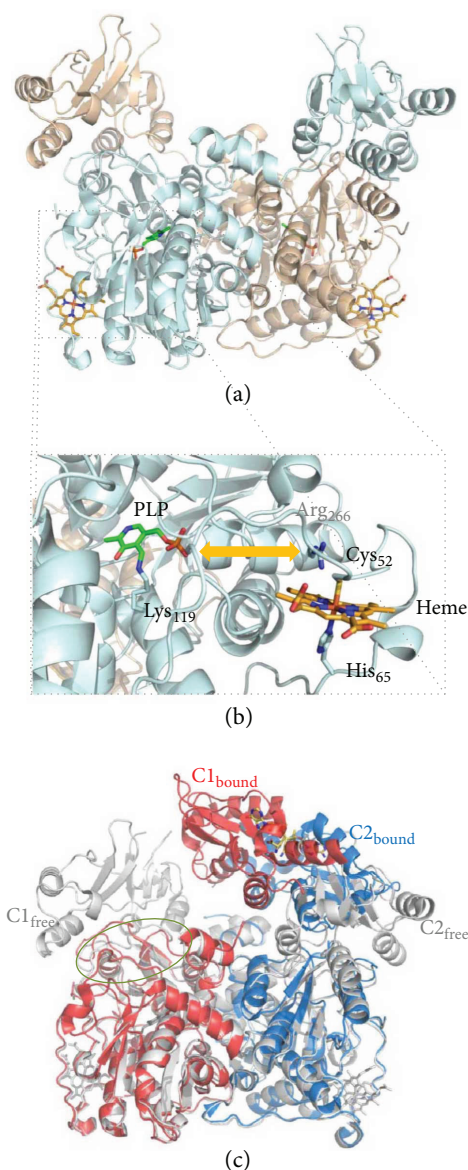
FIGURE 4: Crystallographic structure of human cystathionine β-synthase (CBS). (a) Cartoon representation of the "full-length" human CBS homodimer (PDB ID: 4COO; Δ516–525; 2.0 Å resolution). Green sticks, active site PLP moiety, where H$_2$S production occurs. Orange sticks, regulatory heme *b* where CO or NO binds, resulting in enzyme inhibition. (b) Zoom-in into the catalytic (PLP) and regulatory (heme) sites. The PLP moiety is covalently attached to CBS through Lys$_{119}$ (human CBS numbering), while the *b*-type heme is axially coordinated by Cys$_{52}$ and His$_{65}$. Orange arrow indicates the communication between the heme and PLP sites mediated by the α-helix comprising residues Thr$_{257}$-Gly$_{258}$-Gly$_{259}$-Thr$_{260}$-Ile$_{261}$-Thr$_{262}$-Gly$_{263}$-Ile$_{264}$-Ala$_{265}$-Arg$_{266}$. (c) Structural effect of AdoMet binding. While in AdoMet-free CBS, the C-terminal domain of each monomer (C1$_{free}$ and C2$_{free}$, colored in light gray) blocks the substrate entrance into the active site (green oval circle) of the adjacent monomer, AdoMet binding to the C-terminal domains leads to association of the latter in a disk-like form (C1$_{bound}$ and C2$_{bound}$; PDB ID: 4PCU; Δ516–525 Glu201Ser; 3.58 Å resolution), unblocking the active site and derepressing the enzymatic activity. Figure generated with PyMol 1.8.2.0 [238].

together in a "disc"-like form, similarly to the constitutively activated *Drosophila melanogaster* AdoMet-free CBS [47], the substrate entrance opens, and access to the active site is enhanced (Figure 4(c)), thus increasing enzymatic activity [44, 46, 48]. Each Bateman module contains two putative AdoMet-binding cavities (S1 and S2) with different binding affinities [49]. One of these cavities (S2) is exposed and thus likely represents the primary AdoMet binding site, while the other one (S1) appears to be hindered by bulky hydrophobic residues from the catalytic core [46, 48, 49]. The AdoMet-induced association between adjoining Bateman modules disrupts the interactions between the catalytic and C-terminal regulatory domains and opens the catalytic core to the substrates.

(2) Cystathionine γ-Lyase (CSE). Cystathionine γ-lyase (CSE) is a homotetrameric enzyme constituted by 405-amino-acid-long ~44 kDa monomers, each consisting of two structural domains (Figure 5(a)) [50]. The larger PLP-binding catalytic domain (comprising residues 9–263) assembles as an $\alpha/\beta/\alpha$ fold consisting of a seven-stranded β-sheet (6 parallel and 1 antiparallel) flanked by eight α-helices. The smaller C-terminal domain (residues 264–401) is composed of a β-sheet (4 antiparallel strands) with three helices on one side. Similarly to CBS, the PLP in CSE is anchored through a Schiff base bond between the PLP carbonyl and the ε-amino group of a lysine residue (Lys_{212}) (Figure 5(b)), although other forces are at play to stabilize PLP: π-stacking interactions between the Tyr_{114} phenyl moiety and the PLP pyridine ring, and H-bonds between the PLP phosphate moiety and residues Gly_{90}, Leu_{91}, Ser_{209}, and Thr_{211} from the same subunit and Tyr_{60} and Arg_{62} from the adjacent subunit. Structural studies on CSE in the presence of its inhibitor propargylglycine (PPG) attempted to explain its mode of action [50]. While the lysine-PLP bond appears to remain unaffected, PPG is proposed to covalently bind to Tyr_{114}, becoming a vinyl ether, while also forming H-bonds between its amino group and Glu_{339} and between its carboxyl moiety and Arg_{119} and Arg_{62} from the other monomer. This static position of the covalently bound PPG vinyl ether is such that it extends towards the internal PLP aldimine, thus blocking the cofactor reactivity [50].

(3) Mercaptopyruvate Sulfurtransferase (MST). Human mercaptopyruvate sulfurtransferase (MST) is composed of 297 amino acid residues and assembles as a ~33 kDa monomer consisting of two structurally related domains with a rhodanese-like fold (Figure 6(a)) [43]. The N-terminal (residues 1–138) and C-terminal (residues 165–285) domains are tethered by a 26-amino acid linker that strongly interacts with both domains. The assembly of these structurally related domains could have arisen from gene duplication. Structural studies of MST in the presence of its 3-MP substrate have shown that it binds to cysteine 248 in the active site, which is located in a cleft between the two domains (Figure 6(b)) [43]. The reaction originates a persulfidated CysSSH-activated intermediate. Despite the significant substrate-induced chemical modification of the active site, a comparison between the structures of MST with

(a)

(b)
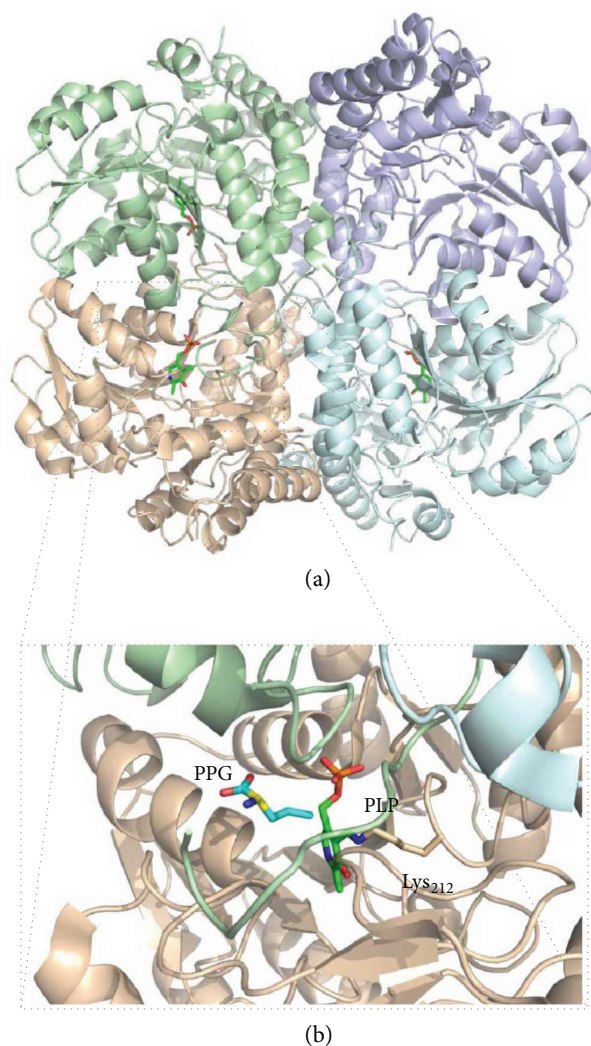
FIGURE 5: Crystallographic structure of human cystathionine γ-lyase (CSE). (a) Cartoon representation of human CSE homotetramer (PDB ID: 3COG; 2.0 Å resolution) cocrystallized with the inhibitor propargylglycine (PPG). Each chain is represented in a different colour. Green sticks, active site PLP moiety where H_2S production occurs. (b) Zoom-in into the catalytic PLP site. The PLP moiety (green sticks) is covalently attached to CSE through Lys_{212} (human CSE numbering); PPG is represented in blue sticks. Figure generated with PyMol 1.8.2.0 [238].

and without bound 3-MP reveals that no major structural differences occur [43]. In a recent report on a compound screening campaign targeting MST, the structures of MST in complex with hit compounds revealed a strong interaction between the persulfidated Cys_{248} and the inhibitors' pyrimidone-like aromatic rings [51], without major structural changes.

2.2. H₂S Catabolism

2.2.1. H₂S: A "Self-Regulatory" Janus Molecule for Cellular Bioenergetics. As mentioned above, while playing a key signaling role only at relatively low, physiological concentrations, at higher concentrations H_2S is potentially toxic,

(a)

(b)
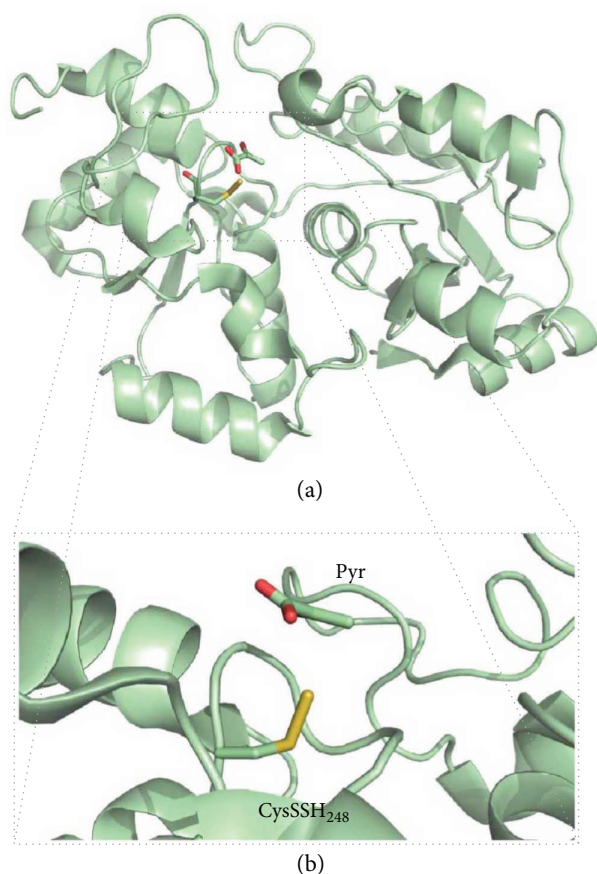
FIGURE 6: Crystallographic structure of human 3-mercaptopyruvate sulfurtransferase (MST). (a) Cartoon representation of human MST monomer (PDB ID: 4JGT; 2.16 Å resolution) cocrystallized with its substrate 3-mercaptopyruvate (3-MP). (b) Zoom-in into the catalytic persulfidated Cys_{248} ($CysSSH_{248}$; human MST numbering) site, after reaction with 3-MP. Pyruvate, a by-product of the reaction of MST with 3-MP, is represented in green sticks. Figure generated with PyMol 1.8.2.0 [238].

FIGURE 7: Mitochondrial sulfide-oxidizing pathway. Scheme depicting the enzymatic components and metabolites involved in sulfide oxidation in the mitochondria. H_2S is initially oxidized by sulfide:quinone oxidoreductase (SQR), which transfers electron equivalents to quinones and generates glutathione persulfide (GSSH) as coproduct. Electrons are transferred to O_2 via complex III (c.III), cytochrome c (Cc), and complex IV (c.IV), contributing to membrane energization and ATP synthesis. GSSH, with O_2 as cosubstrate, is then converted by persulfide dioxygenase (ETHE1) to sulfite (SO_3^{2-}) and GSH. Sulfite can be converted, with GSSH as cosubstrate, into thiosulfate ($S_2O_3^{2-}$) by rhodanese (Rhod), or oxidized into sulfate (SO_4^{2-}) by sulfite oxidase (SOx).

ETHE1 or sulfur dioxygenase), a thiosulfate sulfurtransferase (rhodanese), and a sulfite oxidase (SO_x) (Figure 7). It is to be noted that H_2S oxidation to polysulfide can also be catalyzed by globins (see below) and other proteins, such as catalase and superoxide dismutase, utilizing O_2 or H_2O_2 as electron acceptor [56–59].

From several perspectives, it is fascinating that H_2S oxidation by mitochondria is coupled to energy production, namely, ATP synthesis, as initially demonstrated by investigating the invertebrate *Solemya reidi* [60]. Electrons derived from sulfide oxidation are indeed injected into the respiratory chain at the level of coenzyme Q, thus promoting O_2 consumption and, in turn, energization of the inner mitochondrial membrane. On this basis, H_2S has been recognized as the first inorganic respiratory substrate discovered in mammals [61]. This makes H_2S a very peculiar molecule from a bioenergetic point of view [62], with a dual effect on mitochondrial respiration: stimulatory at low (nanomolar) concentrations when the mitochondrial sulfide oxidation pathway is fully operative or inhibitory at higher (micromolar) concentrations when CcOX activity is impaired and reduced coenzyme Q accumulates, leading to blockage of H_2S detoxification. As remarked recently [63], the system is therefore finely regulated through positive feedback loops so that at lower concentrations sulfide oxidation prevents its own accumulation and consequent inhibition of respiration, whereas at higher concentrations sulfide impairs its own detoxification via inhibition of CcOX. That H_2S can act as an effective substrate of the mitochondrial respiratory chain is in full agreement with the observation that, despite the low K_i value measured with isolated CcOX ($K_i = 0.2 \mu M$

being able to impair cell respiration through inhibition of CcOX [52]. To prevent toxicity, H_2S bioavailability must therefore be finely and differently regulated in different tissues and organs, depending on specific physiological demands. Control of H_2S bioavailability is exerted not only at the level of its biosynthesis but also through enzymatic disposal of such a potentially toxic molecule. In mammals, the ability to detoxify H_2S to thiosulfate and sulfate was demonstrated by metabolic labelling in early studies [53]. More recently, it was discovered that H_2S breakdown is mainly afforded by a mitochondrial enzymatic system (reviewed in [10, 25]), currently designated as "sulfide-oxidizing unit" [54] or "sulfide-oxidizing pathway". Following its initial identification in the lugworm *Arenicola marina* [55], this mitochondrial system has been investigated in more detail. According to current views, this pathway comprises four distinct, yet functionally associated enzymes that together cooperate to catalyze the breakdown of H_2S to thiosulfate and sulfate, the main sulfide catabolites: a sulfide:quinone oxidoreductase (SQR), a persulfide dioxygenase (also known as

FIGURE 8: Structural models of human sulfide quinone oxidoreductase (SQR) and rhodanese (Rhod). (a) Cartoon representation of structural model of human SQR (UniProt accession code: Q9Y6N5.1) generated with Swiss-Model based on the structure of *Acidithiobacillus ferrooxidans* SQR (H198A variant; PDB code: 3SZF; ~19% sequence identity; ~87% sequence coverage) [78]. Flavin adenine dinucleotide (FAD) cofactor in yellow sticks. (b) Zoom-in on the SQR active site comprising the FAD moiety, the active site cysteine residues Cys_{201} and Cys_{379}, and the Tyr_{170} residue which may establish a covalent link with the FAD cofactor. (c) Cartoon representation of structural model of human rhodanese (UniProt accession code: Q16762.4) generated with Swiss-Model based on the structure of the bovine enzyme (PDB code: 1BOH; ~90% sequence identity; 100% sequence coverage). (d) Zoom-in on the Rhod Cys_{248} active site. Figure generated with PyMol 1.8.2.0 [238].

at pH 7.4 [52]), in isolated mitochondria or intact cells, inhibition of respiration only occurs if much higher concentrations of H_2S are administered (micromolar to tens of micromolar; see, for instance, [64, 65]).

The dual effect of H_2S on cell respiration makes investigation of the mitochondrial sulfide-oxidizing activity somewhat challenging from a methodological point of view. Sulfide stimulation of mitochondrial oxygen consumption and consequent energization are indeed best appreciated at low sulfide concentrations, unable to inhibit CcOX. For this reason, most of studies on mitochondrial sulfide oxidation and related bioenergetic effects have been carried out by continuous supply of sulfide at given infusion rates, rather than by sulfide addition as a single bolus (method reviewed in [66]). Using this approach, sulfide oxidation has been quantitatively investigated in several systems, including isolated mitochondria and permeabilized or intact cells from humans and other higher organisms [54, 61, 63, 67–72]. Notably, remarkable differences in terms of H_2S oxidation ability have been reported between human cell lines, spanning from cells in which this catalytic activity is undetectable (as, e.g., in neural cells) to others remarkably active in H_2S removal, like colonocytes [54]. The latter cells are indeed physiologically exposed to massive amounts of H_2S produced by the intestinal microbiota and are therefore likely to have undergone

adaptive mechanisms to prevent H_2S toxicity. In this regard, it is interesting that colonocytes were found to ensure a prominent H_2S-catabolyzing activity even through activity reversal of complex I in the respiratory chain [54].

2.2.2. Components of the Mitochondrial Sulfide-Oxidizing Pathway. The first enzyme operating in the mitochondrial sulfide oxidizing pathway is sulfide:quinone oxidoreductase (SQR, Figure 7). SQR is a member of the protein family of disulfide oxidoreductases, which has been identified in all life domains [73]. It is a membrane-associated protein located at the periplasmic side of the cytoplasmic membrane in prokaryotes and at the inner mitochondrial membrane in eukaryotes. Although no structure of a eukaryotic SQR has thus far been obtained, crystallographic structures of prokaryotic SQRs have been reported [74–76], enabling the construction of a structural model of human SQR (Figures 8(a) and 8(b)). Several structural and amino acid sequence features linked to sulfide oxidation and quinone reduction have allowed for the classification of the SQR family into six subclasses, with human SQR classified as a type II SQR [77]. The main features of type II SQRs, particularly as compared to type I SQRs, are essentially the lack of any extended loops, the poor conservation of quinone-interacting residues, and the substitution of the conserved cysteine covalently linking

the FAD cofactor for a tyrosine (Tyr_{170} according to human SQR numbering), which probably establishes a covalent link with FAD in human SQR via an 8-α-O-tyrosyl bond [77]. SQRs can be monomeric or assemble into dimers or trimers of ~50 kDa subunits [78], each harboring a cysteine disulfide in its active site and a noncovalently bound flavin adenine dinucleotide (FAD) moiety implicated in electron transfer [77]. In mammals, SQR couples H_2S oxidation to the reduction of coenzyme Q, with the concomitant transfer of a sulfur atom to an acceptor that has been proposed to be either sulfite- (SO_3^{2--}) yielding thiosulfate ($S_2O_3^{2-}$) [79–81] or reduced glutathione (GSH) yielding glutathione persulfide (GSSH) [82]. Although the protein displays a higher catalytic efficiency using as cosubstrate sulfite ($k_{cat}/K_M = 2.5 \times 10^6 \, M^{-1} \cdot s^{-1}$) as compared to GSH ($k_{cat}/K_M = 1.6 \times 10^4 \, M^{-1} \cdot s^{-1}$) [83], at physiological concentrations of both cosubstrates, GSH was suggested to be the preferential sulfur acceptor [82–84], at variance from [79–81]. In contrast to the mammalian protein, bacterial SQRs directly release the oxidized sulfur as a soluble polysulfide with up to ten sulfur atoms, instead of reacting with a sulfur acceptor [75, 85]. The reaction mechanism of SQR has been investigated with the isolated protein not only in detergent solution [80, 82, 84] but also after incorporation into nanodiscs [83], where slightly higher catalytic rates have been measured. The postulated mechanism involves (i) reaction of the active site cysteine disulfide with H_2S associated with persulfidation of Cys_{379} (human SQR numbering) to form CysSSH and release of the Cys_{201} thiolate that in turn forms a charge transfer complex with FAD, (ii) transfer of the sulfane sulfur from the persulfidated Cys_{379} to the acceptor with the concomitant reduction of FAD to $FADH_2$, and (iii) oxidation of $FADH_2$ by coenzyme Q. According to kinetic data, the sulfane sulfur transfer step is the rate-limiting one in the reaction.

The next step in the sulfide oxidation pathway is catalyzed by ETHE1 (Figure 7). Mutations in the gene encoding this protein were found to result into an autosomal recessive disorder, known as ethylmalonic encephalopathy, characterized by a severe clinical picture and leading to death during early childhood [86, 87]. The crystallographic structure of human ETHE1 was recently solved (Figure 9) [88]. ETHE1 is a dimeric enzyme, each monomer comprising an $\alpha\beta\beta\alpha$ fold structurally related to dizinc classical metallo-β-lactamases, harboring a mononuclear nonheme iron octahedrally coordinated by two histidines, one aspartate, and three water molecules [88]. The enzyme is proposed to catalyze the oxygenation of the sulfane sulfur atom in the GSSH released from SQR, yielding sulfite [55]. It is important to note that one O_2 molecule is consumed in the reaction.

GSSH and sulfite are further converted into thiosulfate and GSH by rhodanese (Rhod, Figure 7). No structural studies of the human enzyme have been reported, yet a structural model can be obtained based on the ~90% identical bovine homologue (Figures 8(c) and 8(d)) [89]. This protein has a redox-active cysteine (Cys_{248}) in the active site and is highly promiscuous in that it can effectively react with several different substrates. Yet, at physiologically relevant substrate concentrations, the most likely reaction catalyzed by rhodanese was suggested to be the transfer of a sulfur

(a)

(b)
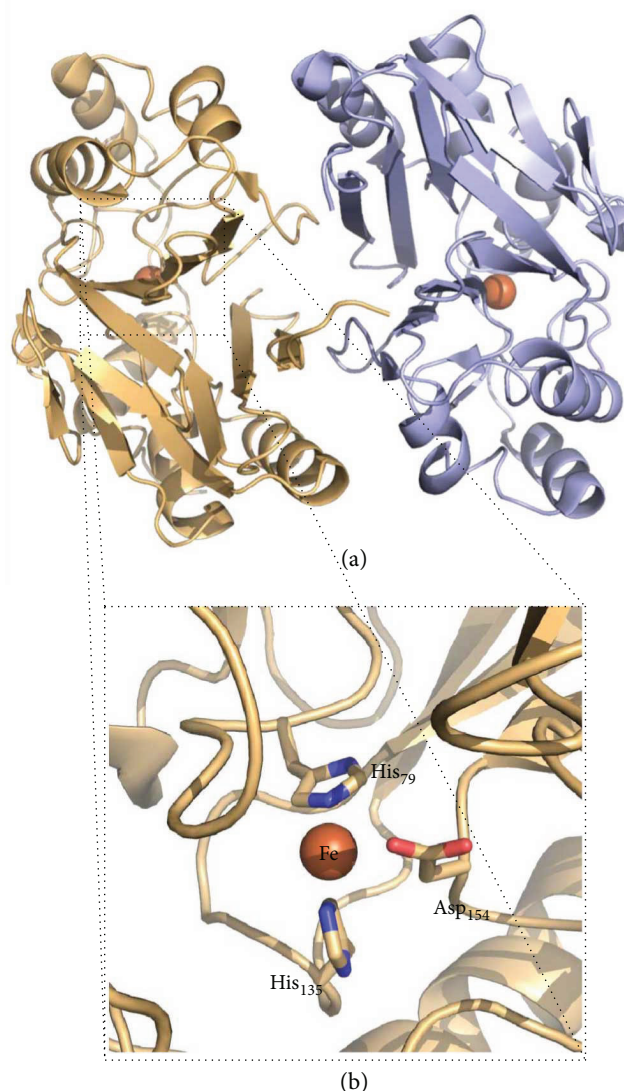
Figure 9: Crystallographic structure of human persulfide dioxygenase (ETHE1). (a) Cartoon representation of human ETHE1 homodimer (PDB ID: 4CHL; 2.61 Å resolution). (b) Zoom-in into the mononuclear nonheme iron catalytic site. Iron ligands (His_{79}, His_{135}, and Asp_{154}; human ETHE1 numbering) are represented in sticks. Figure generated with PyMol 1.8.2.0 [238].

atom from GSSH to sulfite to form thiosulfate [82]. Sulfite oxidase (SOx, Figure 7) catalyzes the last step in the sulfide oxidation pathway. SOx is a multidomain cytochrome b_5 with a molybdenum cofactor [90] and a heme mediating the intramolecular electron transfer from sulfite to cytochrome c. Concomitantly, an oxygen atom is supplied by an H_2O molecule and sulfate (SO_4^{2-}) forms as the end-product of the reaction [90].

Overall, the mitochondrial sulfide-oxidizing pathway couples the oxidation of H_2S to thiosulfate and sulfate with the injection of electrons into coenzyme Q, leading to consumption of 0.79 O_2 per H_2S molecule oxidized, as reported by Goubern and coworkers [61], which is compatible with the predicted value of 0.75. Indeed, based on the postulated

Fe(III)-HS⁻   Sulfheme

(a)   (b)
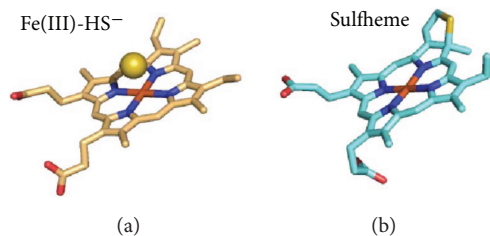
FIGURE 10: Structure of sulfide-reacted heme moieties in globins. (a) Structure of ferric heme moiety (light orange sticks) in human hemoglobin with bound HS⁻ (yellow sphere); PDB entry: 5UCU [115]. (b) Structure of sulfheme moiety (light blue sticks) generated by reaction of horse myoglobin and sulfide, resulting in sulfmyoglobin; PDB entry 1YMC [239].

architecture of the mitochondrial sulfide oxidation pathway presented above, the oxidation of 2 H_2S molecules (involving 2 electrons) is expected to require the consumption of 1.5 O_2 molecules (0.5 by CcOX plus 1 by ETHE1). As O_2 is required for sulfide removal, the efficacy of mitochondrial sulfide oxidation is expected to depend on O_2 availability, clearly vanishing under anoxic conditions. Evidence for a decline of mitochondrial sulfide oxidation at lower O_2 concentrations was preliminarily provided in [69] and, then, substantiated in a later study [63]. To be noted that at very low O_2 concentrations (down to $0.73 \pm 0.04 \mu M$), given a fixed amount of sulfide, a faster onset of cell respiration inhibition was observed at decreasing O_2 concentrations [69], which is consistent with a lower efficacy of sulfide removal but also with a higher control of the respiratory electron transfer chain by CcOX at low O_2 concentration.

Our knowledge of H_2S catabolism and, particularly, of its implication in human physiology and pathophysiology is still rather elusive. Current views of the mitochondrial sulfide oxidation pathway are yet rather patchy and represent a matter of debate. It is likely that the physiological function of this pathway goes well beyond the mere removal/detoxification of H_2S. The impact of this pathway on cell bioenergetics under specific physiological or pathological conditions needs to be better established, as well as its ability to produce bioactive sulfur metabolites (e.g., thiosulfate) whose physiological role has only recently begun to emerge. Finally, it can be anticipated that the mitochondrial sulfide oxidation pathway plays a key role in mediating the intricate interplay between sulfide, O_2, and the other gasotransmitters, but more studies are needed in this direction.

3. Signaling Mediated by Hydrogen Sulfide

The relevance of hydrogen sulfide in mammalian physiology results essentially from its role as a second messenger that transduces signals by interaction with target proteins. The initial classical view of H_2S-mediated signaling initially merely considered the inhibitory properties of hydrogen sulfide towards respiratory CcOX (detailed below) leading to a state of suspended animation. Presently, the signal transducing function of hydrogen sulfide is known to occur via at least two major mechanisms, namely, through (i) interaction with

protein metal centers, particularly heme moieties, and (ii) protein persulfidation (detailed below).

3.1. H_2S and Heme Proteins. Besides being able to promote thiol persulfidation, H_2S can react with protein hemes. As reviewed in Bianco et al. [91], the mechanism and fate of the reaction of H_2S with a heme protein largely depend on several factors, such as the redox and ligation state of the heme iron, the environment in the heme pocket, the protonation state of bound sulfide, and the presence/absence of O_2 or reducing agents in solution. Heme-Fe(III) can bind H_2S as such or as HS⁻ (Figure 10). Stability of one or the other heme adduct generated by reaction with hydrogen sulfide (heme-Fe(III)-H_2S or a heme-Fe(III)-HS⁻) depends on the protein residues in the heme surroundings and, particularly, on the presence of either basic residues able to accept protons from bound H_2S to yield the heme-Fe(III)-HS⁻ species or, alternatively, nonpolar residues stabilizing the fully protonated state of the ligand. Owing to its reducing character, bound sulfide can reduce the heme iron, yielding a heme-Fe(II)-HS· radical adduct that can further react with excess HS⁻/HS· or O_2/H_2O leading, respectively, to formation of polysulfides or thiosulfate. In contrast to these reactions, H_2S can also promote a covalent modification of the heme, yielding the so-called sulfheme derivative with a sulfur atom incorporated into one of the porphyrin pyrrole rings (Figure 10). The mechanism of sulfheme formation is still unclear. Sulfheme can be formed by reaction of H_2S with either the ferrous oxygenated (heme-Fe(II)-O_2 [92]) or the ferryl heme (heme-FeIV=O [93, 94]). However, also in the former case the reaction requires H_2O_2 and thus, likely, the formation of higher valent heme iron intermediates [95, 96]. As reviewed in [5, 91, 95–97], the reactions above have been described by several groups working on numerous hemeproteins, including, among others: globins from mammals, invertebrates, and bacteria; heme-based sensor proteins of diatomic molecules such as O_2, NO, and CO; cytochrome c oxidase; catalase; and peroxidases (lactoperoxidase, myeloperoxidase and thyroid peroxidase).

Because heme proteins can usually react not only with H_2S but also with NO, CO, and O_2, they can play a key role in mediating the crosstalk between these gaseous ligands, namely, controlling each other's biological function. A paradigm of this concept is CcOX. The enzyme, highly reactive with O_2, is indeed a recognized target for all three gasotransmitters (NO, CO, and H_2S). Each of these species can inhibit CcOX, though with markedly different kinetics and mechanisms [29]. While CO can only bind to the fully reduced heme a_3-Cu_B active site, leading to competitive inhibition of the enzyme [98], CcOX inhibition by NO can proceed through two alternative reaction pathways (reviewed in [99–104]): an O_2-competitive pathway, favoured at lower O_2 tension and higher electron flux, leading to a nitrosyl adduct of CcOX with NO bound to ferrous heme a_3, and an O_2-uncompetitive one, prevailing at lower electron flux and higher O_2 tension, whereby an inhibited adduct of enzyme forms with nitrite bound at ferric heme a_3 [29, 105–107]. The mechanism of CcOX inhibition by H_2S has not been investigated as thoroughly as for NO and CO.

Differently from these two species, H_2S does not bind ferrous heme a_3. Based on the postulated mechanism, when the enzyme in turnover with O_2 is exposed to H_2S, oxidized or reduced Cu_B is the primary target site in CcOX. Afterwards, sulfide is thought to be transferred intramolecularly to the nearby ferric heme a_3, resulting in enzyme inhibition [30]. H_2S-inhibited CcOX thus exhibits one sulfide molecule bound to ferric heme a_3 [108, 109] and, possibly, a second one bound to cuprous Cu_B, as revealed by electron paramagnetic resonance (EPR) spectroscopy [110]. Regardless of the exact molecular mechanism, CcOX inhibition by H_2S was demonstrated to be relatively fast (initial rate constant of $2.2 \times 10^4\,M^{-1}\cdot s^{-1}$, as measured at pH 7.4 with the enzyme in turnover with O_2 and cytochrome c [30]), effective ($K_i = 0.2$ μM at pH 7.4), independent of O_2 concentration, and reversible [52]. Similarly to other heme proteins, CcOX inhibition by H_2S was found to be greatly dependent on pH. Acidic conditions remarkably enhance the inhibitory action of sulfide, and consistently, as the pH shifts from 8.05 to 6.28, K_i decreases from 2.6 μM to 0.07 μM [111]. The enhanced efficacy of sulfide inhibition at lower pH suggests that sulfide binds to CcOX either as H_2S (e.g., in fully protonated state) or as HS^- with the concomitant protonation by a protein residue. This is consistent with the active site of the enzyme being located in a nonpolar environment, therefore facilitating the binding of electroneutral or proton-neutralized anionic species [112].

H_2S can also act as a reducing substrate for CcOX [30, 111, 113], when the enzyme is in the so-called pulsed state [30], but the reaction products are yet to be characterized. By reacting with H_2S at relatively low concentrations, heme a_3 in the active site of the enzyme is promptly reduced and, by further reacting with O_2, leads to a ferryl species with optical features indistinguishable from those of the "**P**" catalytic intermediate [30]. Afterwards, the "**F**" ferryl intermediate spontaneously forms on a longer timescale, but it is unclear if the reaction results from autoreduction or electron donation from residual sulfide [30]. CcOX is therefore in principle able to catalyze the oxidative breakdown of H_2S, but the reaction is probably too slow to be physiologically relevant, particularly when compared with the high H_2S-metabolizing activity of SQR.

Another group of proteins whose reactivity with H_2S has been investigated in detail is the globin family. These studies focused primarily, but not exclusively, on human hemoglobin (Hb) and myoglobin (Mb). The reaction of sulfide with Hb has long been known to lead to irreversible covalent conversion of the protein heme to sulfheme (reviewed in [96]); as described above, the modification consists in the incorporation of a sulfur atom into the heme pyrrole B. The resulting protein derivative, named "sulfhemoglobin," exhibits a green color and lower O_2 affinity as compared to the native protein. Accumulation of sulfhemoglobin is therefore associated to toxicity, leading to a rare pathological condition known as "sulfhemoglobinemia." A similar reactivity has been demonstrated also for Mb, leading to formation of "sulfmyoglobin" (Figure 10). Whereas sulfhemoglobinemia likely represents a form of sulfide toxicity, methemoglobinemia, that is, the accumulation

of ferric hemoglobin (metHb) in the blood, has been suggested to protect against sulfide toxicity in mice [114]. In these *in vivo* studies, 2–4 mol of H_2S was inferred to be inactivated per mol of metHb [114]. This superstoichiometric value suggests that metHb is able not only to bind H_2S but also to promote its catalytic breakdown. Consistently, under aerobic conditions metHb was recently demonstrated to bind H_2S, oxidizing it to a mixture of thiosulfate and polysulfides [21]. The reaction, though proceeding at relatively low rates ($3\,min^{-1}$ in the presence of $0.5\,mg\cdot mL^{-1}$ metHb, at pH 7.4 and 25°C [21]), could be of physiological relevance, as Hb-rich red blood cells lack mitochondria and therefore cannot dispose H_2S via the mitochondrial sulfide-oxidizing pathway. Sulfide is a relatively low-affinity ligand for metHb: at pH 7.4 and 37°C, it binds with a k_{on} of $3.2 \times 10^3\,M^{-1}\cdot s^{-1}$ and dissociates from the oxidized heme with a k_{off} of $0.053\,s^{-1}$, yielding a K_D of 17 μM (whose value may be overestimated, given that the H_2S species represents only a fraction of sulfide at pH 7.4). The rate constant for H_2S binding to metHb was found to increase with decreasing pH, and on this basis, H_2S rather than the HS^- species, more abundant at pH 7.4, initially binds to the heme. After binding to the heme iron, H_2S is proposed to deprotonate to HS^-. The postulated $Fe(III)$-HS^- species has been recently detected by X-ray crystallographic analysis of the sulfide-reacted metHb (Figure 10) [115].

Possible mechanisms for polysulfide and thiosulfate formation by metHb have been proposed in [21]. Interestingly, the newly formed polysulfide remains bound to the protein upon heme iron reduction by methionine sulfoxide reductase (MSR). In contrast, it reacts with physiologically relevant, low-molecular-weight (LMW) thiol compounds, such as reduced glutathione (GSH) or cysteine (CysSH), yielding the corresponding persulfides, GSSH and CysSSH, that are eventually released into the solution. In light of the high intracellular concentration of GSH, Hb can act as a source of GSSH that in turn could serve as a persulfide donor in protein persulfidation (detailed below). Therefore, based on its intricate chemistry with sulfide, depending on conditions, Hb can mediate sulfide toxicity via formation of sulfhemoglobin or be protective by promoting sulfide disposal, a particularly relevant function in red blood cells lacking mitochondria. Furthermore, Hb can be viewed as a source of physiologically relevant sulfide oxidation products, namely, thiosulfate and glutathione persulfide (GSSH), whose impact on human physiology is emerging. A somewhat different scenario occurs in atherosclerotic lesions, particularly when they are infiltrated by red blood cells. Indeed, in those lesions, oxidized forms of Hb with the heme in the ferric and ferryl state accumulate and mediate toxicity by promoting radical reactions leading to formation of cross-linked Hb species and lipid modification. Under these circumstances, H_2S was recently reported to exert protective effects, acting as a reductant of ferryl Hb [116].

Another heme protein whose reactivity with sulfide was investigated in depth is human leukocyte myeloperoxidase (MPO). Based on recent studies [117, 118], upon reaction with sulfide, the enzyme does not lead to formation of the sulfheme derivative, at variance with other

heme proteins. Of interest, MPO was reported to catalyze the oxidation of sulfide to sulfane sulfur species both in the presence and in the absence of H_2O_2 [117, 118]. The reaction involves as a central intermediate compound III, a resonance form between the ferrous/dioxygen (Fe(II)-O_2) and ferric/superoxide (Fe(III)-$O_2 \cdot^-$) complex, it is facilitated by ascorbate or SOD and might be of physiological relevance as the formed sulfane sulfur species were proven to oxidize protein cysteine residues to their corresponding per/polysulfide derivatives [117].

3.2. Persulfidation and Persulfide (Bio)chemistry. As mentioned above, many of the signaling functions attributed to H_2S have been shown to be tightly associated with formation of persulfides through the modification of specific cysteine side chains from target proteins, often involving free reactive LMW persulfides (RSSH), particularly cysteine persulfide (CysSSH) and glutathione persulfide (GSSH). Polysulfides are also considered as potentially relevant from a physiological viewpoint, as reviewed elsewhere [119]. However, because they are contaminants of most inorganic H_2S donors employed in research and therefore possibly responsible for some of the effects attributed to H_2S, their (bio)chemistry is still far from being fully understood and will not be detailed herein. The relevance of persulfidation is attested by the fact that deficiency in persulfidated proteins has been associated with different pathologies, including cardiovascular and neurodegenerative (Parkinson's) diseases [120, 121]. Besides its signaling function, persulfidation may also constitute a mechanism to prevent thiol oxidation or electrophilic modification and irreversible damage [122]. The ability of LMW persulfides to readily donate one electron and form a stable perthiyl radical (RSS·), unreactive towards oxygen or NO, led to the proposal of a possible role in redox processes [123]. Recently, the oxidation of cysteine persulfides to perthiosulfenic acid (CysSSOH) observed in different proteins as a consequence of NADPH oxidase activation led to the proposal of this modification as an additional redox-based signaling event [124]. The chemical and biochemical properties, biosynthesis and natural occurrence, analytical detection methods, and cellular longevity of persulfides and polysulfides have all been covered in excellent articles and reviews (e.g., [3, 6, 120, 121, 125–129]). As in other fields focused on reactive molecules, there seem to be controversies as to which species and reactions are more plausible and relevant from a chemical-to-physiological viewpoint. Presently, there is however a consensus that H_2S cannot react directly with protein cysteine thiols. Protein persulfidation, in order to occur, has special requirements both at a "local" (the environment surrounding the target cysteine) and a "global" (redox status, free glutathione/cysteine/H_2S availability) level. Currently, although several possibilities for the formation of persulfidated proteins through posttranslational modification can be envisaged, only four appear to be more plausible (Figure 11(a)). Two of these possibilities involve previous oxidation of the protein target cysteine thiol to a sulfenic moiety (CysSOH), for example, by reaction with hydrogen peroxide, or to a disulfide (CysSSR) by reaction with an oxidized sulfur-containing LMW molecule, for example,

oxidized glutathione (GSSG). Both of these oxidized cysteine residues can then be targeted directly by H_2S, resulting in a persulfidated protein. Reduced cysteine residues (e.g., protein thiols) can be modified to their persulfide derivatives through reaction with a free LMW persulfide (RSSH), such as GSSH or (homo)cysteine persulfide (derived from the H_2S biosynthetic or catabolic pathway [125, 126]), or via reaction with HS·, generated upon reaction of H_2S with metal centers, particularly oxidized protein heme iron. The protein cysteine thiol reaction with HS· should yield a transient CysSSH·$^-$ that, upon reaction with oxygen, yields the protein-bound CysSSH and superoxide anion, similar to that reported for HSSH·$^-$ [3, 130]. In addition to posttranslational persulfidation, it has been quite recently posited that in mammals a major source of persulfidated (and polysulfidated) proteins *in vivo* are actually cysteinyl-tRNA synthetases (CARSs, particularly the mitochondrial CARS2), through cotranslational incorporation of cysteine persulfide or polysulfide at cysteine sites into the nascent polypeptide [131] (Figure 11(b)). From a cellular signaling perspective, the advantage of protein persulfidation by H_2S and/or persulfides is that the resulting species can be reverted to the thiol moiety in different ways, such as direct reaction with reduced glutathione (GSH) or through the thioredoxin system [126], thus affording a reliable switching modification.

As for the LMW persulfides, which are key molecules in protein persulfidation, they are increasingly coming into the limelight due to their intrinsic reactivity (e.g., [125]). Until recently, the two major sources of these persulfides, particularly cysteine persulfide (CysSSH) and glutathione persulfide (GSSH), were considered the enzymes involved in H_2S metabolism. CysSSH is readily generated by the H_2S-synthesizing CBS and CSE, using cystine (CysSSCys) as substrate [125]. Notably, in the course of this reaction, longer polythiolated products with catenated sulfur atoms, such as CysSSSH (synthesized by both CBS and CSE) and CysSSSSH (synthesized by CSE), have been detected. The enzymatic generation of these species further results in appreciable amounts of oxidized polysulfide species like CysSSSCys, CysSSSSCys, and CysSSSSSCys. The newly formed CysSSH and longer cysteine persulfides can then react with reduced glutathione to yield GSSH and $GS(S)_nH$. It should however be noted that, at physiologically relevant substrate concentrations, H_2S rather than CysSSH is expected to be the major product of the transsulfuration pathway enzymes [132], also taking into account that in the cytoplasm, cysteine and reduced glutathione are much more abundant than their oxidation products cystine and GSSG [132]. Recently, MST was also recognized as a source of CysSSH and GSSH, as well as of longer polysulfides, related with its ability to generate other RSS, such as hydrogen persulfide (H_2S_2) and hydrogen trisulfide (H_2S_3) [133, 134]. MST-derived persulfides and polysulfides have been associated with higher cellular levels of protein-bound sulfane sulfur [134, 135]. The MST-catalyzed $CysSS_{(n)}H$ and $GSS_{(n)}H$ production was demonstrated with recombinant MST (wild-type and site-directed variants), MST-expressing COS cells lysates, and mouse brains (cell suspensions and whole

(a)

(b)
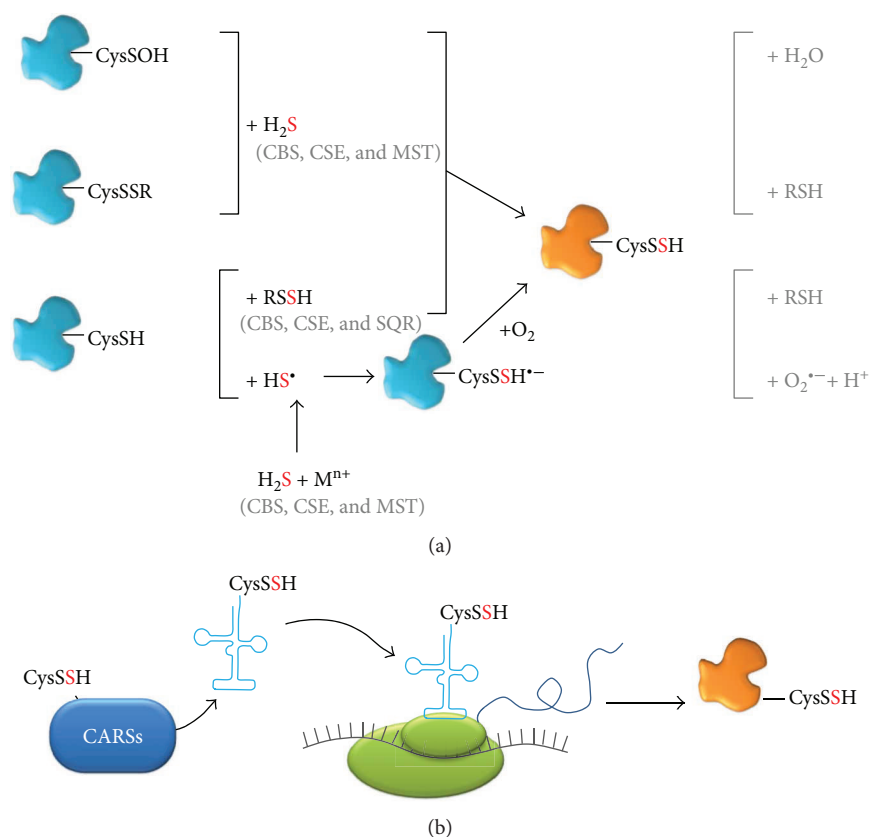
FIGURE 11: Reactions leading to protein persulfidation. Scheme depicting the most plausible *in vivo* reactions leading to cysteine persulfidation in target proteins, through (a) posttranslational modification of cysteine residues or (b) cotranslational incorporation of CysSSH via CysSSH-bound tRNA derived from cysteinyl-tRNA synthetases (CARSs). (a) Proteins with oxidized cysteine residues (CysSSR and CysSOH) can react directly with H_2S (derived from its synthesizing enzymes CBS, CSE, and MST) to yield a protein cysteine persulfide (CysSSH). Proteins with reduced cysteine residues (CysSH) can react with free LMW persulfides (RSSH, such as glutathione persulfide and cysteine persulfide, products of H_2S biosynthetic—CBS, CSE, and MST—or catabolic—SQR—enzymes) or with the HS· radical formed by reaction of H_2S with metal centers (M^{n+}). The resulting protein-bound cysteine perthiyl radical (CysSSH·⁻) can then react with oxygen to yield CysSSH and superoxide anion. (b) Generation of protein cysteine persulfides through cotranslational incorporation of CysSSH. Mammalian cysteinyl-tRNA synthetases (CARSs, dark blue box, which also synthesize free CysSSH from cysteine) catalyze the synthesis of tRNA-bound cysteine persulfides (light blue line), which incorporate CysSSH into the nascent polypeptide (dark blue line) at cysteine sites upon translation (ribosome depicted in green and mRNA in grey).

brains) [133], showing that in the brain LMW persulfides and protein persulfidation are essentially generated via MST and not CBS or CSE [133]. A principal role in CysSSH (and $CysSS_{(n)}H$) synthesis has been recently proposed for mammalian CARSs, particularly the mitochondrial isoform CARS2 [131]. The same report suggests that mitochondria are the key cellular compartments where CysSSH is formed before being released into the cytosol to exert its effects. It is also posited that whereas CARSs may be the major source of CysSSH under physiological conditions, CBS and CSE may still act as major players in CysSSH synthesis in pathophysiological conditions associated with oxidative and electrophilic stress with concomitantly increased cystine concentrations [125, 131, 132].

Besides the LMW persulfides derived from the H_2S-synthesizing enzymes CBS, CSE, and MST [125, 132, 133], GSSH is a metabolic intermediate of the mitochondrial sulfide-oxidizing pathway [126] (Figure 7). Indeed, GSH has been suggested as the preferential sulfur acceptor in the

H_2S oxidation reaction catalyzed by SQR, yielding GSSH [82]. This persulfide is, in turn, the preferential substrate (with sulfite as cosubstrate) for rhodanese to generate thiosulfate as the final oxidation product of sulfide oxidation, together with sulfate [82].

Regardless of how LMW persulfides are generated, their reactivity prompts them to be major signal-transducing species linked to H_2S (patho)physiology. In a nutshell, persulfides are stronger nucleophiles than their thiol counterparts are (yet displaying also a weak electrophilic character). Despite this assumption, only recently it was clearly demonstrated by Cuevasanta et al. [136] that a human serum albumin persulfide derivative displays 20-fold increased reactivity with respect to its thiol counterpart. Persulfides have lower pK_a values than the analogous thiols, thus existing mostly in their anionic nucleophilic RSS⁻ form [3, 6]. Conversely, their weak electrophilicity is exhibited solely in their protonated RSSH form. Interestingly, both the outer sulfhydryl and inner sulfenyl sulfurs have

TABLE 1: Protein targets for cysteine persulfidation and molecular and cellular consequences.

Protein	Target cysteine	Physiological process	Consequences of persulfidation	Refs.
Protein Tyr phosphatase 1B (PTP1B)	Cys_{215}	ER stress response	PTP1B is inhibited, enhancing PERK[a]-mediated phosphorylation of eIF2α[b], suppressing protein translation.	[137]
p65 subunit of nuclear factor κB (NF-κB)	Cys_{38}	NF-κB signaling; apoptosis	Stimulates binding of p65 to ribosomal protein S3, resulting in increased translation of prosurvival genes.	[138]
Inwardly rectifying potassium channel subunit Kir6.1	Cys_{43}	Vasorelaxation and vasodilation	Enhances channel activity through decreased affinity for ATP and increased binding of PtdIns(4,5)P$_2$[c].	[139]

[a]Protein kinase RNA-like ER kinase; [b]eukaryotic translational initiation factor 2α; [c]phosphatidylinositol-4,5-bisphosphate.

electrophilic character, the reaction occurring on either one depending on factors such as steric hindrance or acidity of the leaving group [3]. The ambiguous nucleophilic/electrophilic nature of LMW persulfides, while at the basis of their physiological relevance, accounts for their instability. These species indeed quickly decay or react with other species, particularly oxidants, hampering their characterization both *in vitro* and *in vivo*. This notwithstanding, the molecular details and functional consequences of persulfidation at specific cysteine residues have been demonstrated for a number of targets and shown to regulate several physiological processes (reviewed in, e.g., [127]), such as glycolysis [26], ER stress [137], apoptosis [138], vasorelaxation, and vasodilation [139] (detailed in Table 1). Regarding the latter, H$_2$S was the third gasotransmitter, following NO and CO, to be regarded as an endothelium-derived relaxing factor (EDRF) and as an endothelium-derived hyperpolarizing factor (EDHF), thus regulating vasodilation (detailed below). Despite the relatively few examples available in the literature, protein persulfidation is likely prevalent, yet technically challenging to be detected due to the intrinsic reactivity of persulfides. Using an adaptation of the biotin switch assay modified to detect persulfidated rather than nitrosated proteins, Mustafa et al. reported that 25–50% of hepatic proteins are persulfidated [26]. The extent of protein persulfidation *in vivo* has been further demonstrated by increasingly elaborate and quantitative methodologies [125, 140–143]. It is expected that the number of identified new targets of protein persulfidation will continuously increase, pairing this posttranslational modification with other highly relevant cellular switches.

4. Interplay between Gasotransmitters

4.1. Brief Historical Account of Gasotransmitters. The term "gasotransmitters" [144] has entered the biochemistry and physiology jargon to designate essentially the three small molecules gaseous in nature with demonstrated roles in signal transduction: nitric oxide (NO; although the formally correct abbreviation should be NO·, herein NO will be used for simplicity), carbon monoxide (CO), and hydrogen sulfide (H$_2$S). Arguably, molecular oxygen (O$_2$), although not synthesized endogenously in mammalian cells, could be considered a gasotransmitter due to its gaseous nature, reactivity, and physiological relevance. Besides, O$_2$ is a substrate of the mammalian enzymes that synthesize NO and CO, so O$_2$ levels dictate the bioavailability of the latter.

Gasotransmitter-mediated signaling is an intricate and integrated process involving not only NO, CO, H$_2$S, and O$_2$ but also the collective pool of reactive species (reactive oxygen species (ROS), reactive nitrogen species (RNS), and reactive sulfur species (RSS) resulting from their cross-reactions, establishing a so-called reactive species interactome (RSI) [145]. Irrespectively of the identity of the gasotransmitter molecule or derived species, its signaling mode of action can be narrowed down essentially to two possibilities: interaction with metal centers or modification of cysteine residues in proteins, both resulting either in the activation or in the inactivation of the target protein. The three gasotransmitters NO, CO, and H$_2$S share a common history in that they were initially merely regarded as toxic and poisonous molecules, until the discovery that virtually all life forms, from bacteria to man, are endowed with dedicated synthesizing and detoxifying enzymes and produce or scavenge NO, CO, and H$_2$S to accomplish specific functions. Indeed, in the late 1980s and early 1990s, major advances concerning the role of NO in the regulation of cardiovascular function led to NO being considered Molecule of the Year in 1992 and to the Nobel Prize in Physiology or Medicine being awarded in 1998 to Robert Furchgott, Ferid Murad, and Louis Ignarro Jr "for their discoveries concerning nitric oxide as a signaling molecule in the cardiovascular system" [146]. One of the key findings was the identification of the endothelium-derived relaxing factor (EDRF) as NO [147, 148]. This observation, which revealed beneficial rather than deleterious effects of an otherwise considered toxic molecule, triggered a subfield of biology dedicated to signaling by gaseous second messengers. Indeed, besides other regulatory roles attributed to NO, similar findings were demonstrated for CO, which was also shown to have a role in vasorelaxation [149]. The same function came to be assigned to H$_2$S [17], which also led it to be labeled as an EDRF [127]. The multiple functions of gasotransmitters in human physiology are well attested by the "explosion" of interest that arose since the discovery of NO as a signaling molecule in the mid-1980s, CO in the mid-1990s, and H$_2$S in the 2000s. This is well illustrated by carrying out a Pubmed search querying "gasotransmitters," "nitric oxide," "carbon monoxide," and "hydrogen sulfide" (Figure 12). Altogether, the three gasotransmitters regulate, often through similar molecular processes, vasodilation, energy metabolism, redox homeostasis, apoptosis, cell cycle, reproduction, neuronal
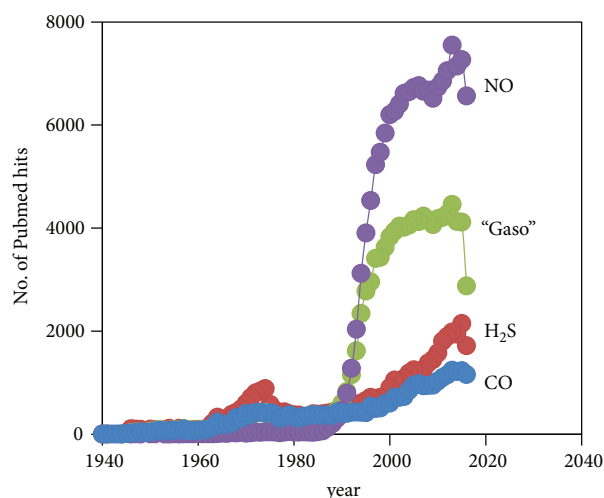
FIGURE 12: Literature on gasotransmitters, H_2S, NO, and CO. Number of articles retrieved from Pubmed queries with the following terms: "hydrogen sulfide" (H_2S), "gasotransmitters" ("gaso"), "nitric oxide" (NO), and "carbon monoxide" (CO).

function, and so on, and dysregulation of the metabolism and/or levels of NO, CO, or H_2S is associated with several pathological conditions, from cardiovascular and neurodegenerative diseases to diabetes and cancer, among others.

A surprising element in gasotransmitter history was the finding that mammals, among many other organisms, encode specialized enzymes that synthesize these previously considered noxious gaseous molecules. NO is enzymatically produced by NO synthases, of which three isoforms have been described and historically classified according to their location or regulation, yet presently considered to be ubiquitous and constitutively expressed: inducible NO synthase (iNOS), endothelial NO synthase (eNOS), and neuronal NO synthase (nNOS) (reviewed, e.g., in [150]). Regardless of the isoform and its localization or regulation, NO synthases catalyze the conversion of arginine and O_2 into NO and citrulline, using electron equivalents derived from NADPH. Besides being synthesized on demand by NO synthases, NO is endogenously generated (i) under hypoxic conditions through nitrite reduction by several heme proteins (including hemoglobin, as reviewed in [151]), (ii) in the digestive tract as an intermediate of bacterial nitrogen metabolism (particularly in the mouth and the gut), and (iii) chemically from nitrite under the acidic environment in the stomach (reviewed, e.g., in [152]). As for CO, it is generated by either isoform of heme oxygenase, HO-1 and HO-2, which catalyze the conversion of heme, with O_2 as cosubstrate, into biliverdin and CO, employing NADPH-derived electron equivalents (reviewed, e.g., in [153]). H_2S synthesis is catalyzed by CBS, CSE and MST, as described above.

As mentioned before, it has become increasingly clear that no gasotransmitter should be regarded as an isolated entity with an independent cellular function and lifespan. Rather, gasotransmitters interact with each other not only by direct cross-reactions that generate other reactive species but also by having cooperative or opposite molecular and cellular consequences towards their targets. Moreover, each gasotransmitter in many ways is able to modulate the synthesis of the others, which represents an additional intricate level of regulation. An example of this modulatory action is described below, concerning the regulation of CBS-catalyzed H_2S production by NO and CO.

4.2. Chemical Bases of the Interplay between H_2S and NO. The biological effects of H_2S and NO are intimately interconnected. The interplay between these two gaseous molecules takes place through numerous mechanisms acting at different levels (reviewed in [154]). Many studies aimed at gaining insight into the chemical foundation of the interaction between H_2S and NO. An extensive analysis has been carried out of the reactivity of sulfide with several NO metabolites, including nitrite [155], peroxynitrite [156, 157], and nitrosothiols [158–163], and with NO releasers such as nitroprusside [163–167]. Despite these efforts, the picture is currently far from being completely clear. As discussed in [5, 168–171], some remarkable discrepancies have indeed emerged, mainly regarding the nature of the species generated in these reactions and their suitability as signaling molecules under physiological conditions.

The first S/N hybrid species suggested to form by reaction of nitrosothiols (e.g., *s*-nitrosoglutathione (GSNO)) with sulfide was thionitrous acid/thionitrite (HSNO/ONS⁻) [161]. In line with previous studies by Whiteman et al. [172, 173], Filipovic et al. [161] reported the formation of HSNO by reaction of H_2S with either GSNO or acidified nitrite, as well as by investigation of the reaction of NO with HS· generated by pulse radiolysis. In addition to HSNO, the reaction of GSNO with sulfide was found to yield also a yellow product assumed to be a mixture of polysulfides. Of interest regarding its potential physiological implications, HSNO was proposed to serve not only as a source of both NO and nitroxyl anion (NO⁻) but also as a donor of nitrosonium ion (NO⁺) to thiols, thereby promoting transnitrosation reactions even across biological membranes [161]. On these bases, HSNO was suggested to be a key species in the interplay between H_2S and NO, sitting at the crossroad between the H_2S and NO signaling pathways.

This view was challenged in subsequent studies by Cortese-Krott et al. [145, 155, 159, 160, 169, 174], who failed to detect HSNO accumulation during the reaction of GSNO with H_2S and claimed HSNO to be too short-lived to accumulate and be identified under physiological conditions, in agreement with Munro and Williams [175] and Williams [176]. Compared to other physiologically relevant nitrosthiols, HSNO was indeed suggested to be much more unstable as it undergoes a facile isomerization by hydrogen shift, leading to formation of four distinct isomers. The yellow product generated by reaction of GSNO with H_2S initially described in [161] was assigned by Cortese-Krott et al. [159] to nitropersulfide (SSNO⁻), a compound discovered and chemically characterized in the '80s [177]. The same research groups reported later [160] that, under physiologically relevant conditions, the reaction between sulfide and NO generates not only SSNO⁻ but also polysulfides and SULFI/NO [ON(NO)SO₃⁻], an additional bioactive

compound consisting of an adduct of two molecules of NO with sulfite. Based on these and further investigations [174], Cortese-Krott et al. reported that SSNO$^-$ is stable in the presence of thiols and cyanides and is able to release NO upon decomposition, targeting the Keap1/Nrf2 redox system, among other possible ones. Overall, this led to the proposal that SSNO$^-$, rather than HSNO, plays a key role in the interplay between NO and H$_2$S under physiological conditions [159]. In line with this proposal, SSNO$^-$ was reported to be very stable under anaerobic conditions, to decay slowly (half life of about 40 minutes) in aqueous buffer under aerobic conditions, and to directly react with deoxygenated metHb with a rate constant of $11\,M^{-1}\cdot s^{-1}$, yielding ferrous nitrosyl Hb (HbNO) presumably via NO release [178]. In contrast, by characterizing pure crystalline SSNO$^-$ prepared as a bis(triphenylphosphine)iminium (PNP$^+$) salt according to [179], Filipovic et al. reported that SSNO$^-$ is a highly unstable species, leading to rapid decomposition with formation of HNO/NO$^-$ in the presence of water, light, or acid and producing HSNO by reaction with H$_2$S, cyanide, and GSH [180, 181].

From the observations reported above, it is clear that additional investigations are needed to reconcile the discrepancies present in the literature and gain further insight into the chemical foundation of the interplay between NO and H$_2$S.

4.3. Modulation of H$_2$S Metabolism by NO and CO. Besides the chemical reactions that define new players in gasotransmitter-mediated signaling, there is an intricate web of cross-regulatory mechanisms whereby each gasotransmitter regulates the homeostasis of the others. While part of that cross-regulation may occur at the transcriptional and translational level, herein we will mainly cover the molecular mechanisms that result from direct interactions between the gasotransmitters and their target proteins, focusing on the modulation by NO and CO of H$_2$S biosynthesis and breakdown.

4.3.1. Modulation of H$_2$S-Generating Enzymes by NO, CO, and Derived Species. The most thoroughly studied H$_2$S-generating enzyme in terms of regulatory mechanisms has certainly been CBS. In what regards its modulation by the other gasotransmitters NO and CO, CBS regulation is centered at its noncatalytic heme bound to the N-terminal domain. This interplay between gasotransmitters results essentially from the fact that H$_2$S production by CBS is reversibly inhibited by NO and CO. The direct effect of this inhibitory mechanism would be that local increases in NO or CO result in decreased H$_2$S synthesis, which has been demonstrated in different cellular models and tissues [182–185]. However, recent evidence suggests that CBS inhibition may in fact result in overall increased H$_2$S production, due to a metabolic switch in the transsulfuration pathway (Figure 1(a)) [11, 186]. In this perspective, inhibiting CBS deviates the transsulfuration branch from cysteine to H$_2$S production via CSE, which has a higher H$_2$S-synthesizing activity, particularly using the accumulated homocysteine also resulting from CBS inhibition [11, 186].

Moreover, the pathophysiological significance of CBS inhibition by gasotransmitters may extend beyond "merely" affecting H$_2$S homeostasis. CBS acts as a metabolic hinge determining the ratio between the remethylation and transsulfuration steps of the methionine cycle (Figure 1(a)). CO inhibition of CBS in various cancer cells has been shown to affect the methylation state of 6-phosphofructo-2-kinase/fructose-2,6-biphosphatase 3 (PFKFB3), suppressing 6-phosphofructo-2-kinase, resulting in a shift of glucose from glycolysis to the pentose phosphate pathway [34, 187].

The regulatory heme-binding domain may be considered a hallmark of CBS evolution, since it is absent from CBS from prokaryotes or unicellular eukaryotes. The low-spin hexacoordinate b-type heme is axially bound to the His$_{65}$ imidazole and Cys$_{52}$ thiolate moieties (human CBS numbering; Figure 4(b)). Besides its regulatory role, the CBS heme has been proposed to have a structural stabilizing effect and contribute to improve CBS folding [188]. After initial submission of this review, a quite interesting observation has been reported, which will once again stir the field of CBS heme regulation. Kumar et al. observed that the N-terminal residues 1–40, so far absent from all CBS crystallographic structures, constitute an intrinsically disordered region that is able to bind heme with Cys and His as axial ligands, in a cysteine-proline-based motif [189]. This observation, deserving further exploration, constitutes an additional level of complexity regarding all the literature on the CBS heme regulation (see below).

The heme regulatory role is essentially related to its redox state and the nature of its endogenous and exogenous ligands. The initial designation of the CBS heme as a redox sensor stemmed from its sensitivity to reducing conditions. Indeed, heme reduction by excess sodium dithionite at 37°C slowly (>20 minutes) inactivates the enzyme, which has been assigned to a ligand switch process in which one of the endogenous ligands of heme iron is replaced by another as yet unknown ligand (Figure 13) [190]. The resulting species has been termed "C424" due to its characteristic UV-visible absorption spectrum, in which the Soret band obtained for reduced CBS with its λ_{max} at 449 nm is shifted to a lower-intensity band centered at 424 nm. Irrespectively of the bound endogenous ligands, once reduced, the heme is able to bind the gasotransmitters CO and NO, which results in reversible enzyme inhibition (Figure 13) [191–195]. Although the low reduction potential (−350 mV, [196]) measured for the CBS heme raised some doubts about the occurrence of reduced CBS heme *in vivo*, the human enzyme methionine synthase reductase (MSR) has been shown to be able to catalyze CBS reduction *in vitro* at the expense of NADPH oxidation. Moreover, MSR is able to generate both the ferrous-CO and the ferrous-NO species of human CBS [191, 197]. Despite the significant distance between the heme and PLP cofactors (~11 Å from edge to edge and ~20 Å from the Fe ion to the pyridoxine ring), communication between them is ensured by a network of molecular interactions occurring at helix 8 (depicted by the yellow arrow in Figure 4(b)) [198, 199]. While at the PLP end of helix 8 the residues Thr$_{257}$ and Thr$_{260}$ establish hydrogen bonds with the PLP
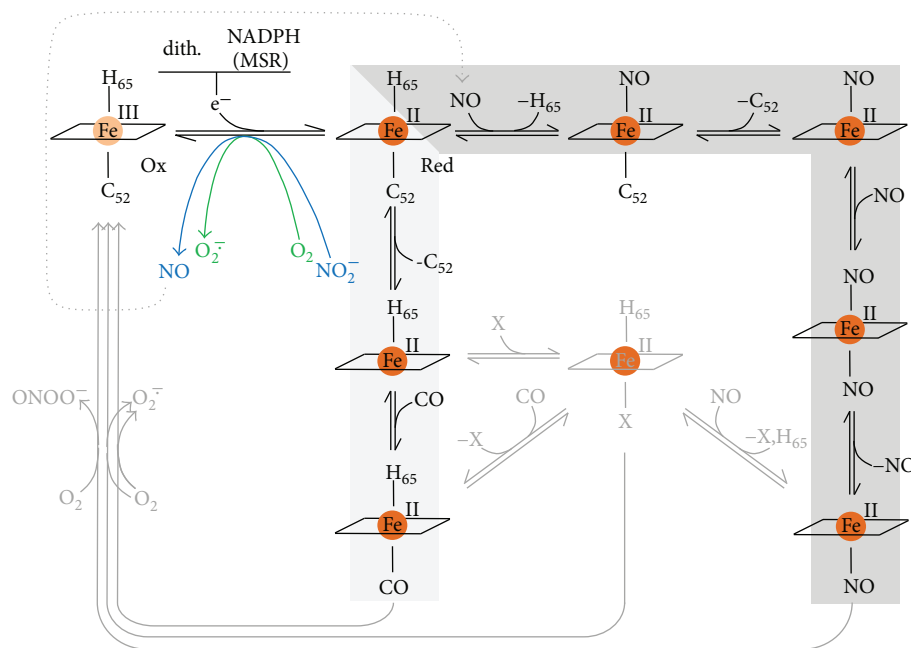
FIGURE 13: Mechanisms of heme reduction and ligand binding to human CBS.

phosphate group, at the heme extremity of this helix Arg_{266} is in electrostatic contact with the heme ligand Cys_{52} thiolate moiety. The relevance of these residues in the allosteric communication between the active (PLP) and regulatory (heme) sites has been further demonstrated in clinically relevant variants [199, 200].

The kinetic characterization of the interplay between the three gasotransmitters centered at CBS has been made possible by taking advantage of the distinct characteristic UV-visible absorption spectra displayed by the heme cofactor in different oxidation and ligation states. Most studies on the CBS redox state and ligand reactivity have thus employed static and time-resolved (stopped-flow) absorption spectroscopy [192–195, 199–204].

The reaction of reduced CBS with CO has been thoroughly characterized *in vitro* and shown to result in a hexacoordinate species in which the endogenous Cys52 ligand has been replaced by CO, with no evidence for stable intermediates. Indeed, the reaction is limited by the slow dissociation of Cys_{52} (0.003–0.017 s^{-1} [192, 195, 197, 204]), as confirmed by laser flash photolysis and time-resolved Raman spectroscopy [192]. Equilibrium titrations revealed that CO binds to ferrous CBS according to two dissociation constants ($K_{d1} = 0.7 – 1.5\,\mu M$ and $K_{d2} = 45 – 68\,\mu M$; $C_{50} \approx 30\,\mu M$), which has been assigned to anticooperativity between paired monomers [192] or differences in the heme microenvironment [194]. The inhibitory effect of CO binding to the ferrous heme in human CBS is characterized by K_i values of 5.6–9.5 μM [194, 204].

Recently, our groups have reported that a clinically relevant variant with a mutation in the N-terminal domain, p.P49L, displays a markedly higher affinity for CO with respect to WT, while showing an essentially WT-like behavior in other functional and structural terms [203]. While this mutation may induce increased flexibility of the loop

containing both heme endogenous ligands, the overall higher proneness to become inhibited by CO may represent a new pathogenic mechanism in classical homocystinuria. Current efforts to develop alternative therapies for classical homocystinuria have essentially focused on chemical and pharmacological chaperones to recover misfolded protein variants originating from missense mutations [205–211] and recently on the development of a PEGylated CBS for enzyme replacement therapy [212–214].

NO binding to reduced CBS is remarkably faster and displays much higher affinity than CO binding. However, initial reports on the reaction between ferrous CBS and NO indicated otherwise. Very low affinity for NO was reported ($K_d = 281\,\mu M$), employing a high excess of sodium dithionite to keep CBS reduced throughout the NO titrations and using a slow NO releaser (diethylamine NONOate) as NO source [193]. Under these conditions, free NO, either unreacted or dissociated from the ferrous-NO CBS adduct, reacts with the excess dithionite and leads to an overestimation of the dissociation constants, as later shown even with minute amounts of excess dithionite [195]. Recently, our groups have shown that NO binding to ferrous CBS occurs with an affinity compatible with a physiological role of NO in controlling CBS function [195]. An apparent K_d of $0.23\,\mu M$ was determined at the lowest dithionite concentration used in that study, which implies that the actual affinity is even higher than measured. Contemporarily, a $K_d = 30\,\mu M$ was determined and still was considered an upper limit for this dissociation constant, as it was measured using NADPH and human MSR as reduction system, therefore involving multiple equilibria (NADPH $\leftrightarrow$ MSR, MSR $\leftrightarrow$ CBS, and CBS $\leftrightarrow$ NO) [191]. As compared to CO, NO binding to reduced CBS not only occurs with markedly higher affinity but is also orders of magnitude faster, as investigated by stopped-flow absorption spectroscopy. Differently from

CO, NO binding results in a pentacoordinate ferrous-NO adduct, where both endogenous ligands have been displaced and a single NO molecule is bound. No reaction intermediates have been detected upon mixing NO with reduced CBS, at least within the time resolution of the stopped-flow equipment. Moreover, also differently from CO, NO binding proceeds with rate constants linearly dependent on NO concentration (up to 800 μM), that is, unlimited by dissociation of the endogenous ligands, yielding a bimolecular rate constant of $\sim 8 \times 10^3 \, M^{-1} \cdot s^{-1}$ (at 25°C). In line with the higher affinity and faster binding of NO with respect to CO, NO dissociation from ferrous CBS is slower than CO dissociation. In mechanistic terms, since NO binding is not rate-limited by the displacement of Cys_{52} (which instead limits CO binding), it has been proposed that NO may initially displace the His_{65} heme ligand (Figure 13). In turn, the absence of evidence for a hexacoordinate intermediate suggests that Cys_{52} is immediately displaced upon NO binding. Finally, although it has been established that the final NO adduct is a pentacoordinate species, it remains to be demonstrated whether NO ends up on the His_{65} or Cys_{52} side of the heme, since both residues are supposed to dissociate from the heme iron. It should be noted that if NO ends up on the Cys52 side, the binding mechanism must involve the formation of a transient bis-NO intermediate (Figure 13). Irrespectively of the mechanistic details, the kinetic and spectroscopic investigations of CBS reduction and CO and NO binding have determined parameters compatible with an *in vivo* role of this regulatory mechanism.

The reaction of reduced CBS with O_2 was also investigated by stopped-flow absorption spectroscopy and shown to be reasonably fast, occurring with a bimolecular rate constant of $\sim 1 \times 10^5 \, M^{-1} \cdot s^{-1}$ (25°C) [202], that is, approximately 10-fold faster than the reaction with NO. Although this reaction reverts CBS back to its active ferric state, it also generates superoxide anion as a reaction product, which may have damaging effects. This oxidation process has indeed been reported to involve a partial heme loss. Superoxide anion promptly reacts with NO (at rates close to the diffusion limit) to yield the powerful oxidant peroxynitrite. Interestingly, it has been shown that CBS heme not only is inactivated by peroxynitrite but also may be a source of it. The reaction of oxidized CBS with peroxynitrite has been shown to result in enzyme inactivation with an IC_{50} of 150 μM, occurring according to a bimolecular rate constant of 2.4–$5 \times 10^4 \, M^{-1} \cdot s^{-1}$ and leading to nitration of Trp_{208}, Trp_{43}, and Tyr_{223}, as well as damaging the heme moiety [215]. Intriguingly, a recent report demonstrated that the reaction between ferrous-NO CBS and O_2, previously shown to revert the heme to its ferric state, yields peroxynitrite [201] (Figure 13). Moreover, the reaction of reduced CBS with nitrite may itself constitute a source of NO [191, 201], which further adds to the complex heme-mediated regulation of H_2S synthesis by CBS (Figure 13).

4.3.2. Effect of AdoMet on CO/NO Binding and Inhibition of H_2S Production by CBS. CBS continues to surprise researchers in the field since regulation of the protein activity not only is intricate but also at times appears odd. It has long been established that AdoMet is an activator

of CBS, increasing its enzymatic activity by 2- to 5-fold. Moreover, AdoMet binding also has a stabilizing effect, particularly under "normal" (nonpathological) conditions [216]. Recently, the structural details of this regulatory mechanism have been elucidated. While the C-terminal regulatory domain from one monomer blocks the substrate entry site in the catalytic core of an adjacent monomer, AdoMet binding to the C-terminal domain (also called Bateman module) causes a domain shift and leads to the association of two C-terminal domains in a disk-like form, unblocking the substrate entrance and thus "activating" (or derepressing) the enzyme [44, 46]. The relevance of this regulatory mechanism is well attested by the fact that some homocystinuric patients express CBS variants with mutations in the C-terminal domain, that are naturally activated (more active than WT) and have limited or absent AdoMet response as the molecular basis of disease [217, 218]. While working on the kinetic characterization of NO and CO binding to human CBS, we noticed that AdoMet has the intriguing effect of eliciting faster and tighter binding of both CO and NO, thus making the enzyme more prone to inhibition by either gasotransmitter [204]. This observation is directly related to the binding of exogenous ligands, since AdoMet had been shown to have no effect on the heme redox properties [196]. Under the same reaction conditions, AdoMet makes CO inhibition >10 times more potent than in its absence ($K_{i(CO,+AdoMet)} = 0.7 \, \mu$M versus $K_{i(CO,-AdoMet)} = 9.5 \, \mu$M) [204]. The kinetic details of this functional effect have been investigated, and it was shown that AdoMet increases CO affinity by ~5-fold and association kinetics by ~10-fold, whereas the effect on NO binding is less drastic (~2-fold higher affinity with respect to AdoMet-free CBS). The latter observation also enforces the previous mechanistic proposal that CO and NO "attack" different sides of the heme. Recently, this observation has been extended to a clinically relevant variant, p.P49L, which displays the same AdoMet response in terms of becoming more sensitive to CO, while being slightly impaired in the AdoMet activation of H_2S production, compared to WT [203]. Irrespectively of the mechanistic details, the AdoMet-induced enhanced CO and NO binding appears as an intricate regulatory mechanism which adds to the complexity of CBS regulation.

4.3.3. Modulation of Sulfide Oxidation by NO. Whereas the effect of CO and NO on H_2S biosynthesis has been investigated in detail, much scarcer is the information on the effect of these two gaseous molecules on H_2S catabolism. Because CO and NO, similarly to cyanide, can both potently inhibit CcOX through different mechanisms (see above), relatively low concentrations of these gasotransmitters are expected to affect mitochondrial sulfide oxidation. Following cell exposure to CO or NO, a transient inhibition of CcOX is indeed expected to occur and lead to electron accumulation in the mitochondrial respiratory chain, eventually impairing quinol oxidation. As a result, SQR-mediated oxidation of sulfide is expected to be impaired as long as CcOX inhibition persists. Accordingly, addition of the NO releaser MAMA NONOate ($\geq$20 μM) or cyanide (260 μM) to colonocytes
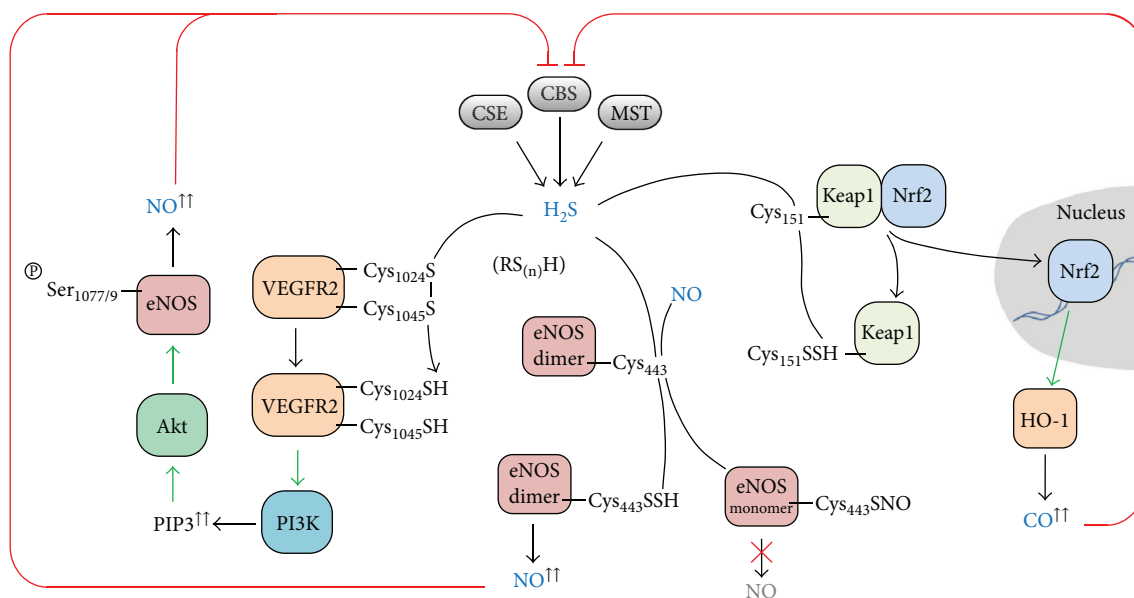
FIGURE 14: H_2S-mediated modulation of nitric oxide and carbon monoxide biosynthesis. Hydrogen sulfide produced by CBS, CSE, and MST, and the related per- and polysulfide species ($RS_{(n)}H$), can modulate NO and CO bioavailability through different mechanisms. Left, representation of sulfide-mediated enhanced eNOS activity: H_2S reduces VEGFR2 Cys_{1024}-Cys_{1045} disulfide, resulting in activation of PI3K; the accumulated PIP3 increases Akt-mediated phosphorylation of eNOS at Ser_{1077} and/or Ser_{1079}, enhancing its NO-synthesizing activity. Center, direct persulfidation of eNOS Cys_{443} sustains the protein catalytic activity by competing with Cys_{443} s-nitrosation, which causes dissociation of the active dimeric into the inactive monomeric form. Right, modulation of CO biosynthesis through increased expression of HO-1, mediated by the Keap1/Nrf2 pathway. Persulfidation of Keap1 Cys_{151}, either by reaction of H_2S with oxidized Cys_{151} or of reduced Cys_{151} with H_2S-derived HS·, causes its dissociation from Nrf2, which can then translocate to the nucleus, where it enhances heme oxygenase HO-1 expression, thus resulting in higher CO levels that may become inhibitory for CBS.

was recently reported to inhibit cellular respiration and its stimulation by 20 μM NaHS [219]. Furthermore, it is worth noting that long-term intraperitoneal or intravenous administration of nitroglycerine in rats was shown to induce decreased rhodanese activity and diminished levels of sulfane sulfur in liver extracts [220]. The observed inhibition of rhodanese was proposed to arise from s-nitrosation of the catalytic cysteine in the protein active site. A cysteine in the isolated rhodanese from bovine liver was indeed shown to be susceptible to s-nitrosation by the NO donors s-nitroso-N-acetylpenicillamine (SNAP) and GSNO, leading to enzyme inhibition [220].

The preliminary information reported above unveils an additional level at which the interplay between the gasotransmitters can be established. A full description of these molecular mechanisms awaits further investigations.

4.3.4. Modulation of NO and CO Synthesis by Hydrogen Sulfide. In light of the crosstalk between gasotransmitters, hydrogen sulfide has been shown to have a role in the control of NO and CO bioavailability under specific (patho)physiological conditions.

As mentioned above, CO is generated by either isoform of heme oxygenase, HO-1 and HO-2 [153]. Several lines of evidence point to a role of hydrogen sulfide in increasing the expression of heme oxygenase, particularly HO-1, and consequently CO levels (mostly evaluated from the abundance of carboxylated hemoglobin), thereby exerting either protective or deleterious effects (e.g., [221–227]). The

underlying regulatory mechanism is proposed to involve the Keap1/Nrf2 system. In particular, persulfidation of Keap1 Cys_{151}, by reaction either of H_2S with oxidized Cys_{151} or of reduced Cys_{151} with H_2S-derived HS· (Figure 11(a)), causes the protein dissociation from Nrf2 that, in turn, translocates into the nucleus, ultimately resulting in increased HO-1 transcription and protein levels (Figure 14) [225]. Another possibility whereby CO production may be modulated resides in the fact that a thiol/disulfide redox switch comprising three Cys-Pro signatures in HO-2 regulates heme binding [228, 229]. The sensitivity of this thiol/disulfide switch to the cellular redox state and possibly to the intracellular sulfide levels may afford another level of H_2S-mediated control of CO levels. Interestingly, the beneficial health effects of certain garlic-derived organosulfur compounds, particularly diallyl disulfide and trisulfide, have been proposed to be related with the modulation of CO production by H_2S via the Keap1/Nrf2 pathway [230–232].

The control of NO biosynthesis by hydrogen sulfide has been investigated in more detail and appears to occur at the transcriptional, translational, and posttranslational levels, involving other signaling pathways, besides a direct inhibition of all NOS isoforms by H_2S. The abundance of data in the literature highlights the fact that the effect of H_2S on the expression and activity of each NOS isoform can vary—sometimes yielding conflicting results—with the model organ, tissue, or cell type investigated and with the nature, concentration, and potency of the employed sulfide donor. Moreover, whereas in some studies "only"

the levels of NO (or nitrite/nitrate) are measured as a function of sulfide exposure, other studies further investigate the NO-mediated cellular and physiological effects of sulfide exposure.

Regulation of eNOS by H_2S has been thoroughly investigated. In different cell types and under different conditions and stimuli, eNOS activation in response to sulfide exposure seems to be mediated by the PIP3/Akt (phosphatidylinositol 3,4,5-trisphosphate/serine/threonine-specific protein kinase) pathway (Figure 14). The molecular mechanism is proposed to involve the reduction by H_2S of the vascular endothelial growth factor receptor 2 (VEGFR2) Cys_{1024}-Cys_{1045} disulfide that in the oxidized state represses its receptor activity. This H_2S-induced disulfide reduction thus prolongs the VEGFR2 activity and consequently the phosphatidylinositol-4,5-bisphosphate 3-kinase (PI3K) activity, yielding an increase in PIP3 levels (which may also be influenced by persulfidation of Cys_{124} in the phosphatase and tensin homolog (PTEN)). The resulting increased Akt activation leads to enhanced eNOS phosphorylation at Ser_{1177} and/or Ser_{1179}, thereby increasing the NO-synthesizing activity. Another level of sulfide-mediated eNOS regulation concerns the direct persulfidation at Cys_{443} (Figure 14). Whereas dimerization appears to be a prerequisite for optimal eNOS activity, s-nitrosation of Cys_{443} induces dimer dissociation into the virtually inactive monomeric form. Sulfide-mediated persulfidation of this residue actively competes with s-nitrosation, thereby maintaining eNOS in the active homodimeric form. Direct *in vitro* inhibition of recombinant eNOS by H_2S is characterized by an extremely high (nonphysiological) IC_{50} of $170\,\mu M$ [233]. Regarding the sulfide-mediated modulation of eNOS expression, various reports have either shown a down- or upregulation of eNOS mRNA and protein levels in response to H_2S exposure. These somehow contradictory results obtained for different model systems (animals, organs, and cells) rule out the establishment of a clear trend, induction versus repression, for sulfide modulation of eNOS expression.

Besides its direct *in vitro* inhibition at nonphysiological H_2S concentrations ($IC_{50} = 210\,\mu M$) [233], sulfide-mediated modulation of iNOS is reported to occur mainly through regulation of its expression. Similarly to eNOS, initial contradictory results indicated either an increase or a decrease in iNOS-mediated NO production in response to sulfide exposure [234]. This controversy was addressed by comparatively investigating the effects of different H_2S donors [235], showing that the rate of H_2S release by the donors is a key determinant for the downstream effects. Subsequent investigations on various models commonly assigned an inhibitory effect of sulfide on iNOS mRNA expression and consequently iNOS-mediated NO production, thereby contributing to the establishment of H_2S as an anti-inflammatory molecule (reviewed, e.g., in [154]).

Currently, the information on nNOS modulation by H_2S is scarce. Besides its inhibition at high nonphysiological sulfide concentrations ($IC_{50} = 130\,\mu M$) [233, 236], nNOS expression seems to be either insensitive to sulfide exposure or decreased upon overexpression of the H_2S-synthesizing CBS in hypertensive (but not normotensive) rats [237].

Altogether, the multiple molecular mechanisms whereby each of the three gasotransmitters may control the bioavailability of the others highlight the intricate signaling mechanisms that govern mammalian (patho)physiology and offer valuable possibilities for pharmacological targeting of each pathway.

5. Concluding Remarks

Hydrogen sulfide evolved from being merely perceived as a toxic and poisonous molecule to a prominent signaling molecule in mammalian physiology, joining nitric oxide and carbon monoxide as the triad of gasotransmitters. The last couple of decades witnessed an accumulation of data showing that (i) H_2S is endogenously synthesized and catabolized by specialized enzymes and kept under a tight control through multiple intricate regulatory mechanisms, (ii) the signaling functions attributed to H_2S are mainly linked to the interaction with and modification of target proteins, via reaction with metal centers (mostly in heme proteins) and through cysteine persulfidation that alters protein structure and function, (iii) dysregulation of H_2S homeostasis is at the basis of several pathologies, including cardiovascular and neurodegenerative diseases and cancer, and (iv) possible mechanisms underlying a functional crosstalk between the three gasotransmitters have been unveiled. The clear link between H_2S metabolism and homeostasis with human health has triggered a strong interest in the discovery and development of pharmacological (synthetic and naturally derived) compounds, either to release H_2S or to modulate the H_2S metabolism enzymes. Despite the accumulated knowledge on hydrogen sulfide biochemistry over the years, all a contribution as this one can amount to be, particularly concerning a field in its infancy, is just a still picture of a fast moving *body*. Indeed, during the writing of this manuscript, several pieces of information even challenging previous observations arose in the literature, further contributing to the complexity of this quickly progressing field.

Abbreviations

3-MP:	3-Mercaptopyruvate
AdoHcy:	S-Adenosyl-L-homocysteine
AdoMet:	S-Adenosyl-L-methionine
ADT-OH:	5-(4-Hydroxyphenyl)-3H-1,2-dithiole-3-thione
Akt:	Serine/threonine-specific protein kinase
AOAA:	Aminooxyacetic acid
AP39:	[10-Oxo-10-(4-(3-thioxo-3H-1,2-dithiol-5yl)phenoxy)decyl) triphenylphosphonium bromide]
ATP:	Adenosine triphosphate
CARSs:	Cysteinyl-tRNA synthetases
CAT:	Cysteine (or aspartate) aminotransferase
CBS:	Cystathionine β-synthase
CcOX:	Mitochondrial cytochrome c oxidase (complex IV)
CO:	Carbon monoxide
CSE:	Cystathionine γ-lyase

CysSOH: Cysteine residue with modified thiol to sulfenic acid
CysSSH: Cysteine persulfide
CysSS$_{(n)}$H: Cysteine polysulfide
CysSSOH: Cysteine perthiosulfenic
CysSSR: Cysteine residues with modified thiol to disulfide
DHLA: Dihydrolipoic acid
EDHF: Endothelium-derived hyperpolarizing factor
EDRF: Endothelium-derived relaxing factor
eIF2α: Eukaryotic translational initiation factor 2α
eNOS: Endothelial nitric oxide synthase
EPR: Electron paramagnetic resonance spectroscopy
ETHE1: Persulfide dioxygenase, or ethylmalonic encephalopathy protein 1
FAD: Flavin adenine dinucleotide
GAPDH: Glyceraldehyde 3-phosphate dehydrogenase
GSNO: S-Nitrosoglutathione
GSSH: Glutathione persulfide
GSS$_{(n)}$H: Glutathione polysulfide
Hb: Hemoglobin
H$_2$S: Hydrogen sulfide
H$_2$S$_2$: Hydrogen persulfide
H$_2$S$_3$: Hydrogen trisulfide
HO-1: Heme oxygenase 1
HO-2: Heme oxygenase 2
HS$^-$: Hydrosulfide
HSNO/ONS$^-$: Thionitrous acid/thionitrite
iNOS: Inducible nitric oxide synthase
Keap1: Kelch-like ECH-associated protein 1
Kir6.1: Inwardly rectifying potassium channel subunit Kir6.1
LMW: Low-molecular-weight
metHb: Ferric hemoglobin
Mb: Myoglobin
MSR: Methionine synthase reductase
MST: 3-Mercaptopyruvate sulfurtransferase
NADPH: Nicotinamide adenine dinucleotide phosphate (reduced form)
NF-κB: Nuclear factor κB
nNOS: Neuronal nitric oxide synthase
NO: Nitric oxide (NO·)
NO$^-$: Nitroxyl anion
NO$^+$: Nitrosonium ion
Nrf2: Nuclear factor erythroid 2-related factor 2
PERK: Protein kinase RNA-like ER kinase
PI3K: Phosphatidylinositol-4,5-bisphosphate 3-kinase
PIP3: Phosphatidylinositol 3,4,5-trisphosphate
PLP: Pyridoxal 5$'$-phosphate
PNP$^+$: Bis(triphenylphosphine)iminium
PPG: Propargylglycine
PtdIns(4,5)P$_2$: Phosphatidylinositol-4,5-bisphosphate
PTEN: Phosphatase and tensin homolog
PTP1B: Protein Tyr phosphatase 1B
Rhod: Rhodanese
RNS: Reactive nitrogen species
ROS: Reactive oxygen species
RSS: Reactive sulfur species
RSS·: Perthiyl radical
S^{2-}: Sulfide
SAHH: S-Adenosyl-L-homocysteine hydrolase
SMCs: Vascular smooth muscle cells
SOx: Sulfite oxidase
SQR: Sulfide:quinone oxidoreductase
SSNO$^-$: Nitropersulfide
Tom20: Translocase of the outer membrane 20
TPP$^+$: Triphenylphosphonium
Trx: Thioredoxin
VEGFR2: Vascular endothelial growth factor receptor 2.

Conflicts of Interest

The authors declare that they have no conflicts of interest.

Acknowledgments

References

[1] B. Ramazzini, *De Morbis Artificum Diatriba*, Baptistam Conzattum, Padova, 1713.

[2] C. W. Scheele, *Chemische Abhandlung von der Luft und dem Feuer*, Magnus Swederus, Upsala, Sweden, 1777.

[3] E. Cuevasanta, M. N. Möller, and B. Alvarez, "Biological chemistry of hydrogen sulfide and persulfides," *Archives of Biochemistry and Biophysics*, vol. 617, pp. 9–25, 2017.

[4] K. R. Olson and K. D. Straub, "The role of hydrogen sulfide in evolution and the evolution of hydrogen sulfide in metabolism and signaling," *Physiology*, vol. 31, no. 1, pp. 60–72, 2016.

[5] Q. Li and J. R. Lancaster Jr, "Chemical foundations of hydrogen sulfide biology," *Nitric Oxide*, vol. 35, pp. 21–34, 2013.

[6] K. Ono, T. Akaike, T. Sawa et al., "Redox chemistry and chemical biology of H$_2$S, hydropersulfides, and derived species: implications of their possible biological activity and utility," *Free Radical Biology and Medicine*, vol. 77, pp. 82–94, 2014.

[7] B. Szczesny, K. Módis, K. Yanagi et al., "AP39, a novel mitochondria-targeted hydrogen sulfide donor, stimulates cellular bioenergetics, exerts cytoprotective effects and protects against the loss of mitochondrial DNA integrity in oxidatively stressed endothelial cells *in vitro*," *Nitric Oxide*, vol. 41, pp. 120–130, 2014.

[8] X. Shen, M. Carlström, S. Borniquel, C. Jädert, C. G. Kevil, and J. O. Lundberg, "Microbial regulation of host hydrogen

sulfide bioavailability and metabolism," *Free Radical Biology and Medicine*, vol. 60, pp. 195–200, 2013.

[9] P. Rose, P. K. Moore, and Y. Z. Zhu, "H$_2$S biosynthesis and catabolism: new insights from molecular studies," *Cellular and Molecular Life Sciences*, vol. 74, no. 8, pp. 1391–1412, 2017.

[10] O. Kabil and R. Banerjee, "Enzymology of H$_2$S biogenesis, decay and signaling," *Antioxidants & Redox Signaling*, vol. 20, no. 5, pp. 770–782, 2014.

[11] R. Banerjee, "Catalytic promiscuity and heme-dependent redox regulation of H$_2$S synthesis," *Current Opinion in Chemical Biology*, vol. 37, pp. 115–121, 2017.

[12] L. Bao, Č. Vlček, V. Pačes, and J. P. Kraus, "Identification and tissue distribution of human cystathionine β-synthase mRNA isoforms," *Archives of Biochemistry and Biophysics*, vol. 350, no. 1, pp. 95–103, 1998.

[13] O. Kabil, V. Vitvitsky, P. Xie, and R. Banerjee, "The quantitative significance of the transsulfuration enzymes for H$_2$S production in murine tissues," *Antioxidants & Redox Signaling*, vol. 15, no. 2, pp. 363–372, 2011.

[14] S. H. Mudd, J. D. Finkelstein, F. Irreverre, and L. Laster, "Transsulfuration in mammals. Microassays and tissue distributions of three enzymes of the pathway," *Journal of Biological Chemistry*, vol. 240, no. 11, pp. 4382–4392, 1965.

[15] S. Saha, P. K. Chakraborty, X. Xiong et al., "Cystathionine β-synthase regulates endothelial function via protein S-sulfhydration," *The FASEB Journal*, vol. 30, no. 1, pp. 441–456, 2016.

[16] Y. Ogasawara, S. Isoda, and S. Tanabe, "Tissue and subcellular distribution of bound and acid-labile sulfur, and the enzymic capacity for sulfide production in the rat," *Biological & Pharmaceutical Bulletin*, vol. 17, no. 12, pp. 1535–1542, 1994.

[17] G. Yang, L. Wu, B. Jiang et al., "H$_2$S as a physiologic vasorelaxant: hypertension in mice with deletion of cystathionine γ-lyase," *Science*, vol. 322, no. 5901, pp. 587–590, 2008.

[18] T. Taniguchi and T. Kimura, "Role of 3-mercaptopyruvate sulfurtransferase in the formation of the iron-sulfur chromophore of adrenal ferredoxin," *Biochimica et Biophysica Acta (BBA) - Enzymology*, vol. 364, no. 2, pp. 284–295, 1974.

[19] N. Nagahara, T. Ito, H. Kitamura, and T. Nishino, "Tissue and subcellular distribution of mercaptopyruvate sulfurtransferase in the rat: confocal laser fluorescence and immunoelectron microscopic studies combined with biochemical analysis," *Histochemistry and Cell Biology*, vol. 110, no. 3, pp. 243–250, 1998.

[20] M. Tomita, N. Nagahara, and T. Ito, "Expression of 3-mercaptopyruvate sulfurtransferase in the mouse," *Molecules*, vol. 21, no. 12, article 1707, 2016.

[21] V. Vitvitsky, P. K. Yadav, A. Kurthen, and R. Banerjee, "Sulfide oxidation by a noncanonical pathway in red blood cells generates thiosulfate and polysulfides," *Journal of Biological Chemistry*, vol. 290, no. 13, pp. 8310–8320, 2015.

[22] O. Kabil and R. Banerjee, "Redox biochemistry of hydrogen sulfide," *Journal of Biological Chemistry*, vol. 285, no. 29, pp. 21903–21907, 2010.

[23] S. E. Bearden, R. S. Beard Jr, and J. C. Pfau, "Extracellular transsulfuration generates hydrogen sulfide from homocysteine and protects endothelium from redox stress," *American Journal of Physiology-Heart and Circulatory Physiology*, vol. 299, no. 5, pp. H1568–H1576, 2010.

[24] O. Kabil, Y. Zhou, and R. Banerjee, "Human cystathionine β-synthase is a target for sumoylation," *Biochemistry*, vol. 45, no. 45, pp. 13528–13536, 2006.

[25] F. Bouillaud and F. Blachier, "Mitochondria and sulfide: a very old story of poisoning, feeding, and signaling?," *Antioxidants & Redox Signaling*, vol. 15, no. 2, pp. 379–391, 2011.

[26] A. K. Mustafa, M. M. Gadalla, N. Sen et al., "H$_2$S signals through protein S-sulfhydration," *Science Signaling*, vol. 2, no. 96, p. ra72, 2009.

[27] K. Módis, Y. J. Ju, A. Ahmad et al., "S-Sulfhydration of ATP synthase by hydrogen sulfide stimulates mitochondrial bioenergetics," *Pharmacological Research*, vol. 113, no. Part A, pp. 116–124, 2016.

[28] M. Fu, W. Zhang, L. Wu, G. Yang, H. Li, and R. Wang, "Hydrogen sulfide (H$_2$S) metabolism in mitochondria and its regulatory role in energy production," *Proceedings of the National Academy of Sciences of the United States of America*, vol. 109, no. 8, pp. 2943–8, 2012.

[29] C. E. Cooper and G. C. Brown, "The inhibition of mitochondrial cytochrome oxidase by the gases carbon monoxide, nitric oxide, hydrogen cyanide and hydrogen sulfide: chemical mechanism and physiological significance," *Journal of Bioenergetics and Biomembranes*, vol. 40, no. 5, pp. 533–539, 2008.

[30] P. Nicholls, D. C. Marshall, C. E. Cooper, and M. T. Wilson, "Sulfide inhibition of and metabolism by cytochrome c oxidase," *Biochemical Society Transactions*, vol. 41, no. 5, pp. 1312–1316, 2013.

[31] J. B. Vicente, F. Malagrinò, M. Arese, E. Forte, P. Sarti, and A. Giuffrè, "Bioenergetic relevance of hydrogen sulfide and the interplay between gasotransmitters at human cystathionine β-synthase," *Biochimica et Biophysica Acta (BBA) - Bioenergetics*, vol. 1857, no. 8, pp. 1127–1138, 2016.

[32] H. Teng, B. Wu, K. Zhao, G. Yang, L. Wu, and R. Wang, "Oxygen-sensitive mitochondrial accumulation of cystathionine β-synthase mediated by Lon protease," *Proceedings of the National Academy of Sciences of the United States of America*, vol. 110, no. 31, pp. 12679–12684, 2013.

[33] C. Szabo, C. Coletta, C. Chao et al., "Tumor-derived hydrogen sulfide, produced by cystathionine-β-synthase, stimulates bioenergetics, cell proliferation, and angiogenesis in colon cancer," *Proceedings of the National Academy of Sciences of the United States of America*, vol. 110, no. 30, pp. 12474–12479, 2013.

[34] T. Yamamoto, N. Takano, K. Ishiwata et al., "Reduced methylation of PFKFB3 in cancer cells shunts glucose towards the pentose phosphate pathway," *Nature Communications*, vol. 5, article 3480, 2014.

[35] A. Davoli, V. Greco, A. Spalloni et al., "Evidence of hydrogen sulfide involvement in amyotrophic lateral sclerosis," *Annals of Neurology*, vol. 77, no. 4, pp. 697–709, 2015.

[36] B. Fräsdorf, C. Radon, and S. Leimkühler, "Characterization and interaction studies of two isoforms of the dual localized 3-mercaptopyruvate sulfurtransferase TUM1 from humans," *Journal of Biological Chemistry*, vol. 289, no. 50, pp. 34543–34556, 2014.

[37] J. D. Finkelstein, "Pathways and regulation of homocysteine metabolism in mammals," *Seminars in Thrombosis and Hemostasis*, vol. 26, no. 3, pp. 219–226, 2000.

[38] T. Majtan, J. Krijt, J. Sokolová et al., "Biogenesis of hydrogen sulfide and thioethers by cystathionine beta-synthase," *Antioxidants & Redox Signaling*, vol. 28, no. 4, pp. 311–323, 2018.

[39] S. Singh, D. Padovani, R. A. Leslie, T. Chiku, and R. Banerjee, "Relative contributions of cystathionine β-synthase and γ-cystathionase to H$_2$S biogenesis via alternative trans-sulfuration reactions," *Journal of Biological Chemistry*, vol. 284, no. 33, pp. 22457–22466, 2009.

[40] T. Chiku, D. Padovani, W. Zhu, S. Singh, V. Vitvitsky, and R. Banerjee, "H$_2$S biogenesis by human cystathionine γ-lyase leads to the novel sulfur metabolites lanthionine and homolanthionine and is responsive to the grade of hyperhomocysteinemia," *Journal of Biological Chemistry*, vol. 284, no. 17, pp. 11601–11612, 2009.

[41] V. Kožich, J. Krijt, J. Sokolová et al., "Thioethers as markers of hydrogen sulfide production in homocystinurias," *Biochimie*, vol. 126, pp. 14–20, 2016.

[42] N. Shibuya, S. Koike, M. Tanaka et al., "A novel pathway for the production of hydrogen sulfide from D-cysteine in mammalian cells," *Nature Communications*, vol. 4, article 1366, 2013.

[43] P. K. Yadav, K. Yamada, T. Chiku, M. Koutmos, and R. Banerjee, "Structure and kinetic analysis of H$_2$S production by human mercaptopyruvate sulfurtransferase," *Journal of Biological Chemistry*, vol. 288, no. 27, pp. 20002–20013, 2013.

[44] J. Ereño-Orbea, T. Majtan, I. Oyenarte, J. P. Kraus, and L. A. Martinez-Cruz, "Structural basis of regulation and oligomerization of human cystathionine β-synthase, the central enzyme of transsulfuration," *Proceedings of the National Academy of Sciences of the United States of America*, vol. 110, no. 40, pp. E3790–E3799, 2013.

[45] M. Meier, M. Janosik, V. Kery, J. P. Kraus, and P. Burkhard, "Structure of human cystathionine β-synthase: a unique pyridoxal 5′-phosphate-dependent heme protein," *The EMBO Journal*, vol. 20, no. 15, pp. 3910–3916, 2001.

[46] J. Ereño-Orbea, T. Majtan, I. Oyenarte, J. P. Kraus, and L. A. Martínez-Cruz, "Structural insight into the molecular mechanism of allosteric activation of human cystathionine β-synthase by S-adenosylmethionine," *Proceedings of the National Academy of Sciences of the United States of America*, vol. 111, no. 37, pp. E3845–E3852, 2014.

[47] M. Koutmos, O. Kabil, J. L. Smith, and R. Banerjee, "Structural basis for substrate activation and regulation by cystathionine beta-synthase (CBS) domains in cystathionine β-synthase," *Proceedings of the National Academy of Sciences of the United States of America*, vol. 107, no. 49, pp. 20958–20963, 2010.

[48] T. J. McCorvie, J. Kopec, S.-J. Hyung et al., "Inter-domain communication of human cystathionine β-synthase: structural basis of S-adenosyl-L-methionine activation," *Journal of Biological Chemistry*, vol. 289, no. 52, pp. 36018–36030, 2014.

[49] A. L. Pey, T. Majtan, J. M. Sanchez-Ruiz, and J. P. Kraus, "Human cystathionine β-synthase (CBS) contains two classes of binding sites for S-adenosylmethionine (SAM): complex regulation of CBS activity and stability by SAM," *Biochemical Journal*, vol. 449, no. 1, pp. 109–121, 2013.

[50] Q. Sun, R. Collins, S. Huang et al., "Structural basis for the inhibition mechanism of human cystathionine γ-lyase, an enzyme responsible for the production of H$_2$S," *Journal of Biological Chemistry*, vol. 284, no. 5, pp. 3076–3085, 2009.

[51] K. Hanaoka, K. Sasakura, Y. Suwanai et al., "Discovery and mechanistic characterization of selective inhibitors of H$_2$S-producing enzyme: 3-mercaptopyruvate sulfurtransferase (3MST) targeting active-site cysteinepersulfide," *Scientific Reports*, vol. 7, article 40227, 2017.

[52] L. C. Petersen, "The effect of inhibitors on the oxygen kinetics of cytochrome *c* oxidase," *Biochimica et Biophysica Acta (BBA) - Bioenergetics*, vol. 460, no. 2, pp. 299–307, 1977.

[53] C. G. Curtis, T. C. Bartholomew, F. A. Rose, and K. S. Dodgson, "Detoxication of sodium ^{35}S-sulphide in the rat," *Biochemical Pharmacology*, vol. 21, no. 17, pp. 2313–2321, 1972.

[54] E. Lagoutte, S. Mimoun, M. Andriamihaja, C. Chaumontet, F. Blachier, and F. Bouillaud, "Oxidation of hydrogen sulfide remains a priority in mammalian cells and causes reverse electron transfer in colonocytes," *Biochimica et Biophysica Acta (BBA) - Bioenergetics*, vol. 1797, no. 8, pp. 1500–1511, 2010.

[55] T. M. Hildebrandt and M. K. Grieshaber, "Three enzymatic activities catalyze the oxidation of sulfide to thiosulfate in mammalian and invertebrate mitochondria," *FEBS Journal*, vol. 275, no. 13, pp. 3352–3361, 2008.

[56] K. R. Olson, Y. Gao, F. Arif et al., "Metabolism of hydrogen sulfide (H$_2$S) and production of reactive sulfur species (RSS) by superoxide dismutase," *Redox Biology*, vol. 15, pp. 74–85, 2018.

[57] K. R. Olson, Y. Gao, E. R. DeLeon et al., "Catalase as a sulfide-sulfur oxido-reductase: an ancient (and modern?) regulator of reactive sulfur species (RSS)," *Redox Biology*, vol. 12, pp. 325–339, 2017.

[58] D. G. Searcy, "HS$^-$:O$_2$ oxidoreductase activity of Cu,Zn superoxide dismutase," *Archives of Biochemistry and Biophysics*, vol. 334, no. 1, pp. 50–58, 1996.

[59] D. G. Searcy, J. P. Whitehead, and M. J. Maroney, "Interaction of Cu,Zn superoxide dismutase with hydrogen sulfide," *Archives of Biochemistry and Biophysics*, vol. 318, no. 2, pp. 251–263, 1995.

[60] M. A. Powell and G. N. Somero, "Hydrogen sulfide oxidation is coupled to oxidative phosphorylation in mitochondria of *Solemya reidi*," *Science*, vol. 233, no. 4763, pp. 563–566, 1986.

[61] M. Goubern, M. Andriamihaja, T. Nubel, F. Blachier, and F. Bouillaud, "Sulfide, the first inorganic substrate for human cells," *The FASEB Journal*, vol. 21, no. 8, pp. 1699–1706, 2007.

[62] C. Szabo, C. Ransy, K. Módis et al., "Regulation of mitochondrial bioenergetic function by hydrogen sulfide. Part I. Biochemical and physiological mechanisms," *British Journal of Pharmacology*, vol. 171, no. 8, pp. 2099–2122, 2014.

[63] A. Abou-Hamdan, C. Ransy, T. Roger, H. Guedouari-Bounihi, E. Galardon, and F. Bouillaud, "Positive feedback during sulfide oxidation fine-tunes cellular affinity for oxygen," *Biochimica et Biophysica Acta (BBA) - Bioenergetics*, vol. 1857, no. 9, pp. 1464–1472, 2016.

[64] X. Leschelle, M. Goubern, M. Andriamihaja et al., "Adaptive metabolic response of human colonic epithelial cells to the adverse effects of the luminal compound sulfide," *Biochimica et Biophysica Acta (BBA) - General Subjects*, vol. 1725, no. 2, pp. 201–212, 2005.

[65] R. Yong and D. G. Searcy, "Sulfide oxidation coupled to ATP synthesis in chicken liver mitochondria," *Comparative Biochemistry and Physiology Part B: Biochemistry and Molecular Biology*, vol. 129, no. 1, pp. 129–137, 2001.

[66] A. Abou-Hamdan, H. Guedouari-Bounihi, V. Lenoir, M. Andriamihaja, F. Blachier, and F. Bouillaud, "Oxidation

of H$_2$S in mammalian cells and mitochondria," *Methods in Enzymology*, vol. 554, pp. 201–228, 2015.

[67] M. Groeger, J. Matallo, O. McCook et al., "Temperature and cell-type dependency of sulfide effects on mitochondrial respiration," *Shock*, vol. 38, no. 4, pp. 367–374, 2012.

[68] N. Helmy, C. Prip-Buus, C. Vons et al., "Oxidation of hydrogen sulfide by human liver mitochondria," *Nitric Oxide*, vol. 41, pp. 105–112, 2014.

[69] J. Matallo, J. Vogt, O. McCook et al., "Sulfide-inhibition of mitochondrial respiration at very low oxygen concentrations," *Nitric Oxide*, vol. 41, pp. 79–84, 2014.

[70] S. Mimoun, M. Andriamihaja, C. Chaumontet et al., "Detoxification of H$_2$S by differentiated colonic epithelial cells: implication of the sulfide oxidizing unit and of the cell respiratory capacity," *Antioxidants & Redox Signaling*, vol. 17, no. 1, pp. 1–10, 2012.

[71] K. Módis, C. Coletta, K. Erdélyi, A. Papapetropoulos, and C. Szabo, "Intramitochondrial hydrogen sulfide production by 3-mercaptopyruvate sulfurtransferase maintains mitochondrial electron flow and supports cellular bioenergetics," *The FASEB Journal*, vol. 27, no. 2, pp. 601–611, 2013.

[72] D. G. Searcy, "Metabolic integration during the evolutionary origin of mitochondria," *Cell Research*, vol. 13, no. 4, pp. 229–238, 2003.

[73] U. Theissen, M. Hoffmeister, M. Grieshaber, and W. Martin, "Single eubacterial origin of eukaryotic sulfide:quinone oxidoreductase, a mitochondrial enzyme conserved from the early evolution of eukaryotes during anoxic and sulfidic times," *Molecular Biology and Evolution*, vol. 20, no. 9, pp. 1564–1574, 2003.

[74] J. A. Brito, F. L. Sousa, M. Stelter et al., "Structural and functional insights into sulfide:quinone oxidoreductase," *Biochemistry*, vol. 48, no. 24, pp. 5613–5622, 2009.

[75] M. M. Cherney, Y. Zhang, M. Solomonson, J. H. Weiner, and M. N. G. James, "Crystal structure of sulfide:quinone oxidoreductase from *Acidithiobacillus ferrooxidans*: insights into sulfidotrophic respiration and detoxification," *Journal of Molecular Biology*, vol. 398, no. 2, pp. 292–305, 2010.

[76] M. Marcia, U. Ermler, G. Peng, and H. Michel, "The structure of *Aquifex aeolicus* sulfide:quinone oxidoreductase, a basis to understand sulfide detoxification and respiration," *Proceedings of the National Academy of Sciences of the United States of America*, vol. 106, no. 24, pp. 9625–9630, 2009.

[77] M. Marcia, U. Ermler, G. Peng, and H. Michel, "A new structure-based classification of sulfide:quinone oxidoreductases," *Proteins: Structure, Function, and Bioinformatics*, vol. 78, no. 5, pp. 1073–1083, 2010.

[78] M. M. Cherney, Y. Zhang, M. N. G. James, and J. H. Weiner, "Structure–activity characterization of sulfide:quinone oxidoreductase variants," *Journal of Structural Biology*, vol. 178, no. 3, pp. 319–328, 2012.

[79] K. D. C. Augustyn, M. R. Jackson, and M. S. Jorns, "Use of tissue metabolite analysis and enzyme kinetics to discriminate between alternate pathways for hydrogen sulfide metabolism," *Biochemistry*, vol. 56, no. 7, pp. 986–996, 2017.

[80] M. R. Jackson, S. L. Melideo, and M. S. Jorns, "Human sulfide:quinone oxidoreductase catalyzes the first step in hydrogen sulfide metabolism and produces a sulfane sulfur metabolite," *Biochemistry*, vol. 51, no. 34, pp. 6804–6815, 2012.

[81] M. R. Jackson, S. L. Melideo, and M. S. Jorns, "Role of human sulfide: quinone oxidoreductase in H$_2$S metabolism," *Methods in Enzymology*, vol. 554, pp. 255–270, 2015.

[82] M. Libiad, P. K. Yadav, V. Vitvitsky, M. Martinov, and R. Banerjee, "Organization of the human mitochondrial hydrogen sulfide oxidation pathway," *Journal of Biological Chemistry*, vol. 289, no. 45, pp. 30901–30910, 2014.

[83] A. P. Landry, D. P. Ballou, and R. Banerjee, "H$_2$S oxidation by nanodisc-embedded human sulfide quinone oxidoreductase," *Journal of Biological Chemistry*, vol. 292, no. 28, pp. 11641–11649, 2017.

[84] T. V. Mishanina, P. K. Yadav, D. P. Ballou, and R. Banerjee, "Transient kinetic analysis of hydrogen sulfide oxidation catalyzed by human sulfide quinone oxidoreductase," *Journal of Biological Chemistry*, vol. 290, no. 41, pp. 25072–25080, 2015.

[85] C. Griesbeck, M. Schütz, T. Schödl et al., "Mechanism of sulfide-quinone reductase investigated using site-directed mutagenesis and sulfur analysis," *Biochemistry*, vol. 41, no. 39, pp. 11552–11565, 2002.

[86] V. Tiranti, P. D'Adamo, E. Briem et al., "Ethylmalonic encephalopathy is caused by mutations in *ETHE1*, a gene encoding a mitochondrial matrix protein," *The American Journal of Human Genetics*, vol. 74, no. 2, pp. 239–252, 2004.

[87] V. Tiranti, C. Viscomi, T. Hildebrandt et al., "Loss of ETHE1, a mitochondrial dioxygenase, causes fatal sulfide toxicity in ethylmalonic encephalopathy," *Nature Medicine*, vol. 15, no. 2, pp. 200–205, 2009.

[88] I. Pettinati, J. Brem, M. A. McDonough, and C. J. Schofield, "Crystal structure of human persulfide dioxygenase: structural basis of ethylmalonic encephalopathy," *Human Molecular Genetics*, vol. 24, no. 9, pp. 2458–2469, 2015.

[89] R. J. Trevino, F. Gliubich, R. Berni et al., "NH$_2$-terminal sequence truncation decreases the stability of bovine rhodanese, minimally perturbs its crystal structure, and enhances interaction with GroEL under native conditions," *Journal of Biological Chemistry*, vol. 274, no. 20, pp. 13938–13947, 1999.

[90] K. Johnson-Winters, G. Tollin, and J. H. Enemark, "Elucidating the catalytic mechanism of sulfite oxidizing enzymes using structural, spectroscopic, and kinetic analyses," *Biochemistry*, vol. 49, no. 34, pp. 7242–7254, 2010.

[91] C. L. Bianco, J. P. Toscano, and J. M. Fukuto, "Chapter 2 – an integrated view of the chemical biology of NO, CO, H$_2$S, and O$_2$," in *Nitric Oxide (Third Edition)*, L. J. Ignarro and B. Freeman, Eds., pp. 9–21, Academic Press, London, UK, 2017.

[92] H. O. Michel, "A study of sulfhemoglobin," *Journal of Biological Chemistry*, vol. 126, no. 1, pp. 323–348, 1938.

[93] J. A. Berzofsky, J. Peisach, and W. E. Blumberg, "Sulfheme proteins. I. Optical and magnetic properties of sulfmyoglobin and its derivatives," *Journal of Biological Chemistry*, vol. 246, no. 10, pp. 3367–3377, 1971.

[94] P. Nicholls, "The formation and properties of sulphmyoglobin and sulphcatalase," *Biochemical Journal*, vol. 81, no. 2, pp. 374–383, 1961.

[95] P. Nagy, "Mechanistic chemical perspective of hydrogen sulfide signaling," *Methods in Enzymology*, vol. 554, pp. 3–29, 2015.

[96] B. B. Ríos-González, E. M. Román-Morales, R. Pietri, and J. López-Garriga, "Hydrogen sulfide activation in hemeproteins: the sulfheme scenario," *Journal of Inorganic Biochemistry*, vol. 133, pp. 78–86, 2014.

[97] R. Pietri, E. Román-Morales, and J. López-Garriga, "Hydrogen sulfide and hemeproteins: knowledge and mysteries," *Antioxidants & Redox Signaling*, vol. 15, no. 2, pp. 393–404, 2011.

[98] B. Chance, M. Erecinska, and M. Wagner, "Mitochondrial responses to carbon monoxide toxicity," *Annals of the New York Academy of Sciences*, vol. 174, pp. 193–204, 1970.

[99] M. Brunori, A. Giuffrè, E. Forte, D. Mastronicola, M. C. Barone, and P. Sarti, "Control of cytochrome *c* oxidase activity by nitric oxide," *Biochimica et Biophysica Acta (BBA) - Bioenergetics*, vol. 1655, no. 1–3, pp. 365–371, 2004.

[100] C. E. Cooper, "Nitric oxide and cytochrome oxidase: substrate, inhibitor or effector?," *Trends in Biochemical Sciences*, vol. 27, no. 1, pp. 33–39, 2002.

[101] C. E. Cooper and C. Giulivi, "Nitric oxide regulation of mitochondrial oxygen consumption II: molecular mechanism and tissue physiology," *American Journal of Physiology-Cell Physiology*, vol. 292, no. 6, pp. C1993–C2003, 2007.

[102] P. Sarti, M. Arese, A. Bacchi et al., "Nitric oxide and mitochondrial complex IV," *IUBMB Life*, vol. 55, no. 10–11, pp. 605–611, 2003.

[103] P. Sarti, E. Forte, D. Mastronicola, A. Giuffrè, and M. Arese, "Cytochrome *c* oxidase and nitric oxide in action: molecular mechanisms and pathophysiological implications," *Biochimica et Biophysica Acta (BBA) - Bioenergetics*, vol. 1817, no. 4, pp. 610–619, 2012.

[104] P. Sarti, A. Giuffrè, M. C. Barone, E. Forte, D. Mastronicola, and M. Brunori, "Nitric oxide and cytochrome oxidase: reaction mechanisms from the enzyme to the cell," *Free Radical Biology and Medicine*, vol. 34, no. 5, pp. 509–520, 2003.

[105] M. G. Mason, P. Nicholls, M. T. Wilson, and C. E. Cooper, "Nitric oxide inhibition of respiration involves both competitive (heme) and noncompetitive (copper) binding to cytochrome *c* oxidase," *Proceedings of the National Academy of Sciences of the United States of America*, vol. 103, no. 3, pp. 708–713, 2006.

[106] D. Mastronicola, M. L. Genova, M. Arese et al., "Control of respiration by nitric oxide in Keilin-Hartree particles, mitochondria and SH-SY5Y neuroblastoma cells," *Cellular and Molecular Life Sciences (CMLS)*, vol. 60, no. 8, pp. 1752–1759, 2003.

[107] P. Sarti, A. Giuffrè, E. Forte, D. Mastronicola, M. C. Barone, and M. Brunori, "Nitric oxide and cytochrome *c* oxidase: mechanisms of inhibition and NO degradation," *Biochemical and Biophysical Research Communications*, vol. 274, no. 1, pp. 183–187, 2000.

[108] P. Nicholls, "The effect of sulphide on cytochrome *aa₃* isosteric and allosteric shifts of the reduced α-peak," *Biochimica et Biophysica Acta (BBA) - Bioenergetics*, vol. 396, no. 1, pp. 24–35, 1975.

[109] P. Nicholls, L. C. Petersen, M. Miller, and F. B. Hansen, "Ligand-induced spectral changes in cytochrome *c* oxidase and their possible significance," *Biochimica et Biophysica Acta (BBA) - Bioenergetics*, vol. 449, no. 2, pp. 188–196, 1976.

[110] B. C. Hill, T. C. Woon, P. Nicholls, J. Peterson, C. Greenwood, and A. J. Thomson, "Interactions of sulphide and other ligands with cytochrome *c* oxidase. An electron-paramagnetic-resonance study," *Biochemical Journal*, vol. 224, no. 2, pp. 591–600, 1984.

[111] P. Nicholls and J. K. Kim, "Sulphide as an inhibitor and electron donor for the cytochrome *c* oxidase system," *Canadian Journal of Biochemistry*, vol. 60, no. 6, pp. 613–623, 1982.

[112] P. R. Rich, B. Meunier, R. Mitchell, and A. John Moody, "Coupling of charge and proton movement in cytochrome c oxidase," *Biochimica et Biophysica Acta (BBA) - Bioenergetics*, vol. 1275, no. 1–2, pp. 91–95, 1996.

[113] P. Nicholls and J. K. Kim, "Oxidation of sulphide by cytochrome *aa₃*," *Biochimica et Biophysica Acta (BBA) - Bioenergetics*, vol. 637, no. 2, pp. 312–320, 1981.

[114] R. P. Smith and R. E. Gosselin, "On the mechanism of sulfide inactivation by methemoglobin," *Toxicology and Applied Pharmacology*, vol. 8, no. 1, pp. 159–172, 1966.

[115] V. Vitvitsky, P. K. Yadav, S. An, J. Seravalli, U. S. Cho, and R. Banerjee, "Structural and mechanistic insights into hemoglobin-catalyzed hydrogen sulfide oxidation and the fate of polysulfide products," *Journal of Biological Chemistry*, vol. 292, no. 13, pp. 5584–5592, 2017.

[116] L. Potor, P. Nagy, G. Méhes et al., "Hydrogen sulfide abrogates hemoglobin-lipid interaction in atherosclerotic lesion," *Oxidative Medicine and Cellular Longevity*, vol. 2018, Article ID 3812568, 16 pages, 2018.

[117] D. Garai, B. B. Ríos-González, P. G. Furtmüller et al., "Mechanisms of myeloperoxidase catalyzed oxidation of H_2S by H_2O_2 or O_2 to produce potent protein Cys-polysulfide-inducing species," *Free Radical Biology and Medicine*, vol. 113, pp. 551–563, 2017.

[118] Z. Pálinkás, P. G. Furtmüller, A. Nagy et al., "Interactions of hydrogen sulfide with myeloperoxidase," *British Journal of Pharmacology*, vol. 172, no. 6, pp. 1516–1532, 2015.

[119] H. Kimura, "Hydrogen polysulfide (H_2S_n) signaling along with hydrogen sulfide (H_2S) and nitric oxide (NO)," *Journal of Neural Transmission*, vol. 123, no. 11, pp. 1235–1245, 2016.

[120] B. D. Paul and S. H. Snyder, "H_2S: a novel gasotransmitter that signals by sulfhydration," *Trends in Biochemical Sciences*, vol. 40, no. 11, pp. 687–700, 2015.

[121] B. D. Paul and S. H. Snyder, "Protein sulfhydration," *Methods in Enzymology*, vol. 555, pp. 79–90, 2015.

[122] R. Millikin, C. L. Bianco, C. White et al., "The chemical biology of protein hydropersulfides: studies of a possible protective function of biological hydropersulfide generation," *Free Radical Biology and Medicine*, vol. 97, pp. 136–147, 2016.

[123] C. L. Bianco, T. A. Chavez, V. Sosa et al., "The chemical biology of the persulfide (RSSH)/perthiyl (RSS·) redox couple and possible role in biological redox signaling," *Free Radical Biology and Medicine*, vol. 101, pp. 20–31, 2016.

[124] D. E. Heppner, M. Hristova, T. Ida et al., "Cysteine perthiosulfenic acid (Cys-SSOH): a novel intermediate in thiol-based redox signaling?," *Redox Biology*, vol. 14, pp. 379–385, 2018.

[125] T. Ida, T. Sawa, H. Ihara et al., "Reactive cysteine persulfides and S-polythiolation regulate oxidative stress and redox signaling," *Proceedings of the National Academy of Sciences of the United States of America*, vol. 111, no. 21, pp. 7606–7611, 2014.

[126] T. V. Mishanina, M. Libiad, and R. Banerjee, "Biogenesis of reactive sulfur species for signaling by hydrogen sulfide oxidation pathways," *Nature Chemical Biology*, vol. 11, no. 7, pp. 457–464, 2015.

[127] B. D. Paul and S. H. Snyder, "H$_2$S signalling through protein sulfhydration and beyond," *Nature Reviews Molecular Cell Biology*, vol. 13, no. 8, pp. 499–507, 2012.

[128] L. B. Poole and C. Schöneich, "Introduction: what we do and do not know regarding redox processes of thiols in signaling pathways," *Free Radical Biology and Medicine*, vol. 80, pp. 145–147, 2015.

[129] M. R. Filipovic, J. Zivanovic, B. Alvarez, and R. Banerjee, "Chemical biology of H$_2$S signaling through persulfidation," *Chemical Reviews*, vol. 118, no. 3, pp. 1253–1337, 2018.

[130] T. N. Das, R. E. Huie, P. Neta, and S. Padmaja, "Reduction potential of the sulfhydryl radical: pulse radiolysis and laser flash photolysis studies of the formation and reactions of ·SH and HSSH·$^-$ in aqueous solutions," *The Journal of Physical Chemistry A*, vol. 103, no. 27, pp. 5221–5226, 1999.

[131] T. Akaike, T. Ida, F. Y. Wei et al., "Cysteinyl-tRNA synthetase governs cysteine polysulfidation and mitochondrial bioenergetics," *Nature Communications*, vol. 8, no. 1, p. 1177, 2017.

[132] P. K. Yadav, M. Martinov, V. Vitvitsky et al., "Biosynthesis and reactivity of cysteine persulfides in signaling," *Journal of the American Chemical Society*, vol. 138, no. 1, pp. 289–299, 2016.

[133] Y. Kimura, S. Koike, N. Shibuya, D. Lefer, Y. Ogasawara, and H. Kimura, "3-Mercaptopyruvate sulfurtransferase produces potential redox regulators cysteine- and glutathione-persulfide (Cys-SSH and GSSH) together with signaling molecules H$_2$S$_2$, H$_2$S$_3$ and H$_2$S," *Scientific Reports*, vol. 7, no. 1, article 10459, 2017.

[134] Y. Kimura, Y. Toyofuku, S. Koike et al., "Identification of H$_2$S$_3$ and H$_2$S produced by 3-mercaptopyruvate sulfurtransferase in the brain," *Scientific Reports*, vol. 5, no. 1, article 14774, 2015.

[135] N. Shibuya, M. Tanaka, M. Yoshida et al., "3-Mercaptopyruvate sulfurtransferase produces hydrogen sulfide and bound sulfane sulfur in the brain," *Antioxidants & Redox Signaling*, vol. 11, no. 4, pp. 703–714, 2009.

[136] E. Cuevasanta, M. Lange, J. Bonanata et al., "Reaction of hydrogen sulfide with disulfide and sulfenic acid to form the strongly nucleophilic persulfide," *Journal of Biological Chemistry*, vol. 290, no. 45, pp. 26866–26880, 2015.

[137] N. Krishnan, C. Fu, D. J. Pappin, and N. K. Tonks, "H$_2$S-induced sulfhydration of the phosphatase PTP1B and its role in the endoplasmic reticulum stress response," *Science Signaling*, vol. 4, no. 203, p. ra86, 2011.

[138] N. Sen, B. D. Paul, M. M. Gadalla et al., "Hydrogen sulfide-linked sulfhydration of NF-κB mediates its antiapoptotic actions," *Molecular Cell*, vol. 45, no. 1, pp. 13–24, 2012.

[139] A. K. Mustafa, G. Sikka, S. K. Gazi et al., "Hydrogen sulfide as endothelium-derived hyperpolarizing factor sulfhydrates potassium channels," *Circulation Research*, vol. 109, no. 11, pp. 1259–1268, 2011.

[140] E. Doka, I. Pader, A. Biro et al., "A novel persulfide detection method reveals protein persulfide- and polysulfide-reducing functions of thioredoxin and glutathione systems," *Science Advances*, vol. 2, no. 1, article e1500968, 2016.

[141] X.-H. Gao, D. Krokowski, B.-J. Guan et al., "Quantitative H$_2$S-mediated protein sulfhydration reveals metabolic reprogramming during the integrated stress response," *eLife*, vol. 4, article e10067, 2015.

[142] S. Longen, F. Richter, Y. Köhler, I. Wittig, K. F. Beck, and J. Pfeilschifter, "Quantitative persulfide site identification (qPerS-SID) reveals protein targets of H$_2$S releasing donors in mammalian cells," *Scientific Reports*, vol. 6, no. 1, article 29808, 2016.

[143] D. Zhang, I. Macinkovic, N. O. Devarie-Baez et al., "Detection of protein S-sulfhydration by a tag-switch technique," *Angewandte Chemie International Edition*, vol. 53, no. 2, pp. 575–581, 2014.

[144] R. Wang, "Two's company, three's a crowd: can H$_2$S be the third endogenous gaseous transmitter?," *The FASEB Journal*, vol. 16, no. 13, pp. 1792–1798, 2002.

[145] M. M. Cortese-Krott, A. Koning, G. G. C. Kuhnle et al., "The reactive species interactome: evolutionary emergence, biological significance, and opportunities for redox metabolomics and personalized medicine," *Antioxidants & Redox Signaling*, vol. 27, no. 10, pp. 684–712, 2017.

[146] "The Nobel prize in physiology or medicine 1998," Nobel Media AB, 2014, http://www.nobelprize.org/nobel_prizes/medicine/laureates/1998/.

[147] L. J. Ignarro, R. E. Byrns, G. M. Buga, and K. S. Wood, "Endothelium-derived relaxing factor from pulmonary artery and vein possesses pharmacologic and chemical properties identical to those of nitric oxide radical," *Circulation Research*, vol. 61, no. 6, pp. 866–879, 1987.

[148] R. M. J. Palmer, A. G. Ferrige, and S. Moncada, "Nitric oxide release accounts for the biological activity of endothelium-derived relaxing factor," *Nature*, vol. 327, no. 6122, pp. 524–526, 1987.

[149] R. Zakhary, S. P. Gaine, J. L. Dinerman, M. Ruat, N. A. Flavahan, and S. H. Snyder, "Heme oxygenase 2: endothelial and neuronal localization and role in endothelium-dependent relaxation," *Proceedings of the National Academy of Sciences of the United States of America*, vol. 93, no. 2, pp. 795–798, 1996.

[150] C. Bogdan, "Nitric oxide and the immune response," *Nature Immunology*, vol. 2, no. 10, pp. 907–916, 2001.

[151] V. Kuhn, L. Diederich, T. C. S. Keller IV et al., "Red blood cell function and dysfunction: redox regulation, nitric oxide metabolism, anemia," *Antioxidants & Redox Signaling*, vol. 26, no. 13, pp. 718–742, 2017.

[152] J. O. Lundberg and E. Weitzber, "Nitric oxide formation from inorganic nitrate," in *Nitric Oxide, Biology and Pathobiology*, L. J. Ignarro and B. A. Freeman, Eds., Academic Press, London, Third edition, 2017.

[153] L. Wu and R. Wang, "Carbon monoxide: endogenous production, physiological functions, and pharmacological applications," *Pharmacological Reviews*, vol. 57, no. 4, pp. 585–630, 2005.

[154] C. G. Kevil, M. M. Cortese-Krott, P. Nagy, A. Papapetropoulos, M. Feelisch, and C. Szabo, "Cooperative interactions between NO and H$_2$S: chemistry, biology, physiology, pathophysiology," in *Nitric Oxide, Biology and Pathobiology*, L. J. Ignarro and B. A. Freeman, Eds., Academic Press, London, Third edition, 2017.

[155] M. M. Cortese-Krott, B. O. Fernandez, M. Kelm, A. R. Butler, and M. Feelisch, "On the chemical biology of the nitrite/sulfide interaction," *Nitric Oxide*, vol. 46, pp. 14–24, 2015.

[156] S. Carballal, M. Trujillo, E. Cuevasanta et al., "Reactivity of hydrogen sulfide with peroxynitrite and other oxidants of biological interest," *Free Radical Biology and Medicine*, vol. 50, no. 1, pp. 196–205, 2011.

[157] E. Cuevasanta, A. Zeida, S. Carballal et al., "Insights into the mechanism of the reaction between hydrogen sulfide and peroxynitrite," *Free Radical Biology and Medicine*, vol. 80, pp. 93–100, 2015.

[158] A. Berenyiova, M. Grman, A. Mijuskovic et al., "The reaction products of sulfide and S-nitrosoglutathione are potent vasorelaxants," *Nitric Oxide*, vol. 46, pp. 123–130, 2015.

[159] M. M. Cortese-Krott, B. O. Fernandez, J. L. T. Santos et al., "Nitrosopersulfide (SSNO⁻) accounts for sustained NO bioactivity of S-nitrosothiols following reaction with sulfide," *Redox Biology*, vol. 2, pp. 234–244, 2014.

[160] M. M. Cortese-Krott, G. G. C. Kuhnle, A. Dyson et al., "Key bioactive reaction products of the NO/H₂S interaction are S/N-hybrid species, polysulfides, and nitroxyl," *Proceedings of the National Academy of Sciences of the United States of America*, vol. 112, no. 34, pp. E4651–E4660, 2015.

[161] M. R. Filipovic, J. L. Miljkovic, T. Nauser et al., "Chemical characterization of the smallest S-nitrosothiol, HSNO; cellular cross-talk of H₂S and S-nitrosothiols," *Journal of the American Chemical Society*, vol. 134, no. 29, pp. 12016–12027, 2012.

[162] X. Teng, T. Scott Isbell, J. H. Crawford et al., "Novel method for measuring S-nitrosothiols using hydrogen sulfide," *Methods in Enzymology*, vol. 441, pp. 161–172, 2008.

[163] K. Ondrias, A. Stasko, S. Cacanyiova et al., "H₂S and HS⁻ donor NaHS releases nitric oxide from nitrosothiols, metal nitrosyl complex, brain homogenate and murine L1210 leukaemia cells," *Pflügers Archiv - European Journal of Physiology*, vol. 457, no. 2, pp. 271–279, 2008.

[164] M. R. Filipovic, M. Eberhardt, V. Prokopovic et al., "Beyond H₂S and NO interplay: hydrogen sulfide and nitroprusside react directly to give nitroxyl (HNO). A new pharmacological source of HNO," *Journal of Medicinal Chemistry*, vol. 56, no. 4, pp. 1499–1508, 2013.

[165] Y. Gao, A. Toubaei, X. Kong, and G. Wu, "Solving the 170-year-old mystery about red-violet and blue transient intermediates in the Gmelin reaction," *Chemistry - A European Journal*, vol. 21, no. 48, pp. 17172–17177, 2015.

[166] J. A. Olabe and V. T. Amorebieta, "P38 mechanism of the reactions of the nitroprusside ion, Fe (CN)₅NO²⁻, with sulfides," *Nitric Oxide*, vol. 31, Supplement 2, p. S52, 2013.

[167] S. L. Quiroga, A. E. Almaraz, V. T. Amorebieta, L. L. Perissinotti, and J. A. Olabe, "Addition and redox reactivity of hydrogen sulfides (H₂S/HS⁻) with nitroprusside: new chemistry of nitrososulfide ligands," *Chemistry - A European Journal*, vol. 17, no. 15, pp. 4145–4156, 2011.

[168] S. Bruce King, "Potential biological chemistry of hydrogen sulfide (H₂S) with the nitrogen oxides," *Free Radical Biology and Medicine*, vol. 55, pp. 1–7, 2013.

[169] M. M. Cortese-Krott, A. R. Butler, J. D. Woollins, and M. Feelisch, "Inorganic sulfur–nitrogen compounds: from gunpowder chemistry to the forefront of biological signaling," *Dalton Transactions*, vol. 45, no. 14, pp. 5908–5919, 2016.

[170] J. M. Fukuto, S. J. Carrington, D. J. Tantillo et al., "Small molecule signaling agents: the integrated chemistry and biochemistry of nitrogen oxides, oxides of carbon, dioxygen, hydrogen sulfide, and their derived species," *Chemical Research in Toxicology*, vol. 25, no. 4, pp. 769–793, 2012.

[171] G. K. Kolluru, S. Yuan, X. Shen, and C. G. Kevil, "H₂S regulation of nitric oxide metabolism," *Methods in Enzymology*, vol. 554, pp. 271–297, 2015.

[172] M. Y. Ali, C. Y. Ping, Y.-Y. P. Mok et al., "Regulation of vascular nitric oxide *in vitro* and *in vivo*; a new role for endogenous hydrogen sulphide?," *British Journal of Pharmacology*, vol. 149, no. 6, pp. 625–634, 2006.

[173] M. Whiteman, L. Li, I. Kostetski et al., "Evidence for the formation of a novel nitrosothiol from the gaseous mediators nitric oxide and hydrogen sulphide," *Biochemical and Biophysical Research Communications*, vol. 343, no. 1, pp. 303–310, 2006.

[174] M. M. Cortese-Krott, D. Pullmann, and M. Feelisch, "Nitrosopersulfide (SSNO⁻) targets the Keap-1/Nrf2 redox system," *Pharmacological Research*, vol. 113, no. Part A, pp. 490–499, 2016.

[175] A. P. Munro and D. L. H. Williams, "Reactivity of sulfur nucleophiles towards S-nitrosothiols," *Journal of the Chemical Society, Perkin Transactions 2*, no. 9, pp. 1794–1797, 2000.

[176] D. L. H. Williams, *Nitrosation Reactions and the Chemistry of Nitric Oxide*, Elsevier, Amsterdam, 2004.

[177] F. Seel and M. Wagner, "Reaction of sulfides with nitrogen monoxide in aqueous-solution," *Zeitschrift für Anorganische und Allgemeine Chemie*, vol. 558, no. 3, pp. 189–192, 1988.

[178] C. Bolden, S. B. King, and D. B. Kim-Shapiro, "Reactions between nitrosopersulfide and heme proteins," *Free Radical Biology and Medicine*, vol. 99, pp. 418–425, 2016.

[179] F. Seel, R. Kuhn, G. Simon, and M. Wagner, "PNP-Perthionitrit und PNP-Monothionitrit / PNP-Perthionitrite and PNP-M onothionitrite," *Zeitschrift für Naturforschung B*, vol. 40, no. 12, pp. 1607–1617, 1985.

[180] R. Wedmann, I. Ivanovic-Burmazovic, and M. R. Filipovic, "Nitrosopersulfide (SSNO⁻) decomposes in the presence of sulfide, cyanide or glutathione to give HSNO/SNO⁻: consequences for the assumed role in cell signalling," *Interface Focus*, vol. 7, no. 2, article 20160139, 2017.

[181] R. Wedmann, A. Zahl, T. E. Shubina et al., "Does perthionitrite (SSNO⁻) account for sustained bioactivity of NO? A (bio)chemical characterization," *Inorganic Chemistry*, vol. 54, no. 19, pp. 9367–9380, 2015.

[182] T. Morikawa, M. Kajimura, T. Nakamura et al., "Hypoxic regulation of the cerebral microcirculation is mediated by a carbon monoxide-sensitive hydrogen sulfide pathway," *Proceedings of the National Academy of Sciences of the United States of America*, vol. 109, no. 4, pp. 1293–1298, 2012.

[183] T. Shintani, T. Iwabuchi, T. Soga et al., "Cystathionine β-synthase as a carbon monoxide–sensitive regulator of bile excretion," *Hepatology*, vol. 49, no. 1, pp. 141–150, 2009.

[184] C. N. Wang, G. L. Duan, Y. J. Liu et al., "Overproduction of nitric oxide by endothelial cells and macrophages contributes to mitochondrial oxidative stress in adrenocortical cells and adrenal insufficiency during endotoxemia," *Free Radical Biology and Medicine*, vol. 83, pp. 31–40, 2015.

[185] M. Kajimura, R. Fukuda, R. M. Bateman, T. Yamamoto, and M. Suematsu, "Interactions of multiple gas-transducing systems: hallmarks and uncertainties of CO, NO, and H₂S gas biology," *Antioxidants & Redox Signaling*, vol. 13, no. 2, pp. 157–192, 2010.

[186] O. Kabil, V. Yadav, and R. Banerjee, "Heme-dependent metabolite switching regulates H₂S synthesis in response to endoplasmic reticulum (ER) stress," *Journal of Biological Chemistry*, vol. 291, no. 32, pp. 16418–16423, 2016.

[187] M. Suematsu, T. Nakamura, Y. Tokumoto, T. Yamamoto, M. Kajimura, and Y. Kabe, "CO-CBS-H₂S axis: from vascular

mediator to cancer regulator," *Microcirculation*, vol. 23, no. 3, pp. 183–190, 2016.

[188] J. Oliveriusová, Vladimír Kery, K. N. Maclean, and J. P. Kraus, "Deletion mutagenesis of human cystathionine β-synthase. Impact on activity, oligomeric status, and *S*-adenosyl-methionine regulation," *Journal of Biological Chemistry*, vol. 277, no. 50, pp. 48386–48394, 2002.

[189] A. Kumar, A. Wißbrock, N. Goradia et al., "Heme interaction of the intrinsically disordered N-terminal peptide segment of human cystathionine-β-synthase," *Scientific Reports*, vol. 8, no. 1, p. 2474.

[190] M. M. Cherney, S. Pazicni, N. Frank, K. A. Marvin, J. P. Kraus, and J. N. Burstyn, "Ferrous human cystathionine β-synthase loses activity during enzyme assay due to a ligand switch process," *Biochemistry*, vol. 46, no. 45, pp. 13199–13210, 2007.

[191] C. Gherasim, P. K. Yadav, O. Kabil, W.-N. Niu, and R. Banerjee, "Nitrite reductase activity and inhibition of H₂S biogenesis by human cystathionine ß-synthase," *PLoS One*, vol. 9, no. 1, article e85544, 2014.

[192] M. Puranik, C. L. Weeks, D. Lahaye et al., "Dynamics of carbon monoxide binding to cystathionine β-synthase," *Journal of Biological Chemistry*, vol. 281, no. 19, pp. 13433–13438, 2006.

[193] S. Taoka and R. Banerjee, "Characterization of NO binding to human cystathionine β-synthase: possible implications of the effects of CO and NO binding to the human enzyme," *Journal of Inorganic Biochemistry*, vol. 87, no. 4, pp. 245–251, 2001.

[194] S. Taoka, M. West, and R. Banerjee, "Characterization of the heme and pyridoxal phosphate cofactors of human cystathionine β-synthase reveals nonequivalent active sites," *Biochemistry*, vol. 38, no. 22, p. 7406, 1999.

[195] J. B. Vicente, H. G. Colaço, M. I. S. Mendes, P. Sarti, P. Leandro, and A. Giuffrè, "NO• binds human cystathionine β-synthase quickly and tightly," *Journal of Biological Chemistry*, vol. 289, no. 12, pp. 8579–8587, 2014.

[196] S. Singh, P. Madzelan, J. Stasser et al., "Modulation of the heme electronic structure and cystathionine beta-synthase activity by second coordination sphere ligands: the role of heme ligand switching in redox regulation," *Journal of Inorganic Biochemistry*, vol. 103, no. 5, pp. 689–697, 2009.

[197] S. Carballal, E. Cuevasanta, I. Marmisolle et al., "Kinetics of reversible reductive carbonylation of heme in human cystathionine β-synthase," *Biochemistry*, vol. 52, no. 26, pp. 4553–4562, 2013.

[198] C. L. Weeks, S. Singh, P. Madzelan, R. Banerjee, and T. G. Spiro, "Heme regulation of human cystathionine β-synthase activity: insights from fluorescence and Raman spectroscopy," *Journal of the American Chemical Society*, vol. 131, no. 35, pp. 12809–12816, 2009.

[199] P. K. Yadav, P. Xie, and R. Banerjee, "Allosteric communication between the pyridoxal 5′-phosphate (PLP) and heme sites in the H₂S generator human cystathionine β-synthase," *Journal of Biological Chemistry*, vol. 287, no. 45, pp. 37611–37620, 2012.

[200] A. T. Smith, Y. Su, D. J. Stevens, T. Majtan, J. P. Kraus, and J. N. Burstyn, "Effect of the disease-causing R266K mutation on the heme and PLP environments of human cystathionine β-synthase," *Biochemistry*, vol. 51, no. 32, pp. 6360–6370, 2012.

[201] S. Carballal, E. Cuevasanta, P. K. Yadav et al., "Kinetics of nitrite reduction and peroxynitrite formation by ferrous

heme in human cystathionine β-synthase," *Journal of Biological Chemistry*, vol. 291, no. 15, pp. 8004–8013, 2016.

[202] S. Carballal, P. Madzelan, C. F. Zinola et al., "Dioxygen reactivity and heme redox potential of truncated human cystathionine β-synthase," *Biochemistry*, vol. 47, no. 10, pp. 3194–3201, 2008.

[203] J. B. Vicente, H. G. Colaço, F. Malagrinò et al., "A clinically relevant variant of the human hydrogen sulfide-synthesizing enzyme cystathionine β-synthase: increased CO reactivity as a novel molecular mechanism of pathogenicity?," *Oxidative Medicine and Cellular Longevity*, vol. 2017, Article ID 8940321, 13 pages, 2017.

[204] J. B. Vicente, H. G. Colaco, P. Sarti, P. Leandro, and A. Giuffrè, "S-Adenosyl-L-methionine modulates CO and NO• binding to the human H₂S-generating enzyme cystathionine β-synthase," *Journal of Biological Chemistry*, vol. 291, no. 2, pp. 572–581, 2016.

[205] J. Kopecká, J. Krijt, K. Raková, and V. Kožich, "Restoring assembly and activity of cystathionine β-synthase mutants by ligands and chemical chaperones," *Journal of Inherited Metabolic Disease*, vol. 34, no. 1, pp. 39–48, 2011.

[206] T. Majtan, L. Liu, J. F. Carpenter, and J. P. Kraus, "Rescue of cystathionine β-synthase (CBS) mutants with chemical chaperones: purification and characterization of eight CBS mutant enzymes," *Journal of Biological Chemistry*, vol. 285, no. 21, pp. 15866–15873, 2010.

[207] T. Majtan, A. L. Pey, J. Ereño-Orbea, L. A. Martínez-Cruz, and J. P. Kraus, "Targeting cystathionine beta-synthase misfolding in homocystinuria by small ligands: state of the art and future directions," *Current Drug Targets*, vol. 17, no. 13, pp. 1455–1470, 2016.

[208] T. Majtan, A. L. Pey, and J. P. Kraus, "Kinetic stability of cystathionine beta-synthase can be modulated by structural analogs of S-adenosylmethionine: potential approach to pharmacological chaperone therapy for homocystinuria," *Biochimie*, vol. 126, pp. 6–13, 2016.

[209] P. Melenovská, J. Kopecká, J. Krijt et al., "Chaperone therapy for homocystinuria: the rescue of CBS mutations by heme arginate," *Journal of Inherited Metabolic Disease*, vol. 38, no. 2, pp. 287–294, 2015.

[210] M. I. S. Mendes, D. E. C. Smith, J. B. Vicente et al., "Small aminothiol compounds improve the function of Arg to Cys variant proteins: effect on the human cystathionine β-synthase p.R336C," *Human Molecular Genetics*, vol. 24, no. 25, pp. 7339–7348, 2015.

[211] L. R. Singh, X. Chen, V. Kožich, and W. D. Kruger, "Chemical chaperone rescue of mutant human cystathionine β-synthase," *Molecular Genetics and Metabolism*, vol. 91, no. 4, pp. 335–342, 2007.

[212] E. M. Bublil, T. Majtan, I. Park et al., "Enzyme replacement with PEGylated cystathionine β-synthase ameliorates homocystinuria in murine model," *Journal of Clinical Investigation*, vol. 126, no. 6, pp. 2372–2384, 2016.

[213] T. Majtan, H. Hůlková, I. Park et al., "Enzyme replacement prevents neonatal death, liver damage, and osteoporosis in murine homocystinuria," *The FASEB Journal*, vol. 31, no. 12, pp. 5495–5506, 2017.

[214] T. Majtan, I. Park, R. S. Carrillo, E. M. Bublil, and J. P. Kraus, "Engineering and characterization of an enzyme replacement therapy for classical homocystinuria," *Biomacromolecules*, vol. 18, no. 6, pp. 1747–1761, 2017.

[215] L. Celano, M. Gil, S. Carballal et al., "Inactivation of cystathionine β-synthase with peroxynitrite," *Archives of Biochemistry and Biophysics*, vol. 491, no. 1–2, pp. 96–105, 2009.

[216] A. Prudova, Z. Bauman, A. Braun, V. Vitvitsky, S. C. Lu, and R. Banerjee, "S-Adenosylmethionine stabilizes cystathionine β-synthase and modulates redox capacity," *Proceedings of the National Academy of Sciences of the United States of America*, vol. 103, no. 17, pp. 6489–6494, 2006.

[217] M. I. S. Mendes, H. G. Colaço, D. E. C. Smith et al., "Reduced response of cystathionine beta-synthase (CBS) to S-adenosylmethionine (SAM): identification and functional analysis of CBS gene mutations in homocystinuria patients," *Journal of Inherited Metabolic Disease*, vol. 37, no. 2, pp. 245–254, 2014.

[218] M. I. S. Mendes, A. S. Santos, D. E. C. Smith et al., "Insights into the regulatory domain of cystathionine beta-synthase: characterization of six variant proteins," *Human Mutation*, vol. 35, no. 10, pp. 1195–1202, 2014.

[219] M. Beaumont, M. Andriamihaja, A. Lan et al., "Detrimental effects for colonocytes of an increased exposure to luminal hydrogen sulfide: the adaptive response," *Free Radical Biology and Medicine*, vol. 93, pp. 155–164, 2016.

[220] I. Kwiecień, M. Sokołowska, E. Luchter-Wasylewska, and L. Włodek, "Inhibition of the catalytic activity of rhodanese by S-nitrosylation using nitric oxide donors," *The International Journal of Biochemistry & Cell Biology*, vol. 35, no. 12, pp. 1645–1657, 2003.

[221] E. D'Araio, N. Shaw, A. Millward, A. Demaine, M. Whiteman, and A. Hodgkinson, "Hydrogen sulfide induces heme oxygenase-1 in human kidney cells," *Acta Diabetologica*, vol. 51, no. 1, pp. 155–157, 2014.

[222] H. Jia, J. Ye, J. You, X. Shi, W. Kang, and T. Wang, "Role of the cystathionine β-synthase/H₂S system in liver cancer cells and the inhibitory effect of quinolone-indolone conjugate QIC2 on the system," *Oncology Reports*, vol. 37, no. 5, pp. 3001–3009, 2017.

[223] K. Kupai, N. Almási, M. Kósa et al., "H₂S confers colonoprotection against TNBS-induced colitis by HO-1 upregulation in rats," *Inflammopharmacology*, vol. 26, no. 2, pp. 479–489, 2018.

[224] M. Shao, C. Zhuo, R. Jiang et al., "Protective effect of hydrogen sulphide against myocardial hypertrophy in mice," *Oncotarget*, vol. 8, no. 14, pp. 22344–22352, 2017.

[225] L. Xie, Y. Gu, M. Wen et al., "Hydrogen sulfide induces Keap1 S-sulfhydration and suppresses diabetes-accelerated atherosclerosis via Nrf2 activation," *Diabetes*, vol. 65, no. 10, pp. 3171–3184, 2016.

[226] C. Y. Zhang, X. H. Li, T. Zhang, J. Fu, and X. D. Cui, "Hydrogen sulfide upregulates heme oxygenase-1 expression in rats with volume overload-induced heart failure," *Biomedical Reports*, vol. 1, no. 3, pp. 454–458, 2013.

[227] S. Zhang, T. Wu, T. Xia, X. Rong, M. Chu, and R. Wu, "Regulation of the heme oxygenase-1/carbon monoxide system by hydrogen sulfide in murine coxsackievirus B3-induced myocarditis," *Cellular and Molecular Biology (Noisy-le-Grand, France)*, vol. 61, no. 2, pp. 69–73, 2015.

[228] L. Yi, P. M. Jenkins, L. I. Leichert, U. Jakob, J. R. Martens, and S. W. Ragsdale, "Heme regulatory motifs in heme oxygenase-2 form a thiol/disulfide redox switch that responds to the cellular redox state," *Journal of Biological Chemistry*, vol. 284, no. 31, pp. 20556–20561, 2009.

[229] L. Yi and S. W. Ragsdale, "Evidence that the heme regulatory motifs in heme oxygenase-2 serve as a thiol/disulfide redox switch regulating heme binding," *Journal of Biological Chemistry*, vol. 282, no. 29, pp. 21056–21067, 2007.

[230] N. E. B. Saidu, I. A. Asali, B. Czepukojc, B. Seitz, C. Jacob, and M. Montenarh, "Comparison between the effects of diallyl tetrasulfide on human retina pigment epithelial cells (ARPE-19) and HCT116 cells," *Biochimica et Biophysica Acta (BBA) - General Subjects*, vol. 1830, no. 11, pp. 5267–5276, 2013.

[231] I. S. Shin, J. Hong, C. M. Jeon et al., "Diallyl-disulfide, an organosulfur compound of garlic, attenuates airway inflammation via activation of the Nrf-2/HO-1 pathway and NF-kappaB suppression," *Food and Chemical Toxicology*, vol. 62, pp. 506–513, 2013.

[232] T. Zeng, C. L. Zhang, F. Y. Song et al., "The activation of HO-1/Nrf-2 contributes to the protective effects of diallyl disulfide (DADS) against ethanol-induced oxidative stress," *Biochimica et Biophysica Acta (BBA) - General Subjects*, vol. 1830, no. 10, pp. 4848–4859, 2013.

[233] S. Kubo, Y. Kurokawa, I. Doe, T. Masuko, F. Sekiguchi, and A. Kawabata, "Hydrogen sulfide inhibits activity of three isoforms of recombinant nitric oxide synthase," *Toxicology*, vol. 241, no. 1–2, pp. 92–97, 2007.

[234] G. S. Oh, H. O. Pae, B. S. Lee et al., "Hydrogen sulfide inhibits nitric oxide production and nuclear factor-κB via heme oxygenase-1 expression in RAW264.7 macrophages stimulated with lipopolysaccharide," *Free Radical Biology and Medicine*, vol. 41, no. 1, pp. 106–119, 2006.

[235] M. Whiteman, L. Li, P. Rose, C. H. Tan, D. B. Parkinson, and P. K. Moore, "The effect of hydrogen sulfide donors on lipopolysaccharide-induced formation of inflammatory mediators in macrophages," *Antioxidants & Redox Signaling*, vol. 12, no. 10, pp. 1147–1154, 2010.

[236] S. Kubo, I. Doe, Y. Kurokawa, H. Nishikawa, and A. Kawabata, "Direct inhibition of endothelial nitric oxide synthase by hydrogen sulfide: contribution to dual modulation of vascular tension," *Toxicology*, vol. 232, no. 1–2, pp. 138–146, 2007.

[237] X.-C. Duan, S.-Y. Liu, R. Guo et al., "Cystathionine-β-synthase gene transfer into rostral ventrolateral medulla exacerbates hypertension via nitric oxide in spontaneously hypertensive rats," *American Journal of Hypertension*, vol. 28, no. 9, pp. 1106–1113, 2015.

[238] *The PyMOL Molecular Graphics System, Version 1.8 Schrödinger*LLC.

[239] S. V. Evans, B. P. Sishta, A. G. Mauk, and G. D. Brayer, "Three-dimensional structure of cyanomet-sulfmyoglobin C," *Proceedings of the National Academy of Sciences of the United States of America*, vol. 91, no. 11, pp. 4723–4726, 1994.

Research Article

Nrf2 Deficiency Unmasks the Significance of Nitric Oxide Synthase Activity for Cardioprotection

Ralf Erkens,[1] Tatsiana Suvorava,[1] Thomas R. Sutton,[2,3] Bernadette O. Fernandez,[2,3] Monika Mikus-Lelinska,[2,3] Frederik Barbarino,[1] Ulrich Flögel,[4] Malte Kelm,[1,5] Martin Feelisch,[2,3] and Miriam M. Cortese-Krott [ID][1]

[1]Cardiovascular Research Laboratory, Division of Cardiology, Pulmonology and Vascular Medicine, Medical Faculty, Heinrich Heine University, Moorenstrasse 5, 40225 Düsseldorf, Germany
[2]Clinical & Experimental Sciences, Faculty of Medicine, University of Southampton, Tremona Road, Southampton SO166YD, UK
[3]NIHR Southampton Biomedical Research Centre, University Hospital Southampton NHS Foundation Trust, Tremona Road, Southampton SO166YD, UK
[4]Department of Molecular Cardiology, Heinrich Heine University, Universitaetsstr. 1, 40225 Düsseldorf, Germany
[5]Cardiovascular Research Institute Düsseldorf (CARID), Medical Faculty, Heinrich Heine University, Moorenstrasse 5, 40225 Düsseldorf, Germany

Correspondence should be addressed to Miriam M. Cortese-Krott; miriam.cortese@uni-duesseldorf.de

Ralf Erkens and Tatsiana Suvorava contributed equally to this work.

The transcription factor nuclear factor (erythroid-derived 2)-like 2 (Nrf2) is a key master switch that controls the expression of antioxidant and cytoprotective enzymes, including enzymes catalyzing glutathione de novo synthesis. In this study, we aimed to analyze whether Nrf2 deficiency influences antioxidative capacity, redox state, NO metabolites, and outcome of myocardial ischemia reperfusion (I/R) injury. In Nrf2 knockout (Nrf2 KO) mice, we found elevated eNOS expression and preserved NO metabolite concentrations in the aorta and heart as compared to wild types (WT). Unexpectedly, Nrf2 KO mice have a smaller infarct size following myocardial ischemia/reperfusion injury than WT mice and show fully preserved left ventricular systolic function. Inhibition of NO synthesis at onset of ischemia and during early reperfusion increased myocardial damage and systolic dysfunction in Nrf2 KO mice, but not in WT mice. Consistent with this, infarct size and diastolic function were unaffected in eNOS knockout (eNOS KO) mice after ischemia/reperfusion. Taken together, these data suggest that eNOS upregulation under conditions of decreased antioxidant capacity might play an important role in cardioprotection against I/R. Due to the redundancy in cytoprotective mechanisms, this fundamental antioxidant property of eNOS is not evident upon acute NOS inhibition in WT mice or in eNOS KO mice until Nrf2-related signaling is abrogated.

1. Introduction

Imbalanced redox equilibria are a hallmark of many pathological processes [1, 2]. An important mechanism by which cells adapt to an altered redox status as a result of a higher oxidative burden, or a compromised reductive capacity, or both, is transcriptional upregulation of a battery of cytoprotective genes. The same genes are also central to the supply with intracellular reducing equivalents required to maintain redox homeostasis and the detoxification of damaging electrophilic by-products of oxidants. The transcription factor Nrf2 is a key master regulator of the expression of genes, encoding antioxidant, detoxifying, and cytoprotective molecules such as heme oxygenase 1 (HO-1), SOD, glutathione S-transferase, glutamate cysteine ligase (an enzyme critical to glutathione biosynthesis), and NADPH quinone

oxidoreductase 1 [3–6]. These genes contain the antioxidant response cis-element (ARE) in their promoters, which is a binding site for Nrf1 and Nrf2 transcription factors. Under steady-state conditions, Nrf2 remains sequestered in the cytoplasm by binding to Kelch-like ECH-associated protein 1 (Keap1). Oxidants and electrophiles induce the release of Nrf2 from the cytosolic complex by oxidation of cysteines within Keap1 and phosphorylation at specific sites [7], thus allowing Nrf2 to shuttle into the nucleus where it heterodimerizes with specific cofactors and coordinates upregulation of cytoprotective genes. Nrf1 serves complementary, but distinct functions including regulation of cell growth and metabolism, heme biosynthesis, and mitochondrial function [8].

Dysfunction in Nrf2-dependent gene regulation has been implicated in the pathogenesis of myocardial and renal ischemia, inflammatory disorders, cancer, and aging [9–12]. Ischemia/reperfusion (I/R) increased Nrf2 dissociation from Keap1, resulting in Nrf2 translocation into the nucleus, binding to the ARE, and activation of phase II detoxifying and antioxidant genes [9]. The Nrf2/ARE pathway affects cell survival through a variety of mediators, including apoptotic proteins such as Bcl-2 and Bax [13] and phase II enzymes such as HO-1 [14]. Moreover, Nrf2 is essential to successful ischemic preconditioning: two cycles of ischemic preconditioning did not result in cardiac protection in the absence of Nrf2 [2]. Likewise, several Nrf2 activators including glucocorticoids [15], endogenous prostaglandin D2 [16], and hydrogen sulfide (H_2S) [17, 18] are cardioprotective in a Nrf2-dependent manner since this cardioprotection was lost in Nrf2 knockout (Nrf2 KO) mice.

Our recent study revealed that Nrf2 KO mice show cardiac hypertrophy, left ventricular diastolic dysfunction, and impaired Ca^{2+} homeostasis [19]. However, we found that vascular function in Nrf2 KO mice was fully preserved via a compensatory upregulation of eNOS. Considering the potent antioxidant and cardioprotective effects of nitric oxide (NO), we surmised that eNOS upregulation in Nrf2 KO mice may affect outcome after acute myocardial infarction. Specifically, we hypothesized that upregulation of eNOS may influence the degree of myocardial I/R injury under conditions of Nrf2 deficiency given the established significance of this transcription factor for cytoprotection and redox regulation.

To test this hypothesis, we first characterized overall thiol and NO metabolic status of Nrf2 KO mice. In a second step, we subjected Nrf2 KO mice to 30 min occlusion of the left anterior descending artery (LAD) followed by 24 h of reperfusion, analyzed infarct size and myocardial function in the presence and absence of a NOS inhibitor, and compared them with wild type (WT) and eNOS KO mice. We found that Nrf2 KO mice show decreased antioxidant capacity (GSH synthesis), yet display preserved redox status and levels of NO metabolites. Moreover, we found an eNOS-dependent cardioprotection against I/R injury in Nrf2 KO mice, which was abrogated by treatment with a NOS inhibitor. Cardioprotection by eNOS-derived NO was neither evident in WT mice treated with a NOS inhibitor nor in eNOS KO mice. Our data suggest that upregulation of eNOS and preserved NO bioavailability protects against myocardial I/R injury whenever antioxidant capacity is compromised like in Nrf2 KO mice. Intriguingly,

due to the redundancy in cytoprotective mechanisms, this fundamental cardioprotective property of eNOS-derived NO is not evident upon acute NOS inhibition in WT or eNOS KO mice until Nrf2-related signaling is impaired.

2. Materials and Methods

2.1. Materials. Unless otherwise specified, chemicals were purchased from Sigma-Aldrich Chemie/Merck (Deisenhofen, Germany). Materials for Western blotting were purchased from Life Technologies (Invitrogen, Darmstadt, Germany).

2.2. Mice. Nrf2 KO/C57BL/6J (BRC number 01390) mice were obtained from Riken (Koyadai, Tsukuba, Ibaraki, Japan) and crossed for more than 10 generations with C57BL/6J. C57BL/6J mice were purchased from Janvier Labs (Le Genest-Saint-Isle, France) and used as WT mouse controls. eNOS KO mice on C57BL/6J background were generously provided by Dr. Axel Gödecke (Heinrich Heine University of Düsseldorf, Germany) [20]. Transgenic mice were bred and housed in the animal facility of the Heinrich Heine University, and male 5-6-month-old mice were used for experiments. All experiments were approved by the North Rhine-Westphalia State Agency for Nature, Environment and Consumer Protection and performed according to the guidelines for the use of experimental animals as given by German law.

2.3. Collection of Blood and Tissues from Nrf2 KO, eNOS KO, and WT Mice. For the analysis of thiols and NO metabolites, blood and organs were collected as described previously [21]. Briefly, mice were anesthetized with isoflurane (2.0%) and killed by exsanguination. Blood was transferred immediately into tubes containing N-ethylmaleimide (NEM)/EDTA (10 : 1 v/v), dissolved in phosphate-buffered solution (PBS) at pH 7.4 (final concentrations: 10 mM NEM, 2 mM EDTA), and centrifuged immediately for 3 min at 3000g. Organs were harvested after 1 min of perfusion with ice cold 10 mM NEM/2 mM EDTA in PBS pH 7.4, blotted dry on filter paper, weighed, snap frozen in liquid nitrogen, and kept at −80°C until later analysis. For Western blot analysis, organs were perfused with PBS pH 7.4 only.

2.4. Determination of Low-Molecular-Weight Thiols and Sulfide by Liquid Chromatography-Mass Spectrometry. Low-molecular-weight thiols and sulfide were measured as their NEM adducts using a Waters Acquity ultra-high pressure liquid chromatography (UHPLC) system coupled with a Xevo triple quadrupole (TQ-S) mass spectrometer. The UHPLC separation used an Acquity UPLC CSH C_{18} (1.7 μm), 2.1 × 100 mm column. Gradient elution was used with the mobile phases consisting of H_2O with 5 mM ammonium formate and 95% acetonitrile (ACN) (eluent A) and 5% H_2O with 5 mM ammonium formate (eluent B). An injection volume of 5 μl was used with a column temperature of 30°C and a flow rate of 0.2 ml/min. The gradient started at 95% A, decreasing down to 40% over 5 min, returning to 95% A by 6 min and allowing the column to equilibrate for another min, resulting in a total run time of 7 min. The elution times of each compound measured were (in min) 0.94 (GSSG), 1.80

(GluCys), 2.00 (GSH), 2.11 (Cys), 2.26 (CysGly), 2.35 (HCys), and 4.80 (sulfide).

2.5. Determination of NO Metabolites. Nitrosated (S-nitroso and N-nitroso) products (RXNO), NO heme, and nitrosyl species were quantified by gas phase chemiluminescence as described [21]. For nitrite/nitrate analysis, NEM-treated samples were deproteinized with ice-cold methanol (1 : 1 v/v), cleared by centrifugation and subjected to analysis by high pressure liquid chromatography using a dedicated nitrite/nitrate analyzer (ENO20, Eicom) as described [22].

2.6. Determination of eNOS Expression by Western Blot Analysis. Lysis of the heart and aorta, sample preparation, and Western blot analysis and detection were carried out as described [19]. Briefly, organs were lysed in RIPA buffer (1% NP40, 0.5% sodium deoxycholate, and 0.1% SDS in PBS pH 7.4) containing a cocktail of protease and phosphatase inhibitors (Pierce), homogenized at 4°C by using Tissue Ruptor (Qiagen, Hilden, Germany), sonicated for 3 min at 4°C, and centrifuged at 4000 ×g for 10 min at 4°C. Total protein concentration of the supernatant was determined by Lowry assay. Samples were loaded in 7% NuPAGE Tris-Acetate precast gels (Invitrogen) and transferred onto PVDF membrane Hybond P (Amersham Biosciences, Munich, Germany). The membranes were blocked for 2 hours with 5% BSA (Bio-Rad) in T-TBS (10 mM Tris, 100 mM NaCl, 0.1% Tween) and incubated overnight at 4°C with a mouse anti-eNOS (1 : 250, custom made from number 624086 anti-eNOS/NOS type III antibody, stock: 1 mg/ml in PBS pH 7.4, BD Bioscience, Erembodegem, Belgium) or monoclonal mouse anti-α-tubulin (1 : 5000, number T6199, Sigma-Aldrich) in T-TBS. After washing for 1 hour in T-TBS, the membranes were incubated with HRP-conjugated goat anti-mouse or anti-rabbit secondary antibodies (1 : 5000; BD Biosciences), and bands were detected using Amersham ECL Select Western Blotting Detection Reagent (number RPN2235, GE Healthcare) and Image Quant (GE Healthcare). Densitometry was carried out using Image Studio Lite software (LI-COR Biotechnology, Lincoln, NE, USA). Detection and quantification of the bands was compared within the linear range of the respective method of analysis.

2.7. Myocardial Ischemia and Reperfusion Protocol. Myocardial ischemia was induced by 30 min of ischemia followed by 24 h of reperfusion in WT, Nrf2 KO, and eNOS KO mice as previously described [23]. Briefly, after skin incision, median sternotomy, and pericardiotomy, the left anterior descending coronary artery was ligated halfway from base to apex with a 7-0 silk suture. Myocardial ischemia was induced for 30 min and confirmed by ST elevation on the electrocardiogram recorded during the ischemic phase and the first minute after reperfusion. Infarct size was evaluated by staining with 2,3,5-triphenyltetrazolium chloride (TTC). Briefly, the hearts were excised and perfused with 0.9% NaCl. The left anterior descending artery was reoccluded in the same location, and 1% Evans Blue dye was injected into the aortic root to delineate the area at risk (AAR) from not-at-risk area. The hearts were frozen at −20°C for

60 min and serially sectioned in 1 mm slices; each slice was weighed and incubated in 1% TTC for 5 min at 37°C. AAR and nonischemic areas were evaluated by computer-assisted planimetry. The size of the myocardial infarct is expressed as a percentage of the infarcted tissue area compared to the total AAR. A subgroup of mice received a continuous intraperitoneal (i.p.) infusion of the NOS inhibitor S-ethylisothiourea hydrobromide (ETU) (1.3 mmol/kg/min) during the ischemic period and in the early reperfusion. Efficient NOS inhibition using this protocol was independently verified by analyzing the concomitant increase in systolic and diastolic blood pressure 15 min after ETU administration as assessed invasively by Millar catheter in anesthetized WT and Nrf2 KO mice [19].

2.8. Analysis of Cardiac Function by High-Resolution Ultrasound and Cardiac Magnetic Resonance Tomography (cMRT). Transthoracic echocardiography was performed as previously described [19]. Left ventricular volume (LV), end-systolic volume (ESV), and end-diastolic volume (EDV), LV ejection fraction (EF), fractional shortening (FS), cardiac output (CO), and stroke volume (SV) were calculated. LV diastolic function was assessed by analysis of the characteristic flow profile of the mitral valve Doppler which was visualized in apical four-chamber view, as described [19]. Cardiac magnetic resonance tomography imaging data were recorded by a Bruker AVANCEIII 9.4 T wide bore NMR spectrometer (Bruker, Rheinstetten, Germany) at 400.13 MHz operated by ParaVision 5.1. Images were acquired using the Bruker microimaging unit Micro 2.5 with actively shielded gradient sets (1.5 T/m) and a 25 mm birdcage resonator, as previously described [24].

2.9. Statistical Analysis. Statistical calculations for each experiment and the number of animals are stated in Results and figure legends. Statistical comparisons between groups were calculated by either Student's t-tests (for 2 groups) or Tukey's multiple comparison post hoc test following one-way ANOVA (for more than two groups). Browne-Forsythe test was performed to check for homoscedasticity of our samples. Post hoc tests were run only if F was not different between the groups and there was no significant variance inhomogeneity. $p < 0.05$ was considered statistically significant.

3. Results

3.1. Decreased Antioxidant Reserve Capacity with Preserved Redox State in Nrf2 KO Mice. It is well known that mice lacking the transcription factor Nrf2 show decreased expression of enzymes involved in glutathione biosynthesis, especially in the liver [25, 26]. To address the question how a lack of Nrf2 affects circulating and tissue thiol metabolic status in the heart and other organs, we assessed the concentration of reduced and oxidized glutathione and some of its precursors in blood and tissues of Nrf2 KO and WT mice. A schematic representation of the main metabolic pathways regulating GSH synthesis is provided in Scheme 1. With the exception of red blood cells, we found that a lack of Nrf2 significantly affects total GSH levels in plasma and

$H_2S \longleftarrow$ Cysteine $\longleftarrow$

Cysteinyl-glycine

Cystine

γ-Glutamyl-cysteine

$\longrightarrow$ Glutathione $\longleftarrow$

Oxidised glutathione
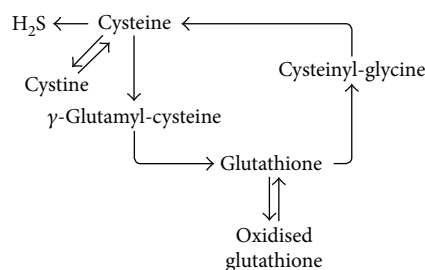
Scheme 1: Simplified schematic representation of the main metabolic pathways involved in the production and degradation of glutathione in mammalian tissues.

all analyzed organs (Table 1), indicating a decreased antioxidant reserve capacity in Nrf2 KO mice as compared to WT mice. Interestingly, the GSH/GSSG ratio in the heart and aorta was similar in Nrf2 KO and WT mice, demonstrating that the redox state in these compartments of Nrf2-deficient mice is fully preserved. We also found that steady-state concentrations of the glutathione precursors, homocysteine, cysteine, and γ-glutamylcysteine, and that of the decomposition product cysteinylglycine were significantly decreased in all organs and in plasma but not in RBCs of Nrf2 KO mice (Table 1). By contrast, RBCs appear to have a peculiar resistance to changes in total thiol levels and displayed a significant increase in their GSH/GSSG ratio under conditions of Nrf2 deficiency. The present study offers evidence of an altered antioxidant capacity in Nrf2 KO mice compared to WT mice, but further examination with a larger cohort of mice is necessary to confirm this finding.

Next, we aimed to analyze how the changes in the thiol metabolic status of Nrf2 KO mice may affect NO metabolism. In good agreement with data published elsewhere [19], we observed an upregulation of eNOS protein in myocardial and vascular tissue of Nrf2 KO mice (Figures 1(a) and 1(b)). Importantly, previous analysis of these mice revealed that the upregulated eNOS in Nrf2 KO mice was functionally active as evidenced by increased flow-mediated vasodilation in vivo and increased carbachol-induced cGMP reposes in aortic rings from Nrf2 KO mice as compared to WT mice [19]. Here, we found that the total levels of nitrite, nitrate, and nitroso species in all compartments were not significantly different between WT and Nrf2 KO mice (Figure 1(c)), except in the aorta. Of note, nitrosyl-hemoglobin levels in RBCs were increased in Nrf2 KO mice as compared to WT mice (Table 2), consistent with the notion of an enhanced NO availability secondary to eNOS upregulation in the vasculature. While total levels of NO-derived species remain essentially unchanged between groups, there are distinct distributions for individual species across groups. Determining whether these trends bear statistical significance, particularly in the case for nitrosation products (RXNO) would require a follow-up study with a larger cohort of mice.

Taken together, these data suggests that Nrf2 KO mice have greatly impaired activity for glutathione synthesis and therefore a diminished antioxidant reserve capacity in all compartments except the erythrocytes, yet overall redox status and total NO metabolite concentrations are well preserved.

3.2. Nrf2 KO Mouse Hearts Are More Resilient toward Myocardial I/R Injury, and This Extra Protection Is Dependent on NOS Activity.

To study the effects of a diminished antioxidant reserve capacity on the susceptibility to myocardial ischemia/reperfusion injury, Nrf2 KO mice were subjected to 30 min occlusion of the left anterior descendent (LAD) artery followed by 24 h of reperfusion, and infarct size and area at risk (AAR) were compared between WT and eNOS KO mice (Figure 2). Unexpectedly, infarct size per AAR was not increased but significantly decreased in Nrf2 KO mice as compared to WT mice ($14.47 \pm 0.7\%$ versus WT mice: $26.68 \pm 2.1\%$ (Figures 2(a) and 2(b)), $n = 9$ each, $p < 0.001$), while the AAR of the left ventricles did not differ between these strains (Figure 2(c)).

We reasoned that the enhanced cardioprotection against I/R injury in Nrf2 KO mice may be a result of compensatory eNOS upregulation. To test this assumption, we treated mice with the NOS inhibitor ETU via continuous i.p. infusion during ischemia and throughout the first 5 minutes of reperfusion. We found that NOS inhibition did not affect infarct size in WT mice, while it significantly increased infarct size in Nrf2 KO mice when compared to untreated controls (Figures 2(a) and 2(b)), such that there was no significant difference between infarct size in the ETU-treated WT and Nrf2 KO mouse hearts. As a further control, the effects of I/R injury were also tested in mice globally deficient for eNOS. Similar to what we observed after acute NOS inhibition in the WT mice, we found no difference in infarct size between eNOS KO and WT mice (Figure 2(a), red boxes).

Taken together, these data demonstrate that upregulation of eNOS in the Nrf2 KO mouse heart accounts for the improved protection of Nrf2 KO mouse myocardium from I/R injury-induced cell death; this cardioprotective property of eNOS is not evident upon acute NOS inhibition in WT or chronic eNOS deficiency in eNOS KO mice but is unmasked when Nrf2-related signaling is impaired.

3.3. In Nrf2 KO Mouse, Systolic and Diastolic Myocardial Functions after Acute Myocardial Infarction (AMI) Are Preserved by NOS.

At baseline conditions, Nrf2 KO mice display well-preserved left ventricular systolic function as measured by cMRT (Table 3), while their left ventricular diastolic function is significantly impaired (Supplementary Table 1). These results fully confirm our previous echocardiographic analyses in Nrf2 KO mice [19]. Of note, Nrf2 KO mice showed some degree of LV hypertrophy as evidenced by increase of the LV mass to body weight ratio (Figure 3(a)). Furthermore, ESV and EDV in Nrf2 KO mice were significantly higher than in WT mice (Supplementary Table 1). Mice lacking eNOS also suffer from cardiac hypertrophy (Figure 3), which was much more prominent than that of Nrf2 KO mice, but was not accompanied by any changes in systolic functional parameters (except for SV) as compared to WT mice (Figure 4, Supplementary Table 1).

Twenty-four hours after AMI, left ventricular systolic function was impaired in WT mice as evidenced by significantly reduced ejection fraction (EF) (Figure 4(a)). In contrast, in Nrf2 KO mice, EF was fully preserved after AMI as compared to baseline (Figure 4(a)). Interestingly, acute

TABLE 1: Concentrations (nM) of low-molecular-weight thiols in blood and tissues of wild type (WT) and Nrf2 KO mice (mean ± SD, $n = 5$ per group).

	WT mice	Nrf2 KO mice	p value (versus WT mice)
Heart			
Total GSH (nM)	144.3 ± 53.11	91.52 ± 12.06	=0.0620 (↓ ns)
GSH (nM)	143.7 ± 52.77	90.77 ± 11.99	=0.0602 (↓ ns)
GSSG (nM)	0.6263 ± 0.427	0.7531 ± 0.352	0.6225
GSH/GSSG	335.0 ± 217.9	140.2 ± 52.51	=0.0887 (↓ ns)
Cys (nM)	16.38 ± 6.976	8.99 ± 1.804	=0.051 (↓ ns)
HCys (nM)	0.6387 ± 0.1949	0.4231 ± 0.06714	↓*0.0475
GluCys (nM)	0.2066 ± 0.03208	0.1852 ± 0.02159	0.2506
Sulfide (nM)	45.9 ± 22.1	28.56 ± 6.597	0.1301
Aorta			
Total GSH (nM)	217.2 ± 73.95	105.9 ± 21.91	↓*0.0121
GSH (nM)	216.4 ± 73.54	105.2 ± 22.2	↓*0.0119
GSSG (nM)	1.099 ± 0.2598	0.7146 ± 0.4136	0.1517
GSH/GSSG	224.8 ± 58.4	186.9 ± 101.2	0.5308
Cys (nM)	54.18 ± 12.78	18.15 ± 3.143	↓***0.0003
HCys (nM)	2.324 ± 0.3268	3.226 ± 2.024	0.3539
GluCys (nM)	0.9574 ± 0.1772	0.6319 ± 0.1166	↓**0.0089
Sulfide (nM)	21.51 ± 5.773	16.78 ± 5.570	0.2237
Liver			
Total GSH (nM)	8097 ± 833.6	4742 ± 2042	↓**0.0094
GSH (nM)	8028 ± 814.8	4592 ± 2025	↓**0.0078
GSSG (nM)	68.61 ± 27.77	150.6 ± 43.52	↑**0.0075
GSH/GSSG	127.2 ± 31.83	31.55 ± 15.14	↓***0.0003
Cys (nM)	204.8 ± 16.85	179.1 ± 52.44	0.3272
HCys (nM)	39.12 ± 7.435	18.18 ± 6.563	↓**0.0015
GluCys (nM)	0.7695 ± 0.04889	0.5463 ± 0.1343	↓**0.0082
CysGly (nM)	96.75 ± 16.4	62.13 ± 21.8	↓*0.0219
Sulfide (nM)	13.19 ± 2.683	15.17 ± 4.521	0.4229
Plasma			
Total GSH (nM)	27,144 ± 8464	16,594 ± 3540	↓*0.0331
GSH (nM)	26,456 ± 8364	16,194 ± 3482	↓*0.0351
GSSG (nM)	688.3 ± 171	399.9 ± 93.14	↓*0.0107
GSH/GSSG	39.04 ± 10.17	41.28 ± 7.372	0.7005
Cys (nM)	11,900 ± 2432	8207 ± 1249	↓*0.0165
HCys (nM)	337 ± 159	209.2 ± 35.86	0.1177
GluCys (nM)	668.8 ± 140.9	320.1 ± 83.34	↓**0.0014
CysGly (nM)	725 ± 186	1422 ± 728.2	= 0.0751 (↓ ns)
Sulfide	332.1 ± 46.77	457.7 ± 386.6	0.4912
Erythrocytes			
Total GSH (nM)	$3.94*10^6 \pm 0.52*10^6$	$3.77*10^6 \pm 0.30*10^6$	0.5570
GSH (nM)	$3.93*10^6 \pm 0.52*10^6$	$3.77*10^6 \pm 0.30*10^6$	0.5583
GSSG (nM)	1058 ± 103.7	781.5 ± 153.3	↓*0.0103
GSH/GSSG	3766 ± 726.2	4946 ± 841	↑*0.0449
Cys (nM)	26,254 ± 10,655	18,796 ± 2980	0.1702
HCys (nM)	754.3 ± 317.9	550.8 ± 104.8	0.2109
GluCys (nM)	286.7 ± 118.3	202.7 ± 44.78	0.1757
CysGly (nM)	11,488 ± 5053	11,772 ± 3183	0.9178
Sulfide (nM)	387.3 ± 69.59	490.7 ± 98.66	0.0917

ns - not significant; ↓ - decreased; ↑ - increased; *$p < 0.05$, **$p < 0.01$, ***$p < 0.001$.
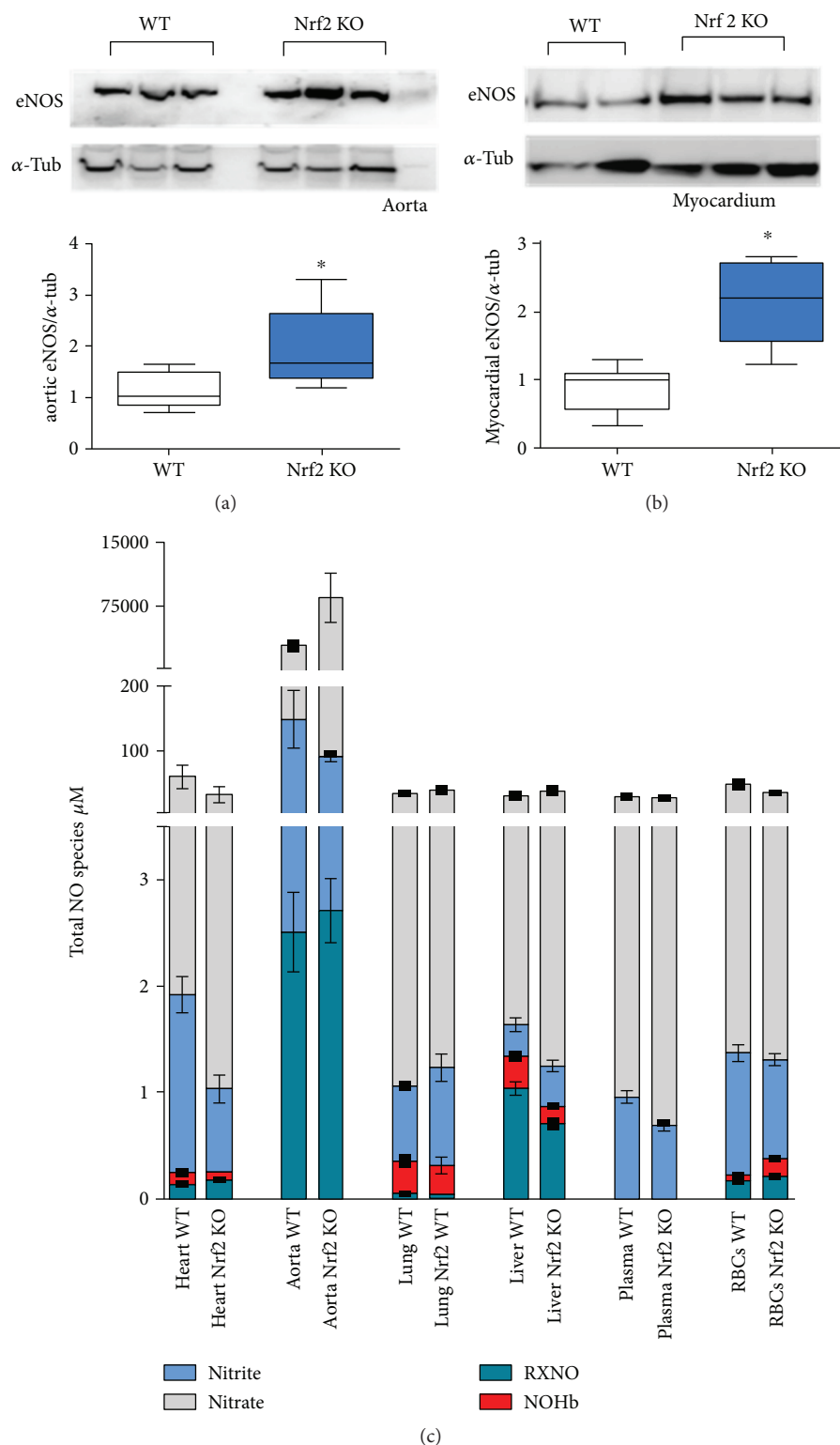
Figure 1: Upregulation of eNOS and preserved total levels of NO metabolites in Nrf2 KO mice. (a) Representative Western blot of eNOS (upper panel) standardized to alpha-tubulin (lower panel) and densitometric analysis of eNOS expression in aorta and (b) heart of WT and Nrf2 KO mice detected by Western blot ($n = 5$ per group, means ± quartiles, $^*p < 0.05$, t-test). (c) Total NO species in different tissues of Nrf2 KO and WT mice ($n = 5$ per group, means ± SEM), (for statistical comparisons and SD please refer also to Table 2).

TABLE 2: Concentrations of nitrite, nitrate, nitrosation products (RXNO), and nitrosyl heme (NO heme) in blood and different tissues of Nrf2 KO mice as compared to WT mice (mean ± SD, $n = 5$ each).

Metabolite	Concentration	WT mice	Nrf2 KO mice	p value (versus WT mice)
Heart				
Nitrite	μM	1.673 ± 0.4005	0.7784 ± 0.8500	↓**0.0039
Nitrate	μM	57.30 ± 40.04	31.22 ± 29.14	ns
RXNO	nM	144.1 ± 26.76	177.4 ± 57.65	ns 0.0603
NO heme	nM	103.8 ± 42.02	79.40 ± 4.777	ns
Aorta				
Nitrite	μM	146.1 ± 99.19	87.49 ± 15.87	ns
Nitrate	μM	2755 ± 1166	8428 ± 4852	ns
RXNO	nM	2506 ± 836.9	2712 ± 1154	ns
NO heme	nM	nd	nd	—
Liver				
Nitrite	μM	0.2970 ± 0.1423	0.3772 ± 0.3052	ns
Nitrate	μM	28.63 ± 9.395	37.17 ± 9.736	ns
RXNO	nM	1040 ± 136	710.1 ± 278.8	↓**0.0019
NO heme	nM	300.0 ± 67.34	162.6 ± 30.52	↓**0.0032
Lung				
Nitrite	μM	0.7026 ± 0.05554	0.9157 ± 0.2999	↑*0.0133
Nitrate	μM	32.40 ± 3.535	38.05 ± 8.71	ns
RXNO	nM	56.56 ± 21.18	42.79 ± 24.02	ns
NO heme	nM	301.6 ± 92.45	275.0 ± 173.8	ns
Plasma				
Nitrite	μM	0.9387 ± 0.1351	0.6771 ± 0.1681	↓**0.0080
Nitrate	μM	27.33 ± 6.395	26.42 ± 7.61	ns
RXNO	nM	21.25 ± 2.7	8.852 ± 1.215	↓****<0.0001
NO heme	nM	nd	nd	—
Erythrocytes				
Nitrite	μM	1.147 ± 0.1761	0.9267 ± 0.1291	ns 0.0545
Nitrate	μM	46.87 ± 12.34	33.75 ± 13.18	ns 0.0514
RXNO	nM	177.8 ± 46.18	213.1 ± 63	ns
NO heme	nM	48.67 ± 15.46	169.0 ± 54.82	↑<0.0001

ns - not significant; ↓ - decreased; ↑ - increased; $^{*}p < 0.05$; $^{**}p < 0.01$; $^{***}p < 0.001$.

NOS inhibition with ETU in Nrf2 KO mice impaired EF after AMI, but did not affect EF in WT mice as compared to untreated mice (Figure 4(a); ETU treatment). Likewise, NOS inhibition significantly decreased CO in Nrf2 KO mice only, but did not affect it in WT mice, pointing to a role of NOS activity in preserving LV systolic function after AMI in Nrf2 KO mice but not in WT mice (Figure 4(b)). Consistent with the results obtained after NOS inhibition in WT mice, CO was not changed after myocardial I/R injury in eNOS KO mice as compared to baseline (Figure 4(b), red boxes). Furthermore, NOS inhibition in Nrf2 KO mice resulted in a significant impairment of cardiac contraction, as indicated by an increase in isovolumetric contraction time (IVCT) measured in apical four-chamber view using pulse wave Doppler (Figure 4(c), Supplementary Table 1, Nrf2 KO + ETU post I/R versus Nrf2 KO post I/R) while NOS inhibition in WT mice had no effect on IVCT, and there was no difference in IVCT in eNOS KO post I/R versus baseline values (Figure 4(c), red boxes).

Assessment of LV diastolic function by mitral flow Doppler imaging showed that Nrf2 KO mice have significant diastolic dysfunction at baseline as evidenced by prolonged DT and IVRT and increased E/A ratio (Supplementary Table 1). Surprisingly, despite the prominent diastolic dysfunction and reduced capacity of myocardial relaxation, LV diastolic dysfunction was not further aggravated by AMI in Nrf2 KO mice as there were no changes in diastolic functional parameters (Figure 5), while E wave DT, IVRT, and total diastolic time were significantly impaired after AMI in WT mice (versus WT baseline, white boxes, Figure 5; Supplementary Table 1). Following administration of the NOS inhibitor, LV DT in Nrf2 KO mice was further impaired (Figure 5(a), red boxes), whereas NOS inhibition in WT mice did not affect DT (Figure 5(a), Supplementary Table 1). Similar to the effects of acute NOS inhibition, LV diastolic functional parameters were not changed post AMI in eNOS KO mice (Figure 5, red boxes); however, these mice exhibited LV diastolic dysfunction at baseline

(a)

(b)

(c)
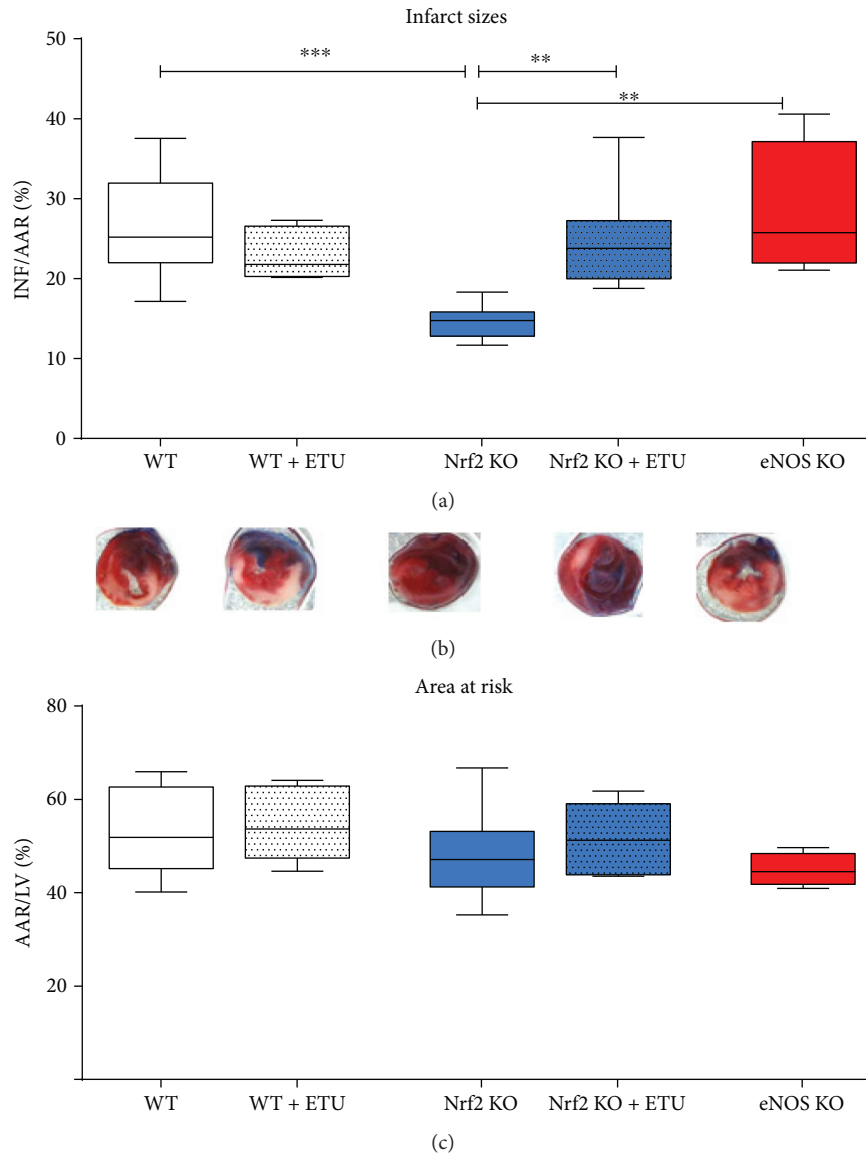
FIGURE 2: NOS-dependent decrease of infarct size in Nrf2 KO mice. (a) Infarct sizes (INF) per area at risk (AAR). Nrf2 KO mice showed a significant decrease in infarct sizes as compared to WT mice. Application of the NOS inhibitor ethylthiourea (ETU) in WT mice did not affect infarct size, whereas ETU application in Nrf2 KO mice increased I/R injury demonstrating the cardioprotective role of NOS activity despite a compromised antioxidative reserve capacity in Nrf2 KO mice. eNOS KO mice showed no differences in I/R injury as compared to WT and WT + ETU mice. WT mice: $n = 9$, Nrf2 KO mice: $n = 8$, eNOS KO mice: $n = 4$-5; Browne-Forsythe test $p = 0.27$, means ± quartiles, one-way ANOVA $**p < 0.01$, $***p < 0.001$. (b) Representative TTC stained heart sections of each strain 24 h after AMI. (c) Comparable values of area at risk/left ventricle demonstrate the reproducibility of the I/R surgery (Browne-Forsythe test $p = 0.24$, means ± quartiles, one-way ANOVA, ns).

which was evidenced by almost twofold increased DT (Supplementary Table 1).

Taken together, these data suggest that Nrf2 KO mice, despite their decreased antioxidant reserve capacity, are more protected against AMI than WT mice, as evidenced by reduced infarct size, maintained systolic function and a lack of postischemic facilitation of LV diastolic dysfunction. Moreover, the results of NOS inhibition experiments revealed the increased infarct size, post AMI impairment of left ventricular systolic dysfunction, and increase of diastolic dysfunction in Nrf2 KO mice demonstrating that NOS-

dependent signaling pathways play a key role in the protection of the heart against I/R injury under conditions of Nrf2 deficiency.

4. Discussion

The main finding of our study is that upregulation of eNOS mediates cardioprotection against I/R under conditions of decreased antioxidant capacity in mice lacking the transcription factor Nrf2. Specifically, we demonstrated that (1) Nrf2 KO mice have a severe decreased antioxidant reserve

TABLE 3: Preserved systolic function in Nrf2 KO mice as measured by cMRT (mean $\pm$ SD, $n = 5$ each).

Parameter	Units	WT mice (mean $\pm$ SD)	Nrf2 KO mice (mean $\pm$ SD)	p value
BM	(g)	35.39 ± 2.55	33.41 ± 2.32	0.228
Age	(d)	219.50 ± 26.48	217.50 ± 28.49	0.911
HF	(min^{-1})	547.42 ± 49.56	519.17 ± 26.36	0.287
EDV	(μl)	52.03 ± 7.61	51.41 ± 5.80	0.888
ESV	(μl)	15.33 ± 3.98	15.89 ± 2.42	0.792
SV	(μl)	36.70 ± 4.38	35.52 ± 4.11	0.668
EF	(%)	70.86 ± 3.99	69.10 ± 2.81	0.439
HZV	(ml/min)	19.98 ± 2.17	18.47 ± 2.49	0.330
m (D)	(mg)	112.17 ± 16.00	119.62 ± 8.54	0.380
rel. m	(mg/g)	3.19 ± 0.56	3.59 ± 0.23	0.177
dmitt (D)	(mm)	1.09 ± 0.06	1.07 ± 0.06	0.646
dmitt (S)	(mm)	1.59 ± 0.10	1.60 ± 0.07	0.844
WVmitt	(%)	145.35 ± 7.31	149.24 ± 9.58	0.487

capacity, characterized by significantly decreased concentration of total glutathione, and of its precursors, but show fully preserved redox status and global NO bioavailability at baseline; (2) following myocardial I/R injury Nrf2 KO mice had a reduced infarct size and (in contrast to WT mice) showed a fully preserved systolic LV function; (3) inhibition of NO synthase activity at the onset of ischemia and during early reperfusion increased myocardial damage and induced systolic dysfunction in Nrf2 KO mice, but not in WT mice; (4) consistent with the results upon acute NOS inhibition in WT mice, infarct size in eNOS KO mice was not different from that in WT mice. Taken together, these data suggest that upregulation of eNOS under conditions of decreased antioxidant capacity due to Nrf2 deficiency likely plays an important role in cardioprotection against I/R injury, while this mechanism of cardioprotection is not evident after acute NOS inhibition in WT or in eNOS KO mice.

4.1. Decreased Antioxidant Capacity and Preserved NO Bioavailability in Nrf2 KO Mice.
Nrf2 is known to play a central role in cellular stress response, adaptation, and resilience [1]. Accordingly, Nrf2 deletion has been shown to result in downregulation of phase 2 detoxifying enzymes (like glutathione S-transferase), antioxidant enzymes (like SOD), and enzymes responsible for glutathione de novo biosynthesis/thiol metabolism (like glutamate cysteine ligase and glutathione synthetase) as assessed in the liver and other organs including the heart [17, 27, 28]; however, a proportion of certain organ-specific Nrf2 target genes is also regulated by other transcription factors, like the aryl hydrocarbon receptor (AhR) [29]. We here provide evidence that thiol metabolism and total antioxidant capacity are strongly impaired in Nrf2 KO mice in all analyzed organs, and this translates into decreased concentrations of glutathione and its precursors, cysteine, homocysteine, and γ-glutamylcysteine. We also found that the changes in glutathione-related aminothiols are tissue-specific. Although this is consistent with the notion of differential expression of Nrf2 target genes among

different organs, a larger cohort of animals is necessary to confirm our findings.

Interestingly, tissue redox status (i.e., the ratio of reduced/oxidized thiols in different organs) in Nrf2 KO mice is not significantly different from that of WT mice, as a result of compensatory alterations of multiple reduced and oxidized thiols. Consistent with a fully preserved redox status, the total levels of NO metabolites remain essentially unchanged between the groups. However, upon observation on these data, there are distinct distributions for individual species across groups. This is particularly the case for nitrosation products (RXNO), exhibiting a p value of 0.0603. Determining whether these trends bear statistical significance would require a follow-up study with a larger cohort of animals. Consistently to preserved levels of NO metabolites, we found that the expression of eNOS was upregulated both in the conduit arteries and in the heart of Nrf2 KO mice as shown by us previously [19] and in this study (which corresponds to increased eNOS-derived NO production with consecutive cGMP-mediated vascular responses). Moreover, this eNOS upregulation translates into elevated nitrosyl-hemoglobin concentrations in RBCs, a good indicator of increased NO bioavailability [21, 30].

Taken together, while the lack of Nrf2 induces a profound decrease in overall antioxidant reserve capacity in all organs, especially in the heart, redox status, total levels of NO metabolites, and NO bioavailability are fully preserved. Further studies with a larger cohort of mice and mice lacking both Nrf2 and eNOS will reveal the causal relationship between lack of Nrf2 and eNOS-derived NO formation to preserve antioxidant capacity and NO bioavailability.

4.2. Nrf2 KO Mice Are Protected against I/R in a NOS-Dependent Fashion.
It is well known that the reoxygenation of the heart during reperfusion is associated with an increase in the production of superoxide and other reactive oxygen species by a variety of enzymes including xanthine oxidase, NADPH oxidases, and respiratory complexes of the mitochondrial electron transport chain. Under these conditions, Nrf2-dependent antioxidant enzymes and the pool of reduced thiols are thought to counterbalance the regional increase in oxidant formation, thereby protecting the myocardium from fatal damage. Thus, lack of Nrf2-dependent protection coupled with downregulation of antioxidant genes and reduced redox capacity of the myocardial and vascular tissues was expected to have detrimental effects in myocardial I/R injury. Moreover, as we previously demonstrated that Nrf2 KO mice have LV diastolic dysfunction (characterized by a decreased cardiac relaxation and impaired Ca^{2+} homeostasis; [19]), one might expect a further impairment of cardiac function in Nrf2 KO mice following AMI secondary to a reduced capacity of myocardial relaxation.

Surprisingly, we found that the Nrf2 KO mouse hearts were fully protected from I/R injury. Specifically, Nrf2 KO mice showed a significantly decreased infarct size and preserved LV systolic function after AMI as compared to WT mice. Furthermore, following I/R injury, we failed to detect any further decline of LV diastolic function in Nrf2 KO mice, which was evident in WT post AMI. The reduced infarct size
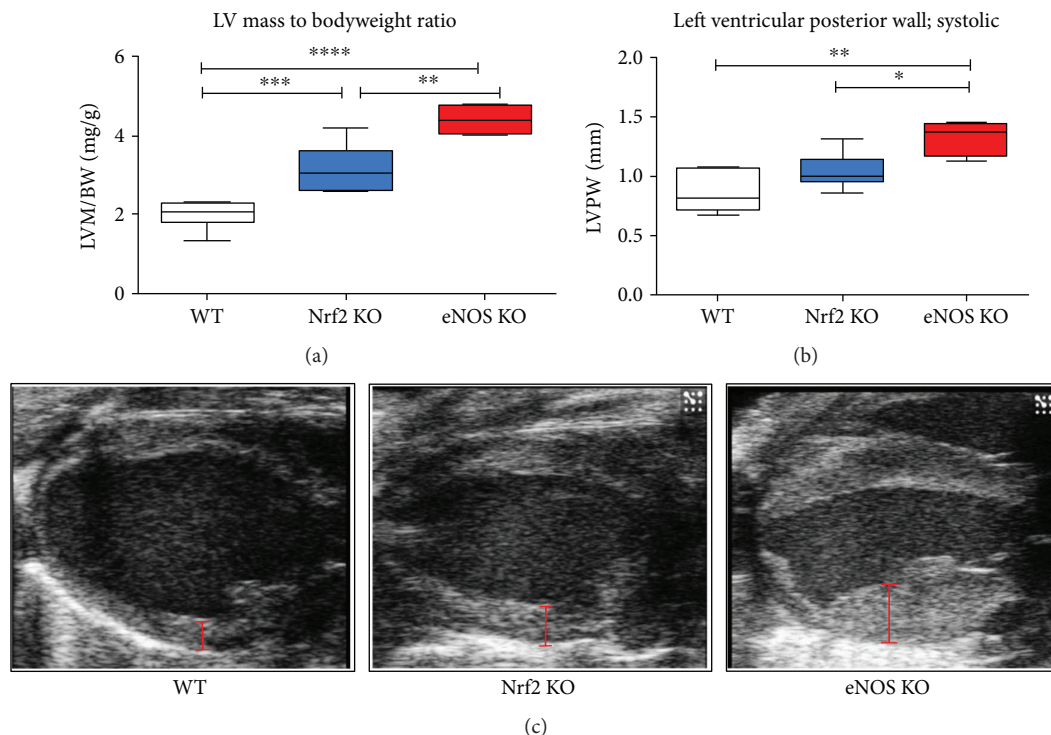
FIGURE 3: Cardiac hypertrophy in Nrf2 KO and eNOS KO mice. (a) LV mass normalized to body weight illustrates cardiac hypertrophy in both Nrf2 KO and eNOS KO mice as compared to WT mice. (b) Diameter of left ventricular posterior wall measured at the end of systole highlights the increase in myocardial hypertrophy in both KO mice. (c) Representative B-mode pictures of the heart from different mouse strains visualize the extent of cardiac hypertrophy. Red bars show the diameter of the left ventricular posterior wall. WT mice: $n = 8$, Nrf2 KO mice: $n = 9$, eNOS KO mice: $n = 4$; Browne-Forsythe test $p > 0.05$, means ± quartiles, one-way ANOVA $^*p < 0.05$, $^{**}p < 0.01$, $^{***}p < 0.001$, $^{****}p < 0.0001$.

after I/R injury in Nrf2 KO mice when compared to WT mice seems to be in contrast to previously published findings on an increased sensitivity of the Nrf2 KO mouse hearts to ischemic reperfusion injury [17]. A possible explanation for these contradictory findings might be the different strains of Nrf2 KO mice used in this and our study, specifically with regard to genetic background. In our study, we used Nrf2 KO mice on a fully backcrossed C57BL/6 background, while others studied Nrf2 KO mice on a SVB background [2, 17, 31]. Of note, Nrf2 KO mice on SVB background do not show LV diastolic dysfunction at baseline (but develop it only after transverse aortic constriction [32]), in addition, they displayed a lupus-like phenotype [33], but the expression of eNOS or NO metabolites were not investigated in these mice. Additional experiments, for example, future studies in Nrf2 KO mice crossbreed with the eNOS-deficient mice, might represent a better approach to study a role of eNOS in cardiovascular protection under conditions of chronic Nrf2 deficiency.

Importantly, the Nrf2 KO mice used in the present study are characterized by upregulation of a fully functional eNOS, which results in hypotension, preserved vascular function *in vivo* (FMD) and ex vivo (aortic ring relaxation), and increased cGMP production in response to pharmacological eNOS stimulation in Nrf2 KO mouse vessels while basal levels of cGMP were not changed [19]. Except of the classical NO-sGC-cGMP signaling, NO can also exert its regulatory effects on protein structure and function through S-

nitrosation of cysteine thiols [34, 35]. Published data demonstrate eNOS-dependent S-nitrosation of many myocardial proteins including beta-arrestin, cardiac ion channels, and GPCR kinase-2, which influence heart contractility and myocyte survival and function [36–40]. S-Nitrosation of these proteins during myocardial I/R can attenuate apoptosis [41] and inflammation [39]. For instance, caspase-3 activity is known to be inhibited by protein S-nitrosation [42]. Furthermore, mitochondrial ROS production can be decreased during I/R, since S-nitrosothiols are able to modify complex I of the mitochondrial electron transfer change [43] and prevent opening of the mitochondrial permeability transition pore [44] and thus may represent cardioprotective action of upregulated eNOS in Nrf2 KO mice. In this study, we could not detect a significant change in total levels of nitroso species in the heart (although a clear trend to increased RXNO levels was observed) which might be due to the fact that the total detected RXNO levels include not only RSNO but also other nitroso species (e.g., RNNO).

Here, we demonstrate that the increase in eNOS activity plays an important fole in cardioprotection against AMI in Nrf2 KO mice. This is supported by our finding that in Nrf2 KO mice, acute NOS inhibition greatly increased infarct size and decreased systolic and diastolic function after I/R, while neither NOS inhibition in WT mice nor chronic global eNOS deficiency in eNOS KO mice affected these parameters. Therefore, eNOS upregulation in Nrf2 KO mice likely
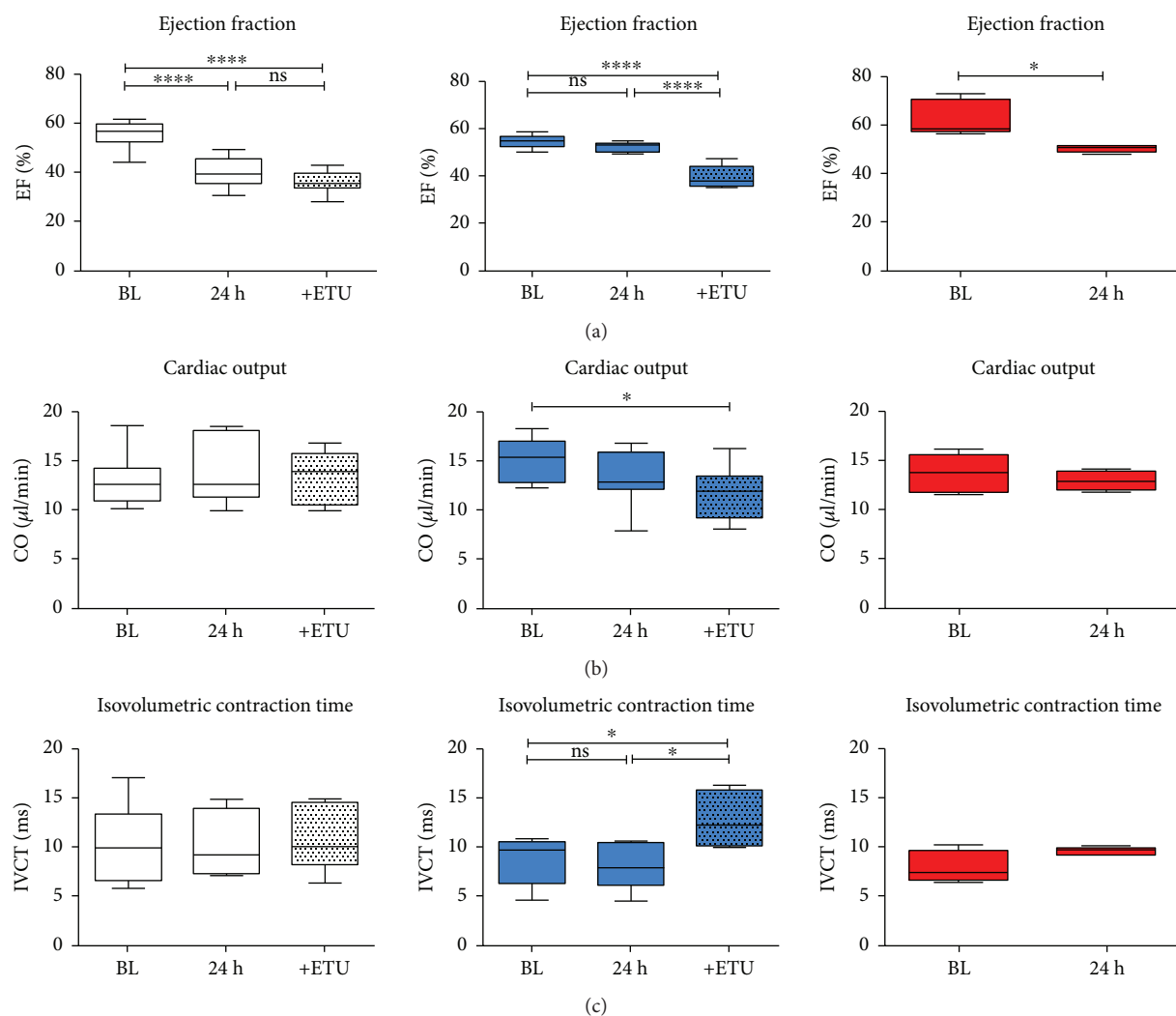
FIGURE 4: Left ventricular systolic function following AMI in Nrf2 KO mice is preserved by NOS. (a) In WT (white box plots) and eNOS KO (red box plots) mice, ejection fraction (EF) was significantly decreased 24 h after AMI, whereas it was essentially unchanged in Nrf2 KO mice (blue box plots). ETU application resulted in an impairment of systolic function in Nrf2 KO mice, but not in WT mice, indicating NOS-dependent preservation of cardiac function in Nrf2 KO mice as compared to WT mice. (b) Cardiac output (CO) was significantly decreased after ETU application in Nrf2 KO mice indicating eNOS-dependent preservation of systolic function after I/R. (c) IVCT was increased after ETU application in Nrf2 KO mice, but not in WT mice. WT mice: $n = 9$, Nrf2 KO mice: $n = 8$; Browne-Forsythe test $p > 0.05$, means ± quartiles, one-way ANOVA, except for eNOS KO mice (red boxes): 4-5, unpaired t-test. $^{*}p < 0.05$ and $^{****}p < 0.0001$.

represents an important protective mechanism that not only protects against myocardial I/R injury but also against impairment of systolic function and the aggravation of diastolic dysfunction after AMI in these mice.

4.3. Role of eNOS-Derived NO in Cardioprotection. Although we found eNOS-derived NO-mediated cardioprotection in Nrf2 KO mice, neither acute NOS inhibition nor global loss of eNOS revealed any cardioprotective effect of NO in the WT mouse hearts. Specifically, eNOS KO mice [20] exhibit no differences in infarct size as compared to the WT mice, which is consistent with the results obtained by acute treatment of WT mice with the NOS inhibitor ETU. Previous reports on the role of eNOS in I/R showed controversial effects, depending on the eNOS KO mouse strain with decreased infarct size in the strain created by Shesely et al. [45] attributed

to iNOS upregulation and increased infarct size and myocardial necrosis [46] in the eNOS KO mouse strain created by Huang et al. [47].

Similar to these two strains, the eNOS KO mouse strain used in the present study (created by Gödecke et al. [20]) shows sustained hypertension, decreased heart rate, increased SV, and cardiac hypertrophy, manifested by increased ventricular wall thickness and mass. However, LV systolic function is fully preserved under basal conditions, as parameters including EF, CO, and FS did not differ between WT and eNOS KO mice. Similar results were reported for the eNOS KO mouse strain generated by Shesely [48]. Likewise, myocardial infarct size and cardiac performance after AMI were not more severe in eNOS KO mice created by Gödecke et al. [20] as compared to WT mice. Accordingly, acute NOS inhibition by ETU in WT mice did neither affect LV function after
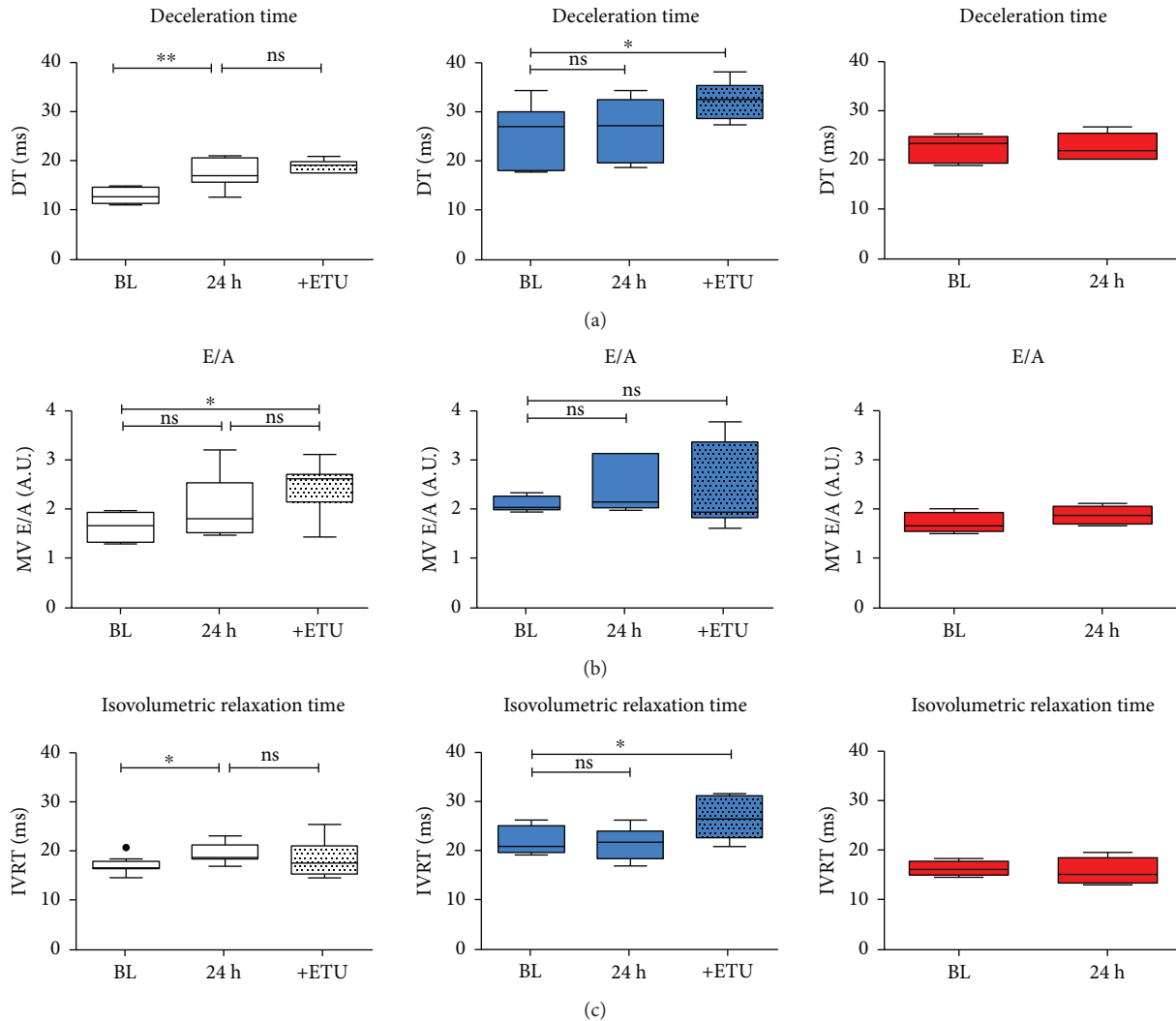
Figure 5: Nrf2 KO mice are protected against impairment of myocardial diastolic function following AMI. (a) I/R injury resulted in an impairment of diastolic function (evaluated with prolonged deceleration time (DT)), (b) E/A relation, and (c) relaxation time (IVRT) in WT mice (white box plots), whereas preexisting diastolic dysfunction was not aggravated in Nrf2 KO mice (blue box plots). In eNOS KO mice (A, red box plots), diastolic dysfunction evidenced by increased DT as compared to WT mice (Supplementary Table 1) was not further exacerbated after AMI. WT mice: $n = 9$, Nrf2 KO mice: $n = 8$; Browne-Forsythe test $p > 0.05$, means ± quartiles, one-way ANOVA $^*p < 0.05$, $^{**}p < 0.01$ except for eNOS KO mice $n = 4$-5, unpaired t-test.

AMI nor infarct size. Therefore, these data clearly demonstrate that lack of eNOS activity is fully compensated by hemodynamic changes and/or cardiac remodeling (on the long term), and the cardioprotective role of eNOS becomes evident only under conditions of a compromised redox reserve like in Nrf2 KO mice. However, the mechanisms of compensation in Nrf2 KO mice treated with NOS inhibitor might differ from the compensation mechanisms of mice chronically deficient for eNOS.

Our experimental setup did not allow us to distinguish between endothelial and other sources of eNOS upregulation in Nrf2 KO mice. However, it has been suggested that activity of endothelial NOS during I/R is of minor importance as compared to the cardiomyocyte-derived NO. Mice with cardiomyocyte-specific overexpression of eNOS displayed significantly decreased infarct size and better preserved cardiac function than mice with systemic eNOS overexpression [49].

In contrast, a study from our laboratory proposed a potential key role of the red blood cell eNOS in cardioprotection against I/R [50]. Specifically, we demonstrated that depletion of circulating blood eNOS increases the severity of myocardial infarction and LV dysfunction suggesting a modulating role of circulating eNOS in an acute model of myocardial I/R. Future studies using tissue-specific transgenic mice with knockin and knockout of key proteins of the eNOS-dependent pathway will help delineating a specific role for eNOS expressed in RBCs and eNOS expressed in other cell types, for example, in endothelium and in cardiomyocytes in conferring cardioprotection against I/R.

Taken together, cardioprotective effects in Nrf2 KO mice were abolished by inhibition of NOS activity in ischemia and early reperfusion, suggesting a role for eNOS in cardioprotection against I/R in Nrf2 deficiency. These data demonstrate that impaired antioxidant defense and decreased redox

reserve in Nrf2 KO mice or decreased NO bioavailability (like in eNOS KO or after NOS inhibition) on their own do not affect myocardial damage after AMI; however, their combination significantly increases myocardial damage and is in line with several recent publications on protective effects of eNOS under conditions of oxidative stress [51, 52].

5. Conclusion

Here, we present experimental evidence that eNOS upregulation under conditions of a compromised antioxidant capacity plays a role in cardioprotection against I/R injury, while eNOS-mediated cardioprotection is not evident after acute NOS inhibition or in eNOS KO mice per se. Although there is overwhelming evidence for associations between oxidative stress and I/R injury, clinical trials consistently failed to demonstrate any cardioprotective effect of antioxidants [53–55]; moreover, high doses of antioxidants may be even harmful [56, 57]. On the contrary, interventions associated with increased eNOS protein expression and improvement of endothelial NO production such as regular exercise training [58], pharmacotherapy with statins [59], and treatment with inhibitors of the renin-angiotensin system [60] have provided superior cardiovascular prevention compared to approaches targeting oxidative stress by applying antioxidants [53–55, 61]. Our results on the beneficial role of eNOS upregulation in cardioprotection under conditions of Nrf2 deficiency and compromised antioxidant status support these data. These results might be also of special importance for the aged organisms, since Nrf2 signaling pathway may substantially contributes to the determination of health span and extension of longevity [62]; and diminished activity of Nrf2 resulting in reduced antioxidative potential, apoptosis, and/or necrosis of the aging myocardium has been reported [63, 64]. Whether the relationship between redox reserve capacity and eNOS-mediated protection may represent one of the key mechanisms underpinning the cardioprotective effects of NO warrants further detailed investigation with larger cohorts of mice and/or mice lacking both eNOS and Nrf2.

Conflicts of Interest

The authors declare that the research was conducted in the absence of any commercial or financial relationships that could be construed as a potential conflict of interest.

Authors' Contributions

Ralf Erkens and Tatsiana Suvorava planned and executed experiments, performed data analysis and interpretation, and wrote the manuscript; Thomas R. Sutton, Bernadette O. Fernandez, Monika Mikus-Lelinska, Frederik Barbarino, and Ulrich Flögel planned and executed experiments and revised the manuscript; Malte Kelm and Martin Feelisch provided substantial intellectual input; Martin Feelisch made substantial contribution in interpretation of the work and critically revised the manuscript; Miriam M. Cortese-Krott designed and coordinated the work and wrote the

manuscript. All authors have given their final approval of the version of the manuscript to be published.

Supplementary Materials

Supplementary Table 1: echocardiographic parameters assessed in vivo by high-resolution ultrasound. Data are reported as mean ± SD; n = number of mice. Differences between the two groups were calculated by unpaired t-test after testing for normal distribution and equal variances; $p < 0.05$ was considered statistically significant and marked in bold. (Supplementary Materials)

References

[1] M. M. Cortese-Krott, A. Koning, G. G. C. Kuhnle et al., "The reactive species interactome: evolutionary emergence, biological significance, and opportunities for redox metabolomics and personalized medicine," *Antioxidants & Redox Signaling*, vol. 27, no. 10, pp. 684–712, 2017.

[2] B. Xu, J. Zhang, J. Strom, S. Lee, and Q. M. Chen, "Myocardial ischemic reperfusion induces de novo Nrf2 protein translation," *Biochimica et Biophysica Acta (BBA) - Molecular Basis of Disease*, vol. 1842, no. 9, pp. 1638–1647, 2014.

[3] E. H. Heiss, D. Schachner, E. R. Werner, and V. M. Dirsch, "Active NF-E2-related factor (Nrf2) contributes to keep endothelial NO synthase (eNOS) in the coupled state role of reactive oxygen species (ROS), eNOS, and heme oxygenase (HO-1) levels," *Journal of Biological Chemistry*, vol. 284, no. 46, pp. 31579–31586, 2009.

[4] T. Ishii, K. Itoh, S. Takahashi et al., "Transcription factor Nrf2 coordinately regulates a group of oxidative stress-inducible genes in macrophages," *Journal of Biological Chemistry*, vol. 275, no. 21, pp. 16023–16029, 2000.

[5] K. Itoh, T. Chiba, S. Takahashi et al., "An Nrf2/small Maf heterodimer mediates the induction of phase II detoxifying enzyme genes through antioxidant response elements," *Biochemical and Biophysical Research Communications*, vol. 236, no. 2, pp. 313–322, 1997.

[6] K. Itoh, N. Wakabayashi, Y. Katoh et al., "Keap1 represses nuclear activation of antioxidant responsive elements by Nrf2 through binding to the amino-terminal Neh2 domain," *Genes & Development*, vol. 13, no. 1, pp. 76–86, 1999.

[7] H. K. Bryan, A. Olayanju, C. E. Goldring, and B. K. Park, "The Nrf2 cell defence pathway: Keap1-dependent and -independent mechanisms of regulation," *Biochemical Pharmacology*, vol. 85, no. 6, pp. 705–717, 2013.

[8] M. Biswas and J. Y. Chan, "Role of Nrf1 in antioxidant response element-mediated gene expression and beyond," *Toxicology and Applied Pharmacology*, vol. 244, no. 1, pp. 16–20, 2010.

[9] Z. A. Shah, R. C. Li, R. K. Thimmulappa et al., "Role of reactive oxygen species in modulation of Nrf2 following ischemic reperfusion injury," *Neuroscience*, vol. 147, no. 1, pp. 53–59, 2007.

[10] A. Lister, T. Nedjadi, N. R. Kitteringham et al., "Nrf2 is overexpressed in pancreatic cancer: implications for cell proliferation and therapy," *Molecular Cancer*, vol. 10, no. 1, p. 37, 2011.

[11] K. Itoh, M. Mochizuki, Y. Ishii et al., "Transcription factor Nrf2 regulates inflammation by mediating the effect of 15-deoxy-$\Delta^{12,14}$-prostaglandin J$_2$," *Molecular and Cellular Biology*, vol. 24, no. 1, pp. 36–45, 2004.

[12] A. A. Shokeir, N. Barakat, A. M. Hussein et al., "Activation of Nrf2 by ischemic preconditioning and sulforaphane in renal ischemia/reperfusion injury: a comparative experimental study," *Physiological Research*, vol. 64, no. 3, pp. 313–323, 2015.

[13] A. Das, B. Gopalakrishnan, O. H. Voss, A. I. Doseff, and F. A. Villamena, "Inhibition of ROS-induced apoptosis in endothelial cells by nitrone spin traps *via* induction of phase II enzymes and suppression of mitochondria-dependent proapoptotic signaling," *Biochemical Pharmacology*, vol. 84, no. 4, pp. 486–497, 2012.

[14] H. J. Kim, M. Zheng, S. K. Kim et al., "CO/HO-1 induces NQO-1 expression via Nrf2 activation," *Immune Network*, vol. 11, no. 6, pp. 376–382, 2011.

[15] S. Tokudome, M. Sano, K. Shinmura et al., "Glucocorticoid protects rodent hearts from ischemia/reperfusion injury by activating lipocalin-type prostaglandin D synthase–derived PGD$_2$ biosynthesis," *Journal of Clinical Investigation*, vol. 119, no. 6, pp. 1477–1488, 2009.

[16] Y. Katsumata, K. Shinmura, Y. Sugiura et al., "Endogenous prostaglandin D$_2$ and its metabolites protect the heart against ischemia–reperfusion injury by activating Nrf2," *Hypertension*, vol. 63, no. 1, pp. 80–87, 2014.

[17] J. W. Calvert, S. Jha, S. Gundewar et al., "Hydrogen sulfide mediates cardioprotection through Nrf2 signaling," *Circulation Research*, vol. 105, no. 4, pp. 365–374, 2009.

[18] B. L. Predmore, K. Kondo, S. Bhushan et al., "The polysulfide diallyl trisulfide protects the ischemic myocardium by preservation of endogenous hydrogen sulfide and increasing nitric oxide bioavailability," *American Journal of Physiology-Heart and Circulatory Physiology*, vol. 302, no. 11, pp. H2410–H2418, 2012.

[19] R. Erkens, C. M. Kramer, W. Luckstadt et al., "Left ventricular diastolic dysfunction in Nrf2 knock out mice is associated with cardiac hypertrophy, decreased expression of SERCA2a, and preserved endothelial function," *Free Radical Biology and Medicine*, vol. 89, pp. 906–917, 2015.

[20] A. Gödecke, U. K. M. Decking, Z. Ding et al., "Coronary hemodynamics in endothelial NO synthase knockout mice," *Circulation Research*, vol. 82, no. 2, pp. 186–194, 1998.

[21] N. S. Bryan, T. Rassaf, R. E. Maloney et al., "Cellular targets and mechanisms of nitros(yl)ation: an insight into their nature and kinetics *in vivo*," *Proceedings of the National Academy of Sciences of the United States of America*, vol. 101, no. 12, pp. 4308–4313, 2004.

[22] D. Z. Levett, B. O. Fernandez, H. L. Riley et al., "The role of nitrogen oxides in human adaptation to hypoxia," *Scientific Reports*, vol. 1, no. 1, p. 109, 2011.

[23] T. Rassaf, M. Totzeck, U. B. Hendgen-Cotta, S. Shiva, G. Heusch, and M. Kelm, "Circulating nitrite contributes to cardioprotection by remote ischemic preconditioning," *Circulation Research*, vol. 114, no. 10, pp. 1601–10, 2014.

[24] F. Bönner, C. Jacoby, S. Temme et al., "Multifunctional MR monitoring of the healing process after myocardial infarction," *Basic Research in Cardiology*, vol. 109, no. 5, p. 430, 2014.

[25] A. Anwar-Mohamed, O. S. Degenhardt, M. A. M. El Gendy, J. M. Seubert, S. R. Kleeberger, and A. O. S. El-Kadi, "The effect of Nrf2 knockout on the constitutive expression of drug metabolizing enzymes and transporters in C57Bl/6 mice livers," *Toxicology In Vitro*, vol. 25, no. 4, pp. 785–795, 2011.

[26] S. C. Lu, "Regulation of glutathione synthesis," *Molecular Aspects of Medicine*, vol. 30, no. 1-2, pp. 42–59, 2009.

[27] Q. Ma, "Role of nrf2 in oxidative stress and toxicity," *Annual Review of Pharmacology and Toxicology*, vol. 53, no. 1, pp. 401–426, 2013.

[28] C. J. Harvey, R. K. Thimmulappa, A. Singh et al., "Nrf2-regulated glutathione recycling independent of biosynthesis is critical for cell survival during oxidative stress," *Free Radical Biology and Medicine*, vol. 46, no. 4, pp. 443–453, 2009.

[29] C. Köhle and K. W. Bock, "Coordinate regulation of phase I and II xenobiotic metabolisms by the Ah receptor and Nrf2," *Biochemical Pharmacology*, vol. 73, no. 12, pp. 1853–1862, 2007.

[30] D. R. Janero, N. S. Bryan, F. Saijo et al., "Differential nitros(yl)ation of blood and tissue constituents during glyceryl trinitrate biotransformation *in vivo*," *Proceedings of the National Academy of Sciences of the United States of America*, vol. 101, no. 48, pp. 16958–16963, 2004.

[31] K. Chan, R. Lu, J. C. Chang, and Y. W. Kan, "NRF2, a member of the NFE2 family of transcription factors, is not essential for murine erythropoiesis, growth, and development," *Proceedings of the National Academy of Sciences of the United States of America*, vol. 93, no. 24, pp. 13943–13948, 1996.

[32] J. Li, T. Ichikawa, L. Villacorta et al., "Nrf2 protects against maladaptive cardiac responses to hemodynamic stress," *Arteriosclerosis, Thrombosis, and Vascular Biology*, vol. 29, no. 11, pp. 1843–1850, 2009.

[33] K. Yoh, K. Itoh, A. Enomoto et al., "Nrf2-deficient female mice develop lupus-like autoimmune nephritis," *Kidney International*, vol. 60, no. 4, pp. 1343–1353, 2001.

[34] N. Gould, P. T. Doulias, M. Tenopoulou, K. Raju, and H. Ischiropoulos, "Regulation of protein function and

signaling by reversible cysteine S-nitrosylation," *Journal of Biological Chemistry*, vol. 288, no. 37, pp. 26473–26479, 2013.

[35] S. M. Haldar and J. S. Stamler, "S-Nitrosylation: integrator of cardiovascular performance and oxygen delivery," *Journal of Clinical Investigation*, vol. 123, no. 1, pp. 101–110, 2013.

[36] E. J. Whalen, M. W. Foster, A. Matsumoto et al., "Regulation of β-adrenergic receptor signaling by S-nitrosylation of G-protein-coupled receptor kinase 2," *Cell*, vol. 129, no. 3, pp. 511–522, 2007.

[37] K. Ozawa, E. J. Whalen, C. D. Nelson et al., "S-Nitrosylation of β-arrestin regulates β-adrenergic receptor trafficking," *Molecular Cell*, vol. 31, no. 3, pp. 395–405, 2008.

[38] D. R. Gonzalez, A. Treuer, Q. A. Sun, J. S. Stamler, and J. M. Hare, "S-Nitrosylation of cardiac ion channels," *Journal of Cardiovascular Pharmacology*, vol. 54, no. 3, pp. 188–195, 2009.

[39] B. Lima, M. T. Forrester, D. T. Hess, and J. S. Stamler, "S-Nitrosylation in cardiovascular signaling," *Circulation Research*, vol. 106, no. 4, pp. 633–646, 2010.

[40] Z. M. Huang, E. Gao, F. V. Fonseca et al., "Convergence of G protein–coupled receptor and S-nitrosylation signaling determines the outcome to cardiac ischemic injury," *Science Signaling*, vol. 6, no. 299, article ra95, 2013.

[41] M. Benhar and J. S. Stamler, "A central role for S-nitrosylation in apoptosis," *Nature Cell Biology*, vol. 7, no. 7, pp. 645-646, 2005.

[42] J. Li, T. R. Billiar, R. V. Talanian, and Y. M. Kim, "Nitric oxide reversibly inhibits seven members of the caspase family via S-nitrosylation," *Biochemical and Biophysical Research Communications*, vol. 240, no. 2, pp. 419–424, 1997.

[43] S. Shiva, Z. Huang, R. Grubina et al., "Deoxymyoglobin is a nitrite reductase that generates nitric oxide and regulates mitochondrial respiration," *Circulation Research*, vol. 100, no. 5, pp. 654–661, 2007.

[44] H. Ohtani, H. Katoh, T. Tanaka et al., "Effects of nitric oxide on mitochondrial permeability transition pore and thiol-mediated responses in cardiac myocytes," *Nitric Oxide*, vol. 26, no. 2, pp. 95–101, 2012.

[45] E. G. Shesely, N. Maeda, H.-S. Kim et al., "Elevated blood pressures in mice lacking endothelial nitric oxide synthase," *Proceedings of the National Academy of Sciences of the United States of America*, vol. 93, no. 23, pp. 13176–13181, 1996.

[46] B. R. Sharp, S. P. Jones, D. M. Rimmer, and D. J. Lefer, "Differential response to myocardial reperfusion injury in eNOS-deficient mice," *American Journal of Physiology-Heart and Circulatory Physiology*, vol. 282, no. 6, pp. H2422–H2426, 2002.

[47] P. L. Huang, Z. Huang, H. Mashimo et al., "Hypertension in mice lacking the gene for endothelial nitric oxide synthase," *Nature*, vol. 377, no. 6546, pp. 239–242, 1995.

[48] X. P. Yang, Y. H. Liu, E. G. Shesely, M. Bulagannawar, F. Liu, and O. A. Carretero, "Endothelial nitric oxide gene knockout mice: cardiac phenotypes and the effect of angiotensin-converting enzyme inhibitor on myocardial ischemia/reperfusion injury," *Hypertension*, vol. 34, no. 1, pp. 24–30, 1999.

[49] J. W. Elrod, J. J. M. Greer, N. S. Bryan et al., "Cardiomyocyte-specific overexpression of NO synthase-3 protects against myocardial ischemia-reperfusion injury," *Arteriosclerosis, Thrombosis, and Vascular Biology*, vol. 26, no. 7, pp. 1517–1523, 2006.

[50] M. W. Merx, S. Gorressen, A. M. Sandt et al., "Depletion of circulating blood NOS3 increases severity of myocardial infarction and left ventricular dysfunction," *Basic Research in Cardiology*, vol. 109, no. 1, p. 398, 2014.

[51] T. Suvorava, N. Nagy, S. Pick et al., "Impact of eNOS-dependent oxidative stress on endothelial function and neointima formation," *Antioxidants & Redox Signaling*, vol. 23, no. 9, pp. 711–723, 2015.

[52] P. Ponnuswamy, A. Schröttle, E. Ostermeier et al., "eNOS protects from atherosclerosis despite relevant superoxide production by the enzyme in apoE$^{-/-}$ mice," *PLoS One*, vol. 7, no. 1, article e30193, 2012.

[53] H. D. Sesso, J. E. Buring, W. G. Christen et al., "Vitamins E and C in the prevention of cardiovascular disease in men: the Physicians' Health Study II randomized controlled trial," *JAMA*, vol. 300, no. 18, pp. 2123–2133, 2008.

[54] K. H. Bønaa, I. Njølstad, P. M. Ueland et al., "Homocysteine lowering and cardiovascular events after acute myocardial infarction," *New England Journal of Medicine*, vol. 354, no. 15, pp. 1578–1588, 2006.

[55] The Heart Outcomes Prevention Evaluation Study Investigators, S. Yusuf, G. Dagenais, J. Pogue, J. Bosch, and P. Sleight, "Vitamin E supplementation and cardiovascular events in high-risk patients," *New England Journal of Medicine*, vol. 342, no. 3, pp. 154–160, 2000.

[56] G. Bjelakovic, D. Nikolova, L. L. Gluud, R. G. Simonetti, and C. Gluud, "Mortality in randomized trials of antioxidant supplements for primary and secondary prevention: systematic review and meta-analysis," *JAMA*, vol. 297, no. 8, pp. 842–857, 2007.

[57] E. R. Miller III, R. Pastor-Barriuso, D. Dalal, R. A. Riemersma, L. J. Appel, and E. Guallar, "Meta-analysis: high-dosage vitamin E supplementation may increase all-cause mortality," *Annals of Internal Medicine*, vol. 142, no. 1, pp. 37–46, 2005.

[58] G. Kojda and R. Hambrecht, "Molecular mechanisms of vascular adaptations to exercise. Physical activity as an effective antioxidant therapy?," *Cardiovascular Research*, vol. 67, no. 2, pp. 187–197, 2005.

[59] U. Laufs, V. La Fata, J. Plutzky, and J. K. Liao, "Upregulation of endothelial nitric oxide synthase by HMG CoA reductase inhibitors," *Circulation*, vol. 97, no. 12, pp. 1129–1135, 1998.

[60] T. G. von Lueder and H. Krum, "RAAS inhibitors and cardiovascular protection in large scale trials," *Cardiovascular Drugs and Therapy*, vol. 27, no. 2, pp. 171–179, 2013.

[61] E. Lonn, S. Yusuf, M. J. Arnold et al., "Homocysteine lowering with folic acid and B vitamins in vascular disease," *New England Journal of Medicine*, vol. 354, no. 15, pp. 1567–1577, 2006.

[62] S. Satta, A. M. Mahmoud, F. L. Wilkinson, M. Y. Alexander, and S. J. White, "The role of Nrf2 in cardiovascular function and disease," *Oxidative Medicine and Cellular Longevity*, vol. 2017, Article ID 9237263, 18 pages, 2017.

[63] S. Zhou, W. Sun, Z. Zhang, and Y. Zheng, "The role of Nrf2-mediated pathway in cardiac remodeling and heart failure," *Oxidative Medicine and Cellular Longevity*, vol. 2014, Article ID 260429, 16 pages, 2014.

[64] J. Kajstura, W. Cheng, R. Sarangarajan et al., "Necrotic and apoptotic myocyte cell death in the aging heart of Fischer 344 rats," *American Journal of Physiology-Heart and Circulatory Physiology*, vol. 271, no. 3, pp. H1215–H1228, 1996.

Research Article

L-Arginine Enhances Protein Synthesis by Phosphorylating mTOR (Thr 2446) in a Nitric Oxide-Dependent Manner in C2C12 Cells

Ruxia Wang, Hongchao Jiao, Jingpeng Zhao, Xiaojuan Wang, and Hai Lin ⓘ

Department of Animal Science, Shandong Key Lab for Animal Biotechnology and Disease Control, Shandong Agricultural University, Tai'an, Shandong, China

Correspondence should be addressed to Hai Lin; hailin@sdau.edu.cn

Muscle atrophy may arise from many factors such as inactivity, malnutrition, and inflammation. In the present study, we investigated the stimulatory effect of nitric oxide (NO) on muscle protein synthesis. Primarily, C2C12 cells were supplied with extra L-arginine (L-Arg) in the culture media. L-Arg supplementation increased the activity of inducible nitric oxide synthase (iNOS), the rate of protein synthesis, and the phosphorylation of mTOR (Thr 2446) and p70S6K (Thr 389). L-NAME, an NOS inhibitor, decreased NO concentrations within cells and abolished the stimulatory effect of L-Arg on protein synthesis and the phosphorylation of mTOR and p70S6K. In contrast, SNP (sodium nitroprusside), an NO donor, increased NO concentrations, enhanced protein synthesis, and upregulated mTOR and p70S6K phosphorylation, regardless of L-NAME treatment. Blocking mTOR with rapamycin abolished the stimulatory effect of both L-Arg and SNP on protein synthesis and p70S6K phosphorylation. These results indicate that L-Arg stimulates protein synthesis via the activation of the mTOR (Thr 2446)/p70S6K signaling pathway in an NO-dependent manner.

1. Introduction

Nitric oxide (NO) is a free radical that is produced by nitric oxide synthase (NOS) enzymes, which catalyze the conversion of L-arginine (L-Arg) to L-citrulline [1]. NO participates in specific signal transduction pathways, representing an important new paradigm in cell communication and signaling processes [2–4].

L-Arg, the precursor to NO, is involved in protein phosphorylation cascades and gene expression [5–7]. L-Arg supplementation enables burn patients to maintain muscle mass [8] and ameliorates muscle dysfunction in *mdx* mice (X-linked muscular dystrophy, a model of Duchenne muscular dystrophy) [9]. Additionally, the concentrations of specific free amino acids, notably arginine and glutamine, are associated with muscle growth and protein synthesis capacity during late pregnancy in well-nourished sheep [10, 11]. However, supplementation with citrulline, the metabolic precursor of arginine, did not result in therapeutically relevant outcomes such as increased skeletal muscle mass and peak muscle force in male mice suffering from 14 d of hindlimb

immobilization [12]. Therefore, further study is required to determine whether L-Arg can stimulate protein synthesis in skeletal muscle tissue. Moreover, skeletal muscle participates in the overall NO metabolism by serving as a nitrate reservoir [13]. L-arginine could protect myocytes from wasting during catabolic conditions in an NO-independent manner [14]. L-citrulline, produced by arginine metabolism, protects skeletal muscle cells from cachectic stimuli in an iNOS-dependent manner [15]. NO is involved in the repair of skeletal muscle injury [16]. The activation of NO during muscle injury is critical in the early phases of the skeletal muscle repair process [17]. The maintenance of NO could ameliorate the symptoms of dystrophy [18, 19]. The age-related muscle refractoriness to exercise can be overcome with NO donor treatment [20]. There is growing evidence that NO is associated with skeletal muscle-wasting diseases, sarcopenia, and cachexia [21, 22]. However, the role of NO in myocyte protein synthesis under normal conditions also needs to be elucidated.

The mammalian target of rapamycin (mTOR), a serine/threonine protein kinase, plays a central role as a nutrient and energy sensor in skeletal muscle. The mTOR signaling

pathway controls cell growth and metabolic progression by phosphorylating two downstream proteins: the eukaryotic initiation factor 4E-binding protein 1 (4E-BP1) and the ribosomal p70S6 kinase1 (p70S6K) [23, 24]. As a crucial component of the anabolic protein synthesis machinery, the mTOR pathway participates in the regulation of protein anabolism in skeletal muscle [25–27]. L-Arg protects muscle cells from wasting *in vitro* in an mTORC1-dependent manner [6, 14]. Therefore, we hypothesized that L-Arg is associated with the regulation of protein anabolism in myocytes through the involvement of the NO and mTOR/p70S6K signaling pathways.

In this study, the effect of L-Arg on myocyte protein synthesis and the involvement of NO were investigated *in vitro* in differentiated mouse C2C12 myoblasts. The protein synthesis rate was estimated with a nonradioactive method by labeling the newly synthesized polypeptides with low concentrations of puromycin and subsequently detecting these proteins with an anti-puromycin antibody [28, 29]. The involvement of the mTOR (Thr 2446)/p70S6K signaling pathway was also evaluated in this study.

2. Materials and Methods

2.1. Cell Culture. Mouse C2C12 myoblasts (China Center for Type Culture Collection, Wuhan, Hubei, CN) were plated and cultured in high-glucose Dulbecco's modified Eagle's medium (DMEM; Thermo Fisher, Shanghai, CN) with 10% fetal bovine serum (Gibco, Grand Island, NY, US) and 1% penicillin/streptomycin (Solarbio, Beijing, CN). At 80% confluence, the cells were induced to differentiate and form myotubes by culturing in DMEM supplemented with 2% horse serum (Gibco, Grand Island, NY, US) for 84 h. Before treatment, the medium was replaced with serum-free DMEM for 12 h. Finally, the C2C12 cells were exposed to the treatments detailed below. Each treatment was performed on 6 or 7 samples ($n = 6$ or 7).

2.2. L-Arginine, L-NAME, and SNP Treatments. The C2C12 cells were subjected to the following treatments: control (basal medium containing 398.7 μM of L-Arg), extra L-arginine supplementation (1 mM; Sigma, Saint Louis, MO, US), N-nitro-L-arginine methyl ester (L-NAME; 10 mM; Sigma, Saint Louis, MO, US), and L-Arg supplementation (1 mM) plus L-NAME (10 mM). The treatment doses were selected based on previous studies [6, 14, 30]. To further evaluate the role of NO, C2C12 cultures were subjected to the following treatments: 1 μM of sodium nitroprusside (SNP; an NO donor; Sigma, Saint Louis, MO, US) or SNP (1 μM) plus L-NAME (10 mM). At 36 h after treatment, puromycin (10 μM; Solarbio, Beijing, CN) was added to the culture media for an additional 30 min, and proteins were extracted from C2C12 cells and used for subsequent analyses.

2.3. Rapamycin Treatment. The C2C12 cells were treated with 100 nM of rapamycin (an inhibitor of p70S6K; Solarbio, Beijing, CN) for 30 min, followed by L-Arg (1 mM) or SNP (1 μM) supplementation for 36 h. Thereafter, puromycin was added to the culture medium for an additional 30 min,

and proteins were extracted from the C2C12 cells and used for subsequent analyses.

2.4. NO Concentration and NOS Activity Assays. NO concentrations in the media and cells were assessed using a commercial kit (Jiancheng Bioengineering Institute, Nanjing, Jiangsu, CN). NO is very chemically active and is thus easily converted into NO_2^- and then NO_3^-. In this reaction system, the concentration of NO_2^- was measured after conversion of NO_3^- into NO_2^- by nitrate reductase. The absorbance of the supernatant was determined at 550 nm using a spectrophotometer (Beijing PGeneral, Beijing, CN). Intracellular NOS activity, including total NOS enzymes (TNOS) and inducible NOS (iNOS), were determined using a commercial kit (Jiancheng Bioengineering Institute, Nanjing, Jiangsu, CN) according to the manufacturer's instructions. In the reaction system, NOS catalyzes L-arginine to produce NO, which reacts with nucleophilic substances to form nonferrous compounds. The absorbance was determined at 530 nm using a UV-2450 spectrophotometer (Beijing PGeneral, Beijing, CN). The experiment was also performed in the absence of calcium and the presence of a calcium chelator to determine the calcium-independent NOS activity, which was taken to represent iNOS activity.

2.5. Protein Preparation and Western Blotting. The cells were washed briefly with PBS (phosphate-buffered saline) and collected in 0.2 mL of RIPA (radio immunoprecipitation assay) lysis buffer (Beyotime, Haimen, Jiangsu, CN). Cell debris were removed by centrifugation at 12,000 ×g for 5 min at 4°C, and the supernatants were used for immunoblotting analysis. The BCA Protein Assay Kit (Beyotime, Nanjing, Jiangsu, CN) was used to determine protein concentrations. Aliquots containing 18 μg of protein were separated by 7.5% SDS polyacrylamide gel electrophoresis, and the separated proteins were transferred onto polyvinylidene fluoride membranes (0.45 μm; Millipore, Boston, MA, USA) at 200 mA for 2 h in western transfer buffer (Beyotime, Nanjing, Jiangsu, CN) containing 20% methanol. Membranes were then blocked for 1 h at room temperature and incubated at 4°C overnight with primary antibodies at an appropriate dilution ratio. The following primary antibodies were used: anti-phospho-4E-BP1 (Thr 37/46), anti-4E-BP1, anti-phospho-p70S6K (Thr 389), anti-p70S6K, anti-phospho-mTOR (Ser 2448), anti-mTOR (Cell Signaling Technologies, Danvers, MA, US), anti-phospho-mTOR (Ser 2481) and anti-phospho-mTOR (Thr 2446) (Abcam, Cambridge, MA, US), anti-mouse puromycin (Kerafast, Boston, MA, US), and anti-β-actin (Beyotime, Nanjing, Jiangsu, CN). After washing, the proteins were probed with horseradish peroxidase-linked anti-rabbit or anti-mouse secondary antibodies with gentle agitation for 4 h. The membranes were subsequently exposed to enhanced chemiluminescence plus western blot detection reagents (Beyotime, Nanjing, Jiangsu, CN). When two different proteins had the same or similar molecular weight, we used different membranes to separately detect them. In contrast, when two proteins were of different molecular weights or when the phosphorylated and total levels of one protein needed to be analyzed, the same membrane was used again.

During this process, the membrane was blocked again and incubated with another antibody after one protein was detected. Finally, the membrane was scanned, and specific bands were quantified using Vilber Fusion FX7 Spectra (Vilber Lourmat, Paris, FR). The band intensity was normalized to the β-actin band in the same sample. For phosphorylated proteins, when the total protein bands showed significant differences in different treatments, the phosphorylated protein bands were normalized to the total protein bands. In contrast, if the total protein bands remained constant among different groups, both the phosphorylated and total protein bands were normalized to β-actin.

2.6. Protein Synthesis Rate Analysis. The protein synthesis rate was detected using a nonradioactive method [28]. The newly synthesized proteins labeled with puromycin were subsequently detected with an anti-puromycin antibody. The accumulation of puromycin-conjugated peptides into nascent peptide chains reflects the rate of protein synthesis [28, 29]. The protein-antibody complexes were detected with ECL Plus A and B (Beyotime, Nanjing, Jiangsu, CN), and the results were quantified using the Fusion FX software (Vilber Lourmat, Paris, FR).

2.7. Statistical Analysis. The data are expressed as the means ± SEM. The results were analyzed using one-way ANOVA and the Statistical Analysis Systems statistical software package (Version 8e; SAS Institute Inc., Cary, NC, US). For the observations of NO, TNOS, and iNOS at 3, 18, and 36 h time points, two-way ANOVA was used to estimate the main effects of L-Arg or L-NAME supplementation and time. Differences between the means were evaluated using Duncan's honestly significant difference tests. Differences were considered as significant at $P < 0.05$ and as approaching significance at $P < 0.10$.

3. Results

3.1. Effect of L-Arg on Protein Synthesis and mTOR and p70S6K Phosphorylation. Compared with the control, L-Arg significantly increased protein synthesis (+70%, $P < 0.05$, Figure 1(a)). The levels of phospho-mTOR (Thr 2446) and phospho-p70S6K (Thr 389) were also significantly increased (+70% and +40%, $P < 0.05$, Figures 1(b) and 1(c), resp.). However, no differences ($P > 0.05$) were observed in the levels of phospho-mTOR (Ser 2448 and Ser 2481) (Figure 1(b)). Additionally, the NO abundance increased significantly in the L-Arg-supplemented culture medium at 3 h (+30%, $P < 0.05$, Figure 2(b)). The concentration of NO in the C2C12 cells and culture media tended to decrease with longer treatment times (−95% and −40%, $P < 0.05$, Figures 2(a) and 2(b), resp.). In contrast, the activities of iNOS and TNOS increased from 3 h to 36 h (+60% and +90%, $P < 0.05$, Figures 2(c) and 2(d), resp.). L-Arg significantly increased the activity of iNOS and TNOS at 3 h (+70% and +30%, $P < 0.05$, Figures 2(c) and 2(d), resp.). The activity of iNOS, however, was somewhat increased at 18 h (+35%, $P = 0.0774$, Figure 2(c)) and clearly increased at 36 h in the C2C12 cells (+65%, $P < 0.05$, Figure 2(c)).

3.2. Effect of L-NAME on Protein Synthesis and mTOR and p70S6K Phosphorylation. L-NAME decreased the NO abundance in the cell-free supernatants (−80%, Figure 2(b)) and NO levels in the C2C12 cells (−80% and −90%, $P < 0.05$) at 18 and 36 h (Figure 2(a)) and tended to decrease NO levels after 36 h treatment in the cell-free supernatants compared with those of the controls (−85%, $P = 0.068$, Figure 2(b)). iNOS activity was not significantly altered ($P > 0.05$) at 3 h, 18 h, and 36 h, whereas TNOS activity was significantly inhibited (−55%, $P < 0.05$) at 18 h (Figure 2(d)) and tended to be suppressed by L-NAME treatment in C2C12 cells at 36 h (−30%, $P = 0.093$) (Figure 2(d)). Compared with controls, however, L-Arg supplementation had no significant influence ($P > 0.05$) on NO concentrations in either the cells or the cell-free supernatant. Conversely, iNOS activity was significantly increased by L-Arg treatment (+60%, $P < 0.05$), regardless of the presence of L-NAME (Figure 2(c)) at 36 h. Additionally, TNOS activity was not altered by treatment with both L-Arg and L-NAME ($P > 0.05$) (Figure 2(d)).

L-NAME treatment significantly decreased ($P < 0.05$) protein synthesis (−25%, Figure 3(a)), as well as the phosphorylated mTOR (Thr 2446) (−40%, Figure 3(b)) and phospho-p70S6K (Thr 389) (−25%, Figure 3(c)) levels in the C2C12 cells. However, this inhibitory effect was significantly reduced by supplementation with 1 mM of L-Arg (+25%, +50%, and +35%, $P < 0.05$, Figures 3(a)–3(c)). In contrast, no difference was detected ($P > 0.05$) in the levels of the total or phosphorylated mTOR (Ser 2448 and Ser 2481) (Figure 3(b)).

3.3. Effect of SNP on Protein Synthesis and mTOR, p70S6K, and 4E-BP1 Phosphorylation. To further evaluate whether NO is involved in the regulation of protein synthesis, we tested the effect of SNP, an NO donor. The results showed that SNP treatment increased NO concentrations in the C2C12 cells (+55%, $P < 0.05$) and in the cell-free supernatants (+80%, $P < 0.05$, Figure 4(a)). Furthermore, iNOS (−60%, $P < 0.05$), but not TNOS ($P > 0.05$), activity was suppressed by SNP treatment (Figure 4(b)).

The results also indicated that SNP significantly increased protein synthesis (+30%, $P < 0.05$, Figure 5(a)), increased the phosphorylation of mTOR (Thr 2446) (35%, $P < 0.05$, Figure 5(b)), and upregulated both total p70S6K and phospho-p70S6K (Thr 389) (+15% and +15%, $P < 0.05$, Figure 5(c)) and phosphor-4E-BP1 (Thr 37/46) levels (+10%, $P < 0.05$, Figure 5(d)). In contrast, phospho-mTOR (Ser 2448 and Ser 2481) levels remained unaltered ($P > 0.05$, Figure 5(d)).

The effect of SNP on L-NAME-induced suppression of protein synthesis was further investigated. L-NAME significantly inhibited the protein synthesis rate (−20%, $P < 0.05$, Figure 6(a)), downregulated the levels of phosphorylated mTOR (Thr 2446) (−60%, $P < 0.05$, Figure 6(b)), and decreased the phosphorylation of p70S6K (Thr 389) (−35%, $P < 0.05$, Figure 6(c)). In contrast, SNP supplementation significantly alleviated the L-NAME-induced inhibition of protein synthesis (+40%, $P < 0.05$, Figure 6(a)). SNP supplementation also upregulated the phosphorylated mTOR (Thr 2446), as well as the total and phosphorylated

(a)

(b)

(c)
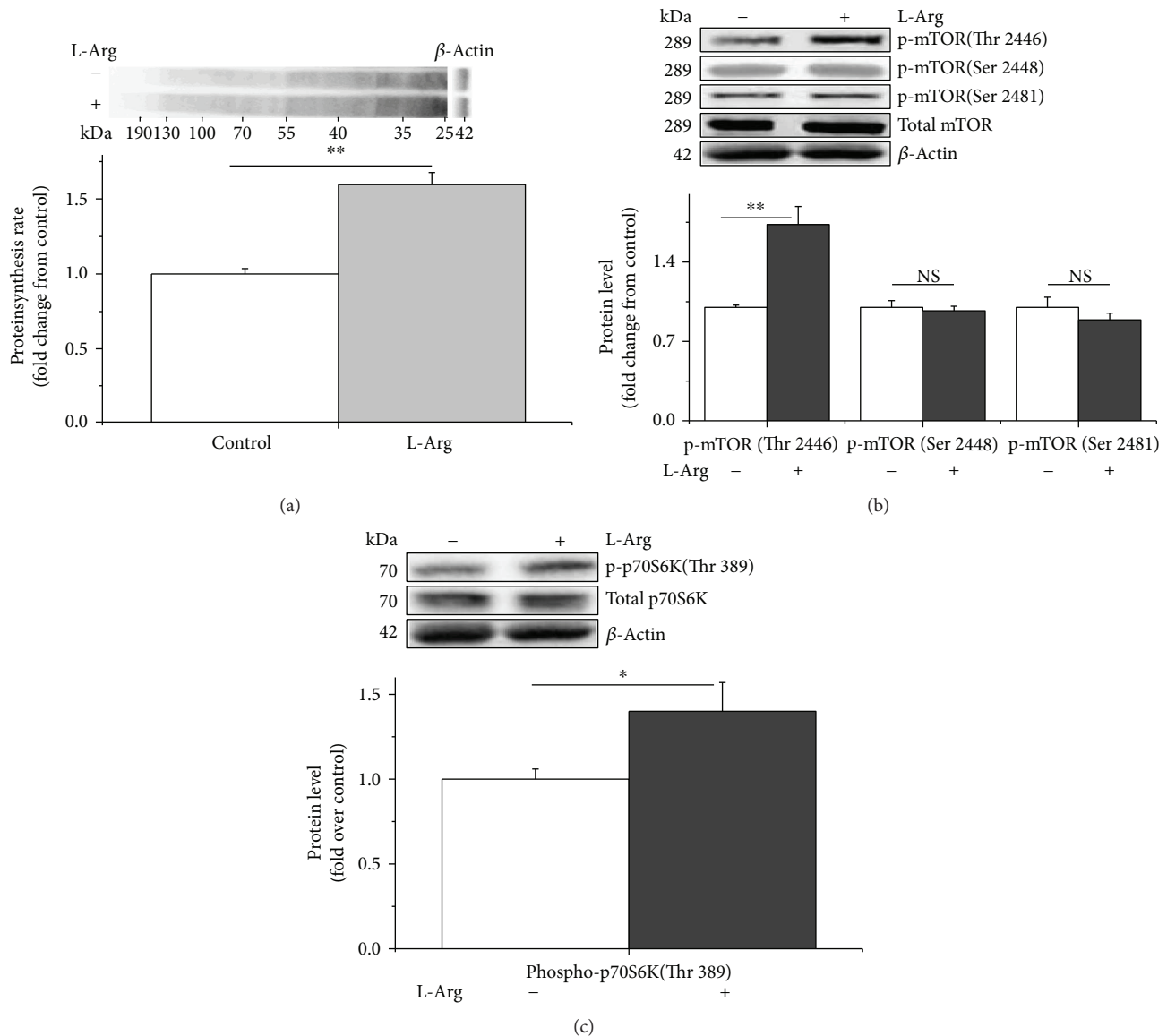
FIGURE 1: L-Arginine enhances protein synthesis by phosphorylating mTOR (Thr 2446) and p70S6K (Thr 389) in C2C12 cells. The protein synthesis rate was evaluated after treatment by supplementation with puromycin ($10\,\mu$M) for 30 min in the cell-free supernatant (a). The levels of phosphorylated mTOR (b) and p70S6K (c) in the C2C12 cells cultured for 36 h in the presence of 1 mM of L-arginine. When the total protein bands showed significant differences with different treatments, the phosphorylated protein bands were normalized to the total protein bands. In contrast, if the total protein bands were similar across different groups, both the phosphorylated and total protein bands were normalized to β-actin. Data are presented as the means ± SEM ($n = 6$); $^{**}P < 0.01$ and $^{*}P < 0.05$ compared with untreated cells. NS, $P > 0.05$.

p70S6K (Thr 389), levels compared with those of the L-NAME treatment (+40% and +35%, $P < 0.05$, Figures 6(b) and 6(c)). However, no difference was detected between the SNP and control treatments ($P > 0.05$). Neither SNP nor L-NAME treatment altered the levels of the phosphorylated mTOR (Ser 2448 and Ser 2481) ($P > 0.05$, Figure 6(b)).

3.4. Effect of Rapamycin Treatment on Protein Synthesis and mTOR and p70S6K Phosphorylation. We further verified whether p70S6K is involved in the stimulatory effect of NO on protein synthesis by blocking mTOR/p70S6K signaling. The results showed that the protein synthesis rate significantly decreased with rapamycin treatment (−20%

and −25%, $P < 0.05$, Figures 7(a) and 7(d)). Meanwhile, rapamycin treatment decreased the levels of total mTOR (−60% and −50%, $P < 0.05$, Figures 7(b) and 7(e)) and p70S6K (Thr 389) phosphorylation (−100% and −100%, $P < 0.05$, Figures 7(c) and 7(f)). Moreover, supplementation with L-Arg or SNP did not reverse the effects of rapamycin treatment on the C2C12 cells ($P > 0.05$) (Figures 7(a) and 7(e)).

4. Discussion

In the present study, we investigated the role of L-Arg on *in vitro* muscle protein synthesis under normal conditions. The results indicated that L-Arg supplementation stimulated
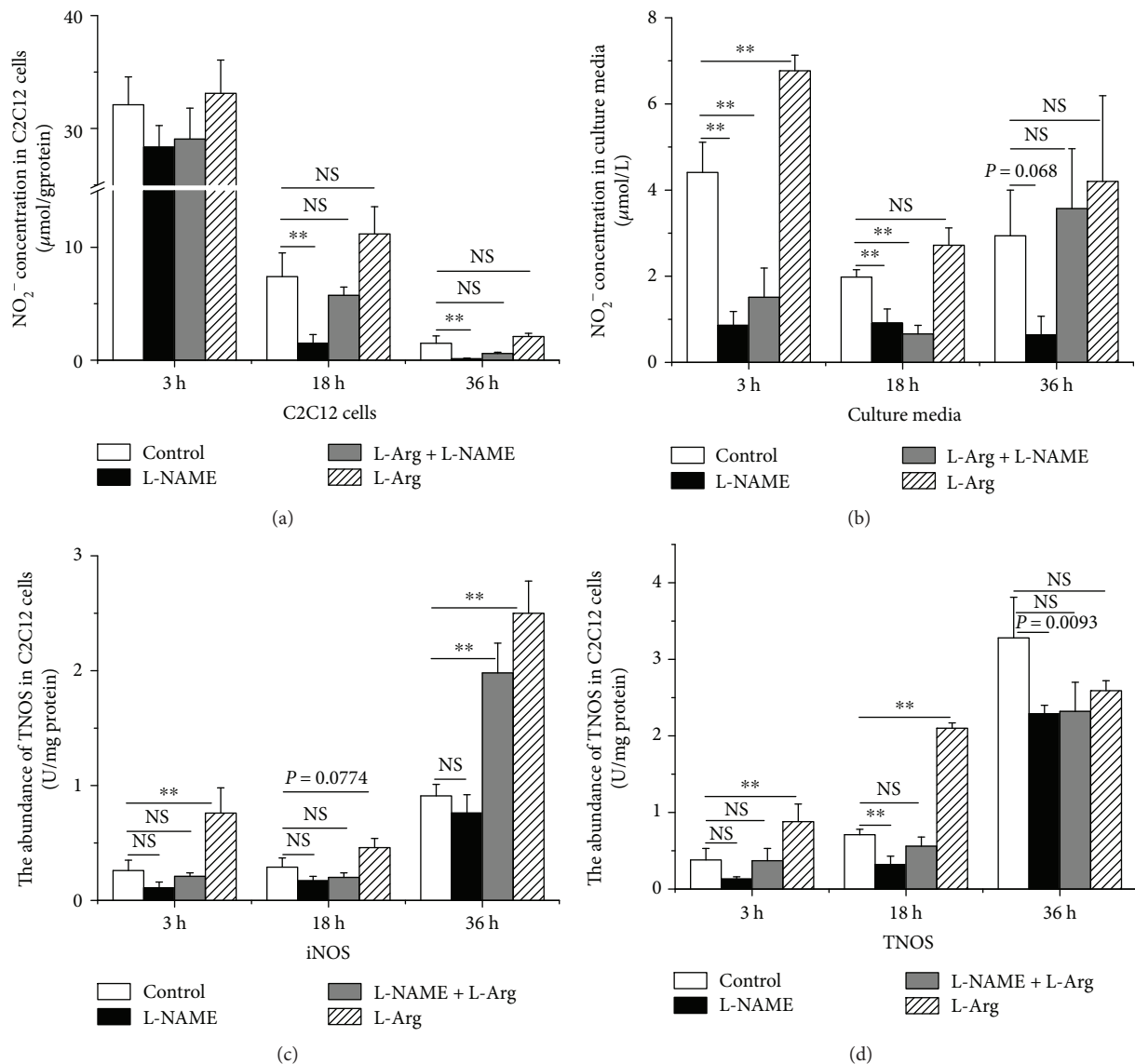
Figure 2: L-Arginine supplementation increases and L-NAME supplementation decreases NO concentrations in C2C12 cells and the culture medium, as well as the activities of inducible nitric oxide synthase (iNOS) and total nitric oxide synthase (TNOS) in C2C12 cells (U/mg protein). NO abundance in C2C12 cells (a) and culture medium (b) was detected after 3 h, 18 h, and 36 h treatments with L-arginine or L-NAME. The activity of NOS-iNOS (c) and TNOS (d) was analyzed following L-arginine or L-NAME supplementation for 3 h, 18 h, and 36 h in C2C12 cells. Data are expressed as the means ± SEM ($n = 7$). **$P < 0.01$ compared with untreated cells. NS, $P > 0.05$.

protein synthesis, increased p70S6K phosphorylation (Thr 389), and upregulated phosphorylated mTOR (Thr 2446) levels. The stimulatory effect of L-Arg on protein synthesis and p70S6K (Thr 389) and mTOR (Thr 2446) phosphorylation was abolished by the presence of L-NAME, an NOS inhibitor. In contrast, SNP, an NO donor, increased protein synthesis and upregulated both p70S6K and mTOR phosphorylation (Thr 389 and Thr 2446, resp.); this effect was not altered by L-NAME. Blocking the phosphorylation of p70S6K with rapamycin, however, abolished the stimulatory effect of both L-Arg and SNP on protein synthesis. These results demonstrate that NO is associated with the regulation of muscle protein synthesis via the mTOR/p70S6K pathway. Moreover, except for one mTOR phosphorylation site (Thr 2446), the phosphorylated levels of

mTOR (Ser 2448 and Ser 2481) were not altered by the L-Arg, L-NAME, or SNP treatment, suggesting that this specific mTOR site (Thr 2446) is the target site involved in the regulation of protein synthesis by NO.

4.1. L-Arg Enhanced Protein Synthesis and the Phosphorylation of p70S6K (Thr 389) and mTOR (Thr 2446).

In animal experiments, L-Arg has been demonstrated to enhance protein synthesis in skeletal muscle [31, 32]. Moreover, L-Arg supplementation is beneficial for the maintenance of muscle mass in burn patients and ameliorates the muscle dysfunction associated with *mdx* mice [8, 9]. The advantageous effect of L-Arg could be partially accounted for by the increased blood circulation in skeletal muscles [33–35].

(a)

(b)

(c)
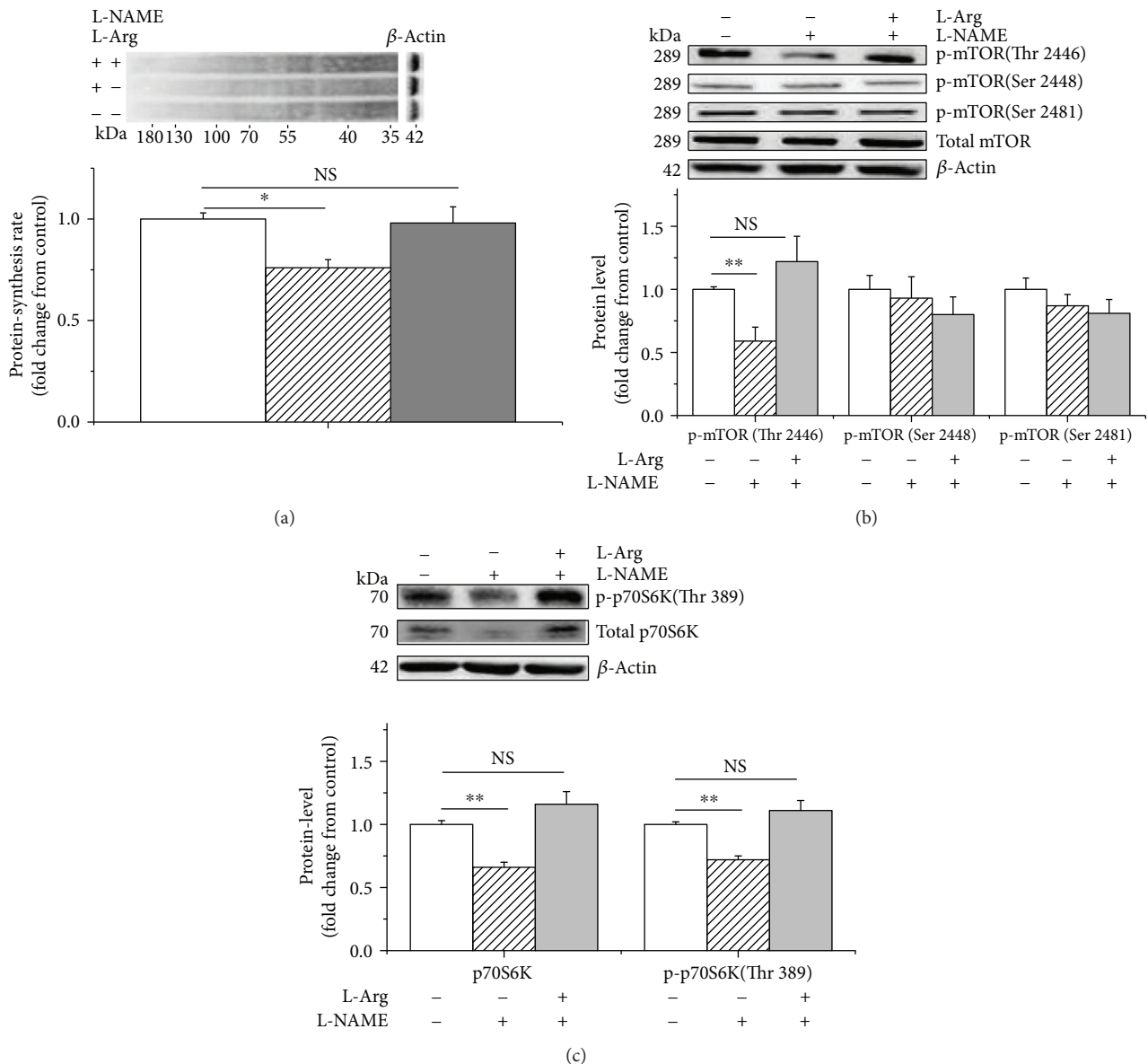
FIGURE 3: L-NAME and L-arginine treatment inhibits and evokes protein synthesis, respectively, in C2C12 cells. The protein synthesis rate was evaluated following treatment by supplementation with puromycin ($10\,\mu$M) for 30 min in the cell-free supernatant (a); the levels of phosphorylated mTOR (b) and p70S6K (c) following L-arginine (1 mM) supplementation in the presence of L-NAME (10 mM). When the total protein bands showed significant differences with different treatments, the phosphorylated protein bands were normalized to the total protein bands. In contrast, if the total protein bands were similar across different groups, both the phosphorylated and total protein bands were normalized to β-actin. Data are presented as the means ± SEM ($n = 6$). $^{**}P < 0.01$ and $^{*}P < 0.05$ compared with untreated cells. NS, $P > 0.05$.

In the present study, we further investigated the direct role of L-Arg in muscle cell protein synthesis. We confirmed the enhancement of protein synthesis in C2C12 cells following L-Arg supplementation, which was in line with the results of [35], in which arginine was found to protect myocytes from wasting by stimulating protein synthesis during catabolic conditions in C2C12 cells. These results suggest that L-Arg stimulates protein synthesis in muscle cells regardless of nutritional status; this finding is supported by the observation of Sales et al. [10, 11], who reported that free amino acids, especially arginine, within muscle cells may be

associated with protein synthesis capacity in fetal lambs of well-nourished sheep.

mTOR complex 1 (mTORC1), consisting of Raptor, GβL, PRAS40, and DEPTOR, phosphorylates 4E-BP1 and p70S6K and thus stimulates protein synthesis [36]. *In vivo*, L-Arg treatment was shown to stimulate p70S6K phosphorylation [32]. Under wasting conditions, arginine treatment increased the levels of phosphorylated mTOR, p70S6K, and 4E-BP1 in C2C12 cells [14]. In line with previous studies, the present results indicated that L-Arg supplementation upregulated p70S6K (Thr 389) and mTOR (Thr 2446)

(a)

(b)
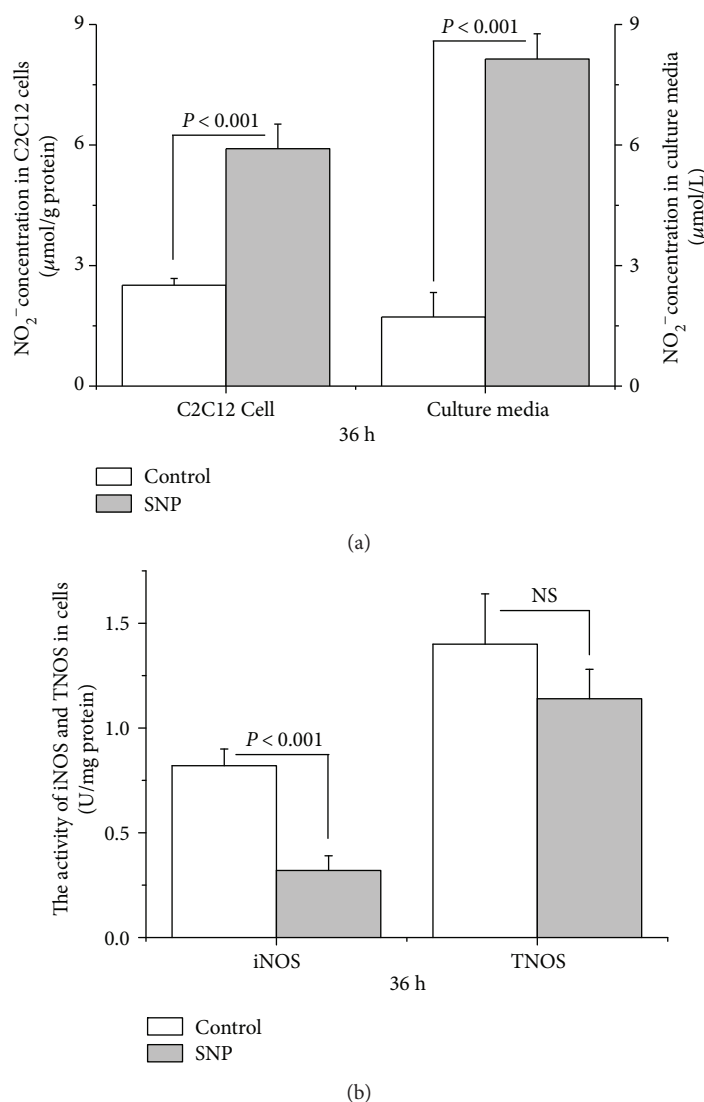
FIGURE 4: SNP supplementation increases NO concentration in C2C12 cells and the culture medium and inhibits the activity of inducible nitric oxide synthase (iNOS) in C2C12 cells (U/mg protein). Data are expressed as the means ± SEM ($n = 7$). NS, $P > 0.05$.

phosphorylation levels, which suggested that the mTOR/p70S6K signaling pathway is an intracellular target of L-Arg. In contrast to the work by Ham et al. [14], who reported that arginine evoked mTOR phosphorylation (Ser 2448) in C2C12 cells under wasting conditions, we observed that L-Arg stimulated the phosphorylation of mTOR at Thr2446, but not at Ser2448 or Ser2481, in C2C12 cells under normal nutritional conditions, suggesting that L-Arg may modulate mTOR activity at different sites according to cellular nutritional state.

4.2. L-Arg-Stimulated Protein Synthesis via NO. In humans, skeletal muscle participates in the overall NO metabolism by serving as a nitrate reservoir [13]. As the precursor of NO, L-Arg has been shown to be involved in protein phosphorylation cascades and gene expression by serving as a cell signaling molecule [5, 37]. Arginine, a conditionally essential amino acid, is known to participate in the production of NO [38]. Under catabolic conditions, L-Arg was also found to

exhibit NO-independent protective effects on muscle wasting [14]. To further investigate the role of NO in the regulation of arginine, we first used L-NAME to suppress NOS activity. The significant decrease in cellular NO concentrations and the suppression of TNOS activity indicated that L-NAME decreased NO production. The decreased protein synthesis and levels of phosphorylated p70S6K (Thr 389) and mTOR (Thr 2446) caused by L-NAME treatment suggested that NO may be involved in muscle cell protein synthesis via the mTOR/p70S6K pathway. The increased NO concentrations in the cell-free supernatant and the restoration of iNOS activity upon treatment with both L-NAME and L-Arg indicated that the suppressive effect of L-NAME on NOS activity could be relieved by L-Arg supplementation. Consistent with this result, L-Arg supplementation reversed the effects of L-NAME on protein synthesis and p70S6K phosphorylation, suggesting that either NO or arginine is involved in the modulation of protein synthesis.

(a)

(b)

(c)

(d)
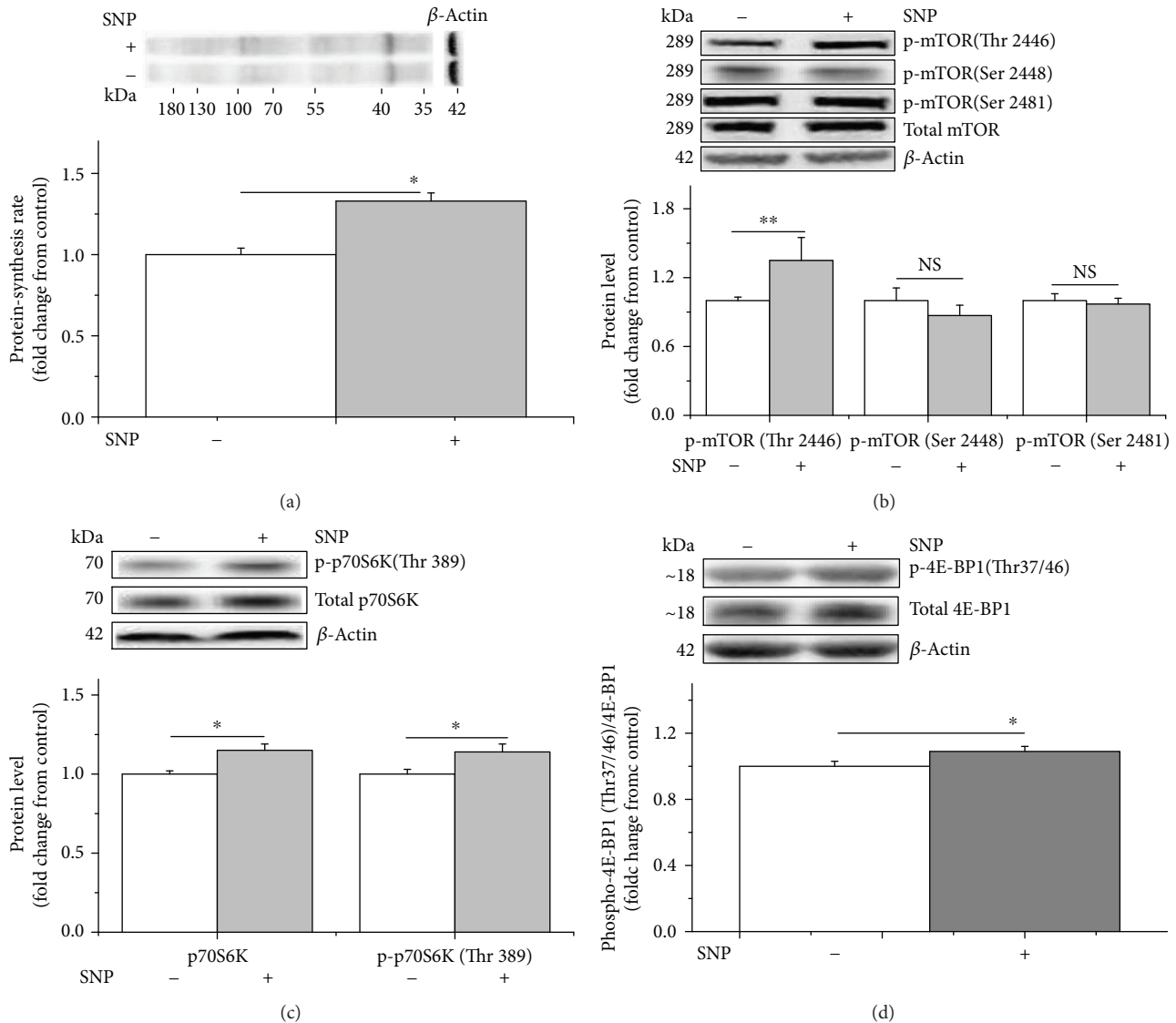
FIGURE 5: SNP treatment increases the protein synthesis rate and the phosphorylated levels of mTOR (Thr 2446), p70S6K (Thr 389), and 4E-BP1 (Thr 37/46) in C2C12 cells. The protein synthesis rate was evaluated following treatment by supplementation with puromycin ($10\,\mu M$) for 30 min in the cell-free supernatant (a). Levels of phosphorylated mTOR (b), p70S6K (c), and 4E-BP1 (d) in C2C12 cells in the presence of $1\,\mu M$ of SNP. When the total protein bands showed significant differences with different treatments, the phosphorylated protein bands were normalized to the total protein bands. In contrast, if the total protein bands were similar across different groups, both the phosphorylated and total protein bands were normalized to β-actin. Data are presented as the means $\pm$ SEM ($n = 6$). $^{**}P < 0.01$ and $^{*}P < 0.05$ compared with untreated cells. NS, $P > 0.05$.

To further verify this hypothesis, we evaluated the effect of SNP, an NO donor, on protein synthesis and p70S6K and mTOR phosphorylation. The elevated NO production in cells and in the media, as well as the decreased iNOS activity, indicated that SNP treatment provides sufficient NO independent of NOS. The increased protein synthesis caused by SNP also suggests that NO, rather than L-Arg, is associated with the regulation of protein synthesis in muscle cells. This hypothesis was confirmed by the observation that the negative effect of L-NAME on protein synthesis could be rescued by SNP supplementation. Therefore, the present results demonstrate that NO, rather than L-Arg, was associated with the regulation of protein synthesis in C2C12 cells, which is consistent with the mechanism in intestinal epithelial cells [39]. This result

was in line with previous work showing that the maintenance of NO could ameliorate dystrophy symptoms [18, 19]. The age-related muscle refractoriness to exercise can be overcome with NO donor treatment [20]. This result, however, contradicted the work of Ham et al., who reported that L-arginine reduces muscle wasting in a dose-dependent manner through NO-independent activation of mTOR [14]. The nutritional status of the cells may account for these different observations. In the present study, we investigated the effect of arginine and NO on protein synthesis and the activation of the mTOR/p70S6K signaling pathway in cells under normal, but not nutrient-deprived, conditions. These results may imply that L-Arg and NO have a positive effect on muscle protein synthesis in a nutritional status-dependent manner.

(a)

(b)

(c)
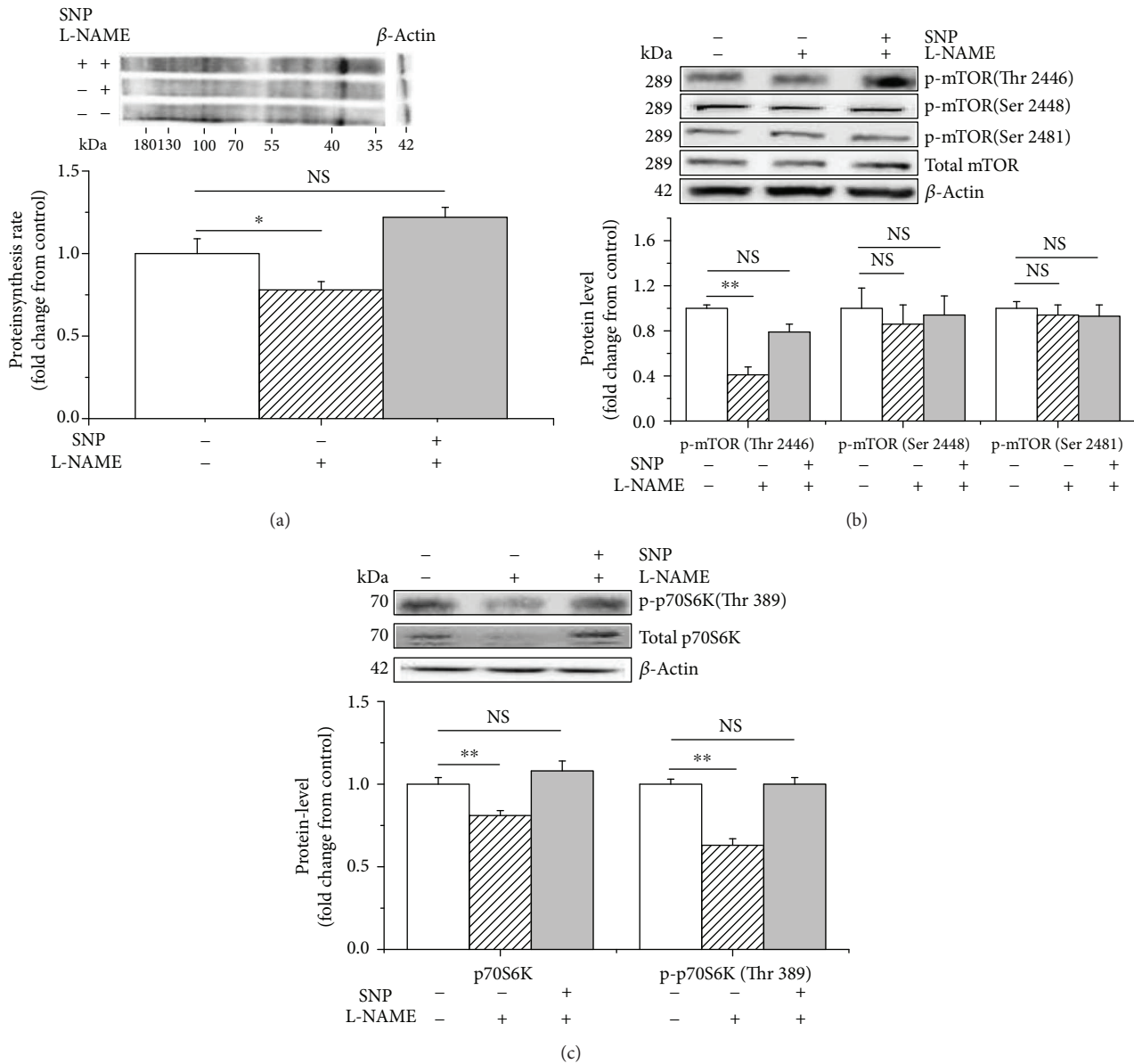
Figure 6: L-NAME and SNP, respectively, inhibit and activate protein synthesis and the phosphorylation of mTOR (Thr 2446) and p70S6K (Thr 389) in C2C12 cells. The protein synthesis rate was evaluated following treatment by supplementation with puromycin (10 μM) for 30 min in the cell-free supernatant (a). The phosphorylation levels of mTOR (b) and p70S6K (c) in C2C12 cells cultured for 36 h in the presence of 1 μM of SNP and 10 mM of L-NAME. When the total protein bands showed significant differences with different treatments, the phosphorylated protein bands were normalized to the total protein bands. In contrast, if the total protein bands were similar across different groups, both the phosphorylated and total protein bands were normalized to β-actin. Data are presented as the means ± SEM ($n = 6$). ${}^{**}P < 0.01$ and ${}^{*}P < 0.05$ compared with untreated cells. NS, $P > 0.05$.

The SNP-induced upregulation of p70S6K and 4E-BP1 phosphorylation suggests that p70S6K and 4E-BP1 are the target proteins of NO, which is consistent with previous studies [40, 41]. However, SNP supplementation only partially restored the downregulation of p70S6K (Thr 389) and mTOR (Thr 2446) phosphorylation by L-NAME. To further clarify the effect of NO on mTOR and p70S6K, the C2C12 cells were treated with rapamycin. The suppression of protein synthesis and inhibition of p70S6K and mTOR phosphorylation by rapamycin indicated that the mTOR/p70S6K pathway is an important pathway in muscle cell

protein synthesis, which is in line with previous studies [42, 43]. The suppressive effect of rapamycin was not reversed by either L-Arg or SNP, which suggests that the regulatory effect of L-Arg or NO on muscle cell protein synthesis is dependent on the phosphorylation of mTOR specifically at Thr 2446 (rather than at Ser 2448 or Ser 2481) to initiate the phosphorylation of p70S6K (Thr 389) and 4E-BP1 (Thr 37/46). Further, the L-Arg- or SNP-induced activation of mTOR (Thr 2446), p70S6K (Thr 389), and 4E-BP1 (Thr 37/46) is consistent with recent research in cocaine treatment [44]. Even though the C-terminus of mTOR contains the

(a)

(b)

(c)

(d)

(e)

(f)
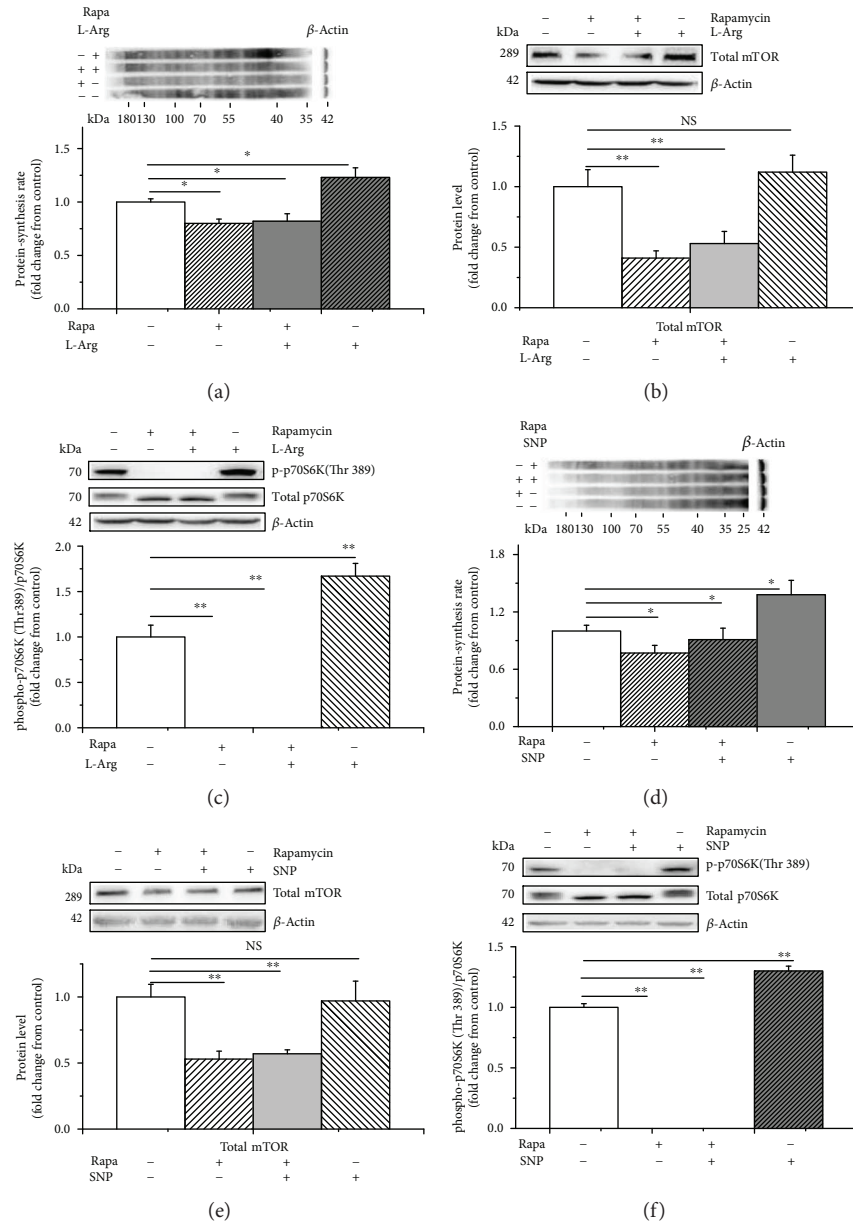
FIGURE 7: Rapamycin inhibits protein synthesis as well as mTOR and p70S6K in C2C12 cells. The protein synthesis rate was evaluated following treatment by supplementation with puromycin (10 μM) for 30 min in the cell-free supernatant (a, d); the level of total mTOR (b, e) and p70S6K (c, f) following treatment with 1 mM of L-arginine or 1 μM of SNP in the presence of rapamycin (100 nM). When the total protein bands showed significant differences with different treatments, the phosphorylated protein bands were normalized to the total protein bands. In contrast, if the total protein bands were similar across different groups, both the phosphorylated and total protein bands were normalized to β-actin. Data are presented as the means $\pm$ SEM ($n = 6$). $^{**}P < 0.01$ and $^{*}P < 0.05$ compared with untreated cells. NS, $P > 0.05$.

phosphorylation sites Thr 2446, Ser 2448, and Ser 2481, which lie within or near a repressor domain and consequently correlate with an increase in activity [45], these sites are regulated by several different kinases including downstream effectors of the mTOR pathway itself or by autophosphorylation. For example, Thr 2446 is a target of AMP-activated protein kinase (AMPK) and S6K [46, 47], which is a novel mammalian target of the rapamycin (mTOR) phosphorylation site regulated by nutrient status [46] and is involved in various metabolic processes. Ser 2481 is an autophosphorylation site that directly monitors the catalytic

activity of both mTORC1 and mTORC2 [48, 49]. The Ser 2448 site is also a key mTOR phosphorylation site and is regulated by Akt and S6K [50, 51]. We made the interesting observation that the phosphorylation status of the Ser 2481 and Ser 2448 sites did not change following L-arginine treatment or SNP supplementation. The specific L-arginine- and SNP-induced mTOR phosphorylation pattern is indicative of upstream signaling, as each phosphorylation site is regulated by different mechanisms.

NO participates in cellular signal transduction mainly through S-nitrosylation of allosteric and active-site cysteine
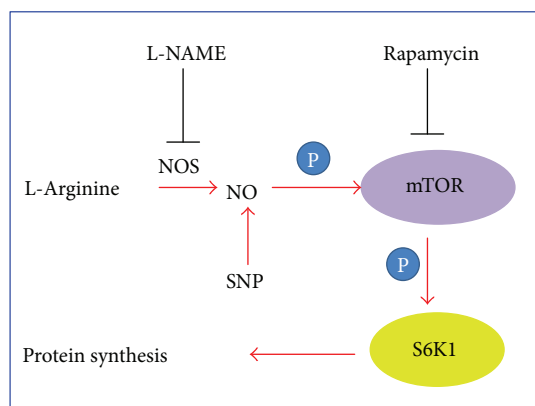
FIGURE 8: The working model of L-arginine/NO in muscle protein synthesis. L-NAME: *N*-nitro-L-arginine methyl ester; NO: nitric oxide; NOS: nitric oxide synthase; SNP: sodium nitroprusside.

thiols within proteins [37, 52, 53]. In aged rats (33 months), the increased phosphorylation of Akt (Ser 473 and Thr 308) in soleus muscles is associated with diminished mTOR phosphorylation, whereas the age-related impairment in Akt kinase activity is associated with increases in Akt S-nitrosylation [54]. Hence, the actions of NO in skeletal muscle under different physiological conditions need to be further investigated.

4.3. The Role of NOS on Muscle Protein Synthesis. NOS has three isoforms: iNOS, nNOS (neuronal NOS, type I), and eNOS (endothelial NOS, type II). In skeletal muscle, nNOS is the major NOS isoform. There is growing evidence that NOS is associated with the development of muscle atrophy. The nNOS/NO system modulates muscle functions such as insulin sensitivity and glucose uptake, muscle contraction, vasodilation, and activation of satellite cells [37, 55, 56]. The translocation of nNOS from the sarcolemma to the cytoplasm, however, is involved in muscle atrophy in an uploading model mimicked by tail suspension [57, 58] and in prolonged alcoholic myopathy [59]. NO signaling is dysregulated during muscular dystrophy due to the disruption of the dystrophin glycoprotein complex (DGC), which anchors nNOS [60]. The inhibition of tendon NOS contributes to the attenuation of atrophy and acceleration of muscle regeneration [61]. On the other hand, iNOS is expressed exclusively in the presence of proinflammatory cytokines. iNOS has been proven to be an important mediator in TNFα-induced cachectic muscle loss and in age-related muscle wasting (sarcopenia) [21]. Under pathological conditions, the activation of iNOS promotes muscle atrophy [62]. NO may exert both protective and pathological effects during muscle wasting, depending on quantitative effects as well as on the spatial arrangement of NOS [22]. L-Citrulline preserves protein synthesis rates and protects myotubes from wasting through induction of the iNOS isoform [15]. In the present study, protein synthesis was suppressed by L-NAME treatment and stimulated by L-Arg. L-NAME suppressed TNOS activity at 18 h ($P < 0.01$) and 36 h ($P = 0.093$) but had little influence on iNOS, suggesting that TNOS may be responsible for blocking protein synthesis. In contrast, L-Arg supplementation

increased iNOS and TNOS at different time points. Hence, the role of iNOS and nNOS on protein synthesis and the mTOR/p70S6K pathway requires further study.

5. Conclusion

In conclusion, our results demonstrate that L-Arg is associated with the regulation of muscle development via the mTOR (Thr 2446)/p70S6K signaling pathway in an NO-dependent manner (Figure 8). These results highlight the potential clinical application of L-Arg or NO for the modulation of muscle metabolism.

Conflicts of Interest

The authors have declared no conflicts of interest.

Authors' Contributions

Ruxia Wang and Hai Lin conceived and designed the experiments; Ruxia Wang performed the experiments; Ruxia Wang and Hai Lin wrote and modified the paper; Hongchao Jiao, Zhao Jingpeng, and Xiaojuan Wang contributed reagents/materials/analysis tools. All the authors read and approved the final manuscript.

Acknowledgments

References

[1] T. Michel and O. Feron, "Nitric oxide synthases: which, where, how, and why?," *The Journal of Clinical Investigation*, vol. 100, no. 9, pp. 2146–2152, 1997.

[2] C. Nathan, "Nitric oxide as a secretory product of mammalian cells," *The FASEB Journal*, vol. 6, no. 12, pp. 3051–3064, 1992.

[3] S. Moncada, R. M. Palmer, and E. A. Higgs, "Nitric oxide: physiology, pathophysiology, and pharmacology," *Pharmacological Reviews*, vol. 43, no. 2, pp. 109–142, 1991.

[4] J. Hemish, N. Nakaya, V. Mittal, and G. Enikolopov, "Nitric oxide activates diverse signaling pathways to regulate gene expression," *Journal of Biological Chemistry*, vol. 278, no. 43, pp. 42321–42329, 2003.

[5] S. M. Morris Jr., "Arginine metabolism: boundaries of our knowledge," *The Journal of Nutrition*, vol. 137, no. 6, pp. 1602S–1609S, 2007.

[6] E. H. Herningtyas, Y. Okimura, A. E. Handayaningsih et al., "Branched-chain amino acids and arginine suppress MaFbx/atrogin-1 mRNA expression via mTOR pathway in C2C12 cell line," *Biochimica et Biophysica Acta (BBA) - General Subjects*, vol. 1780, no. 10, pp. 1115–1120, 2008.

[7] G. Wu, "Amino acids: metabolism, functions, and nutrition," *Amino Acids*, vol. 37, no. 1, pp. 1–17, 2009.

[8] H. Saito, O. Trocki, S. L. Wang, S. J. Gonce, S. N. Joffe, and J. W. Alexander, "Metabolic and immune effects of dietary arginine supplementation after burn," *Archives of Surgery*, vol. 122, no. 7, pp. 784–789, 1987.

[9] E. R. Barton, L. Morris, M. Kawana, L. T. Bish, and T. Toursel, "Systemic administration of L-arginine benefits *mdx* skeletal muscle function," *Muscle & Nerve*, vol. 32, no. 6, pp. 751–760, 2005.

[10] F. Sales, D. Pacheco, H. Blair, P. Kenyon, and S. McCoard, "Muscle free amino acid profiles are related to differences in skeletal muscle growth between single and twin ovine fetuses near term," *SpringerPlus*, vol. 2, no. 1, p. 483, 2013.

[11] F. A. Sales, D. Pacheco, H. T. Blair et al., "Identification of amino acids associated with skeletal muscle growth in late gestation and at weaning in lambs of well-nourished sheep," *Journal of Animal Science*, vol. 92, no. 11, pp. 5041–5052, 2014.

[12] D. J. Ham, T. L. Kennedy, M. K. Caldow, A. Chee, G. S. Lynch, and R. Koopman, "Citrulline does not prevent skeletal muscle wasting or weakness in limb-casted mice," *The Journal of Nutrition*, vol. 145, no. 5, pp. 900–906, 2015.

[13] B. Piknova, J. W. Park, K. M. Swanson, S. Dey, C. T. Noguchi, and A. N. Schechter, "Skeletal muscle as an endogenous nitrate reservoir," *Nitric Oxide*, vol. 47, pp. 10–16, 2015.

[14] D. J. Ham, M. K. Caldow, G. S. Lynch, and R. Koopman, "Arginine protects muscle cells from wasting in vitro in an mTORC1-dependent and NO-independent manner," *Amino Acids*, vol. 46, no. 12, pp. 2643–2652, 2014.

[15] D. J. Ham, B. G. Gleeson, A. Chee et al., "L-Citrulline protects skeletal muscle cells from cachectic stimuli through an *iNOS*-dependent mechanism," *PLoS One*, vol. 10, no. 10, article e0141572, 2015.

[16] L. I. Filippin, M. J. Cuevas, E. Lima, N. P. Marroni, J. Gonzalez-Gallego, and R. M. Xavier, "Nitric oxide regulates the repair of injured skeletal muscle," *Nitric Oxide*, vol. 24, no. 1, pp. 43–49, 2011.

[17] L. I. Filippin, A. J. Moreira, N. P. Marroni, and R. M. Xavier, "Nitric oxide and repair of skeletal muscle injury," *Nitric Oxide*, vol. 21, no. 3-4, pp. 157–163, 2009.

[18] M. Wehling, M. J. Spencer, and J. G. Tidball, "A nitric oxide synthase transgene ameliorates muscular dystrophy in mdx mice," *Journal of Cell Biology*, vol. 155, no. 1, pp. 123–132, 2001.

[19] J. D. Archer, C. C. Vargas, and J. E. Anderson, "Persistent and improved functional gain in mdx dystrophic mice after treatment with L-arginine and deflazacort," *The FASEB Journal*, vol. 20, no. 6, pp. 738–740, 2006.

[20] J. R. S. Leiter, R. Upadhaya, and J. E. Anderson, "Nitric oxide and voluntary exercise together promote quadriceps hypertrophy and increase vascular density in female 18-mo-old mice," *American Journal of Physiology-Cell Physiology*, vol. 302, no. 9, pp. C1306–C1315, 2012.

[21] D. T. Hall, J. F. Ma, S. di Marco, and I. E. Gallouzi, "Inducible nitric oxide synthase (iNOS) in muscle wasting syndrome, sarcopenia, and cachexia," *Aging*, vol. 3, no. 8, pp. 702–715, 2011.

[22] L. M. Leitner, R. J. Wilson, Z. Yan, and A. Gödecke, "Reactive oxygen species/nitric oxide mediated inter-organ communication in skeletal muscle wasting diseases," *Antioxidants & Redox Signaling*, vol. 26, no. 13, pp. 700–717, 2017.

[23] D. C. Fingar, C. J. Richardson, A. R. Tee, L. Cheatham, C. Tsou, and J. Blenis, "mTOR controls cell cycle progression through its cell growth effectors S6K1 and 4E-BP1/eukaryotic translation initiation factor 4E," *Molecular and Cellular Biology*, vol. 24, no. 1, pp. 200–216, 2004.

[24] C. J. Richardson, S. S. Schalm, and J. Blenis, "PI3-kinase and TOR: PIKTORing cell growth," *Seminars in Cell & Developmental Biology*, vol. 15, no. 2, pp. 147–159, 2004.

[25] N. Shimizu, N. Yoshikawa, N. Ito et al., "Crosstalk between glucocorticoid receptor and nutritional sensor mTOR in skeletal muscle," *Cell Metabolism*, vol. 13, no. 2, pp. 170–182, 2011.

[26] C. Rommel, S. C. Bodine, B. A. Clarke et al., "Mediation of IGF-1-induced skeletal myotube hypertrophy by PI(3)K/Akt/mTOR and PI(3)K/Akt/GSK3 pathways," *Nature Cell Biology*, vol. 3, no. 11, pp. 1009–1013, 2001.

[27] T. A. Hornberger and S. Chien, "Mechanical stimuli and nutrients regulate rapamycin-sensitive signaling through distinct mechanisms in skeletal muscle," *Journal Cell Biochemistry*, vol. 97, no. 6, pp. 1207–1216, 2006.

[28] E. K. Schmidt, G. Clavarino, M. Ceppi, and P. Pierre, "SUnSET, a nonradioactive method to monitor protein synthesis," *Nature Methods*, vol. 6, no. 4, pp. 275–277, 2009.

[29] C. A. Goodman, D. M. Mabrey, J. W. Frey et al., "Novel insights into the regulation of skeletal muscle protein synthesis as revealed by a new nonradioactive in vivo technique," *The FASEB Journal*, vol. 25, no. 3, pp. 1028–1039, 2011.

[30] J. H. D. Long, V. A. Lira, Q. A. Soltow, J. L. Betters, J. E. Sellman, and D. S. Criswell, "Arginine supplementation induces myoblast fusion via augmentation of nitric oxide production," *Journal of Muscle Research & Cell Motility*, vol. 27, no. 8, pp. 577–584, 2006.

[31] J. W. Frank, J. Escobar, H. V. Nguyen et al., "Oral *N*-carbamyl-glutamate supplementation increases protein synthesis in skeletal muscle of piglets," *The Journal of Nutrition*, vol. 137, no. 2, pp. 315–319, 2007.

[32] K. Yao, Y. L. Yin, W. Chu et al., "Dietary arginine supplementation increases mTOR signaling activity in skeletal muscle of neonatal pigs," *The Journal of Nutrition*, vol. 138, no. 5, pp. 867–872, 2008.

[33] N. Gokce, "L-arginine and hypertension," *The Journal of Nutrition*, vol. 134, no. 10, pp. 2807S–2811S, 2004.

[34] Y. Nakai, P. Voisine, C. Bianchi et al., "Effects of L-arginine on the endogenous angiogenic response in a model of hypercholesterolemia," *Surgery*, vol. 138, no. 2, pp. 291–298, 2005.

[35] P. Voisine, J. Li, C. Bianchi et al., "Effects of L-arginine on fibroblast growth factor 2–induced angiogenesis in a model of endothelial dysfunction," *Circulation*, vol. 112, no. 9, Supplement, pp. I202–I207, 2005.

[36] J. D. Weber and D. H. Gutmann, "Deconvoluting mTOR biology," *Cell Cycle*, vol. 11, no. 2, pp. 236–248, 2014.

[37] J. S. Stamler and G. Meissner, "Physiology of nitric oxide in skeletal muscle," *Physiological Reviews*, vol. 81, no. 1, pp. 209–237, 2001.

[38] G. Wu and S. M. Morris Jr., "Arginine metabolism: nitric oxide and beyond," *Biochemical Journal*, vol. 336, no. 1, pp. 1–17, 1998.

[39] J. M. Rhoads, Y. Liu, X. Niu, S. Surendran, and G. Wu, "Arginine stimulates cdx2-transformed intestinal epithelial cell migration via a mechanism requiring both nitric oxide and phosphorylation of p70 S6 kinase," *The Journal of Nutrition*, vol. 138, no. 9, pp. 1652–1657, 2008.

[40] L. A. Berven, I. J. Frew, and M. F. Crouch, "Nitric oxide donors selectively potentiate thrombin-stimulated p70^{S6K} activity and morphological changes in Swiss 3T3 cells," *Biochemical and Biophysical Research Communications*, vol. 266, no. 2, pp. 352–360, 1999.

[41] T. Minamino, M. Kitakaze, P. J. Papst et al., "Inhibition of nitric oxide synthesis induces coronary vascular remodeling and cardiac hypertrophy associated with the activation of

p70 S6 kinase in rats," *Cardiovascular Drugs and Therapy*, vol. 14, no. 5, pp. 533–542, 2000.

[42] K. Baar and K. Esser, "Phosphorylation of p70^{S6K} correlates with increased skeletal muscle mass following resistance exercise," *American Journal of Physiology-Cell Physiology*, vol. 276, no. 1, pp. C120–C127, 1999.

[43] S. Fujita, H. C. Dreyer, M. J. Drummond et al., "Nutrient signalling in the regulation of human muscle protein synthesis," *The Journal of Physiology*, vol. 582, no. 2, pp. 813–823, 2007.

[44] L. P. Sutton and M. G. Caron, "Essential role of D1R in the regulation of mTOR complex1 signaling induced by cocaine," *Neuropharmacology*, vol. 99, pp. 610–619, 2015.

[45] C. A. Hoeffer and E. Klann, "mTOR signaling: at the crossroads of plasticity, memory and disease," *Trends in Neurosciences*, vol. 33, no. 2, pp. 67–75, 2010.

[46] S. W. Y. Cheng, L. G. D. Fryer, D. Carling, and P. R. Shepherd, "Thr^{2446} is a novel mammalian target of rapamycin (mTOR) phosphorylation site regulated by nutrient status," *Journal of Biological Chemistry*, vol. 279, no. 16, pp. 15719–15722, 2004.

[47] M. K. Holz and J. Blenis, "Identification of S6 kinase 1 as a novel mammalian target of rapamycin (mTOR)-phosphorylating kinase," *Journal of Biological Chemistry*, vol. 280, no. 28, pp. 26089–26093, 2005.

[48] G. A. Soliman, H. A. Acosta-Jaquez, E. A. Dunlop et al., "mTOR Ser-2481 autophosphorylation monitors mTORC-specific catalytic activity and clarifies rapamycin mechanism of action," *Journal of Biological Chemistry*, vol. 285, no. 11, pp. 7866–7879, 2010.

[49] B. D. Manning, "Comment on "A dynamic network model of mTOR signaling reveals TSC-independent mTORC2 regulation": building a model of the mTOR signaling network with a potentially faulty tool," *Science Signaling*, vol. 5, no. 232, article lc3, 2012.

[50] T. H. Reynolds IV, S. C. Bodine, and J. C. Lawrence Jr., "Control of Ser^{2448} phosphorylation in the mammalian target of rapamycin by insulin and skeletal muscle load," *Journal of Biological Chemistry*, vol. 277, no. 20, pp. 17657–17662, 2002.

[51] G. G. Chiang and R. T. Abraham, "Phosphorylation of mammalian target of rapamycin (mTOR) at Ser-2448 is mediated by p70S6 kinase," *Journal of Biological Chemistry*, vol. 280, no. 27, pp. 25485–25490, 2005.

[52] D. T. Hess, A. Matsumoto, S. O. Kim, H. E. Marshall, and J. S. Stamler, "Protein S-nitrosylation: purview and parameters," *Nature Reviews Molecular Cell Biology*, vol. 6, no. 2, pp. 150–166, 2005.

[53] P. Anand and J. S. Stamler, "Enzymatic mechanisms regulating protein S-nitrosylation: implications in health and disease," *Journal of Molecular Medicine*, vol. 90, no. 3, pp. 233–244, 2012.

[54] M. Wu, A. Katta, M. K. Gadde et al., "Aging-associated dysfunction of Akt/protein kinase B: S-nitrosylation and acetaminophen intervention," *PLoS One*, vol. 4, no. 7, article e6430, 2009.

[55] S. Kapur, S. Bédard, B. Marcotte, C. H. Côté, and A. Marette, "Expression of nitric oxide synthase in skeletal muscle: a novel role for nitric oxide as a modulator of insulin action," *Diabetes*, vol. 46, no. 11, pp. 1691–1700, 1997.

[56] J. E. Anderson, "A role for nitric oxide in muscle repair: nitric oxide–mediated activation of muscle satellite cells," *Molecular Biology of the Cell*, vol. 11, no. 5, pp. 1859–1874, 2000.

[57] N. Suzuki, N. Motohashi, A. Uezumi et al., "NO production results in suspension-induced muscle atrophy through dislocation of neuronal NOS," *The Journal of Clinical Investigation*, vol. 117, no. 9, pp. 2468–2476, 2007.

[58] N. Suzuki, H. Mizuno, H. Warita, S.'. Takeda, Y. Itoyama, and M. Aoki, "Neuronal NOS is dislocated during muscle atrophy in amyotrophic lateral sclerosis," *Journal of the Neurological Sciences*, vol. 294, no. 1-2, pp. 95–101, 2010.

[59] J. Wang, H. Chu, H. Zhao et al., "Nitricoxide synthase-induced oxidative stress in prolonged alcoholic myopathies of rats," *Molecular and Cellular Biochemistry*, vol. 304, no. 1-2, pp. 135–142, 2007.

[60] D. J. Glass, "Two tales concerning skeletal muscle," *The Journal of Clinical Investigation*, vol. 117, no. 9, pp. 2388–2391, 2007.

[61] A. D. Seabra, S. A. S. Moraes, E. J. O. Batista et al., "Local inhibition of nitrergic activity in tenotomized rats accelerates muscle regeneration by increasing fiber area and decreasing central core lesions," *Brazilian Journal of Medical and Biological Research*, vol. 50, no. 3, article e5556, 2017.

[62] M. Assi and A. Rébillard, "The Janus-faced role of antioxidants in cancer cachexia: new insights on the established concepts," *Oxidative Medicine and Cellular Longevity*, vol. 2016, Article ID 9579868, 19 pages, 2016.

Review Article

Genetic Code Expansion: A Powerful Tool for Understanding the Physiological Consequences of Oxidative Stress Protein Modifications

Joseph J. Porter [iD] **and Ryan A. Mehl** [iD]

Department of Biochemistry and Biophysics, Oregon State University, 2011 Agriculture and Life Sciences Building, Corvallis, OR 97331, USA

Correspondence should be addressed to Ryan A. Mehl; ryan.mehl@oregonstate.edu

Posttranslational modifications resulting from oxidation of proteins (Ox-PTMs) are present intracellularly under conditions of oxidative stress as well as basal conditions. In the past, these modifications were thought to be generic protein damage, but it has become increasingly clear that Ox-PTMs can have specific physiological effects. It is an arduous task to distinguish between the two cases, as multiple Ox-PTMs occur simultaneously on the same protein, convoluting analysis. Genetic code expansion (GCE) has emerged as a powerful tool to overcome this challenge as it allows for the site-specific incorporation of an Ox-PTM into translated protein. The resulting homogeneously modified protein products can then be rigorously characterized for the effects of individual Ox-PTMs. We outline the strengths and weaknesses of GCE as they relate to the field of oxidative stress and Ox-PTMs. An overview of the Ox-PTMs that have been genetically encoded and applications of GCE to the study of Ox-PTMs, including antibody validation and therapeutic development, is described.

1. Introduction

It is accepted that posttranslational modifications resulting from oxidation (Ox-PTMs) damage proteins and harm cells. Whether Ox-PTMs can modulate the function of proteins in a specific manner like other PTMs has been a long-standing question [1]. Recent studies have demonstrated that site-specific protein Ox-PTMs can lead to notable gain-of-function alterations that are connected to disease phenotypes. Enzymatic pathways that remove Ox-PTMs have also been identified, providing evidence for dynamic homeostasis with implications for the cellular function of these modifications. Major challenges exist in evaluating effects of Ox-PTMs because of the diversity of mechanisms by which they are formed. The Ox-PTMs result from reactive oxygen species (ROS) (superoxide ($O_2^{\bullet-}$), hydrogen peroxide (H_2O_2), and hydroxyl radical ($OH^{\bullet}$)), reactive nitrogen and oxygen species (RNS) (nitric oxide ($^{\bullet}NO$), nitrogen dioxide ($^{\bullet}NO_2$), and peroxynitrite ($ONOO^-$/$ONOOH$)), and other downstream products interacting with a variety of amino acid residues [2–8].

Elucidating the function of PTMs is notoriously challenging to evaluate because generating the modified proteins *in vivo* or *in vitro* results in a heterogeneous mixture of modified and unmodified proteins. The situation for oxidative stress PTMs is notably more dire because the installation method, diverse and nonspecific chemical reactions from ROS and RNS, produces a heterogeneous mixture of Ox-PTMs on proteins containing multiple different modifications (Figure 1). Each different Ox-PTM needs to be assessed for site-specificity and abundance to identify its effects on protein function. Genetic code expansion (GCE) is particularly well suited to meet these challenges since its core GCE cotranslationally installs the Ox-PTM as a noncanonical amino acid (ncAA). This allows for facile production of homogenously modified protein at genetically programed sites, enabling new approaches for studying Ox-PTMs. GCE can validate Ox-PTM residues identified in oxidative
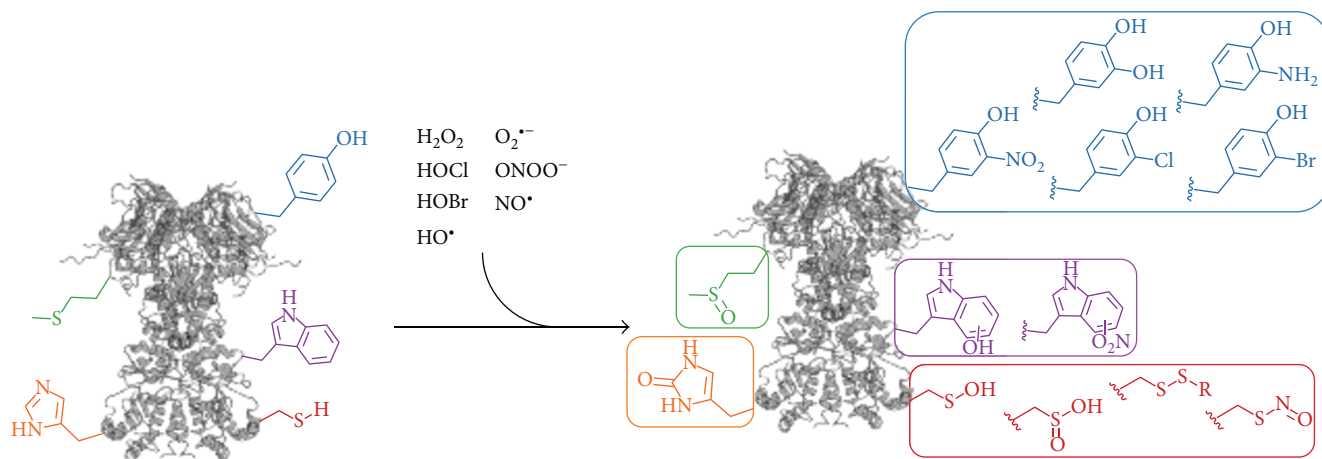
FIGURE 1: A variety of biological oxidants are capable of modifying susceptible amino acid sidechains to their Ox-PTM counterparts. The major groups of amino acids modified are the sulfur containing amino acids (cysteine and methionine) and the aromatic amino acids (tyrosine, tryptophan, and histidine).

stress conditions and explore the functional consequences of a single site of modification. GCE can also be used to develop assays for a particular site of modification on a particular protein and to generate controls for evaluating the selectivity and effectiveness of antibodies for Ox-PTMs. Since GCE functions by generating ncAA-protein in living prokaryotes and eukaryotes, it also allows for the *in vivo* study of homogeneous site-specifically modified protein.

A survey of the literature produces at a minimum 65 reported Ox-PTMs (Figure 2 and Supplementary Table 1). A number of excellent reviews on the ROS and RNS exist and as such we will not discuss them here [9, 10]. Identification of sites and identities of Ox-PTMs has also blossomed as a field of study, and these have been reviewed elsewhere [11, 12]. It is critical to note from studies on the identification of Ox-PTMs that these modifications are often not stable to purification from their native environments and require specialized stabilization or trapping methods [13]. This is important for GCE as these particularly sensitive Ox-PTMs will likewise require chemical caging strategies or stable mimetics for successful genetic incorporation. In this review, we summarize the relevant literature at the intersection of GCE and Ox-PTMs, focusing on the most abundant Ox-PTMs and those amenable to GCE technology (Figure 1). Ox-PTMs of low stability or amino acid cross-links which are not applicable to GCE will not be discussed (3, 7, 9-10, 16, 18–20, 22, 24–26, 31–35, 37–39, 41–44, 46–65 in Figure 2). This review will also highlight the strengths and shortcomings of GCE as applied to the study of Ox-PTMs, outline some of the important considerations when employing GCE, and describe exciting future applications of GCE technology for the oxidative stress field.

2. Genetic Code Expansion Orthogonal Systems

The ability to site-specifically incorporate noncanonical amino acids (ncAAs) into proteins in living cells has emerged

as a powerful method to probe protein structure and function [14, 15]. This capability has been extended to the incorporation of many different PTMs including Ox-PTMs. While cell-free protein synthesis is also developing as a powerful approach for generating modified proteins [16], GCE is a technology that must work inside a living cell. A first consideration for GCE is that the Ox-PTM must be chemically synthesized as an amino acid, which can be challenging for some modifications. The modified amino acid must also be stable to cell culture conditions and be internalized in a cell to concentrations adequate for translation. The stability of an Ox-PTM to cell culture conditions should be evaluated because many Ox-PTMs are redox sensitive and can be toxic to cells at medium concentrations needed for GCE (0.1–1.0 mM). Provided that the Ox-PTM amino acid can pass these initial steps, then selection of GCE components specific for the new amino acid is possible.

Central to GCE technology is an engineered aminoacyl-tRNA synthetase-tRNA pair (aaRS-tRNA) that encodes an ncAA in response to a nonsense (often the amber stop codon) or a frameshift codon (Figure 3). To maintain translational fidelity the aaRS-tRNA pair must also not cross-react with any endogenous aaRS-tRNA pairs in the host organism, that is, this aaRS-tRNA pair must be orthogonal. In general, evolution of an orthogonal aaRS-tRNA pair in a cell requires importing this pair from another domain of life, as the aaRS-tRNA identity elements for recognition are divergent enough to maintain orthogonality. All of the aaRS-tRNA pairs employed so far for GCE were derived from an aaRS-tRNA pair for a canonical amino acid and were altered to instead recognize and charge an ncAA onto the orthogonal tRNA. Generally, this strategy has been more successful when the ncAA of interest resembles the original canonical amino acid (e.g., a modified TyrRS may only accept aromatic amino acids). As this trend exists, it is important to know what orthogonal systems have been used in the past when considering a heretofore unincorporated ncAA. Five main orthogonal pairs have been used, an archaeal TyrRS-tRNA$_{CUA}$ pair
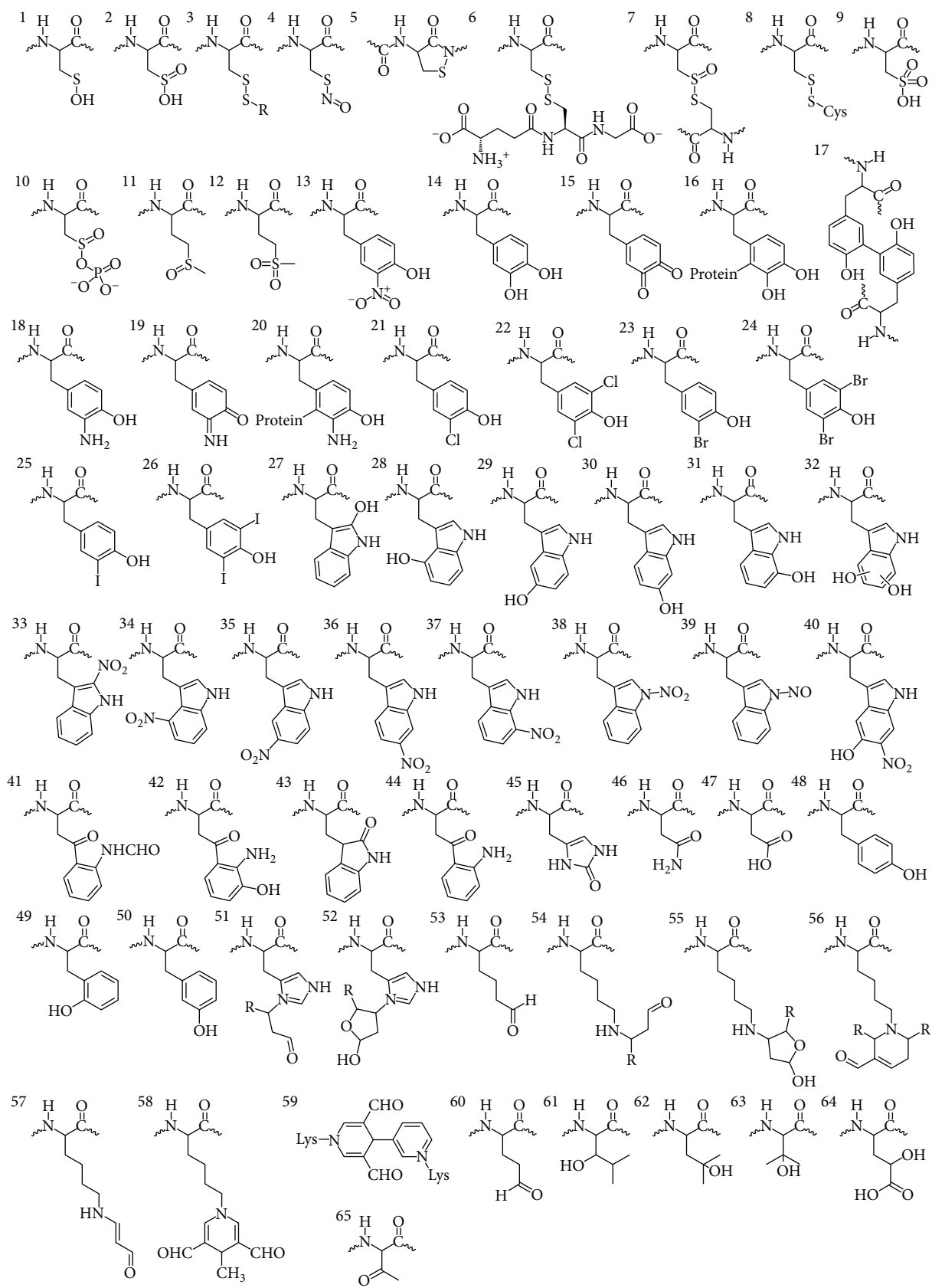
FIGURE 2: Ox-PTMs identified on proteins isolated from conditions of oxidative stress or following *in vitro* reaction with ROS or RNS. For the list of Ox-PTM names and references see the Supplementary Information Table 1.
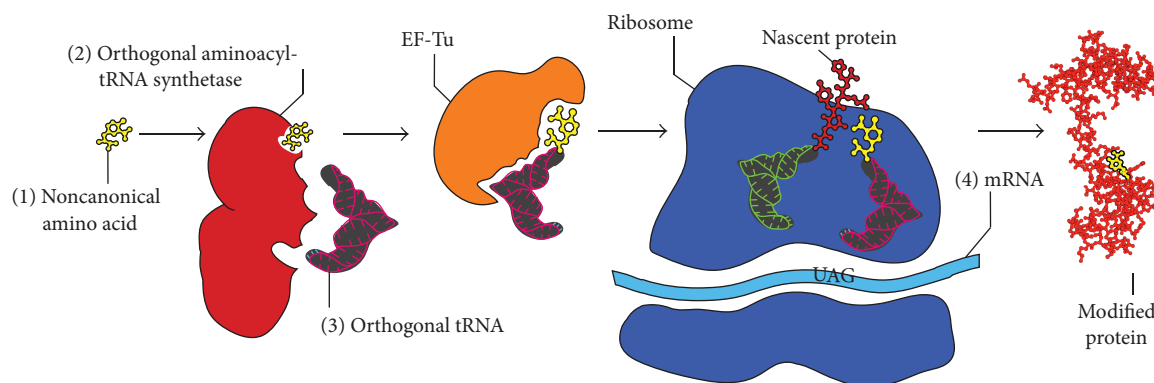
FIGURE 3: Components necessary for genetic code expansion including the noncanonical amino acid of interest (1), an orthogonal aminoacyl tRNA synthetase-tRNA pairs (2) and (3), and an mRNA with an amber stop codon at the site of interest (4).

from *Methanocaldococcus jannaschii (Mj)* has been used extensively in *E. coli* and other bacteria [17]; an *E. coli* LeuRS-tRNA$_{CUA}$ and an *E. coli* TyrRS-tRNA$_{CUA}$ pair have been used in eukaryotes [18, 19]; a pyrrolysyl-aaRS-tRNA pair (PylRS-tRNA$_{CUA}$) derived from several methanogenic archaea (notably *Methanosarcina barkeri* and *Methanosarcina mazei*) is orthogonal in both *E. coli* and eukaryotes [20, 21]; and a liberated *E. coli* TrpRS-tRNA$_{CUA}$ pair orthogonal in both *E. coli* and eukaryotes [22].

3. Developing Orthogonal Pairs

Initially, all orthogonal aaRS-tRNA pairs must be evolved to efficiently incorporate an ncAA of interest. A library of mutations at certain positions is constructed, and a double sieve selection scheme is employed to enrich aaRS variants that incorporate the ncAA of interest but not any of the canonical amino acids [17]. Following a successful selection, several parameters may be used to characterize the effectiveness of the developed aaRS-tRNA pair. The efficiency of the orthogonal pair is a measure of the amount of full length protein produced in the presence of ncAA and is often described by the fluorescence of a reporter protein like GFP or the yield of a purified protein of interest. Fidelity is a parameter that measures the orthogonality of the system. The absolute fidelity of an aaRS-tRNA pair is the amount of full length protein product produced in the absence of ncAA [23]. Relative fidelity is the amount of noncognate amino acid incorporated in the protein of interest in the presence of the ncAA of interest. Relative fidelity is a more useful parameter for characterization of an aaRS-tRNA pair as it is more closely resembles the fidelity of the aaRS under conditions in which it will be used. This parameter is measured by whole protein or tryptic digest mass spectrometry of the purified protein of interest to determine the amount of ncAA incorporation as compared to canonical amino acid. Oftentimes, an evolved orthogonal pair can incorporate a related family of ncAAs, for example, *para*-substituted phenylalanines [24]. This characteristic is called permissivity (sometimes referred to as polyspecificity) of an orthogonal pair [25].

4. Other Considerations and Alternatives to Genetic Code Expansion

There are factors beyond the aaRS/tRNA pair that are also critical for GCE. For a given ncAA to be incorporated by an evolved aaRS-tRNA pair, the ncAA has to meet a set of translational compatibility criteria. The bioavailability of the ncAA has to be taken into account as it must diffuse into, be transported into, or be synthesized within the cell. This is particularly an issue for highly charged amino acids which generally do not diffuse across membranes and a suitable endogenous transporter does not exist. Further, the ncAA of interest needs sufficient stability to persist intracellularly for a timescale on the order of hours to days in order to be incorporated into a protein via translation. Following aminoacylation of the tRNA by the aaRS, the EF-Tu must transport the aminoacyl-tRNA to the ribosome. The EF-Tu has been finely tuned for natural translation and, while it tolerates many ncAAs, those that are highly charged or particularly large are not effectively transported by the EF-Tu. The amino acyl-tRNA then must be decoded on the ribosome. Finally, the installed ncAA also needs to be stable on the protein enabling protein purification and characterization.

A variety of strategies have been employed to overcome these issues with GCE in regard to particular ncAAs. One solution to poor cellular uptake is conversion of the desired ncAA into a dipeptide. Dipeptides have been shown to increase uptake of highly charged or otherwise poorly internalized amino acids via transporters [26, 27]. Alternatively, methylation of the carboxylic acid of certain ncAAs also increases uptake in mammalian cell culture. A third solution is to generate a biosynthetic pathway for the desired ncAA so that it is generated inside the cell of interest [28, 29]. Generally, structural mimics or chemically caged derivatives of ncAAs are used in order to increase stability. For phosphorylated amino acids, both chemical caging [30] and structural mimetics [27, 31] have been used to stabilize the ncAA to allow for ncAA incorporation and characterization of PTM-proteins. Another strategy employed to increase the lifetime of genetically encoded PTM is to knock down the cell's PTM removal pathways. The lifetime of

phosphoserine on proteins is increased by removal of endogenous serine phosphatases, allowing for genuine phosphoserine incorporation [31]. Generally, the EF-Tu transports ncAA aminoacylated-tRNAs efficiently enough to allow for incorporation but some charged ncAAs have required EF-Tu engineering. For initial studies on incorporation of phosphoserine, it was thought that it was necessary to evolve the EF-Tu to allow for the transport of phosphoserylated-tRNA; however, later studies indicated that while this evolved EF-Tu does transport phosphoserylated-tRNA more efficiently, evolution of the EF-Tu was not strictly necessary [31, 32]. The ribosome needs to accommodate the ncAA-tRNA and catalyze peptide chain formation. Chemically acylated tRNA and cell-free synthesis have confirmed that the ribosome is very permissive and ncAAs > 700 Da in size have been incorporated without issue [16]. While an ncAA size limit has been identified for the ribosome exit tunnel using cell-free protein synthesis methods, the vast majority of alpha L-noncanonical amino acids are accepted. Finally, the newly synthesized protein is released from the ribosome and folded, processed, and trafficked to its appropriate location. Since GCE incorporates Ox-PTMs into the primary sequence, altered protein folding pathways and cofactor loading are possible from the modified protein.

Alternative methods to GCE have been developed that may be applicable for particularly metabolically unstable or toxic ncAAs or toxic proteins. Expressed protein ligation (EPL) has emerged as another powerful method to study Ox-PTMs [33]. This method allows the vast chemical space open to solid phase peptide synthesis (SPPS) to be coupled with the robustness of recombinant protein expression. As the ncAA is incorporated via SPPS and then native chemical ligation, novel aaRS/tRNA pairs do not need to be generated. In addition, provided that the sites of modification are within <30 amino acids from one another, it is trivial to incorporate multiple ncAAs. Successful generation of modified histones with EPL also highlights some of the drawbacks of EPL, the site of interest should be within ~50 residues of the N- or C-terminus or a synthesis with three peptides is required, the protein of interest should be able to be refolded from denaturants, and there is some level of sequence requirement both for the intein to generate the α-thioester and for the presence of a cysteine at the site of ligation [34, 35]. The EPL strategy has been used to yield milligram quantities of α-synuclein nitrated selectively at Y39 or Y125 allowing biophysical and biochemical studies of site-specific nitration on α-synuclein structure and function [36]. It is also important to note that the standard desulfurization reaction conditions originally used reduced the incorporated nitrotyrosine to aminotyrosine. This reduction during the desulfurization reaction was prevented with the addition of 2-nitrobenzylamine hydrochloride.

5. Oxidative Modifications of Sulfur Containing Residues

Cysteine Ox-PTMs are abundant modifications with the cysteine sulfur existing in several different oxidation states. Cysteine sulfenic acid (Cys-SOH, 1) is directly generated by the oxidation of cysteine by two-electron oxidants, particularly H_2O_2. The propensity of Cys residues to undergo oxidation is influenced generally by the thiol nucleophilicity, the surrounding protein microenvironment, and the proximity of the target thiol to the ROS source [37]. Accordingly, the susceptibility to oxidation is usually correlated with the Cys pKa. Further, increasing evidence shows that ROS signaling responses are compartmentalized and that spatial regulation of Cys oxidation is key for signaling [38, 39]. Cys-SOH can be overoxidized to cysteine sulfinic acid (Cys-SO$_2$H, 2). As the H_2O_2-mediated pathway of Cys-SOH oxidation proceeds through the sulfenate anion (Cys-SO$^-$), the pKa of Cys-SOH should influence this reaction [39]. With a pKa of ~2, Cys-SO$_2$H exists exclusively in a deprotonated state at physiological pH. The sulfinate group is usually not reducible by typical cellular reductants and as such its further oxidation to sulfonic acid appears to be the only relevant reaction in cells [40]. All of which points to the importance of temporal and spatial control of these protein modifications and the need for tools that enable further investigation.

Cys-SOH has been identified in a relatively small number of proteins, and the identification of this modification remains difficult. The first general analysis of known Cys-SOH modification sites included 47 proteins characterized by crystallography to contain the modification [41]. On the other hand, Cys-SO$_2$H was long considered merely an artifact of protein purification. Increasing evidence however indicates that hyperoxidation to Cys-SO$_2$H in cells is not a rare event. In fact, quantitative analysis of rat liver proteins has shown that ~5% of Cys residues exist as Cys-SO$_2$H [42]. The discovery of sulfiredoxin (Srx), an enzyme that in an ATP-dependent protein reduces Cys-SO$_2$H to Cys-SOH on some peroxiredoxins, has indicated that Cys-SO$_2$H plays a biological role in the redox regulation of peroxiredoxin function [43].

The same electrostatic interactions on the protein that affect the pKa of the Cys thiol also influence the stability of the Cys-SOH. The major factor that increases Cys-SOH stability (or lifetime on a protein) is the absence of proximal thiols capable of generating an intramolecular disulfide (8). It has been also reported that limited solvent access and nearby H-bond acceptors also contribute to Cys-SOH stabilization. In addition to the reaction of Cys-SOH with neighboring cysteine thiols, backbone amide nitrogens can readily react with Cys-SOH to yield a cyclic sulfonamide species (5) [44, 45]. If Cys-SOH modifications are not removed by neighboring Cys residues or amide nitrogens, they can be enzymatically removed. Thioredoxin can directly reduce Cys-SOH to Cys-SH, and Cys-SOH reacts with glutathione to form a mixed disulfide (6), which is later reduced by glutaredoxin. Based on the rate of formation and repair by these mechanisms, the cellular lifetime of sulfenic acid is on the order of minutes, consistent with the lifetime of many PTMs, including phosphorylation [37]. In A431 cells, a peak of protein sulfenylation was observed five minutes after endothelial growth factor stimulation, with a subsequent decay over 30 minutes [39]. Due to the low stability and high turnover rates, monitoring their formation is problematic by direct mass analysis of Cys-SOH. Currently, the use of chemical

probes is the only suitable technique to monitor Cys-SOH formation [46]. The low biological stability of Cys-SOH presents a significant challenge to GCE; however, chemical caging strategies and structural mimetics have been used to overcome this challenge [27, 30, 31]. Since Cys-SO$_2$H is notably more stable, there is a good chance that this oxidation state can be directly incorporated via GCE, although modulation of Srx proteins may be necessary.

The biological impact of protein Cys-SOH formation has been particularly well outlined in protein tyrosine phosphoregulation. Cysteine oxidation controls the activity of both protein tyrosine kinases (PTKs) as well as protein tyrosine phosphatases (PTPs). Sulfenylation of the PTP catalytic Cys residue (pKa 4–6) has emerged as a dynamic mechanism for the inactivation of this protein family [47]. In comparison to PTPs which are always inactivated by ROS, oxidation of PTKs can result in either enhancement or inhibition of kinase activity [48, 49]. It is well established that ROS play a regulatory role for some ion channels, although little is described in terms of the molecular basis for this regulation [50]. Peroxiredoxins (Prxs) are important mediators of H$_2$O$_2$ signaling as they both maintain low levels of H$_2$O$_2$ and are themselves modified to Cys-SOH and Cys-SO$_2$H to modulate H$_2$O$_2$ levels [51].

Cysteine is also S-nitrosylated following the production of NO (4), with implications regarding the influence of NO in cellular transduction [52]. Proteins with a wide variety of functions are found to be endogenously S-nitrosylated in intact cellular systems [53]. Much like other Ox-PTMs, it has become clear that S-nitrosylation and de-nitrosylation are regulated spatially and temporally in the cell [54]. Using the biotin switch methodology (or variations thereof), multiple proteins with the Cys-SNO modification have been isolated [55]. Among the identified proteins is GAPDH, which transnitrosylates and alters the enzymatic activity of SIRT1 [56]. Effector mechanisms for S-nitrosylation include protein-protein interactions, subcellular localization of proteins, and ubiquitylation-dependent protein degradation, which underlie a variety of cellular processes including apoptosis, metabolism, and membrane trafficking. This modification has been implicated in pathophysiological conditions including multiple sclerosis, Parkinson's disease, and asthma [57, 58]. As this Ox-PTM is unstable, genetic incorporation will likely require generation of a structural analogue similar to the methods employed for incorporation of phosphotyrosine and phosphoserine [30, 31]. Clearly, both cysteine oxidation and S-nitrosylation-based Ox-PTMs are of significant biological interest and this is a field ripe for the development of GCE tools.

Methionine sidechains also contain a sulfur atom susceptible to oxidation. ROS and reactive chlorine species are a major source of methionine oxidation yielding methionine sulfoxide (Met-SO, 11) [59, 60]. Methionine is a strongly hydrophobic residue and is generally buried, which protects it from oxidation, although those few surface exposed Met residues are susceptible to oxidation. Methionine oxidation yields two stereoisomers of the sulfoxide, S and R forms. Met-SO formation results in a much more hydrophilic amino acid than Met, which may affect protein structure. Although

Met-SO is a fairly stable product, the sulfur can be further oxidized by strong oxidants to the sulfone (Met-SO$_2$, 12); however, this occurs to a low extent [9]. Met-SO$_2$ is considered an irreversible reaction product and cannot be converted back to Met by cellular reductants. In much the same way as Cys Ox-PTMS, tools to study Met Ox-PTMs are necessary in order to further explore the implications of these modifications.

Under conditions of H$_2$O$_2$ treatment in which Jurkat T-cells were 90% viable, more than 2000 oxidation-sensitive Met residues were identified in the proteome. The majority (84%) of Met-containing peptides contained a low degree of Met-SO (less than 30% oxidized), while only the remaining 16% of peptides were oxidized to a high degree (up to 100% Met-SO) [61]. This significant level of Met oxidation in biological systems requires robust enzymatic repair mechanisms. Methionine sulfoxide reductases (Msrs) efficiently repair Met-SO to Met and are present in all aerobically respiring organisms [62]. Met-SO reductases A and B (MsrA and MsrB) are the prototypical Msrs for the two Met-SO epimers, and while they are similar in neither sequence nor structure, they do share common mechanisms to reduce Met-SO to Met [63].

Methionine oxidation is associated with the aging process and several pathophysiological conditions such as neurodegenerative diseases and cancer [64, 65]. Previously, Met-SO formation under these conditions was regarded only as protein damage. However, Met oxidation is now being acknowledged as a mode of triggering protein activity. The kinase CaMKII and the transcription factor HypT were both found to be activated following oxidation of particular methionines [66, 67]. The polymerization of actin has also been shown to be regulated by the redox state of Met residues, mediated by the concerted and stereo-selective action of Mical proteins and MsrB1 [68].

Oxidized cysteine or methionine residues have yet to be incorporated by GCE. While this should not be an insurmountable challenge, sulfur containing Ox-PTMs do present stability issues. Cys-SOH is not stable on proteins in living cells, so genetic incorporation will require a chemical caging strategy or the use of a mimetic, analogous to what has been done for stable mimetics of phosphorylated serine, threonine, and tyrosine [27, 29–31]. A photocaged Cys-SOH on the protein Gpx3 has been prepared by alkylation of catalytic Cys32 with dimethoxy-o-nitrobenzyl bromide (DMNB-Br), followed by oxidation with H$_2$O$_2$. While the photocaged cysteine sulfenic acid free amino acid was also synthesized with the goal to genetically encode this amino acid, to date, it has not been incorporated via GCE [69]. In order to successfully incorporate Met-SO, modulation of cellular Msr levels will be imperative in order to purify intact modified protein similar to the hurdles of removing cellular phosphatases when incorporating phosphorylated amino acids [31].

6. Ox-PTMs of Aromatic Residues

While the role of sulfur oxidation has been extensively studied, the biological role of Ox-PTMs on aromatic residues

is less clear. Residues susceptible to oxidative or nitrosative modifications include tyrosine, tryptophan, and histidine.

Protein tyrosine nitration (nitroTyr, 13) occurs under basal physiological conditions and is several-fold enhanced under conditions of increased oxidant and $^\bullet$NO formation. Much like other Ox-PTMs, the distribution of tyrosine-nitrated proteins is largely dependent on the proximity to sites of RNS generation [70]. With the advent of proteomic analyses, it has been observed that protein tyrosine nitration occurs on a subset of proteins, and within those proteins, only a subset of tyrosines is nitrated [13, 71–74]. Based on current evidence, the mechanism of protein tyrosine nitration in biological systems is mediated by free radical reactions, implying an intermediate tyrosyl radical and subsequent reactions with either $^\bullet$NO or $^\bullet$NO$_2$ [75]. Other Ox-PTMs may result from this general reaction mechanism as tyrosyl radical may also react with ROS to form L-3,4-dihydroxyphenylalanine (DOPA, 14) or another nearby tyrosine to form the protein-cross-linked dityrosine (17) [76, 77]. Tyrosine is also susceptible to modification by myeloperoxidase- and eosinophil peroxidase-derived hypochlorous and hypobromous acid to form 3-chlorotyrosine (21) and 3-bromotyrosine (23) [13]. As with all Ox-PTMs, it is difficult to establish direct and quantitative relationships between extent of nitration on specific proteins and biological responses in cells and the influence of protein tyrosine nitration is often obscured by the multiplicity of oxidative modifications. GCE has already begun to untangle some of this complexity [78–81].

Mass spectrometry indicates that protein-bound nitroTyr is present in plasma and tissue at levels on the order of 1 μmol of nitroTyr/mol of tyrosine under normal conditions and increases up to 100-fold under conditions of oxidative stress [82, 83]. Over 60 individual proteins have been determined to contain nitroTyr [10] of which several have been investigated further with GCE. Less is known about the abundance of other tyrosine Ox-PTMs although in general they appear to be less abundant and appear on fewer proteins [13].

In contrast to the previously discussed Ox-PTMs, nitroTyr and the other tyrosine Ox-PTMs are generally stable modifications requiring protein turnover to remove the Ox-PTM-modified proteins from the cellular protein pool [84]. A "denitrase" activity, capable of returning nitroTyr to the native tyrosine, has been reported multiple times although the enzyme responsible has not been isolated [85–88]. Tyrosine nitration is abundant in aging tissue and has been linked to pathological conditions including neurodegeneration, atherosclerosis, and cancer [10, 89]. While tyrosine nitration was traditionally thought of as global oxidative damage that accumulates under conditions of oxidative stress, it has become clear that some proteins with nitroTyr modifications at specific sites are capable of mediating biology [79–81]. Currently, it is unclear the structural consequences of adding a meta nitro group to a tyrosine on the proteins that have this clear gain of function. The most obvious two options for altering protein structure are from the pKa change to tyrosine and new interactions afforded by the nitro group. Nitration of tyrosine lowers the pKa of the amino acid from ~10 to near neutral pH, imparting a negative charge, while the nitro group also adds significant steric bulk and new hydrogen bonding groups. GCE is uniquely positioned to determine the structural consequences of PTMs because structural mimics of a PTM can be installed to probe if one chemical feature of a PTM is more critical than another. Possible biological effects due to these alterations to tyrosine properties include changes in protein activity (gain- or loss-of-function), increased protein immunogenicity, interference in tyrosine kinase-dependent regulation, modulation of protein assembly or polymerization, facilitation of protein degradation (turnover), or formation of proteasome resistant protein aggregates [90]. GCE has provided tools to further the molecular understanding of protein tyrosine nitration, and development of new tools promises further control over the study of biological processes associated with this Ox-PTM.

High levels of protein tyrosine halogenation have been detected in several inflammatory conditions including arthritis, some types of cancer, heart disease, cystic fibrosis, and asthma [91–93]. Protein tyrosine halogenation in vivo is a result of the reaction of myeloperoxidase-derived HOCl or eosinophil peroxidase-derived HOBr, yielding 3-chlorotyrosine (21) and 3-bromotyrosine, respectively (23). HOCl and HOBr are strong oxidants and possess potent antibacterial properties, as such they are generated as components of mammalian host defense [94, 95]. However, overproduction or misplaced induction can lead to accumulation of protein modification seen in the above inflammatory conditions. The 3-chlorotyrosine modification along with 3-nitroTyr has been noted in ApoA1 [91, 96]. The interest in these Ox-PTMs has led to the generation of a PylRS-pylT pair that efficiently incorporates both 3-chlorotyrosine and 3-bromotyrosine.

The same conditions that result in protein tyrosine nitration also result in oxidation and nitration of tryptophan residues. A variety of products result from the in vitro reaction of tryptophan with biologically relevant RNS (27–44), but those hydroxytryptophan and nitrotryptophan have been detected in samples from tissue or cell culture, specifically 2-hydroxytryptophan (27), 4-hydroxytryptophan (28), 5-hydroxytryptophan (29), or 6-hydroxytryptophan (30), 6-nitrotryptophan (36), and 5-hydroxy-6-nitrotryptophan (40) [7, 13, 97].

While tyrosine and tryptophan Ox-PTMs occur under the same conditions, several MS studies have indicated that tryptophan modifications are on the order of 10- to 1000-fold less abundant than tyrosine modification [98, 99]. No direct repair mechanisms for tryptophan Ox-PTMs have been noted, indicating that the only path to remove these Ox-PTMs is protein turnover. Although Ox-PTMs occur at a lower rate on tryptophan than on tyrosine, these modifications likely modulate cellular regulation as tryptophan residues are particularly important for specific protein-protein interactions and protein-small molecule recognition [100, 101]. At least one instance of 5-hydroxy-6-nitrotryptophan formation has been reported in the mitochondrial metabolic enzyme succinyl-CoA:3-ketoacid coenzyme A transferase (SCOT). This age-dependent Ox-PTM leads to a 30% increase in SCOT enzymatic activity and is thought to play

a protective role, allowing the heart to better utilize ketone metabolism for energy production [102].

While a novel GCE system for incorporation of tryptophan derivatives has been published and shown to utilize 5-hydroxytryptophan as a substrate, it has not yet been utilized to investigate the effects of this Ox-PTM [22]. As tryptophan Ox-PTMs are generally stable to cellular conditions and the tryptophan-based system can be evolved for other tryptophan-based ncAAs, this system will likely be applicable to the study of tryptophan Ox-PTMs.

Oxidation of histidine to 2-oxohistidine (45) occurs through a radical mechanism in protein, particularly near metal binding sites or in tissue exposed to UV radiation [103]. This Ox-PTM has been noted to occur significantly in Cu, Zn-SOD [104]. Little is known about how widespread this modification is or how it impacts biological function [105]. While a variety of histidine mimics have been genetically encoded via GCE, 2-oxohistidine has not yet been encoded genetically [106]. As 2-oxohistidine is stable enough on proteins to be characterized by X-ray crystallography [107] and given the aforementioned orthogonal system for modified histidine incorporation, it is likely that 2-oxohistidine will be amenable to incorporation by GCE.

7. Ox-PTMs that Have Been Incorporated by GCE

The first PTM genetically encoded was nitroTyr by Neumann and coworkers in 2008 and to date has been the most utilized GCE system for probing Ox-PTMs. An *Mj* orthogonal pair was evolved and subsequently used to confirm a loss of function in site-specifically nitrated MnSOD [78]. Through a novel selection scheme, a second generation *Mj* nitroTyr-RS was then generated with roughly an order of magnitude greater efficiency for producing nitroTyr-proteins [23]. This second generation *Mj* nitroTyr-RS was used to generate all 5 forms of nitrated Hsp90 found in endogenously nitrated Hsp90. This allowed each different site-specifically nitrated form of Hsp90 to be characterized for functional changes *in vitro* and cellular toxicity *in vivo* in different mammalian cell lines. Three of the five nitrated forms had no apparent effect when delivered into PC12 cells at physiologically relevant levels. For nitrated Hsp90, a toxic gain of function and motor neuron cell death occur if Hsp90 is nitrated at either tyrosine 33 or tyrosine 56 in less than 5% of the cellular pool of Hsp90 [79]. This is a key advance in the study of Ox-PTMs because it is the first example of a toxic gain of function confirmed from a single site of modification on a protein. Antibodies to nitrated Hsp90 were then generated, and using GCE was validated to recognize site-specific nitroTyr-33-Hsp90 and nitroTyr-56-Hsp90. These antibodies, now confirmed to recognize the nitration of a specific sites on Hsp90, have been used to monitor formation of toxic nitrated Hsp90 in tissue and track these oxoforms in other pathological states. It was further shown that nitration of Hsp90 at tyrosine 33 downregulates mitochondrial activity [81]. This nitroTyr GCE system has also been used to investigate physiological

role of tyrosine nitration in apolipoprotein A1 (ApoA1), a serum protein that facilitates systemic lipid trafficking. Using mass spectroscopy, three tyrosine residues in ApoA1 were identified as nitration sites. Genetic code expansion allowed the generation and characterization of each nitrated form of ApoA1, and only one nitrated tyrosine had an effect on ApoA1 activity. GCE was used to show that site-specific nitration of ApoA1 at tyrosine 166 results in a 90% reduction in LCAT activity [80]. A site-specific antibody for ApoA1 nitroTyr-166 was also generated in order to monitor this Ox-PTM in the context of atherosclerotic tissue. These antibodies specific for ApoA1 nitroTyr-166 confirmed that only this nitrated variant was removed from human serum and was enriched in atherosclerotic plaques by 1000-fold over nonnitrated ApoA1.

The ability to incorporate the structurally similar 3-chlorotyrosine and 3-bromotyrosine Ox-PTMs with GCE would enable the characterization of these modifications in disease. However, the first and second generation *Mj* nitroTyr synthetase is not permissive to these ncAAs, and synthetases generated for halotyrosine using the *Mj* synthetase system resulted in poor efficiency and fidelity. However, selections for a 3-chlorotyrosine synthetase from the PylRS/pylT pair have yielded aaRSs that have good efficiency and fidelity for halogenated tyrosines. Proteins with site-specifically incorporated 3-chlorotyrosine and 3-bromotyrosine have indicated that currently available commercial antibodies to these modifications are not specific or are not sensitive to these modifications alone. GCE now presents the opportunity to improve on the specificity and sensitivity of antibodies for these modifications.

GCE has also been applied to the site-specific incorporation of the redox-active amino acid DOPA (14). The site-specific incorporation of DOPA is challenging because when this amino acid is added to media, it can react with cellular components, yielding the oxidized ncAA (DOPA quinone, 15) that can serve as an electrophile [108]. To overcome the side reactions in media, a photocaged DOPA has also been encoded [109]. While the GCE of photocaged DOPA was developed for the production of recombinant bioadhesives not for studying oxidative stress, this tool could also be used to evaluate the effects of DOPA containing proteins in disease.

8. Application of GCE to the Study of Ox-PTMs

It has long been known that ROS and RNS modify protein amino acids but it has been challenging to determine the extent of their biological role and abundance. Identifying Ox-PTM formation on a protein is the first step of any investigation into Ox-PTMs followed by verification of biological relevance. The nitroTyr Ox-PTM can be used as an example of how the synergy of new detection methods and GCE can advance the understanding of Ox-PTMs. The earliest manuscripts outlining detection of nitroTyr in proteins were based on methods using HPLC/UV-Vis and amino acid analysis because this Ox-PTM possesses a significant absorbance at 430 nm [110, 111]. A September 2017 PubMed literature survey revealed 5522 manuscripts published with the term

"nitrotyrosine" in the title or abstract. In the first 24 years of research involving nitroTyr, less than 2% of present publications on nitroTyr were published, which was followed by a virtual explosion in the number of papers published on nitro-Tyr in the ensuing years. This rapid increase in nitroTyr research coincides nicely with the development of the first nitroTyr antibodies by Joe Beckman and coworkers in 1994 (Figure 4(a)) [112]. NitroTyr antibodies have been used to detect this modification in tissue via immunohistochemistry, for identification of proteins via Western blot and for enrichment of proteins for proteomic methods. Due in part to access to antibodies as a detection method, nitroTyr now serves as a general biomarker for oxidative stress [113].

The increased interest in the nitroTyr Ox-PTM has spurred numerous methods for identifying nitroTyr proteins including HPLC-based techniques for quantifying total nitroTyr in tissues and lysates and various mass spectrometry methods for identifying sites of nitroTyr modification in proteins [11, 114]. The interest in nitroTyr and its detection in a variety of pathological conditions created the need to generate homogeneous nitrated proteins for characterization which led directly to the first GCE system for nitroTyr incorporation [78]. GCE clearly enables characterization of how a specific Ox-PTM on a protein alters its function but it also allows for analysis of the antibodies generated to detect Ox-PTM proteins. With access to site-specific and homogeneous Ox-PTM protein generated from GCE, the specificity and sensitivity of Ox-PTM antibodies can be determined. The original nitroTyr antibodies generated were a foundational advancement in studying oxidative stress, but as the field progresses, improved antibodies for studying Ox-PTMs are needed. While the development of nitroTyr antibodies lead to the incorporation of nitroTyr via GCE, better detection methods for nitroTyr can now be developed using site-specifically modified protein from GCE (Figure 4(b)).

It has become very clear through GCE that nitroTyr antibodies have wildly different sensitivity depending on the site of protein nitration. All of the currently available Ox-PTM antibodies were developed prior to GCE of Ox-PTM and were validated using methods available at the time of their development [115]. Now, GCE allows for verification that Ox-PTM antibodies are selective for one type of Ox-PTM over others of similar structure. Since antibodies are often generated to proteins that have been exposed to ROS and RNS reagents, not homogeneous Ox-PTM proteins, the resulting antibody specificity might be to a different Ox-PTM than intended. For example, the nitroTyr monoclonal antibody (clone 1A6) indicated a nitrated protein present in aged rat heart mitochondria, but this protein was instead found to contain 5-hydroxy-6-nitrotryptophan, which closely resembles the nitroTyr sidechain [102].

A powerful application of GCE is the ability to confirm that an Ox-PTM modification at a specific location in a protein is detected by an antibody. While nitroTyr-antibodies are specific for the nitroTyr modification, they do not detect all sites of nitration equally. In addition, if there is the ability to detect the modification at one location on a protein and

not another, this can be verified with GCE. A specific peptide sequence containing the desired Ox-PTM can be used to generate antibodies, and then the Ox-PTM antibodies can be screened for selectivity against homogeneous protein generated with GCE. Antibodies specific for nitroTyr-33-Hsp90, nitroTyr-56-Hsp90, and ApoA1 have been generated using this approach [79–81]. These site-specific antibodies have been used to determine the extent of nitration of specific sites in Hsp90 in different cellular contexts and conditions. Unsurprisingly, there exists clear peptide context-dependent sensitivity to the function of nitroTyr antibodies, that is to say, the amino acid sequence of the protein surrounding the Ox-PTM site plays a role in antibody detection sensitivity. In addition to the development of site-specific antibodies, the ability of GCE to produce homogeneously nitrated proteins allows for the characterization of this context dependence that was not possible with existing techniques. While much of the past work on detection of Ox-PTMs with antibodies has focused on nitroTyr, further development of GCE for other Ox-PTMs will lead to exciting advances in Ox-PTM antibody development and validation, particularly for cysteine and methionine oxoforms.

As Ox-PTMs are relevant to disease, the Ox-PTM proteins and their function represent a new class of possible therapeutic targets. Any Ox-PTM protein that shows an undesirable gain-of-function or new interaction could be a therapeutic target. Ox-PTMs present a unique situation insofar as they are not directly enzymatically catalyzed and therefore the PTM "writer" (e.g., kinase) cannot be directly inhibited. This requires the oxidized protein itself to be directly inhibited. For instance, nitrated Hsp90 found in motor neurons under pathological conditions such as ALS and spinal cord injury may present a target for intervention [79]. It has become increasingly clear that the site of protein Ox-PTMs is an important determinant of their biological role. With this in mind, the use of GCE for site-specific PTM incorporation as a means of screening for potential therapeutics against specific Ox-PTMs has been acknowledged [116]. This is clear in the case of Hsp90, which is endogenously nitrated on five tyrosines and of them only nitration of tyrosines 33 and 56 leads to motor neuron cell death, while nitration of tyrosine 33 downregulates mitochondrial activity [79, 81]. Given this clear functional specificity from site-dependence of nitrated Hsp90, it will be desirable to develop sequence-specific inhibitors that target site-specific Ox-PTM proteins. As GCE can produce all possible Ox-PTM forms, the technology will allow for screening of therapeutic compounds against site-specific oxoforms.

9. Conclusions and Perspective

The study of protein Ox-PTMs is hampered by access to defined Ox-PTM proteins. GCE is uniquely suited to overcome this roadblock because it generates site-specific and homogenous Ox-PTM proteins. GCE has been applied to protein tyrosine nitration both to investigate biological effects of particular sites of modification on key proteins and to provide defined Ox-PTM proteins for validating
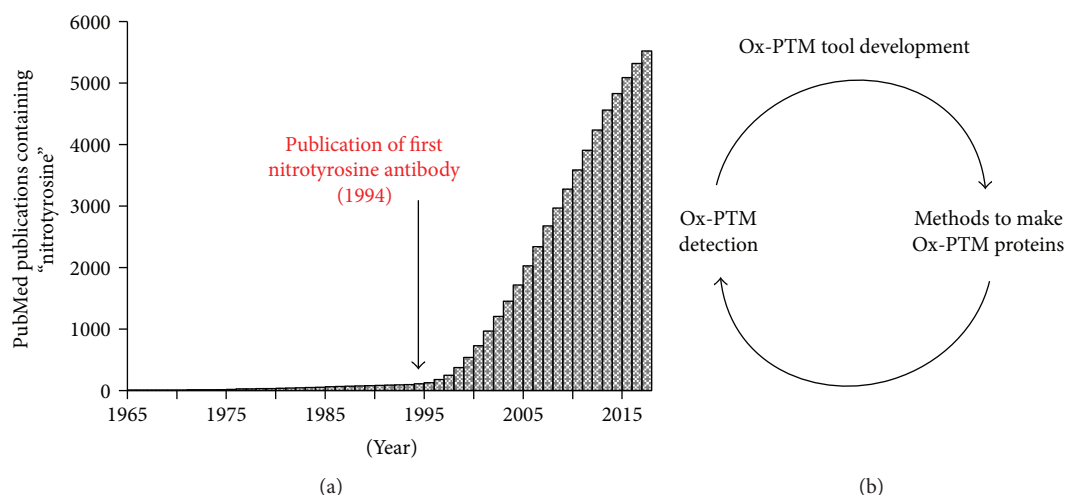
FIGURE 4: (a) Total number of publications on PubMed containing the word 'nitrotyrosine' in the title or abstract published up to the year indicated. The publication of the first nitrotyrosine antibody by Beckman and coworkers in 1994 is denoted with an arrow. (b) The cycle of development of chemical biology tools for studying Ox-PTMs. New methods like development of antibodies allow easier detection of Ox-PTMs, which naturally lead to increased interest and development of new chemical biology tools, including GCE, for studying Ox-PTMs. Tools like GCE allow for development of better detection methods, which further reinforces the cycle.

nitroTyr antibodies. Every newly identified Ox-PTM protein that shows a gain of function can be considered as a therapeutic target since it forms under oxidative stress conditions. As seen with nitrated Hsp90 and ApoA1, the ability to generate Ox-PTM proteins opens the ability to develop screens for therapeutics and identifies their molecular role in disease.

Thus far, the development of GCE methods for Ox-PTMs has relied on researchers from both the oxidative stress field and the GCE fields. NitroTyr was identified in biological samples as a major marker for oxidative stress which prompted those in GCE to develop methods for site-specific incorporation of this Ox-PTM. As those in the oxidative stress field embraced the use of the GCE methods for challenging problems, the GCE tools required refinement and improvement. With this in mind, significant advances in the Ox-PTM field will likely rely on synergy between developments in GCE technology and those applying the tools to challenging Ox-PTM problems.

Conflicts of Interest

The authors declare that there is no conflict of interest regarding the publication of this paper.

Acknowledgments

Supplementary Materials

Table S1: list of Ox-PTMs identified following oxidative stress in cells or exposure of protein *in vitro* to ROS and RNOS. *(Supplementary Material)*

References

[1] M. P. Murphy, A. Holmgren, N. G. Larsson et al., "Unraveling the biological roles of reactive oxygen species," *Cell Metabolism*, vol. 13, no. 4, pp. 361–366, 2011.

[2] K. G. Reddie and K. S. Carroll, "Expanding the functional diversity of proteins through cysteine oxidation," *Current Opinion in Chemical Biology*, vol. 12, no. 6, pp. 746–754, 2008.

[3] C. M. Spickett and A. R. Pitt, "Protein oxidation: role in signalling and detection by mass spectrometry," *Amino Acids*, vol. 42, no. 1, pp. 5–21, 2012.

[4] E. R. Stadtman, "[25] Role of oxidized amino acids in protein breakdown and stability," *Methods in Enzymology*, vol. 258, pp. 379–393, 1995.

[5] A. Drazic and J. Winter, "The physiological role of reversible methionine oxidation," *Biochimica et Biophysica Acta (BBA) - Proteins and Proteomics*, vol. 1844, no. 8, pp. 1367–1382, 2014.

[6] M. B. Feeney and C. Schöneich, "Tyrosine modifications in aging," *Antioxidants & Redox Signaling*, vol. 17, no. 11, pp. 1571–1579, 2012.

[7] T. Nuriel, A. Hansler, and S. S. Gross, "Protein nitrotryptophan: formation, significance and identification," *Journal of Proteomics*, vol. 74, no. 11, pp. 2300–2312, 2011.

[8] K. Uchida, "Histidine and lysine as targets of oxidative modification," *Amino Acids*, vol. 25, no. 3-4, pp. 249–257, 2003.

[9] M. J. Davies, "The oxidative environment and protein damage," *Biochimica et Biophysica Acta (BBA) - Proteins and Proteomics*, vol. 1703, no. 2, pp. 93–109, 2005.

[10] P. Pacher, J. S. Beckman, and L. Liaudet, "Nitric oxide and peroxynitrite in health and disease," *Physiological Reviews*, vol. 87, no. 1, pp. 315–424, 2007.

[11] D. Tsikas and M. W. Duncan, "Mass spectrometry and 3-nitrotyrosine: strategies, controversies, and our current perspective," *Mass Spectrometry Reviews*, vol. 33, no. 4, pp. 237–276, 2014.

[12] C. Batthyany, S. Bartesaghi, M. Mastrogiovanni, A. Lima, V. Demicheli, and R. Radi, "Tyrosine-nitrated proteins: proteomic and bioanalytical aspects," *Antioxidants & Redox Signaling*, vol. 26, no. 7, pp. 313–328, 2017.

[13] A. Bachi, I. Dalle-Donne, and A. Scaloni, "Redox proteomics: chemical principles, methodological approaches and biological/biomedical promises," *Chemical Reviews*, vol. 113, no. 1, pp. 596–698, 2013.

[14] J. W. Chin, "Expanding and reprogramming the genetic code," *Nature*, vol. 550, no. 7674, pp. 53–60, 2017.

[15] A. Dumas, L. Lercher, C. D. Spicer, and B. G. Davis, "Designing logical codon reassignment - expanding the chemistry in biology," *Chemical Science*, vol. 6, no. 1, pp. 50–69, 2015.

[16] R. B. Quast, D. Mrusek, C. Hoffmeister, A. Sonnabend, and S. Kubick, "Cotranslational incorporation of non-standard amino acids using cell-free protein synthesis," *FEBS Letters*, vol. 589, no. 15, pp. 1703–1712, 2015.

[17] L. Wang, A. Brock, B. Herberich, and P. G. Schultz, "Expanding the genetic code of *Escherichia coli*," *Science*, vol. 292, no. 5516, pp. 498–500, 2001.

[18] N. Wu, A. Deiters, T. A. Cropp, D. King, and P. G. Schultz, "A genetically encoded photocaged amino acid," *Journal of the American Chemical Society*, vol. 126, no. 44, pp. 14306-14307, 2004.

[19] J. W. Chin, T. A. Cropp, J. C. Anderson, M. Mukherji, Z. Zhang, and P. G. Schultz, "An expanded eukaryotic genetic code," *Science*, vol. 301, no. 5635, pp. 964–967, 2003.

[20] H. Neumann, S. Y. Peak-Chew, and J. W. Chin, "Genetically encoding N^ε-acetyllysine in recombinant proteins," *Nature Chemical Biology*, vol. 4, no. 4, pp. 232–234, 2008.

[21] T. Mukai, T. Kobayashi, N. Hino, T. Yanagisawa, K. Sakamoto, and S. Yokoyama, "Adding L-lysine derivatives to the genetic code of mammalian cells with engineered pyrrolysyl-tRNA synthetases," *Biochemical and Biophysical Research Communications*, vol. 371, no. 4, pp. 818–822, 2008.

[22] J. S. Italia, P. S. Addy, C. J. J. Wrobel et al., "An orthogonalized platform for genetic code expansion in both bacteria and eukaryotes," *Nature Chemical Biology*, vol. 13, no. 4, pp. 446–450, 2017.

[23] R. B. Cooley, J. L. Feldman, C. M. Driggers et al., "Structural basis of improved second-generation 3-nitro-tyrosine tRNA synthetases," *Biochemistry*, vol. 53, no. 12, pp. 1916–1924, 2014.

[24] S. J. Miyake-Stoner, A. M. Miller, J. T. Hammill et al., "Probing protein folding using site-specifically encoded unnatural amino acids as FRET donors with tryptophan," *Biochemistry*, vol. 48, no. 25, pp. 5953–5962, 2009.

[25] R. B. Cooley, P. A. Karplus, and R. A. Mehl, "Gleaning unexpected fruits from hard-won synthetases: probing principles of permissivity in non-canonical amino acid-tRNA synthetases," *Chembiochem*, vol. 15, no. 12, pp. 1810–1819, 2014.

[26] A. R. Parrish, X. She, Z. Xiang et al., "Expanding the genetic code of *Caenorhabditis elegans* using bacterial aminoacyl-tRNA synthetase/tRNA pairs," *ACS Chemical Biology*, vol. 7, no. 7, pp. 1292–1302, 2012.

[27] X. Luo, G. Fu, R. E. Wang et al., "Genetically encoding phosphotyrosine and its nonhydrolyzable analog in bacteria," *Nature Chemical Biology*, vol. 13, no. 8, pp. 845–849, 2017.

[28] R. A. Mehl, J. C. Anderson, S. W. Santoro et al., "Generation of a bacterium with a 21 amino acid genetic code," *Journal of the American Chemical Society*, vol. 125, no. 4, pp. 935–939, 2003.

[29] M. S. Zhang, S. F. Brunner, N. Huguenin-Dezot et al., "Biosynthesis and genetic encoding of phosphothreonine through parallel selection and deep sequencing," *Nature Methods*, vol. 14, no. 7, pp. 729–736, 2017.

[30] C. Hoppmann, A. Wong, B. Yang et al., "Site-specific incorporation of phosphotyrosine using an expanded genetic code," *Nature Chemical Biology*, vol. 13, no. 8, pp. 842–844, 2017.

[31] D. T. Rogerson, A. Sachdeva, K. Wang et al., "Efficient genetic encoding of phosphoserine and its nonhydrolyzable analog," *Nature Chemical Biology*, vol. 11, no. 7, pp. 496–503, 2015.

[32] H. S. Park, M. J. Hohn, T. Umehara et al., "Expanding the genetic code of *Escherichia coli* with phosphoserine," *Science*, vol. 333, no. 6046, pp. 1151–1154, 2011.

[33] T. W. Muir, "Semisynthesis of proteins by expressed protein ligation," *Annual Review of Biochemistry*, vol. 72, no. 1, pp. 249–289, 2003.

[34] M. Holt and T. Muir, "Application of the protein semisynthesis strategy to the generation of modified chromatin," *Annual Review of Biochemistry*, vol. 84, no. 1, pp. 265–290, 2015.

[35] V. Muralidharan and T. W. Muir, "Protein ligation: an enabling technology for the biophysical analysis of proteins," *Nature Methods*, vol. 3, no. 6, pp. 429–438, 2006.

[36] R. Burai, N. Ait-Bouziad, A. Chiki, and H. A. Lashuel, "Elucidating the role of site-specific nitration of α-synuclein in the pathogenesis of Parkinson's disease via protein semisynthesis and mutagenesis," *Journal of the American Chemical Society*, vol. 137, no. 15, pp. 5041–5052, 2015.

[37] M. Lo Conte and K. S. Carroll, "The redox biochemistry of protein sulfenylation and sulfinylation," *Journal of Biological Chemistry*, vol. 288, no. 37, pp. 26480–26488, 2013.

[38] K. Chen, M. T. Kirber, H. Xiao, Y. Yang, and J. F. Keaney Jr., "Regulation of ROS signal transduction by NADPH oxidase 4 localization," *Journal of Cell Biology*, vol. 181, no. 7, pp. 1129–1139, 2008.

[39] C. E. Paulsen, T. H. Truong, F. J. Garcia et al., "Peroxide-dependent sulfenylation of the EGFR catalytic site enhances kinase activity," *Nature Chemical Biology*, vol. 8, no. 1, pp. 57–64, 2011.

[40] M. A. Wilson, "The role of cysteine oxidation in DJ-1 function and dysfunction," *Antioxidants & Redox Signaling*, vol. 15, no. 1, pp. 111–122, 2011.

[41] F. R. Salsbury Jr., S. T. Knutson, L. B. Poole, and J. S. Fetrow, "Functional site profiling and electrostatic analysis of cysteines modifiable to cysteine sulfenic acid," *Protein Science*, vol. 17, no. 2, pp. 299–312, 2008.

[42] M. Hamann, T. Zhang, S. Hendrich, and J. A. Thomas, "[15] Quantitation of protein sulfinic and sulfonic acid, irreversibly oxidized protein cysteine sites in cellular proteins," *Methods in Enzymology*, vol. 348, pp. 146–156, 2002.

[43] C. Jacob, A. L. Holme, and F. H. Fry, "The sulfinic acid switch in proteins," *Organic & Biomolecular Chemistry*, vol. 2, no. 14, pp. 1953–1956, 2004.

[44] S. R. Lee, K. S. Yang, J. Kwon, C. Lee, W. Jeong, and S. G. Rhee, "Reversible inactivation of the tumor suppressor PTEN by H_2O_2," *Journal of Biological Chemistry*, vol. 277, no. 23, pp. 20336–20342, 2002.

[45] A. Salmeen, J. N. Andersen, M. P. Myers et al., "Redox regulation of protein tyrosine phosphatase 1B involves a sulphenyl-amide intermediate," *Nature*, vol. 423, no. 6941, pp. 769–773, 2003.

[46] S. E. Leonard and K. S. Carroll, "Chemical 'omics' approaches for understanding protein cysteine oxidation in biology," *Current Opinion in Chemical Biology*, vol. 15, no. 1, pp. 88–102, 2011.

[47] J. J. Tanner, Z. D. Parsons, A. H. Cummings, H. Zhou, and K. S. Gates, "Redox regulation of protein tyrosine phosphatases: structural and chemical aspects," *Antioxidants and Redox Signaling*, vol. 15, no. 1, pp. 77–97, 2011.

[48] E. Giannoni, F. Buricchi, G. Raugei, G. Ramponi, and P. Chiarugi, "Intracellular reactive oxygen species activate Src tyrosine kinase during cell adhesion and anchorage-dependent cell growth," *Molecular and Cellular Biology*, vol. 25, no. 15, pp. 6391–6403, 2005.

[49] J. K. Smith, C. N. Patil, S. Patolla, B. W. Gunter, G. W. Booz, and R. J. Duhe, "Identification of a redox-sensitive switch within the JAK2 catalytic domain," *Free Radical Biology & Medicine*, vol. 52, no. 6, pp. 1101–1110, 2012.

[50] M. Y. Song, A. Makino, and J. X.-J. Yuan, "Role of reactive oxygen species and redox in regulating the function of transient receptor potential channels," *Antioxidants and Redox Signaling*, vol. 15, no. 6, pp. 1549–1565, 2011.

[51] S. G. Rhee, "Overview on peroxiredoxin," *Molecules and Cells*, vol. 39, no. 1, pp. 1–5, 2016.

[52] J. S. Stamler, D. I. Simon, J. A. Osborne et al., "S-Nitrosylation of proteins with nitric oxide: synthesis and characterization of biologically active compounds," *Proceedings of the National Academy of Sciences of the United States of America*, vol. 89, no. 1, pp. 444–448, 1992.

[53] D. T. Hess, A. Matsumoto, S. O. Kim, H. E. Marshall, and J. S. Stamler, "Protein S-nitrosylation: purview and parameters," *Nature Reviews Molecular Cell Biology*, vol. 6, no. 2, pp. 150–166, 2005.

[54] J. S. Stamler, S. Lamas, and F. C. Fang, "Nitrosylation: the prototypic redox-based signaling mechanism," *Cell*, vol. 106, no. 6, pp. 675–683, 2001.

[55] R. Li and J. Kast, "Biotin switch assays for quantitation of reversible cysteine oxidation," *Methods in Enzymology*, vol. 585, pp. 269–284, 2017.

[56] M. D. Kornberg, N. Sen, M. R. Hara et al., "GAPDH mediates nitrosylation of nuclear proteins," *Nature Cell Biology*, vol. 12, no. 11, pp. 1094–1100, 2010.

[57] M. W. Foster, T. J. McMahon, and J. S. Stamler, "S-Nitrosylation in health and disease," *Trends in Molecular Medicine*, vol. 9, no. 4, pp. 160–168, 2003.

[58] B. Gaston, J. Reilly, J. M. Drazen et al., "Endogenous nitrogen oxides and bronchodilator S-nitrosothiols in human airways," *Proceedings of the National Academy of Sciences of the United States of America*, vol. 90, no. 23, pp. 10957–10961, 1993.

[59] C. Schoneich, "Methionine oxidation by reactive oxygen species: reaction mechanisms and relevance to Alzheimer's disease," *Biochimica et Biophysica Acta (BBA) - Proteins and Proteomics*, vol. 1703, no. 2, pp. 111–119, 2005.

[60] T. Nauser, J. Pelling, and C. Schoneich, "Thiyl radical reaction with amino acid side chains: rate constants for hydrogen transfer and relevance for posttranslational protein modification," *Chemical Research in Toxicology*, vol. 17, no. 10, pp. 1323–1328, 2004.

[61] B. Ghesquière, V. Jonckheere, N. Colaert et al., "Redox proteomics of protein-bound methionine oxidation," *Molecular & Cellular Proteomics*, vol. 10, no. 5, article M110.006866, 2011.

[62] H. Weissbach, L. Resnick, and N. Brot, "Methionine sulfoxide reductases: history and cellular role in protecting against oxidative damage," *Biochimica et Biophysica Acta (BBA) - Proteins and Proteomics*, vol. 1703, no. 2, pp. 203–212, 2005.

[63] W. T. Lowther, H. Weissbach, F. Etienne, N. Brot, and B. W. Matthews, "The mirrored methionine sulfoxide reductases of *Neisseria gonorrhoeae* pilB," *Nature Structural Biology*, vol. 9, no. 5, pp. 348–352, 2002.

[64] G. H. Kwak, T. H. Kim, and H. Y. Kim, "Down-regulation of MsrB3 induces cancer cell apoptosis through reactive oxygen species production and intrinsic mitochondrial pathway activation," *Biochemical and Biophysical Research Communications*, vol. 483, no. 1, pp. 468–474, 2017.

[65] L. Zhang, S. Peng, J. Sun et al., "A specific fluorescent probe reveals compromised activity of methionine sulfoxide reductases in Parkinson's disease," *Chemical Science*, vol. 8, no. 4, pp. 2966–2972, 2017.

[66] A. Drazic, H. Miura, J. Peschek et al., "Methionine oxidation activates a transcription factor in response to oxidative stress," *Proceedings of the National Academy of Sciences of the United States of America*, vol. 110, no. 23, pp. 9493–9498, 2013.

[67] J. R. Erickson, M. L. A. Joiner, X. Guan et al., "A dynamic pathway for calcium-independent activation of CaMKII by methionine oxidation," *Cell*, vol. 133, no. 3, pp. 462–474, 2008.

[68] B. C. Lee, Z. Péterfi, F. K. W. Hoffmann et al., "MsrB1 and MICALs regulate actin assembly and macrophage function via reversible stereoselective methionine oxidation," *Molecular Cell*, vol. 51, no. 3, pp. 397–404, 2013.

[69] J. Pan and K. S. Carroll, "Light-mediated sulfenic acid generation from photocaged cysteine sulfoxide," *Organic Letters*, vol. 17, no. 24, pp. 6014–6017, 2015.

[70] R. Radi, "Protein tyrosine nitration: biochemical mechanisms and structural basis of functional effects," *Accounts of Chemical Research*, vol. 46, no. 2, pp. 550–559, 2013.

[71] K. S. Aulak, M. Miyagi, L. Yan et al., "Proteomic method identifies proteins nitrated *in vivo* during inflammatory challenge," *Proceedings of the National Academy of Sciences of the United States of America*, vol. 98, no. 21, pp. 12056–12061, 2001.

[72] A. J. Gow, C. R. Farkouh, D. A. Munson, M. A. Posencheg, and H. Ischiropoulos, "Biological significance of nitric oxide-mediated protein modifications," *American Journal of Physiology-Lung Cellular and Molecular Physiology*, vol. 287, no. 2, pp. L262–L268, 2004.

[73] J. Kanski, A. Behring, J. Pelling, and C. Schoneich, "Proteomic identification of 3-nitrotyrosine-containing rat cardiac proteins: effects of biological aging," *American Journal of Physiology-Heart and Circulatory Physiology*, vol. 288, no. 1, pp. H371–H381, 2005.

[74] J. Kanski, S. J. Hong, and C. Schoneich, "Proteomic analysis of protein nitration in aging skeletal muscle and identification of nitrotyrosine-containing sequences *in vivo* by nanoelectrospray ionization tandem mass spectrometry," *Journal of Biological Chemistry*, vol. 280, no. 25, pp. 24261–24266, 2005.

[75] R. Radi, "Nitric oxide, oxidants, and protein tyrosine nitration," *Proceedings of the National Academy of Sciences of the*

United States of America, vol. 101, no. 12, pp. 4003–4008, 2004.

[76] J. W. Heinecke, "Mechanisms of oxidative damage by myeloperoxidase in atherosclerosis and other inflammatory disorders," *The Journal of Laboratory and Clinical Medicine*, vol. 133, no. 4, pp. 321–325, 1999.

[77] J. W. Heinecke, "Mass spectrometric quantification of amino acid oxidation products in proteins: insights into pathways that promote LDL oxidation in the human artery wall," *FASEB Journal*, vol. 13, no. 10, pp. 1113–1120, 1999.

[78] H. Neumann, J. L. Hazen, J. Weinstein, R. A. Mehl, and J. W. Chin, "Genetically encoding protein oxidative damage," *Journal of the American Chemical Society*, vol. 130, no. 12, pp. 4028–4033, 2008.

[79] M. C. Franco, Y. Ye, C. A. Refakis et al., "Nitration of Hsp90 induces cell death," *Proceedings of the National Academy of Sciences of the United States of America*, vol. 110, no. 12, pp. E1102–E1111, 2013.

[80] J. A. DiDonato, K. Aulak, Y. Huang et al., "Site-specific nitration of apolipoprotein A-I at tyrosine 166 is both abundant within human atherosclerotic plaque and dysfunctional," *Journal of Biological Chemistry*, vol. 289, no. 15, pp. 10276–10292, 2014.

[81] M. C. Franco, K. C. Ricart, A. S. Gonzalez et al., "Nitration of Hsp90 on tyrosine 33 regulates mitochondrial metabolism," *Journal of Biological Chemistry*, vol. 290, no. 31, pp. 19055–19066, 2015.

[82] S. J. Nicholls, Z. Shen, X. Fu, B. S. Levison, and S. L. Hazen, "Quantification of 3-nitrotyrosine levels using a benchtop ion trap mass spectrometry method," *Methods in Enzymology*, vol. 396, pp. 245–266, 2005.

[83] M. L. Brennan, W. Wu, X. Fu et al., "A tale of two controversies: defining both the role of peroxidases in nitrotyrosine formation *in vivo* using eosinophil peroxidase and myeloperoxidase-deficient mice, and the nature of peroxidase-generated reactive nitrogen species," *Journal of Biological Chemistry*, vol. 277, no. 20, pp. 17415–17427, 2002.

[84] J. M. Souza, I. Choi, Q. Chen et al., "Proteolytic degradation of tyrosine nitrated proteins," *Archives of Biochemistry and Biophysics*, vol. 380, no. 2, pp. 360–366, 2000.

[85] Y. Kamisaki, K. Wada, K. Bian et al., "An activity in rat tissues that modifies nitrotyrosine-containing proteins," *Proceedings of the National Academy of Sciences of the United States of America*, vol. 95, no. 20, pp. 11584–11589, 1998.

[86] K. S. Aulak, T. Koeck, J. W. Crabb, and D. J. Stuehr, "Dynamics of protein nitration in cells and mitochondria," *American Journal of Physiology-Heart and Circulatory Physiology*, vol. 286, no. 1, pp. H30–H38, 2004.

[87] H. S. Smallwood, N. M. Lourette, C. B. Boschek et al., "Identification of a denitrase activity against calmodulin in activated macrophages using high-field liquid chromatography–FTICR mass spectrometry," *Biochemistry*, vol. 46, no. 37, pp. 10498–10505, 2007.

[88] R. S. Deeb, T. Nuriel, C. Cheung et al., "Characterization of a cellular denitrase activity that reverses nitration of cyclooxygenase," *American Journal of Physiology-Heart and Circulatory Physiology*, vol. 305, no. 5, pp. H687–H698, 2013.

[89] E. Gochman, J. Mahajna, P. Shenzer et al., "The expression of iNOS and nitrotyrosine in colitis and colon cancer in humans," *Acta Histochemica*, vol. 114, no. 8, pp. 827–835, 2012.

[90] J. M. Souza, G. Peluffo, and R. Radi, "Protein tyrosine nitration—functional alteration or just a biomarker?," *Free Radical Biology & Medicine*, vol. 45, no. 4, pp. 357–366, 2008.

[91] B. Shao, M. N. Oda, J. F. Oram, and J. W. Heinecke, "Myeloperoxidase: an oxidative pathway for generating dysfunctional high-density lipoprotein," *Chemical Research in Toxicology*, vol. 23, no. 3, pp. 447–454, 2010.

[92] D. I. Pattison and M. J. Davies, "Kinetic analysis of the reactions of hypobromous acid with protein components: implications for cellular damage and use of 3-bromotyrosine as a marker of oxidative stress," *Biochemistry*, vol. 43, no. 16, pp. 4799–4809, 2004.

[93] E. Thomson, S. Brennan, R. Senthilmohan et al., "Identifying peroxidases and their oxidants in the early pathology of cystic fibrosis," *Free Radical Biology & Medicine*, vol. 49, no. 9, pp. 1354–1360, 2010.

[94] A. Strzepa, K. A. Pritchard, and B. N. Dittel, "Myeloperoxidase: a new player in autoimmunity," *Cellular Immunology*, vol. 317, pp. 1–8, 2017.

[95] J. Wang and A. Slungaard, "Role of eosinophil peroxidase in host defense and disease pathology," *Archives of Biochemistry and Biophysics*, vol. 445, no. 2, pp. 256–260, 2006.

[96] S. L. Hazen and J. W. Heinecke, "3-Chlorotyrosine, a specific marker of myeloperoxidase-catalyzed oxidation, is markedly elevated in low density lipoprotein isolated from human atherosclerotic intima," *The Journal of Clinical Investigation*, vol. 99, no. 9, pp. 2075–2081, 1997.

[97] Y. Huang, J. A. DiDonato, B. S. Levison et al., "An abundant dysfunctional apolipoprotein A1 in human atheroma," *Nature Medicine*, vol. 20, no. 2, pp. 193–203, 2014.

[98] Y. Ishii, A. Ogara, T. Katsumata et al., "Quantification of nitrated tryptophan in proteins and tissues by high-performance liquid chromatography with electrospray ionization tandem mass spectrometry," *Journal of Pharmaceutical and Biomedical Analysis*, vol. 44, no. 1, pp. 150–159, 2007.

[99] H. Kawasaki, A. Shigenaga, M. Uda et al., "Nitration of tryptophan in ribosomal proteins is a novel post-translational modification of differentiated and naive PC12 cells," *Nitric Oxide*, vol. 25, no. 2, pp. 176–182, 2011.

[100] A. A. Bogan and K. S. Thorn, "Anatomy of hot spots in protein interfaces," *Journal of Molecular Biology*, vol. 280, no. 1, pp. 1–9, 1998.

[101] K. Ikeda, B. Yukihiro Hiraoka, H. Iwai et al., "Detection of 6-nitrotryptophan in proteins by Western blot analysis and its application for peroxynitrite-treated PC12 cells," *Nitric Oxide*, vol. 16, no. 1, pp. 18–28, 2007.

[102] I. Rebrin, C. Bregere, S. Kamzalov, T. K. Gallaher, and R. S. Sohal, "Nitration of tryptophan 372 in succinyl-CoA:3-ketoacid CoA transferase during aging in rat heart mitochondria," *Biochemistry*, vol. 46, no. 35, pp. 10130–10144, 2007.

[103] F. Zhao, E. Ghezzo-Schoneich, G. I. Aced, J. Hong, T. Milby, and C. Schoneich, "Metal-catalyzed oxidation of histidine in human growth hormone. Mechanism, isotope effects, and inhibition by a mild denaturing alcohol," *Journal of Biological Chemistry*, vol. 272, no. 14, pp. 9019–9029, 1997.

[104] B. Alvarez, V. Demicheli, R. Durán et al., "Inactivation of human Cu,Zn superoxide dismutase by peroxynitrite and formation of histidinyl radical," *Free Radical Biology & Medicine*, vol. 37, no. 6, pp. 813–822, 2004.

[105] B. Alvarez and R. Radi, "Peroxynitrite reactivity with amino acids and proteins," *Amino Acids*, vol. 25, no. 3-4, pp. 295–311, 2003.

[106] H. Xiao, F. B. Peters, P. Y. Yang, S. Reed, J. R. Chittuluru, and P. G. Schultz, "Genetic incorporation of histidine derivatives using an engineered pyrrolysyl-tRNA synthetase," *ACS Chemical Biology*, vol. 9, no. 5, pp. 1092–1096, 2014.

[107] D. A. K. Traoré, A. E. Ghazouani, L. Jacquamet et al., "Structural and functional characterization of 2-oxo-histidine in oxidized PerR protein," *Nature Chemical Biology*, vol. 5, no. 1, pp. 53–59, 2008.

[108] L. Alfonta, Z. Zhang, S. Uryu, J. A. Loo, and P. G. Schultz, "Site-specific incorporation of a redox-active amino acid into proteins," *Journal of the American Chemical Society*, vol. 125, no. 48, pp. 14662-14663, 2003.

[109] M. Hauf, F. Richter, T. Schneider et al., "Photoactivatable mussel-based underwater adhesive proteins by an expanded genetic code," *Chembiochem*, vol. 18, no. 18, pp. 1819–1823, 2017.

[110] A. J. Furth and D. B. Hope, "Studies on the chemical modification of the tyrosine residue in bovine neurophysin-II," *Biochemical Journal*, vol. 116, no. 4, pp. 545–553, 1970.

[111] S. Beeckmans and L. Kanarek, "The modification with tetranitromethane of an essential tyrosine in the active site of pig fumarase," *Biochimica et Biophysica Acta (BBA) - Protein Structure and Molecular Enzymology*, vol. 743, no. 3, pp. 370–378, 1983.

[112] J. S. Beckmann, Y. Z. Ye, P. G. Anderson et al., "Extensive nitration of protein tyrosines in human atherosclerosis detected by immunohistochemistry," *Biological Chemistry Hoppe-Seyler*, vol. 375, no. 2, pp. 81–88, 1994.

[113] J. Frijhoff, P. G. Winyard, N. Zarkovic et al., "Clinical relevance of biomarkers of oxidative stress," *Antioxidants & Redox Signaling*, vol. 23, no. 14, pp. 1144–1170, 2015.

[114] T. Nuriel, R. S. Deeb, D. P. Hajjar, and S. S. Gross, "Protein 3-nitrotyrosine in complex biological samples: quantification by high-pressure liquid chromatography/electrochemical detection and emergence of proteomic approaches for unbiased identification of modification sites," *Methods in Enzymology*, vol. 441, pp. 1–17, 2008.

[115] Y. Z. Ye, M. Strong, Z. Q. Huang, and J. S. Beckman, "[19] Antibodies that recognize nitrotyrosine," *Methods in Enzymology*, vol. 269, pp. 201–209, 1996.

[116] Z. Y. Buuh, Z. Lyu, and R. E. Wang, "Interrogating the roles of post-translational modifications of non-histone proteins," *Journal of Medicinal Chemistry*, 2017.

Review Article

Dual Roles of Serine-Threonine Kinase Receptor-Associated Protein (STRAP) in Redox-Sensitive Signaling Pathways Related to Cancer Development

Ravi Manoharan [ID],[1] **Hyun-A Seong,**[2] **and Hyunjung Ha** [ID][2]

[1]*Department of Biochemistry, University of Madras, Guindy Campus, Chennai 600025, India*
[2]*Department of Biochemistry, School of Biological Sciences, Chungbuk National University, Cheongju 28644, Republic of Korea*

Correspondence should be addressed to Hyunjung Ha; hyunha@cbnu.ac.kr

Serine-threonine kinase receptor-associated protein (STRAP) is a transforming growth factor β (TGF-β) receptor-interacting protein that has been implicated in both cell proliferation and cell death in response to various stresses. However, the precise roles of STRAP in these cellular processes are still unclear. The mechanisms by which STRAP controls both cell proliferation and cell death are now beginning to be unraveled. In addition to its biological roles, this review also focuses on the dual functions of STRAP in cancers displaying redox dysregulation, where it can behave as a tumor suppressor or an oncogene (i.e., it can either inhibit or promote tumor formation), depending on the cellular context. Further studies are needed to define the functions of STRAP and the redox-sensitive intracellular signaling pathways that enhance either cell proliferation or cell death in human cancer tissues, which may help in the development of effective treatments for cancer.

1. Introduction

Reactive oxygen species (ROS) mediate redox signaling critical for numerous cellular functions [1]. In general, moderate levels of ROS function as signals to activate stress-responsive survival pathways [2]. By contrast, high levels of ROS in cells and tissues can induce cell damage and activate cell death pathways. Therefore, maintenance of moderate levels of ROS in cells is important to support essential signaling pathways without causing cellular damage and death. Under the normal physiological conditions, the redox balance maintains the proper function of redox-sensitive signaling proteins and ensures that cells respond properly to endogenous and exogenous stimuli [3]. However, once redox state is unbalanced, oxidative stress is induced and tumor formation is promoted by initiating an aberrant induction of tumor progression signaling and disruption of cell death signaling [4]. Notably, ROS-sensitive signaling pathways that participate in cell proliferation, differentiation, and cell survival process are frequently elevated in many types of cancers [5].

Cell proliferation and cell death must be regulated to maintain tissue homeostasis in multicellular organisms. This regulation is achieved, in part, through many redox-sensitive intracellular signaling pathways that coordinate the processes of cell proliferation and cell death. These intracellular signaling events are influenced by protein-protein interactions, which involve various signaling molecules and protein modifications, such as protein phosphorylation that either activates or inactivates a target protein to perform a certain function.

Serine-threonine kinase receptor-associated protein (STRAP) was initially identified as a transforming growth factor β (TGF-β) receptor-interacting protein that inhibited TGF-β signaling, probably by stabilizing the association between TGF-β receptors and Smad7 and preventing the binding of Smad2 and Smad3 to TGF-β receptors [6]. STRAP localizes in both the cytoplasm and nucleus [7]. STRAP-deficient mouse embryonic fibroblasts (STRAP$^{-/-}$ MEFs) showed higher levels of TGF-β-mediated transcriptional activation and growth inhibition than their wild-type
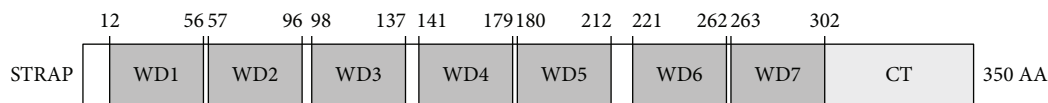
FIGURE 1: Domain structures of STRAP protein. STRAP protein contains seven WD40 repeats (WD1 to 7) and the C-terminal (CT) domain. Numbers indicate the amino acid residues corresponding to the domain boundaries.

counterparts [8]. TGF-β signaling is initiated by the binding of ligands, such as TGF-β1, to type I and II TGF-β receptors on the cell surface. Activated TGF-β receptors directly induce the downstream phosphorylation of the transcription factors Smad2 and Smad3, which undergo rapid homotrimerization and conversion to Co-Smad heterooligomers that contain Smad4. The heteromeric Smad complex then translocates into the nucleus, where it cooperates with other nuclear cofactors to regulate the transcription of target genes [9, 10].

The STRAP gene was first cloned from mouse embryonic [6] and human HepG2 [11] cDNA libraries. The human and mouse STRAP gene encodes a protein of 350 amino acids with a predicted molecular mass of 38 kDa. The full-length STRAP protein includes seven WD40 repeats (WD1 to 7) and a C-terminal (CT) domain (Figure 1). A WD40 repeat is composed of approximately 40 amino acids, often terminating in a tryptophan-aspartic acid (WD) dipeptide [12]. Equally important, WD40 repeats are frequently involved in protein-protein interactions [13]. In fact, the WD40 repeats within STRAP bind to various target proteins, thereby regulating cell proliferation and cell death [14–18]. Moreover, STRAP knockout mice showed embryonic lethality between embryonic days E 10.5 and E 12.5 due to defects in angiogenesis, cardiogenesis, somatogenesis, and neural tube closure, indicating that STRAP is required for normal embryo development [19]. Furthermore, the deregulation of STRAP has been implicated in tumorigenesis [8, 11, 18].

Posttranslational modifications (PTMs), such as protein phosphorylation, are critical for STRAP to exert its biological functions (Figure 2). STRAP stability and activity is mainly regulated by phosphorylation at threonine and serine residues. For instance, phosphorylation of STRAP at Thr[175] and Ser[179] by ASK1 is required for the negative regulation of ASK1 activity [16]. Murine protein serine/threonine kinase 38 (MPK38)-mediated of STRAP at Ser[188] enhanced STRAP stability, thereby inducing the proapoptotic activity of STRAP via redox-sensitive ASK1, TGF-β, p53, and phosphoinositide 3-kinase (PI3K)/3-phosphoinositide-dependent protein kinase-1 (PDK1) signaling [14]. These data indicate that the phosphorylation of STRAP at specific residues plays an important role in determining STRAP-mediated cell proliferation and cell death, although further studies are needed to identify the other phosphorylation sites on STRAP.

Intense research in recent years has revealed that STRAP interacts with many redox-sensitive signaling proteins that regulate various cellular processes such as the cell cycle, proliferation, differentiation, survival, and apoptosis. Under the normal physiological conditions, STRAP promotes cell survival and proliferation and inhibits cell cycle arrest and apoptosis in normal and cancer cells, indicating that STRAP may function as an antiapoptotic protein [8, 16, 20]. By contrast, changes in redox balance induce cell death by STRAP in normal and cancer cells, implying that STRAP may also function as a proapoptotic protein [14, 21]. In this review, we summarize recent progress in understanding the potential cellular and molecular mechanisms of STRAP involved in cell proliferation, survival, and death. We also review the dual roles of STRAP in cancer, which may contribute to the development of a novel therapeutic option for cancer treatment.

2. Regulation of STRAP Activity by Protein-Protein Interactions

2.1. Antiapoptotic Activity of STRAP in Cells. The regulation of cell proliferation in multicellular organisms is a complex process, which is achieved, in part, by crosstalk between cell cycle progression and programmed cell death. STRAP promotes cell proliferation, which may be achieved through the inhibition of apoptosis and the activation of cell growth pathways. Furthermore, numerous STRAP-interacting proteins can positively or negatively regulate STRAP function. The following sections highlight our current understanding of the diverse regulatory mechanisms of STRAP in cell proliferation.

2.1.1. STRAP-Mediated Inhibition of TGF-β Signaling Pathway. Nm23-H1, a tumor suppressor, enhances the STRAP-induced inhibition of TGF-β signaling via a redox-dependent interaction with STRAP [15]. The association of Nm23-H1 with STRAP is mediated by cysteine residues present in each of these two proteins, Cys[145] in Nm23-H1 and Cys[152] and Cys[270] in STRAP. Consistently, this association was dependent on the presence of dithiothreitol or β-mercaptoethanol but not H_2O_2. The coexpression of Nm23-H1 with STRAP promotes the inhibition of TGF-β-induced apoptosis and promotes cell growth by STRAP. Another study suggests that PDK1 also regulates the STRAP-induced inhibition of TGF-β signaling [17]. Notably, PDK1 potentiates the STRAP-induced inhibition of TGF-β signaling by stabilizing the association between Smad7 and TGF-β receptors and preventing the nuclear translocation of Smad3. In addition to Nm23-H1 and PDK1, another STRAP-interacting protein, B-myb, was found to promote the STRAP-induced inhibition of TGF-β signaling. An amino-terminal DNA-binding domain and a region (amino acids 373–468) between the acidic and conserved regions of B-myb mediate the B-myb-STRAP interaction. This binding enhances the STRAP-mediated inhibition of TGF-β signaling by modulating complex formation between TGF-β

(a) Antiapoptotic function of STRAP

(b) Proapoptotic function of STRAP
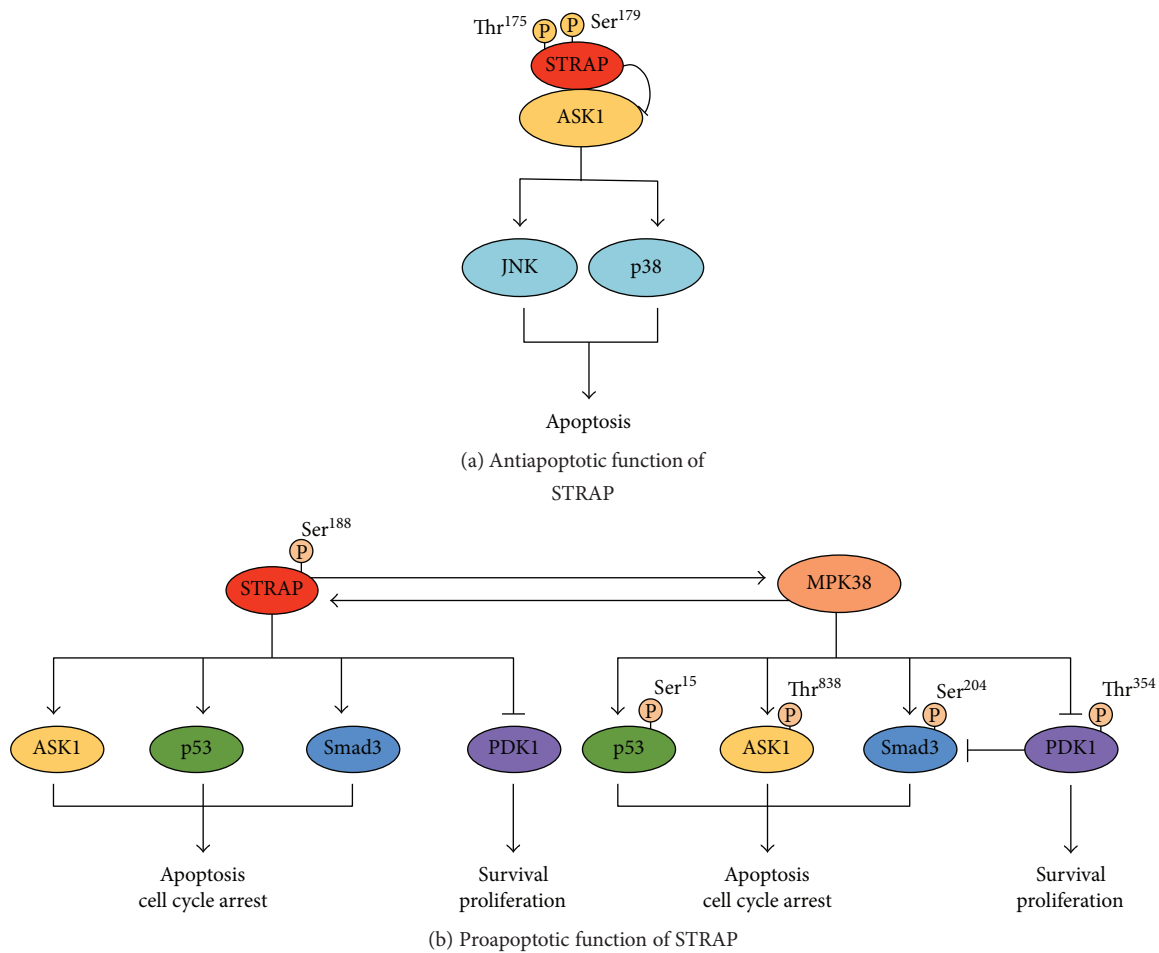
FIGURE 2: Differential regulation of STRAP functions by phosphorylation. (a) STRAP phosphorylation at Thr^{175} and Ser^{179} by ASK1 for STRAP-mediated inhibition of ASK1-induced cell death [16]. (b) STRAP Ser^{188} phosphorylation by MPK38 leads to cell death by modulating both STRAP- and MPK38-mediated ASK1, TGF-β, p53, and PI3K/PDK1 signaling pathways [14]. P: phosphorylated; ASK1: apoptosis signal-regulating kinase 1; PDK1: 3-phosphoinositide-dependent protein kinase-1; MPK38: murine protein serine/threonine kinase 38.

receptors and Smad3 or Smad7. Furthermore, B-myb prevents the translocation of Smad3 in response to TGF-β1 [22]. Collectively, these findings add to the growing evidence that STRAP participates in the negative regulation of TGF-β signaling and subsequently promotes cell growth by directly interacting with many intracellular interacting partners such as Nm23-H1, PDK1, and B-myb.

2.1.2. STRAP-Mediated Inhibition of ASK1 Signaling Pathway. Apart from its role in the TGF-β pathway, as discussed above, STRAP is involved in the suppression of cell death through a redox-dependent interaction with apoptosis signal-regulating kinase 1 (ASK1) [16]. ASK1, a member of the mitogen-activated protein kinase kinase kinase family, is activated by diverse stimuli, including ROS, tumor necrosis factor α (TNF-α), Fas, H_2O_2, and DNA damage. The activation of ASK1 leads to the stimulation of the c-Jun NH_2-terminal kinase (JNK)/p38 signaling pathway, which is essential for cell death [23–25]. ASK1 has emerged as a key regulator of apoptosis, and its inactivation may directly contribute

to the promotion of cell growth. We recently reported that STRAP interacts with ASK1 and subsequently inhibits ASK1 activity. The redox-dependent interaction of ASK1 and STRAP was mediated by cysteine residues present in each of these two proteins, Cys^{1351} and Cys^{1360} in ASK1 and Cys^{152} and Cys^{270} in STRAP. However, this interaction was disrupted by exogenous stimuli, including H_2O_2, TNF-α, endoplasmic reticulum-induced stress (thapsigargin), and calcium overload (ionomycin). Furthermore, ASK1 phosphorylates STRAP at Thr^{175} and Ser^{179}. Phosphorylation at these residues is important for stabilizing complex formation between ASK1 and its negative regulators, thioredoxin and 14-3-3 and/or preventing complex formation between ASK1 and its substrate mitogen-activated protein kinase kinase 3 (MKK3), thereby resulting in the inhibition of ASK1 signaling that regulates JNK and p38 kinases [16]. Consistently, STRAP suppressed H_2O_2-mediated apoptosis in an ASK1 phosphorylation-dependent manner by inhibiting ASK1 activity via direct protein-protein interactions (Figure 2(a)).
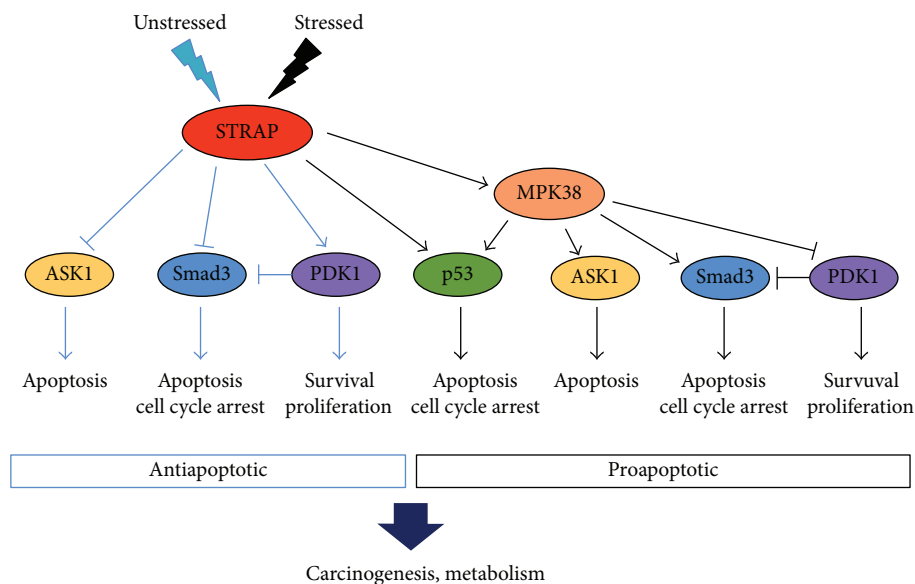
FIGURE 3: Main mechanisms through which STRAP exerts its double-faced role. Under the normal physiological condition, STRAP promotes cell survival and proliferation and inhibits cell cycle arrest and apoptosis, partly by regulating a number of signaling molecules, such as ASK1, Smad3, and PDK1. Upon treatment of cells with ASK1/TGF-β/p53 stimuli, STRAP promotes cell cycle arrest and apoptosis, partly by regulating p53 and MPK38 signaling molecules [14–17, 21, 38–41].

2.1.3. STRAP-Mediated Stimulation of PDK1 Signaling Pathway. PDK1 is a serine-threonine kinase that phosphorylates and activates various downstream targets, including protein kinase C, S6 ribosomal kinase (S6K), glucocorticoid-induced kinase, and AKT1, to induce various cellular responses such as cell survival, proliferation, and differentiation [26–30]. STRAP was also identified as a binding partner of PDK1, an interaction requiring the catalytic domain of PDK1. The interaction between PDK1 and STRAP was increased by insulin treatment but decreased by TGF-β1 treatment. Moreover, STRAP positively regulates the PI3K/PDK1-mediated protection against TNF-α-induced apoptosis, thereby enhancing cell survival [17].

2.1.4. STRAP-Mediated Stimulation of Nm23-H1-Induced Cell Growth. STRAP also regulates cell proliferation by modulating Nm23-H1-mediated signaling. Nm23-H1 was initially identified as a suppressor of metastasis due to its low expression in highly metastatic cell lines and tumors [31]. In addition to its role as a metastatic suppressor, Nm23-H1 also contributes to the proliferation and differentiation of cervical cancer and breast carcinoma cell lines and to the progression of the disease [32, 33]. However, the mechanism by which Nm23-H1 affects cell proliferation is unknown. We recently reported that STRAP interacts with Nm23-H1 in a redox-dependent manner and promotes cell growth. In HaCaT cells, a spontaneously transformed aneuploid immortal keratinocyte cell line, the overexpression of STRAP, but not a STRAP (C152S/C270S) cysteine mutant defective in binding to Nm23-H1, resulted in the promotion of Nm23-H1-induced cell growth [15]. These results indicate the possible involvement of STRAP in Nm23-H1-induced cell growth.

In summary, these findings reveal that STRAP modulates multiple mechanisms that contribute to the reduced sensitivity of cells to apoptosis, thereby promoting cell survival. STRAP is a key signaling molecule that regulates cell proliferation by controlling a broad range of biological processes such as cell growth, cell survival, cell cycle arrest, and apoptosis (Figure 3). The functions of STRAP are achieved through its large number of interacting partners and multiple modes of regulation. Therefore, an important future direction is to identify and characterize additional STRAP-interacting partners to better understand how the specific functions of STRAP are fulfilled through its interacting partners.

2.2. Proapoptotic Activity of STRAP in Cells. Although STRAP promotes cell survival and proliferation by inhibiting apoptosis, recent studies show that STRAP can also mediate cell death depending on the stimulus (Figure 3). Recently, this was supported by reports showing that STRAP associates with the p53 tumor suppressor and subsequently stimulates p53-mediated transcriptional activity [21, 22]. The p53 tumor suppressor is a transcriptional regulator; thus, it can regulate the expression of numerous target genes that induce cell cycle arrest, differentiation, and apoptosis in response to different cellular stresses [34]. p53 activity is modulated by various binding partners that induce the transactivation of target genes and different cellular outcomes [35]. Nm23-H1 and its binding partner STRAP associate with p53 and subsequently potentiate p53-mediated transcription. p53 activation by Nm23-H1 and STRAP is mediated by the removal of mouse double minute 2 homolog (Mdm2), a negative regulator of p53, from the p53-Mdm2 complex. Notably, both Nm23-H1 and STRAP directly interact with the central DNA-binding domain of p53 in a redox-dependent manner,

thereby promoting its functions such as apoptosis and cell cycle arrest [21]. Additional studies suggest that the redox-dependent interaction of STRAP with MPK38 contributes to cell death through ASK1, TGF-β, p53, and PI3K/PDK1 signaling, leading to apoptotic cell death [14]; thus, these findings indicate that STRAP functions as a proapoptotic molecule.

3. Regulation of STRAP Activity by Phosphorylation

Recent studies report that the STRAP-mediated balance between apoptosis and cell proliferation is linked to phosphorylation events, and that STRAP phosphorylation at specific residues plays an important role in determining whether a cell proliferates or dies [14, 16]. MPK38, also known as maternal embryonic leucine zipper kinase, is a member of the AMP-activated protein kinase-related kinase family. It controls a variety of biological processes, including cell proliferation, survival, apoptosis, tumorigenesis, signal transduction, and metabolism [36, 37]. Specifically, MPK38 interacts with and phosphorylates diverse target proteins, thereby regulating their biological functions. For instance, MPK38 phosphorylates ASK1 at Thr^{838} and promotes ASK1-mediated apoptosis [38]. MPK38 also phosphorylates p53 at Ser^{15} [39] and Smad proteins (Ser^{245} of Smad2, Ser^{204} of Smad3, Ser^{343} of Smad4, and Thr^{96} of Smad7) [40], resulting in the stimulation of p53- and TGF-β-induced cell cycle arrest and apoptosis, respectively. In addition, MPK38 inhibits the activity of PDK1 via the phosphorylation of Thr^{354}, which decreases cell survival [41].

3.1. MPK38 Regulates STRAP Activity through Ser^{188} Phosphorylation. Our recent study showed that MPK38 also interacts with STRAP to enhance its apoptotic functions. Phosphorylation of STRAP at Ser^{188} by MPK38 plays a central role in promoting the activation of MPK38-dependent ASK1, TGF-β, and p53 signaling and the inactivation of MPK38-dependent PI3K/PDK1 signaling, eventually leading to apoptotic cell death [14]. STRAP phosphorylation at Ser^{188} by MPK38 also affects complex formation between ASK1 and MKK3, TGF-β receptors and Smad3, p53 and Mdm2, and PDK1 and AKT1, which is critical for the activation of these signaling pathways [14]. Collectively, these studies provide strong evidence that STRAP can affect cell death via two mechanisms by directly regulating these signalings and indirectly regulating these signaling via MPK38 (Figure 2(b)). Although the above study was carried out in cultured cells, a study performed in mice demonstrated that the phosphorylation of STRAP at Ser^{188} also associates with cell proliferation and cell death through these signalings, resulting in apoptotic cell death [14].

3.2. ASK1 Regulates STRAP Activity through Thr^{175}/Ser^{179} Phosphorylation. The phosphorylation of STRAP at specific residues dictates whether the protein will play a role in cell proliferation or cell death. Different upstream signals may regulate STRAP and activate different intracellular signaling pathways, thus leading to distinct cell functions. For example,

STRAP phosphorylation at Thr^{175} and Ser^{179} by ASK1 promotes cell survival and cell proliferation by suppressing apoptosis [16], whereas increased stress induces cell death, which is mediated by MPK38 phosphorylation (Figure 2). Further studies are needed to understand the roles of STRAP in cell proliferation and cell death.

4. Roles of STRAP in Cancer

4.1. Tumor-Promoting Activity of STRAP in Tumor Development

4.1.1. Inhibition of TGF-β Signaling Pathway by STRAP. In general, a balance among cell proliferation, survival, and apoptosis maintains cellular homeostasis [42]. Cancers can occur when this balance is disrupted, either by an increase in cell proliferation or a decrease in cell death [43]. Mounting evidence indicates that STRAP can promote tumor progression by inhibiting apoptosis and activating cell proliferation. Furthermore, STRAP protein expression is elevated in 60% of colorectal, 78% of lung, and 46% of breast carcinomas [8, 11, 44]. The overexpression of STRAP in different cell lines promotes cell proliferation and tumorigenicity in *in vitro* and *in vivo* experiments. For example, the knockdown of endogenous STRAP by STRAP-specific siRNAs decreases tumorigenicity, which clearly supports the role of STRAP in carcinogenesis [8]. Given that TGF-β acts as a tumor suppressor in normal cells, redox-sensitive TGF-β signaling exerts the tumor suppressive effects of TGF-β, thereby inhibiting tumor development [45]. Furthermore, the overexpression of STRAP inhibits TGF-β-mediated growth suppression by increasing Smad7 binding to TGF-β receptors, which induces cell proliferation and tumor development [7]. Studies in various cancer cell lines also demonstrate that STRAP augments cell proliferation and oncogenesis by blocking the antiproliferative effects mediated by TGF-β signaling. Equally important, STRAP$^{-/-}$ MEFs show enhanced TGF-β-mediated transcriptional activation and growth inhibition. For example, STRAP overexpression alleviates the TGF-β-induced inhibition of cell growth and induces the tumorigenicity of lung adenocarcinoma (A549) and colon adenocarcinoma (FET) cells [8], indicating an important role of STRAP in tumor development through negative regulation of TGF-β-mediated growth suppression.

4.1.2. Stimulation of Notch and Wnt/β-Catenin Signaling Pathways by STRAP. A recent study also implicates that STRAP has a role in the progression of colorectal cancers (CRCs). STRAP expression was elevated in all stages of colorectal cancer, and the tumor growth was inhibited in heterozygous STRAP knockout mice. Importantly, STRAP activated Notch signaling by inhibiting polycomb repressive complex 2 assembly, leading to colon carcinogenesis [46]. STRAP also promotes Wnt/β-catenin signaling, leading to the development and progression of CRC. Notably, STRAP binds to GSK-3β and stabilizes β-catenin by inhibiting its ubiquitin-dependent degradation, resulting in the stimulation of Wnt/β-catenin signaling in CRC cells. Consistent

with this observation, the knockdown of STRAP in murine colon carcinoma cell lines inhibited tumorigenesis, invasion, and metastasis, demonstrating that STRAP increases the invasion and metastasis of CRC partly via the inhibition of the ubiquitin-dependent degradation of β-catenin and the enhancement of Wnt/β-catenin signaling [47].

4.1.3. Downregulation of E-cadherin and p21^{Cip1} Promoter Activities by STRAP.

Analysis of clinical data from the cancer genome atlas reveals that the level of STRAP mRNA expression is upregulated in lung adenocarcinoma with metastasis, strongly implying that STRAP participates in the pathology of lung adenocarcinoma metastasis [48]. In addition, STRAP inhibits Sp1-dependent transcription, resulting in the downregulation of the tumor suppressor genes E-cadherin and p21^{Cip1}, thereby promoting tumor progression in non-small-cell lung cancers. Therefore, the increased expression of STRAP in lung cancer contributes to the downregulation of E-cadherin and p21^{Cip1}, which in turn leads to tumor progression [49].

4.1.4. Enhancement of PDK1 Signaling Pathway by STRAP.

Apoptosis, the major form of cellular suicide, is central to various physiological processes, including the maintenance of homeostasis in multicellular organisms. The inhibition of apoptosis can activate cell survival factors that facilitate the continuous proliferation in cancer cells [42]. STRAP promotes tumor progression through the inhibition of apoptosis and the activation of cell survival [15, 16]. The activation of PDK1 signaling has been implicated in cell proliferation, survival, and tumorigenesis [50]. PDK1 also inhibits TGF-β-mediated cell growth arrest and apoptosis by directly interacting with Smad proteins [51], revealing that PDK1 inhibition may be beneficial for tumor suppression. Thus, PDK1 inhibitors are currently being tested as anticancer drugs [52, 53]. STRAP also interacts with PDK1 and promotes the phosphorylation of PDK1 substrates, including S6K, AKT1, and Bad, leading to enhanced cell survival [17]. STRAP also indirectly inhibits cell cycle arrest and apoptosis by promoting the PDK1-mediated suppression of TGF-β signaling, resulting in enhanced cell survival [17]. These results clearly indicate that STRAP promotes cell survival and cell growth via PDK1, thereby contributing to tumor progression.

4.1.5. Stimulation of Nm23-H1 Activity and Inhibition of ASK1 Activity by STRAP.

STRAP was found to potentiate the Nm23-H1-induced growth of HaCaT cells through a redox-dependent interaction with Nm23-H1 [15]. Nm23-H1 was previously reported to affect proliferation and differentiation of cervical cancer and breast carcinoma cell lines [32, 33], suggesting that STRAP may also contribute to the progression of cervical and breast tumors. However, the exact nature of this mechanism is unknown, and further studies are needed to evaluate STRAP and Nm23-H1 activities during tumor progression. On the other hand, ASK1 functions as a tumor suppressor due to its ability to induce apoptosis of both breast cancer and lung adenocarcinoma cell lines [54, 55]. STRAP interacts with ASK1, which inhibits its kinase activity and the subsequent ASK1-induced apoptosis, thereby promoting cell survival and cell growth [16]. Overall, high level of STRAP expression in various cancers implies that STRAP has a role in tumor growth and aggressiveness, and therefore, inhibition of STRAP may be an attractive cancer therapeutic target.

4.2. Tumor Suppressive Activity of STRAP during Tumorigenesis.

STRAP overexpression associates with the progression of many different types of tumors, although several investigators report contradictory results. For example, STRAP directly regulates the most important tumor suppressor, p53, in cervical cancer (HeLa), colorectal carcinoma (HCT116), and breast cancer (MCF7) cell lines. The overexpression of STRAP leads to increased p53-induced apoptosis and decreased cell proliferation, whereas the loss of STRAP has the opposite effects, indicating that STRAP plays a key role in tumor suppression [21, 22]. Given that p53 plays a critical role in numerous cellular processes, including cell cycle arrest, differentiation, apoptosis, and tumor suppression, the loss of p53 function is a common feature of human cancers [56]. Functionally, STRAP and its interacting partner Nm23-H1 directly bind to and stabilize p53 by dissociating Mdm2, resulting in the induction of p53-induced apoptosis and cell cycle arrest [21]. These results indicate that STRAP proteins are also responsible for tumor suppression.

Equally important, the PTM of STRAP by protein kinases, such as ASK1 and MPK38, plays an important role in determining the pro- or antiapoptotic function of STRAP. For example, STRAP phosphorylation at Thr^{175} and Ser^{179} by ASK1 is required for STRAP-mediated inhibition of ASK1-induced cell death [16]. By contrast, MPK38-mediated STRAP phosphorylation at Ser^{188} contributes to the proapoptotic function of STRAP by modulating STRAP-dependent ASK1, TGF-β, p53, and PI3K/PDK1 signaling [14]. However, further studies are needed to clarify the mechanisms regulating STRAP function.

5. Conclusions

STRAP is an even more complex regulator of cellular functions than was previously thought, and its roles in the regulation of the redox-sensitive TGF-β cascade and the promotion of cell growth continue to be investigated. Apart from its role in the TGF-β cascade, additional details on the function and regulation of STRAP are rapidly emerging. For example, recent studies show that STRAP plays a critical role in the regulation of both cell proliferation and cell death in response to various stresses, accompanied by changes in the redox status, by interacting with multiple target proteins. Studies on STRAP-mediated redox signaling that promotes either cell proliferation or cell death, as well as studies on the significance of phosphorylation in these events, are at best preliminary. Therefore, further studies are needed to identify additional STRAP phosphorylation sites involved in the regulation of cell proliferation and cell death.

Although recent studies report conflicting results on the roles of STRAP in cancer, the tumor-promoting effects of STRAP, including the induction of cell proliferation and cell survival and the inhibition of apoptosis, were observed in numerous cancer cells. However, the tumor suppressive effects of STRAP have not yet been confirmed in cancer tissues, although the proapoptotic function of STRAP was observed in normal and cancer cells. Hence, further studies investigating the dual functions of STRAP, as well as its regulation by redox-dependent signaling, which induces either cell death or cell proliferation in human cancers, are needed because they may contribute to the development of more effective cancer treatments.

Conflicts of Interest

The authors declared no conflict of interest.

Acknowledgments

References

[1] J. Zhang, X. Wang, V. Vikash et al., "ROS and ROS-mediated cellular signaling," *Oxidative Medicine and Cellular Longevity*, vol. 2016, Article ID 4350965, 18 pages, 2016.

[2] B. Marengo, M. Nitti, A. L. Furfaro et al., "Redox homeostasis and cellular antioxidant systems: crucial players in cancer growth and therapy," *Oxidative Medicine and Cellular Longevity*, vol. 2016, Article ID 6235641, 16 pages, 2016.

[3] D. Trachootham, W. Lu, M. A. Ogasawara, N. Rivera-Del Valle, and P. Huang, "Redox regulation of cell survival," *Antioxidants & Redox Signaling*, vol. 10, no. 8, pp. 1343–1374, 2008.

[4] A. Acharya, I. Das, D. Chandhok, and T. Saha, "Redox regulation in cancer: a double-edged sword with therapeutic potential," *Oxidative Medicine and Cellular Longevity*, vol. 3, no. 1, pp. 23–34, 2010.

[5] P. Storz, "Reactive oxygen species in tumor progression," *Frontiers in Bioscience*, vol. 10, no. 1–3, pp. 1881–1896, 2005.

[6] P. K. Datta, A. Chytil, A. E. Gorska, and H. L. Moses, "Identification of STRAP, a novel WD domain protein in transforming growth factor-β signaling," *The Journal of Biological Chemistry*, vol. 273, no. 52, pp. 34671–34674, 1998.

[7] P. K. Datta and H. L. Moses, "STRAP and Smad7 synergize in the inhibition of transforming growth factor β signaling," *Molecular and Cellular Biology*, vol. 20, no. 9, pp. 3157–3167, 2000.

[8] S. K. Halder, G. Anumanthan, R. Maddula et al., "Oncogenic function of a novel WD-domain protein, STRAP, in human carcinogenesis," *Cancer Research*, vol. 66, no. 12, pp. 6156–6166, 2006.

[9] J. Massagué, "TGF-β signalling in context," *Nature Reviews Molecular Cell Biology*, vol. 13, no. 10, pp. 616–630, 2012.

[10] Y. Shi and J. Massagué, "Mechanisms of TGF-β signaling from cell membrane to the nucleus," *Cell*, vol. 113, no. 6, pp. 685–700, 2003.

[11] S. Matsuda, R. Katsumata, T. Okuda et al., "Molecular cloning and characterization of human MAWD, a novel protein containing WD-40 repeats frequently overexpressed in breast cancer," *Cancer Research*, vol. 60, no. 1, pp. 13–17, 2000.

[12] C. U. Stirnimann, E. Petsalaki, R. B. Russell, and C. W. Müller, "WD40 proteins propel cellular networks," *Trends in Biochemical Sciences*, vol. 35, no. 10, pp. 565–574, 2010.

[13] D. Li and R. Roberts, "WD-repeat proteins: structure characteristics, biological function, and their involvement in human diseases," *Cellular and Molecular Life Sciences*, vol. 58, no. 14, pp. 2085–2097, 2001.

[14] H.-A. Seong, R. Manoharan, and H. Ha, "A crucial role for the phosphorylation of STRAP at Ser188 by MPK38 in STRAP-dependent cell death through ASK1, TGF-β, p53, and PI3K/PDK1 signaling pathways," *Cell Cycle*, vol. 13, no. 21, pp. 3357–3374, 2014.

[15] H.-A. Seong, H. Jung, and H. Ha, "Nm23-H1 tumor suppressor physically interacts with serine-shreonine kinase receptor-associated protein, a transforming growth factor-β (TGF-β) receptor interacting protein, and negatively regulates TGF-β signaling," *The Journal of Biological Chemistry*, vol. 282, no. 16, pp. 12075–12096, 2007.

[16] H. Jung, H.-A. Seong, R. Manoharan, and H. Ha, "Serine-threonine kinase receptor-associated protein inhibits apoptosis signal-regulating kinase 1 function through direct interaction," *The Journal of Biological Chemistry*, vol. 285, no. 1, pp. 54–70, 2010.

[17] H.-A. Seong, H. Jung, H.-S. Choi, K.-T. Kim, and H. Ha, "Regulation of transforming growth factor-β signaling and PDK1 kinase activity by physical interaction between PDK1 and serine-threonine kinase receptor-associated protein," *The Journal of Biological Chemistry*, vol. 280, no. 52, pp. 42897–42908, 2005.

[18] J. Reiner and P. K. Datta, "TGF-beta-dependent and -independent roles of STRAP in cancer," *Frontiers in Bioscience*, vol. 16, no. 1, pp. 105–115, 2011.

[19] W. V. Chen, J. Delrow, P. D. Corrin, J. P. Frazier, and P. Soriano, "Identification and validation of PDGF transcriptional targets by microarray-coupled gene-trap mutagenesis," *Nature Genetics*, vol. 36, no. 3, pp. 304–312, 2004.

[20] G. Anumanthan, S. K. Halder, D. B. Friedman, and P. K. Datta, "Oncogenic serine-threonine kinase receptor-associated protein modulates the function of Ewing sarcoma protein through a novel mechanism," *Cancer Research*, vol. 66, no. 22, pp. 10824–10832, 2006.

[21] H. Jung, H.-A. Seong, and H. Ha, "Nm23-H1 tumor suppressor and its interacting partner STRAP activate p53 function," *The Journal of Biological Chemistry*, vol. 282, no. 48, pp. 35293–35307, 2007.

[22] H.-A. Seong, R. Manoharan, and H. Ha, "B-MYB positively regulates serine-threonine kinase receptor-associated protein (STRAP) activity through direct interaction," *The Journal of Biological Chemistry*, vol. 286, no. 9, pp. 7439–7456, 2011.

[23] H. Y. Chang, H. Nishitoh, X. Yang, H. Ichijo, and D. Baltimore, "Activation of apoptosis signal-regulating kinase 1 (ASK1) by the adapter protein Daxx," *Science*, vol. 281, no. 5384, pp. 1860–1863, 1998.

[24] H. Ichijo, E. Nishida, K. Irie et al., "Induction of apoptosis by ASK1, a mammalian MAPKKK that activates SAPK/JNK and p38 signaling pathways," *Science*, vol. 275, no. 5296, pp. 90–94, 1997.

[25] M. Saitoh, H. Nishitoh, M. Fujii et al., "Mammalian thiore-doxin is a direct inhibitor of apoptosis signal-regulating kinase (ASK) 1," *The EMBO Journal*, vol. 17, no. 9, pp. 2596–2606, 1998.

[26] B. Vanhaesebroeck and D. R. Alessi, "The PI3K-PDK1 connection: more than just a road to PKB," *Biochemical Journal*, vol. 346, Part 3, pp. 561–576, 2000.

[27] E. Fayard, L. A. Tintignac, A. Baudry, and B. A. Hemmings, "Protein kinase B/Akt at a glance," *Journal of Cell Science*, vol. 118, no. 24, pp. 5675–5678, 2005.

[28] H. J. Hinton, D. R. Alessi, and D. A. Cantrell, "The serine kinase phosphoinositide-dependent kinase 1 (PDK1) regulates T cell development," *Nature Immunology*, vol. 5, no. 5, pp. 539–545, 2004.

[29] C. K. Kikani, L. Q. Dong, and F. Liu, ""New"-clear functions of PDK1: beyond a master kinase in the cytosol?," *Journal of Cellular Biochemistry*, vol. 96, no. 6, pp. 1157–1162, 2005.

[30] A. Mora, D. Komander, D. M. F. van Aalten, and D. R. Alessi, "PDK1, the master regulator of AGC kinase signal transduction," *Seminars in Cell & Developmental Biology*, vol. 15, no. 2, pp. 161–170, 2004.

[31] E. F. Michelotti, S. Sanford, J. M. P. Freije, N. J. MacDonald, P. S. Steeg, and D. Levens, "Nm23/PuF does not directly stimulate transcription through the CT element *in vivo*," *The Journal of Biological Chemistry*, vol. 272, no. 36, pp. 22526–22530, 1997.

[32] Y. Yang, S. Lu, M. F. Li, and Z. H. Wang, "Effects of tumor metastasis suppressor gene nm23-H1 on invasion and proliferation of cervical cancer cell lines," *Ai Zheng*, vol. 28, no. 7, pp. 702–707, 2009.

[33] A. Leone, U. Flatow, K. VanHoutte, and P. S. Steeg, "Transfection of human nm23-H1 into the human MDA-MB-435 breast carcinoma cell line: effects on tumor metastatic potential, colonization and enzymatic activity," *Oncogene*, vol. 8, no. 9, pp. 2325–2333, 1993.

[34] O. Laptenko and C. Prives, "Transcriptional regulation by p53: one protein, many possibilities," *Cell Death & Differentiation*, vol. 13, no. 6, pp. 951–961, 2006.

[35] R. Beckerman and C. Prives, "Transcriptional regulation by P53," *Cold Spring Harbor Perspectives in Biology*, vol. 2, no. 8, article a000935, 2010.

[36] R. Ganguly, A. Mohyeldin, J. Thiel, H. I. Kornblum, M. Beullens, and I. Nakano, "MELK—a conserved kinase: functions, signaling, cancer, and controversy," *Clinical and Translational Medicine*, vol. 4, no. 1, p. 11, 2015.

[37] P. Jiang and D. Zhang, "Maternal embryonic leucine zipper kinase (MELK): a novel regulator in cell cycle control, embryonic development, and cancer," *International Journal of Molecular Sciences*, vol. 14, no. 12, pp. 21551–21560, 2013.

[38] H. Jung, H.-A. Seong, and H. Ha, "Murine protein serine/threonine kinase 38 activates apoptosis signal-regulating kinase 1 via Thr^{838} phosphorylation," *The Journal of Biological Chemistry*, vol. 283, no. 50, pp. 34541–34553, 2008.

[39] H.-A. Seong and H. Ha, "Murine protein serine-threonine kinase 38 activates p53 function through Ser^{15} phosphorylation," *The Journal of Biological Chemistry*, vol. 287, no. 25, pp. 20797–20810, 2012.

[40] H.-A. Seong, H. Jung, and H. Ha, "Murine protein serine/threonine kinase 38 stimulates TGF-β signaling in a

kinase-dependent manner via direct phosphorylation of Smad proteins," *The Journal of Biological Chemistry*, vol. 285, no. 40, pp. 30959–30970, 2010.

[41] H.-A. Seong, H. Jung, R. Manoharan, and H. Ha, "PDK1 protein phosphorylation at Thr^{354} by murine protein serine-threonine kinase 38 contributes to negative regulation of PDK1 protein activity," *The Journal of Biological Chemistry*, vol. 287, no. 25, pp. 20811–20822, 2012.

[42] S. Kalimuthu and K. Se-Kwon, "Cell survival and apoptosis signaling as therapeutic target for cancer: marine bioactive compounds," *International Journal of Molecular Sciences*, vol. 14, no. 2, pp. 2334–2354, 2013.

[43] R. Gerl and D. L. Vaux, "Apoptosis in the development and treatment of cancer," *Carcinogenesis*, vol. 26, no. 2, pp. 263–270, 2005.

[44] C. J. Kim, B. J. Choi, J. H. Song et al., "Overexpression of serine-threonine receptor kinase-associated protein in colorectal cancers," *Pathology International*, vol. 57, no. 4, pp. 178–182, 2007.

[45] J. J. Lebrun, "The dual role of TGFβ in human cancer: from tumor suppression to cancer metastasis," *ISRN Molecular Biology*, vol. 2012, Article ID 381428, 28 pages, 2012.

[46] L. Jin, T. Vu, G. Yuan, and P. K. Datta, "STRAP promotes stemness of human colorectal cancer via epigenetic regulation of the NOTCH pathway," *Cancer Research*, vol. 77, no. 20, pp. 5464–5478, 2017.

[47] G. Yuan, B. Zhang, S. Yang et al., "Novel role of STRAP in progression and metastasis of colorectal cancer through Wnt/β-catenin signaling," *Oncotarget*, vol. 7, no. 13, pp. 16023–16037, 2016.

[48] Y. Wang, R. Han, Z. Chen et al., "A transcriptional miRNA-gene network associated with lung adenocarcinoma metastasis based on the TCGA database," *Oncology Reports*, vol. 35, no. 4, pp. 2257–2269, 2016.

[49] L. Jin and P. K. Datta, "Oncogenic STRAP functions as a novel negative regulator of E-cadherin and p21^{Cip1} by modulating the transcription factor Sp1," *Cell Cycle*, vol. 13, no. 24, pp. 3909–3920, 2014.

[50] J. H. Choi, Y. R. Yang, S. K. Lee et al., "Potential inhibition of PDK1/Akt signaling by phenothiazines suppresses cancer cell proliferation and survival," *Annals of New York Academy of Sciences*, vol. 1138, no. 1, pp. 393–403, 2008.

[51] H.-A. Seong, H. Jung, K.-T. Kim, and H. Ha, "3-phosphoinositide-dependent PDK1 negatively regulates transforming growth factor-β-induced signaling in a kinase-dependent manner through physical interaction with Smad proteins," *The Journal of Biological Chemistry*, vol. 282, no. 16, pp. 12272–12289, 2007.

[52] C. Garcia-Echeverria and W. R. Sellers, "Drug discovery approaches targeting the PI3K/Akt pathway in cancer," *Oncogene*, vol. 27, no. 41, pp. 5511–5526, 2008.

[53] S. F. Barnett, D. Defeo-Jones, S. Fu et al., "Identification and characterization of pleckstrin-homology-domain-dependent and isoenzyme-specific Akt inhibitors," *Biochemical Journal*, vol. 385, no. 2, Part 2, pp. 399–408, 2005.

[54] O. Meurette, S. Stylianou, R. Rock, G. M. Collu, A. P. Gilmore, and K. Brennan, "Notch activation induces Akt signaling via an autocrine loop to prevent apoptosis in breast epithelial cells," *Cancer Research*, vol. 69, no. 12, pp. 5015–5022, 2009.

[55] C. T. Kuo, B. C. Chen, C. C. Yu et al., "Apoptosis signal-regulating kinase 1 mediates denbinobin-induced apoptosis in human lung adenocarcinoma cells," *Journal of Biomedical Science*, vol. 16, no. 1, p. 43, 2009.

[56] F. Toledo and G. M. Wahl, "Regulating the p53 pathway: *in vitro* hypotheses, *in vivo* veritas," *Nature Reviews Cancer*, vol. 6, no. 12, pp. 909–923, 2006.

Review Article

Altered Redox Homeostasis in Branched-Chain Amino Acid Disorders, Organic Acidurias, and Homocystinuria

Eva Richard, Lorena Gallego-Villar, Ana Rivera-Barahona, Alfonso Oyarzábal, Belén Pérez, Pilar Rodríguez-Pombo, and Lourdes R. Desviat (ORCID)

Centro de Biología Molecular Severo Ochoa UAM-CSIC, Centro de Diagnóstico de Enfermedades Moleculares (CEDEM), CIBERER, IdiPaz, Universidad Autónoma de Madrid, Madrid, Spain

Correspondence should be addressed to Lourdes R. Desviat; lruiz@cbm.csic.es

Inborn errors of metabolism (IEMs) are a group of monogenic disorders characterized by dysregulation of the metabolic networks that underlie development and homeostasis. Emerging evidence points to oxidative stress and mitochondrial dysfunction as major contributors to the multiorgan alterations observed in several IEMs. The accumulation of toxic metabolites in organic acidurias, respiratory chain, and fatty acid oxidation disorders inhibits mitochondrial enzymes and processes resulting in elevated levels of reactive oxygen species (ROS). In other IEMs, as in homocystinuria, different sources of ROS have been proposed. In patients' samples, as well as in cellular and animal models, several studies have identified significant increases in ROS levels along with decreases in antioxidant defences, correlating with oxidative damage to proteins, lipids, and DNA. Elevated ROS disturb redox-signaling pathways regulating biological processes such as cell growth, differentiation, or cell death; however, there are few studies investigating these processes in IEMs. In this review, we describe the published data on mitochondrial dysfunction, oxidative stress, and impaired redox signaling in branched-chain amino acid disorders, other organic acidurias, and homocystinuria, along with recent studies exploring the efficiency of antioxidants and mitochondria-targeted therapies as therapeutic compounds in these diseases.

1. Introduction

A growing body of evidence indicates that disruption of redox homeostasis is involved in the pathophysiology of several inborn errors of metabolism (IEMs), including organic acidurias, respiratory chain disorders, fatty acid oxidation disorders, and aminoacidopathies [1–7]. IEMs are defined as genetic defects that affect a metabolic pathway or cellular process and are commonly characterized by a specifically altered biochemical profile that guides the diagnosis [8]. They belong to the category of rare diseases (defined by the EU as those with an incidence lower than 1 in 2000), and most of them are inherited in autosomal recessive fashion. In the classic IEMs, pathology results from accumulation of toxic metabolites and/or from the deficiency or absence of

substrates necessary to perform normal cellular functions. Many of them are systemic, and in most cases, they affect the central nervous system [8].

Several IEMs share common pathomechanisms as a consequence of the accumulation of toxic metabolites; these inhibit specific mitochondrial enzymes and processes, resulting in mitochondrial dysfunction, impaired energy metabolism, increased reactive oxygen species (ROS) levels, altered antioxidant response capability, and increased oxidative stress, resulting in damage to DNA, proteins, and lipids [2, 3, 9, 10]. The brain and heart, frequently affected in IEMs, are energy-demanding organs highly sensitive to oxidative stress due to their high rate of oxygen consumption, substantial iron and polyunsaturated lipid contents, and relatively low activity of their antioxidant defences and repair enzymes

[11]. Metabolic profiling of oxidative stress in IEM patients' samples has documented the correlation between oxidative stress markers and biochemical and clinical parameters [12, 13].

Mitochondria, which are the major energy producers in the cell, and where many important metabolic pathways take place, are the major ROS producers [14]. Mitochondrial ROS is generated, in the form of superoxide anion (O_2^-), at complexes I and III of the electron transport chain and are rapidly converted to hydrogen peroxide (H_2O_2) by the enzyme superoxide dismutase (MnSOD). Mitochondrial matrix complexes such as pyruvate dehydrogenase, alpha-ketoglutarate dehydrogenase, or branched-chain alpha-ketoacid dehydrogenase (BCKDH) can also generate O_2^-. Other cellular sources of ROS exist, and an active interplay between all of them has been documented [15]. To avoid the noxious consequences of ROS, mitochondria express a variety of antioxidant enzymes, including MnSOD, peroxiredoxins, and glutathione peroxidase (GPX) [16]. Among the nonprotein antioxidants, glutathione (L-γ-glutamyl-L-cysteinylglycine) represents the main antioxidant defence present in the cell. An increase in ROS levels correlates with a decrease in reduced glutathione (GSH). Thus, the ratio of oxidized (GSSG) to reduced (GSH) is indicative of cellular redox balance and has been used as a biomarker of oxidative stress in different diseases including IEMs [17–20].

At physiological concentrations, ROS are recognized to act as signaling molecules modifying specific proteins that will transmit a message modulating specific cellular pathways, in what is known as redox signaling [15]. Well-known examples include redox-sensitive changes in conformation and function of receptors, transcription factors, kinases, and phosphatases, which lead to a specific cellular response [15]. At high concentrations, ROS may cause extensive damage to cells, by peroxidation of lipids, carbonylation of proteins, or DNA base oxidation. These toxic effects can disrupt mitochondrial function causing a further increase in ROS production, thus forming a vicious cycle. In cases of chronic, high levels of ROS production, apoptosis or autophagy/mitophagy processes are triggered [16]. All this has led to redefine the concept of oxidative stress, initially conceived as an alteration in the balance between oxidant and antioxidant molecules, to a disturbance in redox signaling with possible molecular and/or cellular damage [15].

In the mitochondria, H_2O_2 is the most likely signal involved in redox signaling and in transcription regulation, through thiol/disulfide exchange reactions [21]. Signal transduction by H_2O_2 may occur via peroxiredoxin-2 and transcription factor STAT3 [22]. H_2O_2 acts on redox-sensitive targets such as transcription factor NRF2 involved in antioxidant response, NFκB protein complex involved in inflammation, stress kinase JNK, and insulin-like growth factor IGF1, linking energy metabolism and inflammatory responses [23]. Oxidative stress and bioenergetics deficits trigger signaling through mitophagy receptors such as ATG32, BCL2-L-13, and FUNDC1, leading to the elimination of damaged mitochondria [24].

In IEMs, as in cardiovascular and neurodegenerative diseases, the production of pathological amounts of ROS resulting in oxidative damage may indeed disturb redox signaling and induce cell stress responses, which may in some cases lead to cell death [1, 25]. However, the exact molecular mechanisms and cellular pathways involved in this progression are scarcely characterized. In some IEMs, specific activation of stress kinases p38 and JNK and of autophagy/mitophagy and apoptotic pathways has been documented [6, 7, 26, 27].

A recent review provided insight into the adaptive stress responses that operate in IEMs, linking mitochondrial biogenesis to cellular antioxidant, anti-inflammatory, protein quality control, and autophagy functions [1]. As a first line of cellular responses to oxidative stress, the expression of antioxidant enzymes and heat-shock proteins increases, along with an upregulation of glycolysis and activation of mitochondrial biogenesis, as occurs in multiple acyl-CoA dehydrogenation deficiency [28]. ROS-mediated activation of AMP-activated protein kinase (AMPK) could be the link between metabolic reprogramming, mitochondrial biogenesis, and activation of cellular stress repair pathways, followed by the progression to proinflammatory responses controlled by signaling pathways mTOR/HIF-1α/NFκB [1].

The presence of interconnected redox-signaling pathways and their alterations in disease contributing to the pathogenesis suggests that specific compounds targeting excessive ROS or mitochondrial dysfunction may show therapeutic potential. This has been explored in some IEMs, in which several antioxidants or mitochondrial biogenesis activators have proven effective in cellular and/or animal models of disease [29–32]. However, clinical efficacy of these approaches remains unproven. In addition, the possible interference of these therapies with cellular redox signaling should be taken into account for careful design and appropriate clinical testing.

In this study, we describe sources of ROS in specific IEMs; we summarize the available data on altered redox homeostasis and oxidative damage in patients' samples and in animal models of disease; we discuss potential implications for redox signaling and describe the recent advances in antioxidant- and mitochondria-targeted therapies for these pathologies. To this aim, we have focused in selected branched-chain amino acid disorders, organic acidurias, and defects leading to the accumulation of homocysteine (homocystinuria) (Figure 1). For other IEMs, namely inherited mitochondrial diseases and fatty acid oxidation disorders, the readers are referred to recent reviews [9, 33].

2. Branched-Chain Amino Acid Disorders and Organic Acidurias

Branched-chain amino acids (BCAAs: Val, Ile, Leu) are essential amino acids not only necessary for protein synthesis but also key nitrogen donors involved in interorgan and intercellular nitrogen shuttling [34] and key nutrient signals involved in important functions including food intake regulation. Leu has long been known as an anabolic nutrient-signaling molecule that stimulates protein synthesis by activation of the mTORC1 pathway in selected tissues [35]. Recently, mitochondrial sirtuin 4 (SIRT4), acting as a lysine
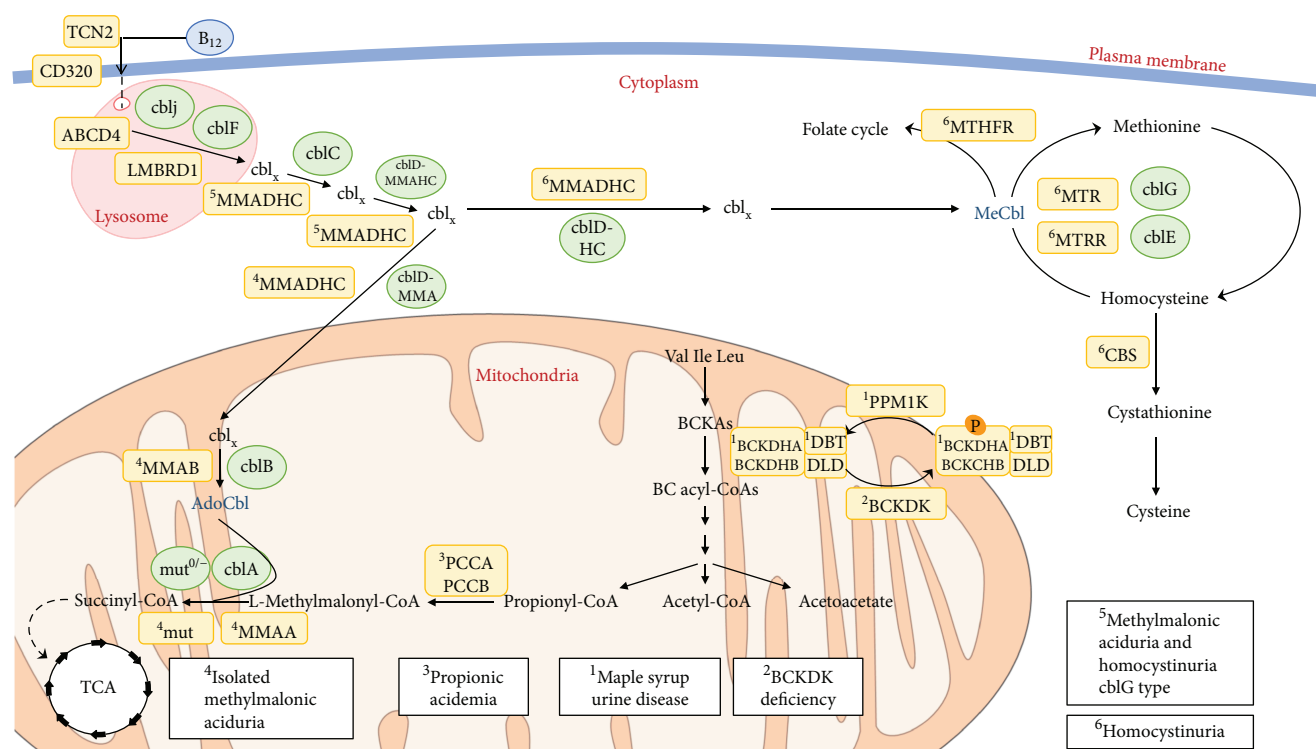
FIGURE 1: Schematics of the metabolic pathways and their cellular localization affected in branched-chain organic acidurias and homocystinuria disorders mentioned in this work. The affected genes and corresponding diseases (in boxes) are shown for each pathway.

deacylase, has been reported to control Leu catabolism and insulin secretion, reinforcing the hypothesis of a possible link between BCAA metabolism and insulin secretion [36]. All these data underscore the critical role of BCAAs metabolism in humans' health and disease, as was evidenced with the characterization of maple syrup urine disease (MSUD) [37] and, more recently, with the description of branched-chain ketoacid dehydrogenase kinase (BCKDK) deficiency [38, 39].

Organic acidurias/acidemias are described as IEMs affecting enzymes, receptors, or transport proteins in the catabolic pathway of amino acids and odd-chain fatty acids and characterized by the abnormal accumulation of organic acids in body fluids [40]. More than 65 organic acidurias have been described, with MSUD, propionic acidemia (PA), and methylmalonic acidurias (MMA) among the most prevalent. A secondary mitochondrial dysfunction induced by accumulating toxic metabolites is an important pathomechanism in these disorders [10]. Patients with organic acidurias show elevated plasma protein carbonyls and lower GSH levels in leukocytes [20]. Here we briefly summarize the published data on branched-chain amino acid disorders and specific organic acidurias with a profile of altered redox homeostasis.

2.1. Disorders Involving Branched-Chain α-Ketoacid Dehydrogenase. MSUD (MIM #248600), caused by the deficiency of branched-chain α-ketoacid dehydrogenase complex (BCKDHc) activity, is characterized by elevated levels of BCAAs and their corresponding α-keto-acids (BCKAs)

in body fluids and tissues, resulting in complex neurological phenotypes [37]. As the important gatekeeping enzyme that it is, BCKDHc is regulated by reversible phosphorylation catalyzed by a specific BCKD kinase (BCKDK) that inhibits BCKDHc function, halting the catabolic pathway of BCAAs [41], and a dephosphorylation catalyzed by the mitochondrial protein phosphatase PP2Cm (encoded by the *PPM1K* gene) that stimulates BCKDHc activity [42]. Optimal BCKDHc activity necessary to maintain BCAA homeostasis is achieved by the coordinated response of BCKDK and PP2Cm activities. Blockage or unrestrained BCAA metabolism through BCKDHc leads to a dysmetabolism of BCAAs resulting in MSUD or BCKDK deficiency (MIM #614923) (Figure 1), two different clinical conditions with a hallmark of neurological perturbation.

MSUD results from mutations in the genes E1α-*BCKDHA* (MIM #608348), E1β-*BCKDHB* (MIM #24861), and E2-*DBT* (MIM #248610) [37]. The disease affects 1 : 185,000 newborns worldwide and is manifested by diverse clinical phenotypes, ranging from the most severe form—seen in 70% of patients with MSUD and associated with a profound neurological impact and high mortality if not treated early—to mild forms that present during early development. The mechanisms underlying brain injury are not completely understood. Different studies have been carried out using chemical induction of the disease by BCAAs or BCKAs in cultured cells [43, 44] and animal models [45–48]. All converge in the identification of oxidative stress, brain energy deficit, and/or alterations in the brain's neurotransmission balance, mostly affecting

glutamate [46], as important neurodegenerative determinants. Recent studies in human peripheral blood mononuclear cells have shown that 10 mM of BCAAs can directly trigger a mechanism that involves the two major ROS sources, NADPH oxidase and mitochondria. BCAAs stimulate the activation of the redox-sensitive transcription factor NFκB resulting in the release of proinflammatory molecules [49].

Increases in lipid and protein oxidation are detected in plasma of MSUD patients [50, 51]. The two branched-chain aminotransferases (BCATs) involved in the conversion of BCAAs in BCKAs contain redox-active cysteine residues and could be affected by an oxidative environment. Their inhibition would provoke a further increase in the BCAA levels that could exacerbate the effect of the blockage [34]. An increased inflammatory profile has also been observed in plasma samples from MSUD patients maintained at low BCAA levels indicating the presence of sustained inflammation and activation of the immune system probably as a result of unbalanced ROS production [52].

On the other hand, mutations in the *PPM1K* gene in human result in a mild increase of BCAA and BCKA levels compatible with a mild variant form of MSUD (Figure 1), which nevertheless results in ROS increases along with the activation of the JNK and p38 MAP kinases [42]. This could be related to its critical role for mitochondrial function and cell survival previously described in animal models [53].

In the reverse of the MSUD metabolic problem, BCKDK patients (MIM #614923) manifest an unrestrained BCAA metabolism with decreased BCAA and BCKA levels, accompanied by neurocognitive phenotypes [38, 39]. However, also in this case, the mitochondrial response to BCKDK deficiency seems to be the increase in O_2^-, alterations in the expression of MnSOD and GPX, and alterations in the bioenergetics' profile with reductions in ATP-linked respiration and intracellular levels. All these data support the hyperfusion response of BCKDK-deficient mitochondria to stress and the altered cell fate observed in patients' fibroblasts [54]. Apart from the canonical ROS-producing sites in mitochondrial electron transfer chain, several reports pointed towards the important role of mitochondrial 2-oxoacid dehydrogenase complexes (2-oxoglutarate dehydrogenase, pyruvate dehydrogenase, and BCKDH) that share the E3 dihydrolipoamide dehydrogenase, as major O_2^-/H_2O_2 producers under conditions of maximum activities of substrate oxidation [55, 56]. Therefore, the most likely result from the uninhibited activity of BCKDHc could be a misbalance in redox equilibrium and an increase in the production of O_2^-/H_2O_2 [54–56].

2.2. Propionic Acidemia. Propionic acidemia (PA, MIM #606054) is one of the most frequent life-threatening organic acidurias, affecting 1 in 100,000 live births worldwide. PA results from mutations in the *PCCA* or *PCCB* gene that encode the α and β subunits of propionyl-CoA carboxylase (PCC), respectively. PCC is a biotin-dependent mitochondrial enzyme that catalyzes the reaction of propionyl-CoA to D-methylmalonyl-CoA, the first step of the propionate oxidation pathway (Figure 1). Propionyl-CoA derives from

the catabolism of certain amino acids including BCAAs (Ile, Val, Thr, and Met), of cholesterol, and from the beta-oxidation of odd chain fatty acids and bacteria gut production [57]. PCC deficiency results in the accumulation and excretion of propionate, 3-hydroxypropionate, methylcitrate, and propionylglycine, which are the biochemical hallmarks for diagnosis [57]. PA leads to a multisystemic disorder that affects the cardiovascular, gastrointestinal, renal, nervous, and immune systems [58, 59]. The clinical outcome varies from a severe neonatal form characterized by ketoacidosis, feeding refusal, lethargy, failure to thrive, seizures, and encephalopathy to a milder-late onset form with metabolic decompensations, failure to thrive, and diverse neurological deficiencies [60–62]. Cardiomyopathy and neurological features are associated with a high morbidity and mortality and have been attributed to bioenergetic failure and intracellular accumulation of toxic metabolites [63, 64].

A number of *in vitro* and *in vivo* studies of propionyl-CoA metabolites have shown inhibition of enzymes involved in energy production pathways, such as respiratory chain complex III [65] and pyruvate dehydrogenase complex [66]. Furthermore, propionyl-CoA reacts with oxaloacetate to produce methylcitrate that inhibits enzymes such as phosphofructokinase aconitase and citrate synthase [67]. In addition, propionate, at concentrations similar to those found in the plasma of PA patients, strongly inhibits oxygen consumption as well as oxidation of pyruvate and alpha-ketoglutarate in rat liver mitochondria [66, 68]. Moreover, the lack of PCC that blocks the anaplerotic biosynthesis of succinyl-CoA from propionyl-CoA may result in diminished TCA cycle activity [69]. This could be especially relevant for the heart and skeletal muscle, for which propionate is a major anaplerotic substrate. Propionic acid was shown to stimulate the production of O_2^- in the presence of Ca^{2+} influx activators in human neutrophils [70], to increase protein carbonylation in rats [71] and to stimulate lipid peroxidation in rat cerebral tissues [72].

The secondary mitochondrial dysfunction in PA is manifested as a decrease in ATP and phospho-creatine production, a decrease in the activity of respiratory chain complexes, mtDNA depletion, and abnormal mitochondrial structures present in PA patients' biopsies. This is evident particularly in high-energy-demanding organs such as the brain and heart [73–75]. In addition, evidence of oxidative stress and cellular damage has been shown in PA patients' fibroblasts through detection of elevated intracellular H_2O_2 levels correlating with the activation of the JNK and p38 pathways [26]. Urinary samples from PA patients show high levels of oxidative stress markers [12].

Alterations in redox homeostasis and mitochondrial function were observed in a hypomorphic mouse model of PA ($Pcca^{-/-}$ (A138T)) [5]. These include increased O_2^- production and *in vivo* mitochondrial H_2O_2 levels, mtDNA depletion, lipid oxidative damage, and tissue-specific alterations in the activities of OXPHOS complexes and in antioxidant defences. An increase in the DNA repair enzyme 8-guanine DNA glycosylase 1 (OGG1) induced by oxidative stress was also found in the liver of PA mice [32]. These

alterations show a good correlation with the altered mitochondrial function and oxidative damage detected in PA patients' samples [12, 73–77].

2.3. Methylmalonic Acidurias.

Methylmalonic acidurias (MMA) include a heterogeneous group of autosomal recessive genetic disorders caused by deficiency of the mitochondrial enzyme methylmalonyl-CoA mutase (MCM) or by defects in cobalamin (cbl) absorption, intracellular cbl trafficking, or synthesis of adenosylcobalamin (Adocbl) and methylcobalamin (Mecbl), which serve as cofactors for MCM and for the cytosolic enzyme methionine synthase, respectively (Figure 1). Two clinical entities have been described: (i) isolated MMA, characterized by methylmalonic acid accumulation and caused by MCM deficiency, defects in Adocbl synthesis, and methylmalonyl-CoA epimerase deficiency and (ii) combined MMA and homocystinuria, characterized by methylmalonic acid and homocysteine accumulation and caused by defects in intracellular cbl metabolism (Figure 1).

2.3.1. Isolated MMA.

MCM (MIM #251000; mut^0 or mut^- enzymatic subtypes), encoded by the *mut* gene, is a mitochondrial matrix enzyme that catalyzes the conversion of L-methylmalonyl-CoA to succinyl-CoA [57]. Biochemically, the disease is characterized by accumulation of methylmalonic acid and by accumulation of propionate, 3-hydroxypropionate, and 2-methylcitrate, due to activation of alternative pathways of propionate oxidation. Clinical presentation varies from a severe, early onset form of the disease, with neonatal ketoacidosis, lethargy, failure to thrive, encephalopathy, and hepatomegaly, to a milder late-onset presentation usually diagnosed during infancy that has a less serious neurological outcome [57]. Neurological symptoms, including psychomotor delay, irritability, lethargy, hypotonia, convulsions, and coma, have been related to a failure in mitochondrial oxidative metabolism. Mitochondrial dysfunction could be due to a combination of the inhibition of specific enzymes and transporters, limitation in the availability of substrates for mitochondrial metabolic pathways, and oxidative damage [78].

Mitochondrial toxicity of methylmalonic acid has been examined *in vitro* using a variety of normal tissues and extracts, including rat brain, mouse muscle, and bovine heart, suggesting an impairment of mitochondrial function, ROS generation, and other secondary metabolic perturbations [72, 79–81]. In addition, 2-methylcitric acid, malonic acid, and propionyl-CoA inhibit respiratory chain and tricarboxylic cycle [82]. In cultured neurons, methylmalonic acid decreases ATP/ADP ratio, collapses ion gradients, causes membrane depolarization, and increases intracellular calcium levels, leading to necrotic and apoptotic cell death [78].

Experimental evidence using patients' samples and a *mut*-knockout mouse identified multiple oxidative phosphorylation (OXPHOS) defects in MMA perturbations in antioxidant defences and resulting oxidative damage, indicating deficient energy metabolism caused by methylmalonyl-CoA accumulation and reduced succinyl-CoA levels [73, 83–86]. Proteomic analysis of patient liver samples by two-dimensional differential in-gel electrophoresis (2D–DIGE) and mass spectrometry (MALDI-MS and LC-MSMS) showed alterations of enzymes involved in free radical scavenging [87]. In patient's fibroblasts, proteomic analysis (2-D DIGE/MALDI-TOF) identified several differentially expressed proteins related to oxidative stress and apoptosis (cytochrome c, MnSOD, and mitochondrial glycerophosphate dehydrogenase) [88]. In a study using high-dimensional flow cytometry, patients with MMA showed lower GSH levels in T lymphocytes, monocytes, and neutrophils, compared to healthy controls [20]. Oxidative damage markers (F-2 isoprostanes and dityrosine) were found increased in urinary samples from MMA patients [12, 89]. Plasma from patients showed significantly higher levels of protein carbonyls as compared to healthy controls [20].

In addition, various parameters of oxidative stress and apoptosis were evaluated in cultured fibroblasts from a spectrum of patients with MMA showing a significant increase in intracellular ROS content, MnSOD protein and apoptosis rate compared to controls [6]. Furthermore, cytochrome c oxidase deficiency was observed in renal tubular megamitochondria from a MMA patient [90], and mitochondrial ultrastructural abnormalities were found in renal samples from MMA mice [89] and in liver samples from MMA mut^0 patients undergoing transplantation [91].

2.3.2. MMA Combined with Homocystinuria.

Cobalamin deficiency type C with methylmalonic aciduria and homocystinuria (cblC; MMACHC; MIM #277400 and #609831) (Figure 1) is the most frequent genetic disorder of vitamin B_{12} metabolism. MMACHC protein is a processing enzyme involved in an early cytoplasmic step in the cofactor-trafficking pathway. It exhibits unusual chemical versatility with demonstrated gluthatione transferase, reductive decyanase, and aquocobalamin reductase activities and converts incoming cobalamin derivatives to an intermediate that can be partitioned into Mecbl and Adocbl synthesis to support cellular needs [92–94]. MMACHC catalyzes the glutathione- (GSH-) dependent dealkylation of alkylcobalamins and the reductive deacyanation of cyanocobalamin [95].

Early-onset patients with cblC disease present multisystem failure while there are late-onset patients exhibiting a milder form, with progressive neurological symptoms and behavioural disturbances [96]. Maculopathy and abnormal vision are extremely common in early-onset patients [97].

Increasing evidence provides support that oxidative stress is closely associated with the physiopathology of this disorder. In this disease, there is a combined contribution of mitochondrial ROS due to accumulation of methylmalonic acid, as well as of homocysteine-derived ROS (see below, the Homocystinuria section). Patient-derived fibroblasts showed elevated ROS, apoptosis, and active phosphorylated forms of p38 and JNK stress-kinase levels [98, 99]. High levels of oxidative damage biomarkers have been found in urinary samples [12]. Decreased levels of proteins involved in cellular detoxification (members of the peroxiredoxin family and isoforms of glutathione-S-transferases) were detected in patient-derived fibroblasts by proteomics techniques [100, 101]. Another proteomic study in patients'

lymphocytes revealed the deregulation in the expression of proteins involved in oxidative stress and cellular detoxification, especially those related to glutathione metabolism [102]. In relation to this, an imbalance of glutathione metabolism was observed in *cblC* blood samples with a significant decrease in total and reduced glutathione, along with an increase in different oxidized glutathione forms [19]. GSH depletion could be the consequence of a reduced synthesis since total glutathione and its rate-limiting precursor (cysteine) is decreased in *cblC* patients [19]. In addition, increased levels of protein-bound glutathione were detected, providing evidence of the impact of changes in glutathione pools in the pathogenesis of *cblC* disease through redox regulation of protein function [19]. Furthermore, two mutant MMACHC proteins exhibited impaired glutathione binding, and stabilization of the cob(II)alamin derivative has been observed in presence of physiologically relevant glutathione concentrations. The preferential stabilization of cob(II)alamin by the mutants with a concomitant increase in GSSG production offers insights into ROS production [103].

2.4. Glutaric Aciduria Type I.

Glutaric aciduria type I (GAI, OMIM #231670) is caused by the deficiency of the mitochondrial enzyme glutaryl-CoA dehydrogenase (GCDH), responsible for the oxidative decarboxylation of glutaryl-CoA to crotonyl-CoA, in the catabolic pathways of lysine and tryptophan [104]. The deficiency causes accumulation of glutarate and 3-hydroxyglutarate, and patients are at risk of acute striatal injury during encephalopathic crises before 4 years of age, frequently precipitated by nonspecific illnesses [105]. These episodes lead to the appearance of neurological symptoms including dystonia, dyskinesia, seizures, and coma [106]. Current treatment for GAI includes dietary lysine restriction and carnitine supplementation, although this does not prevent striatal degeneration in about one-third of the patients. Excitotoxicity, oxidative stress, and mitochondrial dysfunction induced by accumulating metabolites have been associated with brain pathogenesis, although the exact underlying mechanisms remain unclear [4, 107, 108].

Glutaric acid administration induces lipid peroxidation and alterations in antioxidant defences in rats [109]. GCDH-deficient knockout mice ($Gcdh^{-/-}$) show a biochemical phenotype comparable to GAI patients but do not develop striatal degeneration [110]. These mice exhibit protein oxidative damage and reduction of antioxidant defences in the brain when subjected to an acute lysine overload [111]. Indeed, GCDH knockout mice fed on a high-lysine chow represent an animal model of GAI encephalopathy g [112]. In these mice, high concentrations of glutaric acid within neurons were correlated with mitochodrial swelling and biochemical changes (depletion of alpha-ketoglutarate and accumulation of acetyl-CoA) consistent with Krebs cycle disruption [113].

2.5. Other Organic Acidurias.

There are several other organic acidurias in which there is an inhibition of energy metabolism attributed to accumulation of toxic metabolites in mitochondria. These include 3-methylcrotonyl-CoA carboxylase deficiency (MCC, MIM #210200 and #210210), 2-methyl-3-hydroxybutyric aciduria (MOHBA, MIM #20 3750), 3-methylglutaconic aciduria (MHGA, MIM #250 950), D-2-hydroxyglutaric aciduria (D-2-OHGA, MIM #600721), L-2-hydroxyglutaric aciduria (L-2-OHGA, MIM #236792), 3-hydroxy-3-methylglutaric aciduria (3-HMGA, MIM #246450), and ethylmalonic encephalopathy (EE, MIM #602473). Deficiencies in several respiratory chain complexes have been reported in some of these pathologies, such as MOHBA (I and IV) [114], MGA (I and V) [115], D-2-OHGA (V and IV) [116], and EE (IV and II) [117]. Abnormal structure of mitochondria was also found in patients' samples with MHGA [118].

A growing body of experimental evidence indicates that impairment of redox homeostasis induced by the major organic acids accumulating in 3-HMGA contributes to the brain and liver pathophysiology [3]. Lipid and protein damage, along with a decrease of antioxidant defences, have been observed in patients' plasma and urine [3].

A recent transcriptome study in MCC-deficient patient-derived fibroblasts revealed an altered gene expression profile indicative of mitochondrial dysfunction, decreased antioxidant response, and disruption of energy homeostasis [119]. This correlates with previous *in vitro* studies in the cerebral cortex of young rats in which the accumulated metabolites have been shown to disrupt energy homeostasis and cause lipid peroxidation [120].

3. Homocystinuria

In several IEMs, increased ROS causes pathophysiological oxidative damage that is not originated in the mitochondria. This is the case of homocystinuria in which excess homocysteine (Hcy) directly promotes ROS formation. Hcy is a sulphur-containing amino acid derived from the demethylation of the essential amino acid methionine. Autoxidation of two Hcy molecules yields the oxidized disulphide homocystine, two protons and two electrons, generating ROS in the form of O_2^-, hydrogen radical, or H_2O_2 [121]. Formation of mixed disulphides also contributes to the additional formation of ROS [121]. In addition to its inherent reactivity, specific mechanisms such as reduction in bioavailable nitric oxide and decreased glutathione peroxidase activity may play a role in Hcy-induced oxidative stress [122, 123]. Plasma Hcy has been known for decades as a risk marker for cardiovascular disease, which is explained by Hcy-induced oxidative damage in endothelial cells [124]. Induction of NADPH oxidase or downregulation of thioredoxin expression have been postulated as underlying mechanisms [125]. Elevated homocysteine concentration has also been proposed as a risk factor for neurodegenerative diseases inducing neurological dysfunction via oxidative stress [126].

Hcy metabolism stands at the intersection of two pathways: remethylation to methionine and transsulfuration to cystathionine [127]. Inherited homocystinurias have in common accumulation of homocysteine with subsequent neurotoxicity. This group of diseases encompasses two distinctive clinical entities: classical homocystinuria due to

cystathionine β-synthase (CBS) deficiency (transsulfuration pathway) and the rare inborn errors of cobalamin and folate metabolism (remethylation pathway) [128] (Figure 1).

3.1. Homocystinuria due to Cystathionine β-Synthase Deficiency.
Deficiency of cystathionine β-synthase (CBS, MIM #236200) is a disorder of methionine metabolism leading to elevated methionine and an abnormal accumulation of Hcy and its metabolites (homocystine, homocysteine-cysteine complex, and others) in the blood and urine. In the case of excess cellular methionine levels, the transsulfuration pathway plays an important role in Hcy metabolism and converts Hcy into cystathionine with the help of the enzyme CBS (Figure 1). The cystathionine formed is then converted into cysteine by cystathionine γ-lyase. Although the pathophysiology of CBS deficiency is not yet well established, Hcy excess or cysteine deficiency rather than the accumulation of methionine is more likely to cause the pathogenesis of this disease [127]. CBS deficiency is clinically characterized by heterogeneous clinical manifestations in various organs and tissues, such as thinning and lengthening of the long bones, osteoporosis, dislocation of the ocular lens, thromboembolism, and mental retardation [127].

Oxidative stress may play an important role in the pathophysiology of homocystinuria, as deduced from studies carried out in patients and animal models [129]. Protein, lipid, and DNA oxidative damage and decreased antioxidant defences have been found in patients [130–132]. Increases in lipid, protein, and DNA oxidative damage biomarkers have been reported in CBS-deficient mice [133] and in samples from animal models subjected to Hcy administration [134, 135].

3.2. Homocystinuria due to Remethylation Defects.
Remethylation disorders are due to deficiencies of enzymes involved in the remethylation of Hcy to methionine causing homocystinuria. They include defects in methionine synthase (MTR, MIM #156570), methionine synthase reductase (MTRR, MIM #602568), MMADHC 5(MIM #611935), and 5,10-methylene tetrahydrofolate reductase enzyme (MTHFR, MIM #236250) (Figure 1) [136]. Biochemically, these disorders are characterized by Hcy elevation and low-to-normal methionine levels, without urinary methylmalonic acid excretion. Patients present severe clinical symptoms, which are mainly neurological for MTHFR deficiency and neurohematological for MTR and MTRR defects [136]. Two major mechanisms have been proposed to explain the pathogenesis of these diseases: (i) defective methionine synthesis (with a consequent drop in S-adenosylmethionine production and deficiencies of numerous methylation reactions leading to hypomyelination in the central nervous system) [137] and (ii) Hcy excess [127].

Patient-derived fibroblasts with defects in MTR, MTRR, or MTHFR show a significant increase in ROS content, in MnSOD levels, in the rate of apoptosis, and in the levels of the active phosphorylated forms of p38 and JNK stress kinases [7]. Increased mRNA and protein levels of Herp, Grp78, IP$_3$R1, pPERK, ATF4, CHOP, asparagine synthase,

GADD45, and MAM-associated proteins were also found in these cells indicating an increase in endoplasmic reticulum stress and subsequent mitochondrial calcium overload. In addition, an activation of autophagy process and a substantial degradation of altered mitochondria by mitophagy were detected in patient-derived fibroblasts [138].

4. Challenges in ROS Detection

ROS production plays an important role in physiological and pathological processes. In order to understand how they contribute to these cellular processes, it is essential to identify the specific reactive species produced, levels, and subcellular localization. ROS lifetime ranges from nanoseconds to seconds due to their high reactivity and depends on numerous clearance mechanisms such as the intracellular antioxidant levels [139]. Steady state concentration of mitochondrial O_2^- and H_2O_2 have been estimated to be in the picomolar and low nanomolar ranges, respectively. ROS detection thereby requires specific molecular probes that promptly interact with ROS to compete with antioxidants and generate stable products, which can be accurately quantified. However, their very short life span and extremely low concentration and instability, as well as the large diversity of possible chemical reactions, make ROS assessment challenging. Excellent reviews by different authors cover the limitations, progress, and perspectives of the most widely used tools and new approaches described for monitoring ROS detection [139–142]. In this section, we focus on some of the most common detection strategies used to asses oxidative stress in vitro and in vivo in organic acidurias, pointing out some of their methodological constrains and concerns.

Assessment of ROS levels has largely relied on the detection of end products [143]. The small cell-permeable probes $2',7'$-dichlorodihydrofluorescein (H$_2$DCF) and dihydroethidium (DHE) are the most commonly used molecules for intracellular ROS detection of H_2O_2 and O_2^-, respectively. Despite the fact that H$_2$DCF is one of the most commonly used probes, many concerns have been raised regarding its mechanism of action and specificity [144]. For instance, it is known that a host of ROS species such as nitric oxide, peroxynitrite anions (ONOO−), and even organic hydroperoxides can oxidize H$_2$DCF. In addition, redox reactions with DCF and DCFH may lead to generation of the DCF-free radical anion [145], which produces O_2^- and reacts with antioxidants such as thiols and ascorbate [146]. Intracellular ROS generation throughout oxidation of H$_2$DCF has been detected in PA, cobalamin disorders (cblB, cblC, cblE, and cblG), MTHFR deficiency, and MSUD patient-derived fibroblasts [26, 42, 98]. Recently, mitochondrial ROS generation has been measured in the cortex of a mouse model of MMA (induced by MMA and ammonia) [147]. DCF measurements should be carefully considered, and extra controls for the assessment of ROS production are required. Thus, DCF has been suggested as a general oxidative stress indicator instead of serving as a specific proof of H_2O_2 production.

DHE has been extensively used for intracellular O_2^- measurements together with its mitochondrial-targeted analog (MitoSOX). The specificity of DHE and its oxidative

products has been a matter of debate for decades [144]. DHE can form two fluorescent products. One is ethidium, which is formed by nonspecific redox reactions, while the other is 2-hydroxyethidium (2-OH-E+), a specific adduct of O_2^- [148]. The fluorescent spectra of ethidium and 2-OH-E+ overlap, and it is therefore difficult to accurately measure only 2-OH-E+ by simple fluorescent detection methods. However, careful use of specific wavelengths of excitation allows separation of these to signals [149]. DHE staining has been used to measure O_2^- production in brain and heart cryosections of $Pcca^{-/-}$ (A138T) mice [5]. MitoSOX has been used to measure the basal production of mitochondrial O_2^- in cobalamin disorders (cblB and cblE) and in BCKDK-deficient patient-derived fibroblasts [6, 7, 54]. However, the combination of DHE and analytical methods such as high-pressure liquid chromatography and mass spectrometry is essential to validate DHE as a technique to quantify O_2^- [150].

In order to have a better understanding of ROS mitochondrial regulation and its role in oxidative damage and redox signaling, new approaches to measure mitochondrial ROS levels within living organisms are essential. Logan et al. developed a radiometric mass spectrometry probe approach. This method is based on the use of the MitoB probe, which comprises a triphenylphosphonium (TPP) cation driving its accumulation inside the mitochondria, conjugated to an arylboronic acid that reacts with H_2O_2 to form a phenol MitoP. Once MitoB is administrated to the animal, the probe is modified *in vivo* by ROS to generate an exomarker product (MitoP). The MitoB/MitoP ratio allows assessment of the levels of ROS *in vivo* [151, 152]. This technique has been applied to the mouse model of PA, to measure relative levels of H_2O_2 in the liver and heart [5]. The main advantages of this approach are its high selectivity, *in vivo* localization, and the use of analytical techniques such as LC-MS/MS to identify and quantify exomarkers. However, some significant weaknesses are also observed such as its inherently invasive methodology and the time-consuming nature of sample preparation.

Despite the progress achieved in the field of ROS detection, there is a clear need to develop noninvasive, *in vivo*, and more selective methods to address many important questions related to the role of altered redox homeostasis in the pathology of IEMs.

5. Redox-Based Therapeutic Approaches

Most IEMs in which altered redox homeostasis and oxidative damage have been documented as described in this work do not have an effective treatment. Therapy mainly consists on protein restriction and supplementation with special formulas that provide the necessary nutrients for adequate growth and development, as well as the administration of specific compounds aiming to detoxify the accumulated metabolites or to enhance residual enzymatic activities [10, 153]. However, the clinical outcome overall remains unsatisfactory, as multiorgan complications (neurological, cardiac, renal, hematological, and gastrointestinal, among others) persist. In this scenario, antioxidants and mitochondrial activators/

protectors may be beneficial to prevent or ameliorate oxidative damage contributing to organ pathophysiology.

Chemically, antioxidants are reduced compounds that directly react with ROS avoiding the oxidation of a third molecule. The *in vitro* mode of action of nutraceutical and synthetic antioxidants is mainly based on their capacity to act as free radical scavengers. However, *in vivo* antioxidant response depends on distribution, absorption, metabolism, and excretion of the compound, hampering a direct action on ROS. In fact, it is now clear that *in vivo* antioxidants provide indirect cellular and tissue protection against oxidative damage by targeting NRF2 and NAD-dependent protein deacetylase sirtuin-1 (SIRT1) [154, 155], modulating the antioxidant response (Figure 2).

NRF2 transcription factor regulates cellular homeostasis by binding to regulatory DNA regions known as electrophile response elements or EpRE (previously named antioxidant regulatory elements (AREs)). Under oxidative stress, NRF2 translocates to the nucleus, binds to EpRE sequences, and promotes the transcription of antioxidant enzymes, genes of GSH metabolism, and NADPH regeneration (Figure 2) [156].

Antioxidant response can also be driven by SIRT1, a class I histone deacetylase that mediates deacetylation in a NAD+-dependent manner. SIRT1 is mainly localized in the nucleus where, apart from histones, it can interact with and deacetylate peroxisome proliferator-activated receptor gamma coactivator 1-alpha (PGC1α) and Forkhead box protein O3 (FOXOa3) [157, 158]. Deacetylated PGC1α and FOXOa3 have an increased transcriptional activity and promote mitochondrial biogenesis and expression of antioxidant genes (Figure 2). Therefore, NRF2 and SIRT1 activation by polyphenolic compounds represent the main targets for antioxidant therapy to reduce oxidative damage.

Several studies have evaluated different antioxidant compounds as adjuvant therapy in a number of IEMs. The brain is highly sensitive to free radicals due to its high energetic demands, its high lipid content, and its low regeneration capacity. In this context, oxidative damage has been proposed as one of the mechanisms involved in the development of the characteristic neurological symptoms of PA, MMA, MSUD, GAI, and homocystinuria patients. Even though the transport rate of antioxidants through the blood brain barrier is low, different studies have reported a reversion of brain damage after antioxidant treatments in these diseases [159–162].

In organic acidurias, a beneficial effect of L-carnitine supplementation with *in vitro* antioxidant properties has been described [13, 163]. L-carnitine shows antioxidant capacities as it can act as ROS scavenger and reduce lipid peroxidation to an extent comparable to that seen with α-tocopherol [164]. It also protects endogenous antioxidant enzymes from peroxidative damage and induces elevated cellular GSH [31]. L-carnitine supplementation is routinely included in the treatment of PA and MMA, to prevent a secondary carnitine deficiency and to promote detoxification of propionic and methylmalonic acids, which are excreted in the form of carnitine esters. Evaluation of oxidative stress parameters in urine from PA and MMA patients during treatment with L-carnitine- and protein-restricted diet showed
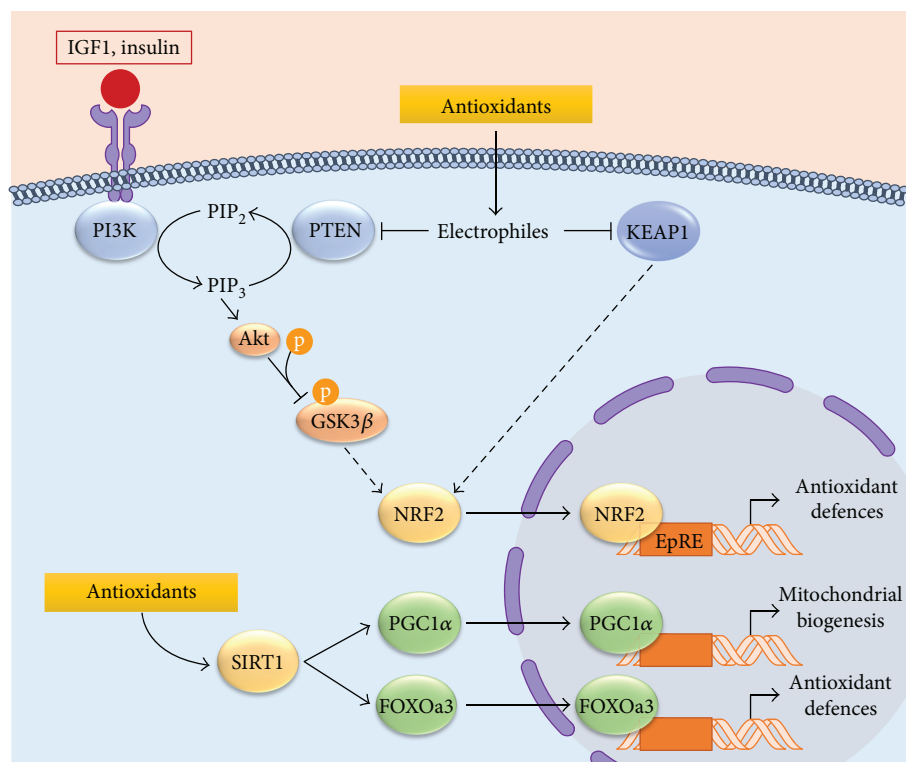
FIGURE 2: NRF2- and SIRT1-signaling pathways targeted by antioxidant compounds. Under normal homeostatic conditions, NRF2 transcriptional activity is inhibited by KEAP1 and PTEN. KEAP1 directly interacts with NRF2 and mediates its ubiquitination and subsequent proteasomal degradation. Furthermore, PTEN eliminates 3-phosphoinositides (PIP_3) required for AKT activation, thus leading to GSK3β activation and NRF2 phosphorylation. *In vivo* antioxidants act as electrophiles that modify and inhibit KEAP1 and PTEN. When KEAP1 is oxidized, its interaction with NRF2 is disrupted and NRF2 half-life increases. Electrophiles also inhibit the redox-sensitive phosphatase PTEN, allowing PIP_3 accumulation, AKT activation, and GSK3β inactivation. In these conditions, NRF2 is translocated to the nucleus where it binds to the electrophile response element (EpRE) and drives the expression of antioxidant defence genes. Additionally, antioxidant compounds modulate SIRT1 pathway favouring the antioxidant defence response and mitochondrial biogenesis by activation of FOXOa3 and PGC1α transcription factors, respectively.

a significant reduction of urinary and plasma biomarkers of oxidative damage to lipids and proteins [13, 163]. L-carnitine treatment was also shown to reduce plasma malondialdehyde concentrations and urine dityrosine and isoprostanes in patients with MSUD [51, 165].

In a MMA patient with optic neuropathy, CoQ_{10} treatment in conjunction with vitamin E resulted in improved visual acuity [166]. Interestingly, treatment of MMA mice with CoQ_{10} and vitamin E showed a significant amelioration in the loss of glomerular filtration rate and a normalization of plasma lipocalin-2 levels [89], indicating that the therapeutic effects are not restricted to the nervous system.

Recently, *in vitro* and *in vivo* studies in PA have also shown the positive effect of antioxidant treatment. Using patients' fibroblasts, different antioxidants (tiron, trolox, resveratrol, and MitoQ) significantly reduced H_2O_2 levels and regulated the expression of antioxidant enzymes [30]. In the hypomorphic mouse model of PA [167], oral treatment with resveratrol and MitoQ protected against lipid and DNA oxidative damage and induced the expression of antioxidant enzymes [32]. In addition to its antioxidant properties, resveratrol exerts different effects

on mitochondrial function and dynamics [168], which clearly contributes to its beneficial effect in IEMs with mitochondrial ROS production, such as organic acidemias and respiratory chain defects [169].

A clinical trial (NCT01793090) is ongoing in patients with MMA cblC-type defect to investigate the safety and efficacy of the EPI-743 compound in relation to visual and neurological impairment. This molecule targets NADPH quinone oxidoreductase 1, thus providing beneficial effects in diseases characterized by oxidative stress and alterations in glutathione redox balance, as is the case of mitochondrial diseases [170].

Taurine, a compound potentially reducing oxidative damage, is being tested in a clinical trial with homocystinuria (CBS-deficient) patients (NCT01192828). Taurine treatment in a mouse model of CBS deficiency reversed GSH depletion with potential beneficial effects [171].

Although the use of antioxidants as potential therapies holds great interest for many diseases (including IEMs) in which oxidative stress plays a pathophysiological role, there is to date limited clinical evidence of their efficacy, which may be related to pharmacokinetic and/or pharmacodynamics
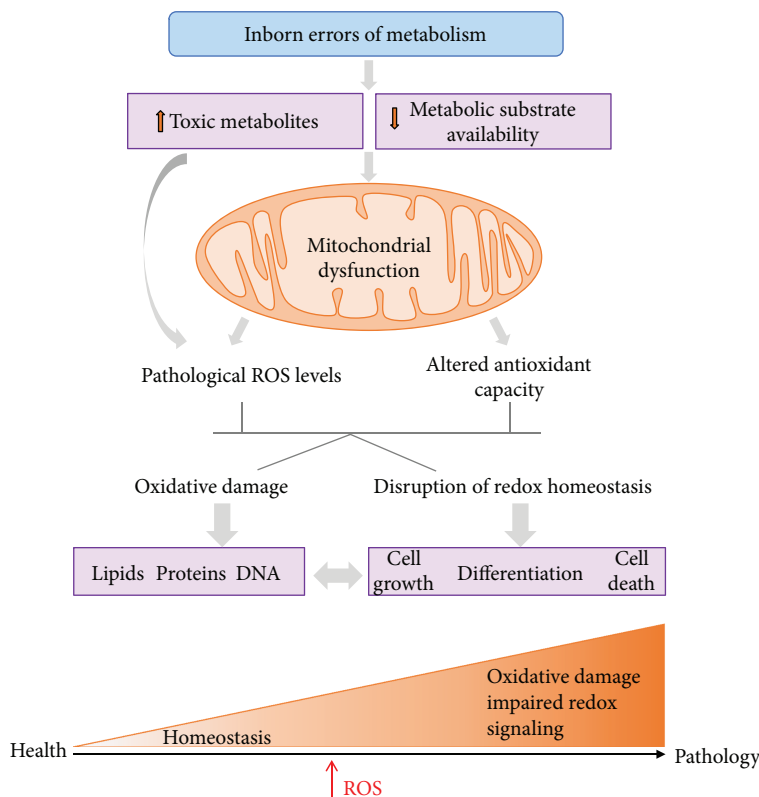
FIGURE 3: ROS and oxidative damage contribute to IEM physiopathology. The scheme shows the consequences of toxic metabolite accumulation in IEMs on mitochondrial function and ROS increase, which in turn results in oxidative damage and alteration in ROS signaling contributing to disease pathology.

reasons [172]. The intracellular levels of the specific antioxidant, its distribution throughout the body, together with the subcellular location are factors that influence the *in vivo* effects. Moreover, antioxidants react with free radicals with the same rate constant as other natural molecules, and their intracellular concentrations cannot overcome this kinetic limitation. Therefore, antioxidant effectiveness *in vivo* could be limited [154].

Throughout the years, different studies have shown both beneficial and adverse effects of antioxidant compounds. *In vitro* β-carotene shows antioxidant and anti-inflammatory effects when administered at low doses whereas prooxidant and proinflammatory responses have been reported at higher concentrations [173, 174]. Similar contradictory results have been obtained in *in vivo* studies. While in a randomized trial dietary consumption of β-carotene and vitamins C and E did not affect cancer incidence and mortality [175], higher doses of these compounds did not show any health beneficial effect. In fact, they could significantly increase the risk of mortality (reviewed in [176, 177]). ROS are required at physiological concentrations for optimal cellular homeostasis [178]. Therefore, free radical scavenging by antioxidants could be undesirable as disruption of redox balance would lead to cellular dysfunction and originate different side effects.

New indirect antioxidant approaches targeting redox enzymes or NRF2 agonists that upregulate cellular antioxidant

defences are promising alternatives that warrant further investigation [155].

6. Conclusions and Future Perspectives

The pathophysiological role of ROS in IEMs has been firmly established in many studies revealing oxidative damage to proteins, lipids, and DNA in patients' samples and animal models, correlating with clinical and biochemical parameters (Figure 3). Consequently, different antioxidants have been successfully used in cellular and animal models of IEMs [30–32, 89, 98]. Despite these positive results, for other diseases, there is no clear conclusion on the efficacy of antioxidant treatments in human clinical trials, which limits the expectations also for IEMs.

In the past years, we have gained deeper insights into the complex and dynamic roles of ROS signals in normal and pathological processes, yet the field of redox signaling in IEMs is still in its infancy. Novel technologies such as redox proteomics [179] or transgenic animals expressing redox reporters [180] are revolutionising the field and represent excellent tools to investigate redox regulatory networks in disease. They may also provide insight to explain the poor performance of antioxidant therapies in clinical trials. In many IEMs, mitochondrial ROS-targeting agents that accumulate in the mitochondria and compounds activating or improving mitochondrial function may constitute a

valid approach. Further preclinical research is warranted to investigate basic mechanisms of redox signaling and their implications for IEM disease progression, as well as exploring the benefits of targeted antioxidant therapies.

Disclosure

Conflicts of Interest

The authors declare that they have no conflicts of interest.

Acknowledgments

References

[1] R. K. J. Olsen, N. Cornelius, and N. Gregersen, "Redox signalling and mitochondrial stress responses; lessons from inborn errors of metabolism," *Journal of Inherited Metabolic Disease*, vol. 38, no. 4, pp. 703–719, 2015.

[2] M. Wajner, A. Latini, A. T. S. Wyse, and C. S. Dutra-Filho, "The role of oxidative damage in the neuropathology of organic acidurias: insights from animal studies," *Journal of Inherited Metabolic Disease*, vol. 27, no. 4, pp. 427–448, 2004.

[3] G. Leipnitz, C. R. Vargas, and M. Wajner, "Disturbance of redox homeostasis as a contributing underlying pathomechanism of brain and liver alterations in 3-hydroxy-3-methylglutaryl-CoA lyase deficiency," *Journal of Inherited Metabolic Disease*, vol. 38, no. 6, pp. 1021–1028, 2015.

[4] M. Wajner and S. I. Goodman, "Disruption of mitochondrial homeostasis in organic acidurias: insights from human and animal studies," *Journal of Inherited Metabolic Disease*, vol. 43, no. 1, pp. 31–38, 2011.

[5] L. Gallego-Villar, A. Rivera-Barahona, C. Cuevas-Martin et al., "In vivo evidence of mitochondrial dysfunction and altered redox homeostasis in a genetic mouse model of propionic acidemia: implications for the pathophysiology of this disorder," *Free Radical Biology and Medicine*, vol. 96, pp. 1–12, 2016.

[6] E. Richard, A. Alvarez-Barrientos, B. Perez, L. R. Desviat, and M. Ugarte, "Methylmalonic acidaemia leads to increased production of reactive oxygen species and induction of apoptosis through the mitochondrial/caspase pathway," *The Journal of Pathology*, vol. 213, no. 4, pp. 453–461, 2007.

[7] E. Richard, L. R. Desviat, M. Ugarte, and B. Perez, "Oxidative stress and apoptosis in homocystinuria patients with genetic remethylation defects," *Journal of Cellular Biochemistry*, vol. 114, no. 1, pp. 183–191, 2013.

[8] E. Morava, S. Rahman, V. Peters, M. R. Baumgartner, M. Patterson, and J. Zschocke, "Quo vadis: the re-definition of "inborn metabolic diseases"," *Journal of Inherited Metabolic Disease*, vol. 38, no. 6, pp. 1003–6, 2015.

[9] R. K. J. Olsen, N. Cornelius, and N. Gregersen, "Genetic and cellular modifiers of oxidative stress: what can we learn from fatty acid oxidation defects?," *Molecular Genetics and Metabolism*, vol. 110, pp. S31–S39, 2013.

[10] E. Richard, P. Rodriguez-Pombo, L. R. Desviat et al., "Mitochondrial organic acidurias. Part II: mitochondrial dysfunction," in *Mitochondrial Pathophysiology*, F. Palau and S. Cadenas, Eds., pp. 173–191, Research Signpost, Kerala, India, 2011.

[11] E. L. Streck, G. A. Czapski, and C. Goncalves da Silva, "Neurodegeneration, mitochondrial dysfunction, and oxidative stress," *Oxidative Medicine and Cellular Longevity*, vol. 2013, Article ID 826046, 2 pages, 2013.

[12] P. J. Mc Guire, A. Parikh, and G. A. Diaz, "Profiling of oxidative stress in patients with inborn errors of metabolism," *Molecular Genetics and Metabolism*, vol. 98, no. 1-2, pp. 173–180, 2009.

[13] G. S. Ribas, G. B. Biancini, C. Mescka et al., "Oxidative stress parameters in urine from patients with disorders of propionate metabolism: a beneficial effect of L-carnitine supplementation," *Cellular and Molecular Neurobiology*, vol. 32, no. 1, pp. 77–82, 2012.

[14] R. J. Mailloux, S. L. McBride, and M. E. Harper, "Unearthing the secrets of mitochondrial ROS and glutathione in bioenergetics," *Trends in Biochemical Sciences*, vol. 38, no. 12, pp. 592–602, 2013.

[15] A. Bindoli and M. P. Rigobello, "Principles in redox signaling: from chemistry to functional significance," *Antioxidants & Redox Signaling*, vol. 18, no. 13, pp. 1557–1593, 2013.

[16] T. Finkel, "Signal transduction by mitochondrial oxidants," *Journal of Biological Chemistry*, vol. 287, no. 7, pp. 4434–4440, 2012.

[17] N. Ballatori, S. M. Krance, S. Notenboom, S. Shi, K. Tieu, and C. L. Hammond, "Glutathione dysregulation and the etiology and progression of human diseases," *Biological Chemistry*, vol. 390, no. 3, pp. 191–214, 2009.

[18] H. Salmi, J. V. Leonard, and R. Lapatto, "Patients with organic acidaemias have an altered thiol status," *Acta Paediatrica*, vol. 101, no. 11, pp. e505–e508, 2012.

[19] A. Pastore, D. Martinelli, F. Piemonte et al., "Glutathione metabolism in cobalamin deficiency type C (cblC)," *Journal of Inherited Metabolic Disease*, vol. 37, no. 1, pp. 125–129, 2014.

[20] K. R. Atkuri, T. M. Cowan, T. Kwan et al., "Inherited disorders affecting mitochondrial function are associated with glutathione deficiency and hypocitrullinemia," *Proceedings of the National Academy of Sciences*, vol. 106, no. 10, pp. 3941–3945, 2009.

[21] M. P. Murphy, "Mitochondrial thiols in antioxidant protection and redox signaling: distinct roles for glutathionylation and other thiol modifications," *Antioxidants & Redox Signaling*, vol. 16, no. 6, pp. 476–495, 2012.

[22] M. C. Sobotta, W. Liou, S. Stöcker et al., "Peroxiredoxin-2 and STAT3 form a redox relay for H2O2 signaling," *Nature Chemical Biology*, vol. 11, no. 1, pp. 64–70, 2015.

[23] F. Yin, H. Sancheti, Z. Liu, and E. Cadenas, "Mitochondrial function in ageing: coordination with signalling and

transcriptional pathways," *The Journal of Physiology*, vol. 594, no. 8, pp. 2025–2042, 2016.

[24] H. Wu, H. Wei, S. A. Sehgal, L. Liu, and Q. Chen, "Mitophagy receptors sense stress signals and couple mitochondrial dynamic machinery for mitochondrial quality control," *Free Radical Biology and Medicine*, vol. 100, pp. 199–209, 2016.

[25] A. Boneh, "Signal transduction in inherited metabolic disorders: a model for a possible pathogenetic mechanism," *Journal of Inherited Metabolic Disease*, vol. 38, no. 4, pp. 729–740, 2015.

[26] L. Gallego-Villar, C. Perez-Cerda, B. Perez et al., "Functional characterization of novel genotypes and cellular oxidative stress studies in propionic acidemia," *Journal of Inherited Metabolic Disease*, vol. 36, no. 5, pp. 731–740, 2013.

[27] P. Alcaide, B. Merinero, P. Ruiz-Sala et al., "Defining the pathogenicity of creatine deficiency syndrome," *Human Mutation*, vol. 32, no. 3, pp. 282–291, 2011.

[28] H. Rocha, R. Ferreira, J. Carvalho et al., "Characterization of mitochondrial proteome in a severe case of ETF-QO deficiency," *Journal of Proteomics*, vol. 75, no. 1, pp. 221–228, 2011.

[29] J. Lopez-Erauskin, S. Fourcade, J. Galino et al., "Antioxidants halt axonal degeneration in a mouse model of X-adrenoleukodystrophy," *Annals of Neurology*, vol. 70, no. 1, pp. 84–92, 2011.

[30] L. Gallego-Villar, B. Perez, M. Ugarte, L. R. Desviat, and E. Richard, "Antioxidants successfully reduce ROS production in propionic acidemia fibroblasts," *Biochemical and Biophysical Research Communications*, vol. 452, no. 3, pp. 457–461, 2014.

[31] G. S. Ribas, C. R. Vargas, and M. Wajner, "L-carnitine supplementation as a potential antioxidant therapy for inherited neurometabolic disorders," *Gene*, vol. 533, no. 2, pp. 469–476, 2014.

[32] A. Rivera-Barahona, E. Alonso-Barroso, B. Perez, M. P. Murphy, E. Richard, and L. R. Desviat, "Treatment with antioxidants ameliorates oxidative damage in a mouse model of propionic acidemia," *Molecular Genetics and Metabolism*, vol. 122, no. 1-2, pp. 43–50, 2017.

[33] G. Hayashi and G. Cortopassi, "Oxidative stress in inherited mitochondrial diseases," *Free Radical Biology and Medicine*, vol. 88, no. Part A, pp. 10–17, 2015.

[34] J. E. Sperringer, A. Addington, and S. M. Hutson, "Branched-chain amino acids and brain metabolism," *Neurochemical Research*, vol. 42, no. 6, pp. 1697–1709, 2017.

[35] J. M. Han, S. J. Jeong, M. C. Park et al., "Leucyl-tRNA synthetase is an intracellular leucine sensor for the mTORC1-signaling pathway," *Cell*, vol. 149, no. 2, pp. 410–424, 2012.

[36] K. A. Anderson, F. K. Huynh, K. Fisher-Wellman et al., "SIRT4 is a lysine deacylase that controls leucine metabolism and insulin secretion," *Cell Metabolism*, vol. 25, no. 4, pp. 838–855.e15, 2017.

[37] D. T. Chuang and V. E. Shi, "Maple syrup urine diesease (branched chain ketoaciduria)," in *The Metabolic and Molecular Basis of Inherited Disease*, C. R. Scriver, A. L. Beaudet, W. Sly, and D. Valle, Eds., pp. 1971–2005, McGraw-Hill, New York, 2001.

[38] G. Novarino, P. El-Fishawy, H. Kayserili et al., "Mutations in BCKD-kinase lead to a potentially treatable form of autism with epilepsy," *Science*, vol. 338, no. 6105, pp. 394–397, 2012.

[39] A. Garcia-Cazorla, A. Oyarzabal, J. Fort et al., "Two novel mutations in the BCKDK (branched-chain keto-acid dehydrogenase kinase) gene are responsible for a neurobehavioral deficit in two pediatric unrelated patients," *Human Mutation*, vol. 35, no. 4, pp. 470–477, 2014.

[40] G. R. D. Villani, G. Gallo, E. Scolamiero, F. Salvatore, and M. Ruoppolo, ""Classical organic acidurias": diagnosis and pathogenesis," *Clinical and Experimental Medicine*, vol. 17, no. 3, pp. 305–323, 2017.

[41] R. A. Harris, M. Joshi, and N. H. Jeoung, "Mechanisms responsible for regulation of branched-chain amino acid catabolism," *Biochemical and Biophysical Research Communications*, vol. 313, no. 2, pp. 391–396, 2004.

[42] A. Oyarzabal, M. Martinez-Pardo, B. Merinero et al., "A novel regulatory defect in the branched-chain α-keto acid dehydrogenase complex due to a mutation in the PPM1K gene causes a mild variant phenotype of maple syrup urine disease," *Human Mutation*, vol. 34, no. 2, pp. 355–362, 2013.

[43] A. Sitta, G. S. Ribas, C. P. Mescka, A. G. Barschak, M. Wajner, and C. R. Vargas, "Neurological damage in MSUD: the role of oxidative stress," *Cellular and Molecular Neurobiology*, vol. 34, no. 2, pp. 157–165, 2014.

[44] P. de Lima Pelaez, C. Funchal, S. O. Loureiro et al., "Branched-chain amino acids accumulating in maple syrup urine disease induce morphological alterations in C6 glioma cells probably through reactive species," *International Journal of Developmental Neuroscience*, vol. 25, no. 3, pp. 181–189, 2007.

[45] W. J. Zinnanti, J. Lazovic, K. Griffin et al., "Dual mechanism of brain injury and novel treatment strategy in maple syrup urine disease," *Brain*, vol. 132, Part 4, pp. 903–918, 2009.

[46] T. Friedrich, A. M. Lambert, M. A. Masino, and G. B. Downes, "Mutation of zebrafish dihydrolipoamide branched-chain transacylase E2 results in motor dysfunction and models maple syrup urine disease," *Disease Models & Mechanisms*, vol. 5, no. 2, pp. 248–258, 2012.

[47] R. Bridi, J. Araldi, M. B. Sgarbi et al., "Induction of oxidative stress in rat brain by the metabolites accumulating in maple syrup urine disease," *International Journal of Developmental Neuroscience*, vol. 21, no. 6, pp. 327–332, 2003.

[48] R. Bridi, C. A. Braun, G. K. Zorzi et al., "α-Keto acids accumulating in maple syrup urine disease stimulate lipid peroxidation and reduce antioxidant defences in cerebral cortex from young rats," *Metabolic Brain Disease*, vol. 20, no. 2, pp. 155–167, 2005.

[49] O. Zhenyukh, E. Civantos, M. Ruiz-Ortega et al., "High concentration of branched-chain amino acids promotes oxidative stress, inflammation and migration of human peripheral blood mononuclear cells via mTORC1 activation," *Free Radical Biology and Medicine*, vol. 104, pp. 165–177, 2017.

[50] A. G. Barschak, A. Sitta, M. Deon et al., "Oxidative stress in plasma from maple syrup urine disease patients during treatment," *Metabolic Brain Disease*, vol. 23, no. 1, pp. 71–80, 2008.

[51] C. P. Mescka, C. A. Y. Wayhs, C. S. Vanzin et al., "Protein and lipid damage in maple syrup urine disease patients: L-carnitine effect," *International Journal of Developmental Neuroscience*, vol. 31, no. 1, pp. 21–24, 2013.

[52] C. P. Mescka, G. Guerreiro, B. Donida et al., "Investigation of inflammatory profile in MSUD patients: benefit of

L-carnitine supplementation," *Metabolic Brain Disease*, vol. 30, no. 5, pp. 1167–1174, 2015.

[53] G. Lu, S. Ren, P. Korge et al., "A novel mitochondrial matrix serine/threonine protein phosphatase regulates the mitochondria permeability transition pore and is essential for cellular survival and development," *Genes & Development*, vol. 21, no. 7, pp. 784–796, 2007.

[54] A. Oyarzabal, I. Bravo-Alonso, M. Sanchez-Arago et al., "Mitochondrial response to the BCKDK-deficiency: some clues to understand the positive dietary response in this form of autism," *Biochimica et Biophysica Acta (BBA) - Molecular Basis of Disease*, vol. 1862, no. 4, pp. 592–600, 2016.

[55] J. Kaplon, L. Zheng, K. Meissl et al., "A key role for mitochondrial gatekeeper pyruvate dehydrogenase in oncogene-induced senescence," *Nature*, vol. 498, no. 7452, pp. 109–112, 2013.

[56] C. L. Quinlan, R. L. S. Goncalves, M. Hey-Mogensen, N. Yadava, V. I. Bunik, and M. D. Brand, "The 2-oxoacid dehydrogenase complexes in mitochondria can produce superoxide/hydrogen peroxide at much higher rates than complex I," *Journal of Biological Chemistry*, vol. 289, no. 12, pp. 8312–8325, 2014.

[57] W. A. Fenton, R. A. Gravel, and L. E. Rosenberg, "Disorders of propionate and methylmalonate metabolism," in *The Metabolic and Molecular Bases of Inherited Disease*, C. R. Scriver, A. L. Beaudet, W. Sly, and D. Valle, Eds., pp. 2165–2190, McGraw-Hill, New York, 2001.

[58] L. Pena and B. K. Burton, "Survey of health status and complications among propionic acidemia patients," *American Journal of Medical Genetics Part A*, vol. 158A, no. 7, pp. 1641–1646, 2012.

[59] L. Pena, J. Franks, K. A. Chapman et al., "Natural history of propionic acidemia," *Molecular Genetics and Metabolism*, vol. 105, no. 1, pp. 5–9, 2012.

[60] S. Kölker, A. G. Cazorla, V. Valayannopoulos et al., "The phenotypic spectrum of organic acidurias and urea cycle disorders. Part 1: the initial presentation," *Journal of Inherited Metabolic Disease*, vol. 38, no. 6, pp. 1041–1057, 2015.

[61] S. Kölker, V. Valayannopoulos, A. B. Burlina et al., "The phenotypic spectrum of organic acidurias and urea cycle disorders. Part 2: the evolving clinical phenotype," *Journal of Inherited Metabolic Disease*, vol. 38, no. 6, pp. 1059–1074, 2015.

[62] S. C. Grünert, S. Müllerleile, L. De Silva et al., "Propionic acidemia: clinical course and outcome in 55 pediatric and adolescent patients," *Orphanet Journal of Rare Diseases*, vol. 8, no. 1, p. 6, 2013.

[63] J. Baruteau, I. Hargreaves, S. Krywawych et al., "Successful reversal of propionic acidaemia associated cardiomyopathy: evidence for low myocardial coenzyme Q10 status and secondary mitochondrial dysfunction as an underlying pathophysiological mechanism," *Mitochondrion*, vol. 17, pp. 150–156, 2014.

[64] M. Nizon, C. Ottolenghi, V. Valayannopoulos et al., "Long-term neurological outcome of a cohort of 80 patients with classical organic acidurias," *Orphanet Journal of Rare Diseases*, vol. 8, no. 1, p. 148, 2013.

[65] S. W. Sauer, J. G. Okun, G. F. Hoffmann, S. Koelker, and M. A. Morath, "Impact of short- and medium-chain organic acids, acylcarnitines, and acyl-CoAs on mitochondrial energy metabolism," *Biochimica et Biophysica Acta (BBA) - Bioenergetics*, vol. 1777, no. 10, pp. 1276–1282, 2008.

[66] N. Gregersen, "The specific inhibition of the pyruvate dehydrogenase complex from pig kidney by propionyl-CoA and isovaleryl-Co-A," *Biochemical Medicine*, vol. 26, no. 1, pp. 20–27, 1981.

[67] S. Cheema-Dhadli, C. C. Leznoff, and M. L. Halperin, "Effect of 2-methylcitrate on citrate metabolism: implications for the management of patients with propionic acidemia and methylmalonic aciduria," *Pediatric Research*, vol. 9, no. 12, pp. 905–908, 1975.

[68] D. A. Stumpf, J. Mcafee, J. K. Parks, and L. Eguren, "Propionate inhibition of succinate:CoA ligase (GDP) and the citric acid cycle in mitochondria," *Pediatric Research*, vol. 14, no. 10, pp. 1127–1131, 1980.

[69] H. Brunengraber and C. R. Roe, "Anaplerotic molecules: current and future," *Journal of Inherited Metabolic Disease*, vol. 29, no. 2-3, pp. 327–331, 2006.

[70] S. Nakao, Y. Moriya, S. Furuyama, R. Niederman, and H. Sugiya, "Propionic acid stimulates superoxide generation in human neutrophils," *Cell Biology International*, vol. 22, no. 5, pp. 331–337, 1998.

[71] F. K. Rigo, L. Pasquetti, C. R. M. Malfatti et al., "Propionic acid induces convulsions and protein carbonylation in rats," *Neuroscience Letters*, vol. 408, no. 2, pp. 151–154, 2006.

[72] F. U. Fontella, V. Pulrolnik, E. Gassen et al., "Propionic and L-methylmalonic acids induce oxidative stress in brain of young rats," *Neuroreport*, vol. 11, no. 3, pp. 541–544, 2000.

[73] Y. de Keyzer, V. Valayannopoulos, J. F. Benoist et al., "Multiple OXPHOS deficiency in the liver, kidney, heart, and skeletal muscle of patients with methylmalonic aciduria and propionic aciduria," *Pediatric Research*, vol. 66, no. 1, pp. 91–95, 2009.

[74] R. Mardach, M. A. Verity, and S. D. Cederbaum, "Clinical, pathological, and biochemical studies in a patient with propionic acidemia and fatal cardiomyopathy," *Molecular Genetics and Metabolism*, vol. 85, no. 4, pp. 286–290, 2005.

[75] M. A. Schwab, S. W. Sauer, J. G. Okun et al., "Secondary mitochondrial dysfunction in propionic aciduria: a pathogenic role for endogenous mitochondrial toxins," *Biochemical Journal*, vol. 398, no. 1, pp. 107–112, 2006.

[76] K. Fragaki, A. Cano, J. F. Benoist et al., "Fatal heart failure associated with CoQ10 and multiple OXPHOS deficiency in a child with propionic acidemia," *Mitochondrion*, vol. 11, no. 3, pp. 533–536, 2011.

[77] S. Yano, S. Yano, L. Li et al., "Infantile mitochondrial DNA depletion syndrome associated with methylmalonic aciduria and 3-methylcrotonyl-CoA and propionyl-CoA carboxylase deficiencies in two unrelated patients: a new phenotype of mtDNA depletion syndrome," *Journal of Inherited Metabolic Disease*, vol. 26, no. 5, pp. 481–488, 2003.

[78] D. R. Melo, A. J. Kowaltowski, M. Wajner, and R. F. Castilho, "Mitochondrial energy metabolism in neurodegeneration associated with methylmalonic acidemia," *Journal of Bioenergetics and Biomembranes*, vol. 43, no. 1, pp. 39–46, 2011.

[79] L. F. Pettenuzzo, C. Ferreira Gda, A. L. Schmidt, C. S. Dutra-Filho, A. T. Wyse, and M. Wajner, "Differential inhibitory effects of methylmalonic acid on respiratory chain complex activities in rat tissues," *International Journal of Developmental Neuroscience*, vol. 24, no. 1, pp. 45–52, 2006.

[80] S. R. Mirandola, D. R. Melo, P. F. Schuck, G. C. Ferreira, M. Wajner, and R. F. Castilho, "Methylmalonate inhibits succinate-supported oxygen consumption by interfering with

mitochondrial succinate uptake," *Journal of Inherited Metabolic Disease*, vol. 31, no. 1, pp. 44–54, 2008.

[81] M. A. Morath, J. G. Okun, I. B. Muller et al., "Neurodegeneration and chronic renal failure in methylmalonic aciduria—a pathophysiological approach," *Journal of Inherited Metabolic Disease*, vol. 31, no. 1, pp. 35–43, 2008.

[82] S. Kolker and J. G. Okun, "Methylmalonic acid—an endogenous toxin?," *Cellular and Molecular Life Sciences*, vol. 62, no. 6, pp. 621–624, 2005.

[83] V. Valayannopoulos, L. Hubert, J. F. Benoist et al., "Multiple OXPHOS deficiency in the liver of a patient with CblA methylmalonic aciduria sensitive to vitamin B(12)," *Journal of Inherited Metabolic Disease*, vol. 32, no. 2, pp. 159–162, 2009.

[84] R. J. Chandler, P. M. Zerfas, S. Shanske et al., "Mitochondrial dysfunction in mut methylmalonic acidemia," *The FASEB Journal*, vol. 23, no. 4, pp. 1252–1261, 2009.

[85] K. Hayasaka, K. Metoki, T. Satoh et al., "Comparison of cytosolic and mitochondrial enzyme alterations in the livers of propionic or methylmalonic acidemia: a reduction of cytochrome oxidase activity," *The Tohoku Journal of Experimental Medicine*, vol. 137, no. 3, pp. 329–334, 1982.

[86] M. A. Cosson, G. Touati, F. Lacaille et al., "Liver hepatoblastoma and multiple OXPHOS deficiency in the follow-up of a patient with methylmalonic aciduria," *Molecular Genetics and Metabolism*, vol. 95, no. 1-2, pp. 107–109, 2008.

[87] M. Caterino, R. J. Chandler, J. L. Sloan et al., "The proteome of methylmalonic acidemia (MMA): the elucidation of altered pathways in patient livers," *Molecular BioSystems*, vol. 12, no. 2, pp. 566–574, 2016.

[88] E. Richard, L. Monteoliva, S. Juarez et al., "Quantitative analysis of mitochondrial protein expression in methylmalonic acidemia by two-dimensional difference gel electrophoresis," *Journal of Proteome Research*, vol. 5, no. 7, pp. 1602–1610, 2006.

[89] I. Manoli, J. R. Sysol, L. Li et al., "Targeting proximal tubule mitochondrial dysfunction attenuates the renal disease of methylmalonic acidemia," *Proceedings of the National Academy of Sciences*, vol. 110, no. 33, pp. 13552–13557, 2013.

[90] Z. K. Zsengeller, N. Aljinovic, L. A. Teot et al., "Methylmalonic acidemia: a megamitochondrial disorder affecting the kidney," *Pediatric Nephrology*, vol. 29, no. 11, pp. 2139–2146, 2014.

[91] Y. Wilnai, G. M. Enns, A. K. Niemi, J. Higgins, and H. Vogel, "Abnormal hepatocellular mitochondria in methylmalonic acidemia," *Ultrastructural Pathology*, vol. 38, no. 5, pp. 309–314, 2014.

[92] J. Kim, C. Gherasim, and R. Banerjee, "Decyanation of vitamin B12 by a trafficking chaperone," *Proceedings of the National Academy of Sciences*, vol. 105, no. 38, pp. 14551–14554, 2008.

[93] J. Kim, L. Hannibal, C. Gherasim, D. W. Jacobsen, and R. Banerjee, "A human vitamin B12 trafficking protein uses glutathione transferase activity for processing alkylcobalamins," *Journal of Biological Chemistry*, vol. 284, no. 48, pp. 33418–33424, 2009.

[94] Z. Li, C. Gherasim, N. A. Lesniak, and R. Banerjee, "Glutathione-dependent one-electron transfer reactions catalyzed by a B_{12} trafficking protein," *Journal of Biological Chemistry*, vol. 289, no. 23, pp. 16487–16497, 2014.

[95] Z. Li, A. Shanmuganathan, M. Ruetz et al., "Coordination chemistry controls the thiol oxidase activity of the B_{12}-trafficking protein CblC," *Journal of Biological Chemistry*, vol. 292, no. 23, pp. 9733–9744, 2017.

[96] J. P. Lerner-Ellis, J. C. Tirone, P. D. Pawelek et al., "Identification of the gene responsible for methylmalonic aciduria and homocystinuria, cblC type," *Nature Genetics*, vol. 38, no. 1, pp. 93–100, 2005.

[97] J. D. Weisfeld-Adams, E. A. McCourt, G. A. Diaz, and S. C. Oliver, "Ocular disease in the cobalamin C defect: a review of the literature and a suggested framework for clinical surveillance," *Molecular Genetics and Metabolism*, vol. 114, no. 4, pp. 537–546, 2015.

[98] E. Richard, A. Jorge-Finnigan, J. Garcia-Villoria et al., "Genetic and cellular studies of oxidative stress in methylmalonic aciduria (MMA) cobalamin deficiency type C (cblC) with homocystinuria (MMACHC)," *Human Mutation*, vol. 30, no. 11, pp. 1558–1566, 2009.

[99] A. Jorge-Finnigan, A. Gamez, B. Perez, M. Ugarte, and E. Richard, "Different altered pattern expression of genes related to apoptosis in isolated methylmalonic aciduria cblB type and combined with homocystinuria cblC type," *Biochimica et Biophysica Acta (BBA) - Molecular Basis of Disease*, vol. 1802, no. 11, pp. 959–967, 2010.

[100] L. Hannibal, P. M. DiBello, M. Yu et al., "The MMACHC proteome: hallmarks of functional cobalamin deficiency in humans," *Molecular Genetics and Metabolism*, vol. 103, no. 3, pp. 226–239, 2011.

[101] L. Hannibal, P. M. DiBello, and D. W. Jacobsen, "Proteomics of vitamin B12 processing," *Clinical Chemistry and Laboratory Medicine*, vol. 51, no. 3, pp. 477–488, 2013.

[102] M. Caterino, A. Pastore, M. G. Strozziero et al., "The proteome of cblC defect: in vivo elucidation of altered cellular pathways in humans," *Journal of Inherited Metabolic Disease*, vol. 38, no. 5, pp. 969–979, 2015.

[103] C. Gherasim, M. Ruetz, Z. Li, S. Hudolin, and R. Banerjee, "Pathogenic mutations differentially affect the catalytic activities of the human B12-processing chaperone CblC and increase futile redox cycling," *Journal of Biological Chemistry*, vol. 290, no. 18, pp. 11393–11402, 2015.

[104] S. Goodman and F. Frerman, "Organic acidemias due to defects in lysine oxidation: 2-ketoadipic acidemia and glutaric acidemia," in *The Metabolic and Molecular Basis of Inherited Disease*, C. R. Scriver, A. L. Beaudet, W. S. Sly, and D. Valle, Eds., pp. 2195–2204, McGraw-Hill Inc, New York, 2001.

[105] S. Kölker, S. F. Garbade, C. R. Greenberg et al., "Natural history, outcome, and treatment efficacy in children and adults with glutaryl-CoA dehydrogenase deficiency," *Pediatric Research*, vol. 59, no. 6, pp. 840–847, 2006.

[106] K. A. Strauss, E. G. Puffenberger, D. L. Robinson, and D. H. Morton, "Type I glutaric aciduria, part 1: natural history of 77 patients," *American Journal of Medical Genetics*, vol. 121C, no. 1, pp. 38–52, 2003.

[107] A. U. Amaral, C. Cecatto, B. Seminotti et al., "Experimental evidence that bioenergetics disruption is not mainly involved in the brain injury of glutaryl-CoA dehydrogenase deficient mice submitted to lysine overload," *Brain Research*, vol. 1620, pp. 116–129, 2015.

[108] S. Kolker, S. W. Sauer, G. F. Hoffmann, I. Muller, M. A. Morath, and J. G. Okun, "Pathogenesis of CNS involvement in disorders of amino and organic acid metabolism,"

Journal of Inherited Metabolic Disease, vol. 31, no. 2, pp. 194–204, 2008.

[109] A. Latini, G. C. Ferreira, K. Scussiato et al., "Induction of oxidative stress by chronic and acute glutaric acid administration to rats," *Cellular and Molecular Neurobiology*, vol. 27, no. 4, pp. 423–438, 2007.

[110] D. M. Koeller, M. Woontner, L. S. Crnic et al., "Biochemical, pathologic and behavioral analysis of a mouse model of glutaric acidemia type I," *Human Molecular Genetics*, vol. 11, no. 4, pp. 347–357, 2002.

[111] B. Seminotti, R. T. Ribeiro, A. U. Amaral et al., "Acute lysine overload provokes protein oxidative damage and reduction of antioxidant defenses in the brain of infant glutaryl-CoA dehydrogenase deficient mice: a role for oxidative stress in GA I neuropathology," *Journal of the Neurological Sciences*, vol. 344, no. 1-2, pp. 105–113, 2014.

[112] W. J. Zinnanti, J. Lazovic, E. B. Wolpert et al., "A diet-induced mouse model for glutaric aciduria type I," *Brain*, vol. 129, no. 4, pp. 899–910, 2006.

[113] W. J. Zinnanti, J. Lazovic, C. Housman et al., "Mechanism of age-dependent susceptibility and novel treatment strategy in glutaric acidemia type I," *Journal of Clinical Investigation*, vol. 117, no. 11, pp. 3258–3270, 2007.

[114] C. Perez-Cerda, J. García-Villoria, R. Ofman et al., "2-Methyl-3-hydroxybutyryl-CoA dehydrogenase (MHBD) deficiency: an X-linked inborn error of isoleucine metabolism that may mimic a mitochondrial disease," *Pediatric Research*, vol. 58, no. 3, pp. 488–491, 2005.

[115] W. Sperl, P. Ješina, J. Zeman et al., "Deficiency of mitochondrial ATP synthase of nuclear genetic origin," *Neuromuscular Disorders*, vol. 16, no. 12, pp. 821–829, 2006.

[116] C. G. da Silva, C. A. J. Ribeiro, G. Leipnitz et al., "Inhibition of cytochrome c oxidase activity in rat cerebral cortex and human skeletal muscle by D-2-hydroxyglutaric acid in vitro," *Biochimica et Biophysica Acta (BBA) - Molecular Basis of Disease*, vol. 1586, no. 1, pp. 81–91, 2002.

[117] D. Zafeiriou, P. Augoustides-Savvopoulou, D. Haas et al., "Ethylmalonic encephalopathy: clinical and biochemical observations," *Neuropediatrics*, vol. 38, no. 2, pp. 78–82, 2007.

[118] S. B. Wortmann, R. J. T. Rodenburg, A. Jonckheere et al., "Biochemical and genetic analysis of 3-methylglutaconic aciduria type IV: a diagnostic strategy," *Brain*, vol. 132, no. 1, pp. 136–146, 2009.

[119] L. Zandberg, H. C. van Dyk, F. H. van der Westhuizen, and A. A. van Dijk, "A 3-methylcrotonyl-CoA carboxylase deficient human skin fibroblast transcriptome reveals underlying mitochondrial dysfunction and oxidative stress," *The International Journal of Biochemistry & Cell Biology*, vol. 78, pp. 116–129, 2016.

[120] Â. Zanatta, A. P. Moura, A. M. Tonin et al., "Neurochemical evidence that the metabolites accumulating in 3-methylcrotonyl-CoA carboxylase deficiency induce oxidative damage in cerebral cortex of young rats," *Cellular and Molecular Neurobiology*, vol. 33, no. 1, pp. 137–146, 2013.

[121] M. R. Hayden and S. C. Tyagi, "Homocysteine and reactive oxygen species in metabolic syndrome, type 2 diabetes mellitus, and atheroscleropathy: the pleiotropic effects of folate supplementation," *Nutrition Journal*, vol. 3, no. 1, 2004.

[122] C. G. Zou and R. Banerjee, "Homocysteine and redox signaling," *Antioxidants & Redox Signaling*, vol. 7, no. 5-6, pp. 547–559, 2005.

[123] D. W. Jacobsen, "Hyperhomocysteinemia and oxidative stress: time for a reality check?," *Arteriosclerosis, Thrombosis, and Vascular Biology*, vol. 20, no. 5, pp. 1182–1184, 2000.

[124] H. J. Blom, "Consequences of homocysteine export and oxidation in the vascular system," *Seminars in Thrombosis and Hemostasis*, vol. Volume 26, no. Number 03, pp. 227–232, 2000.

[125] N. Tyagi, K. C. Sedoris, M. Steed, A. V. Ovechkin, K. S. Moshal, and S. C. Tyagi, "Mechanisms of homocysteine-induced oxidative stress," *American Journal of Physiology-Heart and Circulatory Physiology*, vol. 289, no. 6, pp. H2649–H2656, 2005.

[126] F. Bonetti, G. Brombo, and G. Zuliani, "The relationship between hyperhomocysteinemia and neurodegeneration," *Neurodegenerative Disease Management*, vol. 6, no. 2, pp. 133–145, 2016.

[127] S. H. Mudd, H. L. Levy, and J. P. Kraus, "Disorders of trans-sulfuration," in *The Online Metabolic and Molecular Bases of Inherited Diseases*, K. Kinzler, A. Ballabio, S. E. Antonarakis, A. L. Beaudet, B. Vogelstein, and D. Valle, Eds., McGrall-Hill, New York, 2011.

[128] M. Schiff and H. J. Blom, "Treatment of inherited homocystinurias," *Neuropediatrics*, vol. 43, no. 6, pp. 295–304, 2012.

[129] J. L. Faverzani, T. G. Hammerschmidt, A. Sitta, M. Deon, M. Wajner, and C. R. Vargas, "Oxidative stress in homocystinuria due to cystathionine β-synthase deficiency: findings in patients and in animal models," *Cellular and Molecular Neurobiology*, vol. 37, no. 8, pp. 1477–1485, 2017.

[130] C. S. Vanzin, G. B. Biancini, A. Sitta et al., "Experimental evidence of oxidative stress in plasma of homocystinuric patients: a possible role for homocysteine," *Molecular Genetics and Metabolism*, vol. 104, no. 1-2, pp. 112–117, 2011.

[131] C. S. Vanzin, V. Manfredini, A. E. Marinho et al., "Homocysteine contribution to DNA damage in cystathionine β-synthase-deficient patients," *Gene*, vol. 539, no. 2, pp. 270–274, 2014.

[132] C. S. Vanzin, C. P. Mescka, B. Donida et al., "Lipid, oxidative and inflammatory profile and alterations in the enzymes paraoxonase and butyrylcholinesterase in plasma of patients with homocystinuria due CBS deficiency: the vitamin B12 and folic acid importance," *Cellular and Molecular Neurobiology*, vol. 35, no. 6, pp. 899–911, 2015.

[133] K. Robert, J. Nehme, E. Bourdon et al., "Cystathionine β synthase deficiency promotes oxidative stress, fibrosis, and steatosis in mice liver," *Gastroenterology*, vol. 128, no. 5, pp. 1405–1415, 2005.

[134] E. L. Streck, P. S. Vieira, C. M. Wannmacher, C. S. Dutra-Filho, M. Wajner, and A. T. Wyse, "In vitro effect of homocysteine on some parameters of oxidative stress in rat hippocampus," *Metabolic Brain Disease*, vol. 18, no. 2, pp. 147–154, 2003.

[135] C. Matté, F. M. Stefanello, V. Mackedanz et al., "Homocysteine induces oxidative stress, inflammatory infiltration, fibrosis and reduces glycogen/glycoprotein content in liver of rats," *International Journal of Developmental Neuroscience*, vol. 27, no. 4, pp. 337–344, 2009.

[136] D. Watkins and D. S. Rosenblatt, "Inherited disorders of folate and cobalamin transport amd metabolism," in *The Metabolic and Molecular Bases of Inherited Diseases*, C. R. Scriver, A. L. Beaudet, W. Sly, and D. Valle, Eds., pp. 3897–3933, McGrall-Hill, New York, 2011.

[137] R. Surtees, "Demyelination and inborn errors of the single carbon transfer pathway," *European Journal of Pediatrics*, vol. 157, no. S2, pp. S118–S121, 1998.

[138] A. Martinez-Pizarro, L. R. Desviat, M. Ugarte, B. Perez, and E. Richard, "Endoplasmic reticulum stress and autophagy in homocystinuria patients with remethylation defects," *PLoS One*, vol. 11, no. 3, article e0150357, 2016.

[139] S. I. Dikalov and D. G. Harrison, "Methods for detection of mitochondrial and cellular reactive oxygen species," *Antioxidants & Redox Signaling*, vol. 20, no. 2, pp. 372–382, 2014.

[140] X. Zhang and F. Gao, "Imaging mitochondrial reactive oxygen species with fluorescent probes: current applications and challenges," *Free Radical Research*, vol. 49, no. 4, pp. 374–382, 2015.

[141] B. Kalyanaraman, M. Hardy, R. Podsiadly, G. Cheng, and J. Zielonka, "Recent developments in detection of superoxide radical anion and hydrogen peroxide: opportunities, challenges, and implications in redox signaling," *Archives of Biochemistry and Biophysics*, vol. 617, pp. 38–47, 2017.

[142] K. Debowska, D. Debski, M. Hardy et al., "Toward selective detection of reactive oxygen and nitrogen species with the use of fluorogenic probes – limitations, progress, and perspectives," *Pharmacological Reports*, vol. 67, no. 4, pp. 756–764, 2015.

[143] W. A. Pryor and S. S. Godber, "Noninvasive measures of oxidative stress status in humans," *Free Radical Biology and Medicine*, vol. 10, no. 3-4, pp. 177–184, 1991.

[144] A. C. Ribou, "Synthetic sensors for reactive oxygen species detection and quantification: a critical review of current methods," *Antioxidants & Redox Signaling*, vol. 25, no. 9, pp. 520–533, 2016.

[145] M. Wrona and P. Wardman, "Properties of the radical intermediate obtained on oxidation of $2',7'$-dichlorodihydrofluorescein, a probe for oxidative stress," *Free Radical Biology and Medicine*, vol. 41, no. 4, pp. 657–667, 2006.

[146] C. Rota, C. F. Chignell, and R. P. Mason, "Evidence for free radical formation during the oxidation of $2'$-$7'$-dichlorofluorescin to the fluorescent dye $2'$-$7'$-dichlorofluorescein by horseradish peroxidase:possible implications for oxidative stress measurements," *Free Radical Biology and Medicine*, vol. 27, no. 7-8, pp. 873–881, 1999.

[147] L. F. F. Royes, P. Gabbi, L. R. Ribeiro et al., "A neuronal disruption in redox homeostasis elicited by ammonia alters the glycine/glutamate (GABA) cycle and contributes to MMA-induced excitability," *Amino Acids*, vol. 48, no. 6, pp. 1373–1389, 2016.

[148] H. Zhao, J. Joseph, H. M. Fales et al., "Detection and characterization of the product of hydroethidine and intracellular superoxide by HPLC and limitations of fluorescence," *Proceedings of the National Academy of Sciences*, vol. 102, no. 16, pp. 5727–5732, 2005.

[149] K. M. Robinson, M. S. Janes, M. Pehar et al., "Selective fluorescent imaging of superoxide in vivo using ethidium-based probes," *Proceedings of the National Academy of Sciences*, vol. 103, no. 41, pp. 15038–15043, 2006.

[150] J. Zielonka, M. Hardy, and B. Kalyanaraman, "HPLC study of oxidation products of hydroethidine in chemical and biological systems: ramifications in superoxide measurements," *Free Radical Biology and Medicine*, vol. 46, no. 3, pp. 329–338, 2009.

[151] A. Logan, H. M. Cochemé, P. B. L. Pun et al., "Using exomarkers to assess mitochondrial reactive species in vivo," *Biochimica et Biophysica Acta (BBA) - General Subjects*, vol. 1840, no. 2, pp. 923–930, 2014.

[152] A. Logan, I. G. Shabalina, T. A. Prime et al., "In vivo levels of mitochondrial hydrogen peroxide increase with age in mtDNA mutator mice," *Aging Cell*, vol. 13, no. 4, pp. 765–768, 2014.

[153] B. Merinero, C. Perez-Cerda, L. R. Desviat et al., "Mitochondrial organic acidurias. Part I: biochemical and molecular basis," in *Mitochondrial Pathophysiology*, F. Palau and S. Cadenas, Eds., pp. 145–171, Research Signpost, Kerala (India), 2011.

[154] H. J. Forman, K. J. A. Davies, and F. Ursini, "How do nutritional antioxidants really work: nucleophilic tone and para-hormesis versus free radical scavenging in vivo," *Free Radical Biology and Medicine*, vol. 66, pp. 24–35, 2014.

[155] H. H. H. W. Schmidt, R. Stocker, C. Vollbracht et al., "Antioxidants in translational medicine," *Antioxidants & Redox Signaling*, vol. 23, no. 14, pp. 1130–1143, 2015.

[156] J. D. Hayes and A. T. Dinkova-Kostova, "The Nrf2 regulatory network provides an interface between redox and intermediary metabolism," *Trends in Biochemical Sciences*, vol. 39, no. 4, pp. 199–218, 2014.

[157] A. Brunet, L. B. Sweeney, J. F. Sturgill et al., "Stress-dependent regulation of FOXO transcription factors by the SIRT1 deacetylase," *Science*, vol. 303, no. 5666, pp. 2011–2015, 2004.

[158] S. Nemoto, M. M. Fergusson, and T. Finkel, "SIRT1 functionally interacts with the metabolic regulator and transcriptional coactivator PGC-1α," *Journal of Biological Chemistry*, vol. 280, no. 16, pp. 16456–16460, 2005.

[159] L. F. Pettenuzzo, Patrícia F. Schuck, A. T. S. Wyse et al., "Ascorbic acid prevents water maze behavioral deficits caused by early postnatal methylmalonic acid administration in the rat," *Brain Research*, vol. 976, no. 2, pp. 234–242, 2003.

[160] L. Pettenuzzo, P. F. Schuck, F. Fontella et al., "Ascorbic acid prevents cognitive deficits caused by chronic administration of propionic acid to rats in the water maze," *Pharmacology Biochemistry and Behavior*, vol. 73, no. 3, pp. 623–629, 2002.

[161] C. A. Ribeiro, Â. M. Sgaravatti, R. B. Rosa et al., "Inhibition of brain energy metabolism by the branched-chain amino acids accumulating in maple syrup urine disease," *Neurochemical Research*, vol. 33, no. 1, pp. 114–124, 2008.

[162] F. S. Rodrigues, M. A. Souza, D. V. Magni et al., "N-Acetylcysteine prevents spatial memory impairment induced by chronic early postnatal glutaric acid and lipopolysaccharide in rat pups," *PLoS One*, vol. 8, no. 10, article e78332, 2013.

[163] G. S. Ribas, V. Manfredini, J. F. de Mari et al., "Reduction of lipid and protein damage in patients with disorders of propionate metabolism under treatment: a possible protective role of L-carnitine supplementation," *International Journal of Developmental Neuroscience*, vol. 28, no. 2, pp. 127–132, 2010.

[164] I. Gulcin, "Antioxidant and antiradical activities of L-carnitine," *Life Sciences*, vol. 78, no. 8, pp. 803–811, 2006.

[165] G. Guerreiro, C. P. Mescka, A. Sitta et al., "Urinary biomarkers of oxidative damage in maple syrup urine disease: the L-carnitine role," *International Journal of Developmental Neuroscience*, vol. 42, pp. 10–14, 2015.

[166] S. Pinar-Sueiro, R. Martinez-Fernandez, S. Lage-Medina, L. Aldamiz-Echevarria, and E. Vecino, "Optic neuropathy

in methylmalonic acidemia: the role of neuroprotection," *Journal of Inherited Metabolic Disease*, vol. 33, no. S3, pp. 199–203, 2010.

[167] A. J. Guenzel, S. E. Hofherr, M. Hillestad et al., "Generation of a hypomorphic model of propionic acidemia amenable to gene therapy testing," *Molecular Therapy*, vol. 21, no. 7, pp. 1316–1323, 2013.

[168] M. R. de Oliveira, S. F. Nabavi, A. Manayi, M. Daglia, Z. Hajheydari, and S. M. Nabavi, "Resveratrol and the mitochondria: from triggering the intrinsic apoptotic pathway to inducing mitochondrial biogenesis, a mechanistic view," *Biochimica et Biophysica Acta (BBA) - General Subjects*, vol. 1860, no. 4, pp. 727–745, 2016.

[169] A. Lopes Costa, C. Le Bachelier, L. Mathieu et al., "Beneficial effects of resveratrol on respiratory chain defects in patients' fibroblasts involve estrogen receptor and estrogen-related receptor alpha signaling," *Human Molecular Genetics*, vol. 23, no. 8, pp. 2106–2119, 2014.

[170] A. W. El-Hattab, A. M. Zarante, M. Almannai, and F. Scaglia, "Therapies for mitochondrial diseases and current clinical trials," *Molecular Genetics and Metabolism*, vol. 122, no. 3, pp. 1–9, 2017.

[171] K. N. Maclean, H. Jiang, S. Aivazidis et al., "Taurine treatment prevents derangement of the hepatic γ-glutamyl cycle and methylglyoxal metabolism in a mouse model of classical homocystinuria: regulatory crosstalk between thiol and sulfinic acid metabolism," *The FASEB Journal*, article fj.201700586R, 2018.

[172] O. Firuzi, R. Miri, M. Tavakkoli, and L. Saso, "Antioxidant therapy: current status and future prospects," *Current Medicinal Chemistry*, vol. 18, no. 25, pp. 3871–3888, 2011.

[173] P. Palozza, S. Serini, A. Torsello et al., "Regulation of cell cycle progression and apoptosis by beta-carotene in undifferentiated and differentiated HL-60 leukemia cells: possible involvement of a redox mechanism," *International Journal of Cancer*, vol. 97, no. 5, pp. 593–600, 2002.

[174] S. L. Yeh, H. M. Wang, P. Y. Chen, and T. C. Wu, "Interactions of β-carotene and flavonoids on the secretion of pro-inflammatory mediators in an in vitro system," *Chemico-Biological Interactions*, vol. 179, no. 2-3, pp. 386–393, 2009.

[175] J. Lin, N. R. Cook, C. Albert et al., "Vitamins C and E and beta carotene supplementation and cancer risk: a randomized controlled trial," *Journal of the National Cancer Institute*, vol. 101, no. 1, pp. 14–23, 2009.

[176] G. Bjelakovic, D. Nikolova, L. L. Gluud, R. G. Simonetti, and C. Gluud, "Mortality in randomized trials of antioxidant supplements for primary and secondary prevention: systematic review and meta-analysis," *JAMA*, vol. 297, no. 8, pp. 842–857, 2007.

[177] G. Bjelakovic, D. Nikolova, L. L. Gluud, R. G. Simonetti, and C. Gluud, "Antioxidant supplements for prevention of mortality in healthy participants and patients with various diseases," *Cochrane Database of Systematic Reviews*, no. 3, article CD007176, 2012.

[178] K. R. Martin and J. C. Barrett, "Reactive oxygen species as double-edged swords in cellular processes: low-dose cell signaling versus high-dose toxicity," *Human & Experimental Toxicology*, vol. 21, no. 2, pp. 71–75, 2002.

[179] L. I. Leichert and T. P. Dick, "Incidence and physiological relevance of protein thiol switches," *Biological Chemistry*, vol. 396, no. 5, pp. 389–399, 2015.

[180] Y. Fujikawa, L. P. Roma, M. C. Sobotta et al., "Mouse redox histology using genetically encoded probes," *Science Signaling*, vol. 9, no. 419, p. rs1, 2016.

Research Article

p66^{Shc} Inactivation Modifies RNS Production, Regulates Sirt3 Activity, and Improves Mitochondrial Homeostasis, Delaying the Aging Process in Mouse Brain

Hernán Pérez,[1] Paola Vanesa Finocchietto,[1,2] Yael Alippe,[1] Inés Rebagliati,[1] María Eugenia Elguero,[1] Nerina Villalba,[1] Juan José Poderoso,[1] and María Cecilia Carreras [1,3]

[1]*Laboratory of Oxygen Metabolism, INIGEM-UBA-CONICET, Buenos Aires, Argentina*
[2]*Departamento de Medicina, Facultad de Medicina, Universidad de Buenos Aires, Buenos Aires, Argentina*
[3]*Departamento de Bioquímica Clínica, Facultad de Farmacia y Bioquímica, Universidad de Buenos Aires, Buenos Aires, Argentina*

Correspondence should be addressed to María Cecilia Carreras; carreras@ffyb.uba.ar

Programmed and damage aging theories have traditionally been conceived as stand-alone schools of thought. However, the p66^{Shc} adaptor protein has demonstrated that aging-regulating genes and reactive oxygen species (ROS) are closely interconnected, since its absence modifies metabolic homeostasis by providing oxidative stress resistance and promoting longevity. p66$^{Shc(−/−)}$ mice are a unique opportunity to further comprehend the bidirectional relationship between redox homeostasis and the imbalance of mitochondrial biogenesis and dynamics during aging. This study shows that brain mitochondria of p66$^{Shc(−/−)}$ aged mice exhibit a reduced alteration of redox balance with a decrease in both ROS generation and its detoxification activity. We also demonstrate a strong link between reactive nitrogen species (RNS) and mitochondrial function, morphology, and biogenesis, where low levels of ONOO$^-$ formation present in aged p66$^{Shc(−/−)}$ mouse brain prevent protein nitration, delaying the loss of biological functions characteristic of the aging process. Sirt3 modulates age-associated mitochondrial biology and function via lysine deacetylation of target proteins, and we show that its regulation depends on its nitration status and is benefited by the improved NAD$^+$/NADH ratio in aged p66$^{Shc(−/−)}$ brain mitochondria. Low levels of protein nitration and acetylation could cause the metabolic homeostasis maintenance observed during aging in this group, thus increasing its lifespan.

1. Introduction

Aging is a multifactorial degenerative process that strongly impacts the endocrinology and biochemistry of the brain [1]. Mitochondrial function declines in the normal aging process and increases the incidence of age-related disorders. In accordance with the free radical theory of aging, this process can be ascribed to the oxidative damage caused by the generation of reactive oxygen species (ROS) derived from mitochondrial respiration when O$_2$ is partially reduced [2]. It has been demonstrated that electron transfer leakage throughout the mitochondrial respiratory chain is responsible for the formation of most cellular ROS [3]. In this way, ROS generation depends on mitochondrial activity [4], which by itself can be perceived as a signal sensor and transducer in various enzymatic and gene-mediated physiological and pathophysiological processes [5].

In addition, mitochondrial function and morphology are also modulated by nitric oxide (NO) exposure. NO is a relatively low reactive radical whose derivatives, such as peroxynitrite (ONOO$^-$), can cause nitrosative damage in biomolecules, proteosomic degradation failure, enzymatic activity inhibition, and overall interference of regulatory functions [6]. These processes occur in aging, when the levels of ROS

rise and superoxide anion (O_2^-) conjugates with NO to create reactive nitrogen species (RNS), and their products nitrate (NO_3^-), nitrite (NO_2^-), and peroxynitrite ($ONOO^-$), which have demonstrated a direct role in cellular signaling, vasodilation, immune response, and aging [7–9].

Alterations in ROS/RNS levels have been mechanistically linked with changes in mitochondrial morphology in many studies, suggesting a crosstalk between redox homeostasis and mitochondrial dynamics [10]. Mitochondrial morphology is regulated by continuous fusion and fission events that are essential to maintaining normal mitochondrial function [11]. These fusion/fission processes are finely regulated by the mitochondrial fusion proteins optic atrophy 1 (Opa1), mitofusins 1 and 2 (Mfn1 and Mfn2, resp.) and by the mitochondrial fission proteins dynamin-related protein 1 (Drp1) and fission protein 1 (Fis1). High levels of ROS and RNS, such as those measured in aging models, have been associated with redox-induced posttranslational modifications (i.e., nitration or S-nitrosylation) in several of these proteins and their binding targets, leading to mitochondrial fragmentation [12–14].

Mitochondrial plasticity and density decrease with age, and their capacity for mitochondrial biogenesis is reduced owing to a redox-dependent decline of (peroxisome proliferator-activated receptor γ-coactivator-1α) (PGC-1α) activity [15–17]. PGC-1α is a transcriptional coactivator that enhances the activity of specific transcription factors, in turn coordinating the expression of key nuclear-encoded mitochondrial genes that are required for the proper functioning of the organelle.

A link between mitochondrial biogenesis and mitochondrial morphology has been suggested by the fact that PGC-1α regulates Mfn2 expression. Repression of Mfn2 in cells decreases oxygen consumption, mitochondrial membrane potential, and the expression of oxidative phosphorylation proteins [17].

On the other hand, changes observed in the lysine acetylation profile of proteins or "acetylome" are related to normal aging and age-related diseases [18]. Sirt3, a member of the NAD^+-dependent deacetylase family, is the most studied mitochondrial sirtuin associated with metabolic homeostasis maintenance. Sirt3 is considered a key element to delaying the loss of biological functions during aging [19]. Recent studies have shown that the acetylation levels of mouse mitochondrial proteins are modulated in fasting conditions or during caloric restriction [20]. Additionally, an increase in Sirt3 expression was observed in several tissues under these conditions, suggesting an improvement in the protection against ROS-induced aging [21–24]. SIRT3 stimulates proteins participating in ATP generation, tricarboxylic acid (TCA) cycle, and electron transport chain and stress response [25, 26]. Further, it promotes mitochondrial biogenesis via PGC-1α-mediated inhibition of cellular ROS and delays mitochondrial dynamic age imbalance, deacetylating Opa1 [27, 28].

In the last years, more cases of cooperation between ROS and aging-regulating genes have been established in senescence and aging development [29]. The adaptor protein p66[Shc] is a genetic determinant of lifespan that regulates ROS metabolism and cellular apoptosis. Faced with a stress signal (growth factor, insulin receptor activation, excessive radiation, or oxidative stress), PKCβ phosphorylates p66[Shc] in Ser36, which translocates to mitochondria, oxidizes cytochrome c in the intermembrane space, and prevents electron transfer to cytochrome oxidase, resulting in a higher reduction level of complex III (ubiquinol and cytochromes b-c1) [30]. The inhibition of electron free flow determines the formation of semiubiquinone and the subsequent O_2 monoelectric reduction with O_2^- formation, eventually dismutated to hydrogen peroxide (H_2O_2) by MnSOD [31]. p66[Shc] ablation in mice is translated into a significant decrease in mitochondria-produced ROS and a 30% increase in lifespan [32]. These knockout mice for p66[Shc] (p66[Shc(−/−)]) have been shown to be thinner, to exhibit an increased metabolic rate, and to have less body fat than their wild-type littermates [33]. And more remarkably, they have been described as an animal model of healthy aging with better cognitive abilities at adulthood in a spatial memory task and improved physical performance at senescence [34]. The aim of this study is to deepen the bidirectional relationship between redox homeostasis and the imbalance of mitochondrial dynamics and biogenesis in this model of healthy aging.

2. Materials and Methods

2.1. Mice and Ethics. Dr. P. G. Pellicci at the European Institute of Oncology, Milan, kindly provided 129 p66[Shc] knockout (p66[Shc(−/−)]) breeding pairs for this project. The breeding stocks were backcrossed onto 129/SV mice. A colony was maintained in the animal facility at the School of Pharmacy and Biochemistry of the University of Buenos Aires. Heterozygous Shc KO mice (p66[Shc(+/−)]) were mated to produce the homozygous Shc KO (p66[Shc(−/−)]), and WT control littermates were used for the study. Mice aged 3, 18, and 24 months from both groups were housed in a constant-temperature room (20–24°C) with a 12-hour dark/12-hour light cycle, fed ad libitum with a standard diet and free access to water. Animal experiments were performed in accordance with the principles of laboratory animal care. The Institutional Animal Care and Research Committee of the University of Buenos Aires approved all animal procedures. We made every possible effort to minimize animal suffering and to reduce the number of animals used.

2.2. Mitochondrial Isolation. Mice were deeply anesthetized using ketamine (50 mg/kg) and sacrificed by cervical dislocation. The brains were immediately extracted and homogenized in MSHE buffer (0.22 M mannitol, 70 mM sucrose, 0.5 mM EGTA, 2 mM KHEPES). The homogenate was centrifuged at 800g for 10 min at 4°C. The supernatant was transferred and centrifuged again at 10,000g for 10 min at 4°C in a Sorvall centrifuge. The pellet containing mitochondria was resuspended and isolated at 100,000g by Percoll gradient centrifugation in an ultracentrifuge [35]. Fresh mitochondria were used to determine membrane potential, oxygen consumption, NO production, nNOS activity, and NAD/NADH ratio. For complex activities, MnSOD and catalase activity, and Western blotting determination,

mitochondria were stored at −80°C and then subjected to three freeze/thaw cycles followed by a homogenization step by passage through a 29 G hypodermic needle.

2.3. NOS Activity. Homogenate fractions of brain tissue from control and KO (p66$^{Shc-/-}$) mice were determined by conversion from [3H] L-Arg to [3H] L-citrulline [36] in 50 mM potassium phosphate buffer, pH 7.4, in the presence of 100 μM L-Arg, 0.1 μM [3H] L-Arg (NEN), 0.1 mM NADPH, 0.3 mM CaCl$_2$, 0.1 μM calmodulin, 10 μM tetrahydrobiopterin, 1 μM flavin adenine dinucleotide, 1 μM flavin mononucleotide, 50 mM L-valine, and 1 mg/mL protein. Specific activity was calculated by subtracting the remaining activity in the presence of the NOS inhibitor 5 mM L-NMMA or 2 mM ethylene glycol tetraacetic acid [37].

2.4. Mitochondrial H$_2$O$_2$ Production. Mitochondrial H$_2$O$_2$ production was monitored using a Hitachi F-2000 spectrofluorometer with excitation and emission wavelengths at 315 and 425 nm, respectively [31]. The reaction medium, potassium phosphate buffer (50 mM) and 50 mM L-valine, was supplemented with 10 mM succinate, 12.5 units/mL horseradish peroxidase, 250 M p-hydroxyphenylacetic acid, and 0.15 mg of mitochondrial protein per mL. Mitochondrial preparations were supplemented with 1 μM Mn(III)tetrakis(4-benzoic acid) porphyrin (Cayman Chemical, Ann Arbor, MI) and 0.2 μM antimycin A for a uniform maximal H$_2$O$_2$ production rate [38].

2.5. Antioxidant Enzyme Activities. Mitochondrial Mn-SOD activity was determined by inhibition of cytochrome c reduction at 550 nm in 50 mM potassium phosphate buffer/ 0.1 mM EDTA (pH 7.8) at 25°C, and results were expressed as pmoles SOD per mg of protein [39]. Catalase activity in supernatants was determined by the decrease in H$_2$O$_2$ absorption at 240 nm ($\varepsilon_{240} = 41 \mu M^{-1} cm^{-1}$). The pseudo-first reaction constant (k') expressed as k'/mg protein was calculated and then extrapolated to a calibration curve to obtain U CAT/mg protein [40].

2.6. Oxygen Consumption Rate. Oxygen uptake was determined polarographically with a Clark-type electrode placed in a 3 mL chamber at 30°C, in a reaction medium consisting of 0.23 mM mannitol, 70 mM sucrose, 30 mM Tris-HCl, 4 mM MgCl$_2$, 5 mM Na$_2$HPO$_4$-KH$_2$PO$_4$, and 1 mM EDTA, pH 7.4, saturated with room air (225 μM O$_2$) with 0.5–1 mg mitochondria protein/mL. Oxygen uptake was determined using 6 mM malate-glutamate or succinate as substrates in the presence (state 3) or the absence (state 4) of a phosphate acceptor (0.2 mM ADP). Oxygen uptake was expressed in nanogram atoms of oxygen per minute per milligram of protein. The respiratory control rate was calculated as state 3/ state 4 respiration rate. The P/O ratio was calculated as the ratio of nmoles of added ADP per nanogram atoms of O$_2$ utilized during state 3 [41, 42].

2.7. Mitochondrial Respiratory Chain Complex Activity. Nicotinamide adenine dinucleotide- and succinate-cytochrome c reductase activities (complexes I–III and II–III, resp.) were assayed by cytochrome c reduction at 550 nm with a

Hitachi U3000 spectrophotometer (Hitachi, Tokyo, Japan) at 30°C. Cytochrome oxidase activity (complex IV) was determined by monitoring cytochrome c oxidation at 550 nm ($\varepsilon_{550} = 21 mM^{-1} \times cm^{-1}$); the reaction rate was measured as the pseudo-first-order reaction constant (k') and expressed as k'/min/mg protein [43].

2.8. Mitochondrial Membrane Potential (Ψ) and Mitochondrial NO, ROS, and O$_2^-$ Production. Mitochondrial membrane potential (Ψ) and mitochondrial NO, ROS, and O$_2^-$ production were estimated by flow cytometry (FACSCalibur) using fluorescent dyes 3,3′-dihexyloxacarbocyanine iodide (DiOC6) (200 nM; Molecular Probes), DAF-FM (10 μM; Molecular Probes) with 0.3 mM L-arginine in the presence and absence of the NOS inhibitor (3 mM L-NAME), H$_2$DCFDA (25 μM; Sigma-Aldrich), or MitoSOX (2.5 μM; Molecular Probes), respectively. Fresh brain mitochondria (50 μg protein/mL) were suspended in 0.5 mL of respiration buffer (120 mM KCl, 5 mM KH$_2$PO$_4$, 1 mM EGTA, 3 mM HEPES, and 1 mg/mL fatty acid-free BSA [pH 7.4]). These assays were performed in the dark at 37°C for 15 min. After the incubation period, mitochondria were centrifuged for 5 min at 10,000g for pelleting and washing and then suspended to record the fluorescence intensity.

2.9. NAD/NADH Mitochondrial Ratio and ATP Content. The NAD Cycling Enzyme Mix in Abcam NADH/NAD Quantification Kit was specifically used to recognize NADH/NAD$^+$ in an enzyme cycling colorimetric reaction read at OD 450 nm in a colorimetric microplate reader. Total ATP content was determined in 10 mg of fresh slice brain tissue based on luciferase's requirement for ATP in producing light (emission maximum ~560 nm at pH 7.8) using the ATP bioluminescent assay kit (Molecular Probes).

2.10. SIRT3 Deacetylase Activity. SIRT3 deacetylase activity was determined as described in Cayman's SIRT3 direct fluorescent screening assay kit (item no. 10011566). In a plate, assay buffer, modified p53 acetylated peptide, recombinant Sirt3, and NAD$^+$ were incubated with increased concentrations of ONOO$^-$ (100, 250, and 500 μM) or with purified mitochondrial lysates, final volume 50 μL. Deacetylation reactions were stopped after 2 h of incubation at room temperature by adding 50 μL of stop solution. The fluorophore release by deacetylation of the p53 peptide was analyzed with a fluorometer using an excitation wavelength of 350–360 nm and an emission wavelength of 450–465 nm [44].

2.11. Mitochondrial Morphology. Transmission electron microscopy was performed in 90 nm sections from mouse brains and fixed in 4% paraformaldehyde, 2% glutaraldehyde, and 5% sucrose in PBS, followed by 2 h postfixation in 1% osmium tetroxide and then 1 h in uranyl acetate in 50% ethanol. Samples were washed with 50% ethanol and dehydrated with a graded series of ethanol, clarified with acetone, and embedded in Vestopal. Grids were prepared and stained with uranyl acetate and lead citrate. Samples were observed at 100 kV with a Zeiss EM 109T transmission electron microscope (Zeiss, Oberkochen, Germany). The

TABLE 1: Oxidative parameters in isolated brain mitochondria of wild-type and p66$^{Shc(-/-)}$ aged mice.

	Control (WT 3 mo)	WT 24 mo	p66$^{Shc(-/-)}$ 24 mo
A. H$_2$O$_2$ production rate (nmoles/min/mg prot)			
1. Malate + glutamate	1.66 ± 0.05	2.22 ± 0.1^a	0.97 ± 0.03^b
2. Succinate	1.08 ± 0.05	1.35 ± 0.09^a	0.8 ± 0.1^b
B. Superoxide anion level (AFU)	101 ± 8	194 ± 4.5^a	140 ± 14^b
C. ROS level (AFU)	76 ± 3	111 ± 8^a	82 ± 4^a
D. SOD activity (pmoles/min/mg prot)	2824 ± 309	2305 ± 153^a	2468 ± 94^a
E. Catalase activity (units/mg prot)	32 ± 5	29 ± 4	27 ± 3

Note: data are expressed as the mean ± SEM of the different groups ($n = 6$). Results were contrasted in pairs between the 3-month-old WT control group and the two aged groups (a) as well as between the 24-month-old WT and p66$^{Shc(-/-)}$ groups (b). a and b represent $p < 0.05$, one-way analysis of variance (ANOVA) and Bonferroni post hoc test.

mitochondrial area and length were measured in 400 mitochondria per mouse using the ImageJ software. For the quantification of mitochondrial morphology, we used the criteria described in [45].

2.12. RNA Extraction, Quantitative Real-Time PCR, and mtDNA Content.
Total RNA was extracted with TRIzol Reagent (Invitrogen Corp.). After DNase treatment, 2 μg of samples was reverse-transcribed in duplicate using Taq polymerase and Oligo d(T)$_{16}$. For RT-qPCR studies, cDNA samples were diluted 5-fold, and for mtDNA/nDNA qPCRs, 40 ng of total genomic DNA was used. PCR amplification and analyses were performed with StepOnePlus Real-Time PCR Systems (Thermo Fisher). SYBR® Green PCR Master Mix (Thermo Fisher) was used for all reactions, following the manufacturer's instructions. Total DNA was precipitated with isopropanol (vol. 1:1) from brain tissue samples (~10 mg), homogenized in 20 mg/mL of proteinase K solution, and finally dissolved in Tris-EDTA buffer. The mtDNA/nDNA ratio was calculated using mtDNA primers for the 16S rRNA and nDNA primers for the β-2 microglobulin (β2M) gene [46].

2.13. Western Blots.
15 to 70 μg of protein was electrophoresed on 10–15% vol/vol polyacrylamide SDS-PAGE gels. Proteins were electrophoretically transferred onto PVDF membranes. The membranes were subsequently blocked and, after blocking, were incubated at room temperature with the following antibodies: 1:500 anti-NOS1 (R-20):sc-648, 1:500 anti-Mfn2 (H-68):sc-50331, 1:2000 anti-actin (I-19):sc-1616, and 1:2000 anti-VDAC1 (N-18):sc-8828 were obtained from Santa Cruz, CA. 1:500 anti-OPA1:612607 and 1:1000 anti-DLP1:611113 were obtained from BD Biosciences. 1:1000 anti-phospho-DRP1 (Ser616):#3455 was obtained from Cell Signaling. 1:1000 anti-nitrotyrosine, clone1A6:#05-233 was obtained from EMD Millipore.

2.14. Coimmunoprecipitation.
Mitochondrial proteins (500 μg) were incubated with 4 μg of monoclonal anti-Sirt3 antibody (C73E3) and 30 μL protein A/G PLUS Agarose (Santa Cruz, CA) at 4°C. The beads were then washed three times, suspended in sample buffer, boiled, and centrifuged, and the supernatants were subjected to immunoblotting against monoclonal anti-Sirt3 or anti-nitrotyrosine, clone1A6, antibodies.

2.15. Statistical Analyses.
Statistical analyses were performed using GraphPad Prism 5.01. Data are presented as means ± SEM, and significant differences between groups were assessed using one-way analysis of variance (ANOVA) followed by Bonferroni's multiple comparison test or Dunnett's test [47].

3. Results

3.1. Oxidative Characteristics and ROS Production of Isolated Brain Mitochondria Are Inversely Modified in WT and p66$^{Shc(-/-)}$ Aged Mice.
Aiming at understanding how p66^{Shc} participates in the redox homeostasis balance in aging, several biochemical techniques were used to determine different oxidative parameters in purified brain mitochondria from young (3-month-old) and old (24-month-old) WT and p66$^{Shc-/-}$ mice. As shown in Table 1A, there was a significant increment in H$_2$O$_2$ production by WT mice during aging. This increase in the production rate varied based on the use of malate-glutamate or succinate as the electron transport chain (ETC) substrate, being 33% and 25%, respectively ($p < 0.05$). In turn, p66$^{Shc-/-}$ mice exhibited a significant reduction in total mitochondrial H$_2$O$_2$ production with both substrates when compared to WT mice (41% and 26%, resp., $p < 0.05$) within the aged mouse groups. Concomitantly, superoxide generation (O$_2^-$) and ROS production rate, measured with MitoSOX and H$_2$DCFDA, increased steeply in the WT group during aging (92% and 46%, resp., $p < 0.05$) while in aged KO mice a slight rise was observed in comparison to the young WT control group (38% and 8%, resp., $p < 0.05$) (Table 1B and C).

On the other hand, when the antioxidant detoxification response was analyzed, our results showed that the loss of MnSOD enzymatic activity registered in aging was more pronounced in WT mice than in the aged KO group when contrasted to the 3-month-old WT control (19% and 13%, resp., $p < 0.05$). No changes were observed in catalase activity (Table 1D and E). No differences were detected in any parameters between WT and p66$^{Shc-/-}$ young mouse groups (data not shown).

3.2. nNOS Activity and RNS Production Are Altered in Old Transgenic p66$^{Shc(-/-)}$ Mice. Considering the low levels of ROS production in p66$^{Shc(-/-)}$ aged mice and its key role in RNS formation during aging, it was interesting to assess how the levels of the nNOS enzyme, and its products and byproducts, were modified in old p66$^{Shc(-/-)}$ mouse brains. The absence of p66^{Shc} did not affect nNOS gene transcription or protein levels in the lifespan of mice. Figure 1(a) shows a significant increase in nNOS activity of p66$^{Shc(-/-)}$ mice during the latest stage of life compared to WT mice ($p < 0.05$). However, a not significant increase in nNOS content was observed in both groups during aging by Western blot and real-time PCR (Figure 1(b)). In turn, the increase in nNOS activity registered at 24 mo observed in KO mice correlates with the higher NO content measured at the same period ($p < 0.05$) (Figure 1(c)). Interestingly, aged p66$^{Shc-/-}$ mice did not exhibit the same mitochondrial protein nitration profile as aged WT mice did. The latest showed an increment of nitrated proteins compared to the KO group ($p < 0.05$) (Figure 1(d)), consistent with the reduction in H_2O_2 and O_2^- production, which is necessary for the reaction with NO to form $ONOO^-$.

3.3. Altered ROS and RNS in p66^{Shc} KO Mice Modify Brain Mitochondrial Metabolic Parameters in Aging. To understand the effect of RNS and ROS imbalance on the mitochondrial function of aged p66$^{Shc(-/-)}$ mice, isolated and purified brain mitochondria from both groups were used to assess oxygen consumption in ADP stimulation (stage 3) and resting (stage 4) stages. This allowed the determination of the respiratory control ratio (RCR = E3/E4). Table 2 shows the bioenergetics status measured in brain mitochondria, with malate/glutamate or succinate as oxidizable substrate. Aging decreased the oxygen consumption rate by 25% in stage 3 regardless of the substrate used for the WT group ($p < 0.05$). However, using Mal/Glut as substrate, stage 3 of the respiratory rate was increased by 22% and 68% in aged p66$^{Shc(-/-)}$ mice when compared to the 3-month-old and 24-month-old WT groups, respectively ($p < 0.05$). Meanwhile, this effect decreased by using succinate as substrate with no differences observed between the aged KO and young WT groups and only a 30% increment between the aged KO and the aged WT groups ($p < 0.05$). The respiratory control rates using both Mal/Glut and succinate exhibited an approximate 30% inhibition in aging ($p < 0.05$). In turn, 24-month-old KO mice maintained RCR values similar to those in 3-month-old WT mice (Table 2A). These data suggested an inhibitory effect on the respiratory chain by p66^{Shc} in aged WT mouse brain.

To explain this increase in oxygen consumption rate, the enzymatic activity of the mitochondrial respiratory chain complexes was studied. Results showed that 24-month-old WT mice displayed a higher decrease (48%) in complex I (CI) activity than did aged p66$^{Shc(-/-)}$ mice (34%) when compared to the 3-month-old WT control group ($p < 0.05$) (Table 2). Such decrease in CI activity between the aged groups was noticeable only in the latest stage of life while no differences were observed between the genotypes in previous stages of life (data not shown). Opposite to CI, higher NO concentrations,

such as the one observed in p66$^{Shc(-/-)}$ old mice, could be partially responsible for the greater CIV reversible inhibition shown in 24-month-old p66$^{Shc(-/-)}$ mice (31%) in comparison with the decrease observed in WT aging mice (17%) ($p < 0.05$). No differences were observed in CII–III activity profiles during aging between both genotypes (Table 2B).

Table 2C also shows a decrease in brain tissue ATP content for the aged WT group (65%), although such effect was only partially reverted in aged p66$^{Shc(-/-)}$ mice (35%) ($p < 0.05$). This was extensive to other bioenergetics parameters. When we analyzed the NAD$^+$/NADH ratio, p66$^{Shc(-/-)}$ mice exhibited a milder decrease (32%) in comparison to the 78% reduction observed in the WT group during aging while the mitochondrial membrane potential ($\Delta\Psi$) showed a 14% decrease compared to the 49% decline observed in the same group ($p < 0.05$) (Table 2D and E). Taken together, these results indicate that aged p66$^{Shc(-/-)}$ mice displayed a better mitochondrial function condition compared than aged WT did.

3.4. Mitochondrial Content, Ultrastructure, and Morphology Are Modified in Aged p66$^{Shc(-/-)}$ Mouse Brain. Based on the improved bioenergetics parameters observed in p66$^{Shc(-/-)}$ mice and the already accepted downregulated mitochondrial biogenesis in aging, it is interesting to study how p66^{Shc} impacts on mitochondrial quantity and structure. The mitochondrial content of a sample can be determined using different methods that provide information about mitochondrial biogenesis and tissue's oxidative capacity. Mitochondrial DNA (mtDNA) content relative to nuclear DNA was determined by real-time qPCR in brain samples of the study groups and shown as a percentage of the 3-month-old WT relative mtDNA content. During aging, mitochondrial content was reduced by 30% in the WT group, while in the p66$^{Shc(-/-)}$ group, a 45% increase was observed ($p < 0.05$) (Figure 2(a)).

In accordance with these results, the PGC-1α mRNA expression level declined by 50% in WT mouse brains during aging, whereas in the p66$^{Shc(-/-)}$ group, PGC-1α remained stable through their lives ($p < 0.05$) (Figure 2(b)). Electron microscope images with fresh brain slices showed differences in mitochondrial morphology (Figure 2(c)). For both WT and p66$^{Shc(-/-)}$ 3-month-old mice, normal size and volume mitochondria were observed, with predominantly tubular-shaped mitochondria (70% of total measured mitochondria), while the remaining displayed round (fragmented) morphology. However, at the end of their life, the time point of maximal ROS production, 24-month-old WT mouse brain slices were characterized by decreased tubular mitochondria (−44%) and increased round-shaped mitochondria (+120%) ($p < 0.05$). This age effect in mitochondrial morphology was partially mitigated in 24-month-old p66$^{Shc(-/-)}$ mice, to the extent that both types of mitochondrial populations coexisted in this group (55% tubular mitochondria) showing an intermediate phenotype between 3- and 24-month-old WT mice ($p < 0.05$) (Figure 2(d)).

3.5. The Absence of p66^{Shc} Is Associated with Changes in Mitochondrial Dynamics in Aging. Mitochondrial morphology depends on the interaction among highly dynamic

(a)

(b)

(c)

(d)
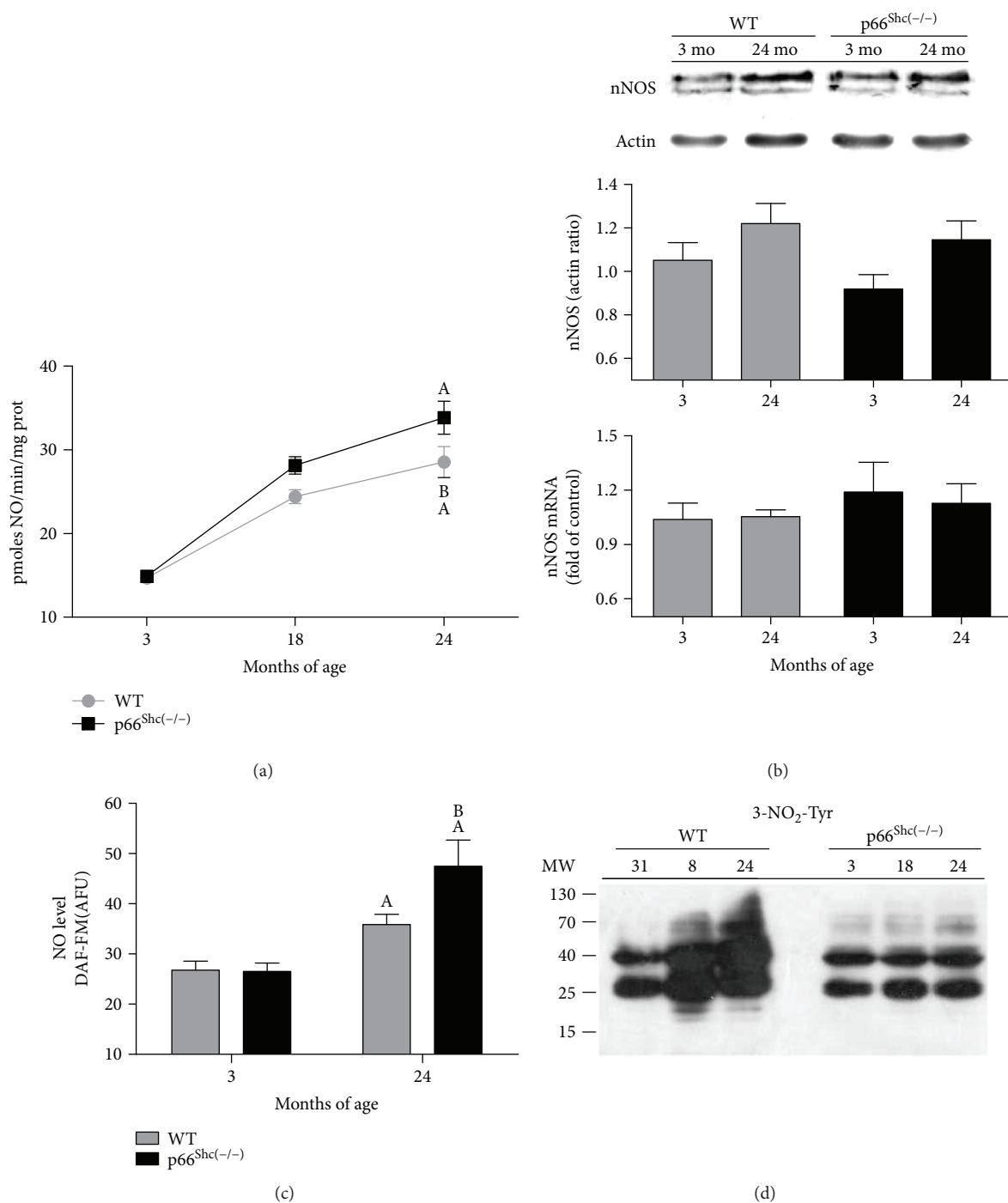
Figure 1: nNOS expression and RNS production in p66$^{Shc(-/-)}$ brain mice during aging. Mice were sacrificed at 3, 18, and 24 months of age. (a) Time course of nNOS activity in mitochondria brain mice measured by 3H-L-citrulline formation ($n = 6$). (b) RT-qPCR and immunoblot of proteins separated using SDS-PAGE from whole brain lysate reveals nNOS mRNA levels and protein expression of mouse brain in WT (grey) and p66$^{Shc(-/-)}$ (black) groups at 3 and 24 months of age. GADPH mRNA levels and actin protein expression were used as housekeeping control and loading control, respectively ($n > 5$, for each experimental group). (c) NO levels were obtained from 50 μg/mL of isolated mitochondria incubated with 0.3 mM L-arginine, 10 μM DAF-FM, and 0.5 μM MitoTracker (per duplicate) at 495 nm (excitation) and 515 nm (emission) in the presence or absence of the NOS inhibitor (3 mM L-NAME) from ($n \geq 6$). (d) Western blot of nitrated proteins from the different groups; membranes were revealed with anti-3-nitrotyrosine antibodies for each group ($n \geq 3$). Values represent means ± standard error of the mean (SEM); A represents $p < 0.05$ compared to the 3-month-old group, and B represents $p < 0.05$ between 24-month-old WT and p66$^{Shc(-/-)}$ groups, one-way analysis of variance (ANOVA) and Bonferroni post hoc test.

TABLE 2: Bioenergetic parameters of isolated brain mitochondria of wild-type and p66$^{Shc(-/-)}$ aged mice.

	Control (WT 3 mo)	WT 24 mo	p66$^{Shc(-/-)}$ 24 mo
A. Oxygen consumption rate			
1. Malate + glutamate			
State 3 (ng at O/min/mg protein)	102 ± 3.6	74 ± 2.4^a	125 ± 4.6^b
Respiratory control (RC)	4.3 ± 0.2	3.3 ± 0.1^a	4.4 ± 0.2
2. Succinate			
State 3 (ng at O/min/mg protein)	116 ± 4.4	84 ± 3.5^a	109 ± 5^a
Respiratory control (RC)	4.1 ± 0.1	3.1 ± 0.1^a	5 ± 0.1^a
B. Respiratory chain complex activity			
1. Complex I (nmol/min/mg protein)	78.4 ± 4.7	37.5 ± 3.1^a	51.8 ± 5.2^b
2. Complex II–III (nmol/min/mg protein)	98.2 ± 9.1	51.1 ± 6.7^a	48.4 ± 4.1^a
3. Complex IV (k'/min/mg protein)	23 ± 0.75	19.1 ± 0.45^a	15.8 ± 1^b
C. ATP synthesis rate (nmol/min/mg protein)	125 ± 1	42 ± 3^a	81 ± 2^b
D. NAD$^+$/NADH$^+$H ratio	5.3 ± 0.7	1.2 ± 0.4^a	2.7 ± 0.5^b
E. Mitochondrial potential, $\Delta\Psi$ (AFU)	601 ± 15	414 ± 25^a	520 ± 16^b

Note: data are expressed as the mean $\pm$ SEM of the different groups ($n = 6$). Results were contrasted in pairs between the 3-month-old WT control group and the two aged groups (a) as well as between both the 24-month old WT and p66$^{Shc(-/-)}$ groups (b). a and b represent $p < 0.05$, one-way analysis of variance (ANOVA) and Bonferroni post hoc test. AFU: arbitrary fluorescence units.

processes, such as the fusion/fission balance. To understand how p66^{Shc} intervenes in mitochondrial dynamics, we analyzed changes in some of the main proteins responsible for the mitochondrial network remodeling. Figure 3(a) shows that in WT mice, the Mfn2 fusion protein content in the mitochondrial fraction decreased with aging (30%), while p66$^{Shc(-/-)}$ mice exhibited a rise in the levels of this protein (25%) ($p < 0.05$). Additionally, Mfn2 mRNA levels during aging remained steady in the WT genotype while the KO group presented a rising tendency which became significant for the 24-month-old group (3-fold increase of control) ($p < 0.05$) (Figure 3(a)). Unlike Mfn2, no differences were registered either in the Opa1 levels in the mitochondrial fraction of the same tissue or in its messenger expression (Figure 3(b)). To further comprehend the effect of p66 in the mitochondrial network, we also studied a mitochondrial fission dynamin-related protein (Drp1). This protein was downregulated (30%) in KO mice during the latest stages of life, while in the WT group an upregulation of Drp1 was observed during aging (50%) ($p < 0.05$). An increase in p-Drp1 (S616) levels is shown in WT mice throughout their lives (2.5-fold) ($p < 0.05$). However, no changes were detected on p-Drp1 (S616) content in p66$^{Shc(-/-)}$ mouse brain during aging (Figure 3(c)). The pattern observed in Drp1 protein levels throughout the lives of both WT and p66$^{Shc(-/-)}$ mouse groups was similar to that of their gene expression, exhibiting a rise in aged WT mouse brain (3-fold) and remaining stable in the p66$^{Shc(-/-)}$ group, as shown in the same figure ($p < 0.05$).

3.6. Sirt3 Activity Is Sensitive to Being Downregulated by Nitration.

To further comprehend how the high levels of RNS, more precisely ONOO$^-$, can modulate the deacetylating capacity of mitochondria, we studied the biochemistry of Sirt3, which is the main protein responsible for this process in this organelle. Its biological activity depends on NAD as a cofactor which increased in old p66$^{Shc(-/-)}$ mice (Table 2D). Using the bioinformatics software GPS (Group-Based Prediction System), which allowed us to predict different posttranslational modifications, we analyzed the murine aminoacidic sequence of Sirt3 deacetylase and detected a tyrosine susceptible to be nitrated at position 100. Such position has been reported to be a part of the NAD-binding domain. With the use of a commercial kit, we tested if Sirt3 activity was sensitive to nitration. Incubating a recombinant Sirt3 (rSirt3) with increasing concentrations of ONOO$^-$ (100, 250, and 500 μM), we observed a decrease in the enzymatic activity by 47%, 55%, and 70%, respectively ($p < 0.05$) (Figure 4(a)). Furthermore, the 3-nitrotyrosine content of the Sirt3 protein immunoprecipitated from purified mitochondria showed a higher increase on Sirt3 nitration in the WT group compared to the p66$^{Shc(-/-)}$ group during aging. No age- or genotype-related differences were observed in the Sirt3 expression levels measured by immunoprecipitation assay with anti-Sirt3 antibodies (Figure 4(b)). In agreement with these results, rSirt3 activity in the presence of the mitochondrial fraction from aged p66$^{Shc(-/-)}$ mouse brain was higher than that observed when challenged with the aged WT mitochondrial fraction ($p < 0.05$). This inhibitory effect was equivalent to the one obtained with 100 μM ONOO$^-$ incubation, while aged p66$^{Shc(-/-)}$ mitochondria with increased NAD/NADH ratio and reduced mitochondrial protein nitration content showed a favorable and less inhibitory environment for rSirt3 activity (33%) ($p < 0.05$) (Figure 4(c)).

4. Discussion

Mitochondria play a key role maintaining cellular metabolic homeostasis during aging [48]. In this study, we show that brain mitochondria of p66$^{Shc(-/-)}$ aged mice exhibit a

(a)

(b)

(c)

(d)
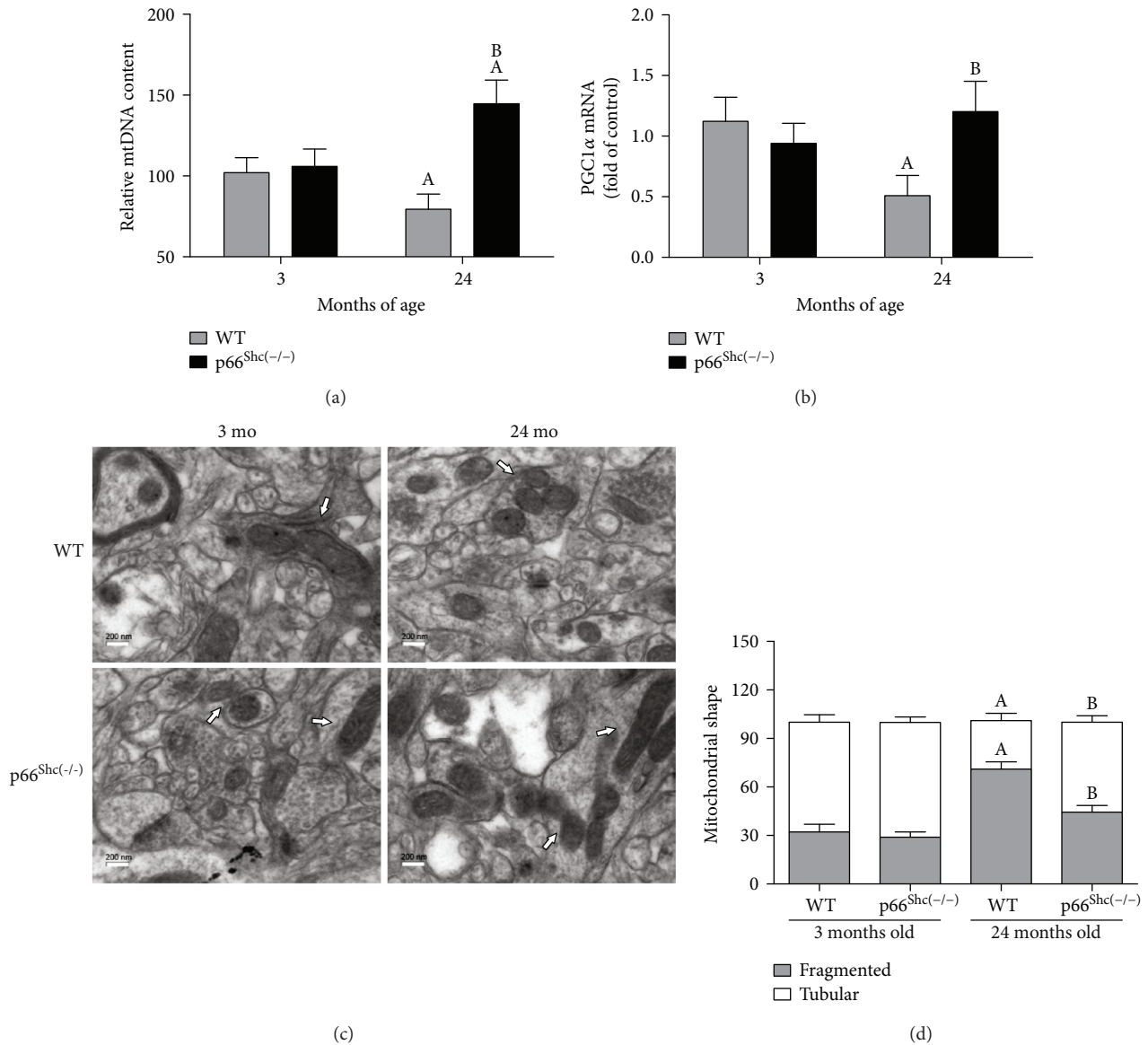
Figure 2: Effects of aging on mitochondrial content, biogenesis, and structure in p66$^{Shc(-/-)}$ mouse brain. (a) Quantification of mtDNA and nuclear DNA by qPCR. (b) The mtDNA/nDNA ratio was calculated from 3- and 24-month WT (grey) and p66$^{Shc(-/-)}$ (black) groups. The mRNA levels of PGC-1α were measured in TRIzol-treated brain extracts from all the studied groups; GADPH mRNA was used as standard ($n = 6$). (c) Mitochondrial morphology was evaluated using electron microscopy of fixed brain slices ($n = 5$ for each experimental group) (magnification:×20,000). (d) At least 300 tubular and fragmented mitochondria were counted per arbitrary area. The percentage distribution of tubular and fragmented brain mitochondria was determined in a minimum of 8–10 random fields at ×4400 magnification to ensure a representative area of analysis ($n = 5$). Mitochondria whose length was more than three times their width were considered tubular, while the remaining round mitochondria were considered fragmented. The analysis was performed by two different investigators in a blinded fashion. Values represent the mean ± SEM; A represents $p < 0.05$ compared to the 3-month-old group, B represents $p < 0.05$ between 24-month-old WT and p66$^{Shc(-/-)}$ groups, one-way analysis of variance (ANOVA) and Bonferroni post hoc test.

reduced alteration of redox balance and a strong link between reactive nitrogen species and mitochondrial function, morphology, and biogenesis [49]. We also demonstrate that sirtuin 3 lysine deacetylase activity is modulated by its nitration status and is enhanced by the improved NAD$^+$/NADH ratio observed in aged p66$^{Shc(-/-)}$ brain mitochondria.

Brain mitochondria of p66$^{Shc(-/-)}$ aged mice exhibit a reduced alteration of redox balance with a decrease both in

ROS generation and in its detoxification activity (Table 1), with this balance being the major determinant of lifespan according to Harman's theory of aging. Although this reduction in the antioxidant response is unexpected, the upregulation of this compensatory mechanism might not be necessary considering this low ROS production condition. Young p66$^{Shc-/-}$ mouse brains show normal baseline levels of intracellular oxidative stress compared to wild types, and other groups reported the upregulation of brain p66-Shc gene
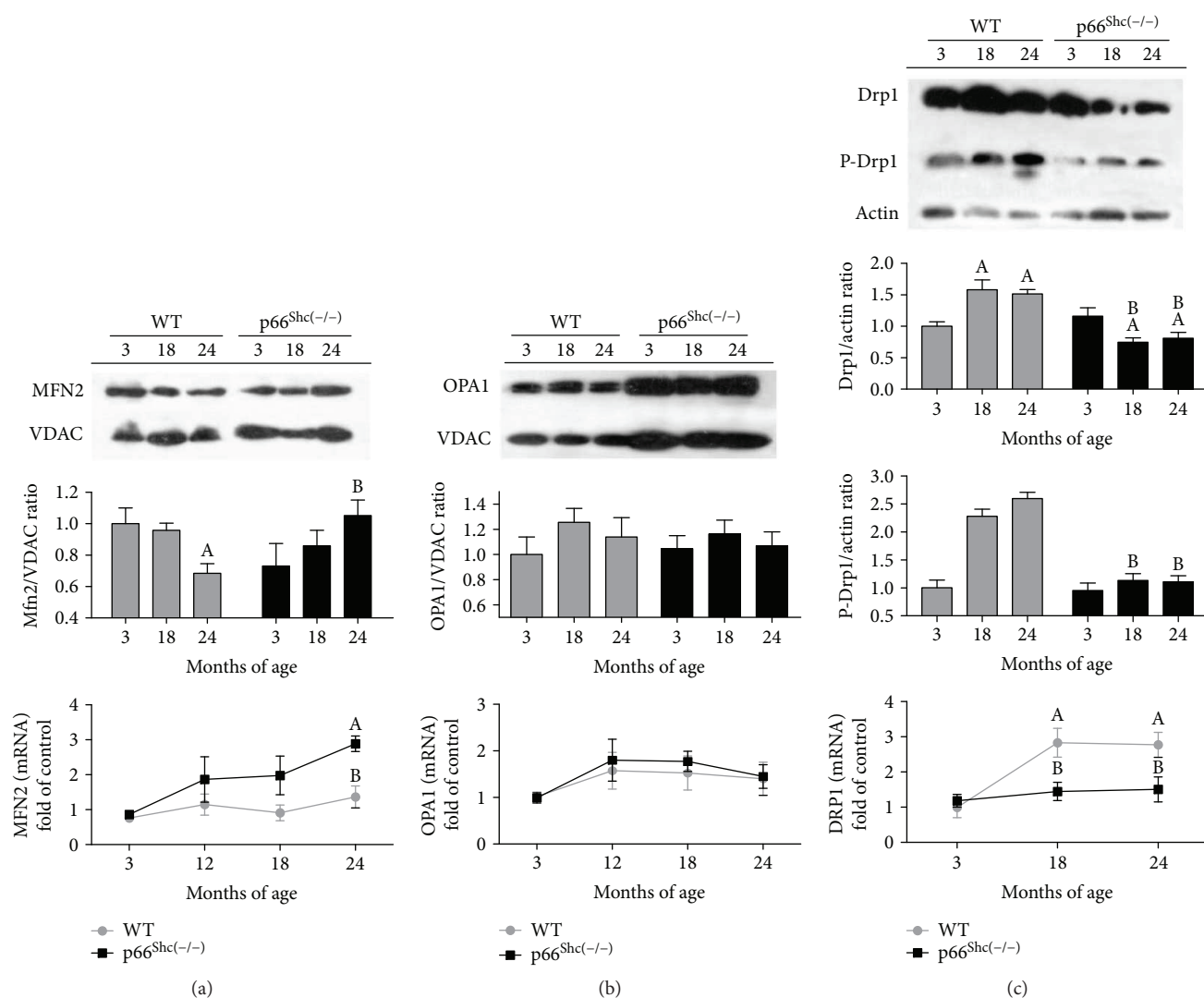
FIGURE 3: Effects of aging on mitochondrial dynamics in p66$^{Shc(-/-)}$ mouse brain. Immunoblot of proteins separated using SDS-PAGE from purified brain mitochondria or whole brain lysate and RT-qPCR of mRNA from TRIzol-treated brain extracts were performed. The expression of the fusion proteins Mfn2 (a) and Opa1 (b), and the fission protein Drp1 (c) with its (S616) phosphorylated active isoform and mRNA levels of mouse brain in WT (grey) and p66$^{Shc(-/-)}$ (black) groups were observed at 3, 18, and 24 months of age. VDAC protein expression in mitochondrial fraction, actin protein expression in whole brain lysates, and GADPH mRNA levels in RT-qPCR were used as standard, respectively ($n > 5$, for each experimental group). Values represent the mean ± SEM; A represents $p < 0.05$ compared to the 3-month-old group, B represents $p < 0.05$ between 18- or 24-month-old WT and p66$^{Shc(-/-)}$ respective groups, one-way analysis of variance (ANOVA) and Bonferroni post hoc test.

expression during aging [50]. These findings can explain the reduced age-related oxidative stress levels observed in p66^{Shc}$^{-/-}$ mice. Therefore, p66^{Shc} can be considered a convergent point between both oxidative stress and programmed genetic theories of aging.

Considerable efforts had been made to understand and explain the effects of oxidants (ROS and RNS) on the resultant oxidative-nitrosative stress on lipids, proteins, and DNA and their contribution to the aging process. During the last years, different groups including ours confirmed that NO is a typical mitochondrial modulator. High levels are harmful and end in protein oxidation and nitration, leading to loss of mitochondrial and cell function, while controlled

levels can induce stress resistance and mitochondrial biogenesis [51]. Considering that mitochondrial NO metabolism involves regulatory aspects of ROS production, RNS markedly contribute to the mitochondrial modulation of life processes [52]. Indeed, a significant nNOS increase in rat brain during aging has been recently proven to correlate with an increase in mitochondrial protein nitration [8]. Our findings show an intensification in nNOS activity and high levels of NO in p66$^{Shc(-/-)}$ mouse brain during aging (Figure 1). However, the rise in NO production is not followed by protein nitration. A similar effect was previously shown in p66$^{Shc(-/-)}$ mice, which are protected against age-related endothelial dysfunction due to the increment of NO bioavailability

(a)   (b)   (c)
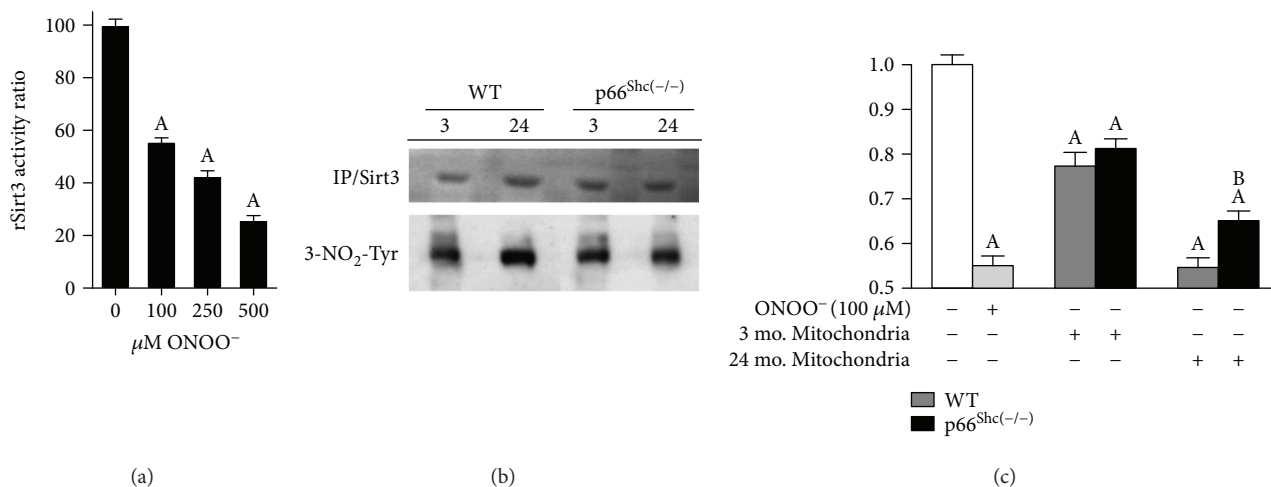
Figure 4: Effect of ONOO⁻ in Sirt3 activity. Recombinant Sirt3 (rSirt3) activity was examined using a fluorometric method. Assays were performed according to the manufacturer's instructions. (a) Recombinant Sirt3 (rSirt3) was incubated with increased concentrations of ONOO⁻ (100, 250, and 500 μM). (b) Immunoprecipitation of Sirt3 was performed from mitochondrial brain lysates incubated with monoclonal anti-Sirt3 antibody and protein A/G PLUS Agarose and then were subjected to immunoblotting against monoclonal anti-Sirt3 or anti-3-nitrotyrosine antibodies. (c) rSirt3 was incubated with 100 μM ONOO⁻ or purified brain mitochondrial lysates from 3- and 24-month WT (grey) and p66$^{Shc(-/-)}$ (black) groups ($n \geq 3$, for each experimental group). Results were contrasted in pairs between rSirt3 and the two aged groups (a) as well as between both the 24-month-old WT and p66$^{Shc(-/-)}$ groups (b). Values represent means ± SEM; A and B represent $p < 0.05$, one-way analysis of variance (ANOVA) and Bonferroni post hoc test.

without protein nitration [53]. This remarkable effect observed in aged p66$^{Shc(-/-)}$ mice could also be caused by their lower H_2O_2 and O_2^- levels, disfavoring the formation of ONOO⁻ by NO breakdown.

Prior evidence has reported a back-and-forth communication flow between changes in ROS/RNS balance and mitochondrial biogenesis, dynamics, and function [10, 54, 55]. This study displays a minor decrease in the respiratory chain complex I (CI) activity with increased oxygen consumption and ATP content in p66$^{Shc(-/-)}$ compared to WT mouse brain during aging, possibly caused by the irreversible nitration of CI at high ONOO⁻ concentrations observed in the last ones (Table 2) [49]. Meanwhile, the inhibition of cytochrome c oxidase (CIV) observed in p66$^{Shc(-/-)}$ brain mitochondria, possibly due to the high levels of steady-state matrix NO concentration, is not enough to counteract this improvement in mitochondrial bioenergetics. Even though NO binds to and reversibly inhibits cytochrome c oxidase-modulating respiration, CI would own the highest level of control in brain mitochondria ETC [56].

Sirt3 is part of the mitochondria-localized sirtuins, modulating acetylation of many proteins that participate in redox regulation [21, 22]. One of the most interesting attributes of Sirt3 is its potential to promote the extension of lifespan [57, 58]. Even though the molecular basis for lifespan extension is not yet clear, the upregulation of Sirt3 expression in long-lived individuals and its physical interaction inside mitochondria with proteins related to the aging process, such as FOXO3a or acetyl-coa synthetase (AceCS2), have been indeed previously studied in literature. The FOXO family transcription factors are human homologs of the daf-16 gene in *Caenorhabditis elegans*, which contributes to the regulation of the nematode lifespan [22]. Additionally, the Sirt3/AceCS2 complex has a role in apoptosis and growth

regulation under certain environmental conditions in a specific type of noncancer epithelial cells [59].

Sirt3/PGC-1α decreased oxidative stress and conferred resistance to oxidative stress-induced damage by regulating antioxidant defense [60]. In aging, the gradual decline in mitochondrial content results from an age-dependent reduction of the PGC-1α level, a key regulator of mitochondrial biogenesis [61, 62]. SIRT3 mediates the reduction of the ROS level by stimulating PGC-1α gene expression, and in turn, PGC-1α induces SIRT3 expression, creating a positive-feedback loop [27]. Aged p66$^{Shc(-/-)}$ mice show high levels of PGC-1α gene expression and increased mitochondrial content compared with their WT littermates (Figure 2). Accordingly, an impaired balance between fission and fusion events may also be related to an age-dependent decline in mitochondrial biogenesis [63].

Mitochondrial morphology depends on the interaction of highly dynamic processes, such as the fusion/fission balance. In aging, given the loss of plasticity of these processes, the maintenance of metabolic homeostasis is compromised. It has been described that ROS-induced mitochondrial depolarization might be responsible for mitochondrial fragmentation [64]. In this work, aged p66$^{Shc(-/-)}$ mouse brain mitochondria present enhanced $\Delta\Psi$ and display filament or tubular shape. This is consistent with the observed Mfn2 upregulation, a GTPase embedded in the mitochondria outer membrane directly involved in its fusion, and with the downregulation of Drp1 expression (Figure 3), a GTPase that generates ring-like structures constricting mitochondria in fission events. Phosphorylation of Drp1 at Ser 616 (S616) by several kinases including the cyclin-dependent kinase (CDK) family promotes mitochondrial fission [65]. We also observe high levels of pDrp1-S616 in WT mouse brains during aging. These findings suggest an intimate relationship

between mitochondrial energetic status and dynamics. Moreover, regulation of these GTPase proteins by posttranslational modification, such as deacetylation by Sirt3 or nitrosylation/nitration by RNS, is extensively described in literature [15, 28].

Interestingly, the utilization of a GPS algorithm predicts the existence of a tyrosine in position 100 of a Sirt3 murine sequence which, as part of the described NAD^+-binding domain, is capable of being nitrated [66]. It is known that the decline in NAD^+ level during aging disrupts nuclear-mitochondrial communication [67]. However, the level of NAD^+ remains stable in p66$^{Shc(-/-)}$ mice throughout their lives. In accordance to these data, we show here that Sirt3 is sensitive to be nitrated and its activity is protected against age-related nitration in brains of aged p66$^{Shc(-/-)}$ mice (Figure 4). These findings suggest a close relationship between RNS and deacetylation activity in brain mitochondria.

In accordance to the free radical theory of aging, this process is triggered and sustained by the deleterious accumulative effect of oxidative damage caused by mitochondrial respiration-generated ROS. On the other hand, the genetic programmed theory asserts that aging and death are necessary parts of evolution, and the low variability in lifespan within species proves that aging is not only a wear-and-tear process [68–72]. Through its capacity to generate hydrogen peroxide (H_2O_2), p66^{Shc} is a clear example of this strong link between oxidative stress and the genetic of aging, and it could be a potential target for anti-aging strategy. The modulation of p66^{Shc} activity could be a candidate for therapeutic intervention for a longer lifespan or higher quality of life.

5. Conclusions

In conclusion, results show the pivotal role of p66^{Shc} inactivation in multiple processes related to aging in mouse brains. Through the modification in ROS/RNS production, which in turn regulates Sirt3 activity, the absence of p66^{Shc} improves mitochondrial dynamics and biogenesis. Taken together, these findings can partially explain the observed delay in the aging of p66$^{Shc(-/-)}$ mouse brains. Moreover, the enhancement in mitochondrial homeostasis can be the underlying cause of the improved cognition and motor function observed in p66^{Shc} KO mice during aging [34]. More studies will still be necessary to fully understand this complex and multifactorial process.

Disclosure

Preliminary data were presented at the LXI Reunión Anual de la Sociedad Argentina de Investigación Clínica, Mar del Plata, Argentina [49].

Conflicts of Interest

The authors declare that they have no conflict of interest.

References

[1] N. A. Bishop, T. Lu, and B. A. Yankner, "Neural mechanisms of ageing and cognitive decline," *Nature*, vol. 464, no. 7288, pp. 529–535, 2010.

[2] D. Harman, "Aging: a theory based on free radical and radiation chemistry," *Journal of Gerontology*, vol. 11, no. 3, pp. 298–300, 1956.

[3] M. P. Murphy, "How mitochondria produce reactive oxygen species," *Biochemical Journal*, vol. 417, no. 1, pp. 1–13, 2009.

[4] D. L. Hoffman and P. S. Brookes, "Oxygen sensitivity of mitochondrial reactive oxygen species generation depends on metabolic conditions," *Journal of Biological Chemistry*, vol. 284, no. 24, pp. 16236–16245, 2009.

[5] F. M. Cerqueira, F. M. Cunha, F. R. M. Laurindo, and A. J. Kowaltowski, "Calorie restriction increases cerebral mitochondrial respiratory capacity in a NO•-mediated mechanism: impact on neuronal survival," *Free Radical Biology & Medicine*, vol. 52, no. 7, pp. 1236–1241, 2012.

[6] A. B. Knott and E. Bossy-Wetzel, "Impact of nitric oxide on metabolism in health and age-related disease," *Diabetes, Obesity and Metabolism*, vol. 12, Supplement 2, pp. 126–133, 2010.

[7] J. J. Poderoso, C. Lisdero, F. Schöpfer et al., "The regulation of mitochondrial oxygen uptake by redox reactions involving nitric oxide and ubiquinol," *Journal of Biological Chemistry*, vol. 274, no. 53, pp. 37709–37716, 1999.

[8] P. Y. Lam, F. Yin, R. T. Hamilton, A. Boveris, and E. Cadenas, "Elevated neuronal nitric oxide synthase expression during ageing and mitochondrial energy production," *Free Radical Research*, vol. 43, no. 5, pp. 431–439, 2009.

[9] R. V. Pérez-Gallardo, R. Noriega-Cisneros, E. Esquivel-Gutiérrez et al., "Effects of diabetes on oxidative and nitrosative stress in kidney mitochondria from aged rats," *Journal of Bioenergetics and Biomembranes*, vol. 46, no. 6, pp. 511–518, 2014.

[10] P. H. G. M. Willems, R. Rossignol, C. E. J. Dieteren, M. P. Murphy, and W. J. H. Koopman, "Redox homeostasis and mitochondrial dynamics," *Cell Metabolism*, vol. 22, no. 2, pp. 207–218, 2015.

[11] H. Chen and D. C. Chan, "Emerging functions of mammalian mitochondrial fusion and fission," *Human Molecular Genetics*, vol. 14, Supplement 2, pp. R283–R289, 2005.

[12] D. H. Cho, T. Nakamura, J. Fang et al., "S-nitrosylation of Drp1 mediates *beta*-amyloid-related mitochondrial fission and neuronal injury," *Science*, vol. 324, no. 5923, pp. 102–105, 2009.

[13] G. P. Leboucher, Y. C. Tsai, M. Yang et al., "Stress-induced phosphorylation and proteasomal degradation of mitofusin 2 facilitates mitochondrial fragmentation and apoptosis," *Molecular Cell*, vol. 47, no. 4, pp. 547–557, 2012.

[14] C. A. Sacksteder, W. J. Qian, T. V. Knyushko et al., "Endogenously nitrated proteins in mouse brain: links to neurodegenerative disease," *Biochemistry*, vol. 45, no. 26, pp. 8009–8022, 2006.

[15] W. Qiang, K. Weiqiang, Z. Qing, Z. Pengju, and L. Yi, "Aging impairs insulin-stimulated glucose uptake in rat skeletal muscle via suppressing AMPKα," *Experimental & Molecular Medicine*, vol. 39, no. 4, pp. 535–543, 2007.

[16] R. M. Reznick, H. Zong, J. Li et al., "Aging-associated reductions in AMP-activated protein kinase activity and mitochondrial biogenesis," *Cell Metabolism*, vol. 5, no. 2, pp. 151–156, 2007.

[17] A. Y. Seo, A. M. Joseph, D. Dutta, J. C. Y. Hwang, J. P. Aris, and C. Leeuwenburgh, "New insights into the role of mitochondria in aging: mitochondrial dynamics and more," *Journal of Cell Science*, vol. 123, no. 15, pp. 2533–2542, 2010.

[18] P. L. Puri and V. Sartorelli, "HDACs and sirtuins: targets for new pharmacological interventions in human diseases," *Pharmacological Research*, vol. 62, no. 1, pp. 1-2, 2010.

[19] B. Kincaid and E. Bossy-Wetzel, "Forever young: SIRT3 a shield against mitochondrial meltdown, aging, and neurodegeneration," *Frontiers in Aging Neuroscience*, vol. 5, 2013.

[20] B. Schwer, M. Eckersdorff, Y. Li et al., "Calorie restriction alters mitochondrial protein acetylation," *Aging Cell*, vol. 8, no. 5, pp. 604–606, 2009.

[21] W. C. Hallows, W. Yu, B. C. Smith et al., "Sirt3 promotes the urea cycle and fatty acid oxidation during dietary restriction," *Molecular Cell*, vol. 41, no. 2, pp. 139–149, 2011.

[22] T. Shi, F. Wang, E. Stieren, and Q. Tong, "SIRT3, a mitochondrial sirtuin deacetylase, regulates mitochondrial function and thermogenesis in brown adipocytes," *Journal of Biological Chemistry*, vol. 280, no. 14, pp. 13560–13567, 2005.

[23] X. Qiu, K. Brown, M. D. Hirschey, E. Verdin, and D. Chen, "Calorie restriction reduces oxidative stress by SIRT3-mediated SOD2 activation," *Cell Metabolism*, vol. 12, no. 6, pp. 662–667, 2010.

[24] D. B. Lombard, F. W. Alt, H. L. Cheng et al., "Mammalian Sir2 homolog SIRT3 regulates global mitochondrial lysine acetylation," *Molecular and Cellular Biology*, vol. 27, no. 24, pp. 8807–8814, 2007.

[25] B. Schwer, J. Bunkenborg, R. O. Verdin, J. S. Andersen, and E. Verdin, "Reversible lysine acetylation controls the activity of the mitochondrial enzyme acetyl-CoA synthetase 2," *Proceedings of the National Academy of Sciences of the United States of America*, vol. 103, no. 27, pp. 10224–10229, 2006.

[26] W. C. Hallows, S. Lee, and J. M. Denu, "Sirtuins deacetylate and activate mammalian acetyl-CoA synthetases," *Proceedings of the National Academy of Sciences of the United States of America*, vol. 103, no. 27, pp. 10230–10235, 2006.

[27] X. Kong, R. Wang, Y. Xue et al., "Sirtuin 3, a new target of PGC-1α, plays an important role in the suppression of ROS and mitochondrial biogenesis," *PloS One*, vol. 5, no. 7, article e11707, 2010.

[28] S. A. Samant, H. J. Zhang, Z. Hong et al., "SIRT3 deacetylates and activates OPA1 to regulate mitochondrial dynamics during stress," *Molecular and Cellular Biology*, vol. 34, no. 5, pp. 807–819, 2014.

[29] A. Raffaello and R. Rizzuto, "Mitochondrial longevity pathways," *Biochimica et Biophysica Acta (BBA) - Molecular Cell Research*, vol. 1813, no. 1, pp. 260–268, 2011.

[30] P. G. Pelicci, "Electron transfer between cytochrome C and p66SHC generates reactive oxygen species that trigger mitochondrial apoptosis," *The FEBS Journal*, vol. 272, Supplement 1, pp. 319-320, 2005.

[31] A. Boveris, N. Oshino, and B. Chance, "The cellular production of hydrogen peroxide," *Biochemical Journal*, vol. 128, no. 3, pp. 617–630, 1972.

[32] E. Migliaccio, M. Giorgio, S. Mele, and G. Pelicci, "The p66^Shc adaptor protein controls oxidative stress response and life span in mammals," *Nature*, vol. 402, no. 6759, pp. 309–313, 1999.

[33] I. Berniakovich, M. Trinei, M. Stendardo et al., "p66^Shc-generated oxidative signal promotes fat accumulation," *Journal of Biological Chemistry*, vol. 283, no. 49, pp. 34283–34293, 2008.

[34] A. Berry, A. Greco, M. Giorgio et al., "Deletion of the lifespan determinant p66^Shc improves performance in a spatial memory task, decreases levels of oxidative stress markers in the hippocampus and increases levels of the neurotrophin BDNF in adult mice," *Experimental Gerontology*, vol. 43, no. 3, pp. 200–208, 2008.

[35] C. Giulivi, J. J. Poderoso, and A. Boveris, "Production of nitric oxide by mitochondria," *Journal of Biological Chemistry*, vol. 273, no. 18, pp. 11038–11043, 1998.

[36] R. G. Knowles and M. Salter, "Measurement of NOS activity by conversion of radiolabeled arginine to citrulline using ion-exchange separation," *Nitric Oxide Protocols*, vol. 100, pp. 67–73, 1998.

[37] M. C. Carreras, M. Melani, N. Riobó, D. P. Converso, E. M. Gatto, and J. J. Poderoso, "Neuronal nitric oxide synthases in brain and extraneural tissues," *Methods in Enzymology*, vol. 359, pp. 413–423, 2002.

[38] M. C. Carreras, D. P. Converso, A. S. Lorenti et al., "Mitochondrial nitric oxide synthase drives redox signals for proliferation and quiescence in rat liver development," *Hepatology*, vol. 40, no. 1, pp. 157–166, 2004.

[39] J. M. McCord and I. Fridovich, "The utility of superoxide dismutase in studying free radical reactions I. Radicals generated by the interaction of sulfite, dimethyl sulfoxide, and oxygen," *Journal of Biological Chemistry*, vol. 244, no. 22, pp. 6056–6063, 1969.

[40] B. Chance, "Special methods: catalase," in *Methods of Biochemical Analysis*, R. Glick, Ed., pp. 408–424, Wiley Interscience, New York, NY, USA, 1954.

[41] R. W. Estabrook, "[7] Mitochondrial respiratory control and the polarographic measurement of ADP: O ratios," *Methods in Enzymology*, vol. 10, pp. 41–47, 1967.

[42] M. C. Carreras, J. G. Peralta, D. P. Converso et al., "Modulation of liver mitochondrial NOS is implicated in thyroid-dependent regulation of O_2 uptake," *American Journal of Physiology-Heart and Circulatory Physiology*, vol. 281, no. 6, pp. H2282–H2288, 2001.

[43] S. M. Cardoso, C. Pereira, and C. R. Oliveira, "Mitochondrial function is differentially affected upon oxidative stress," *Free Radical Biology & Medicine*, vol. 26, no. 1-2, pp. 3–13, 1999.

[44] B. Schwer, B. J. North, R. A. Frye, M. Ott, and E. Verdin, "The human silent information regulator (Sir) 2 homologue hSIRT3 is a mitochondrial nicotinamide adenine dinucleotide–dependent deacetylase," *The Journal of Cell Biology*, vol. 158, no. 4, pp. 647–657, 2002.

[45] A. S. Gonzalez, M. E. Elguero, P. Finocchietto et al., "Abnormal mitochondrial fusion–fission balance contributes to the progression of experimental sepsis," *Free Radical Research*, vol. 48, no. 7, pp. 769–783, 2014.

[46] V. Venegas, J. Wang, D. Dimmock, and L. J. Wong, "Real-time quantitative PCR analysis of mitochondrial DNA content,"

Current Protocols in Human Genetics, vol. 68, pp. 19.7:19.7.1–19.7:19.7.12, 2011.

[47] J. P. Sánchez-Villamil, V. D'Annunzio, P. Finocchietto et al., "Cardiac-specific overexpression of thioredoxin 1 attenuates mitochondrial and myocardial dysfunction in septic mice," *The International Journal of Biochemistry & Cell Biology*, vol. 81, Part B, pp. 323–334, 2016.

[48] M. Gonzalez-Freire, R. De Cabo, M. Bernier et al., "Reconsidering the role of mitochondria in aging," *The Journals of Gerontology: Series A*, vol. 70, no. 11, pp. 1334–1342, 2015.

[49] H. Pérez, M. E. Elguero, N. M. Villalba, Y. Alippe, J. J. Poderoso, and M. C. Carreras, "P66shc and its role in mitochondrial homeostasis throughout the aging process," *Medicina*, vol. 76, Supplement 1, p. 105, 2016.

[50] K. Sone, M. Mori, and N. Mori, "Selective upregulation of p66-Shc gene expression in the liver and brain of aged rats," *Archives of Gerontology and Geriatrics*, vol. 55, no. 3, pp. 744–748, 2012.

[51] E. Nisoli, C. Tonello, A. Cardile et al., "Calorie restriction promotes mitochondrial biogenesis by inducing the expression of eNOS," *Science*, vol. 310, no. 5746, pp. 314–317, 2005.

[52] M. C. Carreras and J. J. Poderoso, "Mitochondrial nitric oxide in the signaling of cell integrated responses," *American Journal of Physiology-Cell Physiology*, vol. 292, no. 5, pp. C1569–C1580, 2007.

[53] P. Francia, C. delli Gatti, M. Bachschmid et al., "Deletion of p66^{Shc} gene protects against age-related endothelial dysfunction," *Circulation*, vol. 110, no. 18, pp. 2889–2895, 2004.

[54] L. Lizana, B. Bauer, and O. Orwar, "Controlling the rates of biochemical reactions and signaling networks by shape and volume changes," *Proceedings of the National Academy of Sciences of the United States of America*, vol. 105, no. 11, pp. 4099–4104, 2008.

[55] C. A. Mannella, W. J. Lederer, and M. S. Jafri, "The connection between inner membrane topology and mitochondrial function," *Journal of Molecular and Cellular Cardiology*, vol. 62, pp. 51–57, 2013.

[56] J. E. Telford, S. M. Kilbride, and G. P. Davey, "Complex I is rate-limiting for oxygen consumption in the nerve terminal," *Journal of Biological Chemistry*, vol. 284, no. 14, pp. 9109–9114, 2009.

[57] G. Rose, S. Dato, K. Altomare et al., "Variability of the *SIRT3* gene, human silent information regulator *Sir2* homologue, and survivorship in the elderly," *Experimental Gerontology*, vol. 38, no. 10, pp. 1065–1070, 2003.

[58] J. Halaschek-Wiener, M. Amirabbasi-Beik, N. Monfared et al., "Genetic variation in healthy oldest-old," *PLoS One*, vol. 4, no. 8, article e6641, 2009.

[59] S. J. Allison and J. Milner, "SIRT3 is pro-apoptotic and participates in distinct basal apoptotic pathways," *Cell Cycle*, vol. 6, no. 21, pp. 2669–2677, 2007.

[60] S. Gounden, A. Phulukdaree, D. Moodley, and A. Chuturgoon, "Increased SIRT3 expression and antioxidant defense under hyperglycemic conditions in HepG2 cells," *Metabolic Syndrome and Related Disorders*, vol. 13, no. 6, pp. 255–263, 2015.

[61] K. R. Short, M. L. Bigelow, J. Kahl et al., "Decline in skeletal muscle mitochondrial function with aging in humans," *Proceedings of the National Academy of Sciences of the United States of America*, vol. 102, no. 15, pp. 5618–5623, 2005.

[62] E. Koltai, N. Hart, A. W. Taylor et al., "Age-associated declines in mitochondrial biogenesis and protein quality control factors are minimized by exercise training," *American Journal of Physiology-Regulatory, Integrative and Comparative Physiology*, vol. 303, no. 2, pp. R127–R134, 2012.

[63] D. A. Chistiakov, I. A. Sobenin, V. V. Revin, A. N. Orekhov, and Y. V. Bobryshev, "Mitochondrial aging and age-related dysfunction of mitochondria," *BioMed Research International*, vol. 2014, Article ID 238463, 7 pages, 2014.

[64] X. Fan, R. Hussien, and G. A. Brooks, "H_2O_2-induced mitochondrial fragmentation in C_2C_{12} myocytes," *Free Radical Biology & Medicine*, vol. 49, no. 11, pp. 1646–1654, 2010.

[65] N. Taguchi, N. Ishihara, A. Jofuku, T. Oka, and K. Mihara, "Mitotic phosphorylation of dynamin-related GTPase Drp1 participates in mitochondrial fission," *Journal of Biological Chemistry*, vol. 282, no. 15, pp. 11521–11529, 2007.

[66] Z. Liu, J. Cao, Q. Ma, X. Gao, J. Ren, and Y. Xue, "GPS-YNO2: computational prediction of tyrosine nitration sites in proteins," *Molecular BioSystems*, vol. 7, no. 4, pp. 1197–1204, 2011.

[67] A. P. Gomes, N. L. Price, A. J. Y. Ling et al., "Declining NAD$^+$ induces a pseudohypoxic state disrupting nuclear-mitochondrial communication during aging," *Cell*, vol. 155, no. 7, pp. 1624–1638, 2013.

[68] I. B. Afanas'ev, "Free radical mechanisms of aging processes under physiological conditions," *Biogerontology*, vol. 6, no. 4, pp. 283–290, 2005.

[69] L. T. Knapp and E. Klann, "Superoxide-induced stimulation of protein kinase C via thiol modification and modulation of zinc content," *Journal of Biological Chemistry*, vol. 275, no. 31, pp. 24136–24145, 2000.

[70] S. Ikeyama, G. Kokkonen, S. Shack, X. T. Wang, and N. J. Holbrook, "Loss in oxidative stress tolerance with aging linked to reduced extracellular signal-regulated kinase and Akt kinase activities," *The FASEB Journal*, vol. 16, no. 1, pp. 114–116, 2002.

[71] Q. Jin, B. S. Jhun, S. H. Lee et al., "Differential regulation of phosphatidylinositol 3-kinase/Akt, mitogen-activated protein kinase, and AMP-activated protein kinase pathways during menadione-induced oxidative stress in the kidney of young and old rats," *Biochemical and Biophysical Research Communications*, vol. 315, no. 3, pp. 555–561, 2004.

[72] S. L. Colombo and S. Moncada, "AMPKα1 regulates the antioxidant status of vascular endothelial cells," *Biochemical Journal*, vol. 421, no. 2, pp. 163–169, 2009.

Review Article

Insights on Localized and Systemic Delivery of Redox-Based Therapeutics

Nicholas E. Buglak (iD),[1,2,3] **Elena V. Batrakova,**[2,4] **Roberto Mota,**[1,2]
and Edward S. M. Bahnson (iD)[1,2,3,5]

[1]*Department of Surgery, Division of Vascular Surgery, University of North Carolina at Chapel Hill, Chapel Hill, NC 27599, USA*
[2]*Center for Nanotechnology in Drug Delivery, University of North Carolina at Chapel Hill, Chapel Hill, NC 27599, USA*
[3]*Curriculum in Toxicology, University of North Carolina at Chapel Hill, Chapel Hill, NC 27599, USA*
[4]*Division of Pharmacoengineering and Molecular Pharmaceutics, University of North Carolina at Chapel Hill, Chapel Hill, NC 27599, USA*
[5]*Department of Cell Biology & Physiology, University of North Carolina at Chapel Hill, Chapel Hill, NC 27599, USA*

Correspondence should be addressed to Edward S. M. Bahnson; edward_bahnson@med.unc.edu

Reactive oxygen and nitrogen species are indispensable in cellular physiology and signaling. Overproduction of these reactive species or failure to maintain their levels within the physiological range results in cellular redox dysfunction, often termed cellular oxidative stress. Redox dysfunction in turn is at the molecular basis of disease etiology and progression. Accordingly, antioxidant intervention to restore redox homeostasis has been pursued as a therapeutic strategy for cardiovascular disease, cancer, and neurodegenerative disorders among many others. Despite preliminary success in cellular and animal models, redox-based interventions have virtually been ineffective in clinical trials. We propose the fundamental reason for their failure is a flawed delivery approach. Namely, systemic delivery for a geographically local disease limits the effectiveness of the antioxidant. We take a critical look at the literature and evaluate successful and unsuccessful approaches to translation of redox intervention to the clinical arena, including dose, patient selection, and delivery approach. We argue that when interpreting a failed antioxidant-based clinical trial, it is crucial to take into account these variables and importantly, whether the drug had an effect on the redox status. Finally, we propose that local and targeted delivery hold promise to translate redox-based therapies from the bench to the bedside.

1. Introduction

Redox reactions are at the center of cellular metabolism and signaling and result in the production of reactive species [1]. Reactive species that stem from oxygen reduction reactions are called reactive oxygen species (ROS) and include free radical and nonradical molecules such as hydroxyl radical ($HO^{\bullet}$), peroxyl ($RO_2^{\bullet}$), superoxide ($O_2^{\bullet-}$), singlet oxygen ($^1O_2$), and hydrogen peroxide (H_2O_2) [2]. Reactive species that stem from nitric oxide metabolism are called reactive nitrogen species (RNS) and include free radical and nonradical molecules such as nitric oxide ($^{\bullet}NO$) itself, nitrite (NO_2^-), nitrogen dioxide ($^{\bullet}NO_2$),

peroxynitrite ($ONOO^-$), dinitrogen trioxide (N_2O_3), and alky peroxynitrite ($ONOOR$) [2]. These species are highly reactive and therefore are capable of forming reversible and irreversible interactions with many different macromolecules throughout the body. Under physiological conditions, the reactive species are in balance with antioxidant defenses which enzymatically and nonenzymatically maintain redox homeostasis. In homeostasis, reactive species fulfill their critical role in cell signaling, migration, proliferation, and metabolism. If the redox balance is skewed towards the reactive species however, either from their overproduction or antioxidant depletion, a pathological condition can ensue. Exposure to cigarette smoke [3], various air pollutants [4, 5],

UV radiation [6], xenobiotics [7], alcohol consumption [8], and different diseases can further exacerbate the pathological cellular state. Consequently, the prolonged redox imbalance can cause aberrant DNA modifications [9], lipid peroxidation [10], peptide chain fragmentation [11], and alterations in signal transduction [12]. This state of cellular redox imbalance, as ROS and RNS overwhelm defense mechanisms, is often referred to as oxidative stress.

Disruption in redox homeostasis can result in undesirable molecular interactions throughout the cell. Impairment at the molecular level can lead to defective organelles, which can translate into cellular dysfunction. In turn, this can cause tissue incompetence ultimately resulting in the development of organ-specific or systemic disease. For this reason, a component of redox dysfunction has been linked to almost all disease states [13, 14] including asthma, hypertension, carcinoma, leukemia, diabetes, Alzheimer's disease, autoimmunity, and infection. The implication of a causative role of ROS and RNS in disease development has led to many studies and clinical trials using antioxidant molecules as therapeutics. Despite our understanding of the biochemical interaction of reactive species and their associations with disease onset, causality has yet to be fully elucidated. It is because of this poorly understood and missing connection that most redox-based therapies have largely been unsuccessful. For the purposes of this review, we evaluate the research with the assumption that reactive species have a causal role in disease onset. Accordingly, we chose to review a range of redox-based molecules, from micronutrients, which have been trialed for decades, to new and emerging small molecules currently entering clinical trials for the first time. Additionally, we highlight cell-mediated drug delivery as a novel approach for administering these therapeutics. Ultimately, this review aims to rationalize the reasons as to why few redox-based therapies succeed.

2. Localized and Targeted versus Systemic Therapy Application

Failure of therapies to date can be attributed to improper route of drug administration, a discrepancy between preventative and remission therapy, wrong dose to achieve desired effect, or the wrong choice in redox-active molecule due to the vast array of reactive moieties between redox-active compounds. We propose that a fundamental issue with most therapeutic approaches up to now has been their method of delivery. For instance, systemic delivery of an antioxidant for the treatment of a geographically local redox imbalance, as with tumors or atherosclerotic lesions, simply may not deliver the therapeutic concentration to the diseased site. The route of administration may not have been fully evaluated or the metabolism of that antioxidant formulation may not have been properly understood before trials began. Moreover, the redox-active therapeutic may interact with and disrupt systems currently at redox homeostasis. This could lead to a state of local reductive or oxidative stress outside of the diseased area as many "antioxidants" have a prooxidant capacity depending on their concentration and redox environment. Following this notion, systemic delivery

of antioxidants to treat a disease with systemic redox imbalance, as in diabetes, may yield the desirable effect. For conditions with localized redox imbalance, however, we suggest the necessity of developing locally delivered or targeted therapeutic strategies that deliver the redox intervention directly and preferentially to the site of disease, hence addressing the redox dysfunction in a local and targeted manner.

3. Micronutrients

Micronutrients are readily obtained through the diet and were among the first molecules with antioxidant properties to be identified. Their chemical structures have redox-sensitive functional groups or radical scavenging moieties. Additionally, some have the capacity to recycle endogenous antioxidants. These molecules were also the first to be trialed as therapeutics. Herein, we discuss several recent trials with the ubiquitous alpha-lipoic acid as well as vitamins A, B_{12}, C, and E.

3.1. Vitamin C. Vitamin C, also known as ascorbic acid or ascorbate, is a water-soluble compound synthesized from glucose by most animals and galactose by plants. Humans and apes are among the few animals that lack the key enzyme required for vitamin C biosynthesis, L-gulonolactone oxidase [15]. As such, ascorbate is obtained externally through the diet or by supplementation. Among its many physiological functions, ascorbate acts as a cofactor for neurotransmitter synthesis as well as collagen synthesis and maintenance [16]. As an antioxidant, ascorbate is capable of recycling oxidized vitamin E to its reduced form [17] and scavenging many different ROS and RNS. The preclinical and clinical studies discussed herein are summarized in Table 1.

Work done by Schoenfeld et al. [18] revitalized the therapeutic potential of ascorbate in treating cancer by describing a potential new mechanism in non-small-cell lung cancer (NSCLC) and glioblastoma (GBM). Cellular work using two NSCLC and two GBM cell lines showed that ascorbate selectively sensitizes these cancer cells to chemotherapeutics and radiation therapy compared to primary bronchial epithelial cells and normal human astrocytes [18]. As previously mentioned, antioxidants can have a prooxidant capacity depending on their redox environment. Here, ascorbate treatment increased steady-state levels of hydrogen peroxide (H_2O_2) and labile iron levels in both cancer cell types, but not in noncancerous cells [18]. The enhanced cancer cell-ascorbate toxicity could be inhibited by preincubation with iron chelators or with catalase, which breaks down H_2O_2. Meanwhile, preincubation with EDTA [18], a known enhancer of iron redox cycling, further increased cancer cell-specific toxicity. Lane et al. [19] reported that ascorbate may also increase intracellular iron uptake by acting on transferrin receptors. The cancer-specific toxicity *in vitro* was recapitulated in mouse xenograft models by Schoenfeld et al. [18] for both NSCLC and GBM using combinations of radiochemotherapy with intraperitoneal injections of ascorbate. Animals treated with all three therapies, compared to radiochemotherapy or ascorbate alone,

TABLE 1: Preclinical and clinical studies using vitamin C.

Route	Vitamin C Results	Reference
Preclinical studies		
In vitro	Pancreatic cancer cell H_2O_2 production increases susceptibility to therapeutic effect of vitamin C	[20]
I.P.	Maintaining a 20 mM plasma concentration of vitamin C is optimal to obtain a therapeutic effect from vitamin C in an induced-tumor mouse model	[20]
In vitro	Vitamin C increases intracellular iron uptake in HUVECs as well as in multiple human cancer cell lines	[19]
In vitro	Vitamin C selectively sensitizes non-small-cell lung cancer and glioblastoma cells to radiation and chemotherapy, while increasing labile iron and H_2O_2 levels	[18]
Clinical studies		
1.25 g (oral) 50 g (I.V.)	Orally administered vitamin C unable to maintain therapeutic plasma concentration	[21]
15–125 g I.V.	High-dose infusion of vitamin C with gemcitabine in stage IV pancreatic cancer patients could achieve stable plasma levels of 20 mM while increasing the mean survival time	[23]
75 g I.V.	Vitamin C infusions were well tolerated and increased average progression-free survival in glioblastoma patients and control rate of disease in non-small-cell lung cancer patients	[18]

I.P.: intraperitoneal; I.V.: intravenous.

exhibited an increased rate of survival [18]. The authors proposed a mechanism inherent to cancer cells whereby superoxide ($O_2^{\bullet-}$) and H_2O_2 disrupt cellular iron metabolism with ascorbate oxidation further increasing intracellular H_2O_2 and labile iron levels. Through the Fenton reaction, H_2O_2 and iron react causing an increased oxidative burden and resulting in the observed cancer-specific ascorbate toxicity [18]. A phase I clinical trial for GBM patients treated with radiation, temozolomide, and intravenous ascorbate infusions showed that ascorbate was well tolerated and increased the average progression-free survival compared to the historical median [18]. Additionally, a phase II clinical trial for NSCLC patients treated with chemotherapy and ascorbate infusions reported an increased disease control rate compared with historical controls [18]. Unfortunately, the efficacy of ascorbate infusions in concert with radiochemotherapy has yet to be determined due to the limited sample size in these two studies.

The ability of ascorbate to specifically target NSCLC and GBM cancer cells without affecting the redox homeostasis of healthy cells makes systemic intravenous administration possible. In this example, the redox modulation happens only in tumor cells where iron metabolism is disrupted, and in this sense, this is an example of targeted therapy. However, a consistent plasma concentration must be maintained and 20 mM has been proposed as the therapeutic optimum [20]. Meanwhile, oral administration is incapable of obtaining and maintaining the required plasma concentrations [21, 22]. These data show the importance of administration route to achieve the desired effect. In the PACMAN study, a phase I clinical trial for stage IV pancreatic cancer, Welsh et al. [23] showed that infusion of high doses of ascorbate together with gemcitabine achieved stable plasma levels around 20 mM. The PACMAN study also revealed that systemically administered ascorbate did not cause an alteration in the erythrocyte reduced to oxidized glutathione (GSH:GSSG) ratio nor in plasma levels of F_2-isoprostane [23], an arachidonic acid peroxidation product commonly used as a biomarker. The mean survival was 12 months, almost double the historic median for gemcitabine-treated patients [23], yet due to the small sample size, no statistically significant conclusion about efficacy can be made. As of June 2017, the PACMAN study is scheduled to enter phase II (NCT02905578), with phase II trials for NSCLC (NCT02905591) and GBM (NCT02344355) scheduled as well. Hopefully, these upcoming and future trials will identify if an intravenous vitamin C formulation is an effective targeted systemic delivery for treating a geographically local redox imbalance.

3.2. Vitamin E. E vitamins are a group of fat-soluble compounds classified as saturated tocopherols or unsaturated tocotrienols, with α, β, γ, and δ isoforms within each group. The most biologically active vitamin E compound in humans is α-tocopherol. Therefore, α-tocopherol will be the vitamin E isoform described henceforth unless otherwise specified. Interestingly, vitamin E has been hypothesized to act only as a peroxyl ($RO_2^{\bullet}$) radical scavenger [17, 24]. As such, vitamin E effectively prevents the peroxyl radical chain reaction-driven lipid peroxidation. A summary of the preclinical and clinical studies discussed can be seen in Table 2.

Being fat soluble, vitamin E is mainly transported by lipoproteins where it prevents lipoprotein oxidation [25]—a redox reaction that drives atherosclerotic plaque development. An atherosclerosis model of rabbits fed a high-cholesterol diet showed that dietary vitamin E supplementation significantly reduced plaque development [26]. Tang et al. showed that vitamin E supplementation reduced plaque development in apolipoprotein E knockout ($ApoE^{-/-}$) mice when administered early, between 6 and 22 weeks of age, yet had no effect on reducing advanced lesions when administered at 30 or 38 weeks [27]. It is worth noting here that α-tocopherol has been shown to have limited antiatherosclerotic potential in rodent models [28]. In both the rabbit model and the $ApoE^{-/-}$ mice, vitamin E activated the nuclear factor erythroid 2-related factor 2 (Nrf2) pathway

TABLE 2: Preclinical and clinical studies using vitamin E.

Route	Vitamin E Results	Reference
Preclinical studies		
In vitro	α-Tocopherol activates Nrf2 in human retinal pigment epithelial cell line ARPE-19, thus inducing transcription of phase II enzymes	[32]
Oral	16 weeks of 1500 IU vitamin E daily is able to rescue Nrf2 function in alveolar macrophages from human atopic asthmatics	[33]
In vitro	α-Tocopheryl succinate activates Nrf2 in PC3 prostate cancer cell line which inhibits NF-κB nuclear translocation and neoplastic activity	[31]
Oral I.M.	Vitamin E significantly reduced atherosclerotic plaque progression in rabbits fed a high-cholesterol diet	[26]
Oral	Vitamin E significantly reduced atherosclerotic plaque progression in ApoE$^{-/-}$ mice	[27]
Oral	Vitamin E deficiency disrupts grass carp growth and physiology while vitamin E supplementation is able to reverse the negative effects	[34]
Clinical studies		
400–800 IU Oral	Daily vitamin E supplementation showed substantial reduction in nonfatal myocardial infarction in patients with angiographically proven coronary atherosclerosis, yet no significant benefit on risk of cardiovascular death was observed	[38]
400 IU Oral	4–6 years of daily vitamin E supplementation showed no therapeutic benefit on cardiovascular events in high-risk patients 55 years of age or older	[39]
100–3200 IU Oral	16 weeks of at least 800 IU/day of vitamin E required to reduce the plasma F2-isoprostane concentration	[40]
400 IU Oral	Daily supplementation of vitamin E only therapeutic in type 2 diabetes with genotype for systemically elevated oxidative stress	[41]
400 IU Oral	Hemodialysis patients experienced reduced rate of plasma MDA level increase following 2 months of vitamin E supplementation.	[44]
400 mg Oral	Patients with Down syndrome had their abnormal superoxide dismutase and catalase activity as well as low levels of reduced glutathione returned to physiological levels following vitamin E supplementation	[45]
2000 IU Oral	Daily high dose of vitamin E slowed the functional decline of Alzheimer's disease patients	[46]
400 IU Oral	Eight weeks of daily vitamin E supplementation increased paraoxonase-1 enzyme activity but did not lower serum malondialdehyde levels in type 2 diabetic patients	[43]
300 mg Oral	Three months of daily vitamin E supplementation significantly reduced serum malondialdehyde levels in insulin-dependent type 2 diabetic patients	[42]
Ointment S.C.	Patients undergoing colorectal cancer surgery exposed to vitamin E at the surgical site experienced a reduced rate of surgical site infection and lowered inflammatory response	[47]

I.M.: intramuscular; S.C.: subcutaneous.

[26, 27], which regulates the expression of antioxidant enzymes [29]. Specifically, Bozaykut et al. [26] showed an increase in the expression of glutathione S-transferase, one downstream enzyme of Nrf2, which is responsible for initiating the function of glutathione (GSH) [30], another major intracellular antioxidant. The Nrf2 pathway has now also been implicated as a vitamin E therapeutic mechanism in *in vitro* models of cancer [31] and macular degeneration [32] as well as in *in vivo* allergy [33] and developmental [34] studies. Furthermore, vitamin E has also been shown to increase peroxisome proliferator-activated receptor gamma (PPARγ) expression [26, 27]. PPARγ is one isoform of the PPAR ligand-activated transcription factors whose activation can be protective against cardiovascular diseases, neurodegenerative disorders, and cancer [35–37]. Thus, Nrf2 and PPAR activation reveal indirect antioxidant properties of vitamin E, which when paired with the direct radical scavenging ability make for a promising therapeutic.

CHAOS [38] and HOPE [39] were two of the first trials using vitamin E in prevention of cardiovascular disease. Both of these trials showed no cardiovascular benefit, which can potentially be attributed to the 400 IU/day [39] or up to 800 IU/day [38] doses used. In 2007, Roberts et al. [40] conducted both a dose-ranging and time-course study in hypercholesterolemic patients to evaluate the pharmacology of vitamin E. This was a beneficial study for future clinical trials as they revealed two critical dosing aspects. First, it took 16 weeks of daily dosing to reduce the plasma F_2-isoprostane concentration [40]. Second, this reduction was only significantly obtained at 1600 IU/day and 3200 IU/day, with a trend towards reduction at 800 IU/day [40]. At the largest dose of natural vitamin E (3200 IU/day), there was a 49% reduction in plasma F_2-isoprostanes, which led the authors to suggest

TABLE 3: Preclinical and clinical studies using alpha-lipoic acid.

Route	Alpha-lipoic acid Results	Reference
Preclinical studies		
Oral	ALA slowed the rate of plaque progression in a diet-induced rabbit atherosclerosis model	[56]
I.P.	ALA reduced lesion size in a diet-induced atherosclerotic mouse model. ALA also reduced vascular smooth muscle cell proliferation and migration *in vitro*	[59]
I.V.	Spleen weight/body weight ratio, levels of H_2O_2, lipid peroxidation, and levels of reduced glutathione returned to physiological levels in LPS-treated rats following ALA injection	[52]
Oral	ALA restored GSH, SOD, and catalase plasma concentrations to physiological levels in a pesticide-induced oxidative stress rat model	[54]
S.C.	ALA restored SOD and catalase concentrations to physiological levels in brain tissue of a phenylketonuria rat model	[55]
I.P.	Kidney mitochondrial function restored in LPS-treated rats following ALA exposure	[53]
Clinical studies		
600–1800 mg Oral	Five weeks of daily ALA supplementation alleviated the pain experienced by diabetics suffering from distal symmetric polyneuropathy.	[61]
600 mg Oral	Four years of daily ALA supplementation improved neuropathic conditions of diabetics suffering from polyneuropathy and the 600 mg dose was well tolerated for an extended period of time	[63]
600 mg Oral	20 weeks of daily ALA supplementation alleviated the pain experienced by diabetics suffering from polyneuropathy	[62]

I.P.: intraperitoneal; I.V.: intravenous; S.C.: subcutaneous.

that the antioxidant potency of vitamin E may not be biologically effective [40]. These studies taken together underline the relevance of selecting the appropriate dose and regimen to achieve a significant effect on redox homeostasis. Only after determining that a treatment actually improves redox function can we assess its antioxidant effect on disease progression and clinical outcomes. A study by Milman et al. [41] showed that daily vitamin E supplementation only had cardiovascular benefit in type 2 diabetics having a haptoglobin 2-2 genotype. The protein produced by this genotype is associated with elevated systemic oxidative stress due to its inferior function compared to the haptoglobin 1-1 genotype protein product. Several studies measured serum malondialdehyde (MDA) levels, a lipid peroxidation product, to assess the benefit of oral vitamin E supplementation. Although a reduction in plasma MDA levels was frequently observed, this systemic decrease in a lipid peroxidation marker did not correlate with improvement of clinical symptoms [42–44]. Thus, translating cellular and animal model work into an effective human therapeutic while also identifying the proper patient population that benefits from the given therapy and relevant biomarkers makes clinical trial design rather difficult.

Patients with ranging neurological disorders have been reported to experience increased levels of systemic oxidative stress [13]. Parisotto et al. [45] compared the blood antioxidant status of children with Down syndrome (DS) before and after 6 months of daily vitamin C and E supplementation. The study showed that DS patients had elevated superoxide dismutase (SOD) and catalase activity yet lower GSH levels, and all could be returned to physiological levels after supplementation [45]. A randomized, double-blind, placebo-controlled, parallel-group trial reported that a high dose of 2000 IU/day of vitamin E slowed the

functional decline of patients with mild to moderate Alzheimer's disease [46]. Both studies highlight how a systemically administered antioxidant can reduce systemic redox imbalance and alleviate symptoms experienced by individuals with neurological disease.

Lastly, Alias et al. [47] showed that subcutaneous application of vitamin E acetate ointment reduced the rate of surgical site infection in colorectal cancer surgery patients, while simultaneously lowering the inflammatory response. The patients underwent a laparoscopic, or minimally invasive, surgery. Patients who received vitamin E treatment had decreased C-reactive protein and a reduced white blood cell count 48 hours after surgery and reported lower postoperative pain [47]. This is an excellent example of a preventative strategy for localized delivery of an antioxidant to mitigate the onset of local redox imbalance.

3.3. Alpha-Lipoic Acid.
The disulfide fatty acid α-lipoic acid (ALA) is an amphipathic molecule both naturally synthesized and obtained through the diet. Virtually ubiquitous throughout the body, ALA and its reduced form, dihydrolipoic acid, have been reported to have numerous antioxidant and anti-inflammatory properties [48]. The therapeutic potential thus stems from the capability of ALA to scavenge reactive species [49, 50], recycle glutathione (GSH) and vitamins C and E [49], chelate divalent transient metal ions [50], and increase glucose uptake [51]. The preclinical and clinical studies described from here on are summarized in Table 3.

Goraca et al. [52] evaluated ALA treatment in a rat model of bacterial infection using lipopolysaccharide (LPS), a major component of the outer membrane of gram-negative bacteria. The spleen of LPS-treated rats had increased levels of hydrogen peroxide (H_2O_2) and lipid peroxidation, an

increased spleen weight/body weight ratio, and decreased levels of GSH [52]. All three of these markers were returned to physiological levels after intravenous ALA injection [52] suggesting that ALA can protect the spleen from an exaggerated inflammatory response. Cimolai et al. [53] showed that intraperitoneal-injected ALA could restore kidney mitochondrial function in rats exposed to LPS. Mignini et al. [54] used a pesticide-induced oxidative stress rat model to evaluate the effects of oral ALA supplementation and showed that ALA could increase plasma GSH concentrations. Additionally, ALA restored SOD and catalase plasma concentrations to physiological levels [54]. Subcutaneous delivery of ALA restored SOD and catalase to physiological levels in the brain tissue of a phenylketonuria rat model [55], a neurological disease that causes systemic phenylalanine accumulation and oxidative stress. Orally administered ALA slowed the rate of plaque progression, lowered plasma F_2-isoprostane levels, decreased lipid accumulation, and reduced collagen deposition in a diet-induced rabbit atherosclerosis model [56]. Furthermore, ALA decreased mRNA expression of vascular cell adhesion molecule-1 (VCAM-1) and of intracellular adhesion molecule-1 (ICAM-1) and reduced NF-κB pathway activity in the rabbit model [56]; all of which are proinflammatory factors associated with plaque development [57, 58]. A diet-induced atherosclerotic mouse model also showed that intraperitoneal ALA delivery could reduce lesion size and VCAM-1 and ICAM-1 expression [59]. Lee et al. [59] showed that ALA could reduce vascular smooth muscle proliferation and migration *in vitro* by attenuating the Ras-MEK1/2-ERK1/2 proliferative pathway. As of June 2017, phase III clinical trials using ALA for atherosclerosis treatment (NCT00764270) and heart disease prevention (NCT00765310) are ongoing.

ALA supplementation has been particularly successful in diabetic patients and has been prescribed for the treatment of diabetic polyneuropathy in Germany for decades [50]. In 2004, Ziegler et al. [60] assessed the role of oxidative stress in the development of diabetic polyneuropathy, a complex neuronal disorder associated with increased morbidity and mortality. Their results showed that systemic redox imbalance was more prominent in diabetics with polyneuropathy than in diabetics without polyneuropathy [60]. The SYDNEY 2 clinical trial assessed the efficacy of orally administered ALA in alleviating pain experienced by diabetic patients with distal symmetric polyneuropathy [61]. The primary measurement in the SYDNEY 2 trial was total symptom score (TSS), a summation of factors related to neuropathic pain where higher scores indicate an increased level of experienced pain. The results revealed that 600 mg of ALA administered orally for 5 weeks improved the positive sensory symptoms of diabetic patients [61]. Similar findings were described by Garcia-Alcala et al., [62] who reported that 20 weeks of ALA treatment resulted in a continuous reduction in TSS. NATHAN 1 was a four-year clinical trial that further assessed ALA treatment for polyneuropathy as well as the safety of prolonged oral administration of 600 mg of ALA [63]. This trial used several comprehensive analyses alongside TSS such as the neuropathy impairment score (NIS)

[64] and the NIS lower limbs score to measure therapeutic outcomes without any direct measurements of changes in redox markers. Improvement of neuropathic impairments, particularly small fiber and muscular function, was ultimately reported, and the 600 mg dose was well tolerated by patients [63]. We guide the readers to an extensive review by Papanas and Ziegler [65] of more trials and relevant meta-analyses regarding ALA in diabetic neuropathy. The success seen in these trials can likely be attributed to the hydrophilic and lipophilic nature of ALA as well as to the delivery route in treating a disorder that stems from a systemic redox imbalance.

3.4. Vitamin A.
A vitamins are a group of unsaturated, fat-soluble organic molecules that elicit pleiotropic effects throughout the body. Physiologically, vitamin A regulates energy homeostasis, lipid metabolism, the immune response, and gene expression for cellular development and differentiation [66–68]. The major signaling mechanism for the regulatory actions of vitamin A is through nuclear retinoic acid receptors. However, signaling through Janus kinase (JAK)/signal transducer and activator of transcription (STAT), mitogen-activated protein kinase (MAPK), and PPAR pathways have also been described [67]. Vitamin A quenches singlet oxygen ($^1O_2$) [69] and prevents lipid peroxidation by scavenging peroxyl ($RO_2^\bullet$) radicals [70], similar to vitamin E. Furthermore, the major active metabolite of vitamin A—retinoic acid—acts as a precursor for rhodopsin, the light-sensitive pigment in the eye responsible for phototransduction [71]. Retinoic acid is obtained through the diet from animal-derived food or from plant-derived precursors like β-carotene and lycopene. Clinical studies using vitamin A are summarized in Table 4.

In accordance with the pleiotropic properties on cellular homeostasis, vitamin A was trialed and is now accepted as a therapeutic for various skin-related conditions. Topically applied β-carotene protected human skin from IR-generated reactive species [72] and orally administered β-carotene reduced UV-induced skin lesions [73]. A randomized, double-blind, vehicle-controlled, clinical trial showed that topical retinol, the alcohol retinoic acid derivative, applied three times a week for 24 weeks reduced the appearance of aging-related fine wrinkles in elderly volunteers by increasing the dermal matrix [74]. Furthermore, topical application of tretinoin or all-*trans* retinoic acid has long been prescribed for the treatment of acne and photoaging [75, 76] and is more effective than orally administered tretinoin in cases of photoaging [77]. The role of these and more vitamin A derivatives in treating skin disease has been reviewed elsewhere [78]. The success of topical vitamin A application provides evidence that identifying the proper antioxidant for a given condition combined with an administration route that localizes the redox intervention results in a successful antioxidant therapy.

3.5. Vitamin B_{12}.
Vitamin B_{12} derivatives or cobalamins (Cbl) are soluble macrocycles belonging to the corrinoid family with a cobalt atom tethered in the center of the corrin plane. They are essential cofactors for two enzymes in

TABLE 4: Clinical studies using vitamin A.

Route	Vitamin A Results	Reference
Clinical studies		
24 mg Oral	12 weeks of daily oral vitamin A reduced UV-induced skin lesions	[73]
0.4% lotion Topical	Topical vitamin A application three times a week for 24 weeks reduced aging-related wrinkles	[74]
0.2% lotion Topical	Topical vitamin A protects skin from IR-generated reactive species	[72]
20 mg Oral 0.05% lotion Topical	Topical vitamin A more effective in treating photoaging than orally administered	[77]

TABLE 5: Preclinical and clinical studies using vitamin B_{12}.

Route	Vitamin B_{12} (cobalamin) Results	Reference
Preclinical studies		
In vitro	Pulse radiolysis determined that the rate constant between Cob(II)alamin and superoxide ($O_2^{\bullet-}$) is 6.8×10^8 M^{-1} s^{-1}, which is within an order of magnitude of cytosolic and mitochondrial superoxide dismutase (SOD)	[79]
In vitro	Cob(II)alamin reacts with $O_2^{\bullet-}$ at a rate similar to that of the SOD	[80]
In vitro	Cyanocobalamin treatment inhibited $O_2^{\bullet-}$-induced damage in human aortic endothelial cells by scavenging intracellular $O_2^{\bullet-}$	[83]
Clinical studies		
0.5 mg Oral	Daily supplementation with folic acid, vitamin B_6, and vitamin B_{12} for one year significantly reduced the carotid intima-media thickness, a marker of atherosclerosis, in at-risk patients	[86]
0.4 mg Oral	Six months of daily folic acid and vitamin B_{12} supplementation improved coronary endothelial function in patients at risk for coronary artery disease	[87]
0.4 mg Oral	Two years of daily supplementation with folic acid and vitamin B_{12} significantly increased coronary blood flow in patients with stable coronary artery disease	[88]
25 or 0.5 mg I.M.	Daily ultrahigh-dose injections (25 mg) of methylcobalamin improved the compound muscle action potentials of patients with amyotrophic lateral sclerosis	[89]
Eyedrops	Eyedrops containing 0.15% hyaluronic acid and vitamin B_{12} reduced oxidative stress markers in the conjunctiva (mucous membrane covering eye) and improved the overall symptoms of patients with chronic dry eye	[90]

I.M.: intramuscular.

mammals: mitochondrial methylmalonyl-CoA mutase and cytosolic methionine synthase. The central cobalt can change its oxidation state between +3 (cob(III)alamin), +2 (cob(II)a-lamin), and +1(cob(I)alamin), which makes these compounds redox active. Moreover, it has been shown that Cbl reacts with $O_2^{\bullet-}$ at rates comparable with that of superoxide dismutase [79, 80]. Hence, it has been suggested that cobalamins modulate inflammation and redox status [81–83] in addition to and independently of their cofactor function. Low serum levels of B_{12} are prevalent in patients with type 2 diabetes mellitus, and there is an association between low levels of B_{12} and markers of oxidative dysfunction [84]. Moreover, levels of B_{12} negatively correlate with fasting glucose, oxidized LDL, and catalase levels in diabetic vegetarians [85]. These findings suggest that Cbl supplementation could be useful in patients with type 2 diabetes mellitus, especially if

they are vegetarians, who are at risk of low B_{12}. Preclinical and clinical work with vitamin B_{12} is summarized in Table 5.

Cobalamin is essential to metabolize homocysteine, an independent risk factor for cardiovascular disease. Hence, researchers have investigated the role of Cbl in cardiovascular disease. One of us was among the first to characterize a redox effect in vascular cells [83] and suggest that it acted by direct scavenging of $O_2^{\bullet-}$ with a high rate constant [80]. In a randomized placebo-controlled trial, a mix of folate, vitamin B_6, and vitamin B_{12} reduced the carotid intima-media thickness in patients at risk of cerebral ischemia [86]. This effect was found to be independent of homocysteine. In a small prospective randomized placebo-controlled trial, Willems et al. [87] demonstrated that treatment with cobalamin in patients with coronary artery disease improved volumetric coronary blood flow. These results

were later confirmed by Bleie et al. [88] showing an increased coronary blood flow in a patient with stable coronary artery disease treated with cobalamin, suggesting that B_{12} improves vascular function.

Cobalamin levels are associated with systemic and central nervous system (CNS) markers of redox dysfunction and inflammation, independently of homocysteine levels [82]. In a controlled, double-blinded study in patients with idiopathic osteoarthritis, Flynn et al. [81] found that Cbl improved handgrip and tenderness compared to NSAID treatment. Regarding effect on the CNS, intramuscular injection of high doses of Cbl improved muscle action potential amplitude in a small double-blind trial in patients with amyotrophic lateral sclerosis [89].

A successful example of local administration of Cbl to reduce redox dysfunction and inflammation was published by Macri et al. [90]. They found that eye drops containing hyaluronic acid and vitamin B_{12} significantly decrease markers of lipid peroxidation and inflammation, improving dry eye symptoms. Although vitamin B_{12} is not classically considered an antioxidant, more evidence accumulates supporting a redox effect of Cbl. Since it is well tolerated and no adverse effects have been reported, exploring further the noncoenzyme and redox effects of Cbl is a promising therapeutic avenue for cardiovascular, neurological, and inflammatory diseases.

4. Enzyme Regulators and Mimetics

The use of stoichiometric antioxidant molecules presents with the problem that they are finite. At the necessary site they may be present in limited concentrations or may not have been recycled after their redox reaction. Accordingly, most cellular redox homeostasis is maintained by enzymes [91]. As we have shown with micronutrients, certain antioxidants can increase enzyme production and function aside from directly inactivating the reactive species. Herein, we analyze several specific enzyme-directed therapeutics and present an overview in Figure 1. Next, we discuss the use of redox enzymes, enzyme mimics, and enzyme regulators.

4.1. NADPH Oxidase Inhibitors. Nicotinamide adenine dinucleotide phosphate (NADPH) oxidases (NOX) are a group of transmembrane enzymes that generate superoxide ($O_2^{\bullet-}$) by transferring electrons from NADPH across a membrane to reduce molecular oxygen [92]. Accordingly, NOX enzymes are present in the plasma membrane, endoplasmic reticulum, mitochondrial membrane, and nuclear membrane, as well as at focal adhesions [93] and invadopodia [94]. In total, there are seven NOX isoforms termed NOX1-5 or DUOX1-2. NOX enzymes are physiologically crucial for the immune response and during angiogenesis; these functions along with enzymatic regulation and localization have been reviewed in extensive detail elsewhere [95]. Pathologically, dysregulated NOX enzymes have been implicated in various cancers [96, 97], neurodegenerative diseases [98], cardiovascular diseases [99], and renal disease [100].

Due to the association of dysregulated NOX with disease onset, it was fitting to pursue direct NOX inhibition as a therapeutic. Triazolopyrimidine derivatives (VAS) and pyrazolo-pyridine dione derivatives (GKT) are two efficacious small molecule inhibitors that have been reported. VAS and GKT successfully mitigate ROS formation and damage in in vitro and in vivo models of disease [101–105]. These two families, and others not covered in this section, have been extensively reviewed elsewhere [106].

Specifically, GKT137831 is a NOX 1 and 4 inhibitor that has been reported to mitigate renal disease [105], attenuate diabetic nephropathy [102], and suppress cardiac fibroblast activity associated with hypertensive heart disease [104]. A randomized, double-blind, placebo-controlled phase II trial using GKT137831 for treating type 2 diabetes with nephropathy was concluded in 2015 (NCT02010242). The drug developer, Genkyotex, reported that GKT137831 was safe and significantly reduced liver enzyme and inflammatory marker levels, with the results unpublished as of June 2017. Currently, Genkyotex is finalizing a phase II study design to treat the liver disease primary biliary cholangitis with GKT137831.

Meanwhile, VAS2870 a NOX 1, NOX 2, and NOX 4 inhibitor has been reported to have protective properties against brain ischemia in mice [101] and to reduce ROS production and radiation-induced phenotypic changes in human pulmonary artery endothelial cells [103]. One challenge for translating the success of VAS molecules to the clinic is their low solubility. Hecht et al. [107] have potentially solved this issue by developing a method that utilizes spray drying, microemulsification, and cyclodextrin incorporation to enhance the solubility and stability of VAS3947 as a model VAS molecule, for oral administration. Ongoing studies with these two classes of molecules will offer a greater understanding of their pharmacological efficacy and the value of targeted NOX inhibition in disease treatment or prevention.

4.2. Nitric Oxide Synthase Inhibitors. Nitric oxide synthase (NOS) represents a group of enzymes that utilize molecular oxygen and NADPH to oxidize L-arginine producing L-citrulline and nitric oxide ($^{\bullet}$NO). There are three NOS isoforms termed neuronal NOS (nNOS or NOS I), inducible NOS (iNOS or NOS II), and endothelial NOS (eNOS or NOS III). Exceptions to the general locations and regulatory mechanisms for each isoform have been extensively reviewed elsewhere [108], but generally, nNOS is found throughout the central (CNS) and peripheral (PNS) nervous systems where $^{\bullet}$NO is implicated in aspects of synaptic plasticity and cellular communication; iNOS is typically found in cells of the immune system where $^{\bullet}$NO is responsible for the cell's cytotoxic properties; eNOS is mostly expressed in endothelial cells where $^{\bullet}$NO causes vasodilation and vasoprotection and prevents platelet aggregation. Therapeutic approaches have been aimed at inhibiting iNOS.

Initially, NOS inhibitors aimed to displace the enzymatic substrate arginine but were clinically ineffective and even increased mortality in the case of L-NMMA treatment for septic shock [109]. To date, the most successful NOS
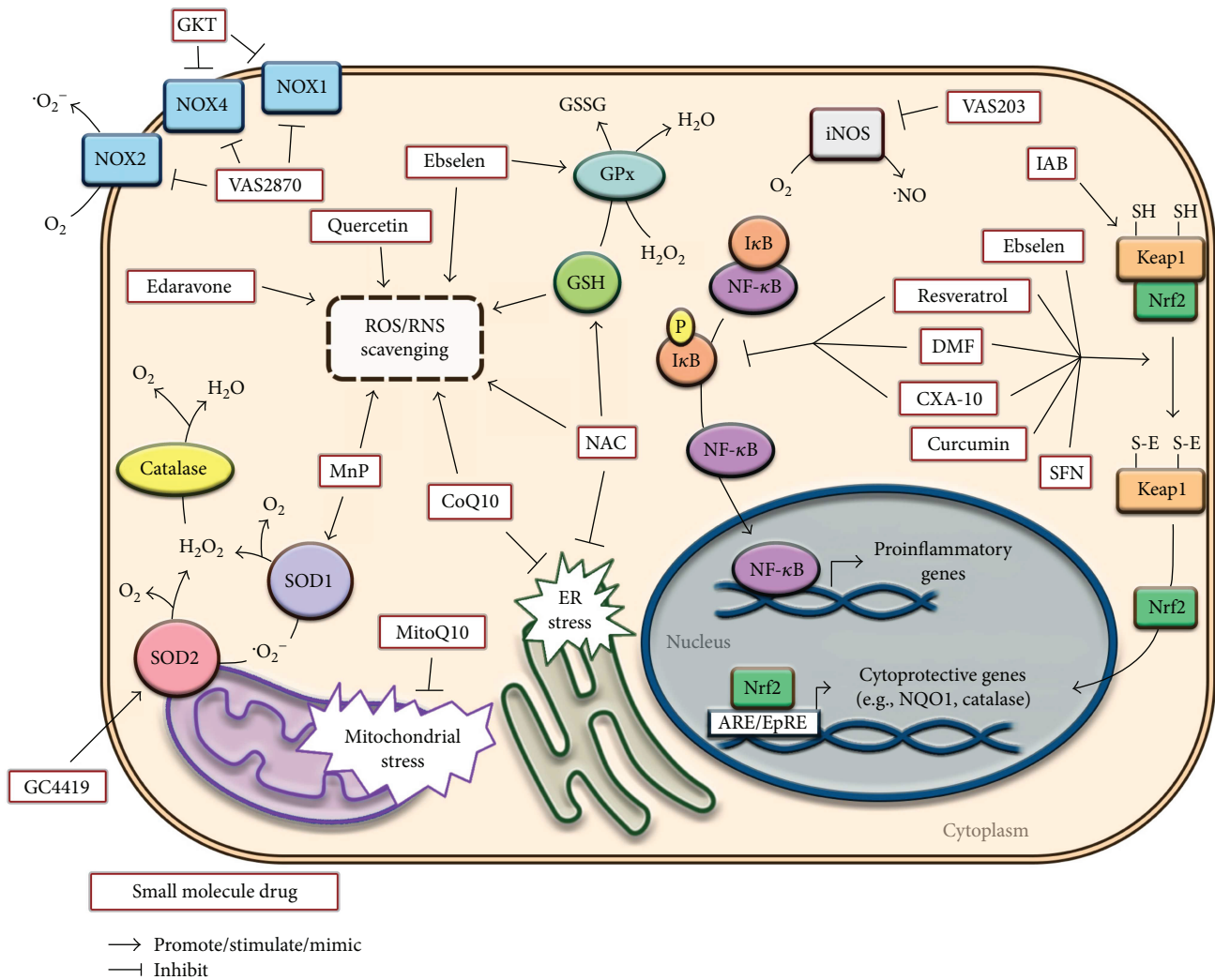
Figure 1: A scheme depicting cellular sites of action of several redox interventions. ARE/EpRE: antioxidant response element/electrophile responsive element; CoQ10: coenzyme Q10; CXA-10: 10-nitro-oleic-acid formulation; DMF: dimethyl fumarate; ER: endoplasmic reticulum; GKT: GKT137831; GPx: glutathione peroxidase; GSH: glutathione; IAB: N-iodoacetyl-N-biotinylhexylenediamine; MnP: manganese porphyrins; NAC: N-acetylcysteine; NOS: nitric oxide synthase; NOX: NADPH oxidase; NQO1: NAD(P)H quinone dehydrogenase 1; Nrf2: nuclear factor erythroid 2-related factor 2; RNS: reactive nitrogen species; ROS: reactive oxygen species; SFN: sulforaphane; SOD: superoxide dismutase.

inhibitor is 4-amino-tetrahydrobiopterin (VAS203), developed by Vasopharm, which is an analogue of the redox-sensitive NOS cofactor tetrahydrobiopterin rather than an arginine analogue [110]. VAS203 is an allosteric iNOS inhibitor and is being trialed for the treatment of traumatic brain injury (TBI). TBI has been shown to cause increased iNOS activity in the brain due to a compromised blood-brain barrier, aside from other major complications [111]. An exploratory phase II placebo-controlled, randomized trial named NOSTRA-II determined that VAS203 may have neuroprotective properties and can be safely administered, although there was reversible kidney damage reported in several patients at the highest tested dose (30 mg/kg) [110]. In light of these findings, a phase I trial to assess renal function impairment in healthy volunteers was concluded in early 2017 with results unreported so far (NCT02992236). As of June 2017, NOSTRA-III—the

placebo-controlled, randomized, double-blind phase III trial—is underway to evaluate the efficacy of VAS203 infusions on clinical outcomes of patients with moderate to severe TBI (NCT02794168).

4.3. Superoxide Dismutase Mimetics. Superoxide dismutase (SOD) is a group of metal-containing enzymes that convert superoxide ($O_2^{\bullet-}$) to hydrogen peroxide (H_2O_2) and/or molecular oxygen. In humans, there are cytosolic (SOD1) and extracellular (SOD3) isoforms which utilize copper and zinc as cofactors while the mitochondrial (SOD2) isoform uses manganese as the cofactor. Manganese porphyrins (MnP) are among the most prominent SOD mimics developed to date. MnPs are made up of a macrocyclic ring structure with manganese found at the center. Other SOD mimics also have similar structures but house a different metal at their center. Further detail of MnP alongside

other prominent mimetics' synthesis, structure, kinetics, and potential therapeutic benefits has been extensively reviewed [112]. The therapeutic efficacy of MnPs is heavily dependent on the redox environment at the time of administration. For instance, MnP administration at the onset of diabetes inhibited oxidative damage in a rat model [113]. When administered after the onset of diabetes, however, the same MnP actually increased oxidative damage [114].

GC4419 is a promising new MnP-like SOD mimetic highly specific for reacting with $O_2^{\bullet -}$. GC4419 has been shown to rescue cell clonogenicity of both a SOD2-*null* human embryonic kidney cell line [115] and radiation or chemotherapy-treated primary human dermal fibroblasts [116]. Intravenous delivery of GC4419 is currently in a phase II clinical trial for alleviating radiation-induced oral mucositis in patients with head and neck cancer (NCT02508389). Galera Therapeutics Inc. is also assessing the tolerability and pharmacokinetics of another SOD mimetic, GC4711, given orally compared to intravenous GC4419 in healthy volunteers (NCT03099824). BMX-001 is a MnP currently in a phase I clinical trial for glioblastoma patients undergoing radiation therapy (NCT02655601). Additionally, a continuous infusion of MnP AEOL 10150 using a subcutaneously implanted osmotic pump was able to significantly reduce radiation-induced injury in a rat model [117] and has proven to be beneficial in a nonhuman primate radiation-induced injury model [118]. As of 2017, Aeolus Pharmaceuticals Inc. is working on moving AEOL 10150 into clinical trials. Of note, MnPs often can react with various species and moieties besides $O_2^{\bullet -}$ which expands their potential outside of being just a SOD mimetic but also complicates their utility.

4.4. Catalase Delivery. Catalase is an antioxidant enzyme that catalyzes the disproportionation of H_2O_2 to O_2 and H_2O; it decreases neuroinflammation and attenuates neurodegeneration in the CNS.

An important component of many metabolic and inflammatory diseases of the CNS involves inflammation [119]. These include Alzheimer's and Parkinson's diseases (AD and PD) [120–122], stroke [123, 124], traumatic brain injury (TBI), multiple sclerosis (MS), age-related macular degeneration (AMD), prion disease, meningitis, encephalitis, human immunodeficiency virus- (HIV-) associated neurocognitive disorders [125, 126], epilepsy, brain cancer, lysosomal storage diseases [127, 128], obesity [129, 130], and even mental health disorders such as depression, autism, and schizophrenia. These diseases are often accompanied by the extensive recruitment of immunocytes. Such inflammatory activities are linked to microglial activation and its secretion of neurotoxic factors. These include ROS and RNS leading to oxidative stress and neuronal injuries [131–134]. Oxidative stress affects neuronal, astrocyte, and microglia function by inducing ion transport and calcium mobilization and activating apoptotic programs. Apoptosis and excitotoxicity are principal causes of mitochondrial-induced neuronal death. Therefore, the need for delivery of potent antioxidants, in particular, catalase to affected brain tissues cannot be overstated.

The administration of catalase has been shown to rescue the primary cultured cerebellar granule cells in *in vitro* models of PD [135, 136]. Thus, addition of catalase to cerebellar granule cells treated with a toxin, 1-methyl-4-phenyl-1,2,3,6-tetrahydropyridine (MPTP) that causes a severe and irreversible parkinsonian syndrome in humans and in nonhuman primates [137], resulted in enhancing their viability by 75% compared to the control cells. Regrettably, the blood-brain barrier (BBB) severely restricts the transport of this potent antioxidant to the brain. Although small lipophilic molecules (MW < 400 kDa) can cross the BBB in pharmacologically significant amounts, effective concentrations of lipid-insoluble drugs (polar molecules and small ions), as well as high molecular weight compounds (peptides, proteins, and nucleic acids), cannot be delivered to the CNS within the limits of clinical toxicity. The inability of most potent therapeutics to cross the BBB following systemic administration necessitates the need to develop unconventional, clinically applicable drug delivery systems for the treatment of brain disorders. Smart, biologically active vehicles are crucial to accomplishing this challenging task.

To this end, immunocytes that include mononuclear phagocytes (dendritic cells, monocytes, and macrophages), neutrophils, and lymphocytes can carry nanoformulated drugs as they readily home to disease sites. Using living cells as drug delivery vehicles, takes advantage of their natural carriage, storage, mobility, and secretory capacity. It offers several benefits over common drug administration regimens; these include targeted drug transport to disease sites, prolonged drug half-lives, time-controlled drug release, and diminished drug immunogenicity and cytotoxicity profiles. Thus, a cell-based delivery system to bring nanoformulated catalase to affected brain regions was developed [138, 139]. The system rests in the abilities of blood-borne macrophages to carry antioxidant proteins across the BBB to the inflamed tissues. Using inflammatory response cells enables targeted drug transport and prolonged circulation times [140], along with reductions in cell and tissue toxicities. In addition, these cells are capable of cell-to-cell transmission of drug-laden nanoparticles that improves their therapeutic outcomes.

One of the main obstacles in utilizing these cells is related to the fact that monocytes efficiently disintegrate and digest all entrapped foreign particles. Therefore, it is crucial to protect the activity of the drug inside this cell carrier [141]. To preclude macrophage-mediated enzyme degradation, catalase was packaged into a block ionomer complex with a cationic block copolymer, poly(ethyleneimine)-poly(ethylene glycol) (PEI-PEG). Overall, the structure and composition of protective nanocontainers play a crucial role in the effectiveness of formulations for cell-based drug delivery systems. For example, a recent study by one of us indicates that structure of block copolymer used for catalase nanoformulation (nanozyme), affects its cytotoxicity, loading, and release capacities, as well as preservation of catalase enzymatic activity inside cell-carriers [142]. Bone marrow-derived macrophages (BMM) carried significant amounts of catalase then slowly released the active enzyme over several days [138]. The enzyme released upon stimulation of nanozyme-loaded cell carriers decomposed microglial H_2O_2

produced upon nitrated alpha-synuclein or tumor necrosis factor alpha- (TNF-α-) induced activation *in vitro*. A significant amount of catalase was detected in brains of mice after transfer of BMM loaded with nanoformulated catalase following MPTP intoxication. It was demonstrated that such nanozyme-loaded BMM injected into MPTP-intoxicated mice reduce neuroinflammation and attenuate nigrostriatal degeneration [139]. This signified a neuroprotective effect of nanozyme-loaded monocytes in MPTP-induced neurodegeneration.

Another approach to targeted cell-mediated brain delivery of catalase is to utilize macrophages transfected *ex vivo* with a plasmid DNA (pDNA) encoding catalase [143]. Systemic administration of pretransfected macrophages produced month-long expression levels of catalase in the brain resulting in threefold reductions in inflammation and complete neuroprotection in mouse models of PD. This resulted in significant improvements in motor functions in PD mice. Mechanistic studies revealed that transfected macrophages secreted extracellular vesicles, exosomes, packed with catalase genetic material, pDNA and mRNA, active catalase, and NF-κB, a transcription factor involved in the encoded gene expression. Exosomes efficiently transfer their contents to contiguous neurons resulting in de novo protein synthesis in target cells. Thus, genetically modified macrophages serve as a highly efficient system for reproduction, packaging, and targeted gene and drug delivery to treat inflammatory and neurodegenerative disorders [143]. Of note, a proper differentiation of drug carriers into particular subtypes may further boost the therapeutic efficiency of cell-based drug formulations [144]. Alternatively, activated macrophages phenotype (M2) utilized in these studies did not promote further inflammation in the brain, resulting in a subtle, but statistically significant effect on neuronal regeneration and repair *in vivo*.

Even though this modality of antioxidant enzyme delivery has not moved to clinical trials yet, it is a promising approach to deliver redox-active enzymes in a targeted manner and to overcome several of the obstacles related to delivery of proteins and delivery to the CNS.

5. Small Molecule Antioxidants

Small (MW <250 kDA) molecule antioxidants have desirable pharmacokinetic properties able to exponentially enhance antioxidant defense by directly acting on signaling pathways [145]. Phenolic groups dominate this class but there are multiple other species with unique antioxidant properties [146]. In this section, we will discuss some of the most commonly used and already developed small molecule antioxidants and highlight emerging formulations (Figure 1).

5.1. Electrophiles. Electrophilic small molecules are potent activators of the nuclear factor erythroid 2-related factor 2 (Nrf2) pathway. Nrf2 is a transcription factor that induces the production of antioxidant and detoxification enzymes controlled by an enhancer sequence called the antioxidant response element/electrophile responsive element (ARE/EpRE). The identification of Nrf2 as the critical transcription factor in this pathway was only recognized in 1997 [29]. This discovery triggered tremendous progress in understanding the increased efficacy of small molecule antioxidants in therapeutic applications. Under homeostatic conditions, Nrf2 is sequestered to the cytoplasm by the actin-bound inhibitor Kelch-like ECH-associated protein 1 (Keap1). Keap1 subjects Nrf2 to polyubiquitination and degradation via the proteasome. During redox imbalance, or if the cell is exposed to electrophilic small molecules, key cysteine residues on Keap1 are oxidized causing a conformational change that releases Nrf2. Under these conditions, Nrf2 is able to translocate to the nucleus where it forms heterodimers with Maf proteins and binds ARE/EpRE. Nrf2 binding to ARE/EpRE results in transcription of cytoprotective enzymes such as catalase, glutathione S-transferase, NAD(P)H quinone oxidoreductase 1, SOD 1, heme oxygenase 1, and many more.

5.1.1. Sulforaphane. Sulforaphane (SFN) is an isothiocyanate metabolite found in cruciferous vegetables, such as broccoli, and is one of the most widely studied electrophilic Nrf2 inducers. The anticarcinogenic properties of broccoli were attributed to SFN when it was first identified as a phase II metabolic enzyme inducer in 1992 [147]. After the characterization of the Nrf2/Keap1 pathway, SFN was identified as a Nrf2 inducer further describing its potential in anticancer therapy [148]. Since then, oral administration of SFN has been shown to improve behavioral symptoms of young men with autism spectrum disorder [149] and is being further evaluated for this condition (NCT02561481, NCT02879110, and NCT02909959). SFN has also been shown to improve fasting glucose in obese patients with dysregulated type 2 diabetes [150] and is currently in a phase II clinical trial (NCT02801448). As a redox-based therapeutic, SFN is making headway in animal models of atherosclerosis. Angioplasty with stent placement is the most common surgical intervention for treating atherosclerosis or a stenotic vessel. A major complication following angioplasty is vessel reocclusion or restenosis. Currently, restenosis is best inhibited by chemotherapy-eluting stents, yet they create a favorable local environment for thrombosis [151]. Yoo et al. [152] showed that local application of SFN at the site of arterial injury inhibits restenosis in an angioplasty-injury rat model. This was attributed to the Nrf2-activating properties of SFN, which likely inhibits the phenotypic change in vascular smooth muscles that drives restenosis. Multiple other groups have since successfully inhibited restenosis using SFN in similar animal models [153, 154]. One of us has been studying local delivery of other electrophiles such as cinnamic aldehyde as a therapy to inhibit restenosis. Development of a delivery vehicle that specifically targets the site of an atherosclerotic plaque could provide a novel antioxidant approach for treating vasculopathies and improving surgical outcomes and is the current focus of our lab.

5.1.2. Dimethyl Fumarate. Dimethyl fumarate (DMF) is an esterified fumaric acid that can inhibit NF-κB activation [155]. DMF effectively increases relapsing-remitting multiple sclerosis patient quality of life when administered orally as

a delayed-release conformation, termed BG00012 [156] (NCT00420212). DMF interacts with GSH under specific conditions in the bloodstream which limits this absorption route and bioavailability, justifying why recent studies mostly use limited and/or low doses of DMF [157]. New formulations of DMF or newly synthesized derivatives could improve the pharmacokinetics of this compound and provide useful new approaches.

5.1.3. Nitro-Oleic Acid. Nitro-oleic acid is one of the many nitrated fatty acids naturally present in human and animal tissues. Nitrated fatty acids result from $^\bullet$NO-derived species reacting with unsaturated fatty acids resulting in $^\bullet NO_2$ addition at a double bond [158]. Nitro-oleic acid has been shown to have cytoprotective properties through Nrf2 and PPARγ activation and NF-κB inhibition [158]. CXA-10 is an orally administered 10-nitro-oleic-acid compound developed by Complexa Inc. CXA-10 has been trialed in five phase I clinical trials related to kidney injury as of 2017 (NCT02313064, NCT02127190, NCT02248051, NCT02460146, and NCT02547402) with differentiated safety in over 100 subjects reported as well as activation of target genes and inhibition of disease-related fibrotic and inflammatory biomarkers. Notably, the metabolic profile of patients in NCT02127190 has recently been characterized [159]. CXA-10 is set to enter phase II trials in 2018 for the treatment of pulmonary arterial hypertension and focal segmental glomerulosclerosis, two life-threatening diseases with a severely poor prognosis. These and future trials using nitrated lipids may yield effective redox-based therapies.

5.1.4. Synthetic Electrophiles. Recently, there has been a surge in development of ARE-/EpRE-inducing molecules. Such molecules include N-iodoacetyl-N-biotinylhexylenediamine (IAB) which modifies Keap1 [160] but so far has a minimum effect on Nrf2 activation due to cytotoxicity and engagement with intracellular proteins [161]. Dai et al. [162] recently showed that several new formulations of Pyrazino[2,1-*a*]isoquinolin analogues, compounds originally designed for their antifungal properties [163], have potential as inducers of the Nrf2 pathway. Future studies using novel formulations may yield exciting therapeutics in the upcoming years. Moreover, testing new synthetic electrophilic compounds using novel platforms for targeted delivery could offer significant advances in redox medicine.

5.2. Nitric Oxide and Related Compounds. $^\bullet$NO is a small nitrogen-centered free radical gas that can diffuse several cell diameters from its production site. As mentioned above, it is synthesized by nitric oxide synthases (NOS). It serves as a neurotransmitter involved in memory and learning, and as a signaling molecule controlling vascular tone, cell proliferation, and cell survival. During inflammation an inducible form of NOS (iNOS) produces large quantities of $^\bullet$NO involved in host protection against pathogens. Because of its role in vascular homeostasis, its potential therapeutic role in vascular disease has been extensively studied and is reviewed elsewhere [164]. Direct inhalation of $^\bullet$NO is the simplest way to deliver it. Inhaled $^\bullet$NO has been clinically

used to treat pulmonary hypertension and acute respiratory distress syndrome. However, a recent systematic review analyzing 14 different trials shows that even though inhaled nitric oxide improves oxygenation, there is no reduction in mortality [165]. On the other hand, inhalational $^\bullet$NO appears to be beneficial for respiratory failure in terms of infants after meta-analysis of 16 studies [166]. $^\bullet$NO reduced mortality and/or use of extracorporeal membrane oxygenation. Moreover, inhalational $^\bullet$NO reduces development of chronic lung disease and use of extracorporeal membrane oxygenation in newborns with persistent pulmonary hypertension [167]. Similarly, Miller et al. [168] conducted a randomized study in infants with pulmonary hypertension after congenital heart surgery. They found that inhalation of $^\bullet$NO lessens the risk of pulmonary hypertensive crises and shortens postoperative recovery [168].

Since $^\bullet$NO is highly reactive, inhalational $^\bullet$NO is mostly a local intervention to the airways. When it comes to systemic administration, different strategies have been used to increase $^\bullet$NO: administration of its precursors L-arginine, use of $^\bullet$NO donors, or use of other $^\bullet$NO bioactive compounds such as nitrates, nitrite, or S-nitrosothiols. A systematic review in 2017 that included 5 completed clinical trials assessing the use of glyceryl trinitrate in patients with stroke concluded that there is no evidence to recommend use of this drug in stroke [169]. The amount of preclinical data suggesting a beneficial effect of increasing $^\bullet$NO for the treatment of vascular disease has not led to a successful clinical translation. Even though there are several attempts to increase $^\bullet$NO via systemic administration of L-arginine or nitric oxide donors, they have failed to improve vascular outcomes (reviewed in [164] and [170]). A large prospective multicenter, randomized trial studying the effect of $^\bullet$NO donors on restenosis after balloon angioplasty showed a modest improvement on angiographic restenosis but no differences in clinical outcomes [171]. These negative results highlight the issue of attempting to treat a localized $^\bullet$NO deficiency at sites of arterial disease via a systemic approach. Hence, numerous attempts to deliver bioactive $^\bullet$NO locally aim at overcoming the problems with systemic delivery. Endolumenal delivery of $^\bullet$NO via a permeable balloon catheter inhibits restenosis in the rat carotid balloon injury model [172]. We have shown that an S-nitrosated nanofiber targeted to sites of arterial injury significantly inhibits restenosis in the rat balloon carotid injury model [173].

Further evidence that targeted or localized approaches result in successful clinical application of $^\bullet$NO-based therapies is provided from fields that lend themselves to formulations for local delivery. One such field is dermatology, and the anti-inflammatory and antimicrobial properties of $^\bullet$NO show promise to treat acne vulgaris [174]. Results of a phase II clinical trial (NCT01844752) show that a topical formulation of $^\bullet$NO decreases inflammatory and noninflammatory lesions in subjects with acne vulgaris [175].

5.3. Flavonoids. Flavonoids are a group of naturally occurring compounds found in many fruits and vegetables as well as beverages such as tea and wine. The flavonoid active compounds are secondary metabolites that have been proven

beneficiary in protecting against atherosclerotic disease progression [176]. Flavonoids were initially identified for their direct scavenging properties but recent findings point out that the indirect antioxidant effects are of greater biological relevance and better support the use of these compounds as therapeutics [177]. Accordingly, flavonoids have been ascribed to anti-inflammatory, anticancer, and antithrombotic properties with dose-dependent effects [178].

5.3.1. Curcumin. *Curcuma longa*, turmeric, is the yellow-pigmented spice commonly used in curries that is comprised of naturally occurring phenolic compounds called curcuminoids. Curcumin is the most abundant of the curcuminoids and is classified as a linear diarylheptanoid with multiple functional groups. In mice, curcumin has been shown to induce Nrf2 nuclear translocation and induction of ARE/EpRE signaling [179]. Curcumin has been shown to inhibit gastric tumor growth by disrupting cellular bioenergetics [180] and to reduce the atherogenic and dyslipidemic panel in patients with chronic disease [181, 182]. Multiple studies show adjunct supplementation of curcumin with other active ingredients induces redox homeostasis in metabolic syndrome [183]. Of note, curcumin has been extensively pursued as a therapeutic with over $150 million in federal funds linked to biomedical studies, yet no conclusive therapeutic effects in humans have been determined to date [184]. Nelson et al. [184] recently published an extensive review describing some considerations to explain the pitfalls of using curcumin. In general, the poor absorption of curcumin and limited abundance of the active compound may hinder its therapeutic potential as a systemic agent. Furthermore, they classify curcumin as a pan-assay interference compound which may show activity in an assay by interfering with the readout rather than by the specific compound/target interaction the assay aims to assess. Nevertheless, because of its lipophilic characteristics, curcumin could still be considered a good agent for synergic localized or targeted therapy if better formulations arise. Indeed, nanoparticle-encapsulated curcumin has been shown to have antimicrobial properties and to promote wound healing in an *in vivo* murine wound model [185].

5.3.2. Quercetin. Quercetin is a polyphenolic, pigmented flavonoid found in capers and onions that acts as an ROS scavenger. Quercetin has been proposed to have antioxidant effects in inducible vascular models of disease [186, 187], while also exhibiting anti-inflammatory and antineoplastic properties in several other models [188–190]. Unfortunately, most flavonoids are not readily absorbed by the human intestine which severely limits the bioavailability and overall therapeutic potential of quercetin [191]. It has failed to exhibit the anticipated preventative effects on serum phospholipids in healthy subjects as a supplement over an 8-week period [192]. Also, no significant changes in endothelial function or $^{\bullet}$NO production were reported after 50–400 mg doses of water-dissolved quercetin extract were given to healthy subjects [193] (ACTRN12615001338550). It has been reported that a food matrix, as in onion powder rather than extract, significantly increases the bioavailability

of quercetin in animals and humans [194]. Burak et al. [195] recently showed that the use of concomitant onion skin extract, instead of quercetin dehydrate alone, significantly increased the oral bioavailability of quercetin in healthy subjects. Extracting quercetin during food processing may be the factor limiting bioavailability of this flavonoid. As such, combinatorial therapy with other antioxidants, as has recently been trialed [196], may enhance quercetin delivery and overall benefit.

5.3.3. Resveratrol. Resveratrol is a natural phenol found in berries. It is the most studied flavonoid in scientific research and has the potential to induce Sirtuin-1 activity [197] and modulate Nrf2 [198] and NF-κB [199]. *In vitro* studies indicate anti-inflammatory effects from resveratrol in multiple cell lines [200, 201]. In human keratinocytes, it has been shown to reduce H_2O_2-induced production of ROS [202]. It also has proven preventive antioxidant therapeutic effects in multiple animal injury models [203–205]. In chickens, resveratrol induces redox balance via heat shock protein regulation in immuno-competent tissues [206]. In clinical studies, oral supplementation in adult smokers significantly decreased acute phase markers and triglycerides but did not alter chronic disease markers, weight, and blood pressure [207]. Topical application of resveratrol and vitamin E increased skin pigmentation and elasticity by altering heme oxygenase 1 and other collagen-specific targeting genes [208]. Orally administered resveratrol reduced cardiovascular disease risk in hypercholesterolemia patients and also increased serum vitamin E levels [209]. Apostolidou et al. [209] highlight the synergistic properties of resveratrol and vitamin E in decreasing cardiovascular disease risk. This illustrates the great potential that flavonoids, specifically resveratrol, might have as a joint therapy with other antioxidant molecules.

5.4. Thiol Molecules

5.4.1. Glutathione. Glutathione (GSH) is a nonprotein, tripeptide thiol and one of the most abundant antioxidants in the body. In its reduced form, GSH is integral for cellular metabolism and maintaining cellular redox homeostasis. Work done by Mischley et al. [210] suggested that intranasal delivery may be able to augment GSH levels within the nervous system of patients with Parkinson's disease. In a follow-up phase II trial, however, there was no significant improvement in motor function from intranasal GSH delivery compared to the placebo [211]. In 2015, Schmitt et al. [212] showed that sublingual GSH was absorbed more effectively than oral supplementation by bypassing hepatic metabolism, potentially revealing a compelling new delivery approach. Several clinical trials assessing the benefit of oral GSH delivery are currently underway for growth improvement in children with cystic fibrosis (NCT03020719) and overall health of adults with a history of malnutrition (NCT03166371). Future work will dictate whether the therapeutic benefits of GSH can be through isolated administration or will continue to rely on intracellular upregulation by exogenous agents.

5.4.2. N-Acetylcysteine. N-acetylcysteine (NAC) is a prodrug thiol and precursor for cysteine and GSH. NAC treatment has been promising in *in vitro* [213] and *in vivo* [214] models but has fallen short in clinical trials similarly to most other antioxidants. NAC was ineffective in randomized clinical studies of arterial disease [215] and in attenuating nephrotoxicity [216]. Kazemi et al. [217] found no association from a high dose of prophylactic NAC given orally before and after surgery in preventing postoperative atrial fibrillation. A clinical trial evaluating NAC administered with amiodarone, which helps regulate heart rhythm, in preventing atrial fibrillation after thoracic surgery is currently in phase III (NCT02750319). Synergic NAC administration has been promising in treating infection [218] and reflux disease [219]. Trials using NAC with L-carnitine for polycystic ovary syndrome (NCT03164421) and with the drug minocycline for the treatment of bipolar depression (NCT02719392) are currently underway. As of 2017, there are over 70 other ongoing clinical trials using NAC as a sole therapeutic or together with other antioxidant molecules or drugs which will broaden our understanding of this unique prodrug.

5.5. Other Scavenging Molecules

5.5.1. Coenzyme Q10 and MitoQ10. Coenzyme Q10 (CoQ10) is a lipid-soluble ubiquinol antioxidant with high functionality in the Golgi apparatus and endoplasmic reticulum [220]. CoQ10 has been shown to reduce oxidative stress by modulating UBIAD1 and eNOS enzymatic activity in cardiovascular tissues [221]. A research group from Linköping University in Sweden has published multiple papers using oral administration of CoQ10 in clinical studies. The results show a direct effect on serum selenium levels which corresponds with decreased cardiovascular mortality rate in elderly patients [222]. CoQ10 in joint administration with selenium modified over 100 different microRNA expression levels in healthy elderly patients [223]. Lastly, the joint administration with selenium for 4 years increased insulin-like growth factor-1, which has implications of anti-inflammatory and antioxidative effects, further explaining the observed reduction in cardiovascular mortality in these trials [224]. Yet, a 300 mg oral dose of CoQ10 12 hours postprocedure did not reduce periprocedural myocardial injury in patients with elective percutaneous coronary interventions but did decrease C-reactive protein [225]. MitoQ10 is a 3rd generation derivate of CoQ10 that has an added positive charge with direct targeting for the mitochondria. Even though this approach does not target a specific organ or tissue, it directs the redox intervention to a specific organelle. MitoQ10 administered in drinking water jointly with Losartan prevented hypertensive disease and consequent rat myocardial hypertrophy [226]. In a clinical trial, orally administered MitoQ10 showed no therapeutic benefit as a Parkinson's disease-modifying therapy [227]. MitoQ10 is currently in clinical trials for improving physiological function of middle-aged and older adults (NCT02597023), attenuating chronic kidney disease (NCT02364648), and reducing fatigue experienced by patients with multiple sclerosis

(NCT03166800). The benefits of these two therapeutics appear yet to come, especially for MitoQ10 as it advances into promising clinical trials.

5.5.2. Ebselen. Ebselen is a synthetic selenoorganic molecule with antioxidant, anti-inflammatory, antimicrobial, and antifungal properties. This molecule is capable of catalytically scavenging hydrogen peroxide and organic hydroperoxides, at the expense of cellular thiols, thus mimicking glutathione peroxidase [228]. Additionally, ebselen can react with $ONOO^-$ ($k = 10^6\,M^{-1}\,s^{-1}$) providing another possible mechanism of redox modulation [229]. Moreover, the ability of ebselen to react with cellular thiols makes ebselen a weak electrophile capable of activating Nrf2 [230]. SPI-1005 is an oral formulation of ebselen developed by Sound Pharmaceuticals Inc. that has undergone phase I trials for hearing loss (NCT01452607) and Meniere's disease (NCT02603081) and phase II trials for preventing noise-induced temporary auditory threshold shifts (NCT01444846) [231]. Currently, ebselen is in phase II trials to prevent ototoxicity (NCT02819856), as well as noise-induced (NCT02779192) and chemotherapy-induced (NCT01451853) hearing loss. Preclinical evidence suggested that ebselen improves insulin secretion and pancreatic islet viability in murine models of diabetes [232, 233]; however, ebselen failed to improve glycemia and vascular function in a small clinical trial with diabetic patients [234]. Importantly, this trial measured redox markers and showed that the ebselen dose and regimen used did not reduce any systemic markers of oxidative stress, suggesting that redox regulation was not achieved. The failure of this trial should not be taken to imply that redox imbalance is not at the core of the disease. Rather, as the redox state was not altered, this suggests that a wrong dose, improper administration route, or perhaps even the wrong redox-active molecule was used. Ongoing work with different formulations of selenoorganic molecules [235] may yield new and interesting therapeutics.

5.5.3. Edaravone. Edaravone is a synthetic reactive species scavenging antioxidant previously named MCI-186. Edaravone has been reported to specifically quench hydroxyl radicals, thus preventing lipid peroxidation, and has been used for the treatment of ischemia-reperfusion injury in Japan for more than a decade [236]. Edaravone was rebranded as Radicava in 2017 after its approval by the U.S. Food and Drug Administration (FDA) for the treatment of amyotrophic lateral sclerosis (ALS) [237], a rare neurodegenerative disease that effects voluntary muscle movement. This designation was made after the conclusion of the final phase III trial in October of 2017 (NCT01492686). Radicava treatment significantly reduced the rate of disability progression experienced by patients with ALS. The FDA approval of an antioxidant molecule shows promise that identifying the proper disease and patient population for a given molecule can result in a successful drug campaign and, more importantly, in an effective redox-based therapy.

6. Conclusion

A causal relationship linking redox dysfunction with disease would predict successful translation to the clinic of therapies aimed at restoring redox homeostasis. However, the complexity of cellular redox reactions continues to thwart the utility of antioxidants as effective therapeutics in disease prevention and treatment. The first trials aimed at restoring redox homeostasis utilized antioxidants for their direct scavenging and redox cycling properties but were largely unsuccessful. Current evidence suggests that using molecules to upregulate endogenous antioxidant enzyme expression can have useful therapeutic benefits. Likewise, inhibition of ROS/RNS producing enzymes or inhibiting pathways that promote excess ROS/RNS generation could ultimately yield a greater efficacy than attempting to scavenge these species directly. Early failures of redox-active molecules in clinical trials may reflect the wrong choice of therapeutic, the wrong dose, or wrong selection of a patient population that would benefit the most from the intervention. Not accounting for these possibilities might lead to the conclusion that redox dysfunction is not part of the disease etiology. Importantly, few studies actually assess the effect of the redox intervention on redox biomarkers. If an antioxidant fails to improve primary outcomes, it is important to know if it actually affects redox markers. If the intervention does not improve redox status, then it is likely that the selection of drug, dose, or route of administration was not ideal. This issue does not have a clear solution since there is not a consensus as to what biomarkers to use when assessing redox function *in vivo*. Having some evidence that the tested drug actually improves redox homeostasis, however, allows for the identification of a subset of patients that are more likely to benefit from the redox intervention. For example, the use of tirapazamine, a reductively activated drug to potentiate chemotherapy in patients with squamous cell carcinoma, showed a promising significant effect in patients with hypoxic tumors [238]. However, in a large phase III trial without selection for hypoxia, addition of tirapazamine to chemoradiotherapy showed no improvement in outcomes [239]. This highlights the need to identify the patient population that is most likely to benefit from the intervention. Failure to identify this subpopulation could dilute the patient pool potentially masking beneficial effects. Similarly, the example shows the importance of measuring the specific conditions related to the expected mechanism of action. Current studies address several of these issues. Importantly, many successful clinical trials have exploited local delivery or a targeted effect to specific cells. The realization that local and targeted drug delivery could directly address the problem of systemic effect of redox therapies opens a new and exciting avenue for translational redox research. As the drug delivery field develops new and better ways to precisely target therapeutic payloads to tissue sites, we can specifically address local redox dysfunction.

Conflicts of Interest

The authors declare that there are no conflicts of interest regarding the publication of this review.

References

[1] D. P. Jones, "Redefining oxidative stress," *Antioxidants & Redox Signaling*, vol. 8, no. 9-10, pp. 1865–1879, 2006.

[2] B. Halliwell, "Free radicals, proteins and DNA: oxidative damage versus redox regulation," *Biochemical Society Transactions*, vol. 24, no. 4, pp. 1023–1027, 1996.

[3] S. P. Faux, T. Tai, D. Thorne, Y. Xu, D. Breheny, and M. Gaca, "The role of oxidative stress in the biological responses of lung epithelial cells to cigarette smoke," *Biomarkers*, vol. 14, Supplement 1, pp. 90–96, 2009.

[4] N. Li, M. Hao, R. F. Phalen, W. C. Hinds, and A. E. Nel, "Particulate air pollutants and asthma. A paradigm for the role of oxidative stress in PM-induced adverse health effects," *Clinical Immunology*, vol. 109, no. 3, pp. 250–265, 2003.

[5] R. M. Babadjouni, D. M. Hodis, R. Radwanski et al., "Clinical effects of air pollution on the central nervous system; a review," *Journal of Clinical Neuroscience*, vol. 43, pp. 16–24, 2017.

[6] J. D'Orazio, S. Jarrett, A. Amaro-Ortiz, and T. Scott, "UV radiation and the skin," *International Journal of Molecular Sciences*, vol. 14, no. 6, pp. 12222–12248, 2013.

[7] V. M. Costa, F. Carvalho, J. A. Duarte, L. Bastos Mde, and F. Remiao, "The heart as a target for xenobiotic toxicity: the cardiac susceptibility to oxidative stress," *Chemical Research in Toxicology*, vol. 26, no. 9, pp. 1285–1311, 2013.

[8] M. Galicia-Moreno and G. Gutierrez-Reyes, "The role of oxidative stress in the development of alcoholic liver disease," *Revista de Gastroenterología de México*, vol. 79, no. 2, pp. 135–144, 2014.

[9] A. Barzilai and K. Yamamoto, "DNA damage responses to oxidative stress," *DNA Repair*, vol. 3, no. 8-9, pp. 1109–1115, 2004.

[10] A. Ayala, M. F. Munoz, and S. Arguelles, "Lipid peroxidation: production, metabolism, and signaling mechanisms of malondialdehyde and 4-hydroxy-2-nonenal," *Oxidative Medicine and Cellular Longevity*, vol. 2014, Article ID 360438, 31 pages, 2014.

[11] H. M. Stringfellow, M. R. Jones, M. C. Green, A. K. Wilson, and J. S. Francisco, "Selectivity in ROS-induced peptide backbone bond cleavage," *The Journal of Physical Chemistry A*, vol. 118, no. 48, pp. 11399–11404, 2014.

[12] V. Cecarini, J. Gee, E. Fioretti et al., "Protein oxidation and cellular homeostasis: emphasis on metabolism," *Biochimica et Biophysica Acta (BBA) - Molecular Cell Research*, vol. 1773, no. 2, pp. 93–104, 2007.

[13] B. Uttara, A. V. Singh, P. Zamboni, and R. T. Mahajan, "Oxidative stress and neurodegenerative diseases: a review of upstream and downstream antioxidant therapeutic options," *Current Neuropharmacology*, vol. 7, no. 1, pp. 65–74, 2009.

[14] H. N. Siti, Y. Kamisah, and J. Kamsiah, "The role of oxidative stress, antioxidants and vascular inflammation in cardiovascular disease (a review)," *Vascular Pharmacology*, vol. 71, pp. 40–56, 2015.

[15] M. Nishikimi, R. Fukuyama, S. Minoshima, N. Shimizu, and K. Yagi, "Cloning and chromosomal mapping of the human nonfunctional gene for L-gulono-gamma-lactone oxidase, the enzyme for L-ascorbic acid biosynthesis missing in man," *The Journal of Biological Chemistry*, vol. 269, no. 18, pp. 13685–13688, 1994.

[16] R. Figueroa-Mendez and S. Rivas-Arancibia, "Vitamin C in health and disease: its role in the metabolism of cells and redox state in the brain," *Frontiers in Physiology*, vol. 6, p. 397, 2015.

[17] M. G. Traber and J. F. Stevens, "Vitamins C and E: beneficial effects from a mechanistic perspective," *Free Radical Biology & Medicine*, vol. 51, no. 5, pp. 1000–1013, 2011.

[18] J. D. Schoenfeld, Z. A. Sibenaller, K. A. Mapuskar et al., "O2$^-$ and H2O2$^-$mediated disruption of Fe metabolism causes the differential susceptibility of NSCLC and GBM cancer cells to pharmacological ascorbate," *Cancer Cell*, vol. 31, no. 4, pp. 487–500.e8, 2017.

[19] D. J. Lane, S. Chikhani, V. Richardson, and D. R. Richardson, "Transferrin iron uptake is stimulated by ascorbate via an intracellular reductive mechanism," *Biochimica et Biophysica Acta (BBA) - Molecular Cell Research*, vol. 1833, no. 6, pp. 1527–1541, 2013.

[20] J. Du, S. M. Martin, M. Levine et al., "Mechanisms of ascorbate-induced cytotoxicity in pancreatic cancer," *Clinical Cancer Research*, vol. 16, no. 2, pp. 509–520, 2010.

[21] S. J. Padayatty, H. Sun, Y. Wang et al., "Vitamin C pharmacokinetics: implications for oral and intravenous use," *Annals of Internal Medicine*, vol. 140, no. 7, pp. 533–537, 2004.

[22] J. Verrax and P. B. Calderon, "Pharmacologic concentrations of ascorbate are achieved by parenteral administration and exhibit antitumoral effects," *Free Radical Biology & Medicine*, vol. 47, no. 1, pp. 32–40, 2009.

[23] J. L. Welsh, B. A. Wagner, T. J. van't Erve et al., "Pharmacological ascorbate with gemcitabine for the control of metastatic and node-positive pancreatic cancer (PACMAN): results from a phase I clinical trial," *Cancer Chemotherapy and Pharmacology*, vol. 71, no. 3, pp. 765–775, 2013.

[24] M. G. Traber and J. Atkinson, "Vitamin E, antioxidant and nothing more," *Free Radical Biology & Medicine*, vol. 43, no. 1, pp. 4–15, 2007.

[25] D. Li, S. Devaraj, C. Fuller, R. Bucala, and I. Jialal, "Effect of alpha-tocopherol on LDL oxidation and glycation: in vitro and in vivo studies," *Journal of Lipid Research*, vol. 37, no. 9, pp. 1978–1986, 1996.

[26] P. Bozaykut, B. Karademir, B. Yazgan et al., "Effects of vitamin E on peroxisome proliferator-activated receptor γ and nuclear factor-erythroid 2-related factor 2 in hypercholesterolemia-induced atherosclerosis," *Free Radical Biology & Medicine*, vol. 70, pp. 174–181, 2014.

[27] F. Tang, M. Lu, S. Zhang et al., "Vitamin E conditionally inhibits atherosclerosis in ApoE knockout mice by anti-

[28] C. Suarna, B. J. Wu, K. Choy et al., "Protective effect of vitamin E supplements on experimental atherosclerosis is modest and depends on preexisting vitamin E deficiency," *Free Radical Biology & Medicine*, vol. 41, no. 5, pp. 722–730, 2006.

[29] K. Itoh, T. Chiba, S. Takahashi et al., "An Nrf2/small Maf heterodimer mediates the induction of phase II detoxifying enzyme genes through antioxidant response elements," *Biochemical and Biophysical Research Communications*, vol. 236, no. 2, pp. 313–322, 1997.

[30] J. D. Hayes, J. U. Flanagan, and I. R. Jowsey, "Glutathione transferases," *Annual Review of Pharmacology and Toxicology*, vol. 45, no. 1, pp. 51–88, 2005.

[31] I. Bellezza, A. Tucci, F. Galli et al., "Inhibition of NF-κB nuclear translocation via HO-1 activation underlies alpha-tocopheryl succinate toxicity," *The Journal of Nutritional Biochemistry*, vol. 23, no. 12, pp. 1583–1591, 2012.

[32] Z. Feng, Z. Liu, X. Li et al., "α-Tocopherol is an effective phase II enzyme inducer: protective effects on acrolein-induced oxidative stress and mitochondrial dysfunction in human retinal pigment epithelial cells," *The Journal of Nutritional Biochemistry*, vol. 21, no. 12, pp. 1222–1231, 2010.

[33] R. Dworski, W. Han, T. S. Blackwell, A. Hoskins, and M. L. Freeman, "Vitamin E prevents NRF2 suppression by allergens in asthmatic alveolar macrophages in vivo," *Free Radical Biology & Medicine*, vol. 51, no. 2, pp. 516–521, 2011.

[34] J. H. Pan, L. Feng, W. D. Jiang et al., "Vitamin E deficiency depressed fish growth, disease resistance, and the immunity and structural integrity of immune organs in grass carp (Ctenopharyngodon idella): Referring to NF-κB, TOR and Nrf2 signaling," *Fish & Shellfish Immunology*, vol. 60, pp. 219–236, 2017.

[35] M. Fidaleo, F. Fanelli, M. P. Ceru, and S. Moreno, "Neuroprotective properties of peroxisome proliferator-activated receptor alpha (PPARα) and its lipid ligands," *Current Medicinal Chemistry*, vol. 21, no. 24, pp. 2803–2821, 2014.

[36] S. P. Lakshmi, A. T. Reddy, A. Banno, and R. C. Reddy, "PPAR agonists for the prevention and treatment of lung cancer," *PPAR Research*, vol. 2017, Article ID 8252796, 8 pages, 2017.

[37] M. Chandra, S. Miriyala, and M. Panchatcharam, "PPARγ and its role in cardiovascular diseases," *PPAR Research*, vol. 2017, Article ID 6404638, 10 pages, 2017.

[38] N. G. Stephens, A. Parsons, P. M. Schofield, F. Kelly, K. Cheeseman, and M. J. Mitchinson, "Randomised controlled trial of vitamin E in patients with coronary disease: Cambridge Heart Antioxidant Study (CHAOS)," *The Lancet*, vol. 347, no. 9004, pp. 781–786, 1996.

[39] Heart outcomes prevention evaluation study investigators, S. Yusuf, G. Dagenais, J. Pogue, J. Bosch, and P. Sleight, "Vitamin E supplementation and cardiovascular events in high-risk patients," *The New England Journal of Medicine*, vol. 342, no. 3, pp. 154–160, 2000.

[40] L. J. Roberts 2nd, J. A. Oates, M. F. Linton et al., "The relationship between dose of vitamin E and suppression of oxidative stress in humans," *Free Radical Biology & Medicine*, vol. 43, no. 10, pp. 1388–1393, 2007.

[41] U. Milman, S. Blum, C. Shapira et al., "Vitamin E supplementation reduces cardiovascular events in a subgroup of middle-

aged individuals with both type 2 diabetes mellitus and the haptoglobin 2-2 genotype: a prospective double-blinded clinical trial," *Arteriosclerosis, Thrombosis, and Vascular Biology*, vol. 28, no. 2, pp. 341–347, 2008.

[42] I. P. Chatziralli, G. Theodossiadis, P. Dimitriadis et al., "The effect of vitamin E on oxidative stress indicated by serum malondialdehyde in insulin-dependent type 2 diabetes mellitus patients with retinopathy," *The Open Ophthalmology Journal*, vol. 11, no. 1, pp. 51–58, 2017.

[43] M. Rafraf, B. Bazyun, M. A. Sarabchian, A. Safaeiyan, B. P. Gargari, and E. Vitamin, "Improves serum paraoxonase-1 activity and some metabolic factors in patients with type 2 diabetes: no effects on nitrite/nitrate levels," *Journal of the American College of Nutrition*, vol. 35, no. 6, pp. 521–528, 2016.

[44] A. Ahmadi, N. Mazooji, J. Roozbeh, Z. Mazloom, and J. Hasanzade, "Effect of alpha-lipoic acid and vitamin E supplementation on oxidative stress, inflammation, and malnutrition in hemodialysis patients," *Iranian Journal of Kidney Diseases*, vol. 7, no. 6, pp. 461–467, 2013.

[45] E. B. Parisotto, T. R. Garlet, V. L. L. O. Cavalli et al., "Antioxidant intervention attenuates oxidative stress in children and teenagers with down syndrome," *Research in Developmental Disabilities*, vol. 35, no. 6, pp. 1228–1236, 2014.

[46] M. W. Dysken, M. Sano, S. Asthana et al., "Effect of vitamin E and memantine on functional decline in Alzheimer disease: the TEAM-AD VA cooperative randomized trial," *JAMA*, vol. 311, no. 1, pp. 33–44, 2014.

[47] D. Alias, J. Ruiz-Tovar, A. Moreno et al., "Effect of subcutaneous sterile vitamin E ointment on incisional surgical site infection after elective laparoscopic colorectal cancer surgery," *Surgical Infections*, vol. 18, no. 3, pp. 287–292, 2017.

[48] F. A. Moura, K. Q. de Andrade, J. C. Dos Santos, and M. O. Goulart, "Lipoic acid: its antioxidant and anti-inflammatory role and clinical applications," *Current Topics in Medicinal Chemistry*, vol. 15, no. 5, pp. 458–483, 2015.

[49] B. C. Scott, O. I. Aruoma, P. J. Evans et al., "Lipoic and dihydrolipoic acids as antioxidants. A critical evaluation," *Free Radical Research*, vol. 20, no. 2, pp. 119–133, 2009.

[50] L. Packer, E. H. Witt, and H. J. Tritschler, "Alpha-lipoic acid as a biological antioxidant," *Free Radical Biology & Medicine*, vol. 19, no. 2, pp. 227–250, 1995.

[51] R. C. Eason, H. E. Archer, S. Akhtar, and C. J. Bailey, "Lipoic acid increases glucose uptake by skeletal muscles of obese-diabetic ob/ob mice," *Diabetes, Obesity & Metabolism*, vol. 4, no. 1, pp. 29–35, 2002.

[52] A. Goraca, H. Huk-Kolega, P. Kleniewska, A. Piechota-Polanczyk, and B. Skibska, "Effects of lipoic acid on spleen oxidative stress after LPS administration," *Pharmacological Reports*, vol. 65, no. 1, pp. 179–186, 2013.

[53] M. C. Cimolai, V. Vanasco, T. Marchini, N. D. Magnani, P. Evelson, and S. Alvarez, "α-Lipoic acid protects kidney from oxidative stress and mitochondrial dysfunction associated to inflammatory conditions," *Food & Function*, vol. 5, no. 12, pp. 3143–3150, 2014.

[54] F. Mignini, C. Nasuti, D. Fedeli et al., "Protective effect of alpha-lipoic acid on cypermethrin-induced oxidative stress in Wistar rats," *International Journal of Immunopathology and Pharmacology*, vol. 26, no. 4, pp. 871–881, 2013.

[55] T. B. Moraes, C. E. D. Jacques, A. P. Rosa et al., "Role of catalase and superoxide dismutase activities on oxidative stress in the brain of a phenylketonuria animal model and the effect of lipoic acid," *Cellular and Molecular Neurobiology*, vol. 33, no. 2, pp. 253–260, 2013.

[56] Z. Ying, N. Kherada, B. Farrar et al., "Lipoic acid effects on established atherosclerosis," *Life Sciences*, vol. 86, no. 3-4, pp. 95–102, 2010.

[57] Y. Nakashima, E. W. Raines, A. S. Plump, J. L. Breslow, and R. Ross, "Upregulation of VCAM-1 and ICAM-1 at atherosclerosis-prone sites on the endothelium in the ApoE-deficient mouse," *Arteriosclerosis, Thrombosis, and Vascular Biology*, vol. 18, no. 5, pp. 842–851, 1998.

[58] K. Brand, S. Page, G. Rogler et al., "Activated transcription factor nuclear factor-kappa B is present in the atherosclerotic lesion," *Journal of Clinical Investigation*, vol. 97, no. 7, pp. 1715–1722, 1996.

[59] W. R. Lee, A. Kim, K. S. Kim et al., "Alpha-lipoic acid attenuates atherosclerotic lesions and inhibits proliferation of vascular smooth muscle cells through targeting of the Ras/MEK/ERK signaling pathway," *Molecular Biology Reports*, vol. 39, no. 6, pp. 6857–6866, 2012.

[60] D. Ziegler, C. G. Sohr, and J. Nourooz-Zadeh, "Oxidative stress and antioxidant defense in relation to the severity of diabetic polyneuropathy and cardiovascular autonomic neuropathy," *Diabetes Care*, vol. 27, no. 9, pp. 2178–2183, 2004.

[61] D. Ziegler, A. Ametov, A. Barinov et al., "Oral treatment with alpha-lipoic acid improves symptomatic diabetic polyneuropathy: the SYDNEY 2 trial," *Diabetes Care*, vol. 29, no. 11, pp. 2365–2370, 2006.

[62] H. Garcia-Alcala, C. I. Santos Vichido, S. Islas Macedo et al., "Treatment with α-lipoic acid over 16 weeks in type 2 diabetic patients with symptomatic polyneuropathy who responded to initial 4-week high-dose loading," *Journal of Diabetes Research*, vol. 2015, Article ID 189857, 8 pages, 2015.

[63] D. Ziegler, P. A. Low, W. J. Litchy et al., "Efficacy and safety of antioxidant treatment with α-lipoic acid over 4 years in diabetic polyneuropathy: the NATHAN 1 trial," *Diabetes Care*, vol. 34, no. 9, pp. 2054–2060, 2011.

[64] L. Turner-Stokes, A. Thu, H. Williams, R. Casey, H. Rose, and R. J. Siegert, "The neurological impairment scale: reliability and validity as a predictor of functional outcome in neurorehabilitation," *Disability and Rehabilitation*, vol. 36, no. 1, pp. 23–31, 2014.

[65] N. Papanas and D. Ziegler, "Efficacy of α-lipoic acid in diabetic neuropathy," *Expert Opinion on Pharmacotherapy*, vol. 15, no. 18, pp. 2721–2731, 2014.

[66] H. H. Conaway, P. Henning, and U. H. Lerner, "Vitamin a metabolism, action, and role in skeletal homeostasis," *Endocrine Reviews*, vol. 34, no. 6, pp. 766–797, 2013.

[67] Z. Al Tanoury, A. Piskunov, and C. Rochette-Egly, "Vitamin A and retinoid signaling: genomic and nongenomic effects," *Journal of Lipid Research*, vol. 54, no. 7, pp. 1761–1775, 2013.

[68] C. C. Brown and R. J. Noelle, "Seeing through the dark: new insights into the immune regulatory functions of vitamin A," *European Journal of Immunology*, vol. 45, no. 5, pp. 1287–1295, 2015.

[69] P. Di Mascio, S. Kaiser, and H. Sies, "Lycopene as the most efficient biological carotenoid singlet oxygen quencher," *Archives of Biochemistry and Biophysics*, vol. 274, no. 2, pp. 532–538, 1989.

[70] L. Tesoriere, M. Ciaccio, A. Bongiorno, A. Riccio, A. M. Pintaudi, and M. A. Livrea, "Antioxidant activity of all-trans-retinol in homogeneous solution and in phosphatidyl-choline liposomes," *Archives of Biochemistry and Biophysics*, vol. 307, no. 1, pp. 217–223, 1993.

[71] R. Hubbard and G. Wald, "Cis-trans isomers of vitamin a and retinene in the rhodopsin system," *The Journal of General Physiology*, vol. 36, no. 2, pp. 269–315, 1952.

[72] M. E. Darvin, J. W. Fluhr, M. C. Meinke, L. Zastrow, W. Sterry, and J. Lademann, "Topical beta-carotene protects against infra-red-light-induced free radicals," *Experimental Dermatology*, vol. 20, no. 2, pp. 125–129, 2011.

[73] U. Heinrich, C. Gärtner, M. Wiebusch et al., "Supplementation with beta-carotene or a similar amount of mixed carotenoids protects humans from UV-induced erythema," *The Journal of Nutrition*, vol. 133, no. 1, pp. 98–101, 2003.

[74] R. Kafi, H. S. Kwak, W. E. Schumacher et al., "Improvement of naturally aged skin with vitamin a (retinol)," *Archives of Dermatology*, vol. 143, no. 5, pp. 606–612, 2007.

[75] S. Kang and J. J. Voorhees, "Photoaging therapy with topical tretinoin: an evidence-based analysis," *Journal of the American Academy of Dermatology*, vol. 39, no. 2, Supplement 2, pp. S55–S61, 1998.

[76] H. E. Baldwin, M. Nighland, C. Kendall, D. A. Mays, R. Grossman, and J. Newburger, "40 years of topical tretinoin use in review," *Journal of Drugs in Dermatology*, vol. 12, no. 6, pp. 638–642, 2013.

[77] E. Bagatin, L. R. S. Guadanhim, M. M. S. S. Enokihara et al., "Low-dose oral isotretinoin versus topical retinoic acid for photoaging: a randomized, comparative study," *International Journal of Dermatology*, vol. 53, no. 1, pp. 114–122, 2014.

[78] L. Beckenbach, J. M. Baron, H. F. Merk, H. Loffler, and P. M. Amann, "Retinoid treatment of skin diseases," *European Journal of Dermatology*, vol. 25, no. 5, pp. 384–391, 2015.

[79] R. S. Dassanayake, D. E. Cabelli, and N. E. Brasch, "Pulse radiolysis studies on the reaction of the reduced vitamin B_{12} complex Cob(II)alamin with superoxide," *ChemBioChem*, vol. 14, no. 9, pp. 1081–1083, 2013.

[80] E. Suarez-Moreira, J. Yun, C. S. Birch, J. H. Williams, A. McCaddon, and N. E. Brasch, "Vitamin B_{12} and redox homeostasis: Cob(II)alamin reacts with superoxide at rates approaching superoxide dismutase (SOD)," *Journal of the American Chemical Society*, vol. 131, no. 42, pp. 15078-15079, 2009.

[81] M. A. Flynn, W. Irvin, and G. Krause, "The effect of folate and cobalamin on osteoarthritic hands," *Journal of the American College of Nutrition*, vol. 13, no. 4, pp. 351–356, 1994.

[82] J. Guest, A. Bilgin, B. Hokin, T. A. Mori, K. D. Croft, and R. Grant, "Novel relationships between B12, folate and markers of inflammation, oxidative stress and NAD(H) levels, systemically and in the CNS of a healthy human cohort," *Nutritional Neuroscience*, vol. 18, no. 8, pp. 355–364, 2015.

[83] E. S. Moreira, N. E. Brasch, and J. Yun, "Vitamin B_{12} protects against superoxide-induced cell injury in human aortic endothelial cells," *Free Radical Biology & Medicine*, vol. 51, no. 4, pp. 876–883, 2011.

[84] M. Y. Al-Maskari, M. I. Waly, A. Ali, Y. S. Al-Shuaibi, and A. Ouhtit, "Folate and vitamin B12 deficiency and hyperhomocysteinemia promote oxidative stress in adult type 2 diabetes," *Nutrition*, vol. 28, no. 7-8, pp. e23–e26, 2012.

[85] Y. J. Lee, M. Y. Wang, M. C. Lin, and P. T. Lin, "Associations between vitamin B-12 status and oxidative stress and inflammation in diabetic vegetarians and omnivores," *Nutrients*, vol. 8, no. 3, p. 118, 2016.

[86] U. Till, P. Röhl, A. Jentsch et al., "Decrease of carotid intima-media thickness in patients at risk to cerebral ischemia after supplementation with folic acid, vitamins B6 and B12," *Atherosclerosis*, vol. 181, no. 1, pp. 131–135, 2005.

[87] F. F. Willems, W. R. Aengevaeren, G. H. Boers, H. J. Blom, and F. W. Verheugt, "Coronary endothelial function in hyperhomocysteinemia: improvement after treatment with folic acid and cobalamin in patients with coronary artery disease," *Journal of the American College of Cardiology*, vol. 40, no. 4, pp. 766–772, 2002.

[88] O. Bleie, S. Elin, M. Ueland Per et al., "Coronary blood flow in patients with stable coronary artery disease treated long term with folic acid and vitamin B12," *Coronary Artery Disease*, vol. 22, no. 4, pp. 270–278, 2011.

[89] R. Kaji, M. Kodama, A. Imamura et al., "Effect of ultrahigh-dose methylcobalamin on compound muscle action potentials in amyotrophic lateral sclerosis: a double-blind controlled study," *Muscle & Nerve*, vol. 21, no. 12, pp. 1775–1778, 1998.

[90] A. Macri, C. Scanarotti, A. M. Bassi et al., "Evaluation of oxidative stress levels in the conjunctival epithelium of patients with or without dry eye, and dry eye patients treated with preservative-free hyaluronic acid 0.15% and vitamin B12 eye drops," *Graefe's Archive for Clinical and Experimental Ophthalmology*, vol. 253, no. 3, pp. 425–430, 2015.

[91] H. Sies, "Oxidative stress: a concept in redox biology and medicine," *Redox Biology*, vol. 4, pp. 180–183, 2015.

[92] J. D. Lambeth, "NOX enzymes and the biology of reactive oxygen," *Nature Reviews Immunology*, vol. 4, no. 3, pp. 181–189, 2004.

[93] L. L. Hilenski, R. E. Clempus, M. T. Quinn, J. D. Lambeth, and K. K. Griendling, "Distinct subcellular localizations of Nox1 and Nox4 in vascular smooth muscle cells," *Arteriosclerosis, Thrombosis, and Vascular Biology*, vol. 24, no. 4, pp. 677–683, 2004.

[94] B. Diaz, G. Shani, I. Pass, D. Anderson, M. Quintavalle, and S. A. Courtneidge, "Tks5-dependent, nox-mediated generation of reactive oxygen species is necessary for invadopodia formation," *Science Signaling*, vol. 2, no. 88, article ra53, 2009.

[95] K. Bedard and K. H. Krause, "The NOX family of ROS-generating NADPH oxidases: physiology and pathophysiology," *Physiological Reviews*, vol. 87, no. 1, pp. 245–313, 2007.

[96] J. Morry, W. Ngamcherdtrakul, and W. Yantasee, "Oxidative stress in cancer and fibrosis: opportunity for therapeutic intervention with antioxidant compounds, enzymes, and nanoparticles," *Redox Biology*, vol. 11, pp. 240–253, 2017.

[97] A. C. Little, A. Sulovari, K. Danyal, D. E. Heppner, D. J. Seward, and A. van der Vliet, "Paradoxical roles of dual oxidases in cancer biology," *Free Radical Biology & Medicine*, vol. 110, pp. 117–132, 2017.

[98] Z. Nayernia, V. Jaquet, and K. H. Krause, "New insights on NOX enzymes in the central nervous system," *Antioxidants & Redox Signaling*, vol. 20, no. 17, pp. 2815–2837, 2014.

[99] G. R. Drummond and C. G. Sobey, "Endothelial NADPH oxidases: which NOX to target in vascular disease?," *Trends in Endocrinology and Metabolism*, vol. 25, no. 9, pp. 452–463, 2014.

[100] C. E. Holterman, N. C. Read, and C. R. Kennedy, "Nox and renal disease," *Clinical Science*, vol. 128, no. 8, pp. 465–481, 2015.

[101] C. Kleinschnitz, H. Grund, K. Wingler et al., "Post-stroke inhibition of induced NADPH oxidase type 4 prevents oxidative stress and neurodegeneration," *PLoS Biology*, vol. 8, no. 9, article e1000479, 2010.

[102] J. C. Jha, S. P. Gray, D. Barit et al., "Genetic targeting or pharmacologic inhibition of NADPH oxidase nox4 provides renoprotection in long-term diabetic nephropathy," *Journal of the American Society of Nephrology*, vol. 25, no. 6, pp. 1237–1254, 2014.

[103] S. H. Choi, M. Kim, H. J. Lee, E. H. Kim, C. H. Kim, and Y. J. Lee, "Effects of NOX1 on fibroblastic changes of endothelial cells in radiation induced pulmonary fibrosis," *Molecular Medicine Reports*, vol. 13, no. 5, pp. 4135–4142, 2016.

[104] N. K. Somanna, A. J. Valente, M. Krenz, W. P. Fay, P. Delafontaine, and B. Chandrasekar, "The Nox1/4 dual inhibitor GKT137831 or Nox4 knockdown inhibits angiotensin-II-induced adult mouse cardiac fibroblast proliferation and migration. AT1 physically associates with Nox4," *Journal of Cellular Physiology*, vol. 231, no. 5, pp. 1130–1141, 2016.

[105] S. P. Gray, J. C. Jha, K. Kennedy et al., "Combined NOX1/4 inhibition with GKT137831 in mice provides dose-dependent reno- and atheroprotection even in established micro- and macrovascular disease," *Diabetologia*, vol. 60, no. 5, pp. 927–937, 2017.

[106] S. Altenhofer, K. A. Radermacher, P. W. Kleikers, K. Wingler, and H. H. Schmidt, "Evolution of NADPH oxidase inhibitors: selectivity and mechanisms for target engagement," *Antioxidants & Redox Signaling*, vol. 23, no. 5, pp. 406–427, 2015.

[107] N. Hecht, N. Terveer, C. Schollmayer, U. Holzgrabe, and L. Meinel, "Opening NADPH oxidase inhibitors for in vivo translation," *European Journal of Pharmaceutics and Biopharmaceutics*, vol. 115, pp. 206–217, 2017.

[108] U. Forstermann and W. C. Sessa, "Nitric oxide synthases: regulation and function," *European Heart Journal*, vol. 33, no. 7, pp. 829–837, 2012.

[109] A. Lopez, J. A. Lorente, J. Steingrub et al., "Multiple-center, randomized, placebo-controlled, double-blind study of the nitric oxide synthase inhibitor 546C88: effect on survival in patients with septic shock," *Critical Care Medicine*, vol. 32, no. 1, pp. 21–30, 2004.

[110] J. F. Stover, A. Belli, H. Boret et al., "Nitric oxide synthase inhibition with the antipterin VAS203 improves outcome in moderate and severe traumatic brain injury: a placebo-controlled randomized phase IIa trial (NOSTRA)," *Journal of Neurotrauma*, vol. 31, no. 19, pp. 1599–1606, 2014.

[111] K. Wada, K. Chatzipanteli, R. Busto, and W. D. Dietrich, "Role of nitric oxide in traumatic brain injury in the rat," *Journal of Neurosurgery*, vol. 89, no. 5, pp. 807–818, 1998.

[112] I. Batinic-Haberle, A. Tovmasyan, and I. Spasojevic, "An educational overview of the chemistry, biochemistry and therapeutic aspects of Mn porphyrins – from superoxide dismutation to H2O2-driven pathways," *Redox Biology*, vol. 5, pp. 43–65, 2015.

[113] L. Benov and I. Batinic-Haberle, "A manganese porphyrin suppresses oxidative stress and extends the life span of streptozotocin-diabetic rats," *Free Radical Research*, vol. 39, no. 1, pp. 81–88, 2005.

[114] D. K. Ali, M. Oriowo, A. Tovmasyan, I. Batinic-Haberle, and L. Benov, "Late administration of Mn porphyrin-based SOD mimic enhances diabetic complications," *Redox Biology*, vol. 1, no. 1, pp. 457–466, 2013.

[115] K. Cramer-Morales, C. D. Heer, K. A. Mapuskar, and F. E. Domann, "SOD2 targeted gene editing by CRISPR/Cas9 yields human cells devoid of MnSOD," *Free Radical Biology & Medicine*, vol. 89, pp. 379–386, 2015.

[116] K. A. Mapuskar, K. H. Flippo, J. D. Schoenfeld et al., "Mitochondrial superoxide increases age-associated susceptibility of human dermal fibroblasts to radiation and chemotherapy," *Cancer Research*, vol. 77, no. 18, pp. 5054–5067, 2017.

[117] Z. N. Rabbani, I. Batinic-Haberle, S. Poulton, M. S. Anscher, M. W. Dewhirst, and Z. Vujaskovic, "Long-term administration of a small molecular weight catalytic metalloporphyrin antioxidant, AEOL 10150, protects lungs from radiation-induced injury," *International Journal of Radiation Oncology Biology Physics*, vol. 63, no. 2, pp. S84–S580, 2005.

[118] T. J. MacVittie, A. Gibbs, A. M. Farese et al., "AEOL 10150 mitigates radiation-induced lung injury in the nonhuman primate: morbidity and mortality are administration schedule-dependent," *Radiation Research*, vol. 187, no. 3, pp. 298–318, 2017.

[119] V. H. Perry, M. D. Bell, H. C. Brown, and M. K. Matyszak, "Inflammation in the nervous system," *Current Opinion in Neurobiology*, vol. 5, no. 5, pp. 636–641, 1995.

[120] R. D. Brinton, "A women's health issue: Alzheimer's disease and strategies for maintaining cognitive health," *International Journal of Fertility and Women's Medicine*, vol. 44, no. 4, pp. 174–185, 1999.

[121] I. Gozes, "Neuroprotective peptide drug delivery and development: potential new therapeutics," *Trends in Neurosciences*, vol. 24, no. 12, pp. 700–705, 2001.

[122] R. A. Kroll and E. A. Neuwelt, "Outwitting the blood-brain barrier for therapeutic purposes: osmotic opening and other means," *Neurosurgery*, vol. 42, no. 5, pp. 1083–1099, 1998.

[123] V. E. Koliatsos, R. E. Clatterbuck, H. J. W. Nauta et al., "Human nerve growth factor prevents degeneration of basal forebrain cholinergic neurons in primates," *Annals of Neurology*, vol. 30, no. 6, pp. 831–840, 1991.

[124] D. Dogrukol-Ak, W. A. Banks, N. Tuncel, and M. Tuncel, "Passage of vasoactive intestinal peptide across the blood-brain barrier," *Peptides*, vol. 24, no. 3, pp. 437–444, 2003.

[125] A. Bachis and I. Mocchetti, "Brain-derived neurotrophic factor is neuroprotective against human immunodeficiency virus-1 envelope proteins," *Annals of the New York Academy of Sciences*, vol. 1053, no. 1, pp. 247–257, 2005.

[126] J. Ying Wang, F. Peruzzi, A. Lassak et al., "Neuroprotective effects of IGF-I against TNFα-induced neuronal damage in HIV-associated dementia," *Virology*, vol. 305, no. 1, pp. 66–76, 2003.

[127] R. J. Desnick and E. H. Schuchman, "Enzyme replacement and enhancement therapies: lessons from lysosomal disorders," *Nature Reviews Genetics*, vol. 3, no. 12, pp. 954–966, 2002.

[128] A. Urayama, J. H. Grubb, W. S. Sly, and W. A. Banks, "Developmentally regulated mannose 6-phosphate receptor-mediated transport of a lysosomal enzyme across the blood-brain barrier," *Proceedings of the National Academy of*

Sciences of the United States of America, vol. 101, no. 34, pp. 12658–12663, 2004.

[129] W. A. Banks and C. R. Lebel, "Strategies for the delivery of leptin to the CNS," *Journal of Drug Targeting*, vol. 10, no. 4, pp. 297–308, 2002.

[130] W. A. Banks, "Is obesity a disease of the blood-brain barrier? Physiological, pathological, and evolutionary considerations," *Current Pharmaceutical Design*, vol. 9, no. 10, pp. 801–809, 2003.

[131] P. L. McGeer, S. Itagaki, B. E. Boyes, and E. G. McGeer, "Reactive microglia are positive for HLA-DR in the substantia nigra of Parkinson's and Alzheimer's disease brains," *Neurology*, vol. 38, no. 8, pp. 1285–1291, 1988.

[132] J. Busciglio and B. A. Yankner, "Apoptosis and increased generation of reactive oxygen species in Down's syndrome neurons in vitro," *Nature*, vol. 378, no. 6559, pp. 776–779, 1995.

[133] M. Ebadi, S. K. Srinivasan, and M. D. Baxi, "Oxidative stress and antioxidant therapy in Parkinson's disease," *Progress in Neurobiology*, vol. 48, no. 1, pp. 1–19, 1996.

[134] D. C. Wu, P. Teismann, K. Tieu et al., "NADPH oxidase mediates oxidative stress in the 1-methyl-4-phenyl-1,2,3,6-tetrahydropyridine model of Parkinson's disease," *Proceedings of the National Academy of Sciences of the United States of America*, vol. 100, no. 10, pp. 6145–6150, 2003.

[135] K. N. Prasad, W. C. Cole, A. R. Hovland et al., "Multiple antioxidants in the prevention and treatment of neurodegenerative disease: analysis of biologic rationale," *Current Opinion in Neurology*, vol. 12, no. 6, pp. 761–770, 1999.

[136] R. A. Gonzalez-Polo, G. Soler, A. Rodriguezmartin, J. M. Moran, and J. M. Fuentes, "Protection against MPP+ neurotoxicity in cerebellar granule cells by antioxidants," *Cell Biology International*, vol. 28, no. 5, pp. 373–380, 2004.

[137] J. W. Langston and I. Irwin, "MPTP: current concepts and controversies," *Clinical Neuropharmacology*, vol. 9, no. 6, pp. 485–507, 1986.

[138] E. V. Batrakova, S. Li, A. D. Reynolds et al., "A macrophage-nanozyme delivery system for Parkinson's disease," *Bioconjugate Chemistry*, vol. 18, no. 5, pp. 1498–1506, 2007.

[139] A. M. Brynskikh, Y. Zhao, R. L. Mosley et al., "Macrophage delivery of therapeutic nanozymes in a murine model of Parkinson's disease," *Nanomedicine*, vol. 5, no. 3, pp. 379–396, 2010.

[140] Y. Zhao and M. J. . Haney, "Active targeted macrophage-mediated delivery of catalase to affected brain regions in models of parkinson's disease," *Journal of Nanomedicine & Nanotechnology*, vol. 01, no. S4, 2011.

[141] M. Fujiwara, J. D. Baldeschwieler, and R. H. Grubbs, "Receptor-mediated endocytosis of poly(acrylic acid)-conjugated liposomes by macrophages," *Biochimica et Biophysica Acta (BBA) - Biomembranes*, vol. 1278, no. 1, pp. 59–67, 1996.

[142] Y. Zhao, M. J. Haney, N. L. Klyachko et al., "Polyelectrolyte complex optimization for macrophage delivery of redox enzyme nanoparticles," *Nanomedicine*, vol. 6, no. 1, pp. 25–42, 2011.

[143] M. J. Haney, Y. Zhao, E. B. Harrison et al., "Specific transfection of inflamed brain by macrophages: a new therapeutic strategy for neurodegenerative diseases," *PLoS One*, vol. 8, no. 4, article e61852, 2013.

[144] N. L. Klyachko, M. J. Haney, Y. Zhao et al., "Macrophages offer a paradigm switch for CNS delivery of therapeutic proteins," *Nanomedicine*, vol. 9, no. 9, pp. 1403–1422, 2014.

[145] W. Hur and N. S. Gray, "Small molecule modulators of antioxidant response pathway," *Current Opinion in Chemical Biology*, vol. 15, no. 1, pp. 162–173, 2011.

[146] D. Sikazwe, A. Grillo, S. Ramsinghani, J. Davis, K. McQuiston, and S. Y. Ablordeppey, "Small diverse antioxidant functionalities for oxidative stress disease drug discovery," *Mini Reviews in Medicinal Chemistry*, vol. 12, no. 8, pp. 768–774, 2012.

[147] Y. Zhang, P. Talalay, C. G. Cho, and G. H. Posner, "A major inducer of anticarcinogenic protective enzymes from broccoli: isolation and elucidation of structure," *Proceedings of the National Academy of Sciences of the United States of America*, vol. 89, no. 6, pp. 2399–2403, 1992.

[148] R. K. Thimmulappa, K. H. Mai, S. Srisuma, T. W. Kensler, M. Yamamoto, and S. Biswal, "Identification of Nrf2-regulated genes induced by the chemopreventive agent sulforaphane by oligonucleotide microarray," *Cancer Research*, vol. 62, no. 18, pp. 5196–5203, 2002.

[149] K. Singh, S. L. Connors, E. A. Macklin et al., "Sulforaphane treatment of autism spectrum disorder (ASD)," *Proceedings of the National Academy of Sciences of the Unites States of America*, vol. 111, no. 43, pp. 15550–15555, 2014.

[150] A. S. Axelsson, E. Tubbs, B. Mecham et al., "Sulforaphane reduces hepatic glucose production and improves glucose control in patients with type 2 diabetes," *Science Translational Medicine*, vol. 9, no. 394, artcile eaah4477, 2017.

[151] N. G. Kounis, I. Koniari, A. Roumeliotis et al., "Thrombotic responses to coronary stents, bioresorbable scaffolds and the Kounis hypersensitivity-associated acute thrombotic syndrome," *Journal of Thoracic Disease*, vol. 9, no. 4, pp. 1155–1164, 2017.

[152] S. H. Yoo, Y. Lim, S. J. Kim et al., "Sulforaphane inhibits PDGF-induced proliferation of rat aortic vascular smooth muscle cell by up-regulation of p53 leading to G1/S cell cycle arrest," *Vascular Pharmacology*, vol. 59, no. 1-2, pp. 44–51, 2013.

[153] N. M. Shawky, P. Pichavaram, G. S. G. Shehatou et al., "Sulforaphane improves dysregulated metabolic profile and inhibits leptin-induced VSMC proliferation: implications toward suppression of neointima formation after arterial injury in western diet-fed obese mice," *The Journal of Nutritional Biochemistry*, vol. 32, pp. 73–84, 2016.

[154] N. M. Shawky and L. Segar, "Sulforaphane inhibits platelet-derived growth factor-induced vascular smooth muscle cell proliferation by targeting mTOR/p70S6kinase signaling independent of Nrf2 activation," *Pharmacological Research*, vol. 119, pp. 251–264, 2017.

[155] G. O. Gillard, B. Collette, J. Anderson et al., "DMF, but not other fumarates, inhibits NF-κB activity in vitro in an Nrf2-independent manner," *Journal of Neuroimmunology*, vol. 283, pp. 74–85, 2015.

[156] M. Kita, R. J. Fox, R. Gold et al., "Effects of delayed-release dimethyl fumarate (DMF) on health-related quality of life in patients with relapsing-remitting multiple sclerosis: an integrated analysis of the phase 3 DEFINE and CONFIRM studies," *Clinical Therapeutics*, vol. 36, no. 12, pp. 1958–1971, 2014.

[157] N. M. de Bruin, K. Schmitz, S. Schiffmann et al., "Multiple rodent models and behavioral measures reveal unexpected responses to FTY720 and DMF in experimental autoimmune encephalomyelitis," *Behavioural Brain Research*, vol. 300, pp. 160–174, 2016.

[158] B. A. Freeman, P. R. Baker, F. J. Schopfer, S. R. Woodcock, A. Napolitano, and M. d'Ischia, "Nitro-fatty acid formation and signaling," *Journal of Biological Chemistry*, vol. 283, no. 23, pp. 15515–15519, 2008.

[159] S. R. Salvatore, D. A. Vitturi, M. Fazzari, D. K. Jorkasky, and F. J. Schopfer, "Evaluation of 10-nitro oleic acid bioelimination in rats and humans," *Scientific Reports*, vol. 7, no. 7, article 39900, 2017.

[160] F. Hong, K. R. Sekhar, M. L. Freeman, and D. C. Liebler, "Specific patterns of electrophile adduction trigger Keap1 ubiquitination and Nrf2 activation," *Journal of Biological Chemistry*, vol. 280, no. 36, pp. 31768–31775, 2005.

[161] D. Lin, S. Saleh, and D. C. Liebler, "Reversibility of covalent electrophile-protein adducts and chemical toxicity," *Chemical Research in Toxicology*, vol. 21, no. 12, pp. 2361–2369, 2008.

[162] H. Dai, Q. Jiao, T. Liu, Q. You, and Z. Jiang, "Development of novel Nrf2/ARE inducers bearing Pyrazino[2,1-a]isoquinolin scaffold with potent in vitro efficacy and enhanced physicochemical properties," *Molecules*, vol. 22, no. 9, 2017.

[163] H. Tang, C. H. Zheng, J. Zhu, B. Y. Fu, Y. J. Zhou, and J. G. Lv, "Design and synthesis of novel pyrazino[2,1-a]isoquinolin derivatives with potent antifungal activity," *Archiv der Pharmazie*, vol. 343, no. 6, pp. 360–366, 2010.

[164] K. M. Vural and M. Bayazit, "Nitric oxide: implications for vascular and endovascular surgery," *European Journal of Vascular and Endovascular Surgery*, vol. 22, no. 4, pp. 285–293, 2001.

[165] F. Gebistorf, O. Karam, J. Wetterslev, and A. Afshari, "Inhaled nitric oxide for acute respiratory distress syndrome (ARDS) in children and adults," *Cochrane Database of Systematic Reviews*, no. 6, article CD002787, 2016.

[166] K. J. Barrington, N. Finer, T. Pennaforte, and G. Altit, "Nitric oxide for respiratory failure in infants born at or near term," *Cochrane Database of Systematic Reviews*, vol. 1, article CD000399, 2001.

[167] R. H. Clark, T. J. Kueser, M. W. Walker et al., "Low-dose nitric oxide therapy for persistent pulmonary hypertension of the newborn. Clinical inhaled nitric oxide research group," *The New England Journal of Medicine*, vol. 342, no. 7, pp. 469–474, 2000.

[168] O. I. Miller, S. F. Tang, A. Keech, N. B. Pigott, E. Beller, and D. S. Celermajer, "Inhaled nitric oxide and prevention of pulmonary hypertension after congenital heart surgery: a randomised double-blind study," *The Lancet*, vol. 356, no. 9240, pp. 1464–1469, 2000.

[169] P. M. Bath, K. Krishnan, and J. P. Appleton, "Nitric oxide donors (nitrates), L-arginine, or nitric oxide synthase inhibitors for acute stroke," *Cochrane Database of Systematic Reviews*, vol. 4, article CD000398, 2002.

[170] D. A. Popowich, V. Varu, and M. R. Kibbe, "Nitric oxide: what a vascular surgeon needs to know," *Vascular*, vol. 15, no. 6, pp. 324–335, 2007.

[171] J. M. Lablanche, G. Grollier, J. R. Lusson et al., "Effect of the direct nitric oxide donors linsidomine and molsidomine on angiographic restenosis after coronary balloon angioplasty. The ACCORD study angioplastic coronaire corvasal diltiazem," *Circulation*, vol. 95, no. 1, pp. 83–89, 1997.

[172] G. E. Havelka, E. S. Moreira, M. P. Rodriguez et al., "Nitric oxide delivery via a permeable balloon catheter inhibits neointimal growth after arterial injury," *The Journal of Surgical Research*, vol. 180, no. 1, pp. 35–42, 2013.

[173] E. S. Bahnson, H. A. Kassam, T. J. Moyer et al., "Targeted nitric oxide delivery by supramolecular nanofibers for the prevention of restenosis after arterial injury," *Antioxidants & Redox Signaling*, vol. 24, no. 8, pp. 401–418, 2016.

[174] M. Qin, A. Landriscina, J. M. Rosen et al., "Nitric oxide-releasing nanoparticles prevent propionibacterium acnes-induced Inflammation by both clearing the organism and inhibiting microbial stimulation of the innate immune response," *Journal of Investigative Dermatology*, vol. 135, no. 11, pp. 2723–2731, 2015.

[175] H. Baldwin, D. Blanco, C. McKeever et al., "Results of a phase 2 efficacy and safety study with SB204, an investigational topical nitric oxide-releasing drug for the treatment of acne vulgaris," *The Journal of Clinical and Aesthetic Dermatology*, vol. 9, no. 8, pp. 12–18, 2016.

[176] C. Ferri and D. Grassi, "Antioxidants and beneficial microvascular effects: is this the remedy?," *Hypertension*, vol. 55, no. 6, pp. 1310-1311, 2010.

[177] H. Sies, "Polyphenols and health: update and perspectives," *Archives of Biochemistry and Biophysics*, vol. 501, no. 1, pp. 2–5, 2010.

[178] S. Wang, C. Yang, H. Tu et al., "Characterization and metabolic diversity of flavonoids in citrus species," *Scientific Reports*, vol. 7, no. 1, article 10549, 2017.

[179] Y. Nolvachai and P. J. Marriott, "GC for flavonoids analysis: past, current, and prospective trends," *Journal of Separation Science*, vol. 36, no. 1, pp. 20–36, 2013.

[180] L. Wang, X. Chen, Z. Du et al., "Curcumin suppresses gastric tumor cell growth via ROS-mediated DNA polymerase γ depletion disrupting cellular bioenergetics," *Journal of Experimental & Clinical Cancer Research*, vol. 36, no. 1, p. 47, 2017.

[181] M. Funamoto, Y. Sunagawa, Y. Katanasaka et al., "Highly absorptive curcumin reduces serum atherosclerotic low-density lipoprotein levels in patients with mild COPD," *International Journal of Chronic Obstructive Pulmonary Disease*, vol. 11, pp. 2029–2034, 2016.

[182] Y. Panahi, N. Khalili, E. Sahebi et al., "Curcuminoids modify lipid profile in type 2 diabetes mellitus: a randomized controlled trial," *Complementary Therapies in Medicine*, vol. 33, pp. 1–5, 2017.

[183] Y. Panahi, M. S. Hosseini, N. Khalili, E. Naimi, M. Majeed, and A. Sahebkar, "Antioxidant and anti-inflammatory effects of curcuminoid-piperine combination in subjects with metabolic syndrome: a randomized controlled trial and an updated meta-analysis," *Clinical Nutrition*, vol. 34, no. 6, pp. 1101–1108, 2015.

[184] K. M. Nelson, J. L. Dahlin, J. Bisson, J. Graham, G. F. Pauli, and M. A. Walters, "The essential medicinal chemistry of curcumin," *Journal of Medicinal Chemistry*, vol. 60, no. 5, pp. 1620–1637, 2017.

[185] A. E. Krausz, B. L. Adler, V. Cabral et al., "Curcumin-encapsulated nanoparticles as innovative antimicrobial and wound

healing agent," *Nanomedicine: Nanotechnology, Biology and Medicine*, vol. 11, no. 1, pp. 195–206, 2015.

[186] I. Tinay, T. E. Sener, O. Cevik et al., "Antioxidant agent quercetin prevents impairment of bladder tissue contractility and apoptosis in a rat model of ischemia/reperfusion injury," *LUTS: Lower Urinary Tract Symptoms*, vol. 9, no. 2, pp. 117–123, 2017.

[187] L. Xiao, L. Liu, X. Guo et al., "Quercetin attenuates high fat diet-induced atherosclerosis in apolipoprotein E knockout mice: a critical role of NADPH oxidase," *Food and Chemical Toxicology*, vol. 105, pp. 22–33, 2017.

[188] K. M. Doersch and M. K. Newell-Rogers, "The impact of quercetin on wound healing relates to changes in αV and β1 integrin expression," *Experimental Biology and Medicine*, vol. 242, no. 14, pp. 1424–1431, 2017.

[189] A. I. Abd El-Fattah, M. M. Fathy, Z. Y. Ali, A. E. A. El-Garawany, and E. K. Mohamed, "Enhanced therapeutic benefit of quercetin-loaded phytosome nanoparticles in ovariectomized rats," *Chemico-Biological Interactions*, vol. 271, pp. 30–38, 2017.

[190] N. M. Al-Rasheed, L. Fadda, H. A. Attia, I. A. Sharaf, A. M. Mohamed, and N. M. Al-Rasheed, "Pulmonary prophylactic impact of melatonin and/or quercetin: a novel therapy for inflammatory hypoxic stress in rats," *Acta Pharmaceutica*, vol. 67, no. 1, pp. 125–135, 2017.

[191] J. Terao, "Factors modulating bioavailability of quercetin-related flavonoids and the consequences of their vascular function," *Biochemical Pharmacology*, vol. 139, pp. 15–23, 2017.

[192] C. Burak, S. Wolffram, B. Zur et al., "Effects of the flavonol quercetin and α-linolenic acid on n-3 PUFA status in metabolically healthy men and women: a randomised, double-blinded, placebo-controlled, crossover trial," *The British Journal of Nutrition*, vol. 117, no. 05, pp. 698–711, 2017.

[193] N. P. Bondonno, C. P. Bondonno, L. Rich et al., "Acute effects of quercetin-3-O-glucoside on endothelial function and blood pressure: a randomized dose-response study," *The American Journal of Clinical Nutrition*, vol. 104, no. 1, pp. 97–103, 2016.

[194] Y. Kashino, K. Murota, N. Matsuda et al., "Effect of processed onions on the plasma concentration of quercetin in rats and humans," *Journal of Food Science*, vol. 80, no. 11, pp. H2597–H2602, 2015.

[195] C. Burak, V. Brüll, P. Langguth et al., "Higher plasma quercetin levels following oral administration of an onion skin extract compared with pure quercetin dihydrate in humans," *European Journal of Nutrition*, vol. 56, no. 1, pp. 343–353, 2017.

[196] M. Torella, F. del Deo, A. Grimaldi et al., "Efficacy of an orally administered combination of hyaluronic acid, chondroitin sulfate, curcumin and quercetin for the prevention of recurrent urinary tract infections in postmenopausal women," *European Journal of Obstetrics, Gynecology, and Reproductive Biology*, vol. 207, pp. 125–128, 2016.

[197] F. J. Alcain and J. M. Villalba, "Sirtuin activators," *Expert Opinion on Therapeutic Patents*, vol. 19, no. 4, pp. 403–414, 2009.

[198] S. Li, G. Zhao, L. Chen et al., "Resveratrol protects mice from paraquat-induced lung injury: the important role of SIRT1 and NRF2 antioxidant pathways," *Molecular Medicine Reports*, vol. 13, no. 2, pp. 1833–1838, 2016.

[199] Y. Tian, J. Ma, W. Wang et al., "Resveratrol supplement inhibited the NF-κB inflammation pathway through activating AMPKα-SIRT1 pathway in mice with fatty liver," *Molecular and Cellular Biochemistry*, vol. 422, no. 1-2, pp. 75–84, 2016.

[200] J. Schwager, N. Richard, F. Widmer, and D. Raederstorff, "Resveratrol distinctively modulates the inflammatory profiles of immune and endothelial cells," *BMC Complementary and Alternative Medicine*, vol. 17, no. 1, p. 309, 2017.

[201] M. R. Farag, M. Alagawany, and V. Tufarelli, "In vitro antioxidant activities of resveratrol, cinnamaldehyde and their synergistic effect against cyadox-induced cytotoxicity in rabbit erythrocytes," *Drug and Chemical Toxicology*, vol. 40, no. 2, pp. 196–205, 2017.

[202] J. R. Moyano-Mendez, G. Fabbrocini, D. de Stefano et al., "Enhanced antioxidant effect of trans-resveratrol: potential of binary systems with polyethylene glycol and cyclodextrin," *Drug Development and Industrial Pharmacy*, vol. 40, no. 10, pp. 1300–1307, 2013.

[203] X. Huang, W. Zhao, D. Hu et al., "Resveratrol efficiently improves pulmonary function via stabilizing mast cells in a rat intestinal injury model," *Life Sciences*, vol. 185, pp. 30–37, 2017.

[204] H. Zhang, H. Yan, X. Zhou et al., "The protective effects of resveratrol against radiation-induced intestinal injury," *BMC Complementary and Alternative Medicine*, vol. 17, no. 1, p. 410, 2017.

[205] S. Cho, K. Namkoong, M. Shin et al., "Cardiovascular protective effects and clinical applications of resveratrol," *Journal of Medicinal Food*, vol. 20, no. 4, pp. 323–334, 2017.

[206] L. L. Liu, J. H. He, H. B. Xie, Y. S. Yang, J. C. Li, and Y. Zou, "Resveratrol induces antioxidant and heat shock protein mRNA expression in response to heat stress in black-boned chickens," *Poultry Science*, vol. 93, no. 1, pp. 54–62, 2014.

[207] S. Bo, G. Ciccone, A. Castiglione et al., "Anti-inflammatory and antioxidant effects of resveratrol in healthy smokers a randomized, double-blind, placebo-controlled, crossover trial," *Current Medicinal Chemistry*, vol. 20, no. 10, pp. 1323–1331, 2013.

[208] P. Farris, M. Yatskayer, N. Chen, Y. Krol, and C. Oresajo, "Evaluation of efficacy and tolerance of a nighttime topical antioxidant containing resveratrol, baicalin, and vitamin e for treatment of mild to moderately photodamaged skin," *Journal of Drugs in Dermatology*, vol. 13, no. 12, pp. 1467–1472, 2014.

[209] C. Apostolidou, K. Adamopoulos, S. Iliadis, and C. Kourtidou-Papadeli, "Alterations of antioxidant status in asymptomatic hypercholesterolemic individuals after resveratrol intake," *International Journal of Food Sciences and Nutrition*, vol. 67, no. 5, pp. 541–552, 2015.

[210] L. K. Mischley, K. E. Conley, E. G. Shankland et al., "Central nervous system uptake of intranasal glutathione in Parkinson's disease," *NPJ Parkinson's Disease*, vol. 2, no. 1, article 16002, 2016.

[211] L. K. Mischley, R. C. Lau, E. G. Shankland, T. K. Wilbur, and J. M. Padowski, "Phase IIb study of intranasal glutathione in Parkinson's disease," *Journal of Parkinson's Disease*, vol. 7, no. 2, pp. 289–299, 2017.

[212] B. Schmitt, M. Vicenzi, C. Garrel, and F. M. Denis, "Effects of N-acetylcysteine, oral glutathione (GSH) and a novel sublingual form of GSH on oxidative stress markers: a comparative crossover study," *Redox Biology*, vol. 6, pp. 198–205, 2015.

[213] V. Plaisance, S. Brajkovic, M. Tenenbaum et al., "Endoplasmic reticulum stress links oxidative stress to impaired pancreatic beta-cell function caused by human oxidized LDL," *PLoS One*, vol. 11, no. 9, article e0163046, 2016.

[214] K. Eakin, R. Baratz-Goldstein, C. G. Pick et al., "Efficacy of N-acetyl cysteine in traumatic brain injury," *PLoS One*, vol. 9, no. 4, article e90617, 2014.

[215] J. Stark, "Oxidativ stressz es atherosclerosis," *Orvosi Hetilap*, vol. 156, no. 28, pp. 1115–1119, 2015.

[216] I. Karimzadeh, H. Khalili, S. Dashti-Khavidaki et al., "N-acetyl cysteine in prevention of amphotericin- induced electrolytes imbalances: a randomized, double-blinded, placebo-controlled, clinical trial," *European Journal of Clinical Pharmacology*, vol. 70, no. 4, pp. 399–408, 2014.

[217] B. Kazemi, F. Akbarzadeh, N. Safaei, A. Yaghoubi, K. Shadvar, and K. Ghasemi, "Prophylactic high-dose oral-N-acetylcysteine does not prevent atrial fibrillation after heart surgery: a prospective double blind placebo-controlled randomized clinical trial," *Pacing and Clinical Electrophysiology*, vol. 36, no. 10, pp. 1211–1219, 2013.

[218] A. Karbasi, S. Hossein Hosseini, M. Shohrati, M. Amini, and B. Najafian, "Effect of oral N-acetyl cysteine on eradication of helicobacter pylori in patients with dyspepsia," *Minerva Gastroenterologica e Dietologica*, vol. 59, no. 1, pp. 107–112, 2013.

[219] P. Dabirmoghaddam, A. Amali, M. Motiee Langroudi, M. R. Samavati Fard, M. Hejazi, and M. Sharifian Razavi, "The effect of N-acetyl cysteine on laryngopharyngeal reflux," *Acta Medica Iranica*, vol. 51, no. 11, pp. 757–764, 2013.

[220] F. L. Crane, "Biochemical functions of coenzyme Q10," *Journal of the American College of Nutrition*, vol. 20, no. 6, pp. 591–598, 2001.

[221] V. Mugoni, A. Camporeale, and M. M. Santoro, "Ubiad1 is an antioxidant enzyme that regulates eNOS activity by CoQ10 synthesis," *Cell*, vol. 152, no. 3, pp. 504–518, 2013.

[222] U. Alehagen, J. Alexander, and J. Aaseth, "Supplementation with selenium and coenzyme Q10 reduces cardiovascular mortality in elderly with low selenium status. A secondary analysis of a randomised clinical trial," *PLoS One*, vol. 11, no. 7, article e0157541, 2016.

[223] U. Alehagen, P. Johansson, J. Aaseth, J. Alexander, and D. Wagsater, "Significant changes in circulating microRNA by dietary supplementation of selenium and coenzyme Q10 in healthy elderly males. A subgroup analysis of a prospective randomized double-blind placebo-controlled trial among elderly Swedish citizens," *PLoS One*, vol. 12, no. 4, article e0174880, 2017.

[224] U. Alehagen, P. Johansson, J. Aaseth, J. Alexander, and K. Brismar, "Increase in insulin-like growth factor 1 (IGF-1) and insulin-like growth factor binding protein 1 after supplementation with selenium and coenzyme Q10. A prospective randomized double-blind placebo-controlled trial among elderly Swedish citizens," *PLoS One*, vol. 12, no. 6, article e0178614, 2017.

[225] N. Aslanabadi, N. Safaie, Y. Asgharzadeh et al., "The randomized clinical trial of coenzyme Q10 for the prevention of periprocedural myocardial injury following elective percutaneous coronary intervention," *Cardiovascular Therapeutics*, vol. 34, no. 4, pp. 254–260, 2016.

[226] J. McLachlan, E. Beattie, M. P. Murphy et al., "Combined therapeutic benefit of mitochondria-targeted antioxidant, MitoQ10, and angiotensin receptor blocker, losartan, on cardiovascular function," *Journal of Hypertension*, vol. 32, no. 3, pp. 555–564, 2014.

[227] B. J. Snow, F. L. Rolfe, M. M. Lockhart et al., "A double-blind, placebo-controlled study to assess the mitochondria-targeted antioxidant MitoQ as a disease-modifying therapy in Parkinson's disease," *Movement Disorders*, vol. 25, no. 11, pp. 1670–1674, 2010.

[228] H. Sies, "Ebselen, a selenoorganic compound as glutathione peroxidase mimic," *Free Radical Biology & Medicine*, vol. 14, no. 3, pp. 313–323, 1993.

[229] H. Masumoto and H. Sies, "The reaction of ebselen with peroxynitrite," *Chemical Research in Toxicology*, vol. 9, no. 1, pp. 262–267, 1996.

[230] T. Sakurai, M. Kanayama, T. Shibata et al., "Ebselen, a selenoorganic antioxidant, as an electrophile," *Chemical Research in Toxicology*, vol. 19, no. 9, pp. 1196–1204, 2006.

[231] J. Kil, E. Lobarinas, C. Spankovich et al., "Safety and efficacy of ebselen for the prevention of noise-induced hearing loss: a randomised, double-blind, placebo-controlled, phase 2 trial," *The Lancet*, vol. 390, no. 10098, pp. 969–979, 2017.

[232] J. Mahadevan, S. Parazzoli, E. Oseid et al., "Ebselen treatment prevents islet apoptosis, maintains intranuclear Pdx-1 and MafA levels, and preserves β-cell mass and function in ZDF rats," *Diabetes*, vol. 62, no. 10, pp. 3582–3588, 2013.

[233] X. Wang, J. W. Yun, and X. G. Lei, "Glutathione peroxidase mimic ebselen improves glucose-stimulated insulin secretion in murine islets," *Antioxidants & Redox Signaling*, vol. 20, no. 2, pp. 191–203, 2014.

[234] J. A. Beckman, A. B. Goldfine, J. A. Leopold, and M. A. Creager, "Ebselen does not improve oxidative stress and vascular function in patients with diabetes: a randomized, crossover trial," *American Journal of Physiology-Heart and Circulatory Physiology*, vol. 311, no. 6, pp. H1431–H1436, 2016.

[235] N. V. Barbosa, C. W. Nogueira, P. A. Nogara, A. F. de Bem, M. Aschner, and J. B. T. Rocha, "Organoselenium compounds as mimics of selenoproteins and thiol modifier agents," *Metallomics*, vol. 9, no. 12, pp. 1703–1734, 2017.

[236] K. Kikuchi, S. Tancharoen, N. Takeshige et al., "The efficacy of edaravone (radicut), a free radical scavenger, for cardiovascular disease," *International Journal of Molecular Sciences*, vol. 14, no. 7, pp. 13909–13930, 2013.

[237] J. D. Rothstein, "Edaravone: a new drug approved for ALS," *Cell*, vol. 171, no. 4, p. 725, 2017.

[238] D. Rischin, R. J. Hicks, R. Fisher et al., "Prognostic significance of [18F]-misonidazole positron emission tomography-detected tumor hypoxia in patients with advanced head and neck cancer randomly assigned to chemoradiation with or without tirapazamine: a substudy of trans-tasman radiation oncology group study 98.02," *Journal of Clinical Oncology*, vol. 24, no. 13, pp. 2098–2104, 2006.

[239] D. Rischin, L. J. Peters, B. O'Sullivan et al., "Tirapazamine, cisplatin, and radiation versus cisplatin and radiation for advanced squamous cell carcinoma of the head and neck (TROG 02.02, HeadSTART): a phase III trial of the trans-tasman radiation oncology group," *Journal of Clinical Oncology*, vol. 28, no. 18, pp. 2989–2995, 2010.

Review Article

Reactive Oxygen Species in Chronic Obstructive Pulmonary Disease

Samia Boukhenouna,[1,2] Mark A. Wilson,[3] Karim Bahmed,[1,2] and Beata Kosmider [1,2,4]

[1]*Department of Thoracic Medicine and Surgery, Temple University, Philadelphia, PA 19140, USA*
[2]*Center for Inflammation, Translational and Clinical Lung Research, Temple University, Philadelphia, PA 19140, USA*
[3]*Redox Biology Center and Department of Biochemistry, University of Nebraska, Lincoln, NE 68588, USA*
[4]*Department of Physiology, Temple University, Philadelphia, PA 19140, USA*

Correspondence should be addressed to Beata Kosmider; beata.kosmider@temple.edu

Chronic obstructive pulmonary disease (COPD) includes chronic bronchitis and emphysema. Environmental exposure, primarily cigarette smoking, can cause high oxidative stress and is the main factor of COPD development. Cigarette smoke also contributes to the imbalance of oxidant/antioxidant due to exogenous reactive oxygen species (ROS). Moreover, endogenously released ROS during the inflammatory process and mitochondrial dysfunction may contribute to this disease progression. ROS and reactive nitrogen species (RNS) can oxidize different biomolecules such as DNA, proteins, and lipids leading to epithelial cell injury and death. Various detoxifying enzymes and antioxidant defense systems can be involved in ROS removal. In this review, we summarize the main findings regarding the biological role of ROS, which may contribute to COPD development, and cytoprotective mechanisms against this disease progression.

1. Introduction

Chronic obstructive pulmonary disease (COPD) is a major health problem that is becoming the leading cause of morbidity and mortality throughout the world [1]. This disease is characterized by chronic inflammation, remodeling of the small airways, and destruction of the lung parenchyma [2]. It is believed that oxidative stress is increased in patients with COPD due to chronic exposure to cigarette smoke, a main risk factor, which contains a high concentration of oxidants and reactive oxygen species (ROS) (Figure 1) [3]. Other factors can also contribute to COPD development, such as bacterial and viral infections. Disease development is linked to a protease/antiprotease imbalance [4] that may lead to the lack of the protection against elastolytic enzymes. This imbalance may also create the disproportion of oxidant/antioxidant due to high endogenous ROS released by inflammatory cells such as neutrophils, macrophages, and structural cells, for example, epithelial and endothelial cells [1]. However, cells can be protected against oxidative stress by

enzymatic and nonenzymatic antioxidant systems [5]. Preclinical studies and clinical trials have shown that antioxidant molecules such as small thiol molecules (N-acetyl-L-cysteine and carbocysteine) [6–8], antioxidant enzymes (glutathione peroxidases) [9], activators of Nrf2-regulted antioxidant defense system (sulforaphane) [10, 11], and vitamins, for example, C, E, and D [12–14], can boost the endogenous antioxidant system and reduce oxidative stress. In addition, they may slow the progression of COPD. In this review, we focus on the mechanism of action of endogenous and exogenous ROS that can contribute to this disease development and the cytoprotective role of antioxidant molecules [15].

2. Chronic Obstructive Pulmonary Disease

COPD is the fourth leading cause of death in the United States [16] and is set to become the third cause of mortality in 2020 worldwide [17]. COPD is as a common, preventable, and treatable disease, characterized by persistent airflow limitation that is usually progressive and associated with an
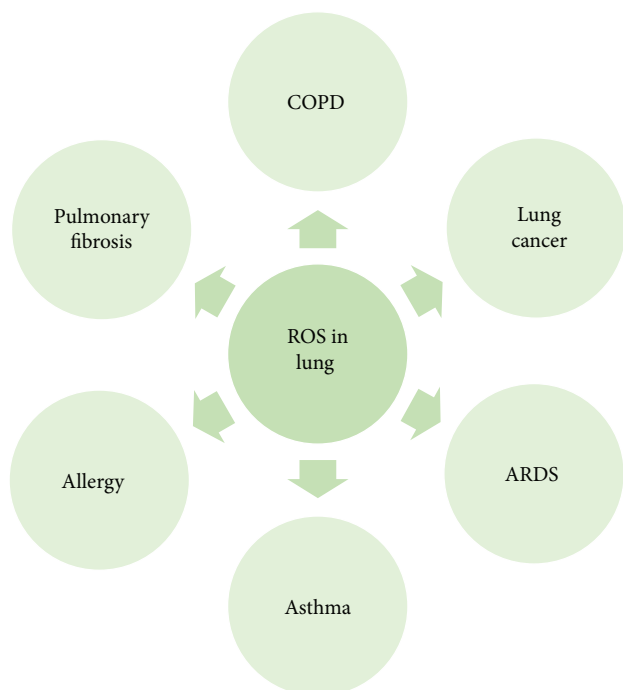
FIGURE 1: Potential contribution of ROS to various lung disease development. ROS—reactive oxygen species; COPD—chronic obstructive pulmonary disease; ARDS—acute respiratory distress syndrome.

enhanced chronic inflammatory response in the airways and the lung to noxious particles or gases. The most commonly encountered risk factor for COPD is cigarette smoke [2]. Moreover, outdoor, occupational, and indoor air pollution may contribute to this disease development. COPD refers mainly to two types: chronic bronchitis and emphysema. Chronic bronchitis is defined as the presence of a cough and sputum production for at least three months in each of two consecutive years [16, 18]. Emphysema is characterized by the destruction of the alveoli, the tiny air sacs in the lung where the exchange of oxygen and carbon dioxide takes place, which results in a decreased level of oxygen in the blood (hypoxemia) combined with an increased level of carbon dioxide in the blood (hypercapnia). Tuder et al. [19, 20] indicated that cigarette smoke could induce alveolar wall destruction by the interaction of apoptosis, oxidative stress, and protease/antiprotease imbalance. This may cause emphysema, which leads to the progressive and relentless loss of lung function due to the destruction of lung parenchyma and chronic inflammation. Furthermore, studies from animal models indicate that 4- to 6-month exposure to cigarette smoke leads to emphysema development in mice, rats, and rabbits [21–23]. Exacerbations of COPD are of major global importance [24]. Exacerbations are defined as sustained worsening of the patient's condition of the stable state and beyond normal day-to-day variations that is acute in onset and may warrant additional treatment in a patient with underlying COPD [25]. It has been reported that exacerbations are also involved in emphysema progression in patients with COPD [26]. Bacteria, viruses, and environmental

agents account for the vast majority of episodes of exacerbation. Exacerbation, systemic inflammation, ROS generation, alterations of metabolism, cardiovascular events, and lung cancer contribute to the overall disease severity and untimely death [2, 20].

3. Oxidative Damage of Biological Molecules

Exposure to exogenous sources of ROS such as cigarette smoke, air pollutants, or endogenously released ROS from leukocytes and macrophages involved in the inflammatory process can induce oxidative stress and the oxidant/antioxidant imbalance (Figure 2) [15]. Neutrophils have a key role in inflammatory processes and have been implicated in the development and progression of all of the pulmonary features of COPD through the release of destructive mediators such as neutrophil elastase and matrix metalloproteinases. Moreover, pulmonary neutrophilic inflammation is a feature of cigarette smoking, but importantly, in patients with COPD, it is sustained even following smoking cessation [27, 28]. Activated immune cells such as neutrophils and macrophages release ROS as a part of the inflammatory process [29]. ROS can react with biological molecules such as lipid, protein, DNA, RNA, and mitochondrial DNA and leads to epithelial cell injury and death (Figure 3), which contribute to COPD development.

During the respiratory burst, neutrophil myeloperoxidase catalyzes the oxidation of chloride ions (Cl^-) by hydrogen peroxide (H_2O_2) to generate the anionic ROS hypochlorite (OCl-) or its conjugate acid, hypochlorous acid (HOCl) (Figure 4(a)) [27]. The concentration of HOCl in the interstitial fluids of inflamed tissue has been estimated to reach more than 5 mM. HOCl has high reactivity, rapidly reacts with a variety of biomolecules, and cannot reach distant intracellular targets [30]. However, reaction of HOCl with amines can generate much more stable chloramines that can diffuse greater distances [27]. Only a few low molecular weight amines, such as nicotine in cigarette smoke, have been found to form chloramines that can cross cellular membranes and mediate HOCl-induced intracellular protein damage [31].

At the molecular level, ROS may induce lipid peroxidation (Figure 4(b)) and yield products such as malondialdehyde, which has the ability to inactivate many cellular proteins by generating protein cross-linkages [32]. This may stimulate pulmonary inflammation [33], promoting alveolar wall destruction and emphysema development. Another product of lipid peroxidation is 4-hydroxy-2,3-nonenal, which has many cytotoxic effects [34]. It has been shown to cause cytoplasmic Ca^{2+} accumulation, induce expression of proinflammatory cytokines and NF-κB, mitochondrial dysfunction, and apoptosis. The end products of lipid peroxidation such as ethane, pentane, and 8-isoprostane are elevated in the breath and serum of patients with COPD [35].

ROS can also cause reversible and irreversible protein modifications. Protein s-sulfenation, s-nitrosylation, s-glutathionylation, disulfides, thiosulfinates, sulfenamides, sulfinamides, and persulfides are reversible modifications [36, 37]. They are involved in redox regulation of protein functions by ROS and RNS. Moreover, these modifications play
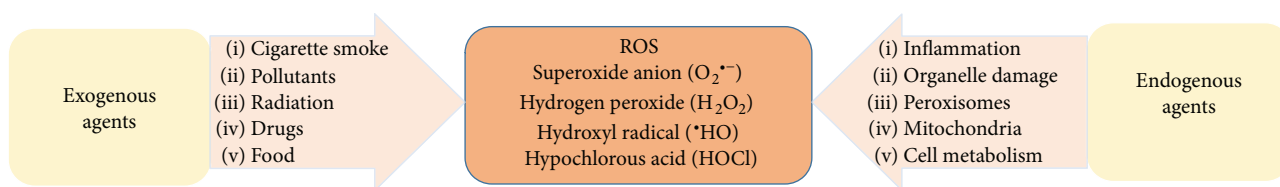
FIGURE 2: Exogenous and endogenous sources of ROS such as superoxide anions, hydrogen peroxide, hydroxyl radicals, and hypochlorous acid in cells.
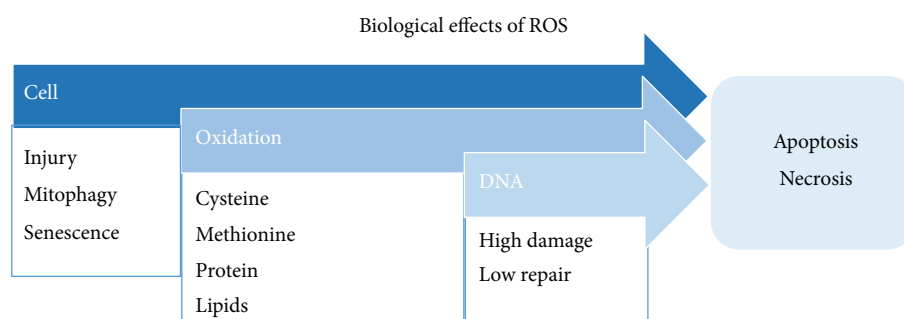

FIGURE 3: ROS reaction with various biomolecules such as proteins, lipids, and DNA may cause cell injury leading to apoptosis and necrosis.

$$H_2O_2 + Cl^- \rightarrow OCl^- + H_2O$$

$$RH + {}^\bullet OH \rightarrow H_2O + R^\bullet$$
$$R^\bullet + O_2 \rightarrow ROO^\bullet$$
$$ROO^\bullet + RH \rightarrow ROOH + R^\bullet$$

(a) (b)

$$Q^\bullet + QH_2 \rightarrow 2H^+ + 2Q^{\bullet-}$$
$$Q^{\bullet-} + O_2 \rightarrow Q + O_2^{\bullet-}$$
$$O_2^{\bullet-} + 2H^+ \rightarrow H_2O_2$$

$$O_2^{\bullet-} + NO^\bullet \rightarrow ONOO^-$$

(c) (d)

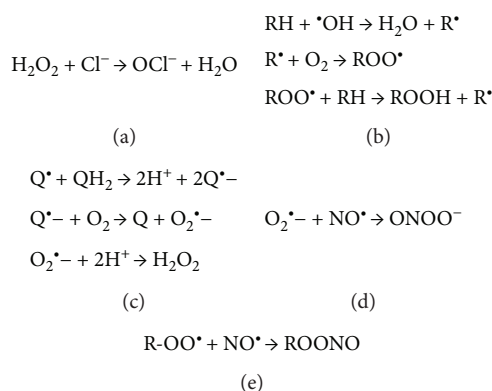$$R\text{-}OO^\bullet + NO^\bullet \rightarrow ROONO$$

(e)

FIGURE 4: The mechanism of ROS interaction with biomolecules. (a) Hypochlorite anion production catalyzed by myeloperoxidase; (b) lipid peroxidation; (c) production of hydrogen peroxide; (d) peroxynitrite generation; (e) production of alkyl peroxynitrites. H_2O_2—hydrogen peroxide; ^-OCl—hypochlorite anion; RH—unsaturated lipid; $^\bullet OH$—hydroxyl radical; $R^\bullet$—lipid radical; $ROO^\bullet$—lipid peroxyl radical; ROOH—lipid peroxide; Q/QH_2—quinone/hydroquinone; $O_2^{\bullet-}$—superoxide anion; $NO^\bullet$—nitric oxide; $ONOO^-$—peroxynitrite; ROONO—alkyl peroxynitrites.

important roles in health because they contribute to regulation of cellular defense systems and protection against oxidative stress. Protein carbonyls, nitrotyrosines, sulfinic acids, sulfonic acids, and sulfonamides are irreversible modifications [37, 38]. Oxidation of proteins may lead to activation of NF-κB, p38 MAPK, induction of inflammatory genes, and inhibition of the activity of endogenous antiproteases, which may contribute to this disease pathogenesis [39]. Although, irreversibly oxidized proteins are often indicators of high oxidative stress and oxidative damage and are detected in lung diseases, they may also be present under normal conditions.

Moreover, ROS can also induce RNA, DNA, and mitochondrial DNA (mtDNA) damage. Studies suggest that RNA is more vulnerable to oxidative damage than other cellular components [40]. RNA could have enhanced susceptibility for oxidative attack because of its widespread cytosolic distribution, single-stranded structure, absence of protective histones, and lack of an advanced repair mechanism [41]. More than 20 different types of base damage by hydroxyl radicals have been identified [40].

The most prevalent oxidized base in RNA is 8-hydroxyguanosine (8-OHG). The highly reactive hydroxyl radical first reacts with guanine to form a C8-OH adduct radical. Then, the loss of an electron and proton generates 8-OHG (an oxidized RNA nucleoside). It is worth to notice that RNA oxidation is more prevalent than DNA oxidation in alveolar wall cells in emphysema [41]. However, DNA oxidation promotes microsatellite instability, inhibits methylation, and accelerates telomere shortening.

8-hydroxy-2′-deoxyguanosine (8-OHdG) is a product of oxidized DNA and widely used as a marker of oxidative cellular damage. Moreover, p53 mutation, observed in lung cancer, is linked to a direct DNA damage due to exposure to carcinogens in cigarette smoke [42]. It is worth noting that patients with emphysema have a high risk of lung cancer development [43]. ROS are also the main source of mtDNA damage and mutagenesis [44]. The main products of mtDNA base damage are thymine glycol among pyrimidines and 8-OHdG among purines. The former has low mutagenicity, whereas the latter upon replication can cause characteristic G→T transversions. MtDNA with oxidative damage may lead to mitochondrial dysfunction in alveolar epithelial cells [45].

4. Reactive Oxygen Species

It is believed that oxidative stress induced by cigarette smoke and oxidative cell damage play a pivotal role in the COPD development [7]. Cigarette smoke is a complex mixture of numerous free radicals and ROS that can be divided into two phases: tar (particle) and gas. Tar phase covers about 10^{17} relatively long-lived radical molecules per gram, for example, quinone/hydroquinone (Q/QH_2) radicals that can reduce oxygen to produce superoxide anion ($O_2^{\bullet-}$) leading the generation of H_2O_2 (Figure 4(c)) and hydroxyl radical ($^\bullet OH$) [3, 46]. Primary among highly reactive ROS is $^\bullet OH$, which can damage all types of macromolecules upon collision, thus having a diffusion-limited lifetime of approximately 1 nanosecond [47]. Hydroxyl radicals can be generated by Fenton chemistry involving H_2O_2 and either ferrous iron (Fe(II)) or cuprous copper (Cu(I)), which constitute dangerous intersections of metal and redox homeostasis. Particulate matter (PM) pollutants were shown to be iron-rich and to increase oxidative stress, providing opportunity for damaging Fenton chemistry to occur and generate $^\bullet OH$ in the lung [48]. Less reactive than $^\bullet OH$ but still dangerous is the superoxide radical anion ($O_2^{\bullet-}$), which can participate in one electron redox chemistry, predominantly with metals and flavin cofactors. In contrast, H_2O_2 is a relatively stable, neutral ROS that can diffuse significant distances from its site of production [47]. Unlike the superoxide radical anion, H_2O_2 participates primarily in two-electron redox chemistry, predominantly with sulfur-containing moieties in the cell. However, H_2O_2 can also participate in some one-electron chemistry with transition metals (see above for a discussion of Fenton reaction). H_2O_2 can serve as a signaling molecule at low concentrations as well as a damage agent at higher concentrations and thus has a complex cellular role that is defined by overlapping mechanisms of H_2O_2 detection, signal transduction, and destruction [49, 50]. Moreover, HOCl generated in the presence of H_2O_2 can further lead to formation of more toxic ROS such as $^\bullet OH$ [27]. The high reactivity of the hypochlorite anion (^-OCl) means that it is fairly indiscriminate in modifying its targets, typically with second order rate constants of $10^5–10^7 M^{-1} s^{-1}$ [51]. In proteins, cysteine, histidine, and methionine are among the favored residues for modification. Primary amines, such as those found in the sidechain of lysine, can also be

modified to chloramines by ^-OCl. In total, high ROS levels may cause lung tissue damage and respiratory problems via modification of diverse target molecules via distinct, ROS-specific mechanisms.

Gas phase of cigarette smoke contains much more reactive molecules than tar. This phase consists of 10^{15} organic and inorganic radicals per puff [3], for example, nitric oxide ($NO^\bullet$), nitrogen dioxide, and peroxynitrite ($ONOO^-$). Cigarette smoke contains 74.5–1008 ppm $NO^\bullet$ [52] and thus represents one of the main ROS and reactive nitrogen species (RNS) to which smokers are exposed. $NO^\bullet$ has a short half-life ($t_{1/2}\sim0.09$ to $2 s$) [53]; however, it reacts quickly (second order rate constant $\sim2.4 \pm 0.3 \times 10^6 M^{-2} s^{-1}$) [54] with $O_2^{\bullet-}$ to form peroxynitrite ($ONOO^-$) (Figure 4(d)). Peroxynitrite is a RNS that is involved in many physiological and pathological processes [55, 56]. Peroxynitrite possesses a very strong oxidation and nitration capabilities, leading to damaging molecules in cells, such as DNA and proteins. A second order reaction depends on the concentrations of one second order reactant or two first order reactants, which are $O_2^{\bullet-}$ and $NO^\bullet$ in the case of peroxynitrite generation. $NO^\bullet$ can also react with organic lipid peroxyl radicals ($ROO^\bullet$) present in cigarette smoke to form alkyl peroxynitrites (ROONO) (Figure 4(e)), which are cytotoxic species. Moreover, $NO^\bullet$ and $O_2^{\bullet-}$ are produced by inflammatory cells such as macrophages, by nitric oxide synthases (NOSs) and NADPH oxidase complexes (NOXs), respectively. Furthermore, ROS and RNS can be released by a noncontrolled process as byproducts during mitochondrial respiration, peroxisomal metabolism [57], and protein folding maturation process in the endoplasmic reticulum [58]. Their increased formation leads to oxidative stress and lung damage.

5. Mitochondrial Dysfunction

Mitochondria are dynamic intracellular organelles that constantly change in shape, size, number, and distribution through constitutive cycles of fusion and fission [59]. Mitochondrial fusion contributes to maintain intact mitochondrial DNA copies, mitochondrial membrane components, and matrix metabolites. Mitochondrial fission plays a role in the segregation of dysfunctional mitochondria from the pool of mitochondria. Accordingly, mitochondrial fission is highly correlated with cell apoptosis [60]. Specifically, mitochondrial fission is achieved by phosphorylation of Drp1 at Ser616, which promotes the recruitment of Drp1 from the cytosol to the mitochondrial surface by human fission protein-1. The possible mechanism indicates that oxidative stress triggers mitochondrial fission and loss by enhancing Drp1 translocation from the cytosol. Cigarette smoking-induced mitochondrial ROS can accelerate phosphorylation of Drp1. Therefore, prolonged oxidative stress can cause an imbalance in fission-fusion, resulting in mitochondrial fragmentation, which may contribute to cell death.

Mitochondria may serve as sensors to detect perturbations of intracellular homeostasis, including oxidative stress [61]. Histone proteins are reported to protect DNA from a variety of potentially dangerous ROS, such as $^\bullet OH$. High sensitivity of mtDNA to damage caused by oxidative stress is

related to the proximity to the source of ROS, the lack of protective histones, and a relatively inefficient mtDNA repair [62]. This may induce the synthesis of defective mitochondrial electron transport chain subunits, further resulting in the decreasing transmembrane potential and leading to the abnormal overproduction of ROS, which damage cells [59]. This further contributes to disturbances in the redox balance leading to the imbalance between the oxidants and antioxidants in the cell. Finally, this cause mitochondrial dysfunction, permeabilization of the outer mitochondrial membrane, release of apoptotic proteins, and cell death [63]. Specifically, $O_2^{\bullet-}$ can lead to mitochondrial depolarization by facilitating cytochrome c release. Mitochondrial dysfunction has been reported in airway smooth muscle cells obtained from smokers and patients with COPD [64]. These cells were unable to provide adequate respiration and had a severely reduced respiratory reserve capacity. Bronchial epithelial cells obtained from ex-smokers with COPD showed damaged mitochondria, with depletion of cristae, increased branching, elongation, and swelling [65]. Moreover, mitochondrial dysfunction in patients with COPD is associated with excessive mitochondrial ROS levels, which contribute to enhanced inflammation [64].

Damaged or dysfunctional mitochondria are cleared from the cells by the autophagy-dependent turnover of mitochondria (mitophagy) [66]. Mitophagy is considered a homeostatic program that maintains a healthy mitochondrial population for cytoprotective roles in disease pathogenesis [67]. In contrast, mitophagy may be also a possible effector of cell death programs. Recent studies indicate that mitophagy is associated with epithelial cell death in COPD, specifically involving necroptosis, a form of programmed necrosis, in response to cigarette smoke exposure. In cultured pulmonary epithelial cells, cigarette smoke caused mitochondrial dysfunction associated with a decline of mitochondrial membrane potential and increased mitochondrial ROS production. Furthermore, it was reported that mild and transient oxidative stress induced by H_2O_2 does not damage mitochondria, but rather initiates a ROS signaling cascade, leading to the induction of selective mitophagy [68]. This in turn would promote the selective removal of damaged mitochondria. Prolonged and more excessive ROS triggers early phase of autophagic process, including cytoprotection. However, higher ROS concentrations may overload this and other quality control systems, leading to permanent cell damage and reduced viability. Based on these observations, ROS can act as signaling molecules influencing cell fate. Redox regulation can promote both survival, for example, during starvation. On the other hand, if the prosurvival attempt fails, high oxidative stress causes cell death [69]. Taken together, studies suggest that mitochondrial dysfunction induced by oxidative stress is a key contributor to the pathophysiology of COPD. Targeting mitochondrial ROS represents a promising therapeutic approach in patients with this disease.

6. Antioxidant Defenses against ROS

Cells mount a diverse and robust defense against ROS, which includes an overlapping array of enzyme activities that are
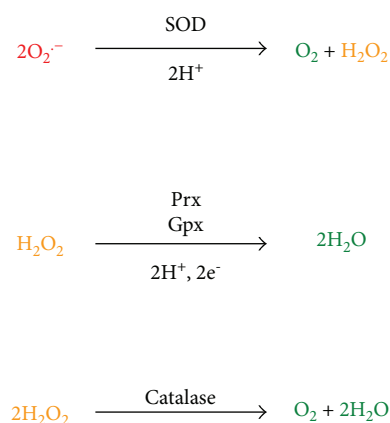

Figure 5: Primary enzymatic means of ROS detoxification. The relative reactivity of the ROS is indicated by color, ranging from highly reactive (red) to inert (green). SOD—superoxide dismutases; Prxs—peroxiredoxins; Gpxs—glutathione peroxidases.

specific for particular ROS. Of the common ROS, only $^{\bullet}OH$ is so reactive that there are no effective enzymatic detoxification strategies (see above for a discussion of $^{\bullet}OH$). Because $^{\bullet}OH$ is so indiscriminately destructive, no mechanisms in the cell can effectively counter it. Although glutathione (GSH) has been suggested as a general redox buffer against this and other ROS, recent work suggests that GSH exerts its antioxidant effect mostly through enzymatic pathways such as glutaredoxins or as the reductant for glutathione peroxidases [70]. Tocopherol and ascorbate form moderately stable radicals and thus can act as "sinks" for $^{\bullet}OH$ and other radicals, although $^{\bullet}OH$ will react with the first molecule it encounters, which is unlikely to be a small molecule antioxidant.

Another radical ROS is $O_2^{\bullet-}$. The superoxide anion is detoxified by the action of the metalloenzyme superoxide dismutase (SOD), which converts $O_2^{\bullet-}$ to H_2O_2 and O_2 (Figure 5).

Being a dismutation, there is no net change in redox state and thus no electrons are required for the balanced reaction [71]. Various SODs exist and are classified according to the metals present in their active sites, which in humans are the Cu-Zn SODs (SOD1; intracellular, SOD3; extracellular) and Mn-SOD (SOD2, mitochondrial). Notably, the Cu-Zn and Mn-SODs have completely different three-dimensional structures as a consequence of being members of different fold families, suggestive of convergent evolution [72]. SODs are highly efficient enzymes, dismutating $O_2^{\bullet-}$ with a $k_{cat}/K_M \sim 7 \times 10^9\,M^{-1}\,s^{-1}$, which exceeds the "diffusion limit" of $\sim 10^9\,M^{-1}\,s^{-1}$. Enzymes operating at the diffusion limit successfully catalyze their reaction nearly every time they encounter substrate (i.e., they are catalytically "perfect"), which would seem to place an upper limit on enzyme catalytic efficiency. However, because $O_2^{\bullet-}$ is an anion, the electrostatic properties of SOD are important and have been evolutionarily optimized to guide this negatively charged substrate toward a positively charged patch near the SOD active site. In this manner, SOD electrostatically "funnels" substrate toward its active site and thus exceeds the theoretical diffusion limit on catalytic efficiency

[73]. Therefore, SOD is remarkably proficient at removing $O_2^{\bullet-}$, although one of its products is H_2O_2, another ROS. Extracellular $O_2^{\bullet-}$ produced by neutrophils is considered a major source of alveolar and bronchial epithelial cell damage, and the SOD system is an important component in the pulmonary defense against hyperoxic injury [74, 75].

The predominant enzymes that handle hydrogen peroxide are the peroxiredoxins (Prxs), a collection of thiol-dependent enzymes that convert peroxides into water (when H_2O_2 is the substrate; Figure 5) or alcohols (when organic peroxides of the general formula ROOH are the substrate). Their high cellular concentration and fast rate of reaction of Prxs with peroxides ($k_{cat}/K_M \sim 10^6$-$10^7 M^{-1} s^{-1}$) mean that they are likely the first molecules in the cell that react with this ROS [76]. Therefore, Prxs have been postulated to be both the front-line defense against elevated peroxide and to mediate initial homeostatic or proliferative peroxide signaling events [77]. In addition to their role in directly detoxifying H_2O_2, the Prxs also indirectly decrease the levels of hypochlorite (^-OCl) and hydroxyl radical ($^\bullet OH$) by reducing the concentration of the peroxide reactant that generates these secondary ROS.

There are six Prxs in mammals, divided into 1-Cys or 2-Cys classes depending on the number of critical cysteine residues in their active sites. Regardless of class, all Prx reduce peroxides via the initial formation of a cysteine sulfenic acid (Cys-SOH) at a highly reactive, peroxidatic cysteine active site residue. The peroxide-derived oxygen atom of the cysteine sulfenic acid intermediate is released as water during the resolution of the sulfenic acid by the attack of a second thiol, either donated by another cysteine residue in the protein (the resolving cysteine in the 2-Cys Prxs) or from small molecule thiols such as glutathione (in 1-Cys Prxs). Therefore, Prx catalysis results in disulfide-containing enzymes that must be reduced by thioredoxin or glutaredoxin in order to restore the resting enzyme and complete the catalytic cycle. This process is dependent on reductases that ultimately obtain electrons from NADPH, thereby coupling Prx-dependent ROS detoxification to the pentose phosphate pathway, which generates NADPH. Prxs I, II, III, and V are the isoforms that are most highly expressed in healthy lung epithelium [78]. Additional evidence suggests that the 1-Cys Prx VI is important specifically for the defense against lipid peroxides in the lung [79]. A further point of particular interest is that Prx VI also possesses phospholipase A2 activity and it is thought to play an important role in the metabolism of lung surfactant phospholipids that appears to be independent of its peroxidase function.

Glutathione peroxidases (Gpxs) are an intriguing class of oxidative stress defense enzymes that typically (though not always) feature a selenocysteine residue in their active sites. Selenocysteine, sometimes called the 21st amino acid, is sometimes found in the active sites of redox-active enzymes [80]. The Gpxs detoxify peroxides using a catalytic strategy that is broadly similar to the Prxs (see above), involving the transient oxidation of an active site residue (cysteine in the Prxs, selenocysteine in the Gpxs) to a monooxygenated form, either cysteine-sulfenic acid (Cys-SOH) in the Prxs or seleno-cysteine selenenic acid (Sec-SeOH) in the Gpxs. In the Gpxs,

this Sec-SeOH is resolved by the sequential action of two molecules of GSH. The first GSH attacks the Sec-SeOH to form a Se-S bond with the enzyme and liberates water (Figure 5). The second GSH regenerates the free enzyme and produces oxidized glutathione disulfide (GSSG) with the first GSH. As such, Gpx activity is critically linked to the cellular glutathione pool, and the released GSSG is reduced to GSH by NADPH-dependent glutathione reductase. Interestingly, Gpx1 deficiency results in only lung modest phenotypes in mouse models; however, alteration of pulmonary immune function has been noted [81]. In general, it is likely that the multiple Prx and Gpx isoforms present in mammals have significantly overlapping activities and that redundancy has evolved in the biochemical mechanisms for removing peroxides.

A curiosity of the cellular defense against peroxides is that it contains so many enzymes apparently dedicated to this task. Catalases are also hydrogen peroxide detoxifying enzymes that, unlike the Prxs and Gpxs, use a reductase-independent, hemedependent chemistry to convert H_2O_2 to O_2 (Figure 5). The hemedependent peroxidases are a related family of enzymes that convert H_2O_2 to water, and some enzymes have both activities in a single polypeptide. Catalases are fast enzymes, with k_{cat} values of $\sim 10^7 s^{-1}$ but also have very high K_M values of $\sim 1 M$ for peroxide. Therefore, catalases are far from their maximum rate when presented with the nM-μM levels of H_2O_2 present in cells and are likely to be kinetically outcompeted by the Prxs. This may result in differing kinetic regimes in which the Prxs and catalases operate, allowing effective response over a range of peroxide insult, from chronic low level (Prxs) to acute high level stress (catalases) [82]. Catalases are expressed in alveolar epithelial cells and may play a particularly important role in acute stress caused by bolus H_2O_2 generation, which occurs during reoxygenation injury in the lung [83].

7. Lung Aging

The ability to prevent the oxidative damage to the lung tissue and the potential to regenerate injured cells are two key determinants of aging [84]. While still an area of controversy, reports indicate that exposure to cigarette smoke, ROS, and other environmental stressors may accelerate biological processes associated with normal aging [85, 86]. Moreover, recent epidemiological study has suggested that about half of patients with COPD fail to achieve full lung function in adolescence and early adulthood. In these individuals, this disease might develop as a consequence of the "normal" decline in lung function with age. Similar to emphysema, lung aging is characterized by a decrease in the density and an increase in the diameter of the membranous bronchioles. However, unlike emphysema, there are no differences in alveolar attachments. COPD may represent an accelerated (or normal) form of lung aging.

8. Conclusions

We highlighted how environmental exposure to cigarette smoke and endogenous ROS generated during inflammatory

processes induce high oxidative stress, which may contribute to COPD development. We summarized the reactivity of the most biologically relevant ROS and RNS, which can oxidize different biomolecules such as DNA, proteins, and lipids. We also reviewed how oxidant molecules (ROS) can be reduced or destroyed by diverse cytoprotective mechanisms focusing on the enzymatic protection afforded by SODs, Prxs, Gpxs, and catalases. Antioxidant systems, for example, GSH, vitamins A, C, and E, and carotenoids, are important and can intersect with other pathways [39]. Under very high oxidative stress conditions present in patients with COPD, these mechanisms may not correctly play their protective role, which may contribute to exacerbation.

Conflicts of Interest

The authors declare no conflict of interest.

Acknowledgments

References

[1] P. A. Kirkham and P. J. Barnes, "Oxidative stress in COPD," *Chest*, vol. 144, no. 1, pp. 266–273, 2013.

[2] J. C. Hogg and R. M. Senior, "Chronic obstructive pulmonary disease - part 2: pathology and biochemistry of emphysema," *Thorax*, vol. 57, no. 9, pp. 830–834, 2002.

[3] W. A. Pryor and K. Stone, "Oxidants in cigarette smoke. Radicals, hydrogen peroxide, peroxynitrate, and peroxynitrite," *Annals of the New York Academy of Sciences*, vol. 686, no. 1 Tobacco Smoki, pp. 12–27, 1993.

[4] B. M. Fischer, E. Pavlisko, and J. A. Voynow, "Pathogenic triad in COPD: oxidative stress, protease-antiprotease imbalance, and inflammation," *International Journal of Chronic Obstructive Pulmonary Disease*, vol. 6, pp. 413–421, 2011.

[5] B. Halliwell, "Antioxidants in human health and disease," *Annual Review of Nutrition*, vol. 16, no. 1, pp. 33–50, 1996.

[6] P. N. R. Dekhuijzen, "Antioxidant properties of N-acetylcysteine: their relevance in relation to chronic obstructive pulmonary disease," *The European Respiratory Journal*, vol. 23, no. 4, pp. 629–636, 2004.

[7] I. Rahman and W. MacNee, "Antioxidant pharmacological therapies for COPD," *Current Opinion in Pharmacology*, vol. 12, no. 3, pp. 256–265, 2012.

[8] E. M. Messier, B. J. Day, K. Bahmed et al., "N-acetylcysteine protects murine alveolar type II cells from cigarette smoke injury in a nuclear erythroid 2-related factor-2-independent manner," *American Journal of Respiratory Cell and Molecular Biology*, vol. 48, no. 5, pp. 559–567, 2013.

[9] R. Vlahos and S. Bozinovski, "Glutathione peroxidase-1 as a novel therapeutic target for COPD," *Redox Report*, vol. 18, no. 4, pp. 142–149, 2013.

[10] D. Malhotra, R. K. Thimmulappa, N. Mercado et al., "Denitrosylation of HDAC2 by targeting Nrf2 restores glucocorticosteroid sensitivity in macrophages from COPD patients," *The Journal of Clinical Investigation*, vol. 121, no. 11, pp. 4289–4302, 2011.

[11] R. K. Thimmulappa, K. H. Mai, S. Srisuma, T. W. Kensler, M. Yamamoto, and S. Biswal, "Identification of Nrf2-regulated genes induced by the chemopreventive agent sulforaphane by oligonucleotide microarray," *Cancer Research*, vol. 62, no. 18, pp. 5196–5203, 2002.

[12] T. C. Wu, Y. C. Huang, S. Y. Hsu, Y. C. Wang, and S. L. Yeh, "Vitamin E and vitamin C supplementation in patients with chronic obstructive pulmonary disease," *International Journal for Vitamin and Nutrition Research*, vol. 77, no. 4, pp. 272–279, 2007.

[13] A. Schols, "Nutrition as a metabolic modulator in COPD," *Chest*, vol. 144, no. 4, pp. 1340–1345, 2013.

[14] E. M. Messier, K. Bahmed, R. M. Tuder, H. W. Chu, R. P. Bowler, and B. Kosmider, "Trolox contributes to Nrf2-mediated protection of human and murine primary alveolar type II cells from injury by cigarette smoke," *Cell Death & Disease*, vol. 4, no. 4, article e573, 2013.

[15] I. Rahman and W. MacNee, "Role of oxidants/antioxidants in smoking-induced lung diseases," *Free Radical Biology & Medicine*, vol. 21, no. 5, pp. 669–681, 1996.

[16] D. L. Hoyert and J. Xu, "Deaths: preliminary data for 2011," *National Vital Statistics Reports*, vol. 61, no. 6, pp. 1–51, 2012.

[17] G. Viegi, S. Maio, F. Pistelli, S. Baldacci, and L. Carrozzi, "Epidemiology of chronic obstructive pulmonary disease: health effects of air pollution," *Respirology*, vol. 11, no. 5, pp. 523–532, 2006.

[18] J. Smith and A. Woodcock, "Cough and its importance in COPD," *International Journal of Chronic Obstructive Pulmonary Disease*, vol. 1, no. 3, pp. 305–314, 2006.

[19] R. M. Tuder, S. McGrath, and E. Neptune, "The pathobiological mechanisms of emphysema models: what do they have in common?," *Pulmonary Pharmacology & Therapeutics*, vol. 16, no. 2, pp. 67–78, 2003.

[20] R. M. Tuder and I. Petrache, "Pathogenesis of chronic obstructive pulmonary disease," *The Journal of Clinical Investigation*, vol. 122, no. 8, pp. 2749–2755, 2012.

[21] M. P. Goldklang, Y. Tekabe, T. Zelonina et al., "Single-photon emission computed tomography/computed tomography imaging in a rabbit model of emphysema reveals ongoing apoptosis in vivo," *American Journal of Respiratory Cell and Molecular Biology*, vol. 55, no. 6, pp. 848–857, 2016.

[22] J. E. Radder, A. D. Gregory, A. S. Leme et al., "Variable susceptibility to cigarette smoke-induced emphysema in 34 inbred strains of mice implicates Abi3bp in emphysema susceptibility," *American Journal of Respiratory Cell and Molecular Biology*, vol. 57, no. 3, pp. 367–375, 2017.

[23] J. Wei, G. Fan, H. Zhao, and J. Li, "Heme oxygenase-1 attenuates inflammation and oxidative damage in a rat model of smoke-induced emphysema," *International Journal of Molecular Medicine*, vol. 36, no. 5, pp. 1384–1392, 2015.

[24] B. R. Celli and P. J. Barnes, "Exacerbations of chronic obstructive pulmonary disease," *The European Respiratory Journal*, vol. 29, no. 6, pp. 1224–1238, 2007.

[25] S. Burge and J. A. Wedzicha, "COPD exacerbations: definitions and classifications," *European Respiratory Journal*, vol. 21, pp. 46s–53s, 2003.

[26] N. Tanabe, S. Muro, T. Hirai et al., "Impact of exacerbations on emphysema progression in chronic obstructive pulmonary

disease," *American Journal of Respiratory and Critical Care Medicine*, vol. 183, no. 12, pp. 1653–1659, 2011.

[27] S. A. Salama, H. H. Arab, H. A. Omar, I. A. Maghrabi, and R. M. Snapka, "Nicotine mediates hypochlorous acid-induced nuclear protein damage in mammalian cells," *Inflammation*, vol. 37, no. 3, pp. 785–792, 2014.

[28] S. Hobbins, I. L. Chapple, E. Sapey, and R. A. Stockley, "Is periodontitis a comorbidity of COPD or can associations be explained by shared risk factors/behaviors?," *International Journal of Chronic Obstructive Pulmonary Disease*, vol. Volume 12, pp. 1339–1349, 2017.

[29] M. Meijer, G. T. Rijkers, and F. J. van Overveld, "Neutrophils and emerging targets for treatment in chronic obstructive pulmonary disease," *Expert Review of Clinical Immunology*, vol. 9, no. 11, pp. 1055–1068, 2014.

[30] D. I. Pattison, C. L. Hawkins, and M. J. Davies, "What are the plasma targets of the oxidant hypochlorous acid? A kinetic modeling approach," *Chemical Research in Toxicology*, vol. 22, no. 5, pp. 807–817, 2009.

[31] S. A. Salama and R. M. Snapka, "Amino acid chloramine damage to proliferating cell nuclear antigen in mammalian cells," *In Vivo*, vol. 26, no. 4, pp. 501–517, 2012.

[32] G. M. Siu and H. H. Draper, "Metabolism of malonaldehyde in vivo and in vitro," *Lipids*, vol. 17, no. 5, pp. 349–355, 1982.

[33] I. Rahman and I. M. Adcock, "Oxidative stress and redox regulation of lung inflammation in COPD," *The European Respiratory Journal*, vol. 28, no. 1, pp. 219–242, 2006.

[34] M. Breitzig, C. Bhimineni, R. Lockey, and N. Kolliputi, "4-Hydroxy-2-nonenal: a critical target in oxidative stress?," *American Journal of Physiology Cell Physiology*, vol. 311, no. 4, pp. C537–C543, 2016.

[35] I. Horvath, W. MacNee, F. J. Kelly et al., "Haemoxygenase-1 induction and exhaled markers of oxidative stress in lung diseases, summary of the ERS research seminar in Budapest, Hungary, September, 1999," *The European Respiratory Journal*, vol. 18, no. 2, pp. 420–430, 2001.

[36] Z. Cai and L. J. Yan, "Protein oxidative modifications: beneficial roles in disease and health," *Journal of Biochemical and Pharmacological Research*, vol. 1, no. 1, pp. 15–26, 2013.

[37] C. E. Paulsen and K. S. Carroll, "Cysteine-mediated redox signaling: chemistry, biology, and tools for discovery," *Chemical Reviews*, vol. 113, no. 7, pp. 4633–4679, 2013.

[38] J. Cai, Y. Chen, S. Seth, S. Furukawa, R. W. Compans, and D. P. Jones, "Inhibition of influenza infection by glutathione," *Free Radical Biology & Medicine*, vol. 34, no. 7, pp. 928–936, 2003.

[39] P. Kirkham and I. Rahman, "Oxidative stress in asthma and COPD: antioxidants as a therapeutic strategy," *Pharmacology & Therapeutics*, vol. 111, no. 2, pp. 476–494, 2006.

[40] Q. Kong and C. L. Lin, "Oxidative damage to RNA: mechanisms, consequences, and diseases," *Cellular and Molecular Life Sciences*, vol. 67, no. 11, pp. 1817–1829, 2010.

[41] G. Deslee, J. C. Woods, C. Moore et al., "Oxidative damage to nucleic acids in severe emphysema," *Chest*, vol. 135, no. 4, pp. 965–974, 2009.

[42] D. L. Gibbons, L. A. Byers, and J. M. Kurie, "Smoking, p53 mutation, and lung cancer," *Molecular Cancer Research*, vol. 12, no. 1, pp. 3–13, 2014.

[43] A. L. Durham and I. M. Adcock, "The relationship between COPD and lung cancer," *Lung Cancer*, vol. 90, no. 2, pp. 121–127, 2015.

[44] I. Shokolenko, N. Venediktova, A. Bochkareva, G. L. Wilson, and M. F. Alexeyev, "Oxidative stress induces degradation of mitochondrial DNA," *Nucleic Acids Research*, vol. 37, no. 8, pp. 2539–2548, 2009.

[45] S. J. Kim, P. Cheresh, D. Williams et al., "Mitochondria-targeted Ogg1 and aconitase-2 prevent oxidant-induced mitochondrial DNA damage in alveolar epithelial cells," *The Journal of Biological Chemistry*, vol. 289, no. 9, pp. 6165–6176, 2014.

[46] D. F. Church and W. A. Pryor, "Free-radical chemistry of cigarette smoke and its toxicological implications," *Environmental Health Perspectives*, vol. 64, pp. 111–126, 1985.

[47] C. C. Winterbourn, "Reconciling the chemistry and biology of reactive oxygen species," *Nature Chemical Biology*, vol. 4, no. 5, pp. 278–286, 2008.

[48] S. Yi, F. Zhang, F. Qu, and W. Ding, "Water-insoluble fraction of airborne particulate matter (PM_{10}) induces oxidative stress in human lung epithelial A549 cells," *Environmental Toxicology*, vol. 29, no. 2, pp. 226–233, 2014.

[49] E. A. Veal, A. M. Day, and B. A. Morgan, "Hydrogen peroxide sensing and signaling," *Molecular Cell*, vol. 26, no. 1, pp. 1–14, 2007.

[50] H. S. Marinho, C. Real, L. Cyrne, H. Soares, and F. Antunes, "Hydrogen peroxide sensing, signaling and regulation of transcription factors," *Redox Biology*, vol. 2, pp. 535–562, 2014.

[51] C. L. Hawkins, D. I. Pattison, and M. J. Davies, "Hypochlorite-induced oxidation of amino acids, peptides and proteins," *Amino Acids*, vol. 25, no. 3-4, pp. 259–274, 2003.

[52] D. C. Chambers, W. S. Tunnicliffe, and J. G. Ayres, "Acute inhalation of cigarette smoke increases lower respiratory tract nitric oxide concentrations," *Thorax*, vol. 53, no. 8, pp. 677–679, 1998.

[53] D. D. Thomas, X. Liu, S. P. Kantrow, and J. R. Lancaster, "The biological lifetime of nitric oxide: implications for the perivascular dynamics of NO and O_2," *Proceedings of the National Academy of Sciences of the United States of America*, vol. 98, no. 1, pp. 355–360, 2001.

[54] R. S. Lewis and W. M. Deen, "Kinetics of the reaction of nitric oxide with oxygen in aqueous solutions," *Chemical Research in Toxicology*, vol. 7, no. 4, pp. 568–574, 1994.

[55] G. Ferrer-Sueta and R. Radi, "Chemical biology of peroxynitrite: kinetics, diffusion, and radicals," *ACS Chemical Biology*, vol. 4, no. 3, pp. 161–177, 2009.

[56] R. Radi, "Peroxynitrite, a stealthy biological oxidant," *The Journal of Biological Chemistry*, vol. 288, no. 37, pp. 26464–26472, 2013.

[57] M. Fransen, M. Nordgren, B. Wang, and O. Apanasets, "Role of peroxisomes in ROS/RNS-metabolism: implications for human disease," *Biochimica et Biophysica Acta (BBA) - Molecular Basis of Disease*, vol. 1822, no. 9, pp. 1363–1373, 2012.

[58] E. Zito, E. P. Melo, Y. Yang, A. Wahlander, T. A. Neubert, and D. Ron, "Oxidative protein folding by an endoplasmic reticulum-localized peroxiredoxin," *Molecular Cell*, vol. 40, no. 5, pp. 787–797, 2010.

[59] A. Sureshbabu and V. Bhandari, "Targeting mitochondrial dysfunction in lung diseases: emphasis on mitophagy," *Frontiers in Physiology*, vol. 4, 2013.

[60] Y. Jiang, X. Wang, and D. Hu, "Mitochondrial alterations during oxidative stress in chronic obstructive pulmonary disease," *International Journal of Chronic Obstructive Pulmonary Disease*, vol. Volume 12, pp. 1153–1162, 2017.

[61] L. Galluzzi, O. Kepp, and G. Kroemer, "Mitochondria: master regulators of danger signalling," *Nature Reviews Molecular Cell Biology*, vol. 13, no. 12, pp. 780–788, 2012.

[62] M. F. Alexeyev, "Is there more to aging than mitochondrial DNA and reactive oxygen species?," *The FEBS Journal*, vol. 276, no. 20, pp. 5768–5787, 2009.

[63] M. Madesh, W. X. Zong, B. J. Hawkins et al., "Execution of superoxide-induced cell death by the proapoptotic Bcl-2-related proteins Bid and Bak," *Molecular and Cellular Biology*, vol. 29, no. 11, pp. 3099–3112, 2009.

[64] C. H. Wiegman, C. Michaeloudes, G. Haji et al., "Oxidative stress-induced mitochondrial dysfunction drives inflammation and airway smooth muscle remodeling in patients with chronic obstructive pulmonary disease," *The Journal of Allergy and Clinical Immunology*, vol. 136, no. 3, pp. 769–780, 2015.

[65] R. F. Hoffmann, S. Zarrintan, S. M. Brandenburg et al., "Prolonged cigarette smoke exposure alters mitochondrial structure and function in airway epithelial cells," *Respiratory Research*, vol. 14, no. 1, p. 97, 2013.

[66] T. Ahmad, I. K. Sundar, C. A. Lerner et al., "Impaired mitophagy leads to cigarette smoke stress-induced cellular senescence: implications for chronic obstructive pulmonary disease," *The FASEB Journal*, vol. 29, no. 7, pp. 2912–2929, 2015.

[67] K. Mizumura, S. M. Cloonan, K. Nakahira et al., "Mitophagy-dependent necroptosis contributes to the pathogenesis of COPD," *The Journal of Clinical Investigation*, vol. 124, no. 9, pp. 3987–4003, 2014.

[68] M. Frank, S. Duvezin-Caubet, S. Koob et al., "Mitophagy is triggered by mild oxidative stress in a mitochondrial fission dependent manner," *Biochimica et Biophysica Acta (BBA) - Molecular Cell Research*, vol. 1823, no. 12, pp. 2297–2310, 2012.

[69] S. Marchi, C. Giorgi, J. M. Suski et al., "Mitochondria-ros crosstalk in the control of cell death and aging," *Journal of Signal Transduction*, vol. 2012, Article ID 329635, 17 pages, 2012.

[70] C. Berndt, C. H. Lillig, and L. Flohe, "Redox regulation by glutathione needs enzymes," *Frontiers in Pharmacology*, vol. 5, 2014.

[71] J. M. McCord and I. Fridovich, "Superoxide dismutase. An enzymic function for erythrocuprein (hemocuprein)," *The Journal of Biological Chemistry*, vol. 244, no. 22, pp. 6049–6055, 1969.

[72] M. V. Omelchenko, M. Y. Galperin, Y. I. Wolf, and E. V. Koonin, "Non-homologous isofunctional enzymes: a systematic analysis of alternative solutions in enzyme evolution," *Biology Direct*, vol. 5, no. 1, p. 31, 2010.

[73] J. J. Perry, D. S. Shin, E. D. Getzoff, and J. A. Tainer, "The structural biochemistry of the superoxide dismutases," *Biochimica et Biophysica Acta (BBA) - Proteins and Proteomics*, vol. 1804, no. 2, pp. 245–262, 2010.

[74] M. F. Tsan, "Superoxide dismutase and pulmonary oxygen toxicity," *Experimental Biology and Medicine*, vol. 214, no. 2, pp. 107–113, 1997.

[75] M. F. Tsan, "Superoxide dismutase and pulmonary oxygen toxicity: lessons from transgenic and knockout mice (review)," *International Journal of Molecular Medicine*, vol. 7, no. 1, pp. 13–19, 2001.

[76] A. Perkins, K. J. Nelson, D. Parsonage, L. B. Poole, and P. A. Karplus, "Peroxiredoxins: guardians against oxidative stress and modulators of peroxide signaling," *Trends in Biochemical Sciences*, vol. 40, no. 8, pp. 435–445, 2015.

[77] L. B. Poole, A. Hall, and K. J. Nelson, "Overview of peroxiredoxins in oxidant defense and redox regulation," *Current Protocols in Toxicology*, 2011, Chapter 7, Unit 7.9.

[78] J. H. Park, Y. S. Kim, H. L. Lee et al., "Expression of peroxiredoxin and thioredoxin in human lung cancer and paired normal lung," *Respirology*, vol. 11, no. 3, pp. 269–275, 2006.

[79] Y. Manevich and A. B. Fisher, "Peroxiredoxin 6, a 1-Cys peroxiredoxin, functions in antioxidant defense and lung phospholipid metabolism," *Free Radical Biology & Medicine*, vol. 38, no. 11, pp. 1422–1432, 2005.

[80] R. J. Hondal, S. M. Marino, and V. N. Gladyshev, "Selenocysteine in thiol/disulfide-like exchange reactions," *Antioxidants & Redox Signaling*, vol. 18, no. 13, pp. 1675–1689, 2013.

[81] S. Bouch, M. O'Reilly, J. B. de Haan, R. Harding, and F. Sozo, "Does lack of glutathione peroxidase 1 gene expression exacerbate lung injury induced by neonatal hyperoxia in mice?," *American Journal of Physiology-Lung Cellular and Molecular Physiology*, vol. 313, no. 1, pp. L115–L125, 2017.

[82] A. V. Peskin, F. M. Low, L. N. Paton, G. J. Maghzal, M. B. Hampton, and C. C. Winterbourn, "The high reactivity of peroxiredoxin 2 with H_2O_2 is not reflected in its reaction with other oxidants and thiol reagents," *The Journal of Biological Chemistry*, vol. 282, no. 16, pp. 11885–11892, 2007.

[83] R. M. Jackson, W. J. Russell, and C. F. Veal, "Endogenous and exogenous catalase in reoxygenation lung injury," *Journal of Applied Physiology*, vol. 72, no. 3, pp. 858–864, 1992.

[84] V. Conti, G. Corbi, V. Manzo, G. Pelaia, A. Filippelli, and A. Vatrella, "Sirtuin 1 and aging theory for chronic obstructive pulmonary disease," *Analytical Cellular Pathology*, vol. 2015, Article ID 897327, 8 pages, 2015.

[85] G. S. Budinger, R. A. Kohanski, W. Gan et al., "The intersection of aging biology and the pathobiology of lung diseases: a joint NHLBI/NIA workshop," *The Journals of Gerontology. Series A, Biological Sciences and Medical Sciences*, vol. 72, no. 11, pp. 1492–1500, 2017.

[86] K. Ito and P. J. Barnes, "COPD as a disease of accelerated lung aging(a)," *Revista Portuguesa de Pneumologia*, vol. 15, no. 4, pp. 743–746, 2009.